VIRAL INFECTION AT THE MATERNAL-FETAL INTERFACE

EDITED BY: Abhay P. S. Rathore, Vivian Vasconcelos Costa and Ashley L. St John
PUBLISHED IN: Frontiers in Immunology

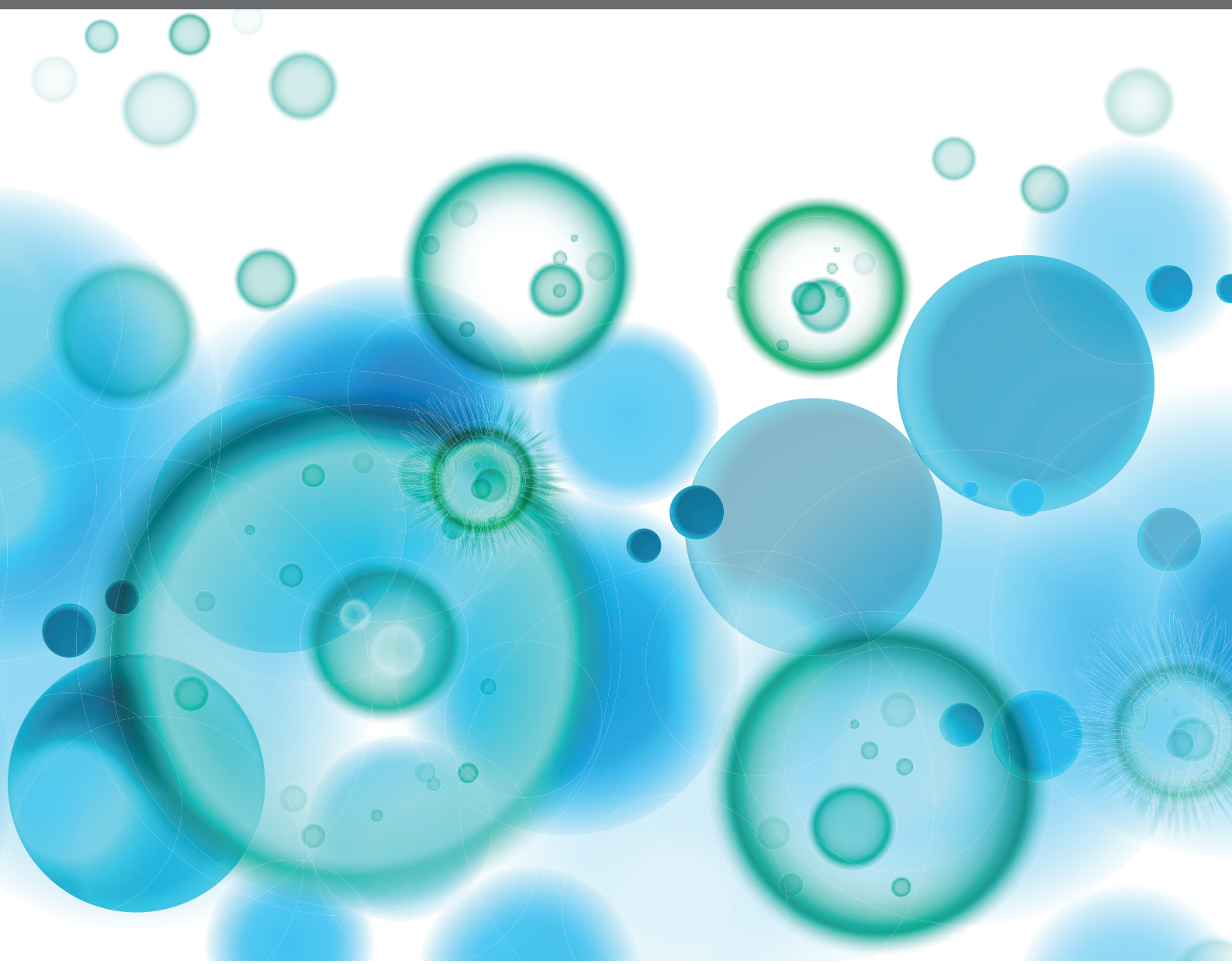

frontiers Research Topics

ISSN 1664-8714
ISBN 978-2-88974-586-9
DOI 10.3389/978-2-88974-586-9

About Frontiers

Frontiers is more than just an open-access publisher of scholarly articles: it is a pioneering approach to the world of academia, radically improving the way scholarly research is managed. The grand vision of Frontiers is a world where all people have an equal opportunity to seek, share and generate knowledge. Frontiers provides immediate and permanent online open access to all its publications, but this alone is not enough to realize our grand goals.

Frontiers Journal Series

The Frontiers Journal Series is a multi-tier and interdisciplinary set of open-access, online journals, promising a paradigm shift from the current review, selection and dissemination processes in academic publishing. All Frontiers journals are driven by researchers for researchers; therefore, they constitute a service to the scholarly community. At the same time, the Frontiers Journal Series operates on a revolutionary invention, the tiered publishing system, initially addressing specific communities of scholars, and gradually climbing up to broader public understanding, thus serving the interests of the lay society, too.

Dedication to Quality

Each Frontiers article is a landmark of the highest quality, thanks to genuinely collaborative interactions between authors and review editors, who include some of the world's best academicians. Research must be certified by peers before entering a stream of knowledge that may eventually reach the public - and shape society; therefore, Frontiers only applies the most rigorous and unbiased reviews.
Frontiers revolutionizes research publishing by freely delivering the most outstanding research, evaluated with no bias from both the academic and social point of view. By applying the most advanced information technologies, Frontiers is catapulting scholarly publishing into a new generation.

What are Frontiers Research Topics?

Frontiers Research Topics are very popular trademarks of the Frontiers Journals Series: they are collections of at least ten articles, all centered on a particular subject. With their unique mix of varied contributions from Original Research to Review Articles, Frontiers Research Topics unify the most influential researchers, the latest key findings and historical advances in a hot research area! Find out more on how to host your own Frontiers Research Topic or contribute to one as an author by contacting the Frontiers Editorial Office: frontiersin.org/about/contact

VIRAL INFECTION AT THE MATERNAL-FETAL INTERFACE

Topic Editors:
Abhay P. S. Rathore, Duke University, United States
Vivian Vasconcelos Costa, Federal University of Minas Gerais, Brazil
Ashley L. St John, Duke-NUS Medical School, Singapore

Citation: Rathore, A. P. S., Costa, V. V., St John, A. L., eds. (2022). Viral Infection at the Maternal-Fetal Interface. Lausanne: Frontiers Media SA.
doi: 10.3389/978-2-88974-586-9

Table of Contents

frontiers in Immunology

EDITORIAL
published: 04 February 2022
doi: 10.3389/fimmu.2022.828681

Editorial: Viral Infection at the Maternal-Fetal Interface

Abhay P. S. Rathore[1*], *Vivian Vasconcelos Costa*[2,3,4] *and Ashley L. St. John*[5,6,7]

[1] Department of Pathology, Duke University Medical Center, Durham, NC, United States, [2] Research Group in Arboviral Diseases, Institute of Biological Sciences, Universidade Federal de Minas Gerais, Belo Horizonte, Brazil, [3] Center for Drug Research and Development of Pharmaceuticals, Institute of Biological Sciences, Universidade Federal de Minas Gerais, Belo Horizonte, Brazil, [4] Departament of Morphology, Institute of Biological Sciences, Universidade Federal de Minas Gerais, Belo Horizonte, Brazil, [5] Program in Emerging Infectious Diseases, Duke-National University of Singapore (NUS), Singapore, Singapore, [6] Department of Microbiology and Immunology, Yong Loo Lin School of Medicine, National University of Singapore (NUS), Singapore, Singapore, [7] SingHealth Duke-National University of Singapore (NUS) Global Health Institute, Singapore, Singapore

Keywords: viruses, maternal-fetal, COVID - 19, Zika, CMV, HIV, maternal immunity

Editorial on the Research Topic

Viral Infection at the Maternal-Fetal Interface

The emergence of infections such as Zika virus (ZIKV) has highlighted the importance of understanding diseases that can be transferred vertically from mother to the fetus. Viruses constitute a large proportion of TORCH pathogens [Toxoplasmosis, Other (syphilis, varicella-zoster, parvovirus B19, Zika), Rubella, Cytomegalovirus (CMV), and Herpes infections], which can result in congenital infections impacting neonatal health and neurodevelopment. Maternal and fetal immunity are critical for infection clearance, while pathogens have evolved to evade both innate and adaptive immune responses that restrict infection spread. In this collection of research articles and reviews, researchers have discussed the interplay between a mothers' immunity and the fetal developing immune system as well as the consequences to fetal health during congenital viral infections.

The human full-term pregnancy is approximately 40 weeks and divided in to three trimesters reflecting stages of development. Gestational age at the time of exposure to infections is one of the important determinants of congenital disease outcomes. For example, ZIKV infection during the first trimester of pregnancy is associated with a higher risk of developing birth defects such as microcephaly and ocular defects in newborns (1). This was elegantly supported by Newman et al. in a study mimicking the sexual transmission of ZIKV infection by intravaginal inoculation of ZIKV in rhesus macaques during developmental time points consistent with the first trimester of pregnancy. The pregnant females exposed to ZIKV during early gestation were found to have non-viable embryos and viral RNA was detected in the demised embryos, supporting a risk of pregnancy loss during early gestation. In contrast to ZIKV, CMV infections are associated with adverse fetal health outcomes when infection occurs during the late gestation periods of second-third trimester (2). To address the increased susceptibility of CMV infection during late gestation, Berkebile et al. used a Guinea pig model of CMV infection. When guinea pigs were infected at days 21 and 35 of gestation (equivalent to mid to late gestational time points in humans), maternal and placental viral load did not differ between the two infection groups. However, transcriptome analysis revealed significant changes in transcripts associated with immune activation in the gestational day 35 infection group

OPEN ACCESS

Edited and reviewed by:
Alexis M. Kalergis, Pontificia Universidad Católica de Chile, Chile

****Correspondence:***
Abhay P. S. Rathore
abhay.rathore@duke.edu

Specialty section:
This article was submitted to Viral Immunology, a section of the journal Frontiers in Immunology

Received: *03 December 2021*
Accepted: *17 January 2022*
Published: *04 February 2022*

Citation:
Rathore APS, Costa VV and St. John AL (2022) Editorial: Viral Infection at the Maternal-Fetal Interface. Front. Immunol. 13:828681. doi: 10.3389/fimmu.2022.828681

suggesting placental sensitization to injury during late gestation CMV infection. In contrast to ZIKV infection, which is acute and is mainly transferred *in utero* (3), HIV transmission from mother to child can occur during various stages of pregnancy and at the time of birth or after birth. This complex nature of HIV transmission from mother to child was reviewed for this collection by Amin et al. They elaborately discussed HIV infection in the context of early life immune responses and viral persistence. Together these studies emphasize the importance of infection timing during pregnancy and early life to immune and functional outcomes of viral infections.

The placenta is a unique organ that emerges in the context of pregnancy to provide nourishment and gas exchange for the developing fetus (4). This critical role is balanced by the need for immune functions that protect mother and developing fetus from adverse outcomes, including congenital infections. The structure of the placenta is central to this role, with the maternal decidua segregated from the placenta through a network of tight barriers involving the syncytiotrophoblast cells and fetal endothelium, where active transport processes are involved in allowing specific substances and molecules to pass from mother to fetus. The complexities of the maternal-fetal interactions at the placental interface are emphasized by the presence of the fully functional maternal immune system, which must interact with newly developing fetal immunity. Thus, during healthy pregnancies, immune responses at the maternal-fetal interface are characterized by immune tolerance (5), which must be balanced with the need to provide protection from pathogens. This complexity in the maternal immune system is highlighted by Moström et al. utilizing a pregnancy model of rhesus macaques. Various innate and adaptive cell populations were profiled in the maternal decidua and in the peripheral blood of pregnant mothers. When comparing healthy and ZIKV-infected pregnancies, signatures of immune suppression with reduced recruitment of functional cytotoxic T cells were observed in ZIKV-infected pregnancies, suggesting reduced capacity for infection clearance.

Viral infection at the maternal-fetal interface could cause placental insufficiency resulting in intra uterine growth restriction (IUGR) and thereby limiting normal fetal growth (6). Experimentally, using wildtype and type-I interferon deficient mice, Andrade et al. show that ZIKV infection resulted in the release of proinflammatory mediators and disrupted the abca1 transporter in the placenta, leading to placental insufficiency and IUGR. In humans, Ronchi et al. utilized morphometric analysis of placenta tissue from ZIKV- and HIV-infected pregnant women. Their data revealed pathological similarities such as increased numbers of knots, sprouts, and $CD163^{+}$ Hofbauer cell hyperplasia with more pronounced Hofbauer cell hyperplasia in ZIKV compared to HIV infected pregnancies. Morphologic features of the placenta were also investigated by Rebutini et al. in the context of maternal SARS-CoV-2 infection. Although SARS-CoV-2 is not well established to vertically transmit from mother to fetus (7, 8), this report highlights its potential of maternal viral infection to influence fetal outcomes by impacting the placental tissue. Strikingly, the authors observed both maternal and fetal malperfusion during COVID-19, and found that pregnant women with SARS-CoV-2 infection were more likely to display chronic histiocytic intervillositis, which is an inflammatory disorder involving infiltration of histiocytes/macrophages into the placenta (9). These reports providing comparisons of the virus-induced changes to the placental ultrastructure in the context of chronic versus acute viral infections highlight that there are likely similar pathways that are triggered to restrict viral infection during pregnancy at the maternal-fetal interface and that these could influence the health of the placental tissue.

Recognizing breast feeding as another important component of maternal-infant exchange with the potential to influence immunity and infection, García et al. characterized the influence of SARS-CoV-2 infection on immune compounds in breast milk. Using a case control study design, they revealed a profile of immune activation that could be detected in the form of higher levels of pro-inflammatory cytokines such as Eotaxin, IP-10, MIP-1α, and RANTES, as well as several growth factors. The pro-inflammatory profile of breast milk from SARS-CoV-2 convalescent mothers is likely supportive of the role of breast milk in providing immune protection to infants from viral infections to which they are likely to be exposed post-partum.

Maternal adaptive immune responses that are pre-existing also have the potential to influence fetal outcomes during pregnancy. In the context of flavivirus infections, exposure to multiple flaviviruses in a lifetime is common, and these heterologous immune responses are often cross-reactive but non-neutralizing and cannot induce full protection against closely related viruses (10). Antibodies against dengue virus for example, have been shown to enhance replication of ZIKV through both antibody-dependent enhancement of infection (ADE) involving uptake of virus/antibody immune complexes *via* Fc receptors on permissive cells such as monocytes, or through transplacental trafficking using the FcRN receptor (11, 12). Acklin et al. addressed the question of whether West Nile Virus (WNV) antibodies could influence ZIKV pathogenesis in a murine model using $STAT2^{-/-}$ mice to enhance disease severity. They found similar resorption rates, fetal and placental sizes and virus infection levels in the presence of human WNV-specific antibodies in mice, in spite of those antibodies promoting efficient ADE *in vitro*, suggesting WNV-specific antibodies to have negligible influence on enhancement of ZCS.

Adaptive immune responses in donors with a history of ZIKV infection during pregnancy were examined in depth by Badolato-Corrêa et al. Extensive characterization of antigen-specific CD4 and CD8 T cells highlighted the rapid decay of ZIKV-specific CD8 T cells relative to CD4 T cells in the months following infection resolution. Interestingly, the authors highlight that there were not significant differences between the T cell responses of mothers with asymptomatic children, versus children with ZCS. This study suggests that similar memory T cell responses are induced by mild and severe congenital disease in the context of ZIKV infection.

Finally, one study investigated whether interventions could be used to prevent fetal complications or severe outcomes of infection. Marim et al. demonstrated that targeting of fetal kynurenine pathway signaling during ZIKV infection in mice could improve neurological outcomes of congenital infection.

Together the articles in this Research Topic advance our understanding of immunological mechanisms promoting health or disease at the maternal-fetal interface during viral infections.

AUTHOR CONTRIBUTIONS

All authors contributed to the article and approved the submitted version.

FUNDING

The authors acknowledge funding from NRF-CRP17-2017-04.

REFERENCES

1. Brasil P, Pereira JP Jr, Moreira ME, Ribeiro Nogueira RM, Damasceno L, Wakimoto M, et al. Zika Virus Infection in Pregnant Women in Rio De Janeiro. *N Engl J Med* (2016) 375(24):2321–34. doi: 10.1056/NEJMoa1602412
2. Bodeus M, Hubinont C, Goubau P. Increased Risk of Cytomegalovirus Transmission In Utero During Late Gestation. *Obstet Gynecol* (1999) 93(5 Pt 1):658–60. doi: 10.1016/S0029-7844(98)00538-9
3. Mlakar J, Korva M, Tul N, Popovic M, Poljsak-Prijatelj M, Mraz J, et al. Zika Virus Associated With Microcephaly. *N Engl J Med* (2016) 374(10):951–8. doi: 10.1056/NEJMoa1600651
4. Gude NM, Roberts CT, Kalionis B, King RG. Growth and Function of the Normal Human Placenta. *Thromb Res* (2004) 114(5-6):397–407. doi: 10.1016/j.thromres.2004.06.038
5. Aluvihare VR, Kallikourdis M, Betz AG. Regulatory T Cells Mediate Maternal Tolerance to the Fetus. *Nat Immunol* (2004) 5(3):266–71. doi: 10.1038/ni1037
6. Peleg D, Kennedy CM, Hunter SK. Intrauterine Growth Restriction: Identification and Management. *Am Fam Physician* (1998) 58(2):453–60, 466-7.
7. Edlow AG, Li JZ, Collier AY, Atyeo C, James KE, Boatin AA, et al. Assessment of Maternal and Neonatal SARS-CoV-2 Viral Load, Transplacental Antibody Transfer, and Placental Pathology in Pregnancies During the COVID-19 Pandemic. *JAMA Netw Open* (2020) 3(12):e2030455. doi: 10.1001/jamanetworkopen.2020.30455
8. Vivanti AJ, Vauloup-Fellous C, Prevot S, Zupan V, Suffee C, Do Cao J, et al. Transplacental Transmission of SARS-CoV-2 Infection. *Nat Commun* (2020) 11(1):3572. doi: 10.1038/s41467-020-17436-6
9. Boyd TK, Redline RW. Chronic Histiocytic Intervillositis: A Placental Lesion Associated With Recurrent Reproductive Loss. *Hum Pathol* (2000) 31 (11):1389–96. doi: 10.1016/S0046-8177(00)80009-X
10. Rathore APS, St John AL. Cross-Reactive Immunity Among Flaviviruses. *Front Immunol* (2020) 11:334. doi: 10.3389/fimmu.2020.00334
11. Rathore APS, Saron WAA, Lim T, Jahan N, St John AL. Maternal Immunity and Antibodies to Dengue Virus Promote Infection and Zika Virus-Induced Microcephaly in Fetuses. *Sci Adv* (2019) 5(2):eaav3208. doi: 10.1126/sciadv.aav3208
12. Brown JA, Singh G, Acklin JA, Lee S, Duehr JE, Chokola AN, et al. Dengue Virus Immunity Increases Zika Virus-Induced Damage During Pregnancy. *Immunity* (2019) 50(3):751–62.e5. doi: 10.1016/j.immuni.2019.01.005

Conflict of Interest: The authors declare that the research was conducted in the absence of any commercial or financial relationships that could be construed as a potential conflict of interest.

frontiers in Immunology

ORIGINAL RESEARCH
published: 12 February 2021
doi: 10.3389/fimmu.2021.610456

Differential Longevity of Memory CD4 and CD8 T Cells in a Cohort of the Mothers With a History of ZIKV Infection and Their Children

Jessica Badolato-Corrêa[1†], Fabiana Rabe Carvalho[2†], Iury Amancio Paiva[1], Débora Familiar-Macedo[1], Helver Gonçalves Dias[1], Alex Pauvolid-Corrêa[3,4], Caroline Fernandes-Santos[1], Monique da Rocha Queiroz Lima[1], Mariana Gandini[5], Andréa Alice Silva[2], Silvia Maria Baeta Cavalcanti[6], Solange Artimos de Oliveira[7], Renata Artimos de Oliveira Vianna[7], Elzinandes Leal de Azeredo[1], Claudete Aparecida Araújo Cardoso[2,7], Alba Grifoni[8], Alessandro Sette[8,9], Daniela Weiskopf[8] and Luzia Maria de-Oliveira-Pinto[1]*

[1] Laboratory of Viral Immunology, Fundação Oswaldo Cruz, Rio de Janeiro, Brazil, [2] Multiuser Laboratory for Research in Nephrology and Medical Science, School of Medicine, Universidade Federal Fluminense, Niterói, Brazil, [3] Department of Veterinary Integrative Biosciences, Texas A&M University, College Station, TX, United States, [4] Laboratory of Respiratory Viruses and Measles, Fiocruz, Rio de Janeiro, Brazil, [5] Laboratory of Cellular Microbiology, Fundação Oswaldo Cruz, Rio de Janeiro, Brazil, [6] Laboratory of Virological Diagnosis, Biomedical Institute, Universidade Federal Fluminense, Niterói, Brazil, [7] Department of Maternal and Child, School of Medicine, Universidade Federal Fluminense, Niterói, Brazil, [8] Center for Infectious Disease and Vaccine Research, La Jolla Institute for Immunology (LJI), San Diego, CA, United States, [9] Division of Infectious Diseases and Global Public Health, Department of Medicine, University of California, San Diego, San Diego, CA, United States

OPEN ACCESS

Edited by:
Ashley L. St John,
Duke-NUS Medical School, Singapore

Reviewed by:
Nina Le Bert,
Duke-NUS Medical School, Singapore
Abhay P. S. Rathore,
Duke University, United States

***Correspondence:**
Luzia Maria de-Oliveira-Pinto
lpinto@ioc.fiocruz.br

[†] These authors have contributed equally to this work

Specialty section:
This article was submitted to Viral Immunology, a section of the journal Frontiers in Immunology

Received: 25 September 2020
Accepted: 22 January 2021
Published: 12 February 2021

Citation:
Badolato-Corrêa J, Carvalho FR, Paiva IA, Familiar-Macedo D, Dias HG, Pauvolid-Corrêa A, Fernandes-Santos C, Lima MRQ, Gandini M, Silva AA, Baeta Cavalcanti SM, de Oliveira SA, de Oliveira Vianna RA, de Azeredo EL, Cardoso CAA, Grifoni A, Sette A, Weiskopf D and de-Oliveira-Pinto LM (2021) Differential Longevity of Memory CD4 and CD8 T Cells in a Cohort of the Mothers With a History of ZIKV Infection and Their Children. Front. Immunol. 12:610456. doi: 10.3389/fimmu.2021.610456

Background: Zika virus (ZIKV) infection causes for mild and self-limiting disease in healthy adults. In newborns, it can occasionally lead to a spectrum of malformations, the congenital Zika syndrome (CZS). Thus, little is known if mothers and babies with a history of ZIKV infection were able to develop long-lasting T-cell immunity. To these issues, we measure the prevalence of ZIKV T-cell immunity in a cohort of mothers infected to the ZIKV during pregnancy in the 2016–2017 Zika outbreak, who gave birth to infants affected by neurological complications or asymptomatic ones.

Results: Twenty-one mothers and 18 children were tested for IFN-γ ELISpot and T-cell responses for flow cytometry assays in response to CD4 ZIKV and CD8 ZIKV megapools (CD4 ZIKV MP and CD8 ZIKV MP). IFN-γ ELISpot responses to ZIKV MPs showed an increased CD4 and CD8 T-cell responses in mothers compared to children. The degranulation activity and IFN-γ-producing CD4 T cells were detected in most mothers, and children, while in CD8 T-cells, low responses were detected in these study groups. The total Temra T cell subset is enriched for IFN-γ+ CD4 T cells after stimulation of CD4 ZIKV MP.

Conclusion: Donors with a history of ZIKV infection demonstrated long-term CD4 T cell immunity to ZIKV CD4 MP. However, the same was not observed in CD8 T cells with the ZIKV CD8 MP. One possibility is that the cytotoxic and pro-inflammatory activities of CD8 T cells are markedly demonstrated in the early stages of infection, but less detected in the disease resolution phase, when the virus has already been eliminated. The

responses of mothers' T cells to ZIKV MPs do not appear to be related to their children's clinical outcome. There was also no marked difference in the T cell responses to ZIKV MP between children affected or not with CZS. These data still need to be investigated, including the evaluation of the response of CD8 T cells to other ZIKV peptides.

Keywords: Zika, T cells, memory, pregnancy, congenital Zika syndrome (CZS)

INTRODUCTION

The emergence of ZIKV in dengue-endemic regions creates a potentially alarming scenario, as those caused by the ZIKV epidemic spread across countries, especially the Americas, during 2015–2016 (1, 2). At present, half of the world's population is considered at risk of dengue virus (DENV), and cases of ZIKV continue to be reported globally (3, 4).

DENV and ZIKV are members of the family *Flaviviridae* and are among the several medically important viruses (5). Both are spread *via* the bite of infected mosquitoes, *Aedes spp*., whose ecological niches expand beyond the tropical and sub-tropical regions (6). Moreover, ZIKV can be transmitted *via* sexual contact (7, 8). It persists for weeks in the reproductive tract (9–11) and undergoes vertical transmission from a mother to fetus (12–15). During Latin America and French Polynesia outbreaks, ZIKV infection typically produces mild symptoms that resolve rapidly. However, when an infection occurs during pregnancy, occasional vertical transmission can lead to a spectrum of devastating neurodevelopmental aberrations, collectively referred to as congenital Zika syndrome (CZS) (16). Conflicting data sets indicate that infants born to mothers infected with ZIKV during pregnancy carry up to 42% risk of developing overt clinical or neuroimaging abnormalities (17–21).

ZIKV is closely related to four serotypes of DENV. They are a positive-sense, single-stranded enveloped RNA virus. The genome encodes a polyprotein, which is processed into three structural proteins [the capsid (C), premembrane (prM), and the envelope (E) protein] and seven non-structural proteins (NS1, NS2A, NS2B, NS3, NS4A, NS4B, and NS5) (22). DENV and ZIKV share 55.1–56.3% amino acid sequence identity (23).

Tonnerre et al. performed a remarkably interesting longitudinal study with samples from 10 non-pregnant women with ZIKV-confirmed acute infection. For the T cell response, the authors confirmed different virus-specific targets for CD4 and CD8 T cells (24). They found that previous DENV infections largely affect the humoral response to ZIKV, with effects on the T cell side limited to increasing the frequency of ZIKV-specific CD8 T cells in some patients (24, 25).

Although viral infections are common during pregnancy, transplacental passage, and fetal infection appear to be the exception rather than the rule. Viral infections during pregnancy have been linked to adverse pregnancy outcomes and birth defects in offspring. Unfortunately, there are limited therapeutic or preventive tools to protect both mother and fetus during pandemics (26).

In the present study, we studied ZIKV memory T cell responses from a cohort of mothers infected with ZIKV during pregnancy in the 2016–2017 Zika outbreak who gave birth to infants affected by neurological complications or asymptomatic ones. These donors with a history of ZIKV infection were evaluated in 2018–2019, 2–3 years after ZIKV infection. This cohort provides a unique opportunity to study ZIKV immunity in an infection occurring during pregnancy and compare it with longitudinal follow-up samples.

MATERIALS AND METHODS

Study Design, Volunteers, and Samples

A cross-sectional study was carried out in pregnant mothers infected with ZIKV and children born to mothers who reported rash during pregnancy overlapping with the ZIKV Public Health Emergency of National Concern in Brazil period (November 2015 and May 2017). These donors' cohort was referred from the Exanthematic Diseases Unit at the Hospital Universitário Antonio Pedro of the Universidade Federal Fluminense (HUAP/UFF) located in Niteroi, Rio de Janeiro (Brazil). Laboratory evidence for ZIKV infection during pregnancy was based on a mother's positive quantitative real-time (qRT)-PCR test result on serum and/or urine samples, done at the flavivirus reference laboratory of Rio de Janeiro State (LACEN, RJ, Brazil) and confirmed by Multiuser Laboratory for Research Support in Nephrology and Medical Science (LAMAP, UFF, Brazil) (27). A qRT-PCR positive test result at any point after maternal rash onset confirmed the ZIKV infection within the first 5 days of rash and/or the urine sample was tested by the 14th day. So, we included 21 pregnant mothers who presented rash, with or without other clinical symptoms suggestive of arbovirus infections, such as arthralgia, myalgia, fever, headache, and conjunctival hyperemia. The exclusion criteria were mothers who were positive with a qRT-PCR for other arboviruses such as chikungunya and dengue. Moreover, mothers who presented positive test results to syphilis, toxoplasmosis, rubella, cytomegalovirus, and HIV infection were excluded. All serology tests were performed by the Service of Clinical Pathology (HUAP, UFF Brazil) (**Figure 1**). Three mothers were infected in the first trimester of pregnancy, 14 in the second trimester, 3 in the third trimester, and 1 before pregnancy (**Table 1**), thus making any laboratory diagnosis of acute Zika infection in babies impossible.

Eighteen children aged 17–38 months with a history of intrauterine exposure to ZIKV were classified as asymptomatic or with CZS if the test was negative for other congenital infections. The asymptomatic ZIKV group (positive maternal qRT-PCR, $n = 9$) consisted of patients with maternal exposure to ZIKV during pregnancy and no clinical evidence of CZS.

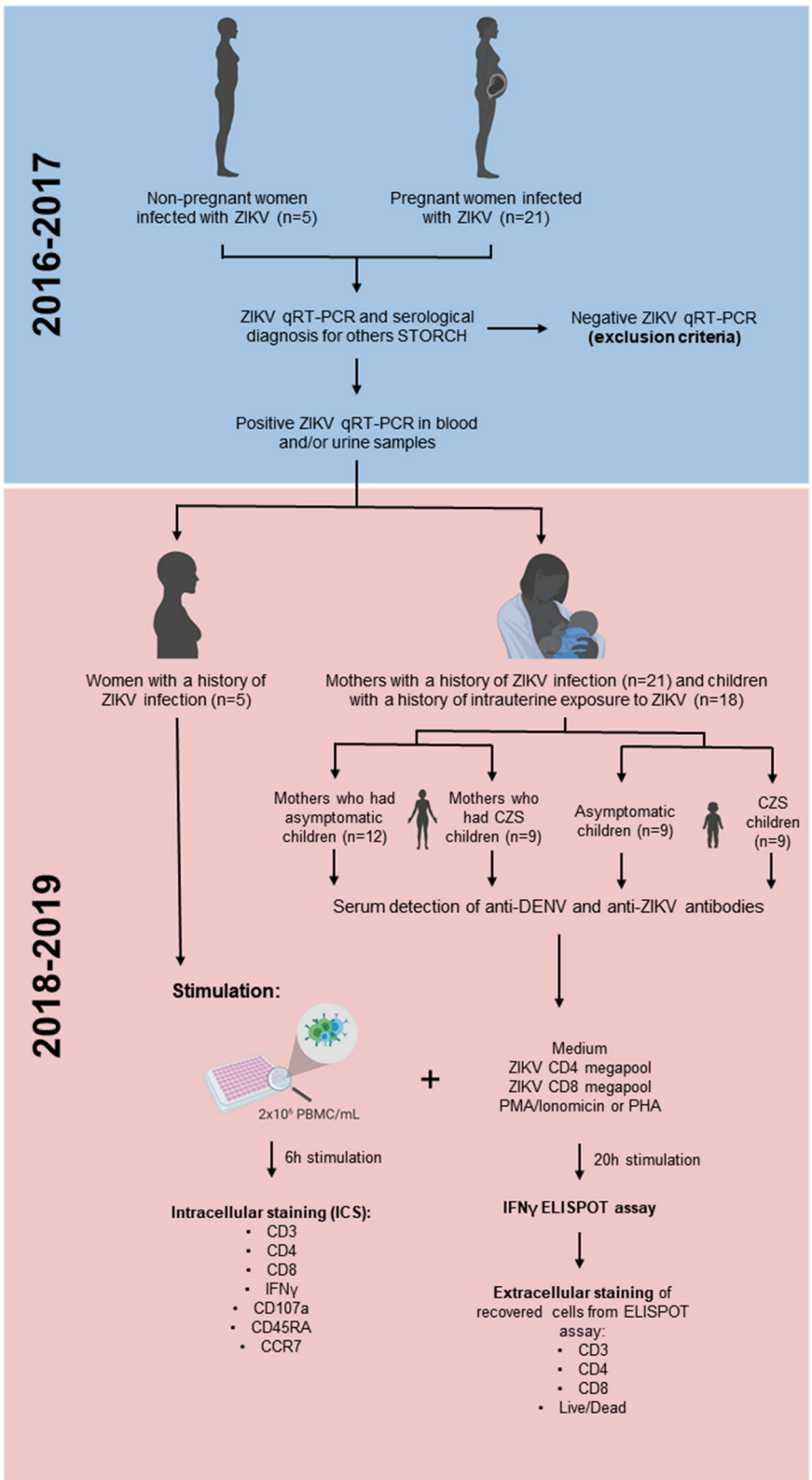

FIGURE 1 | The experimental design used in this study.

TABLE 1 | Characteristics of the recovered mothers infected to Zika virus during pregnancy and their intrauterine exposed children recruited from 2018 to 2019.

Group	Outcome at birth	ID	Age[a,b]	Illness time[b]	Gestational trimester at onset rash	State	RT-aPCR ZIKV	ZIKV anti-IgG	DENV anti-IgG	PRNT 90 ZIKV	PRNT 90 DENV-1	CD4+CD3+ T cells	CD8+CD3+ T cells	CD4/CD8
Women		W1	40	36		RJ	pos	pos	pos	<10	≥10	77.5	13.8	5.6
		W2	40	40		RJ	pos	pos	pos	<10	<10	74.2	18.0	4.1
		W3	23	38		RJ	pos	pos	pos	<10	≥10	60.1	29.4	2.0
		W4	25	42		RJ	pos	pos	pos	<10	≥10	58.9	22.2	2.7
		W5	27	35		RJ	pos	pos	pos	<10	≥10	76.3	20.0	3.8
			27.0 (23–40)[a]	38.0 (35–42)								69.9 (41.5–76.7)	20.0 (13.8–29.4)	3.8 (2–5.6)
Mothers	Asympt.	M1	22	38	3rd	RJ	pos	pos	neg	160	<10	81.6	9.81	8.3
	Asympt.	M2	36	40	3rd	RJ	pos	pos	pos	>320	≥10	65.2	22.3	2.9
	Asympt.	M3	37	38	2nd	RJ	pos	pos	pos	>320	≥10	62.5	16.5	3.8
	Asympt.	M4	23	24	2nd	RJ	pos	pos	neg	>320	<10	66.6	20.2	3.3
	Asympt.	M5	27	40	2nd	RJ	pos	pos	neg	>320	≥10	71.9	19.5	3.7
	Asympt.	M6	33	38	2nd	RJ	pos	pos	pos	<10	<10	61.0	29.2	2.1
	Asympt.	M7	37	38	2nd	RJ	pos	pos	pos	>320	≥10	73.7	21.1	3.5
	Asympt.	M8	41	x	2nd	RJ	pos	neg	neg	>320	<10	61.6	31.1	2.0
	Asympt.	M9	21	38	2nd	RJ	pos	pos	pos	>320	≥10	72.9	17.1	4.3
	Asympt.	M10	32	40	2nd	RJ	pos	pos	pos	>320	≥10	66.9	20.7	3.2
	Asympt.	M11	30	39	2nd	RJ	pos	pos	pos	>320	≥10	69.5	5.49	12.7
	Asympt.	M12	33	39	2nd	RJ	pos	pos	pos	>320	≥10	66.0	16.7	4.0
			32.5 (21–41)[a]	38.0 (24–40)								66.8 (61–81.6)	19.9 (5.5–31.1)	3.6 (2–12.7)
Mothers	CZS	M13	24	23	1st	RJ	pos	pos	neg	>320	<10	71.6	21.6	3.3
	CZS	M14	42	39	2nd	RJ	pos	pos	pos	>320	<10	67.1	22.5	3.0
	CZS	M15	25	37	3rd	RJ	pos	pos	neg	>320	≥10	66.0	17.4	3.8
	CZS	M16	21	42	1st	RJ	pos	pos	pos	>320	≥10	57.4	24.3	2.4
	CZS	M17	40	40	2nd	RJ	pos	pos	pos	>320	≥10	76.5	17.7	4.3
	CZS	M18	41	36	2nd	RJ	pos	pos	pos	>320	<10	71.3	22.3	3.2
	CZS	M19	28	38	2nd	RJ	pos	pos	pos	>320	≥10	80.5	13.9	5.8
	CZS	M20	21	39	before	RJ	pos	pos	pos	>320	<10	62.7	23.2	2.7
	CZS	M21	28	41	1st	RJ	pos	neg	pos	>320	≥10	78.9	14.9	5.3
			28.0 (21–42)[a]	39.0 (23–42)								71.3 (57.4–80.5)	21.6 (13.9–24.3)	3.3 (2.4–5.8)
Children	Asympt.	C1	35	36		RJ	x	neg	neg	x	x	56.1	29.2	1.9
	Asympt.	C2	29	38		RJ	x	neg	neg	<10	≥10	63.9	25.3	2.5
	Asympt.	C3	31	38		RJ	x	neg	pos	x	x	59.2	17.3	3.4

(Continued)

TABLE 1 | Continued

Group	Outcome at birth	ID	Age[a,b]	Illness time[b]	Gestational trimester at onset rash	State	RT-aPCR ZIKV	ZIKV anti-IgG	DENV anti-IgG	PRNT 90 ZIKV	PRNT 90 DENV-1	CD4+CD3+ T cells	CD8+CD3+ T cells	CD4/CD8
	Asympt.	C4	34	37		RJ	x	pos	pos	>320	≥10	80.0	15.2	5.3
	Asympt.	C5	41	39		RJ	x	neg	neg	<10	≥10	70.9	19.4	3.7
	Asympt.	C6	32	38		RJ	x	neg	neg	<10	<10	54.7	30.7	1.8
	Asympt.	C7	38	37		RJ	x	neg	neg	<10	<10	53.5	35.5	1.5
	Asympt.	C8	24	39		RJ	x	neg	neg	<10	≥10	72.6	15.3	4.7
	Asympt.	C9	x	x		RJ	x	neg	neg	<10	≥10	74.1	8.12	9.1
			33.0 (24–41)[b]	38 (24–39)								67.4 (53.5–80.2)	18.4 (14.2–35.5)	3.5 (1.5–5.4)
Children	CZS	C10	29	46		RJ	x	neg	neg	<10	≥10	41.5	31.3	1.3
	CZS	C11	17	26		RJ	x	neg	pos	<10	≥10	58.8	32.9	1.8
	CZS	C12	22	22		RJ	x	neg	pos	160	≥10	80.3	11.7	6.9
	CZS	C13	30	30		RJ	x	x	x	x	x	74.8	11.7	6.4
	CZS	C14	23	38		RJ	x	neg	neg	<10	≥10	76.9	7.37	10.4
	CZS	C15	24	40		RJ	x	neg	neg	<10	≥10	50.9	35.1	1.5
	CZS	C16	32	35		RJ	x	neg	pos	<10	<10	76.5	11.3	6.8
	CZS	C17	32	43		RJ	x	neg	pos	<10	≥10	64.1	29.8	2.2
	CZS	C18	29	30		RJ	x	pos	pos	<10	<10	69.9	18.6	3.8
			29.0 (17–32)[b]	36.5 (22–46)								69.9 (41.5–80.3)	18.6 (7.4–35.1)	3.8 (1.3–10.4)

Age[a], years.
Age[b], months.
Illness time[b], months.
median (minimum–maximum)[a].

The CZS ZIKV group (positive maternal qRT-PCR, $n = 9$) consisted of patients with exposure to ZIKV during pregnancy and with clinical evidence of CZS. Under both ZIKV conditions, mothers had negative results for other infectious agents (syphilis, toxoplasmosis, rubella, cytomegalovirus, and HIV). All participants were clinically evaluated by a multidisciplinary team and are included in an ongoing clinical follow-up program (28). Neuroimaging, such as skull ultrasound, CT or MRI, was performed to investigate radiological factors compatible with congenital infectious diseases. In symptomatic children, according to the Ministry of Health of Brazil, the presence of CZS is defined by maternal ZIKV infection confirmed through qRT-PCR, with two or more clinical parameters, such as microcephaly or other neurological changes; visual or auditory anomalies; and functional disorders, such as irritability, dysphagia, and spasms (29). However, even if the mother has compatible symptoms and is qRT-PCR ZIKV+, it is not possible to state what exposure children who were born asymptomatic had (**Figure 1**).

From 2018 to 2019, blood donations from these donors with a history of ZIKV infection were collected at HUAP/UFF to be used in our study. Previous exposure to DENV or ZIKV were determined by the presence of detectable DENV-specific immunoglobulin G (IgG) titers (30) or ZIKV-specific IgG titers (31) (**Table 1**).

As a control group, we had 5 non-pregnant women infected with ZIKV in the same timeframe (2015–2017). These controls were invited to participate in this study because they had confirmed the diagnosis of ZIKV by qRT-PCR and had positive anti-ZIKV IgG serology. All participants were similar in age compared to the group of mothers (**Table 1**). DENV and chikungunya RNA were not detected in all tested patients, excluding coinfections.

Detection of Dengue IgG and Zika Antibodies With an in-House ELISA

Serum samples were tested using ELISA IgG specific for ZIKV and DENV. Detection of dengue-specific IgG antibodies (Panbio, Australian) and Zika-specific IgG antibodies (Euroimmun, Germany) was performed according to the manufacturer's protocol. These ELISAs were standardized to be used as recommended after studies by the Brazilian Ministry of Health. However, there are concerns about the genuine potential for serological cross-reactivity as a confounding factor in ELISA screening.

The Plaque Reduction Neutralization Test (PRNT)

The PRNT was performed for the laboratory confirmation of Zika cases. The ZIKV/H.sapiens/Brasil/ES2916/2015 strain identified in the State of Espírito Santo, Brazil was used. The cutoff value for PRNT positivity was defined as 90% ($PRNT_{90}$). Samples with neutralizing antibodies for ZIKV were also submitted to $PRNT_{90}$ for dengue virus serotype 1 (DENV-1 from West Pacific). Reference viruses were provided by Laboratório de Flavivírus (LABFLA) of Fiocruz from their arbovirus stocks. The $PRNT_{90}$ was performed to determine the maximum plasma dilution (1:10–1:320) needed to reduce arbovirus plaque formation by 90% among Vero ATCC CCL-81 cells, following standard protocols (32, 33). All plasma was heat-inactivated (56°C, 30 min) before neutralization testing. Next, a final volume of each inactivated sample and virus mixture was transferred to a well-containing Vero cells and then initially screened at a dilution of 1:10 in 6-well-plates at 37°C for 60 min. Those that neutralized ZIKV by at least 90% were further tested at serial 2-fold dilutions to determine 90% endpoint titers. Plasma samples were considered to have DENV-neutralizing antibodies when a plasma dilution of at least $\geq$10 reduced no $<$90% of the formation of DENV viral plaques.

PBMC Isolation

Briefly, peripheral blood mononuclear cells (PBMCs) and plasma were isolated by Ficoll-Paque PLUS density gradient centrifugation (GE Healthcare, United States) and frozen in fetal bovine serum (FBS, Gibco, Invitrogen Co, United States) containing 10% (vol/vol) dimethyl sulfoxide (DMSO) (Sigma-Aldrich, United States). Cells were thawed on the day of the experiment and were used directly for *in vitro* assay.

ZIKV CD4 and CD8 MegaPools Description

ZIKV CD4 and CD8 megapool peptides (MP) have been designed and validated, as previously reported (34, 35). Briefly, a consensus sequence was generated by MAFFT alignment after querying the availability of NCBI polyprotein ZIKV sequences and BLAST to a corresponding ZIKV isolate being able to represent most of the viral sequence analyzed (ID: 64320) (36). Two different strategies have been then applied based on the ZIKV polyprotein sequence to predict CD4 and CD8 epitopes using the TepiTool (37) available in the immune epitope database analysis resource (IEDB-AR) (38). Specifically, to design the ZIKV CD4 MP, the "7-allele-method" (39) was applied with a cutoff of $\leq$20, while, for the ZIKV CD8 MP, the epitopes were predicted using the panel of 27 most frequent A and B alleles with custom selection to consider both 9-mers and 10-mers for the prediction (40) and consensus percentile rank cutoff $\leq$1.5. The resulting predicted epitopes have been separately clustered for CD4 and CD8 using an IEDB cluster 2.0 tool, applying the cluster-break method with a 70% cutoff for sequence identity (41). The corresponding peptides derived by the bioinformatic analyses were synthesized as a crude material (A&A, San Diego, CA), resuspended in DMSO, and pooled according to CD4 or CD8 MP composition followed by sequential lyophilization.

Thus, the MP approach was designed by taking into account the 27 most frequent HLA class I allelic variants worldwide, thus making it possible to capture reactivity independently from geographical location, as previously shown in the context of both ZIKV- and DENV-specific CD8+ T cell responses (25, 40, 42, 43). While we cannot rule out the possibility that the specific population considered might express an allelic variant that is infrequent in the worldwide population, the MPs are still designed to provide a worldwide population coverage of 90% or more.

IFN-γ ELISpot Assay

Frozen collected PBMCs were assayed for IFN-γ cell responses, as previously described (44). Briefly, mouse anti-human IFN-γ antibody (clone 1-DK1; Mabtech) was added to 96-well-plates (Multiscreen HTS; Millipore) coated at 2.5 μg/ml, diluted in phosphate buffer saline (PBS), pH 7.2–7.4 (Sigma-Aldrich). PBMCs were then added in triplicate to wells (2×10^5 cells/well) in the presence or not of ZIKV MPs at 1 μg/ml, followed by incubation at 37°C, 5% CO_2 for 18–20 h. After washing with PBS–Tween 20, 1 μg/ml of IgG biotinylated anti-human IFN-γ (clone 7-B6-1; Mabtech) was added and incubated for 2 h at room temperature. After washing, streptavidin–alkaline phosphatase substrate (Mabtech) was prepared and added to the plate, for 1 h at room temperature. Plates were washed, and alkaline phosphatase substrate of 5-bromo-4-chloro-3-indolyl-phosphate/nitro blue tetrazolium chloride (BCIP-NBT) from KPL (Gaithersburg) was added after allowing spots to develop. The reaction was stopped by washing with tap water. Spots were counted using an automated ELISpot reader (ImmunoSpot1S6UV Ultra, Cleveland). The number of IFN-γ-producing cells was expressed as spot-forming cells (SFC) relative to 10^6 PBMCs. Values were calculated by subtracting the number of spots detected in unstimulated control wells. Values were considered positive if they were equal or >20 spots and at least two times above the mean of unstimulated control wells. The stimulation with phytohemagglutinin (PHA, 5 μg/mL) was done for all individuals analyzed as a positive control of *in vitro* stimulation.

We have previously established an approach in which, prior to initiating the ELISpot assay, we recovered stimulated PBMCs for 20 h and stained with Abs listed in **Supplementary Table 1** for extracellular staining used for flow cytometry experiments.

Intracellular Cytokine Staining

Peripheral blood mononuclear cells (2×10^5 cells/well) were cultured for 6 h with 1 μg/ml ZIKV MPs and brefeldin A (44). Subsequently, the stimulated PBMC were stained with the Abs used for flow cytometry experiments listed in **Supplementary Table 1**. The intracellular cytokine staining (ICS) was performed, permeabilized with saponin (0.05%), and stained with anti-IFNγ antibody. The stimulation with phorbol and ionomycin myristate acetate (PMA plus ionomycin) was performed on all individuals analyzed as a positive control of *in vitro* stimulation. The data were collected using BD FACSAria III flow cytometer and analyzed using FlowJo 10.5.2 software (Tree Star1, USA).

Statistical Analysis

Comparisons between different groups were performed using either the non-parametric Mann–Whitney rank sum test or the parametric unpaired *t*-test (two-tailed analyses). When data followed a normal distribution, the paired Wilcoxon's test was used. Outcome variables were compared among the groups of study using the Kruskal–Wallis test followed by the Dunn's multiple comparisons test. Multiple comparison tests were used to compute *post-hoc* comparisons for all pairs of groups. The statistical significance of differences in frequency of "Responders" was performed using the Fisher's exact test. The planned statistical comparisons rely on the accurate classification of outcome and detection of arbovirus infections and CZS in infants. Data in all figure parts in which error bars are shown were presented as the median with interquartile range (25–75%). An analysis was performed with GraphPad PRISM (version 5) (GraphPad Software). The value of $p < 0.05$ was considered statistically significant.

RESULTS

Detection of ZIKV and DENV-Specific IgG Antibodies by Commercial ELISA and of Neutralizing Antibodies to ZIKV and DENV

Zika virus (ZIKV)- and DENV-specific IgG antibody detection was initially determined using the commercial capture ELISA assay. Out of the 21 symptomatic mothers tested, who were qRT-PCR ZIKV+, 14 (66.7%) had both anti-ZIKV IgG and anti-DENV IgG. Similar percentages were observed between mothers who had asymptomatic children (8 out of 12; 66.7%) and those who had children with CZS (6 out of 9; 66.7%). Five out of 21 (23.8%) had anti-ZIKV IgG but not anti-DENV IgG, and similar percentages were also observed between those who had asymptomatic children (3 out of 12; 25%) and those who had children with CZS (2 out of 9; 22.2%). Only one mother who had a child with CZS (1 out of 21; 4.8%) had anti-DENV IgG but not anti-ZIKV IgG. Another mother who had a child with CZS (1 out of 21; 4.8%) had neither anti-DENV IgG nor anti-ZIKV IgG.

Regarding the 18 children with a history of intrauterine exposure to ZIKV, it was not possible to perform the assay on one child with CZS because the sample volume was insufficient. Most of the children, i.e., 10 out of 17 (58.8%), had neither anti-DENV IgG nor anti-ZIKV IgG, among whom seven were asymptomatic (7 out 9; 77.8%) and three had CZS (3 out of 8; 37.5%). Five out of 17 (29.4%) had anti-DENV IgG but not anti-ZIKV IgG, among whom one was asymptomatic (1 out 9; 11.1%) and four had CZS (4 out of 8; 50%). Two out of 17 (11.8%) had both anti-ZIKV IgG and anti-DENV IgG: one was asymptomatic (1 out of 9) and another had CZS (1 out 8). None of them had anti-ZIKV IgG but not anti-ZIKV IgG.

To confirm previous ZIKV and DENV exposure, plasma samples were tested using $PRNT_{90}$ for the detection of ZIKV and DENV-1-neutralizing antibodies. We could not perform PRNT for all four DENV serotypes since the plasma volume was insufficient for this. Thus, we chose to evaluate DENV-1 since this had the highest prevalence in Rio de Janeiro in the period in which the samples were collected (2015–2016) (45). Out of 19 mothers who had anti-ZIKV IgG, 18 (94.7%) presented with ZIKV-neutralizing antibodies with $PRNT_{90}$ titer > 320, thus confirming the exposure to ZIKV. Interestingly, out of 14 mothers who had both anti-ZIKV IgG and anti-DENV IgG that were detectable, 10 had a $PRNT_{90}$ titer for ZIKV and DENV, thus indicating exposure to both viruses, while 3 presented a $PRNT_{90}$ titer for ZIKV and 1 did not have any detectable $PRNT_{90}$ titer. Regarding the children, it was not possible to perform PRNT on three of them because the sample volume was insufficient. Thus,

two out of 15 children had both anti-ZIKV IgG and anti-DENV IgG that were detectable, and 1 asymptomatic child presented both ZIKV and DENV-neutralizing antibodies.

The frequency of T cell subpopulations was assessed by flow cytometry assay. Data on the percentage of CD4 and CD8 T cells and the ratio between the two subpopulations showed no statistically significant difference between the two donor cohorts (**Table 1**).

Detection of IFN-γ-Producing Cells in Response to ZIKV Peptides in Women and Mothers With a History of ZIKV Infection, but Not in Children With a History of Intrauterine Exposure to ZIKV

Next, we focused on the analysis of T cell responses in donors with a history of ZIKV infection. *Ex vivo* T cell responses to CD4 and CD8 ZIKV MPs (CD4 ZIKV MP and CD8 ZIKV MP) employing the ELISpot assay were measured to quantify the number of IFN-γ secreting cells. The general characteristics of these donors' cohorts are summarized in **Table 1**.

To ensure the comparable quality of samples, we first compared responses induced by the positive control stimulus PHA. As expected, T cells from women (non-pregnant women infected with ZIKV, see **Figure 1** in Materials and Methods) and mothers (pregnant mothers infected with ZIKV, see **Figure 1** in Materials and Methods) with a history of ZIKV infection responded to PHA with values above 250 SFC per 10^6 PBMC, as well as most of the children with a history of intrauterine exposure to ZIKV (from children born to mothers infected with ZIKV during pregnancy, see **Figure 1** in Materials and Methods). One of the samples collected from children responded to PHA with just over 70 SFC per 10^6 PBMC, which resulted in 15 times greater stimulation with PHA compared to the medium; therefore, we decided to maintain this child from the analysis (**Figure 2A**).

In the ELISpot assay, we were able to successfully detect T cell responses using CD4 ZIKV MP and CD8 ZIKV MP. The T cells of all non-pregnant women responded to ZIKV CD4 MP and four out of the five responded to CD8 MP. The frequency of responders was slightly lower in mothers, so the CD4 T cells of 8 out of 10 mothers responded to ZIKV CD4 MP and 6 out of 10 responded to ZIKV CD8 MP. These data demonstrated an important reactivity of donors exposed to ZIKV, both in frequency and magnitude of CD4 and CD8 T cell responses to ZIKV peptides. However, children's T cell responses to ZIKV MP were uncommon as no child responded to CD4 ZIKV MP and only 2 out of 11 responded to CD8 ZIKV MP (**Figure 2B**).

The T cells of all mothers who had asymptomatic children responded to CD4 ZIKV MP and 4 out of the 5 responded to CD8 ZIKV MP. Among those who had children with CZS, the T cells of 3 out of 5 responded to CD4 ZIKV MP and 2 out of 5 to CD8 ZIKV MP. No significant difference was found between the two groups of mothers regarding the magnitude or frequency of responses to the ZIKV MP (**Figure 2C**).

Regarding children, regardless of the clinical outcome, T cells did not respond to CD4 ZIKV MP, and only 1 out of 5 asymptomatic and 1 out of 6 with CZS responded to the CD8 ZIKV MP (**Figure 2D**).

Higher CD4 T Cell Degranulation Ability Compared to CD8 T Cell Degranulation in Donors With a History of ZIKV Infection

Cytotoxic activity is one of the key components of the virus-specific protective immunity (25). In this study, we measured the degranulation capacity of T cells by staining of the expression of the CD107a molecule (**Figure 3A**). Our results were very surprising since we detected an increase in the magnitude of the CD107a-expressing CD4 T cells after stimulation with CD4 ZIKV MP. This response was more intense in mothers and children and less in women. Thus, regarding the response of CD4 T cells to CD4 ZIKV MP, 10 out of 12 mothers, 5 out of 9 children and 2 out of 5 women were responsive to CD4 ZIKV MP with an increase in the frequency and magnitude of CD107a-expressing CD4 T cells. In contrast, no donor responded to CD8 ZIKV MP by inducing the CD107a-expressing CD8 T cell responses (**Figure 3B**).

Further analysis revealed that the response of CD4 T cells to CD4 ZIKV MP was similar among mothers who had asymptomatic or SCZ children (**Figure 3C**). Among children, this response was also independent of whether they had neurological impairment associated with ZIKV (**Figure 3D**).

Higher IFN-γ Producing ZIKV CD4 T Cell Responses Persist in Donors With a History of ZIKV Infection by ICS Assay

By using a ZIKV MP stimulation and ICS assays (**Figure 4A**), we were able to determine the responding T cell subsets as well as the memory subset. Donors cells with a history of ZIKV infection were stimulated with polyclonal PMA plus ionomycin, confirming the viability of all samples (**Figure 4B**).

In a further series of experiments, CD4 T cells from all donors responded to the CD4 ZIKV MP in terms of frequency and magnitude of responses.

CD4 T cells responded to the CD4 ZIKV MP with IFN-γ production in most donors exposed to ZIKV; 3 out of 5 women, 10 out of 13 mothers, and 8 out of 13 children. Regarding the responses of CD8 T cells after stimulation with CD8 ZIKV MP, we observed a lower frequency of responders in all groups: only one out of 5 women, 3 out of 13 mothers, and only 1 out of 13 children (**Figure 4C**). Thus, all donors showed appreciable reactivity, both in terms of increased frequency and magnitude of IFN-γ-producing CD4 responses but a lower response for CD8 responses.

We went to see if there is a difference between the groups of mothers and children. The CD4 T cells of all mothers who had asymptomatic children responded to CD4 ZIKV MP with IFN-γ production, while 4 out of 7 mothers who had CZS children responded, but this difference was not statistical. Regarding CD8 T cell responses, CD8 ZIKV MP responses were remarkably close (**Figure 4D**). Among children, T cell responses to ZIKV MP were quite similar, therefore, regardless of whether they had any neurological impairment associated with ZIKV (**Figure 4E**).

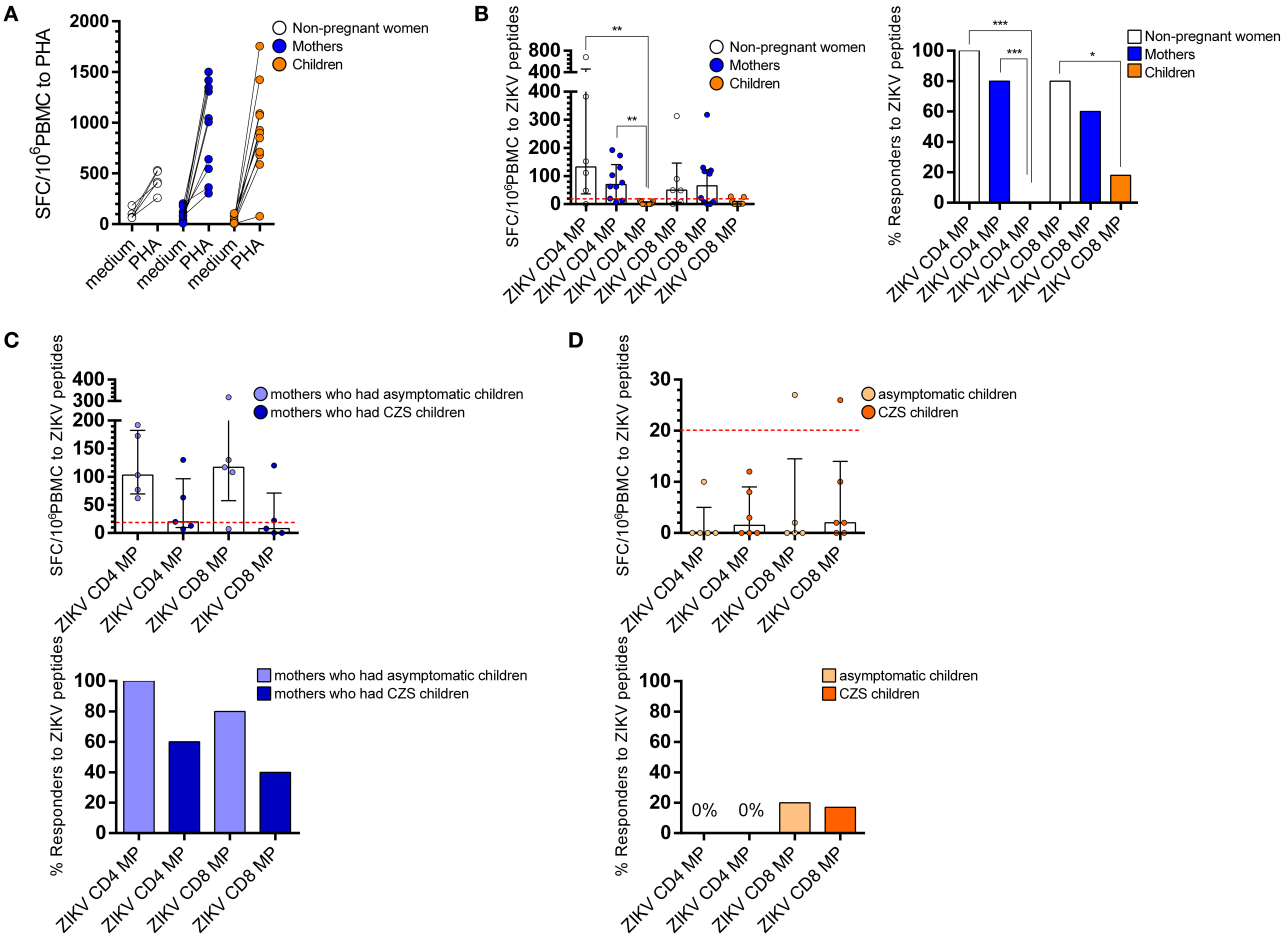

FIGURE 2 | *Ex vivo* reactivity to CD4 and CD8 ZIKV MPs in donors with a history of ZIKV infection. T cell response to by ELISpot *ex vivo* experiments are shown for women (from non-pregnant women infected with ZIKV, white, $n = 5$), mothers (from pregnant mothers infected with ZIKV, blue, $n = 10$), and children (from children born to mothers infected with ZIKV during pregnancy, orange, $n = 11$) with a history of ZIKV infection. In **(A)**, T cell response to PHA stimulation and, in **(B)**, the magnitude of CD4 and CD8 T cell reactivity to ZIKV MPs are expressed as medians and interquartile range (25th and 75th percentiles). Donors were considered "Responders" if the net SFC/106 PBMC after ZIKV MP was ≤20 after 20 h of *in vitro* stimulation. **(C)** CD4 and CD8 T cell reactivity to a ZIKV MP are shown among mothers who had asymptomatic children (light blue) compared with those who had CZS children (dark blue). **(D)** CD4 and CD8 T cell reactivity to ZIKV MPs are shown among children grouped in asymptomatic children (light orange) compared with CZS children (dark orange). Responses were expressed as the number of IFN-g-secreting cells per 106 PBMC. Statistical differences were tested using the one-way analysis of variance (ANOVA) and the Kruskal-Wallis test followed by the Dunn's multiple comparisons test. Bars represent median with interquartile range. Statistical significance for differences in the frequency of "Responders" was performed using Fisher's exact test. $^*p < 0.05$, $^{**}p < 0.001$, $^{***}p < 0.001$. ZIKV, Zika virus; MP, megapool peptide; CZS, congenital Zika syndrome; PBMC, peripheral blood mononuclear cell.

Regarding the IFN-γ producing CD4 and CD8 T cells, we observed that there is a greater degree of reactivity of CD4 T cells after CD4 ZIKV MP compared to CD8 T cells after CD8 ZIKV MP in all studied groups (**Figure 4F** and **Supplementary Figure 1**). We performed an analysis of the mother and child pairs to assess whether the responses agreed (pairs tested $n = 7$). Only two of the seven mother and child pairs responded to CD4 ZIKV MP. For the response of CD8 T cells to CD8 ZIKV MP, in 4 pairs, mothers and children did not respond to CD8 ZIKV MP and, in three cases, mothers responded, but children did not (**Figure 4G**).

When the ELISpot and ICS data for all mothers, relating to CD4 ZIKV MP or CD8 ZIKV MP, were combined, we found a significant positive correlation between ELISpot and ICS ($p = 0.002$ for CD4 ZIKV MP and $p = 0.008$ for CD8 ZIKV MP; the Wilcoxon signed-rank test). Thus, in a broad and collective sense, ICS does not fundamentally conflict with ELISpot in the group of mothers. A similar analysis was performed for children, but no significant correlation between ELISpot and ICS was found for either CD4 ZIKV MP or CD8 ZIKV MP (the Wilcoxon signed-rank test). In the ELISpot 20-h cultures, we evaluated susceptibility to death of PBMCs. In particular, the children's PBMCs had a viability ≥100%. We speculate that the kinetics of cytokine production may have more influence on children's PBMCs than on those of their mothers. Other kinetics should therefore be evaluated in future studies.

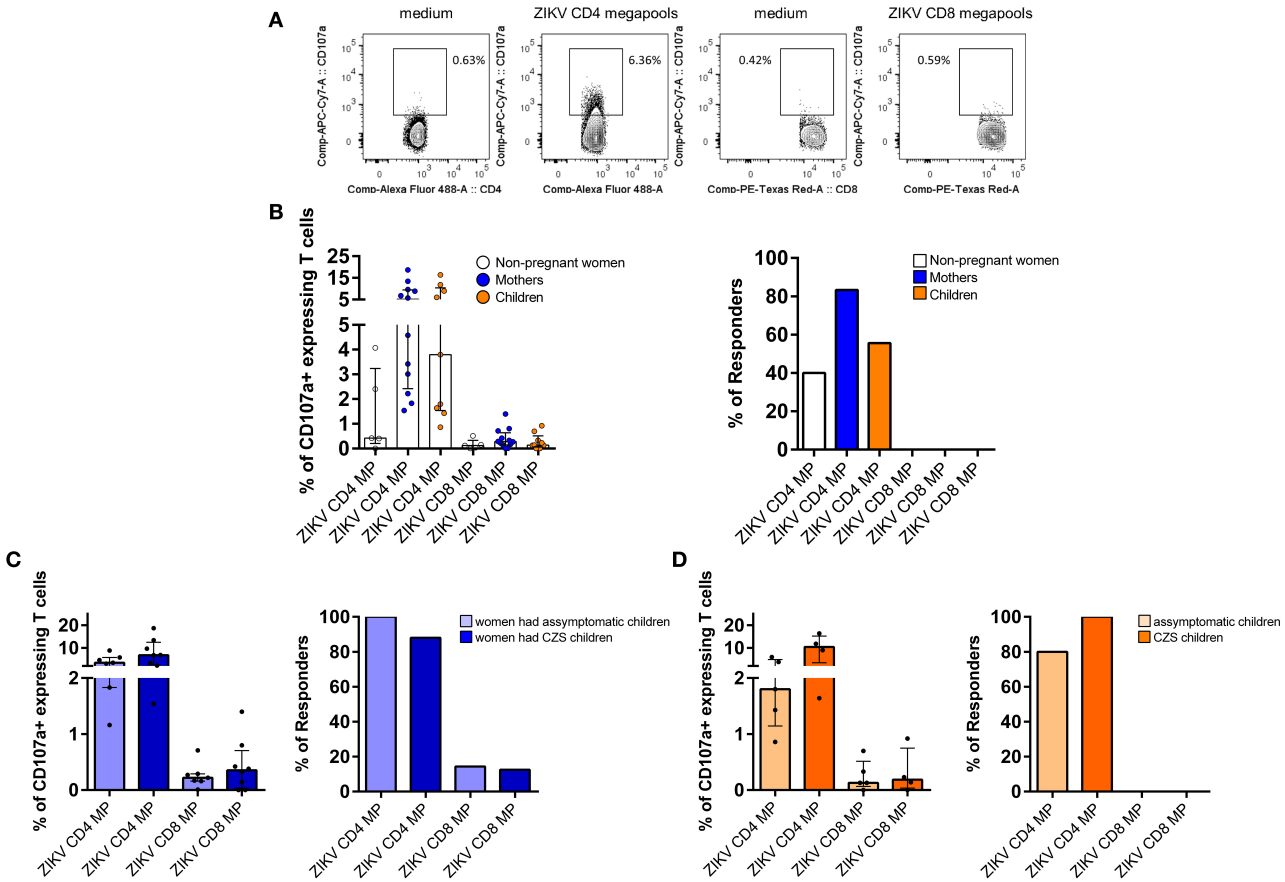

FIGURE 3 | Degranulation activity of T cells from donors with a history of ZIKV infection after ZIKV MP *in vitro* stimulation. **(A)** Gating strategies to the flow cytometry profiles of the degranulation activity of CD4 and CD8 T cells measured by CD107a mobilization after stimulation with ZIKV MPs are shown in a representative of one of the women (from non-pregnant women infected with ZIKV, white, $n = 5$), mothers (from pregnant mothers infected with ZIKV, blue, $n = 12$), and children (from children born to mothers infected with ZIKV during pregnancy, orange, $n = 9$) with a history of ZIKV infection. **(B)** Cumulative data (medians and interquartile range) of the proportion of CD107a+ cells among CD4 and CD8 T cells after ZIKV MP stimulation. Regarding the criteria of positivity of the assay or "Responder," the background in the unstimulated controls was subtracted to ZIKV peptide conditions, and the responder was considered as those who had two times more CD107a-positive cells after subtraction of the background. **(C)** CD4 and CD8 T cell reactivity to ZIKV MPs are shown among mothers who had asymptomatic children (light blue) compared with those who had CZS children (dark blue). **(D)** CD4 and CD8 T cell reactivity to ZIKV MPs are shown among asymptomatic children (light orange) compared with CZS children (dark orange). The magnitude of responses is expressed in medians and interquartile range, and statistical analyses were performed with Mann-Whitney U-test. No statistical difference was found. ZIKV, Zika virus; MP, megapool peptide; CZS, congenital Zika syndrome.

Additionally, we have measured IL-8 levels by ELISA in PBMC supernatants from ZIKV donors recovered from the 20-h cultures for the ELISPOT assay. No statistical difference was found between the groups when comparing the different conditions (data not shown).

The Memory CD4 T Cells Re-Expressing CD45RA (Temra) in Donors With a History of ZIKV Infection Is Enriched for ZIKA-Specific T Cells

We initially analyzed the expression of CD45RA and CCR7 on the total CD4 and CD8 population (**Figure 5A**). In women, the majority of the unspecific CD4 T cells displayed a frequency of naïve (Tn, CD45RA+CCR7+; 50%) phenotype followed by the central memory (Tcm, CD45RA-CCR7+; 37%) phenotype, effector memory (Tem, CD45RA–CCR7–; 15%) phenotype, and finally by effector memory re-expressing CD45RA (Temra, CD45RA+CCR7–; 0.9%) phenotype. In mothers, it was observed that a similar frequency of the unspecific CD4 T cells displayed a Tcm (47%) phenotype and a Tn (41%) phenotype, and then an Tem (11%) phenotype, followed by a Temra (0.5%). As expected, in children, the most CD4 T cells exhibited a Tn (72%) phenotype, followed by a Tcm (23%) phenotype, an Tem (4%) phenotype, and an Temra (0.4%) phenotype (**Figure 5B**).

For the unspecific CD8 T cells, women, mothers, and children had a comparable frequency of all subsets of T cells, exhibiting predominantly a Tn cell (64% in women, 58% in mothers, and 63% in children), followed by a Tem phenotype (23% in women and 16% in both mothers and children donors), a Temra (9, 15, and 11%, respectively), and lastly

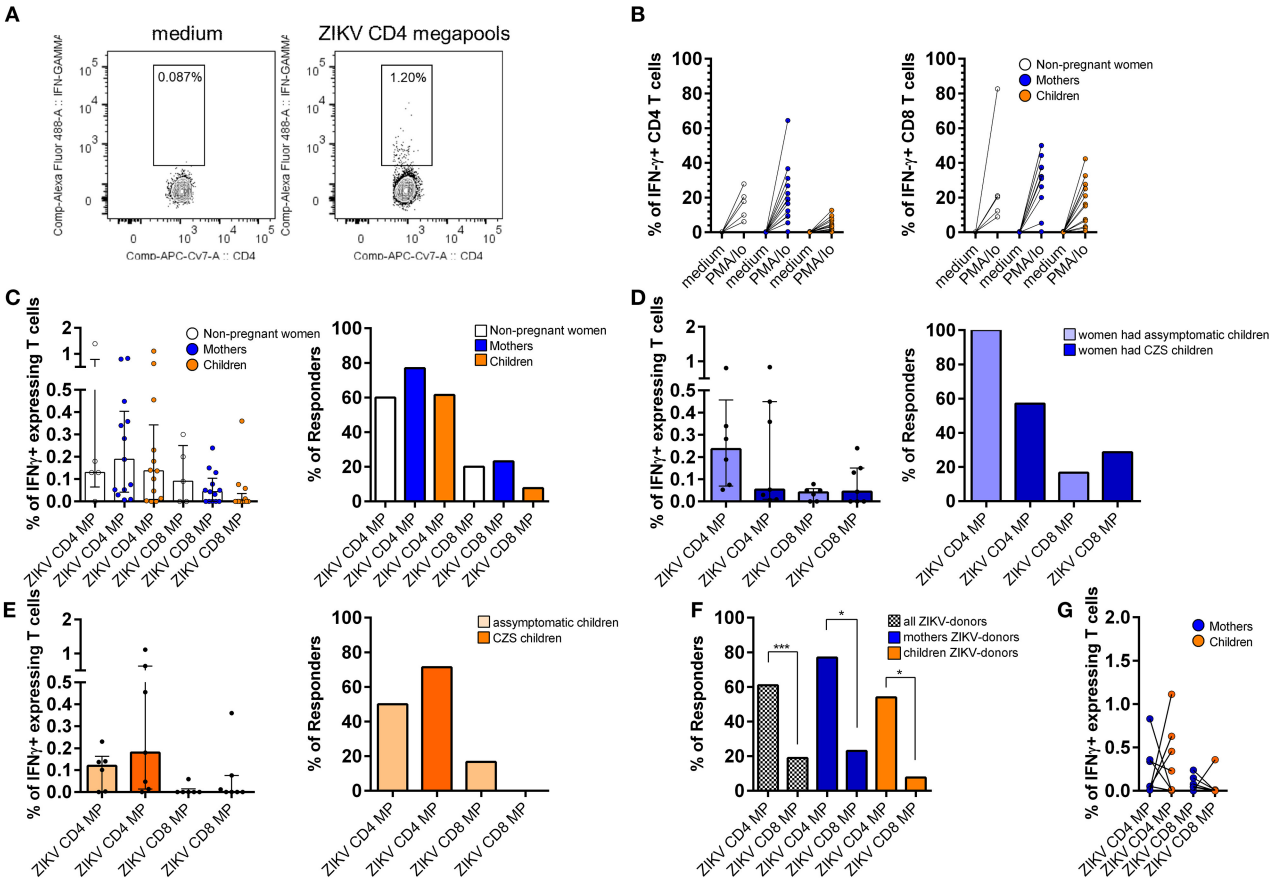

FIGURE 4 | *Ex vivo* reactivity with IFN-γ production of donors with a history with ZIKV infection to CD4 and CD8 ZIKV MPs. CD4 and CD8 ZIKV-restricted responses in women (from non-pregnant women infected with ZIKV, white, $n = 5$), mothers (from pregnant mothers infected with ZIKV, blue, $n = 13$), and children (from children born to mothers infected with ZIKV during pregnancy, orange, $n = 13$) with a history of ZIKV infection after 6-h of *in vitro* stimulation. **(A)** Gating strategy to the flow cytometry plots identifies IFN-g-producing ZIKV-specific T cells. **(B)** Each data point represents the response of a single donor tested with the PMA + io and **(C-E)** two different sets of two protein pools, ZIKV CD4 MP and ZIKV CD8 MP. **(C)** Magnitude of CD4 and CD8 responses and frequency of responders (right) were performed from women, mothers, and children donors to the ZIKV CD4 or CD8 MPs. **(D,E)** Each group is further divided into asymptomatic or CZS. **(D)** Magnitude of CD4 and CD8 responses (left) and frequency of responders (right) were performed from mothers who had asymptomatic children (light blue, $n = 6$) and those who had children with CZS (dark blue, $n = 7$) to the ZIKV CD4 or CD8 peptides. **(E)** Magnitude of CD4 and CD8 responses (left) and frequency of responders (right) were performed from asymptomatic children (light orange, $n = 6$) and CZS children (dark orange, $n = 7$) to the ZIKV CD4 or CD8 MPs. **(F)** Frequency of responders were performed from all (dashed white, $n = 31$), mothers (blue, $n = 13$), and children (orange, $n = 13$) donors to the ZIKV CD4 or CD8 MPs. **(G)** The frequencies of ZIKV-specific IFN-γ-positive CD4 and CD8 cells were compared between the mother-child pairs (tested pairs $n = 7$). The p-values were calculated using the paired t-test. The magnitude of responses is expressed medians and interquartile range, and statistical analyses were performed with the Mann-Whitney U-test. Statistical significance for differences in frequency of responders was performed using a Fisher test. Asterisks indicate significant differences (*$p < 0.05$, ***$p < 0.001$). ZIKV, Zika virus; MP, megapool peptide; CZS, congenital Zika syndrome; INF, interferon.

a Tcm cell (6, 10, and 7%, respectively) (**Figure 5B**). Thus, the majority of unspecific CD4 and CD8 T cells are in the Tn population.

To further determine the memory T cell responses to ZIKV MP, we compared it to responding IFN-γ-secreting Tn out of the total of Tn cells, responding IFN-γ-secreting Tcm out of the total of Tcm cells, responding IFN-γ-secreting Tem out of the total of Tem cells, and finally responding IFN-γ-secreting Temra out of the total of Temra cells (**Figure 5A**).

Further analysis demonstrated that phenotypic analysis of the total of Temra subsets is enriched for responding IFN-γ-secreting CD4 T cells for ZIKV epitopes in women, mothers, and children (**Figure 5C**). In terms of the IFN-γ+-responding CD8 T cells for ZIKV epitopes, no difference was seen in the frequency of Tn or Tcm phenotype in donors with a history of ZIKV infection (**Figure 5C**).

DISCUSSION

In the present study, we aimed to evaluate the T cell response in donors with a history of ZIKV infection during pregnancy. Regarding the few current studies that raise the same questions, our group has progressed when compared to non-pregnant

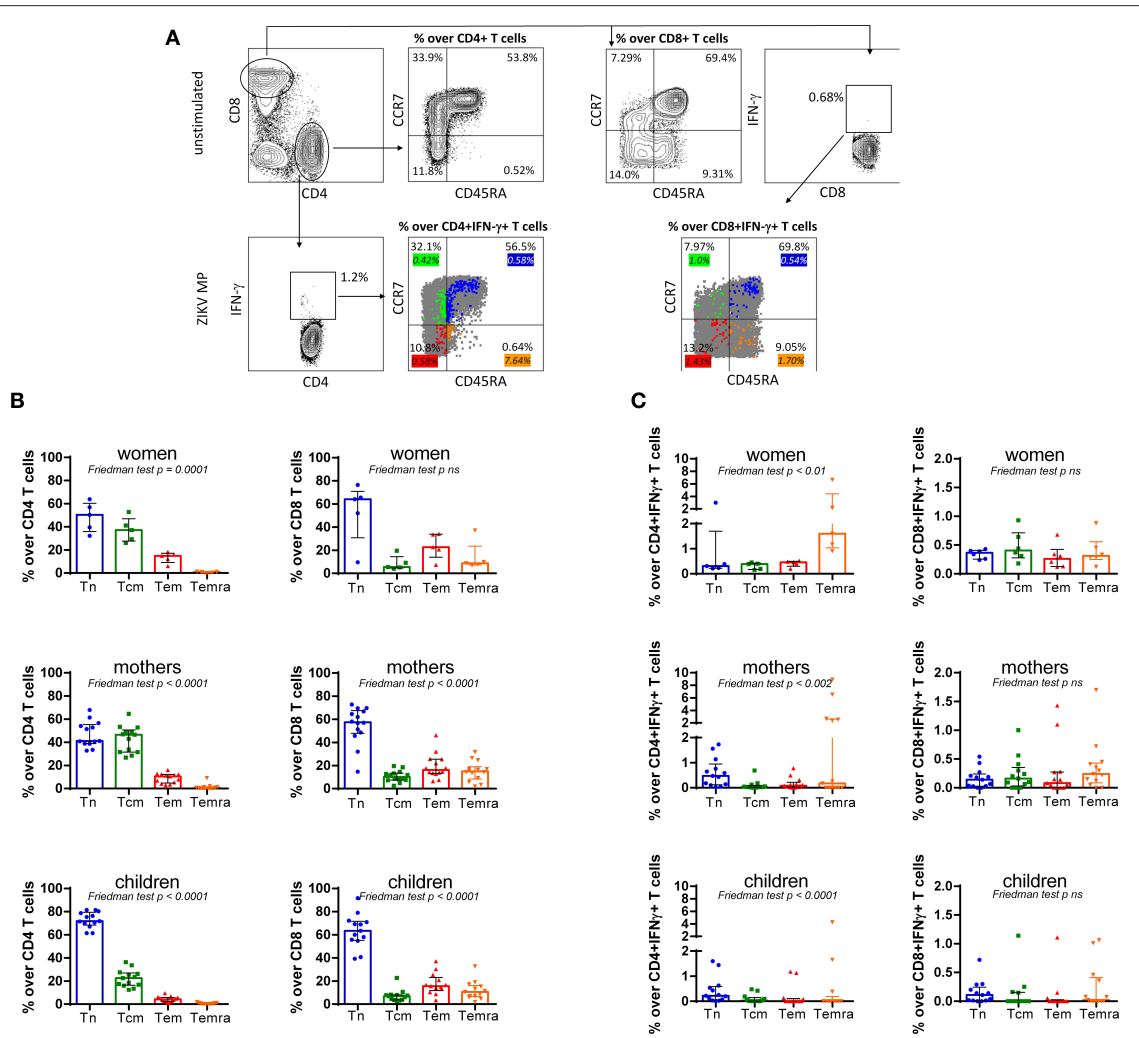

FIGURE 5 | Subpopulations of specific memory from ZIKV donors with a history of ZIKV infection. (A) Gating strategy to identify the CD4 T cell and CD8 T cell subsets, and of the T cell memory subpopulations. Lymphocytes were identified and electronically gated on orthogonal light scatter signals and CD3 immunopositivity. Then, CD3+CD4+T cells and CD3+CD8+T cells were identified. Gating on CD3+CD4+T cells or CD3+CD8+T cells, Tn and Tcm cells were identified as CD45RA negative/positive and CCR7 negative/positive. In unstimulated cells, the percentage of unspecific CD4 and CD8 T cell subsets [Tn: CD45RA+CCR7+; Tcm: CD45RA−CCR7+; effector memory (Tem): CD45RA−CCR7− and effector memory re-expressing CD45RA T cells (Temra): CD45RA+CCR7−] was gated in a representative subject with a history of ZIKV. The percentage values are represented in the graphs. To determine the memory T cell responses to ZIKV MP, the percentage of CD4 and CD8 T cell subsets were demonstrated. The color values represent the frequency of the responding IFN-γ-secreting Tn out of the total of Tn cells, responding IFN-g-secreting Tcm out of the total of Tcm cells, responding IFN-γ-secreting Tem out of the total of Tem cells, and responding IFN-γ-secreting Temra out of the total of Temra cells. The color percentage values are represented in the graphs. **(B)** Percentage of unspecific CD4 and CD8 T cell subsets (Tn, Tcm, Tem, and Temra) gated in unstimulated cells from women (from non-pregnant women infected with ZIKV), mothers (from pregnant mothers infected with ZIKV), and children (from children born to mothers infected with ZIKV during pregnancy) with a history of ZIKV. **(C)** The phenotypic analysis of the responding IFN-γ-secreting T cells for ZIKV epitopes out of a total of Tn or Tcm cell subsets in women, mothers, and children. Data are expressed as median ± the interquartile range for each cohort (n = 5-13 in both panels). Differences between T cell subsets among cohorts were analyzed using the Friedman test. Each data point represents a single donor determination. ZIKV, Zika virus; MP, megapool peptide; CZS, congenital Zika syndrome; INF, interferon; Tn, naïve T cell; Tcm, central memory T cell; Tem, effector memory T cell; Temra, effector memory re-expressing CD45RA T cell.

women, pregnant mothers, and both asymptomatic and CZS children born to mothers infected with ZIKV during pregnancy.

It is essential to understand the repertoires of the ZIKV effector T cell response to the point of extrapolating if the development of a non-protective immunity in mothers is related to the affected children. In addition, in pregnancy and congenital infection scenarios, it is not known if there is a development of long-lasting T cell immunity to ZIKV. To address these issues, the ZIKV T cell immunity in a cohort of mothers infected with ZIKV during pregnancy and children affected (or not) by neurological complications was assessed 2–3 years after the initial infection.

If previous DENV cross-reactive immunity contributes or not to protection against ZIKV infection during pregnancy, it

is still unclear. During the Brazilian ZIKV epidemic (2016–2017), 94 pregnant women who gave birth to infants with or without microcephaly were evaluated. Based on previous studies, DENV immunity is not a prerequisite for ZIKV entry into the fetal compartment (46). Halai et al. supported Araújo's findings (47). In contrast, ZIKV-infected human placental tissues showed increased replication in the presence of DENV antibodies, dependent on FcγR engagement (48). In mouse models, the presence of DENV-specific antibodies in ZIKV-infected pregnant mice significantly increased fetal resorption in immune-compromised mice (48) and also displayed CZS, including microcephaly, in immune-competent mice (49, 50).

Thus, conflicting datasets regarding the impact of ADE (antibody-dependent enhancement) on congenital malformations in babies have emerged from different studies, including mouse and non-human primates' models and human donors. Based on Zimmerman's review, additional prospective epidemiologic studies, *ex vivo* studies, and animal model experimentation are needed to fully dissect the complex risk factors and pathways through which ZIKV can seed and infect the fetal compartment (51).

Even so, this can be framed if the mothers' ZIKV T cell effector immune response repertoires are "weak" to the point of not giving protective immunity to the affected children. So far, data addressing this issue is only available in the murine model (52). The authors evaluated adapted mouse models established for ZIKV infection during pregnancy. Interestingly, they observed a reduction in a load of ZIKV in maternal and fetal tissues and an increase in fetal viability and growth in immune mice to DENV compared to non-immune mice. The depletion or genetic deficiency of CD8 T cells nullified this effect, even under ADE conditions (52). A single study on pregnancy and immunity to ZIKV in human patients was recently developed by Reynolds et al. The authors showed that almost all mothers with a history of ZIKV infection have serological evidence of immunity to dengue, suggesting that their children who had microcephaly were born to mothers' immune to DENV. In addition, they showed that different viral products can induce a multifunctional response to E and NS1 antigens and also immunoregulatory responses to NS5 and C ZIKV proteins, which could impact immunopathogenesis (53). From our dataset, it is not yet clear if children who had microcephaly were born of mothers with "an altered" T cell responses. It would be necessary to have acute samples of pregnant mothers to answer this question with greater propriety.

Outside the context of donors infected during pregnancy or by congenital infection, several studies have been evaluating the T cell responses to ZIKV proteins in human donors immune or not to DENV. It is known that ZIKV-reactive T cells in the acute phase of infection are detected earlier and in greater magnitude in DENV-immune patients. Conversely, the pattern of CD4 responses to ZIKV-restricted class II peptides was remarkably similar in acute and convalescent phases, while a lower frequency and magnitude of responses were observed with the CD8 counterpart (44). In another study, Grifoni's data indicated an immunological signature for CD8 T cell responses reproducible and temporally stable after Ag-specific stimulation even 1–2 years after ZIKV infection (25). Moreover, circulating tetramer-positive ZIKV-specific CD8 T cells peaked at early convalescence day post-infection with elevated levels persisting for months from a volunteer woman (54). On the other hand, whereas C-, prM-, E-, and NS5-specific cytokine-expressing CD4 T cells were readily detected in all patients tested, absent or low detection of functional CD8 effector T cells against peptides spanning ZIKV C, prM, E, and NS5 was identified (55). We agree with Lai's study using peptides that span all 10 ZIKV proteins. Our data indicate that after *in vitro* stimulation with the ZIKV MP, CD4 T cells maintain their degranulation and IFN-γ production capacity, which was not observed by CD8 T cells. One possibility is that the cytotoxic and pro-inflammatory activities of CD8 T cells are high at an early stage of ZIKV infection but do not persist in the disease resolution phase when the virus has apparently been eliminated. Our experimental design was based on well-established protocols, with stimulation with ZIKV or DENV MP of cells cultured for 6 h to perform a flow cytometry assay or for 20 h for the ELISpot assay (25, 34, 42, 44, 56). Additionally, studies have already been carried out on *in vitro* expansion of peptide-specific T cells for 14 days (34, 56, 57). Thus, our future proposal is to perform *in vitro* expansion of peptide-specific T cells in the kinetics of up to 14 days, in order to confirm our observations on the role of CD8 T cells.

The protective role of CD8 T cells has been demonstrated in several studies using mouse models. Huang's study demonstrated that an adoptive transfer of ZIKV-immune CD8 T cells can protect against ZIKV infection (58). Indeed, polyfunctional, cytotoxic CD8 T cells are activated (59), reducing ZIKV burden, and, in the same sense, CD8 depletion or genetic absence resulted in greater ZIKV infection and mortality in mice (60). Moreover, ZIKV-specific and ZIKV/DENV cross-reactive CD8 T cells in DENV-immune mice expanded post-ZIKV challenge and reduced infectious ZIKV levels, and CD8 T cell depletion confirmed this protection (61). Nevertheless, within a susceptible mouse model, CD8 T cells appear as an important mediator of ZIKV neuropathogenesis (62, 63). It is currently impossible to determine what the impact of the short duration of ZIKV-specific CD8 T cells will be for donors with a history of ZIKV infection. Unfortunately, only with the emergence of new ZIKV epidemics, this issue can be assessed.

In relation to ZIKV-specific CD4 T cell responses in Zika patients, Koblischke et al. showed a strong impact of structural ZIKV protein on immunodominant CD4 T cell responses (64). Interestingly, most of the CD4 Temra cells are DENV-specific in donors with previous DENV infection (43). Patil et al. revealed in patients with dengue that these CD4 T cells in the Temra subsets are highly enriched with CD4 cytotoxic T lymphocytes expressing several genes linked to cytotoxic and costimulatory function, compared with CD4 T cells in the Tcm and Tem subsets (65). Tian et al. revealed that the CD4 Temra cells can be subdivided into two major subsets between DENV-immune individuals based on the expression of the adhesion G protein-coupled receptor GPR56. While GPR56+ Temra cells display a transcriptional and proteomic program with cytotoxic features, GPR56+ Temra cells have higher levels of clonal expansion and contain the majority of virus-specific Temra cells (66). Overall,

like DENV infection, our data indicate that the Temra CD4 T cell subset is enriched for responding IFN-γ-secreting CD4 T cells for ZIKV epitopes in donors with a history of ZIKV infection. Future efforts will be underway in our laboratory to assess whether the heterogeneity of CD4 Temra T cells could provide insights to differentiate the outcome of the child's congenital infection in T cell responses against ZIKV.

Some limitations should be considered when interpreting our findings. First, to understand the evolution of the acquired ZIKV immunity, the best would be a "longitudinal study" in which donors were monitored in the acute and convalescent phases and after complete recovery from the disease. Second, the diagnosis of ZIKV through qRT-PCR was not made in newborns, so we cannot affirm that they were vertically infected, especially in asymptomatic cases. Recently, Ribeiro et al. published data from analyses on the positivity of PRNT and serological tests among a total of 88 children in northeastern Brazil who presented clinical cases of CZS between 2016 and 2018. Six (6.8%) were positive for IgG anti-ZIKV, and 2 (2.3%) of them were ZIKV $PRNT_{90}$-positive (67). Although our initial goal was not to make correlations like those made by Ribeiro et al., our data are very close. In our study, only 2 out of 17 children (11.8%) had anti-ZIKV IgG (but also anti-DENV IgG), and 2 out of 15 (13.3%) were ZIKV and DENV $PRNT_{90}$-positive. This frequency of positivity was much lower than we expected, as were the data of Ribeiro et al. Like in their study, our data cannot be attributed to problems in the execution of $PRNT_{90}$, since the protocol established by Baer and Kehn-Hall (36) was strictly followed. The ZIKV/H.sapiens/Brasil/ES2916/2015 strain was identified in the State of Espírito Santo at the time of the CZS epidemic in Brazil (68). In a case report, it was shown that a child was positive for ZIKV IgG at birth and at the age of 12 months but was negative at 21 and 24 months of age. The child's mother was ZIKV RT-PCR, IgM, IgG, and PRNT-positive during the pregnancy. Three hypotheses were raised by the authors of that study: (a) low and transient ZIKV viremia could lead to the lack of detection of the antigen and absence of a strong immune response in the child; (b) specific and direct tropism of ZIKV to the central nervous system could cause ZIKV to become a silent virus that would escape the host's response; and (c) ZIKV could prevent the triggering of a strong innate immune response because active viral replication might have ceased during intrauterine life or shortly thereafter (69). Moreover, methodologically, the use of the recombinant NS1 antigen as a target in the commercial kit may explain the low anti-ZIKV IgG seropositivity in newborns (70).

Third, it was not possible to carry out many analyzes of paired mothers and children, mainly due to the clinical complications of the children during the study, which made it difficult to define a close association between the immunity of mothers and the clinical outcome of their children. Fourth, a caveat to this study is that the T cell responses detected after ZIKV MP restimulations may actually cover specific ZIKV responses and responses from cross-reactions due to previous flavivirus infections, particularly DENV.

Given the similarity between DENV and ZIKV and their common regions of endemicity, questions have arisen about whether immunity to one virus can provide cross-protection against another. Grifoni et al. published data that demonstrated that the degree of MP sequence homology for different flaviviruses directly influenced cross-reactivity in terms of CD4 and CD8 T cell responses. It is important to note that the CD8 MP of ZIKV used in our study was provided by Dr. Sette's team and, therefore, is the same as used by Grifoni et al. According to them, 33% of the DENV and ZIKV CD8 MP have homology $\geq$70% of sequence similarity with the consensus sequence, which in fact means that one-third of the peptides present in the MPs that we tested can cross-react with DENV (34). Here, our data showed that more than 70% of mothers who had both anti-ZIKV IgG and anti-DENV IgG had a $PRNT_{90}$ test positive for ZIKV and DENV. Among the children, 50% of those who had both anti-ZIKV IgG and anti-DENV IgG presented ZIKV and DENV-neutralizing antibodies. Several human studies have investigated cross-reactivity in T cell responses, targeting a variety of viral proteins (71). Grifoni et al. found that prior DENV exposure did not have any impact on the CD4 T cell response to ZIKV infection: patients in the acute phase of ZIKV infection had more IFN-γ+ CD8 T cells after restimulation with ZIKV-derived peptides (44). However, prior DENV immunity did not have any impact on either the transcriptional profile of the CD8 T cells or the capacity of CD4 or CD8 T cells to produce IFN-γ at later stages of infection (25). Therefore, we have no way of knowing with certainty whether the T cell response that we are evaluating is directed only to primary ZIKV infection and not to DENV. We believe that the most important thing is that, despite the high degree of cross-reactivity between T cell responses to DENV and ZIKV, no indication has yet been provided that this may have a negative impact on disease outcomes.

Our data did not show any notable differences between children with CZS and asymptomatic children or between mothers who gave birth to children with CZS and those who gave birth to asymptomatic children, 2–3 years after primary infection. Recently, Macedo-da-Silva et al. used the same cohort of children as in our study, also in the recovery phase. They demonstrated that asymptomatic children presented changes in proteins that participated in processes relating to neuronal death and cerebrovascular abnormalities, low regulation of proteins relating to vision, and increased activity of metalloproteinases, namely MMP-2 and MMP-9, associated with neuronal death. Interestingly, these changes are not common among control children, but they are also characteristic of children with CZS (72). Together with Macedo-da-Silva et al. we think that, perhaps, marked differences between the groups occurred in the acute phase of Zika but were not so evident in the recovery phase.

In summary, we studied donors with a history of ZIKV infection that occurred in the 2016–2017 outbreak in Brazil, including non-pregnant women, mothers infected with ZIKV during pregnancy, and children with a history of intrauterine exposure. In general, donors demonstrated long-term immunity from CD4 T cells to ZIKV CD4 MP, but the same was not observed in CD8 T cells with ZIKV CD8 MP. It is possible that the cytotoxic and pro-inflammatory activities of CD8 T cells are markedly exhibited in the early stages of the disease but less detected in the resolution phase. The responses of mothers'

T cells and children's T cells to ZIKV MPs do not appear to be related to the clinical outcome. These data still need to be investigated, including the evaluation of CD8 T cell response to other ZIKV peptides.

STUDY APPROVAL

These patients were recruited from the Exanthematic Diseases Unit at the Hospital Universitário Antonio Pedro of the Universidade Federal Fluminense, Niteroi city, RJ, Brazil. All activities were performed after obtaining the informed consent of mothers and parents of children. This approved study is titled "Clinical follow-up of pregnant women with rash and their children: prospective study cohort" with approval number 56913416.9.0000.5243.

DATA AVAILABILITY STATEMENT

The raw data supporting the conclusions of this article will be made available by the authors, without undue reservation.

ETHICS STATEMENT

The studies involving human participants were reviewed and approved by these patients were recruited from the Exanthematic Diseases Unit at the HUAP/UFF, Niteroi city, RJ, Brazil. All activities were performed after obtaining the informed consent of mothers and parents of children. This approved study is titled Clinical follow-up of pregnant women with rash and their children: prospective study cohort with approval number 56913416.9.0000.5243. Written informed consent to participate in this study was provided by the participants' legal guardian/next of kin.

AUTHOR CONTRIBUTIONS

JB-C, IAP and, DF-M developed and performed experiments, analyzed, and interpreted data. HGD, AP-C, and CF-S clinically characterized patients for the study including the PRNT90 trials for ZIKV and DENV-1 and additional cytokines ELISA. MG made the sample acquisitions on the flow cytometer. FRC, AAS, RAOV, and CAAC recruited the clinical cohort for the study. FRC, MRQL, AAS, SMBC, and CAAC clinically characterized patients for the study including DENV IgG and ZIKV IgG ELISA. SAO, ELA, and CAAC helped prepare the manuscript. AG, AS, and DW designed and validated the ZIKV megapools. LMO-P and JB-C conceived and designed the study, interpreted the data, and wrote the manuscript. CAAC and LMO-P supervised the research. All the authors discussed the results and commented on the manuscript.

ACKNOWLEDGMENTS

JB-C, FRC, IAP, DF-M, HGD, and CF-S are recipient of doctoral fellowship from Brazilian research institutions CNPq, CAPES and IOC/Fiocruz. This work was funded by the National Institutes of Health contract Nr. 75N9301900065 (AS and DW). This study was financed in part by the Coordination for the Improvement of Higher Education Personnel (Coordenação de Aperfeiçoamento de Pessoal de Nível Superior - CAPES) - Finance Code 001. We thank children and their families that participated in the study, the Multi-function Laboratory to support research in Nephrology and Medical Sciences/LAMAP, the Clinical Research Unit/UPC, Zika Collaborative Group, and Dr. Remberto Mauricio de la Cruz Vargas Vilte for his valuable and stimulating scientific discussions. We also thank the Laboratório de Flavivírus (LabFLA) of Fiocruz, which provided reference viruses from their arbovirus stocks.

SUPPLEMENTARY MATERIAL

The Supplementary Material for this article can be found online at: https://www.frontiersin.org/articles/10.3389/fimmu.2021.610456/full#supplementary-material

REFERENCES

1. Perkins TA, Siraj AS, Ruktanonchai CW, Kraemer MU, Tatem AJ. Model-based projections of Zika virus infections in childbearing women in the Americas. *Nat Microbiol.* (2016) 1:16126. doi: 10.1038/nmicrobiol.2016.126
2. Fauci AS, Morens DM. Zika virus in the Americas–yet another arbovirus threat. *N Engl J Med.* (2016) 374:601–4. doi: 10.1056/NEJMp1600297
3. Brady OJ, Gething PW, Bhatt S, Messina JP, Brownstein JS, Hoen AG, et al. Refining the global spatial limits of dengue virus transmission by evidence-based consensus. *PLoS Negl Trop Dis.* (2012) 6:e1760. doi: 10.1371/journal.pntd.0001760
4. Brady OJ, Hay SI. The first local cases of Zika virus in Europe. *Lancet.* (2019) 394:1991–2. doi: 10.1016/S0140-6736(19)32790-4
5. Bhatt S, Gething PW, Brady OJ, Messina JP, Farlow AW, Moyes CL, et al. The global distribution and burden of dengue. *Nature.* (2013) 496:504–7. doi: 10.1038/nature12060
6. Messina JP, Kraemer MU, Brady OJ, Pigott DM, Shearer FM, Weiss DJ, et al. Mapping global environmental suitability for Zika virus. *Elife.* (2016) 19:e15272. doi: 10.7554/eLife.15272.017
7. D'Ortenzio E, Matheron S, Yazdanpanah Y, de Lamballerie X, Hubert B, Piorkowski G, et al. Evidence of sexual transmission of Zika virus. *N Engl J Med.* (2016) 374:2195–8. doi: 10.1056/NEJMc1604449
8. Fréour T, Mirallié S, Hubert B, Splingart C, Barrière P, Maquart M, et al. Sexual transmission of Zika virus in an entirely asymptomatic couple returning from a Zika epidemic area, France, April 2016. *Euro Surveill.* (2016) 21:23. doi: 10.2807/1560-7917
9. Govero J, Esakky P, Scheaffer SM, Fernandez E, Drury A, Platt DJ, et al. Zika virus infection damages the testes in mice. *Nature.* (2016) 540:438–42. doi: 10.1038/nature20556
10. Ma W, Li S, Ma S, Jia L, Zhang F, Zhang Y, et al. Zika virus causes testis damage and leads to male infertility in mice. *Cell.* (2017) 168:542. doi: 10.1016/j.cell.2017.01.009
11. Tang WW, Young MP, Mamidi A, Regla-Nava JA, Kim K, Shresta S. A mouse model of Zika virus sexual transmission and vaginal viral replication. *Cell Rep.* (2016) 17:3091–8. doi: 10.1016/j.celrep.2016.11.070
12. Cugola FR, Fernandes IR, Russo FB, Freitas BC, Dias JL, Guimarães KP, et al. The Brazilian Zika virus strain causes birth defects in experimental models. *Nature.* (2016) 534:267–71. doi: 10.1038/nature18296

13. Miner JJ, Cao B, Govero J, Smith AM, Fernandez E, Cabrera OH, et al. Zika virus infection during pregnancy in mice causes placental damage and fetal demise. *Cell.* (2016) 165:1081–91. doi: 10.1016/j.cell.2016.05.008
14. Venturi G, Zammarchi L, Fortuna C, Remoli ME, Benedetti E, Fiorentini C, et al. An autochthonous case of Zika due to possible sexual transmission, Florence, Italy, (2014). *Euro Surveill.* (2016) 21:30148. doi: 10.2807/1560-7917.ES.2016.21.8.30148
15. Yockey LJ, Varela L, Rakib T, Khoury-Hanold W, Fink SL, et al. Vaginal exposure to Zika virus during pregnancy leads to fetal brain infection. *Cell.* (2016) 166:1247–56. doi: 10.1016/j.cell.2016.08.004
16. Lima GP, Rozenbaum D, Pimentel C, Frota ACC, Vivacqua D, Machado ES, et al. Factors associated with the development of congenital Zika syndrome: a case-control study. *BMC Infect Dis.* (2019) 19:277. doi: 10.1186/s12879-019-3908-4
17. Brasil P, Pereira JP Jr, Moreira ME, Ribeiro Nogueira RM, Damasceno L, Wakimoto M, et al. Zika virus infection in pregnant women in Rio de Janeiro. *N Engl J Med.* (2016) 375:2321–34. doi: 10.1056/NEJMoa1602412
18. Costa F, Sarno M, Khouri R, de Paula Freitas B, Siqueira I, Ribeiro GS, et al. Emergence of congenital Zika syndrome: viewpoint from the front lines. *Ann Intern Med.* (2016) 164:689–91. doi: 10.7326/M16-0332
19. França GV, Schuler-Faccini L, Oliveira WK, Henriques CM, Carmo EH, Pedi VD, et al. Congenital Zika virus syndrome in Brazil: a case series of the first 1501 livebirths with complete investigation. *Lancet.* (2016) 388:891–7. doi: 10.1016/S0140-6736(16)30902-3
20. Kleber de Oliveira W, Cortez-Escalante J, De Oliveira WT, do Carmo GM, Henriques CM, Coelho GE, et al. Increase in reported prevalence of microcephaly in infants born to women living in areas with confirmed Zika virus transmission during the first trimester of pregnancy - Brazil, 2015. *MMWR Morb Mortal Wkly Rep.* (2016) 65:242–7. doi: 10.15585/mmwr.mm6509e2
21. Mlakar J, Korva M, Tul N, Popović M, Poljšak-Prijatelj M, Mraz J, et al. Zika virus associated with microcephaly. *N Engl J Med.* (2016) 374:951–8. doi: 10.1056/NEJMoa1600651
22. Hamel R, Dejarnac O, Wichit S, Ekchariyawat P, Neyret A, Luplertlop N, et al. Biology of Zika virus infection in human skin cells. *J Virol.* (2015) 89:8880–96. doi: 10.1128/JVI.00354-15
23. Ngono AE, Shresta S. Immune response to dengue and Zika. *Annu Rev Immunol.* (2018) 36:279–308. doi: 10.1146/annurev-immunol-042617-053142
24. Tonnerre P, Melgaço JG, Torres-Cornejo A, Pinto MA, Yue C, Blümel J, et al. Evolution of the innate and adaptive immune response in women with acute Zika virus infection. *Nat Microbiol.* (2020) 5:76–83. doi: 10.1038/s41564-019-0618-z
25. Grifoni A, Costa-Ramos P, Pham J, Tian Y, Rosales SL, Seumois G, et al. Cutting edge: transcriptional profiling reveals multifunctional and cytotoxic antiviral responses of Zika virus-specific CD8+ T cells. *J Immunol.* (2018) 201:3487–91. doi: 10.4049/jimmunol.1801090
26. Racicot K, Mor G. Risks associated with viral infections during pregnancy. *J Clin Invest.* (2017) 127:1591–9. doi: 10.1172/JCI87490
27. Lanciotti RS, Kosoy OL, Laven JJ, Velez JO, Lambert AJ, Johnson AJ, et al. Genetic and serologic properties of Zika virus associated with an epidemic, yap state, Micronesia, 2007. *Emerg Infect Dis.* (2008) 14:1232–9. doi: 10.3201/eid1408.080287
28. Vianna RAO, Lovero KL, Oliveira SA, Fernandes AR, Santos TCSD, Lima LCSS, et al. Children born to mothers with rash during Zika virus epidemic in Brazil: first 18 months of life. *J Trop Pediatr.* (2019) 65:592–602. doi: 10.1093/tropej/fmz019
29. Brazil. Ministry of Health of Brazil. *Health Surveillance Department. Zika Virus in Brazil : the SUS response (electronic resource)/Ministry of Health of Brazil, Health Surveillance Department*. Brasilia: Ministry of Health of Brazil (2017).
30. Miagostovich MP, Nogueira RM, dos Santos FB, Schatzmayr HG, Araújo ES, Vorndam V. Evaluation of an IgG enzyme-linked immunosorbent assay for dengue diagnosis. *J Clin Virol.* (1999) 14:183–9. doi: 10.1016/S1386-6532(99)00059-1
31. Steinhagen K, Probst C, Radzimski C, Schmidt-Chanasit J, Emmerich P, van Esbroeck M, et al. Serodiagnosis of Zika virus (ZIKV) infections by a novel NS1-based ELISA devoid of cross-reactivity with dengue virus antibodies: a multicohort study of assay performance, 2015 to 2016. *Euro Surveill.* (2016) 21:30426. doi: 10.2807/1560-7917.ES.2016.21.50.30426
32. Russell PK, Nisalak A, Sukhavachana P, Vivona S. A plaque reduction test for dengue virus neutralizing antibodies. *J Immunol.* (1967) 99:285–90.
33. Roehrig JT, Hombach J, Barrett AD. Guidelines for plaque-reduction neutralization testing of human antibodies to dengue viruses. *Viral Immunol.* (2008) 21:123–32. doi: 10.1089/vim.2008.0007
34. Grifoni A, Voic H, Dhanda SK, Kidd CK, Brien JD, Buus S, et al. T cell responses induced by attenuated flavivirus vaccination are specific and show limited cross-reactivity with other flavivirus species. *J Virol.* (2020) 94:e00089–20. doi: 10.1128/JVI.00089-20
35. Grifoni A, Tian Y, Sette A, Weiskopf D. Transcriptomic immune profiles of human flavivirus-specific T-cell responses. *Immunology.* (2020) 160:3–9. doi: 10.1111/imm.13161
36. Xu X, Vaughan K, Weiskopf D, Grifoni A, Diamond MS, Sette A, et al. Identifying candidate targets of immune responses in Zika virus based on homology to epitopes in other flavivirus species. *PLoS Curr.* (2016) 8. doi: 10.1371/currents.outbreaks.9aa2e1fb61b0f632f58a098773008c4b
37. Paul S, Sidney J, Sette A, Peters B. TepiTool: a pipeline for computational prediction of T cell epitope candidates. *Curr Protoc Immunol.* (2016) 114:18.19.1–24. doi: 10.1002/cpim.12
38. Dhanda SK, Mahajan S, Paul S, Yan Z, Kim H, Jespersen MC et al. IEDB-AR: immune epitope database-analysis resource in 2019. *Nucleic Acids Res.* (2019) 47:W502–6. doi: 10.1093/nar/gkz452
39. Paul S, Lindestam Arlehamn CS, Scriba TJ, Dillon MB, Oseroff C, Hinz D et al. Development and validation of a broad scheme for prediction of HLA class II restricted T cell epitopes. *J Immunol Methods.* (2015) 422:28–34. doi: 10.1016/j.jim.2015.03.022
40. Paul S, Weiskopf D, Angelo MA, Sidney J, Peters B, Sette A. HLA class I alleles are associated with peptide-binding repertoires of different size, affinity, and immunogenicity. *J Immunol.* (2013) 191:5831–9. doi: 10.4049/jimmunol.1302101
41. Dhanda SK, Vaughan K, Schulten V, Grifoni A, Weiskopf D, Sidney J, et al. Development of a novel clustering tool for linear peptide sequences. *Immunology.* (2018) 155:331–45. doi: 10.1111/imm.12984
42. Weiskopf D, Angelo MA, de Azeredo EL, Sidney J, Greenbaum JA, Fernando AN, et al. Comprehensive analysis of dengue virus-specific responses supports an HLA-linked protective role for CD8+ T cells. *Proc Natl Acad Sci USA.* (2013) 110:E2046–53. doi: 10.1073/pnas.1305227110
43. Weiskopf D, Bangs DJ, Sidney J, Kolla RV, De Silva AD, de Silva AM, et al. Dengue virus infection elicits highly polarized CX3CR1+ cytotoxic CD4+ T cells associated with protective immunity. *Proc Natl Acad Sci USA.* (2015) 112:E4256–63. doi: 10.1073/pnas.1505956112
44. Grifoni A, Pham J, Sidney J, O'Rourke PH, Paul S, Peters B, et al. Prior dengue virus exposure shapes T cell immunity to Zika virus in humans. *J Virol.* (2017) 91:e01469–17. doi: 10.1128/JVI.01469-17
45. Secretaria Estadual de Saúde do Rio de Janeiro. *Boletim Epidemiológico 005/2016.* Rio de Janeiro: Secretaria Estadual de Saúde do Rio de Janeiro (2016).
46. de Araújo TVB, Rodrigues LC, de Alencar Ximenes RA, de Barros Miranda-Filho D, Montarroyos UR, de Melo APL, et al. Association between Zika virus infection and microcephaly in Brazil, January to May, 2016: preliminary report of a case-control study. *Lancet Infect Dis.* (2016) 16:1356–3. doi: 10.1016/S1473-3099(16)30318-8
47. Halai UA, Nielsen-Saines K, Moreira ML, de Sequeira PC, Junior JPP, de Araujo Zin A, et al. Maternal Zika virus disease severity, virus load, prior dengue antibodies, and their relationship to birth outcomes. *Clin Infect Dis.* (2017) 65:877–83. doi: 10.1093/cid/cix472
48. Brown JA, Singh G, Acklin JA, Lee S, Duehr JE, Chokola AN, et al. Dengue virus immunity increases Zika virus-induced damage during pregnancy. *Immunity.* (2019) 50:751–62. doi: 10.1016/j.immuni.2019.01.005
49. Camargos VN, Foureaux G, Medeiros DC, da Silveira VT, Queiroz-Junior CM, Matosinhos ALB, et al. In-depth characterization of congenital Zika syndrome in immunocompetent mice: antibody-dependent enhancement and an antiviral peptide therapy. *EBioMedicine.* (2019) 44:516–29. doi: 10.1016/j.ebiom.2019.05.014

50. Rathore APS, Saron WAA, Lim T, Jahan N, St John AL. Maternal immunity and antibodies to dengue virus promote infection and Zika virus-induced microcephaly in fetuses. *Sci Adv.* (2019) 5:eaav3208. doi: 10.1126/sciadv.aav3208
51. Zimmerman MG, Wrammert J, Suthar MS. Cross-reactive antibodies during Zika virus infection: protection, pathogenesis, and placental seeding. *Cell Host Microbe.* (2020) 27:14–24. doi: 10.1016/j.chom.2019.12.003
52. Regla-Nava JA, Elong Ngono A, Viramontes KM, Huynh AT, Wang YT, Nguyen AT, et al. Cross-reactive dengue virus-specific CD8+ T cells protect against Zika virus during pregnancy. *Nat Commun.* (2018) 9:3042. doi: 10.1038/s41467-018-05458-0
53. Reynolds CJ, Suleyman OM, Ortega-Prieto AM, Skelton JK, Bonnesoeur P, Blohm A, et al. T cell immunity to Zika virus targets immunodominant epitopes that show cross-reactivity with other Flaviviruses. *Sci Rep.* (2018) 8:672. doi: 10.1038/s41598-017-18781-1
54. Ricciardi MJ, Magnani DM, Grifoni A, Kwon YC, Gutman MJ, Grubaugh ND, et al. Ontogeny of the B- and T-cell response in a primary Zika virus infection of a dengue-naïve individual during the 2016 outbreak in Miami, FL. *PLoS Negl Trop Dis.* (2017) 11:e0006000. doi: 10.1371/journal.pntd.0006000
55. Lai L, Rouphael N, Xu Y, Natrajan MS, Beck A, Hart M, et al. Innate, T-, and B-cell responses in acute human Zika patients. *Clin Infect Dis.* (2018) 66:1–10. doi: 10.1093/cid/cix732
56. Angelo MA, Grifoni A, O'Rourke PH, Sidney J, Paul S, Peters B, et al. Human CD4+ T cell responses to an attenuated tetravalent dengue vaccine parallel those induced by natural infection in magnitude, HLA restriction, and antigen specificity. *J Virol.* (2017) 91:e02147–16. doi: 10.1128/JVI.02147-16
57. Grifoni A, Moore E, Voic H, Sidney J, Phillips E, Jadi R, et al. Characterization of magnitude and antigen specificity of HLA-DP, DQ, and DRB3/4/5 restricted DENV-specific CD4+ T cell responses. *Front Immunol.* (2019) 10:1568. doi: 10.3389/fimmu.2019.01568
58. Huang H, Li S, Zhang Y, Han X, Jia B, Liu H, et al. CD8+ T cell immune response in immunocompetent mice during Zika virus infection. *J Virol.* (2017) 91:e00900–17. doi: 10.1128/JVI.00900-17
59. Pardy RD, Rajah MM, Condotta SA, Taylor NG, Sagan SM, Richer MJ. Analysis of the T cell response to Zika virus and identification of a novel CD8+ T cell epitope in immunocompetent mice. *PLoS Pathog.* (2017) 13:e1006184. doi: 10.1371/journal.ppat.1006184
60. Elong Ngono A, Vizcarra EA, Tang WW, Sheets N, Joo Y, Kim K, et al. Mapping and role of the CD8+ T cell response during primary Zika virus infection in mice. *Cell Host Microbe.* (2017) 21:35–46. doi: 10.1016/j.chom.2016.12.010
61. Wen J, Tang WW, Sheets N, Ellison J, Sette A, Kim K, et al. Identification of Zika virus epitopes reveals immunodominant and protective roles for dengue virus cross-reactive CD8+ T cells. *Nat Microbiol.* (2017) 2:17036. doi: 10.1038/nmicrobiol.2017.36
62. Manangeeswaran M, Ireland DD, Verthelyi D. Zika (PRVABC59) infection is associated with T cell infiltration and neurodegeneration in CNS of immunocompetent neonatal C57Bl/6 mice. *PLoS Pathog.* (2016) 12:e1006004. doi: 10.1371/journal.ppat.1006004
63. Jurado KA, Yockey LJ, Wong PW, Lee S, Huttner AJ, Iwasaki A. Antiviral CD8 T cells induce Zika-virus-associated paralysis in mice. *Nat Microbiol.* (2018) 3:141–7. doi: 10.1038/s41564-017-0060-z
64. Koblischke M, Stiasny K, Aberle SW, Malafa S, Tsouchnikas G, Schwaiger J, et al. Structural influence on the dominance of virus-specific CD4 T cell epitopes in Zika virus infection. *Front Immunol.* (2018) 9:1196. doi: 10.3389/fimmu.2018.02083
65. Patil VS, Madrigal A, Schmiedel BJ, Clarke J, O'Rourke P, de Silva AD, et al. Precursors of human CD4+ cytotoxic T lymphocytes identified by single-cell transcriptome analysis. *Sci Immunol.* (2018) 3:eaan8664. doi: 10.1126/sciimmunol.aan8664
66. Tian Y, Babor M, Lane J, Schulten V, Patil VS, Seumois G, et al. Unique phenotypes and clonal expansions of human CD4 effector memory T cells re-expressing CD45RA. *Nat Commun.* (2017) 8:1473. doi: 10.1038/s41467-017-01728-5
67. Ribeiro MRC, Khouri R, Sousa PS, Branco MRFC, Batista RFL, Costa EPF, et al. Plaque reduction neutralization test (PRNT) in the congenital Zika syndrome: positivity and associations with laboratory, clinical, and imaging characteristics. *Viruses.* (2020) 12:1244. doi: 10.3390/v12111244
68. Pauvolid-Corrêa A, Gonçalves Dias H, Marina Siqueira Maia L, Porfírio G, Oliveira Morgado T, Sabino-Santos G, et al. Zika virus surveillance at the human-animal interface in west-central Brazil, 2017-2018. *Viruses.* (2019) 11:1164. doi: 10.3390/v11121164
69. Sulleiro E, Frick MA, Rodó C, Espasa M, Thome C, Espiau M, et al. The challenge of the laboratory diagnosis in a confirmed congenital Zika virus syndrome in utero: a case report. *Medicine.* (2019) 98:1–6. doi: 10.1097/MD.0000000000015532
70. Robbiani DF, Olsen PC, Costa F, Wang Q, Oliveira TY, Nery N Jr, et al. Risk of Zika microcephaly correlates with features of maternal antibodies. *J Exp Med.* (2019) 216:2302–15. doi: 10.1084/jem.20191061
71. Pardy RD, Richer MJ. Protective to a T: the role of T cells during Zika virus infection. *Cells.* (2019) 8:820. doi: 10.3390/cells8080820
72. Macedo-da-Silva J, Rosa-Fernandes L, Barbosa RH, Angeli CB, Carvalho FR, de Oliveira Vianna RA, et al. Serum proteomics reveals alterations in protease activity, axon guidance, and visual phototransduction pathways in infants with in utero exposure to Zika virus without congenital Zika syndrome. *Front Cell Infect Microbiol.* (2020) 10:577819. doi: 10.3389/fcimb.2020.577819

Conflict of Interest: The authors declare that the research was conducted in the absence of any commercial or financial relationships that could be construed as a potential conflict of interest.

frontiers in Immunology

ORIGINAL RESEARCH
published: 17 May 2021
doi: 10.3389/fimmu.2021.686437

Early Embryonic Loss Following Intravaginal Zika Virus Challenge in Rhesus Macaques

*Christina M. Newman[1], Alice F. Tarantal[2,3], Michele L. Martinez[2,3], Heather A. Simmons[4], Terry K. Morgan[5], Xiankun Zeng[6], Jenna R. Rosinski[1], Mason I. Bliss[7], Ellie K. Bohm[8], Dawn M. Dudley[1], Matthew T. Aliota[8], Thomas C. Friedrich[7], Christopher J. Miller[3,9] and David H. O'Connor[1,4]**

[1] Pathology and Laboratory Medicine, University of Wisconsin-Madison, Madison, WI, United States, [2] Pediatrics, Cell Biology and Human Anatomy, School of Medicine, University of California, Davis, CA, United States, [3] California National Primate Research Center, University of California, Davis, CA, United States, [4] Wisconsin National Primate Research Center, University of Wisconsin-Madison, Madison, WI, United States, [5] Pathology, Oregon Health and Sciences University, Portland, OR, United States, [6] Pathology Division, United States Army Medical Research Institute of Infectious Diseases, Frederick, MD, United States, [7] Pathobiological Sciences, University of Wisconsin-Madison, Madison, WI, United States, [8] Veterinary and Biomedical Sciences, University of Minnesota, Saint Paul, MN, United States, [9] Pathology, Microbiology, and Immunology, School of Veterinary Medicine, Center for Immunology and Infectious Diseases, University of California, Davis, CA, United States

OPEN ACCESS

Edited by:
Abhay P. S. Rathore, Duke University, United States

Reviewed by:
Ashley L. St John, Duke-NUS Medical School, Singapore
Stephen Kent, The University of Melbourne, Australia

***Correspondence:**
David H. O'Connor
dhoconno@wisc.edu

Specialty section:
This article was submitted to Viral Immunology, a section of the journal Frontiers in Immunology

Received: *26 March 2021*
Accepted: *04 May 2021*
Published: *17 May 2021*

Citation:
Newman CM, Tarantal AF, Martinez ML, Simmons HA, Morgan TK, Zeng X, Rosinski JR, Bliss MI, Bohm EK, Dudley DM, Aliota MT, Friedrich TC, Miller CJ and O'Connor DH (2021) Early Embryonic Loss Following Intravaginal Zika Virus Challenge in Rhesus Macaques. Front. Immunol. 12:686437. doi: 10.3389/fimmu.2021.686437

Zika virus (ZIKV) is an arthropod-borne virus (arbovirus) and is primarily transmitted by *Aedes* species mosquitoes; however, ZIKV can also be sexually transmitted. During the initial epidemic and in places where ZIKV is now considered endemic, it is difficult to disentangle the risks and contributions of sexual versus vector-borne transmission to adverse pregnancy outcomes. To examine the potential impact of sexual transmission of ZIKV on pregnancy outcome, we challenged three rhesus macaques (*Macaca mulatta*) three times intravaginally with 1 x 10^7 PFU of a low passage, African lineage ZIKV isolate (ZIKV-DAK) in the first trimester (~30 days gestational age). Samples were collected from all animals initially on days 3 through 10 post challenge, followed by twice, and then once weekly sample collection; ultrasound examinations were performed every 3-4 days then weekly as pregnancies progressed. All three dams had ZIKV RNA detectable in plasma on day 3 post-ZIKV challenge. At approximately 45 days gestation (17-18 days post-challenge), two of the three dams were found with nonviable embryos by ultrasound. Viral RNA was detected in recovered tissues and at the maternal-fetal interface (MFI) in both cases. The remaining viable pregnancy proceeded to near term (~155 days gestational age) and ZIKV RNA was detected at the MFI but not in fetal tissues. These results suggest that sexual transmission of ZIKV may represent an underappreciated risk of pregnancy loss during early gestation.

Keywords: Zika virus, macaques, pregnancy, intravaginal infection, embryonic loss

INTRODUCTION

Zika virus (ZIKV) emerged from relative obscurity five years ago to sweep through tropical and subtropical regions of the Western hemisphere. More than a million cases between 2015 and 2018 were reported in Pan American Health Organization (PAHO) regions alone (1). While ZIKV primarily causes mild febrile illness or asymptomatic infections in a majority of individuals, infection during pregnancy can result in a range of adverse outcomes including fetal loss and a constellation of birth defects now known as congenital Zika syndrome (CZS) (2–4). Human infection with ZIKV can occur following mosquito-borne, vertical, and sexual transmission (5–7). While mosquito-borne transmission from infected *Aedes* species mosquitoes is thought to be the most common route of infection in endemic areas, the contribution of sexual transmission in epidemics remains poorly understood, in part because during an outbreak, both transmission routes occur simultaneously and can be challenging to disentangle (8).

Sexual transmission of ZIKV was first documented in 2008 when a scientist working in Senegal became infected and, upon his return to the United States, infected his wife (9). Throughout the ZIKV outbreak in 2015 and 2016, additional sexually-transmitted infections were documented (10–14). The majority of sexually-transmitted cases in non-endemic areas are likely the result of infection of the primary cases during travel, followed by inadvertent transmission to the secondary cases upon returning home (7). As previously mentioned, sexually-transmitted ZIKV infections in endemic areas or areas experiencing active outbreaks are difficult to differentiate from mosquito-transmitted infections because there may be an individual risk of exposure by either route. Epidemiological data suggest that sexual transmission occurs primarily male-to-female through vaginal contact, even weeks after clinical symptom resolution, which suggests that sexual transmission of ZIKV does pose at least a theoretical risk to pregnant women (15). Furthermore, the ZIKV viral RNA (vRNA) load in human semen has been reported to range from the hundreds to tens of millions of copies per milliliter, with values as high as $3.98x10^8$ copies/ml reported (16–18). The testes in particular, were found to be a ZIKV reservoir in animal models (19, 20). In addition, studies have recently shown that intimate partners of household index cases are more likely to also be positive or show serologic evidence of ZIKV infection relative to other members of the same household (21).

Overall, we have limited information regarding the risk of ZIKV sexual transmission to pregnant women and their developing fetuses (14). Studies have shown that other sexually transmitted ascending vaginal infections are associated with an increased risk of pre-term labor and other poor outcomes (22). Whether an ascending intravaginal ZIKV infection poses a higher risk to pregnancy than mosquito-borne infection is currently unknown. Pregnant women or women trying to become pregnant may be less likely to utilize condoms, a recommended strategy for the prevention of sexual transmission of ZIKV (23, 24). Furthermore, a woman might not be aware of a pregnancy during early gestation and unfortunately, existing data suggest that the highest risk for developmental anomalies associated with ZIKV infection is during the first trimester, a critical developmental time period (25–27). Additionally, ZIKV infection during pregnancy has also been associated with an increased risk for spontaneous abortion in both humans and nonhuman primates (28, 29).

Animal models have played a critical role in improving our understanding of the natural history and pathogenesis of ZIKV. To-date, both murine and nonhuman primate (NHP) models have been utilized to examine aspects of sexual transmission of ZIKV (19, 20, 30, 31). Studies in these models have shown persistent shedding of vRNA from the reproductive tract, infection of the female reproductive tract *via* a vaginal exposure route, and fetal effects as a result of vaginal exposure or sexual transmission in mice (20, 30–39). Although studies in pregnant olive baboons have shown that intravaginal challenge with infected baboon semen during mid-gestation can result in productive maternal infection and vRNA detection in some maternal tissues and placentas, to date, studies in NHP have not shown clear evidence of vertical transmission associated with maternal ZIKV infection by the intravaginal route (33).

Because infection during the first trimester is associated with the highest risk for adverse pregnancy outcomes and, since women may be unaware of a pregnancy and may potentially be less likely to utilize barrier methods to prevent sexually-transmitted ZIKV infections during the early first trimester (23, 24), we designed a proof-of-concept study in which we challenged three gravid rhesus macaques (*Macaca mulatta*) intravaginally with ZIKV. Our goal was to investigate the potential impact of intravaginal ZIKV challenge during the first trimester on fetal and pregnancy outcomes and to develop a model for sexual transmission during early pregnancy.

METHODS

Ethics Statement

All animal procedures conformed to the requirements of the Animal Welfare Act and protocols were approved prior to implementation by the Institutional Animal Care and Use Committee (IACUC) at the University of California, Davis. Activities related to animal care, housing, and diet were performed according to California National Primate Research Center (CNPRC) standard operating procedures (SOPs). SOPs for colony related procedures are reviewed and approved by the UC Davis IACUC.

Study Design

Female rhesus macaques (*Macaca mulatta*, N=3) were time-mated and identified as pregnant by ultrasound according to established methods (40). Prior to study assignment normal embryonic growth and development were confirmed by ultrasound. Females were challenged in the first trimester at approximately 30 days gestational age (trimesters divided by 55-day increments; term 165 ± 10 days) with $1x10^7$ PFU ZIKV-DAK three times intravaginally at approximately two-hour intervals

(**Table 1** and **Figure 1**). Pregnancies were monitored by ultrasound every 3-4 days post-challenge and then weekly from day 50 onward throughout the study period. Standardized parameters were assessed including fetal growth (greatest length then biparietal and occipitofrontal diameters, head and abdominal circumferences, humerus and femur lengths) and structural development, amniotic fluid volumes and placental parameters, and compared to normal growth and developmental trajectories for the species (40). Dams were weighed at each sedation and blood samples were collected daily from day 3 through day 10 post-challenge, followed by bi-weekly until maternal plasma vRNA loads were undetectable, and then weekly until hysterotomy. Plasma and peripheral blood mononuclear cells (PBMCs) were isolated at all time points, and serum was collected on days 0, 14, and 24 post-challenge (dams 049-102 and 049-103), and on days 0, 14, 27, and 122 post-challenge for dam 049-101. Urine was collected by ultrasound-guided cystocentesis (~1 ml) on days 7, 10, 14, 21, and 24 post-challenge (dams 049-102 and 049-103) and on days 7, 10, 14, 27, and 122 post-challenge for dam 049-101. Hysterotomies were performed for dam 049-102 and 049-103 at the end of the first trimester (post-detection of nonviable embryos by ultrasound) and near term (~155 days gestational age) for dam 049-101.

Virus Challenge Preparation and Infection

ZIKV strain Zika virus/A.africanus-tc/Senegal/1984/DAK AR 41524 (ZIKV-DAK; GenBank: KX601166) was originally isolated from *Aedes luteocephalus* mosquitoes in Senegal in 1984. One round of amplification on *Aedes pseudocutellaris* cells, followed by amplification on C6/36 cells and two rounds of amplification on Vero cells, were used to prepare a master stock obtained from BEI Resources (Manassas, VA). Challenge stocks were prepared from this master stock by inoculation onto a confluent monolayer of C6/36 mosquito cells as described previously (41). Prior to administration, the ZIKV-DAK stock was diluted to $1x10^7$ PFU in 1 ml sterile saline and delivered *via* a 1 ml tuberculin syringe (37). Animals were inoculated three times intravaginally under ketamine sedation at approximately two-hour intervals using a previously described method (37).

Blood Processing and Plasma vRNA Loads

Plasma and PBMCs were isolated from blood placed in EDTA vacutainers and processed at 1500 RPM for 15 minutes according to standard protocols. Serum was isolated from whole blood collected into glass vacutainers without additives. Viral RNA was extracted from 300 µl plasma as previously described with a Maxwell 16 MDx instrument (Promega, Madison, WI) and evaluated using qRT-PCR (42). RNA concentration was determined by interpolation onto an internal standard curve of seven ten-fold serial dilutions of a synthetic ZIKV RNA segment based on Zika virus/Human/French Polynesia/10087PF/2013 (ZIKV-FP). The limit of quantification of the ZIKV qRT-PCR assay is estimated to be 100 copies vRNA/ml plasma or serum.

Hysterotomy and Tissue Collection

Dams 049-102 and 049-103 were scheduled for hysterotomies in the late first trimester (nonviable embryos detected 3 days prior to hysterotomy). The hysterotomy for dam 049-101 was performed at approximately 155 days gestational age according

TABLE 1 | Dam information on day 0 of study.

Dam ID	Weight (kg)	Age (y)	Gestational Age (days)	Scheduled hysterotomy (days)	Virus	Dose (PFU)	Challenge #
049-101	5.55	6.93	29	155	ZIKV-DAK	$1x10^7$	3
049-102	7.40	11.83	32	155	ZIKV-DAK	$1x10^7$	3
049-103	8.43	12.83	31	155	ZIKV-DAK	$1x10^7$	3

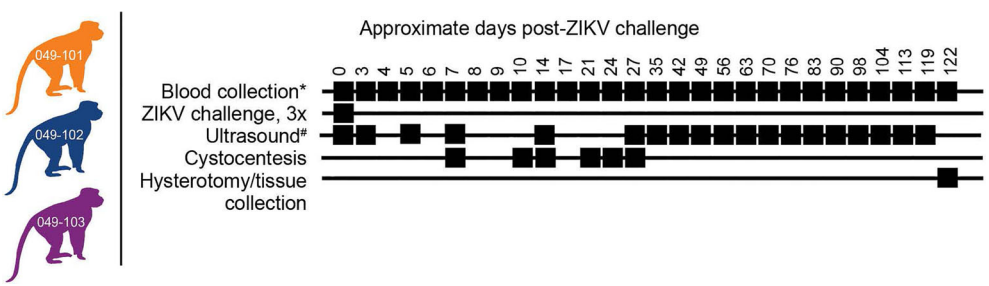

FIGURE 1 | Study design. Three female rhesus macaques were time-mated, confirmed pregnant by ultrasound, and challenged intravaginally at 30 days (+/-2) gestational age with $1x10^7$ PFU ZIKV-DAK three times at two-hour intervals. Blood collection* denotes plasma and PBMC isolation at every sampling time point while serum collection was planned only on days 0, 14, 27, and 122 post-ZIKV challenge. Ultrasound# denotes ultrasound imaging was performed every 3-4 days during early gestation, then weekly thereafter. Hysterotomies were originally planned for each animal at approximately 122 days post-ZIKV challenge.

to the original study design (**Figure 1**) and following established protocols (43). The gestational sac was removed for fetal tissue assessments, with a modified collection protocol for nonviable specimens (see below). For the fetus from dam 049-101 amniotic fluid, fetal blood, and fetal cerebrospinal fluid were collected, then fetal body weights and measures (biparietal and occipitofrontal diameters, abdominal and arm circumferences, hand and foot lengths, humerus and femur lengths, crown-rump length) were assessed. The left cerebral hemisphere and left eye were collected under aseptic conditions and shipped with cold packs to Wisconsin by overnight delivery for additional assessments (see below). Specimens collected for qRT-PCR for vRNA analysis included dura mater; right cerebral hemisphere (frontal, parietal, temporal, occipital lobes); cerebellum (right and left) and midbrain; right optic nerve; right eye (cornea, retina, sclera); spinal cord (cervical, thoracic, lumbar); right and left parotid glands, submandibular, and salivary glands; omentum; thymus; spleen; liver (right, left, quadrate, caudate lobes); pancreas; right and left adrenal glands and kidneys; right and left axillary and inguinal lymph nodes; diaphragm; tracheobronchial and mesenteric lymph nodes; right and left thyroids; trachea; esophagus; pericardium; aorta; right and left atria and ventricles; lung lobes (right and left; all lobes); reproductive tract including right and left gonads; urinary bladder; gastrointestinal tract (stomach, duodenum, jejunum, ileum, colon; meconium), skin, skeletal muscle, and bone marrow (**Table 2**). The placenta was weighed and assessed including disk measurements (primary and secondary for bidiscoid placentas; primary disk only for monodiscoid), umbilical cord and membrane insertion sites, blood vessel distribution, cut surfaces, and examined for the presence of infarcts. Decidua, membranes, umbilical cord, and multiple sections of the placental disks were collected. All specimens were quick frozen in triplicate over liquid nitrogen for qRT-PCR analysis or collected into RNAlater (cat# R0901, Sigma-Aldrich, St. Louis, MO). Multiple blocks of tissues were collected in histology cassettes fixed in 10% buffered formalin, embedded, sectioned (5-6 μm) and stained with hematoxylin and eosin (H&E) or used for *in situ* hybridization (ISH).

For dams 049-102 and 049-103 a modified collection was performed, consistent with the early developmental stage of the conceptus (**Table 2**). Decidua, membranes, umbilical cord, and multiple sections of the placental disks were collected as noted above.

Fresh samples collected from the 049-101 fetus (left cerebral hemisphere and left eye) were shipped with cold packs for additional assessments as noted above; the eye was analyzed by the Comparative Ocular Pathology Laboratory of Wisconsin

TABLE 2 | Fetal and maternal-fetal interface tissues collected at hysterotomy.

Dam ID	Organ System/Tissue	Tissue samples tested (N)	Tissue samples qRT-PCR positive (N)	Positive tissue vRNA copies/mg (± SD)
049-101	integumentary	3	0	0.0
	musculoskeletal	2	0	0.0
	nervous	14	0	0.0
	endocrine	7	0	0.0
	lymphatic	8	0	0.0
	cardiovascular	4	0	0.0
	respiratory	10	0	0.0
	digestive	12	0	0.0
	urinary	3	0	0.0
	reproductive	3	0	0.0
	other	8	0	0.0
	primary placental disk	3	2	$0.66x10^{2a}$ (± $0.51x10^{2}$)
	primary placental disk	3	3	$1.59x10^{3a}$ (± $1.20x10^{3}$)
	placenta with decidua	18	3	$8.13x10^{2a}$ (± $3.97x10^{2}$)
	placenta without decidua	18	6	$6.45x10^{2a}$ (± $6.10x10^{2}$)
	decidua	18	3	0.0
049-102	nervous (brain)	1	1	$2.06x10^{3}$
	digestive (liver)	1	1	$1.23x10^{4}$
	umbilical cord	1	1	$8.37x10^{3}$
	membranes	1	1	$4.87x10^{3}$
	primary placental disk	3	3	$4.96x10^{3a}$ (± $4.00x10^{3}$)
	secondary placental disk	3	3	$3.61x10^{3a}$ (± $1.16x10^{3}$)
	decidua	1	0	0.0
049-103	nervous (brain)	1	1	$1.74x10^{5}$
	digestive (liver)	1	1	$7.42x10^{4}$
	umbilical cord	1	1	$7.13x10^{4}$
	amnion	1	1	$7.08x10^{2}$
	chorionic jelly	1	1	$3.54x10^{3}$
	membranes (amnion and chorion)	1	1	$4.74x10^{3}$
	primary placental disk	3	3	$1.98x10^{3a}$ (± $1.13x10^{3}$)
	secondary placental disk	3	3	$3.40x10^{3a}$ (± $2.18x10^{3}$)
	decidua	1	0	0.0

[a]*mean vRNA load of multiple positive tissue samples.*

(COPLOW). Placental tissues from all dams and tissues for the fetus from dam 049-101 were assessed as described previously in Koenig et al. (44).

Tissue, Urine, and Amniotic Fluid vRNA Loads

Maternal-fetal interface (MFI) and fetal tissue vRNA loads were determined from approximately 20 mg of each specimen. ZIKV RNA was isolated from tissues using the Qiagen AllPrep DNA/RNA Mini Kit (cat# 80284, Qiagen, Germantown MD) using the QIAcube following the manufacturer's protocol. Viral RNA was isolated from 140 µl maternal urine or amniotic fluid using the QIAmp Viral RNA minikit (cat# 52904, Qiagen, Germantown MD) following the manufacturer's protocol. Following isolation, cDNA synthesis was performed using the Qiagen Sensiscript RT kit (cat# 205213, Qiagen, Germantown MD) according to the manufacturer's protocol. Quantification of vRNA load was performed by real-time PCR using the Taqman amplification system and the QuantStudio 12 K Flex Real-Time PCR System (ThermoFisher Scientific, Grand Island, NY) as described previously (43). The estimated limit of quantification of the assay is 50-100 ZIKV RNA copies/mg tissue (average = 75 copies/mg).

In Situ Hybridization (ISH)

ISH probes against the ZIKV genome were commercially purchased (cat# 468361, Advanced Cell Diagnostics, Newark, CA). ISH was performed using the RNAscope® Red 2.5 kit (cat# 322350, Advanced Cell Diagnostics, Newark, CA) according to the manufacturer's protocol. After deparaffinization with xylene, a series of ethanol washes, and peroxidase blocking, sections were heated with the antigen retrieval buffer and then digested by proteinase. Sections were then exposed to the ISH target probe and incubated at 40°C in a hybridization oven for two-hours. After rinsing, ISH signal was amplified using the provided pre-amplifier followed by the amplifier-containing labelled probe binding sites, and developed with a Fast Red chromogenic substrate for 10 minutes at room temperature. Sections were then stained with hematoxylin, air-dried, and mounted.

Plaque Reduction Neutralization Tests (PRNT)

Titers of ZIKV neutralizing antibodies were determined using plaque reduction neutralization tests (PRNT) on Vero cells (ATCC #CCL-81) with a cutoff value of 90% ($PRNT_{90}$) (45). Neutralization curves were generated in GraphPad Prism (San Diego, CA) and the resulting data were analyzed by nonlinear regression to estimate the dilution of serum required to inhibit 90% Vero cell culture infection (45, 46).

RESULTS

Repeated Intravaginal ZIKV Challenge Results in Infection In Pregnant Macaques

All three dams had detectable ZIKV RNA in plasma by 3 days post intravaginal ZIKV challenge (**Figure 2**). ZIKV RNA loads peaked on day 5 for dams 049-101 and 049-102, and on day 6 for dam 049-103. Peak vRNA loads ranged from $1.57x10^4$ copies/ml for 049-101 to $1.30x10^5$ copies/ml for 049-103 (**Figure 2**). The latest detectable plasma vRNA load for animal 049-101 was on day 24 post-challenge ($1.56x10^2$ copies/ml). Dam 049-103 had a detectable plasma vRNA load until day 14 ($2.46x10^3$ copies/ml) but was negative on day 17 (the next time point samples were collected). Dam 049-102 was consistently positive for ZIKV vRNA until day 14, was negative on day 17, and then positive again on days 21 and 24 post challenge. Dam 049-102 was positive for ZIKV RNA in blood plasma collected at hysterotomy, the last time point sampled for the study. Overall, maternal plasma vRNA loads for dams 049-101, 049-102, and 049-103 were somewhat delayed compared to animals subcutaneously inoculated with French Polynesian or Puerto Rican ZIKV isolates in our previous studies, but were consistent in magnitude with previous observations (42, 48, 49). In addition, maternal plasma vRNA loads peaked within a time period similar to subcutaneously inoculated animals infected with the same ZIKV isolate (ZIKV-DAK) (47) (**Figure 2**).

Embryonic Demise Following Intravaginal ZIKV Infection During Early Pregnancy

Ultrasound examinations indicated that the embryos of dams 049-102 and 049-103 were nonviable at approximately 17-18 days post-challenge. Hysterotomies were subsequently scheduled and performed and each dam's final blood and urine samples were collected (**Figure 3A**). Embryo and placental tissues from dams 049-102 and 049-103 were collected for vRNA analysis, histopathological assessment, and ISH. Dam 049-101's pregnancy progressed normally and sampling continued until the study endpoint and near-term hysterotomy at approximately 155 days gestational age (**Figure 3A**). All fetal and placental measurements for 049-101 were recorded and were considered within normal limits for gestational age (**Table 3**) (40).

MFI, Tissues, and Amniotic Fluid Are ZIKV RNA Positive in Nonviable Embryos

ZIKV RNA was detected in the amniotic fluid from the conceptus of both dams 049-102 and 049-103 at $3.87x10^3$ and $7.38x10^3$ copies/ml respectively at the time of hysterotomy (subsequent to embryonic death). In addition, ZIKV RNA was detected in the brain and liver of both non-viable embryos, as well as in MFI tissues including the primary and secondary placental disks and membranes (amnion and chorion) (**Figure 3B**). The highest tissue vRNA burden was detected in the brain of the embryo from dam 049-102 ($1.74x10^5$ copies/mg). ZIKV RNA was not detected in amniotic fluid collected from the fetus of dam 049-101 at hysterotomy. Although a large number of fetal and MFI tissues were assessed following hysterotomy, the presence of ZIKV RNA was only detected in a subset of sections of MFI tissues from 049-101 (**Table 2** and **Figure 3C**). The decidua from all three dams were negative for ZIKV RNA by qRT-PCR. Similarly, ZIKV RNA was not detected in the urine for any of the dams at any of the time points sampled. Overall, these results highlight the focal nature of ZIKV RNA detection in

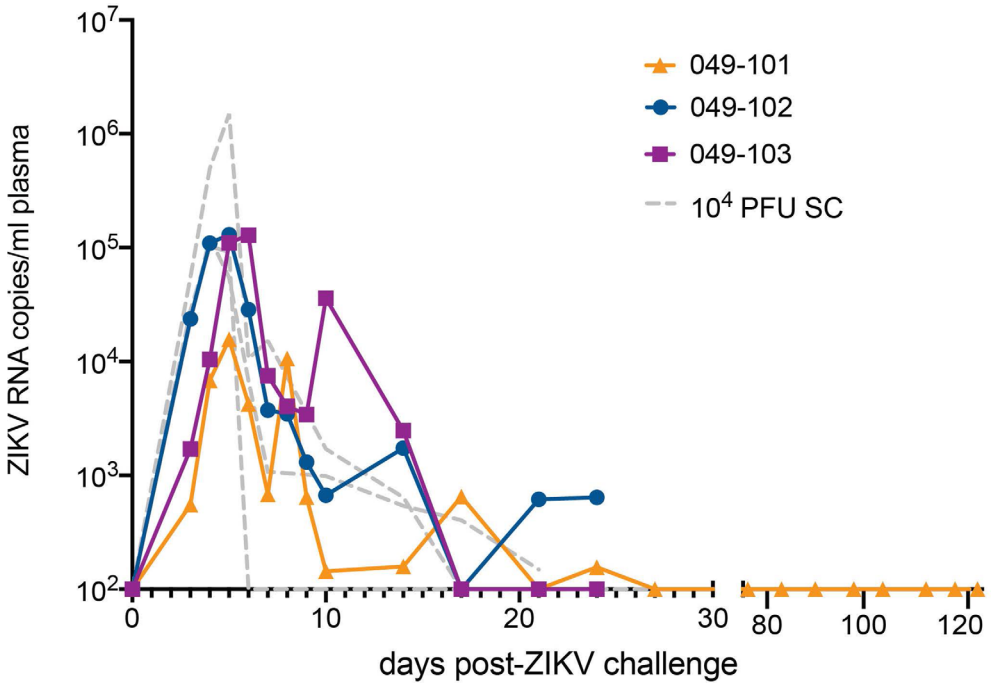

FIGURE 2 | Intravaginal ZIKV challenge resulted in detection of vRNA in plasma for all three dams. The x-axis shows days post-ZIKV challenge. The y-axis starts at the estimated limit of quantification of the qRT-PCR assay ($1x10^2$ copies/ml) and is shown as copies/ml plasma on the log scale. Plasma vRNA loads are displayed for dam 049-101 as orange triangles, for dam 049-102 as blue circles, and for dam 049-103 as magenta squares. For comparison, ZIKV plasma vRNA loads are also shown for three pregnant macaques subcutaneously (SC) inoculated with $1x10^4$ PFU ZIKV-DAK and are displayed as gray dashed lines and noted as 10^4 PFU SC in the legend (47).

fetal and MFI tissues following infection during pregnancy. For a number of tissues, multiple samples were collected for vRNA analysis but ZIKV was only detected in a subset of those samples (**Table 2**).

Changes in Placental Tissues Following Intravaginal ZIKV Infection Are Non-Specific

Histopathological assessments of the placentas of dams 049-102 and 049-103 following embryonic demise showed generalized, non-specific mild necrosis (**Table 4** and **Supplemental Figures 1–3**). In particular, the secondary placental disk from dam 049-102 showed intervillous hemorrhage and parenchymal ischemia (**Supplemental Figures 2A, B**). In addition, the decidua from dam 049-102 showed some evidence of minimal focal necrosis (**Supplemental Figure 2C**). Placentas from both dam 049-102 and dam 049-103 had minimal to mild multifocal villous mineralization. The secondary placental disk of dam 049-103 showed acute neutrophilic inflammation, mild focal ischemia, and hemorrhage (**Supplemental Figure 3B**). Similar to the placentas from the other two dams, the placenta of dam 049-101 showed mild, multifocal villous mineralization, findings which have previously been observed in control placentas. Focal hemorrhage of the primary placental disk basal plate was also noted for dam 049-101 (**Supplemental Figure 1A**). In addition, decidual tissue from dam 049-101 showed mild, multifocal muscularization of the decidual arteries (**Supplemental Figure 1B**). Overall, changes in the placental tissues were mild and not associated with any specific pathological processes. Assessment of fetal tissues from dam 049-101 showed normal brain and eye morphology with no identified lesions.

ZIKV Genomic RNA Is Detected in MFI Tissues From Demise Cases but Not From the Near-Term Pregnancy

Tissue sections from decidua, primary placental disks, and secondary placental disks (bidiscoid placentas) were assessed by ZIKV ISH using RNAscope (see *Methods*). ZIKV genomic RNA was detected in both the primary and secondary placental disks from dams 049-102 and 049-103 (**Figure 4**). No ZIKV RNA was detected by RNAscope in the primary placental disk from dam 049-101, nor any of the decidua sections from any of the pregnancies. The lack of ZIKV RNA in the decidua sections by ISH was consistent with the tissue vRNA assessment by qRT-PCR.

Animals Infected Intravaginally With ZIKV During Pregnancy Develop Neutralizing Antibodies

Serum neutralizing antibody titers (nAbs) against ZIKV were evaluated for dams 049-102 and 049-103 on days 0, 14, and 24

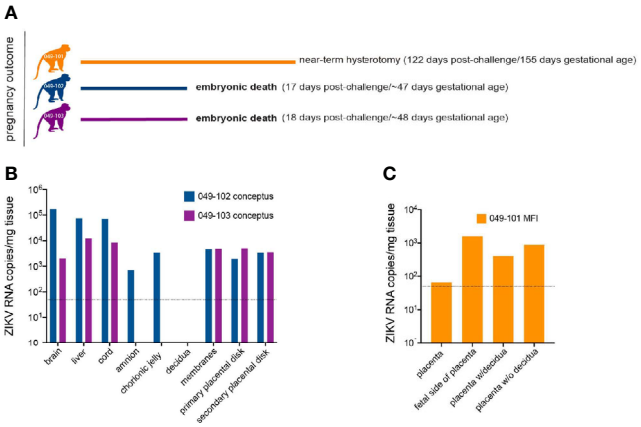

FIGURE 3 | Pregnancy outcomes and maternal-fetal interface (MFI) and fetal tissue vRNA loads. **(A)** Pregnancy outcomes for three dams intravaginally inoculated 3x with ZIKV at approximately 30 days gestation. Two dams (049-102 and 049-103) were determined by ultrasound to have nonviable embryos at approximately 17-18 days post-ZIKV challenge. Hysterotomies and embryo and MFI tissue collections were performed 3 days after detection. Dam 049-101's pregnancy continued until scheduled hysterotomy and extensive tissue collection at approximately 155 days gestational age. **(B)** Average ZIKV vRNA loads for positive embryo and MFI tissues collected at hysterotomy from dams 049-102 (blue) and 049-103 (magenta) following embryonic death at approximately 17-18 days post-ZIKV challenge. The dashed line represents the average of the estimated limit of detection (50-100 copies/mg, average: 75 copies/mg tissue) for the qRT-PCR assay. **(C)** Average ZIKV vRNA loads for positive MFI tissues collected at hysterotomy from dam 049-101 (orange) at approximately 122 days post-ZIKV infection. Fetal tissues were negative for ZIKV RNA by qRT-PCR. The dashed line represents the average of the estimated limit of detection (50-100 copies/mg, average: 75 copies/mg tissue) for the qRT-PCR assay.

TABLE 3 | 049-101 fetal and placental measurements (~155 days gestation, 122 days post challenge).

Tissue	Measure (mm)	Weight (g)
whole body	180.0	405.75
biparietal diameter	52.3	–
head circumference	186.0	–
r./l. femur	52.8/53.0	–
brain	–	54.42
cerebrum	–	50.2
cerebellum with midbrain	–	3.31
cerebellum without midbrain	–	2.47
r./l. eye	13.6/13.8	1.34/1.35
r./l. thyroid	–	0.07/0.07
thymus	–	1.42
spleen	–	0.58
liver	–	12.08
r./l. adrenal	–	0.12/0.17
r./l. kidney	–	1.00/0.99
lung lobes	–	8.76
r./l. testis	–	0.06/0.06
placenta	145.0 x 85.0	159.19

Measurements were considered to be within normal limits by ultrasound and gross assessment (40). R, right; L, left.

post-challenge by 90% plaque reduction neutralization tests ($PRNT_{90}$). Serum samples from 0, 14, 27, and 122 days post-challenge collected from dam 049-101 were similarly assessed. Samples collected on day 0 (pre-challenge) from all animals were negative for ZIKV nAbs. Neutralizing Ab titers above 1:10 are indicative of immunity against ZIKV. Serum collected on day 14 post-challenge from all animals neutralized ZIKV-DAK at levels considered protective by $PRNT_{90}$ (between 1:100 and 1:1000 for each animal). Serum collected on day 24 post-challenge from dams 049-102 and 049-103, and on day 27 post-challenge from dam 049-101 showed an increased neutralization response relative to baseline (day 0) and day 14 for each individual animal (**Figure 5**). By day 122 post-challenge, the ZIKV nAb response for animal 049-101 was lower than on days 14 or 27, but still demonstrated a strong protective response ($PRNT_{90}$ titer approximately 1:300) (**Figure 5**). These results suggest that all animals developed a nAb response against ZIKV following intravaginal ZIKV challenge consistent with findings previously noted for rhesus dams infected subcutaneously (42, 48, 49).

DISCUSSION

Here we describe a proof-of-concept study that indicates intravaginal challenge with ZIKV during early pregnancy results in productive maternal infection and suggests that infection by this route can result in embryonic demise. ZIKV RNA was detected at the MFI and in embryonic tissues, as well as in the amniotic fluid from the pregnancies of dams 049-102 and 049-103, supporting a role for ZIKV in the adverse pregnancy outcomes for these animals. Although ZIKV was detected by qRT-PCR in the MFI tissues from dam 049-101, no vRNA was detected in fetal tissues directly. Interestingly, although vRNA was detectable in the placenta of dam 049-101 by qRT-PCR, it was not detected by ISH. Given the focal nature of ZIKV RNA detected in the placental tissue samples collected from dam 049-101, it is likely that the samples evaluated by ISH were simply from areas without vRNA present (**Table 2**). In order to assess

TABLE 4 | Histopathological assessment of placental tissues from all animals and fetal tissues from 049-101.

Dam ID	Tissue	Findings
049-101	primary placental disk	focally extensive hemorrhage within the basal plate; mild multifocal villous mineralization
	decidua	mild multifocal persistent muscularization of decidual arteries
	fetal brain	no pathological changes
	fetal eye	no pathological changes
	fetal lung	mild bilateral diffuse intra-alveolar squamous cells, similar to control
049-102	primary placental disk	minimal multifocal villous mineralization
	secondary placental disk	intervillous hemorrhage and parenchymal ischemia with acute intervillous inflammation involving the lateral margin; not associated with specific pathologic process
	decidua	minimal focal necrosis
049-103	primary placental disk	mild multifocal mineralization of the anchoring villi
	secondary placental disk	mild focal parenchymal ischemia with coagulative necrosis and acute neutrophilic inflammation and mild multifocal villous mineralization
	decidua	minimal multifocal decidual necrosis with rare neutrophils

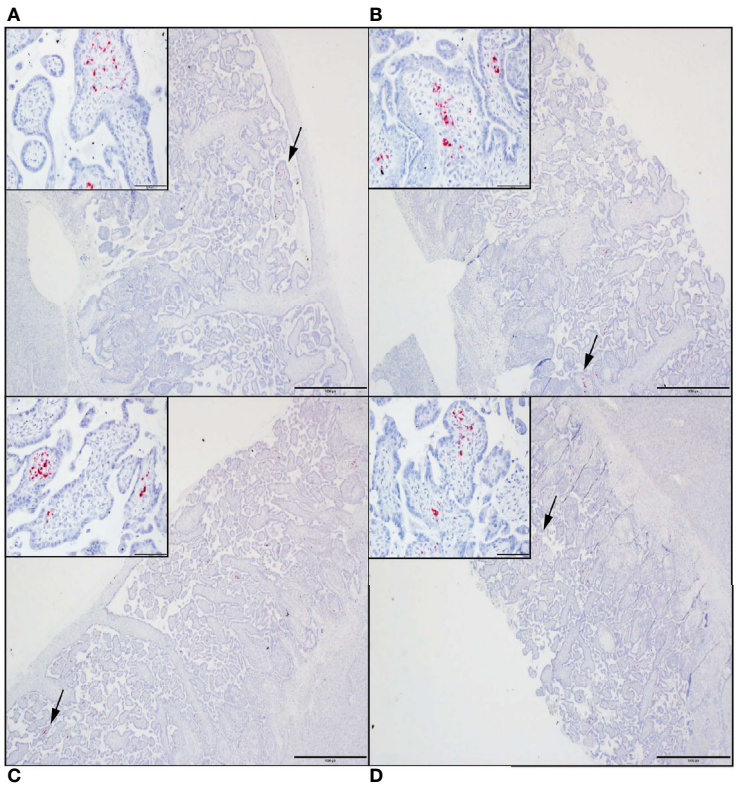

FIGURE 4 | ZIKV genomic RNA was detected by *in situ* hybridization (ISH) in placental tissues collected from dams 049-102 and 049-103, but not from dam 049-101. For all images, red coloration is indicative of positive staining for ZIKV genomic RNA. Overall, positive staining is focal but visible in multiple areas. Insets show high magnification of the areas denoted by the black arrows in each larger panel. Representative images are shown of **(A)** primary placental disk from 049-103, **(B)** secondary placental disk from 049-103, **(C)** primary placental disk from 049-102, and **(D)** secondary placental disk from 049-102. Scale bar = 1000 micrometers.

transmission in these studies we intentionally avoided any intrauterine sampling to ensure no confounding variables. Because vRNA was not detected in any fetal tissues, our results may suggest that vertical transmission did not occur between dam 049-101 and the developing fetus. Alternatively, the results may suggest immunologic elimination of virus at later gestational ages as previously suggested by a study using direct fetal ZIKV inoculation (43). Our decision to challenge the animals in this study early in pregnancy (~30 days gestation) was based on findings in humans suggesting that during the first trimester, ZIKV infection is associated with a higher risk of adverse fetal and pregnancy outcomes (27, 43, 50–53). In addition, we hypothesized that early pregnancy, possibly before a woman knows she is pregnant, may be a period of especially high risk for

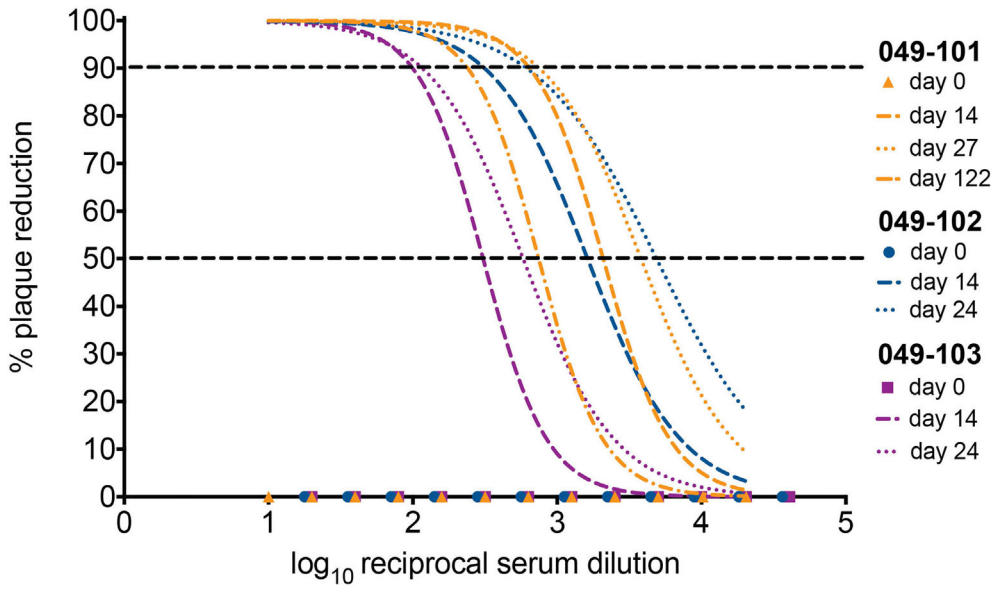

FIGURE 5 | All three dams developed neutralizing antibodies (nAbs) against ZIKV as detected by $PRNT_{90}$ following intravaginal ZIKV infection. The x-axis is the log10 reciprocal serum dilution and the y-axis is the percent plaque reduction for ZIKV-DAK. Day 0 for all animals is shown as symbols with 049-101 represented by orange triangles, 049-102 represented by blue circles, and 049-103 represented by magenta squares. Dashed gray horizontal lines indicate the $PRNT_{90}$ and $PRNT_{50}$ cut-offs, respectively. Neutralization curves were generated using non-linear regression to estimate the dilution of serum required to inhibit 90% of Vero cell culture infection. Neutralization curves are shown for days 14 (dashed lines) and 24 (dotted lines) for dams 049-102 (blue) and 049-103 (magenta), and for days 14, 27, and 122 (dashed and dotted line) for dam 049-101 (orange).

sexual transmission of ZIKV because precautions against this transmission route, such as condoms, may not be utilized (23, 24). Overall, our results suggest that sexual transmission of ZIKV during early pregnancy may represent a significant risk for adverse outcomes.

Our results indicating early demise as a result of ZIKV infection are consistent with those described previously in a cross-center, cross-NHP species study (29). Interestingly, our finding that 2 of 3 (~66%) pregnancies resulted in nonviable embryos following intravaginal ZIKV infection during early pregnancy represents a higher rate of loss than the ~26% previously reported for NHP (29). We acknowledge this loss rate is based on small animal numbers and could change as more animals are studied. Despite this higher rate compared to other NHP models reported to date, both early gestation and near term reflect periods of higher rates of spontaneous loss for macaques (54). While the loss rate reported in our study may be higher than the background rate of early loss in humans during the first trimester, data are very limited regarding the rate at which ZIKV-associated loss occurs in humans during the first trimester. A rate of approximately 11% was recently reported in a study during a period of epidemic transmission in Manaus, Brazil (55–58), although as noted, in many cases women may not be aware of an early pregnancy, thus the rate of loss could actually be higher. Additional studies with larger animal numbers will be necessary to determine the impact of the challenge dose, virus isolate, gestational age, and route of infection on pregnancy loss and how this relates to rates of spontaneous loss in early gestation.

Some limitations of this study include the use of a relatively high dose of ZIKV to inoculate the dams, the inclusion of multiple challenges over a short timeframe, and the small number of animals included in the study. The dose of inoculum chosen for this study is representative of the high end of the ZIKV vRNA range reportedly detected in human semen, which can be up to 100,000 times higher than that in blood (16–18). In part, this dose was chosen due to the small number of animals included, our interest in the impact of intravaginal ZIKV exposure early in pregnancy, and the need to maximize chances of successful infection during early gestation. Previous studies in nonpregnant NHP have shown that intravaginal ZIKV inoculation results in successful infection after a single challenge approximately 33-75 percent of the time (31, 37, 59). In pregnant olive baboons, a single intravaginal inoculation mid-gestation with semen containing ZIKV (originating from French Polynesia or Puerto Rico) resulted in 4 of 6 animals developing detectable vRNA in blood, with an additional animal having detectable vRNA in blood after a second inoculation (33). This was the rationale for the choice to perform repeat challenges at two-hour intervals in this study: in order to maximize the likelihood of establishing a productive infection in our small cohort within a single day. We acknowledge that it is difficult to determine whether the inoculation route played a significant role in our observed outcomes or whether the cumulative inoculum dose, virus isolate, timing of infection, or some combination of these factors played a role in the observed outcomes. Future studies

modeling sexual transmission should aim to determine which of these factors significantly impact pregnancy outcome.

We chose to utilize a low passage African ZIKV isolate (ZIKV-DAK) rather than a more contemporary isolate such as the commonly utilized PRVABC59 because, although it is also low passage, recent studies have suggested that this virus may have an attenuated phenotype and is not as pathogenic as ZIKV-DAK in mice (41, 60). In addition, ZIKV was first isolated from a febrile rhesus macaque in the Zika Forest near Entebbe, Uganda in 1947 (61, 62). Since that time, serologic and molecular (RNA or virus isolation) evidence of continued circulation in Africa has been intermittently reported in humans, animals, and mosquitoes (63–67). Prior to a report from Guinea-Bissau from 2016, during which an outbreak and subsequent identification of infant microcephaly cases was attributed to an African lineage virus, there were no reports of ZIKV impacting pregnancies and infant development in Africa (63, 68). This has led to a number of hypotheses as to why, which includes, but is not limited to the following: widespread immunity in populations of childbearing age due to infection earlier in life; masking of ZIKV-associated adverse outcomes due to a high number of other, co-circulating pathogens in many populations, such as malaria; or embryonic loss during very early pregnancy simply unrecognized due to unknown status or inconsistent access to prenatal care (63, 64, 69). The data generated in this work supports the latter hypothesis of early loss. In reality, depending on the region, many of these factors could be playing an additive role in low and/or underreporting of ZIKV-associated pregnancy outcomes in Africa. Whether the early pregnancy losses observed in our study were due to increased pathogenicity of the African ZIKV isolate utilized relative to other isolates, the intravaginal route of infection, or both will require additional studies.

Many key questions remain with regard to understanding how different ZIKV geographic isolates may differentially impact pregnancy and fetal developmental outcomes. This study suggests that NHP models may be able to differentiate pregnancy outcomes between different isolates. Route of maternal infection may also play a role in pregnancy outcomes, at least in the case of NHP, as intravenous and intra-amniotic ZIKV infections in combination during pregnancy have been associated with a trend toward lower fetal survival rates across multiple studies compared to subcutaneous infections (29). However, both routes of ZIKV infection have been previously shown to result in early pregnancy loss in macaques, in particular when maternal infection occurred in the first trimester (29). Zika virus infection of common marmoset dams *via* an intramuscular route during the first or second trimesters has also been shown to result in spontaneous pregnancy loss (70). In the case of the marmosets, the timing of pregnancy loss (16-18 days post-infection) was very similar to that reported here for intravaginal inoculation (70). Overall, our study suggests that intravaginal infection during early pregnancy may also lower survival rates in macaques. Ultimately, our study was designed to balance all of the potential influential factors previously mentioned within the constraints of a proof-of-concept study and the requirement for challenge and infection to occur during early pregnancy in order to evaluate this question.

Our results suggest that low passage, African lineage virus (ZIKV-DAK) has the potential to result in embryonic demise in rhesus macaques when infection occurs intravaginally and in early pregnancy. To our knowledge, this is the first NHP study to show clear evidence of vertical transmission of ZIKV following intravaginal infection, which has only previously been observed in mice (20, 30, 36). NHP, due to susceptibility without immune modulation, as well as having significant similarities to human pregnancy, may provide better approximations for human infections than other animal models (71). Furthermore, this is the first NHP study to show that African lineage ZIKV infection during pregnancy has the potential to result in severe fetal outcomes. Taken together, our results suggest that additional attention should be given to ongoing perinatal surveillance in African communities and to promoting awareness regarding the risks of sexual transmission of ZIKV in endemic areas.

DATA AVAILABILITY STATEMENT

The raw data supporting the conclusions of this article will be made available by the authors, without undue reservation.

ETHICS STATEMENT

The animal study was reviewed and approved by University of California, Davis Institutional Animal Care and Use Committee.

AUTHOR CONTRIBUTIONS

CN, AT, CM, and DHO designed the study. AT provided animal oversight and monitoring, ultrasound imaging, and performed all sample collections. AT and CM performed animal infections. AT, MM, MB, XZ, HS, TM, MA, EB analyzed samples. CN, DD, and JR curated data. CN and JR prepared the figures. CN prepared the initial manuscript draft. All authors contributed to the article and approved the submitted version.

FUNDING

DHHS/PHS/NIH R01 A|1116382-01A1, NIH P51 OD011107 and NIH S10 OD016261.

ACKNOWLEDGMENTS

We thank the research, animal care, and veterinary staff at the California National Primate Research Center for caring for the animals and supporting this study amid the emerging SARS-CoV-2 pandemic. We also thank DHHS/PHS/NIH for providing

the supplemental funding for R01 A1116382-01A1 that allowed this work to be completed. These studies were also supported by the California National Primate Research Center base operating grant #OD011107. *In vivo* imaging was performed with instrumentation funded by an NIH S10 grant #OD016261.

SUPPLEMENTARY MATERIAL

The Supplementary Material for this article can be found online at: https://www.frontiersin.org/articles/10.3389/fimmu.2021.686437/full#supplementary-material

REFERENCES

1. *Zika Cumulative Cases*. PAHO. Available at: https://www.paho.org/hq/index.php?option=com_content&view=article&id=12390:zika-cumulative-cases&Itemid=42090&lang=en (Accessed March 22, 2021).
2. Moore CA, Staples JE, Dobyns WB, Pessoa A, Ventura CV, Fonseca EB da, et al. Characterizing the Pattern of Anomalies in Congenital Zika Syndrome for Pediatric Clinicians. *JAMA Pediatr* (2017) 171:288–95. doi: 10.1001/jamapediatrics.2016.3982
3. van der Eijk AA, van Genderen PJ, Verdijk RM, Reusken CB, Mögling R, van Kampen JJA, et al. Miscarriage Associated With Zika Virus Infection. *N Engl J Med* (2016) 375:1002–4. doi: 10.1056/NEJMc1605898
4. Azevedo RSS, Araujo MT, Oliveira CS, Filho AJM, Nunes BTD, Henriques DF, et al. Zika Virus Epidemic in Brazil. II. Post-Mortem Analyses of Neonates With Microcephaly, Stillbirths, and Miscarriage. *J Clin Med Res* (2018) 7:496–508. doi: 10.3390/jcm7120496
5. Tabata T, Petitt M, Puerta-Guardo H, Michlmayr D, Wang C, Fang-Hoover J, et al. Zika Virus Targets Different Primary Human Placental Cells, Suggesting Two Routes for Vertical Transmission. *Cell Host Microbe* (2016) 20:155–66. doi: 10.1016/j.chom.2016.07.002
6. Gregory CJ, Oduyebo T, Brault AC, Brooks JT, Chung K-W, Hills S, et al. Modes of Transmission of Zika Virus. *J Infect Dis* (2017) 216:S875–83. doi: 10.1093/infdis/jix396
7. Counotte MJ, Kim CR, Wang J, Bernstein K, Deal CD, Broutet NJN, et al. Sexual Transmission of Zika Virus and Other Flaviviruses: A Living Systematic Review. *PloS Med* (2018) 15:e1002611. doi: 10.1371/journal.pmed.1002611
8. de Barros ACWG, Santos KG, Massad E, Coelho FC. Sex-Specific Asymmetrical Attack Rates in Combined Sexual-Vectorial Transmission Epidemics. *Microorganisms* (2019) 7:112–25. doi: 10.3390/microorganisms7040112
9. Foy BD, Kobylinski KC, Chilson Foy JL, Blitvich BJ, Travassos da Rosa A, Haddow AD, et al. Probable Non-Vector-Borne Transmission of Zika Virus, Colorado, USA. *Emerg Infect Dis* (2011) 17:880–2. doi: 10.3201/eid1705.101939
10. McCarthy M. Zika Virus was Transmitted by Sexual Contact in Texas, Health Officials Report. *BMJ* (2016) 352:i720. doi: 10.1136/bmj.i720
11. D'Ortenzio E, Matheron S, Yazdanpanah Y, de Lamballerie X, Hubert B, Piorkowski G, et al. Evidence of Sexual Transmission of Zika Virus. *N Engl J Med* (2016) 374:2195–8. doi: 10.1056/NEJMc1604449
12. Deckard DT, Chung WM, Brooks JT, Smith JC, Woldai S, Hennessey M, et al. Male-to-Male Sexual Transmission of Zika Virus–Texas, January 2016. *MMWR Morb Mortal Wkly Rep* (2016) 65:372–4. doi: 10.15585/mmwr.mm6514a3
13. Davidson A, Slavinski S, Komoto K, Rakeman J, Weiss D. Suspected Female-to-Male Sexual Transmission of Zika Virus - New York City, 2016. *MMWR Morb Mortal Wkly Rep* (2016) 65:716–7. doi: 10.15585/mmwr.mm6528e2
14. Yarrington CD, Hamer DH, Kuohung W, Lee-Parritz A. Congenital Zika Syndrome Arising From Sexual Transmission of Zika Virus, a Case Report. *Fertil Res Pract* (2019) 5:1. doi: 10.1186/s40738-018-0053-5
15. Turmel JM, Abgueguen P, Hubert B, Vandamme YM, Maquart M, Le Guillou-Guillemette H, et al. Late Sexual Transmission of Zika Virus Related to Persistence in the Semen. *Lancet* (2016) 387:2501. doi: 10.1016/S0140-6736(16)30775-9
16. Musso D, Richard V, Teissier A, Stone M, Lanteri MC, Latoni G, et al. Recipient Epidemiology and Donor Evaluation Study (Reds-III) ZIKV Study Group. Detection of Zika Virus RNA in Semen of Asymptomatic Blood Donors. *Clin Microbiol Infect* (2017) 23:1001.e1–3. doi: 10.1016/j.cmi.2017.07.006
17. Mead PS, Duggal NK, Hook SA, Delorey M, Fischer M, Olzenak McGuire D, et al. Zika Virus Shedding in Semen of Symptomatic Infected Men. *N Engl J Med* (2018) 378:1377–85. doi: 10.1056/NEJMoa1711038
18. Mansuy JM, Dutertre M, Mengelle C, Fourcade C, Marchou B, Delobel P, et al. Zika Virus: High Infectious Viral Load in Semen, a New Sexually Transmitted Pathogen? *Lancet Infect Dis* (2016) 16:405. doi: 10.1016/S1473-3099(16)00138-9
19. McDonald EM, Duggal NK, Brault AC. Pathogenesis and Sexual Transmission of Spondweni and Zika Viruses. *PloS Negl Trop Dis* (2017) 11:e0005990. doi: 10.1371/journal.pntd.0005990
20. Duggal NK, Ritter JM, Pestorius SE, Zaki SR, Davis BS, Chang G-JJ, et al. Frequent Zika Virus Sexual Transmission and Prolonged Viral RNA Shedding in an Immunodeficient Mouse Model. *Cell Rep* (2017) 18:1751–60. doi: 10.1016/j.celrep.2017.01.056
21. Rosenberg ES, Doyle K, Munoz-Jordan JL, Klein L, Adams L, Lozier M, et al. Prevalence and Incidence of Zika Virus Infection Among Household Contacts of Patients With Zika Virus Disease, Puerto Rico, 2016-2017. *J Infect Dis* (2019) 220:932–9. doi: 10.1093/infdis/jiy689
22. Racicot K, Cardenas I, Wünsche V, Aldo P, Guller S, Means RE, et al. Viral Infection of the Pregnant Cervix Predisposes to Ascending Bacterial Infection. *J Immunol* (2013) 191:934–41. doi: 10.4049/jimmunol.1300661
23. Teasdale CA, Abrams EJ, Chiasson MA, Justman J, Blanchard K, Jones HE. Sexual Risk and Intravaginal Practice Behavior Changes During Pregnancy. *Arch Sex Behav* (2017) 46:539–48. doi: 10.1007/s10508-016-0818-z
24. Salvesen von Essen B, Kortsmit K, Warner L, D'Angelo DV, Shulman HB, Virella WH, et al. Preventing Sexual Transmission of Zika Virus Infection During Pregnancy, Puerto Rico, USA, 20161. *Emerg Infect Dis* (2019) 25:2115–9. doi: 10.3201/eid2511.190915
25. Hoen B, Schaub B, Funk AL, Ardillon V, Boullard M, Cabié A, et al. Pregnancy Outcomes After ZIKV Infection in French Territories in the Americas. *N Engl J Med* (2018) 378:985–94. doi: 10.1056/NEJMoa1709481
26. Lin HZ, Tambyah PA, Yong EL, Biswas A, Chan S-Y. A Review of Zika Virus Infections in Pregnancy and Implications for Antenatal Care in Singapore. *Singapore Med J* (2017) 58:171–8. doi: 10.11622/smedj.2017026
27. Kleber de Oliveira W, Cortez-Escalante J, De Oliveira WTGH, do Carmo GMI, Henriques CMP, Coelho GE, et al. Increase in Reported Prevalence of Microcephaly in Infants Born to Women Living in Areas With Confirmed Zika Virus Transmission During the First Trimester of Pregnancy - Brazil, 2015. *MMWR Morb Mortal Wkly Rep* (2016) 65:242–7. doi: 10.15585/mmwr.mm6509e2
28. Pomar L, Malinger G, Benoist G, Carles G, Ville Y, Rousset D, et al. Association Between Zika Virus and Fetopathy: A Prospective Cohort Study in French Guiana. *Ultrasound Obstet Gynecol* (2017) 49:729–36. doi: 10.1002/uog.17404
29. Dudley DM, Van Rompay KK, Coffey LL, Ardeshir A, Keesler RI, Bliss-Moreau E, et al. Miscarriage and Stillbirth Following Maternal Zika Virus Infection in Nonhuman Primates. *Nat Med* (2018) 24:1104–7. doi: 10.1038/s41591-018-0088-5
30. Duggal NK, McDonald EM, Ritter JM, Brault AC. Sexual Transmission of Zika Virus Enhances In Utero Transmission in a Mouse Model. *Sci Rep* (2018) 8:4510. doi: 10.1038/s41598-018-22840-6
31. Haddow AD, Perez-Sautu U, Wiley MR, Miller LJ, Kimmel AE, Principe LM, et al. Modeling Mosquito-Borne and Sexual Transmission of Zika Virus in an Enzootic Host, the African Green Monkey. *PloS Negl Trop Dis* (2020) 14:e0008107. doi: 10.1371/journal.pntd.0008107
32. Schmidt JK, Mean KD, Puntney RC, Alexander ES, Sullivan R, Simmons HA, et al. Zika Virus in Rhesus Macaque Semen and Reproductive Tract Tissues: A Pilot Study of Acute Infection†. *Biol Reprod* (2020) 103:1030–42. doi: 10.1093/biolre/ioaa137
33. Gurung S, Nadeau H, Maxted M, Peregrine J, Reuter D, Norris A, et al. Maternal Zika Virus (Zikv) Infection Following Vaginal Inoculation With ZIKV-Infected Semen in Timed-Pregnant Olive Baboons. *J Virol* (2020) 94:1–16. doi: 10.1128/JVI.00058-20
34. Peregrine J, Gurung S, Lindgren MC, Husain S, Zavy MT, Myers DA, et al. Zika Virus Infection, Reproductive Organ Targeting, and Semen Transmission in the Male Olive Baboon. *J Virol* (2019) 94:1–16. doi: 10.1128/JVI.01434-19
35. Woollard SM, Olwenyi OA, Dutta D, Dave RS, Mathews S, Gorantla S, et al. Preliminary Studies on Immune Response and Viral Pathogenesis of Zika

Virus in Rhesus Macaques. *Pathogens* (2018) 7:70–81. doi: 10.3390/pathogens7030070
36. Winkler CW, Woods TA, Rosenke R, Scott DP, Best SM, Peterson KE. Sexual and Vertical Transmission of Zika Virus in Anti-Interferon Receptor-Treated Rag1-Deficient Mice. *Sci Rep* (2017) 7:7176. doi: 10.1038/s41598-017-07099-7
37. Carroll T, Lo M, Lanteri M, Dutra J, Zarbock K, Silveira P, et al. Zika Virus Preferentially Replicates in the Female Reproductive Tract After Vaginal Inoculation of Rhesus Macaques. *PloS Pathog* (2017) 13:e1006537. doi: 10.1371/journal.ppat.1006537
38. Tang WW, Young MP, Mamidi A, Regla-Nava JA, Kim K, Shresta S. A Mouse Model of Zika Virus Sexual Transmission and Vaginal Viral Replication. *Cell Rep* (2016) 17:3091–8. doi: 10.1016/j.celrep.2016.11.070
39. Yockey LJ, Varela L, Rakib T, Khoury-Hanold W, Fink SL, Stutz B, et al. Vaginal Exposure to Zika Virus During Pregnancy Leads to Fetal Brain Infection. *Cell* (2016) 166:1247–56.e4. doi: 10.1016/j.cell.2016.08.004
40. TA F. Ultrasound Imaging in Rhesus (*Macaca mulatta*) and Long-Tailed (*Macaca fascicularis*) Macaques: Reproductive and Research Applications. *Lab Primate* (2005), 317–52. doi: 10.1016/b978-012080261-6/50020-9
41. Jaeger AS, Murrieta RA, Goren LR, Crooks CM, Moriarty RV, Weiler AM, et al. Zika Viruses of African and Asian Lineages Cause Fetal Harm in a Mouse Model of Vertical Transmission. *PloS Negl Trop Dis* (2019) 13:e0007343. doi: 10.1371/journal.pntd.0007343
42. Dudley DM, Aliota MT, Mohr EL, Weiler AM, Lehrer-Brey G, Weisgrau KL, et al. A Rhesus Macaque Model of Asian-lineage Zika Virus Infection. *Nat Commun* (2016) 7:12204. doi: 10.1038/ncomms12204
43. Tarantal AF, Hartigan-O'Connor DJ, Penna E, Kreutz A, Martinez ML, Noctor SC. Fetal Rhesus Monkey First Trimester Zika Virus Infection Impacts Cortical Development in the Second and Third Trimesters. *Cereb Cortex* (2020) 31:2309–21. doi: 10.1093/cercor/bhaa336
44. Koenig MR, Razo E, Mitzey A, Newman CM, Dudley DM, Breitbach ME, et al. Quantitative Definition of Neurobehavior, Vision, Hearing and Brain Volumes in Macaques Congenitally Exposed to Zika Virus. *PloS One* (2020) 15:e0235877. doi: 10.1371/journal.pone.0235877
45. Breitbach ME, Newman CM, Dudley DM, Stewart LM, Aliota MT, Koenig MR, et al. Primary Infection With Dengue or Zika Virus Does Not Affect the Severity of Heterologous Secondary Infection in Macaques. *PloS Pathog* (2019) 15:e1007766. doi: 10.1371/journal.ppat.1007766
46. Lindsey HS, Calisher CH, Mathews JH. Serum Dilution Neutralization Test for California Group Virus Identification and Serology. *J Clin Microbiol* (1976) 4:503–10.
47. Crooks CM, Weiler AM, Rybarczyk SL, Bliss M, Jaeger AS, Murphy ME, et al. African-Lineage Zika Virus Replication Dynamics and Maternal-Fetal Interface Infection in Pregnant Rhesus Macaques. *Cold Spring Harbor Lab* (2020). doi: 10.1101/2020.11.30.405670
48. Nguyen SM, Antony KM, Dudley DM, Kohn S, Simmons HA, Wolfe B, et al. Highly Efficient Maternal-Fetal Zika Virus Transmission in Pregnant Rhesus Macaques. *PloS Pathog* (2017) 13:e1006378. doi: 10.1371/journal.ppat.1006378
49. Mohr EL, Block LN, Newman CM, Stewart LM, Koenig M, Semler M, et al. Ocular and Uteroplacental Pathology in a Macaque Pregnancy With Congenital Zika Virus Infection. *PloS One* (2018) 13:e0190617. doi: 10.1371/journal.pone.0190617
50. Honein MA, Dawson AL, Petersen EE, Jones AM, Lee EH, Yazdy MM, et al. Birth Defects Among Fetuses and Infants of US Women With Evidence of Possible Zika Virus Infection During Pregnancy. *JAMA* (2017) 317:59–68. doi: 10.1001/jama.2016.19006
51. Peña F, Pimentel R, Khosla S, Mehta SD, Brito MO. Zika Virus Epidemic in Pregnant Women, Dominican Republic, 2016-2017. *Emerg Infect Dis* (2019) 25:247–55. doi: 10.3201/eid2502.181054
52. Ospina ML, Tong VT, Gonzalez M, Valencia D, Mercado M, Gilboa SM, et al. Zika Virus Disease and Pregnancy Outcomes in Colombia. *N Engl J Med* (2020) 383:537–45. doi: 10.1056/NEJMoa1911023
53. Ades AE, Soriano-Arandes A, Alarcon A, Bonfante F, Thorne C, Peckham CS, et al. Vertical Transmission of Zika Virus and its Outcomes: A Bayesian Synthesis of Prospective Studies. *Lancet Infect Dis* (2020) 21:537–45. doi: 10.1016/S1473-3099(20)30432-1
54. Hendrie TA, Peterson PE, Short JJ, Tarantal AF, Rothgarn E, Hendrie MI, et al. Frequency of Prenatal Loss in a Macaque Breeding Colony. *Am J Primatol* (1996) 40:41–53. doi: 10.1002/(SICI)1098-2345(1996)40:1<41::AID-AJP3>3.0.CO;2-0
55. Brasil P, Pereira JP Jr, Moreira ME, Ribeiro Nogueira RM, Damasceno L, Wakimoto M, et al. Zika Virus Infection in Pregnant Women in Rio De Janeiro. *N Engl J Med* (2016) 375:2321–34. doi: 10.1056/NEJMoa1602412
56. Cohain JS, Buxbaum RE, Mankuta D. Spontaneous First Trimester Miscarriage Rates Per Woman Among Parous Women With 1 or More Pregnancies of 24 Weeks or More. *BMC Pregnancy Childbirth* (2017) 17:437. doi: 10.1186/s12884-017-1620-1
57. Redivo E de F, Bôtto Menezes C, da Costa Castilho M, Brock M, da Silva Magno E, Gomes Saraiva M das G, et al. Zika Virus Infection in a Cohort of Pregnant Women With Exanthematic Disease in Manaus, Brazilian Amazon. *Viruses* (2020) 12:1362–77. doi: 10.3390/v12121362
58. Oliver A, Overton C. Diagnosis and Management of Miscarriage. *Practitioner* (2014) 258:25–8.
59. Haddow AD, Nalca A, Rossi FD, Miller LJ, Wiley MR, Perez-Sautu U, et al. High Infection Rates for Adult Macaques After Intravaginal or Intrarectal Inoculation With Zika Virus. *Emerg Infect Dis* (2017) 23:1274–81. doi: 10.3201/eid2308.170036
60. Duggal NK, McDonald EM, Weger-Lucarelli J, Hawks SA, Ritter JM, Romo H, et al. Mutations Present in a Low-Passage Zika Virus Isolate Result in Attenuated Pathogenesis in Mice. *Virology* (2019) 530:19–26. doi: 10.1016/j.virol.2019.02.004
61. Dick GWA, Kitchen SF, Haddow AJ. Zika Virus. I. Isolations and Serological Specificity. *Trans R Soc Trop Med Hyg* (1952) 46:509–20. doi: 10.1016/0035-9203(52)90042-4
62. Dick GWA. Zika Virus. II. Pathogenicity and Physical Properties. *Trans R Soc Trop Med Hyg* (1952) 46:521–34. doi: 10.1016/0035-9203(52)90043-6
63. Nutt C, Adams P. Zika in Africa-the Invisible Epidemic? *Lancet* (2017) 389:1595–6. doi: 10.1016/S0140-6736(17)31051-6
64. Marchi S, Viviani S, Montomoli E, Tang Y, Boccuto A, Vicenti I, et al. Zika Virus in West Africa: A Seroepidemiological Study Between 2007 and 2012. *Viruses* (2020) 12:641–70. doi: 10.3390/v12060641
65. McCrae AW, Kirya BG. Yellow Fever and Zika Virus Epizootics and Enzootics in Uganda. *Trans R Soc Trop Med Hyg* (1982) 76:552–62. doi: 10.1016/0035-9203(82)90161-4
66. Dick GW. Epidemiological Notes on Some Viruses Isolated in Uganda; Yellow Fever, Rift Valley Fever, Bwamba Fever, West Nile, Mengo, Semliki Forest, Bunyamwera, Ntaya, Uganda S and Zika Viruses. *Trans R Soc Trop Med Hyg* (1953) 47:13–48. doi: 10.1016/0035-9203(53)90021-2
67. Kirya BG. A Yellow Fever Epizootic in Zika Forest, Uganda, During 1972: Part 1: Virus Isolation and Sentinel Monkeys. *Trans R Soc Trop Med Hyg* (1977) 71:254–60. doi: 10.1016/0035-9203(77)90020-7
68. Rosenstierne MW, Schaltz-Buchholzer F, Bruzadelli F, Có A, Cardoso P, Jørgensen CS, et al. Zika Virus Igg in Infants With Microcephaly, Guinea-Bissau, 2016. *Emerg Infect Dis* (2018) 24:948–50. doi: 10.3201/eid2405.180153
69. Sheridan MA, Yunusov D, Balaraman V, Alexenko AP, Yabe S, Verjovski-Almeida S, et al. Vulnerability of Primitive Human Placental Trophoblast to Zika Virus. *Proc Natl Acad Sci USA* (2017) 114:E1587–96. doi: 10.1073/pnas.1616097114
70. Seferovic M, Sánchez-San Martín C, Tardif SD, Rutherford J, Castro ECC, Li T, et al. Experimental Zika Virus Infection in the Pregnant Common Marmoset Induces Spontaneous Fetal Loss and Neurodevelopmental Abnormalities. *Sci Rep* (2018) 8:6851. doi: 10.1038/s41598-018-25205-1
71. Dudley DM, Aliota MT, Mohr EL, Newman CM, Golos TG, Friedrich TC, et al. Using Macaques to Address Critical Questions in Zika Virus Research. *Annu Rev Virol* (2019) 6:481–500. doi: 10.1146/annurev-virology-092818-015732

Conflict of Interest: The authors declare that the research was conducted in the absence of any commercial or financial relationships that could be construed as a potential conflict of interest.

frontiers in Immunology

ORIGINAL RESEARCH
published: 21 May 2021
doi: 10.3389/fimmu.2021.680246

ZIKV Disrupts Placental Ultrastructure and Drug Transporter Expression in Mice

Cherley Borba Vieira Andrade[1], Victoria Regina de Siqueira Monteiro[1], Sharton Vinicius Antunes Coelho[2], Hanailly Ribeiro Gomes[1], Ronny Paiva Campos Sousa[1], Veronica Muller de Oliveira Nascimento[1], Flavia Fonseca Bloise[1], Stephen Giles Matthews[3,4,5,6], Enrrico Bloise[7], Luciana Barros Arruda[2] and Tania Maria Ortiga-Carvalho[1]

[1] Institute of Biophysics Carlos Chagas Filho, Federal University of Rio de Janeiro, Rio de Janeiro, Brazil, [2] Institute of Microbiology Paulo de Góes, Federal University of Rio de Janeiro, Rio de Janeiro, Brazil, [3] Department of Physiology, Faculty of Medicine, University of Toronto, Toronto, ON, Canada, [4] Department of Obstetrics & Gynecology, Faculty of Medicine, University of Toronto, Toronto, ON, Canada, [5] Department of Medicine, Faculty of Medicine, University of Toronto, Toronto, ON, Canada, [6] Lunenfeld-Tanenbaum Research Institute, Mount Sinai Hospital, Toronto, ON, Canada, [7] Department of Morphology, Federal University of Minas Gerais, Belo Horizonte, Brazil

OPEN ACCESS

Edited by:
Abhay P. S. Rathore, Duke University, United States

Reviewed by:
Satoru Watanabe, Duke-NUS Medical School, Singapore
Ashley L. St. John, Duke-NUS Medical School, Singapore

***Correspondence:**
Tania Maria Ortiga-Carvalho
taniaort@biof.ufrj.br

Specialty section:
This article was submitted to Viral Immunology, a section of the journal Frontiers in Immunology

Received: *13 March 2021*
Accepted: *30 April 2021*
Published: *21 May 2021*

Citation:
Andrade CBV, Monteiro VRdS, Coelho SVA, Gomes HR, Sousa RPC, Nascimento VMdO, Bloise FF, Matthews SG, Bloise E, Arruda LB and Ortiga-Carvalho TM (2021) ZIKV Disrupts Placental Ultrastructure and Drug Transporter Expression in Mice. Front. Immunol. 12:680246. doi: 10.3389/fimmu.2021.680246

Congenital Zika virus (ZIKV) infection can induce fetal brain abnormalities. Here, we investigated whether maternal ZIKV infection affects placental physiology and metabolic transport potential and impacts the fetal outcome, regardless of viral presence in the fetus at term. Low (10^3 PFU-$ZIKV_{PE243}$; low ZIKV) and high ($5x10^7$ PFU-$ZIKV_{PE243}$; high ZIKV) virus titers were injected into immunocompetent (ICompetent C57BL/6) and immunocompromised (ICompromised A129) mice at gestational day (GD) 12.5 for tissue collection at GD18.5 (term). High ZIKV elicited fetal death rates of 66% and 100%, whereas low ZIKV induced fetal death rates of 0% and 60% in C57BL/6 and A129 dams, respectively. All surviving fetuses exhibited intrauterine growth restriction (IUGR) and decreased placental efficiency. High-ZIKV infection in C57BL/6 and A129 mice resulted in virus detection in maternal spleens and placenta, but only A129 fetuses presented virus RNA in the brain. Nevertheless, pregnancies in both strains produced fetuses with decreased head sizes ($p<0.05$). Low-ZIKV-A129 dams had higher IL-6 and CXCL1 levels ($p<0.05$), and their placentas showed increased CCL-2 and CXCL-1 contents ($p<0.05$). In contrast, low-ZIKV-C57BL/6 dams had an elevated CCL2 serum level and increased type I and II IFN expression in the placenta. Notably, less abundant microvilli and mitochondrial degeneration were evidenced in the placental labyrinth zone (Lz) of ICompromised and high-ZIKV-ICompetent mice but not in low-ZIKV-C57BL/6 mice. In addition, decreased placental expression of the drug transporters P-glycoprotein (P-gp) and breast cancer resistance protein (Bcrp) and the lipid transporter Abca1 was detected in all ZIKV-infected groups, but Bcrp and Abca1 were only reduced in ICompromised and high-ZIKV ICompetent mice. Our data indicate that gestational ZIKV infection triggers specific proinflammatory responses and affects placental turnover and

transporter expression in a manner dependent on virus concentration and maternal immune status. Placental damage may impair proper fetal-maternal exchange function and fetal growth/survival, likely contributing to congenital Zika syndrome.

Keywords: ZIKV, placenta, P-glycoprotein (P-gp) breast cancer resistance protein (BCRP), ABCA1, ABCG1, ultrastructure, cytokine, chemokine 2

INTRODUCTION

Congenital Zika virus (ZIKV) infection can be associated with adverse pregnancy outcomes. Neonates born from ZIKV-positive pregnancies may develop severe neurological abnormalities, placental pathologies and intrauterine growth restriction (IUGR), among other complications (1). ZIKV vertical transmission has become a major public health issue worldwide, especially in Brazil, where more than 200,000 ZIKV-positive cases have been confirmed and over 2,000 congenital microcephaly births have been reported (2–6). These numbers represent a 20-fold rise in the incidence of congenital microcephaly in Brazil during the years of the ZIKV pandemic, with similar increases reported elsewhere in Latin America (2, 3, 7). Importantly, while the ZIKV pandemic is currently thought to be controlled, evidence points to a possible silent ZIKV spread across the Americas (8, 9), highlighting the need for improved knowledge of the possible routes of vertical ZIKV transmission and its association with disruptive inflammatory and developmental phenotypes and the need for new avenues of prevention and treatment.

Previous studies have investigated the possible pathways involved in vertical ZIKV transmission. Miranda and colleagues (10) showed that in humans, ZIKV infection changed the pattern of tight junction proteins, such as claudin-4, in syncytiotrophoblasts. Jurado et al. (2016) suggested that the migratory activities of Hofbauer cells (feto-placental macrophages) could help disseminate ZIKV to the fetal brain (11). Other recent studies have shown that placental villous fibroblasts, cytotrophoblasts, endothelial cells and Hofbauer cells are permissive to ZIKV, and placentae from ZIKV-infected women had chorionic villi with a high mean diameter (11–14). Furthermore, in 2019, Rathore et al. demonstrated that pregnant mice carrying high levels of antibodies against dengue virus (DENV) exhibited increased ZIKV vertical transmission associated with severe microcephaly-like syndrome, demonstrating another possible mechanism of antibody-dependent vertical ZIKV transmission (15). However, at present, further studies are required to identify the precise mechanism of maternal-fetal ZIKV transmission.

Many mouse models have been developed to identify how ZIKV overcomes placental defenses. Initially, limited information was obtained due to the apparent inability of the virus to infect wild-type (WT) mice (16). ZIKV NS5 targets the interferon signaling pathway in humans but not in mice (17). Thus, WT mice show no clear evidence of clinical disease (17, 18) and are of limited use in modeling the disease. However, mice lacking an interferon signaling response show evidence of disease and have been widely used to investigate ZIKV infection during pregnancy (8, 17, 19).

The interferon system, especially type III interferon, is a key mechanism of host defense and a viral target for immune evasion (20). Type III interferons have a role in protection against ZIKV infection in human syncytiotrophoblasts from term placenta (21). Luo et al. have shown that inhibition of Toll-like receptors 3 and 8 inhibits the cytokine output of ZIKV-infected trophoblasts (22). In addition, viral replication coincides with the induction of proinflammatory cytokines, such as interleukin [IL]-6. This cytokine has a crucial role in inflammation and affects the homeostatic processes related to tissue injury and activation of stress-related responses (23, 24). ZIKV infection can trigger an inflammatory response with IL-6 release (11, 25).

Maternal infection has profound effects on placental permeability to drugs and environmental toxins. Changes in the expression and function of specific ABC transporters in the placenta and yolk sac following infective and inflammatory stimuli have been demonstrated (26–30). ABC transporters are efflux transporters that control the biodistribution of several endogenous and exogenous substrates, including xenobiotics (antiretrovirals and synthetic glucocorticoids), steroid hormones (estrogens and androgens), nutrients (folate and cholesterol) and immunological factors (chemokines and cytokines) within the maternal-fetal interface (31). The best described ABC transporters in the placenta are P-glycoprotein (P-gp; also known as multidrug resistance protein 1, MDR1), breast cancer resistance protein (Bcrp) and the lipid Abca1 and Abcg1 transporters. P-gp and Bcrp transporters are responsible for preventing fetal accumulation of xenobiotics and environmental toxins that may be present in the maternal circulation, whereas Abca1 and Abcg1 control the placental exchange of cytotoxic oxysterol and lipid permeability throughout pregnancy; therefore, they play an important role in fetal protection and placental lipid homeostasis (26).

Despite the limited number of studies showing ZIKV infection in immunocompetent mice, intrauterine inoculation with a high virus titer was previously demonstrated to result in decreased fetal viability, with worse outcomes following infection in early gestation (32). In another report, intravenous infection on a very early embryonic day resulted in fetal demise even though the virus was not found in the fetal compartment in most of the treated animals (33). In the present study, we hypothesize that maternal exposure to ZIKV affects placental function, including placental ultrastructure and ABC transporter (P-gp, Bcrp, Abca1 and Abcg1) protein expression, even in the absence of vertical transmission and that these effects are dependent on viral infective titers and maternal immune status.

MATERIALS AND METHODS

Virus Preparation and Storage

The Brazilian $ZIKV_{PE243}$ (GenBank ref. number KX197192) strain was isolated from a febrile case during the ZIKV outbreak in the state of Pernambuco, Brazil and was kindly provided by Dr Ernesto T. Marques Jr. (Centro de Pesquisa Aggeu Magalhães, FIOCRUZ, PE). Viruses were propagated in C6/36 cells, and viral titers were determined by plaque assays in Vero cells, as previously described (34). Supernatants of noninfected C6/36 cells cultured under the same conditions were used as mock controls.

Animal Experimentation and Study Design

Two mouse strains were used in the study: immunocompetent (ICompetent) C57BL/6 and immunocompromised (ICompromised) (type 1 *Ifnr*-deficient) A129 strains. Since we were unable to consistently produce viable pregnancies by mating A129 males and females in our experimental settings, we mated A129 females (n=15) with C57BL/6 males (n=4) to produce ICompromised C57BL6/A129 pregnancies, whereas ICompetent C57BL/6 pregnancies were obtained by mating male (n=6) and female (n=35) C57BL/6 mice (8-10 weeks old). Animals were kept in a controlled temperature room (23°C) with a light/dark cycle of 12 hours and *ad libitum* access to water and food. After detection of the proestrous/estrous phase *via* vaginal cytology, copulation was confirmed by visualization of the vaginal plug and considered gestational day 0.5 (GD0.5). Maternal weight was monitored for confirmation of pregnancy; thus, females were weighed on GD0.5 and GD12.5, and females with a weight gain greater than 3 g were considered pregnant and entered randomly in the experimental groups. Experimental protocols were approved by the Animal Care Committee of the Health Sciences Center, Federal University of Rio de Janeiro (CEUA-036/16 and 104/16) and registered with the Brazilian National Council for Animal Experimentation Control.

On GD12.5, pregnant mice (ICompetent and ICompromised pregnancies) were injected with a single intravenous (i.v.) titer of ZIKV or mock control. ICompetent and ICompromised pregnant mice were randomly subdivided into three experimental groups: the mock (control) group, which received an injection of supernatant from noninfected C6/36 cells (ICompetent mock and ICompromised mock); the high-ZIKV-titer group, inoculated with $5x10^7$ plaque-forming units (PFU) of $ZIKV_{PE243}$ (ICompetent high and ICompromised high); and the ZIKV low-titer group, injected with 10^3 PFU of $ZIKV_{PE243}$ (ICompetent low and ICompromised low).

On the morning of GD18.5, all animals were euthanized with a sodium phenobarbital overdose of 300 mg/kg. Maternal blood was collected *via* cardiac puncture, centrifuged (10 min, 4000 g) and stored at -20°C. The maternal brain and spleen and all placentae and all fetuses were dissected, collected and weighed, followed by fetal head isolation and measurement. The three placentae closest to the mean weight in a litter were selected for further analysis and cut in half using umbilical cord insertion as a reference (35–37). One-half of the placental disk was frozen in liquid nitrogen for qPCR, and the other half was fixed overnight in buffered paraformaldehyde (4%, Sigma-Aldrich, Brazil) for ultrastructural and protein expression/localization analysis. Matched fetal heads, maternal brains and spleens were frozen in liquid nitrogen for qPCR. Of important note, all fetuses obtained from ICompromised pregnancies were heterozygous.

ZIKV RNA Quantification *via* RT-qPCR

ZIKV load was evaluated in maternal blood, brains and spleens and in the placentae and fetal heads. Brains, spleens, placentae and fetal heads were macerated in RPMI medium (Gibco™ RPMI 1640 Medium) normalized by the ratio of 0.2 mg of tissue to every 1 µl of medium and plotted per gram of tissue. The macerated volume was centrifuged at 4500 g for 5 min to remove tissue residues, and then, 500 µl of the centrifuged volume was used for RNA extraction using 1 mL of TRIzol reagent (Life Technologies, Thermo Fischer, USA). Treatment with DNase I (Ambion, Thermo Fischer, USA) was performed to prevent contamination by genomic DNA. cDNA was synthesized using a cDNA High Capacity Kit (Applied Biosystems, Thermo Fischer, USA) according to the manufacturer's instructions by subjecting the samples to the following cycle: 25°C for 10 min, 37°C for 120 min and 85°C for 5 min. qPCR was performed using a StepOnePlus Real-Time qPCR system, TaqMan Master Mix Reagents (Applied Biosystems, Thermo Fischer, USA) and primers and probes specific for the protein E sequence (38). Samples were then subjected to the following cycle: 50°C for 2 min, followed by 40 cycles of 95°C for 10 min, 95°C for 15 sec, and 60°C for 1 min.

RT-qPCR

The placenta was macerated in 1.5 mL of TRIzol reagent (Life Technologies, Thermo Fischer, USA). RNA extraction was performed following the manufacturer's protocol. cDNA was prepared using High Capacity cDNA Reverse Transcription Kit (Applied Biosystems, CA, USA). The reaction was carried out for selected genes using intron-spanning primers (**Table 1**) and the StepOnePlus Real-Time PCR system (Life Technologies, Thermo Fischer, USA). Samples were subjected to the following cycle: 95°C for 10 min, followed by 40 amplification cycles consisting of DNA denaturation for 30 sec at 95°C and annealing of primers for 30 sec at 60°C. The threshold cycle (Ct) was determined for each gene of interest and for the reference genes glycerol 3-phosphate dehydrogenase (*Gapdh*) and RNA Polymerase II Subunit A (*Polr2a)*. The relative expression of each gene was calculated using $2^{-\Delta\Delta CT}$ (39) and graphically expressed as the fold-increase. The efficiency was calculated using the standard curve method. The melting curves were analyzed for each sample.

Detection of Cytokines and Chemokines In Maternal Serum and the Placenta

Initially, placental tissue was homogenized in extraction buffer (50 mM Tris, 150 mM NaCl, 1X Triton, 0.1% SDS, 5 mM EDTA, 5 mM NaF, 50 mM sodium pyrophosphate, 1 mM sodium

TABLE 1 | Primer sequences for the real-time PCR assay.

Gene	Primer sequences	GenBank accession no.
ZIKV	5'CCGCTGCCCAACACAAG3' 5'CCACTAACGTTCTTTTGCAGACAT3'	
Il6	5'TCATATCTTCAACCAAGAGGTA3' 5'CAGTGAGGAATGTCCACAAACTG3'	NM_031168.2
Il1b	5'GTAATGAAAGACGGCACACC3' 5'ATTAGAAACAGTCCAGCCCA3'	XM_006498795.4
Il10	5'TAAGGGTTACTTGGGTTGCCAAG3' 5'CAAATGCTCCTTGATTTCTGGGC3'	NM_010548.2
Ifng	5'AGCAACAGCAAGGCGAAAA3' 5'CTGGACCTGTGGGTTGTTGA3'	NM_008337.4
Ifn1	5'CTGGAGCAGCTGAATGGAAAG3' 5'CTTGAAGTCCGCCCTGTAGGT3'	NM_010510.1
Gapdh	5'CTTTGTCAAGCTCATTTCCTGG3' 5'TCTTGCTCAGTGTCCTTGC3'	XM_017321385.2
Tnf	5'CCTCACACTCAGATCATCTTCTCA3' 5'TGGTTCTCTTTGAGATCCATGC3'	NM_013693.3
Polr2a	5'TCTGCCAAGAATGTGACGCT3' 5'CCAAGCGGCAAAGAATGTCC3'	NM_001291068.1

orthovanadate, pH 7.4) containing complete protease inhibitor cocktail (Roche Applied Science, Germany) with TissueLyser LT (Qiagen, Germany). The protein concentration of each sample was analyzed using a Pierce™ BCA Protein Assay Kit (Thermo Scientific, USA) according to the manufacturer's instructions. Analysis of the cytokines IL-6 and IL-1β and the chemokines monocyte chemoattractant protein-1 (MCP-1/CCL2) and chemokine (C-X-C motif) ligand 1 (CXCL1) in maternal serum and placenta was performed with MILLIPLEX MAP Mouse Cytokine/Chemokine Magnetic Bead Panel – Immunology Multiplex Assays (MCYTOMAG-70K, Merck Millipore, Germany) following the manufacturer's recommendations. The plate with samples and magnetic beads was analyzed on a MAGPIX® System (Merck Millipore, Germany). The analyses were performed using Luminex xPonent® for MAGPIX® v software. 4.2 (Luminex Corp., USA). For each reaction well, the MAGPIX Luminex® platform reports the median fluorescence intensity (MFI) for each of the analytes in the sample. The levels of each analyte were then calculated against the standard curve. The ratio between the value obtained and the protein quantification for each sample was determined and plotted.

Virus Titration by Plaque Assay

Blood from mock- and $ZIKV_{PE243}$-infected mice was collected from the base of the tail at 4 hours, 48 hours and 144 hours following the appropriate treatments and subsequently centrifuged at 400 g for 30 min for plasma separation. Samples obtained at different periods post infection were titrated using a plaque assay. Vero cells (obtained from ATCC® CCL81™) (African green monkey kidney epithelial cell line) were plated in 24-well plates at $4x10^4$ cells per well in Dulbecco's modified Eagle's medium (DMEM) (GIBCO, Thermo Fisher, USA) supplemented with 5% fetal bovine serum (FBS) (GIBCO, Thermo Fisher, USA) and 1% gentamicin (10 μg/ml) (GIBCO, Thermo Fisher, USA) and cultured overnight for complete adhesion at 37°C with 5% CO_2. Then, the medium was removed, and the cells were washed with 1x PBS and incubated with serial (base 10) dilutions of virus in FBS-free medium. After 90 min of incubation under gentle shaking, the medium was removed, and the cells were washed with 1x PBS and cultured with 1.5% carboxymethylcellulose (CMC) supplemented with 1% FBS (GIBCO, Thermo Fisher, USA). After 5 days, the cells were fixed overnight with 4% formaldehyde and stained with 1% crystal violet in 20% methanol (ISOFAR, Brazil) for 1 hour. Plaques were counted, and the virus yield was calculated and expressed as plaque-forming units per milliliter (PFU/ml).

Histological, Immunohistochemistry, and TUNEL Analyses of the Placenta

Placental fragments were fixed overnight and subjected to dehydration (increasing ethanol series; ISOFAR, Brazil), diaphanization with xylol (ISOFAR, Brazil) and paraffin (Histopar, Easypath, Brazil). Sections (5 μm) were prepared using a Rotatory Microtome CUT 5062 (Slee Medical GmbH, Germany) and subjected to immunohistochemistry and TUNEL analyses.

For immunohistochemistry, blocking of endogenous peroxidase was performed with 3% hydrogen peroxide diluted in PBS, followed by microwave antigenic recovery in Tris-EDTA (pH=9) and sodium citrate (pH=6) buffers (15 min for Tris-EDTA buffer and 8 min for citrate buffer). Sections were washed in PBS + 0.2% Tween and exposed to 3% PBS/BSA for 1 hour. Sections were then incubated overnight at 4°C with the following primary antibodies: anti-Ki-67 (1:100 – [M3064]; Spring Bioscience, USA), anti-P-gp (1:500 – Mdr1[sc-55510]; Santa Cruz Biotechnology, USA), anti-Bcrp (1:100 – Bcrp [MAB4146]; Merck Millipore, USA), anti-Abcg1 (1:100 – [PA5-13462]; Thermo Fisher Scientific, USA) or anti-Abca1 (1:100 – [ab18180]; Abcam Plc, UK). The next day, sections were incubated with the biotin-conjugated secondary antibody SPD-060 (Spring Bioscience, USA) for 1 hour at room temperature. Three washes were performed with PBS + 0.2% Tween followed by incubation with streptavidin (SPD-060 - Spring Bioscience, USA) for 30 min. Sections were stained with 3,3-diamino-benzidine (DAB) (SPD-060 - Spring Bioscience, USA), counterstained with hematoxylin (Proquímios, Brazil), dehydrated, diaphanized and mounted with a coverslip and Entellan (Merck, Germany).

For analysis of apoptotic nuclei, terminal deoxynucleotidyl transferase dUTP nick-end labeling (TUNEL) staining was performed using an ApopTag® In Situ Peroxidase Detection Kit (S7100, Merck Millipore, USA) according to the manufacturer's recommendations and as previously described (36). All negative controls were prepared with omission of the primary antibody.

Image acquisition was performed using a high-resolution Olympus DP72 (Olympus Corporation, Japan) camera coupled

to an Olympus BX53 light microscope (Olympus Corporation, Japan). For nuclear quantification of Ki-67 and TUNEL immunolabeling, Stepanizer software (40) was used. For this analysis, we evaluated 15 images from different random fields of the Lz (labyrinth zone) and Jz (junctional zone) for each animal, in a total of five animals from each ICompetent group and three animals from each ICompromised group. A total of 360 digital images (40X) randomly captured per placental region (180 Lz imagens and 180 Jz images) were evaluated in each experimental group. The total number of immunolabeled Ki-67 or TUNEL nuclei in each digital image was normalized by the total image area to obtain an index of the estimated number of proliferative and apoptotic nuclei in the entire histological section analyzed. Analysis was undertaken by two investigators blinded to the treatment.

Quantification of P-gp, Bcrp, Abca1 and Abcg1 staining was performed using the Image-Pro Plus, version 5.0 software (Media Cybernetics, USA) mask tool. The percentage of viable tissue area was considered upon exclusion of negative spaces. A total of 360 digital images (40X) randomly captured per placental region (180 Lz imagens and 180 Jz images) were evaluated in each experimental group. Analysis was undertaken by two investigators blinded to the treatment.

Transmission Electron Microscopy (TEM)

Sections of the placental Lz and Jz were fixed in paraformaldehyde 4% (Sigma-Aldrich, Brazil) for 48 hours, postfixed with osmium tetroxide (Electron Microscopy Sciences, USA) and potassium ferrocyanide (Electron Microscopy Sciences, USA) for 60 min and dehydrated with an increasing series of acetone (30%, 50%, 70%, 90% and two of 100%) (ISOFAR, Brazil). Sections were subsequently embedded with EPOXI resin (Electron Microscopy Sciences, USA) in acetone (1:2, 1:1 and 2:1, respectively) followed by EPOXI pure resin. After polymerization, ultrafine sections (70 nm) were prepared (Leica Microsystems, USA) and collected into 300 mesh copper grids (Electron Microscopy Sciences, USA). Tissue was contrasted with uranyl acetate and lead citrate and visualized using a JEOL JEM-1011 transmission electron microscope (JEOL, Ltd., Akishima, Tokyo, Japan). Digital micrographs were captured using an ORIUS CCD digital camera (Gatan, Inc., Pleasanton, California, EUA) at 6000× magnification. An overall qualitative analysis of the Lz and Jz in different groups was performed by investigating the ultrastructural characteristics of the mitochondria and the ER cisterns. The qualitative evaluation consisted of analyzing disruption of the mitochondrial membranes, mitochondrial morphology, preservation of mitochondrial cristae and matrix intensity (41). Ultrastructural analysis of nuclear morphology and the presence of microvilli in trophoblast sinusoidal giant cells was also undertaken. Analysis of ER cisterns was performed by evaluating the dilation of their lumen (42).

Statistical Analysis

GraphPad Prism 8 software (GraphPad Software, Inc., USA) was used for statistical analysis. A D'Agostino & Pearson normality test was used to evaluate normal distribution, and outliers were identified using a Grubbs test. The data are expressed as the mean ± SEM or individual values. One-way ANOVA followed by Tukey's posttest was used for comparisons between different inbred groups, whereas Student's t-test or a nonparametric Mann-Whitney test was performed to compare the outbred groups. Differences were considered significant when $p<0.05$. Pregnancy parameters were evaluated using the mean value of all fetuses and placentae in a litter per dam and not the individual conceptus, i.e., the mean value. In **Figures 1**, **2**, "n" represents the number of dams. For MET and immunostaining data, placentae closest to the mean weight of all placentae were selected from each litter; "n" represents the number of litters (35–37).

RESULTS

Weight Gain During Pregnancy Is Dependent on Maternal Immune Status in ZIKV-Infected Mice

To determine the effect of ZIKV infection on fetal and placental phenotypes at term (GD18.5), we infected Immunocompetent (ICompetent) C57BL/6 and immunocompromised (ICompromised) A129 mice with ZIKV at GD12.5 (**Figure 1A**). Given the very distinct susceptibility of C57BL/6 and A129 mice to ZIKV, systemic infection models were established by injecting high ($5x10^7$ PFU) and low (10^3 PFU) virus inoculum titers. As shown in **Figure 1B**, ICompetent C57BL/6 mice in all groups and ICompromised A129 dams inoculated with mock and low ZIKV titers exhibited higher maternal weight at GD18.5 than at GD12.5 and GD0.5 ($p<0.05$). On the other hand, ICompromised A129 mice presented significant weight loss at GD18.5, despite showing an increase at GD12.5 in relation to GD0.5 (**Figure 1B**).

Immunocompetent and Immunocompromised Mice Have Distinct Term Placental and Fetal Phenotypes in Response to High and Low ZIKV Titer Challenges in Mid-Pregnancy

The fetuses from C57BL/6 dams and sires were called ICompetent. The fetuses from the mating of A129 dams and C57BL/6 sires were called ICompromised. High-ZIKV ICompetent mice exhibited 34% fetal loss, whereas high-ZIKV-A129 mice had 100% fetal loss (**Figure 1C**). In the low-ZIKV groups, C57BL/6 mice had no (0%) fetal death, while A129 mice exhibited a 42% fetal death rate (**Figure 1C**). Fetal and fetal head sizes were decreased in A129 mice compared to those in C57BL/6 dams infected with the high ZIKV titer ($p=0.05$; **Figures 1D–G**). However, no changes in fetal weight or fetal head size were observed when the mice were infected with the low ZIKV titer (**Figures 1D–G**).

ZIKV Is Detected in the Fetal Brain of ICompromised, but Not ICompetent Mice

ZIKV RNA was detected in the spleens of pregnant ICompetent C57BL/6 mice inoculated with the highest ZIKV titer, confirming acute systemic infection. Viral RNA was also detected in the majority of the placentae of those mice (**Figures 2A, B**) but not in the maternal and fetal C57BL/6 brains (**Figures 2A, B**), suggesting

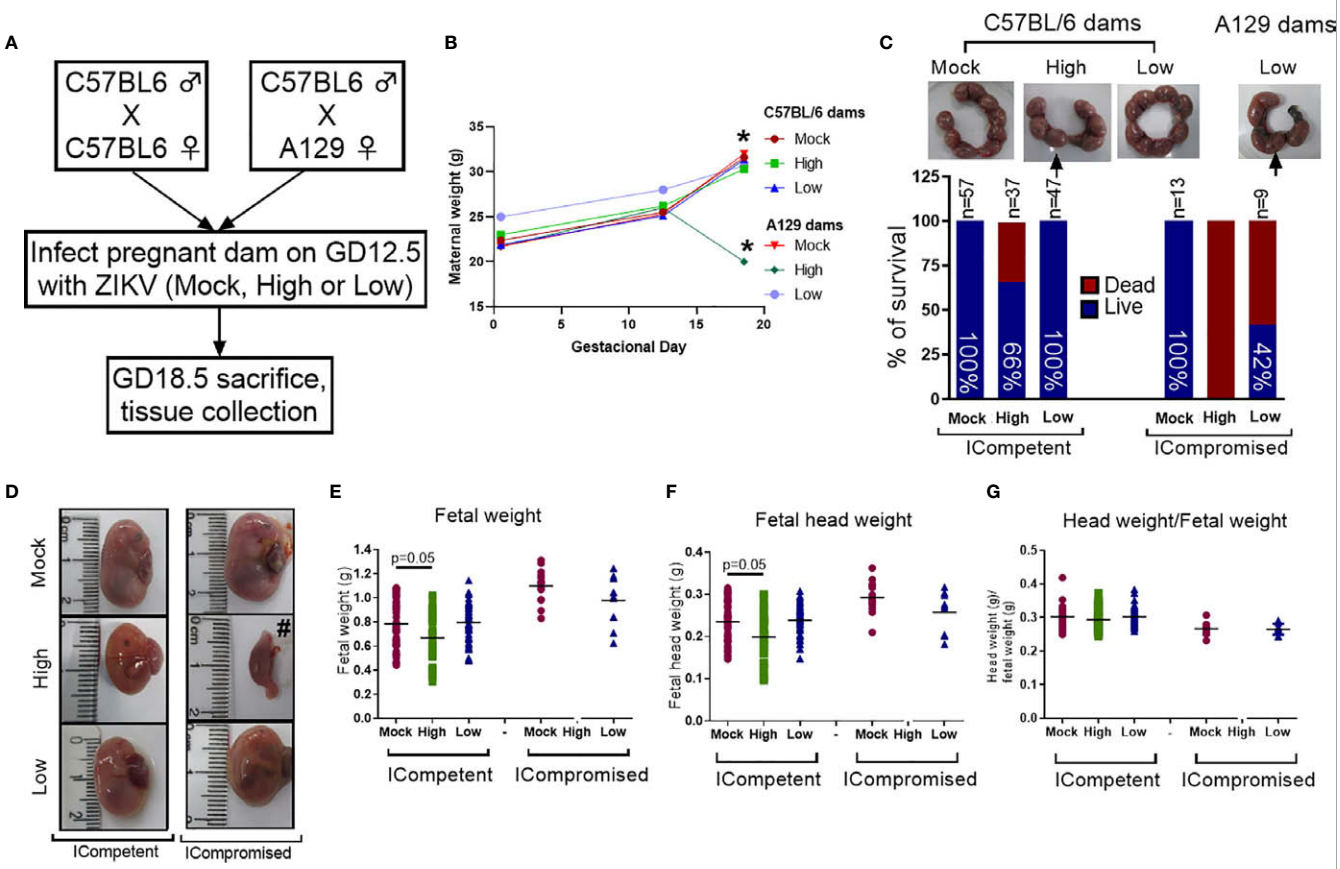

FIGURE 1 | ZIKV infection induced fetal changes during pregnancy. **(A)** Experimental design: matings of C57BL/6 dams x C57BL/6 sires (mock n=11 dams; high ZIKV n=15 dams; low ZIKV n=9 dams) and A129 dams x C57BL/6 sires (n=3 dams/group). The mock control consisted of noninfected C6/36 cell supernatants; high ZIKV titers consisted of $5x10^7$ plaque-forming units (PFU) of $ZIKV_{PE243}$, and low ZIKV titers consisted of 10^3 PFU of $ZIKV_{PE243}$. Fetuses from C57BL/6 dams and sires were termed ICompetent, whereas fetuses from A129 dams and C57BL/6 sires were termed ICompromised. **(B)** Maternal weight gain throughout pregnancy. **(C)** Uterine horn and survival rates following ZIKV exposure (arrows show resorption sites). **(D)** Fetal/reabsorption images (#=example of fetal reabsorption). **(E)** Fetal weight, **(F)** fetal head weight and **(G)** fetal head weight/fetal weight ratio. One-way ANOVA followed by Tukey's posttest was used to assess changes among ICompetent groups, whereas an unpaired Student's t-test or nonparametric Mann-Whitney test was used to assess differences between ICompromised groups. Values are the mean of individual plotted values. *p < 0.05, one-way ANOVA.

that the virus was not transmitted to the fetuses. In contrast, ZIKV RNA was detected in all analyzed organs from ICompromised A129 dams, including the maternal brain and spleen and the placenta and fetal brain (**Figures 2A, B**). Viremia in maternal plasma was evaluated at 4, 48 and 144 hours after infection. Within 4 hours, the presence of the virus was verified in the serum (high ICompetent=637.5 PFU/mL, low ICompetent=740 PFU/mL and low ICompromised=325 PFU/mL), indicating that the virus was correctly inoculated. Afterwards, ZIKV RNA was detected in ICompromised dams at 48 and 144 hours post inoculation but not in ICompetent dams (**Figure 2C**).

ZIKV Infection Induces Distinct Systemic and Placental Inflammatory Responses in ICompetent and ICompromised Mice

The maternal serum and placental protein levels of specific cytokines and chemokines related to fetal death and preterm delivery (43–45) were evaluated to probe whether midgestation ZIKV infection would induce a maternal inflammatory response at term in our two distinct models. Since A129 infected with $5x10^7$ ZIKV-PFU showed 100% fetal loss, we proceeded using $5x10^7$ PFU inoculation in C57BL/6 mice and 10^3 PFU inoculation in both C57BL/6 and A129 mice.

CCL2 was elevated in the serum of low-ZIKV ICompetent mice, but no other alteration was systemically detected in any ICompetent mice at this time point (**Figures 3A, B**). On the other hand, ICompromised dams showed significantly increased CXCL1 and IL-6 levels in the serum and a strong trend for an enhancement in CCL2 (**Figure 3C**). Analysis of cytokine and chemokine expression in the placenta demonstrated that the CXCL1 and CCL2 chemokines were also upregulated in ICompromised but not ICompetent mice (**Figures 3D–F**). Surprisingly, IL-6 protein expression was augmented in the placenta of some of the low-ZIKV ICompetent mice (58%;

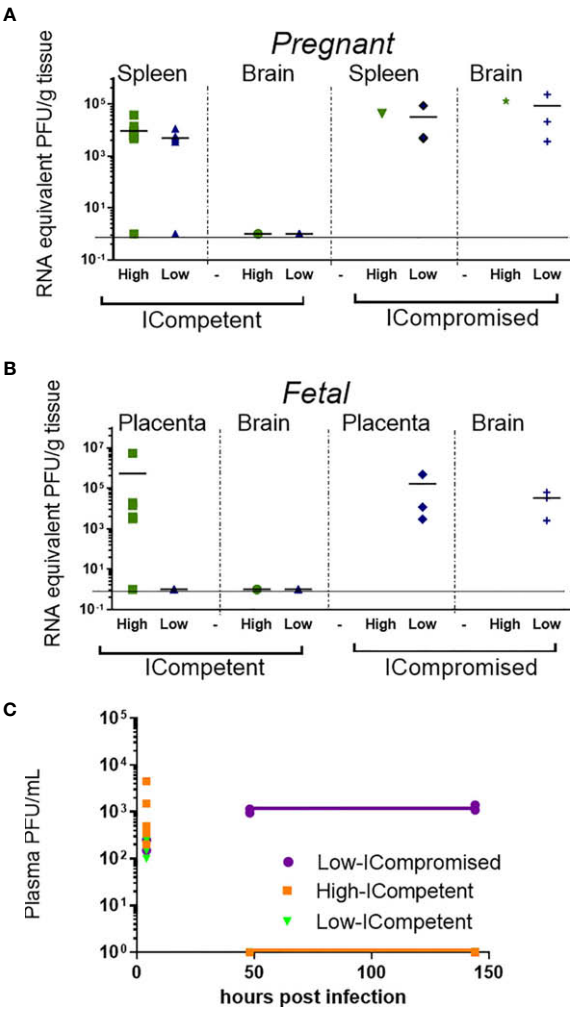

FIGURE 2 | Viral load detection in maternal and fetal tissues after ZIKV infection. Pregnant ICompetent and ICompromised mice were inoculated i.v. with low and high doses of ZIKV. **(A, B)** ZIKV RNA was measured *via* RT-qPCR in tissue samples obtained from maternal spleen and brain **(A)** and from placenta and fetal brain **(B)**. **(C)** The presence of ZIKV infectious particles in the plasma of infected dams was evaluated with a plaque assay 4, 48, and 144 hours post infection in ICompetent (mock n=11 dams; high ZIKV n=15 dams; low ZIKV n=9 dams) and ICompromised (mock n=3 dams; high ZIKV n=3 dams; low ZIKV n=3 dams) mice.

p<0.05) but not in high-ZIKV mice or ICompromised mice (**Figures 3D–F**).

We also assessed the placental mRNA expression of a range of cytokines related to placental infective responses: *Ifng, Il6, Ifn1, Tnf, Il1b* and *Il10*. All the infected mice showed a significant increase in *Tnf* mRNA expression, with higher levels detected in ICompetent mice (**Figures 3G-I**). The low-ZIKV ICompetent mice presented modest but significant *Ifn1* expression, which was not detected in the high-ZIKV group (**Figure 3G**). Additionally, both low-ZIKV-infected groups (ICompetent and ICompromised) presented increased *Ifng* mRNA expression (**Figures 3G, I**, p< 0.05). Interestingly, placental *Il6* mRNA levels were only elevated in ICompromised pregnancies compared to mock pregnancies (p=0.05) (**Figure 3I**). *Il1b* and *Il10* remained unchanged in all groups analyzed (**Figures 3G–I**).

ZIKV Affects Placental Proliferation and Apoptosis in a Viral Load- and Maternal Immune Status-Dependent Manner

We did not observe changes in placental weight or in the fetal: placental weight ratio in any of the groups investigated (data not shown). However, since we detected the presence of ZIKV RNA in the placentas, we investigated the cellular proliferation (Ki-67$^+$ cells) and apoptotic ratio in the Lz and Jz of the mouse placenta. Increased Ki-67 staining was observed in the Lz of high- and low-ZIKV-treated ICompetent animals compared to mock animals (**Figures 4A–D**, p=0.005 and p=0.015), whereas the apoptotic ratio in the Lz was increased in high-ZIKV dams and decreased in low-ZIKV dams (p=0.01, **Figures 4E–H**). Although no differences were observed in Ki67 staining (**Figures 5A-D**), a similar apoptotic pattern was detected in the Jz of ICompetent pregnancies (p=0.008 and p=0.004, respectively; **Figures 5E–H**). In contrast, in ICompromised dams, Lz Ki-67 staining was decreased (p=0.001; **Figures 4I–L**), while the apoptotic reaction was increased in ZIKV-infected animals (p=0.05; **Figures 4M–P**). Jz from ICompromised offspring exhibited increased Ki-67 labeling and no differences in the apoptotic reaction (p=0.001; **Figures 5I–P**).

Placental Ultrastructure Is Differently Impacted by High- and Low-Titer ZIKV Infection in ICompetent and ICompromised Trocaria Strains of Mice

Lz ultrastructural analyses of ICompetent and ICompromised-mock animals detected sinusoidal trophoblastic giant cells exhibiting regular microvilli, euchromatic nuclei, preserved mitochondrial ultrastructure and regular narrow ER cisternae (**Figures 6A, B**). In sharp contrast, high-ZIKV ICompetent (**Figure 6C**) infected placentae showed fewer villi in the sinusoidal giant trophoblastic cells, degenerated mitochondria, granular ER with dilated cisterns and euchromatic nuclei. The sinusoidal giant trophoblastic cells in the low-ZIKV ICompetent mice (**Figure 6D**) also had fewer villi and degenerated mitochondria than those in the mock placentae, but no effect on the ER or euchromatic nuclei observed. Low-ZIKV ICompromised infected placentae (**Figure 6E**) showed fewer villi in the sinusoidal giant trophoblastic cells, degenerated mitochondria, granular ER with dilated cisterns and euchromatic nuclei.

The Jz of mock ICompetent and ICompromised placentae (**Figures 7A, B**) exhibited euchromatic nuclei, with evident heterochromatin, preserved mitochondria and narrow cisternae in a granular ER. High-ZIKV ICompetent Jz had degenerated mitochondria, granular ER with dilated cisterns and euchromatic nuclei (**Figure 7C**). Low-ZIKV ICompetent (**Figure 7D**) placentae exhibited euchromatic nuclei with evident heterochromatin, preserved mitochondria and narrow cisternae in a granular ER, whereas low-ZIKV ICompromised placentae

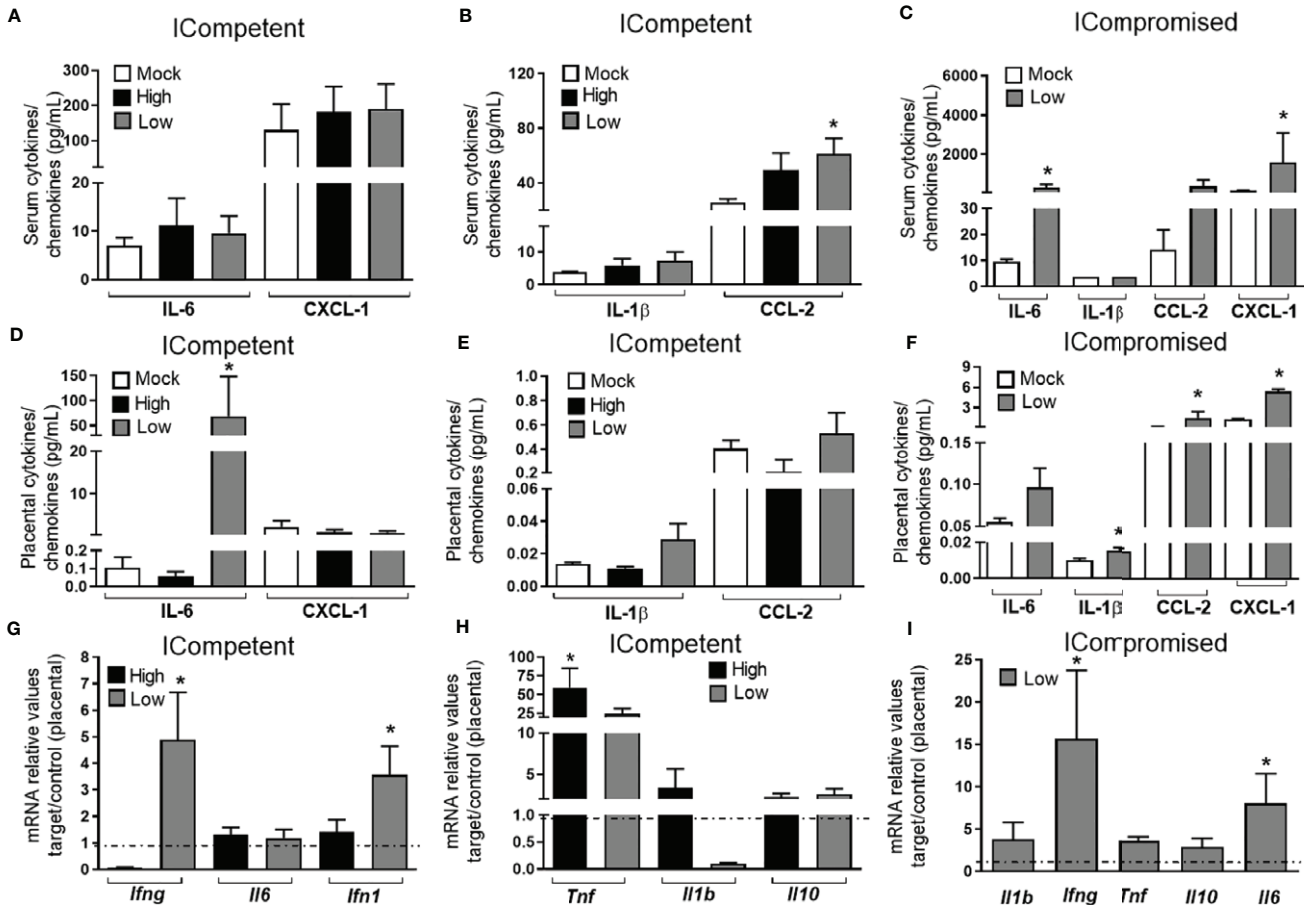

FIGURE 3 | ZIKV during pregnancy promotes an inflammatory response in the maternal serum and in the placenta. Levels of IL-1β, IL-6, CCL-2 and CXCL-1 in the maternal serum **(A–C)** and placenta **(D–F)** at GD18.5 in matings of C57BL/6 dams x C57BL/6 sires (ICompetent fetuses - mock n=11 dams; high ZIKV n=15 dams; low ZIKV n=9 dams) and A129 dams x C57BL/6 sires (ICompromised fetuses n=3 dams/group). Placental mRNA expression **(G–I)** of *Ifng*, *Ifn1, Il1b, Il6, Il10* and *Tnf*. Broken lines show the expression levels in both lineages in the mock group. One-way ANOVA followed by Tukey's posttest was used to assess changes among ICompetent groups, whereas an unpaired Student's t-test or nonparametric Mann-Whitney test was used to assess differences between ICompromised groups. The values are expressed as the mean ± SEM. *P < 0.05.

had degenerated mitochondria, granular ER with dilated cisterns and euchromatic nuclei (**Figure 7E**).

ZIKV Differentially Affects Placental Expression of Drug and Lipid ABC Transporter Systems

Evaluation of key ABC transporters in the Lz of mock and ZIKV-infected ICompetent and ICompromised placentae revealed that immunolabeling of the drug P-gp and Bcrp efflux transporter systems was primarily present at the cellular membranes of the sinusoidal trophoblastic giant cells, with diffuse cytoplasmic Bcrp staining. Labeling of the Abca1 and Abcg1 lipid efflux transporters was moderately and heterogeneously distributed within the Lz. Less Lz-P-gp was observed in ICompetent mice infected with both high- and low-ZIKV infective regimens than in mock-treated animals (p=0.001 and p=0.002, respectively; **Figures 8A–E**), whereas reduced Bcrp and Abca1 staining was observed in high-ZIKV-infected mice (p=0.003 and p=0.004, **Figures 8F–J** and **8K–O**, respectively). No changes in Abcg1 were observed in any of the ICompetent experimental groups (**Figures 8P–T**). P-gp, Bcrp and Abca1 transporter immunostaining was downregulated in ICompromised low ZIKV-treated animals (p=0.001, p=0.05 and p=0.05, **Figures 9A–D**, **9E–H** and **9I–L**, respectively). No changes in Abcg1 were observed in any of the ICompromised experimental groups (**Figures 9M–P**).

Next, the impact of ZIKV on ABC transporters in the Jz layer (structural and endocrine layers of the mouse placenta) was assessed. P-gp and Bcrp were predominantly localized at the cellular membranes of spongiotrophoblast cells, whereas Abca1 and Abcg1 exhibited membrane and cytoplasmic staining. P-gp staining was decreased in Jz cells from the low-ZIKV ICompromised placentae (p=0.006), with no other alterations observed (**Figures 10A–T**, **11A–P**).

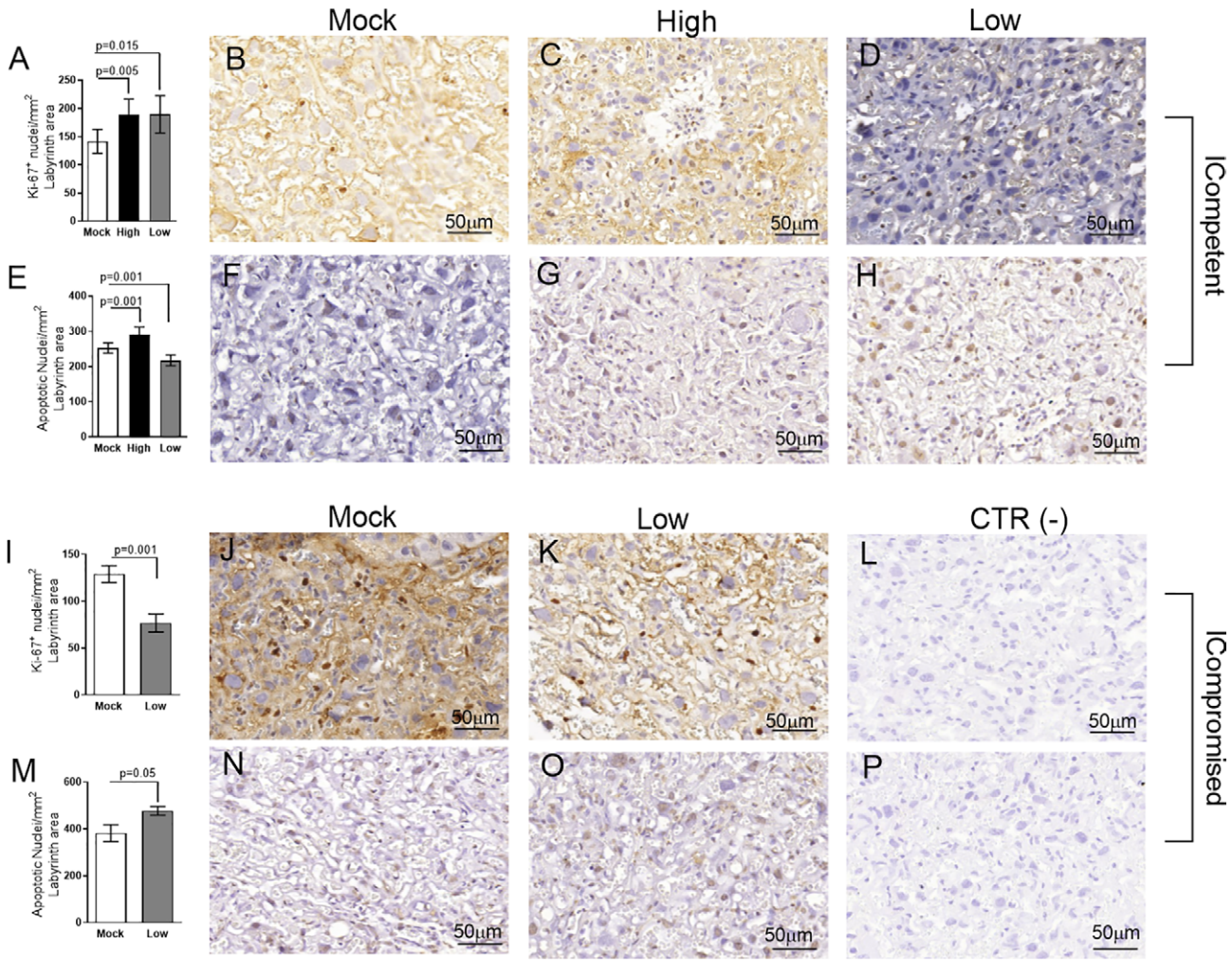

FIGURE 4 | Labyrinthine remodeling in ICompetent and ICompromised placentae is affected by gestational ZIKV infection. A total of 180 digital images (40X) randomly captured from the whole labyrinth zone (Lz) of each placenta per dam were evaluated. Immunolabeled nuclei from each digital image were quantified and normalized by the total digital image area to obtain an index of the estimated number of proliferative and apoptotic nuclei in the entire histological section. **(A, I)** Quantification and **(B–D, J, K)** representative photomicrographs of Ki-67^{+} stained nuclei in the Lz of ICompetent (n=6 placentae from 6 independent dams/group) and ICompromised (n=3 placentae from 3 independent dams/group) placentae, respectively. **(E, M)** Quantification and **(F–H, N, O)** representative photomicrographs of apoptotic nuclei (TUNEL) in the Lz of ICompetent (n=5 placentae from 5 independent dams/group) and ICompromised (n=3 placentae from 3 independent dams/group) placentae, respectively. **(L, P)** Negative controls. One-way ANOVA followed by Tukey's posttest was used to assess changes among ICompetent groups, whereas an unpaired Student's t-test or nonparametric Mann-Whitney test was used to assess differences between ICompromised groups. The values are expressed as the mean ± SEM. Images were captured at 40X. Scale bar=50 μm.

DISCUSSION

In this study, we investigated several fetal and placental features at term (GD18.5) in ICompetent (C57BL/6) and ICompromised (A129) females exposed to ZIKV at mid-pregnancy (GD12.5). Fetal survival rates, systemic and placental inflammatory responses, placental ultrastructure and cell turnover, as well as the expression of key drug (P-gp and Bcrp) and lipid (Abca1) efflux transporter systems in the placenta, were consistently impacted by ZIKV in both strains. The magnitude of the effects was clearly related to the infective titer (high and low) of ZIKV and maternal immune status (ICompetent-C57BL/6 x and ICompromised-A129), and fetal alterations were not exclusively dependent on virus detection in the fetuses.

Infection of ICompetent mice with ZIKV did not result in viremia in the initial postinoculation phase, although viral RNA was detected in the maternal spleen in both the high- and low-ZIKV groups, confirming systemic infection. This is consistent with a previous report (46). Our data demonstrate that pregnant ICompetent C57BL/6 mice were more susceptible to high ZIKV titers than to low ZIKV infective. Since viral RNA was only detected in the placentae of high ZIKV-infected mice, fetal survival rates and weights were impacted to a greater extent in those mice. Strikingly, even though the virus was not present in

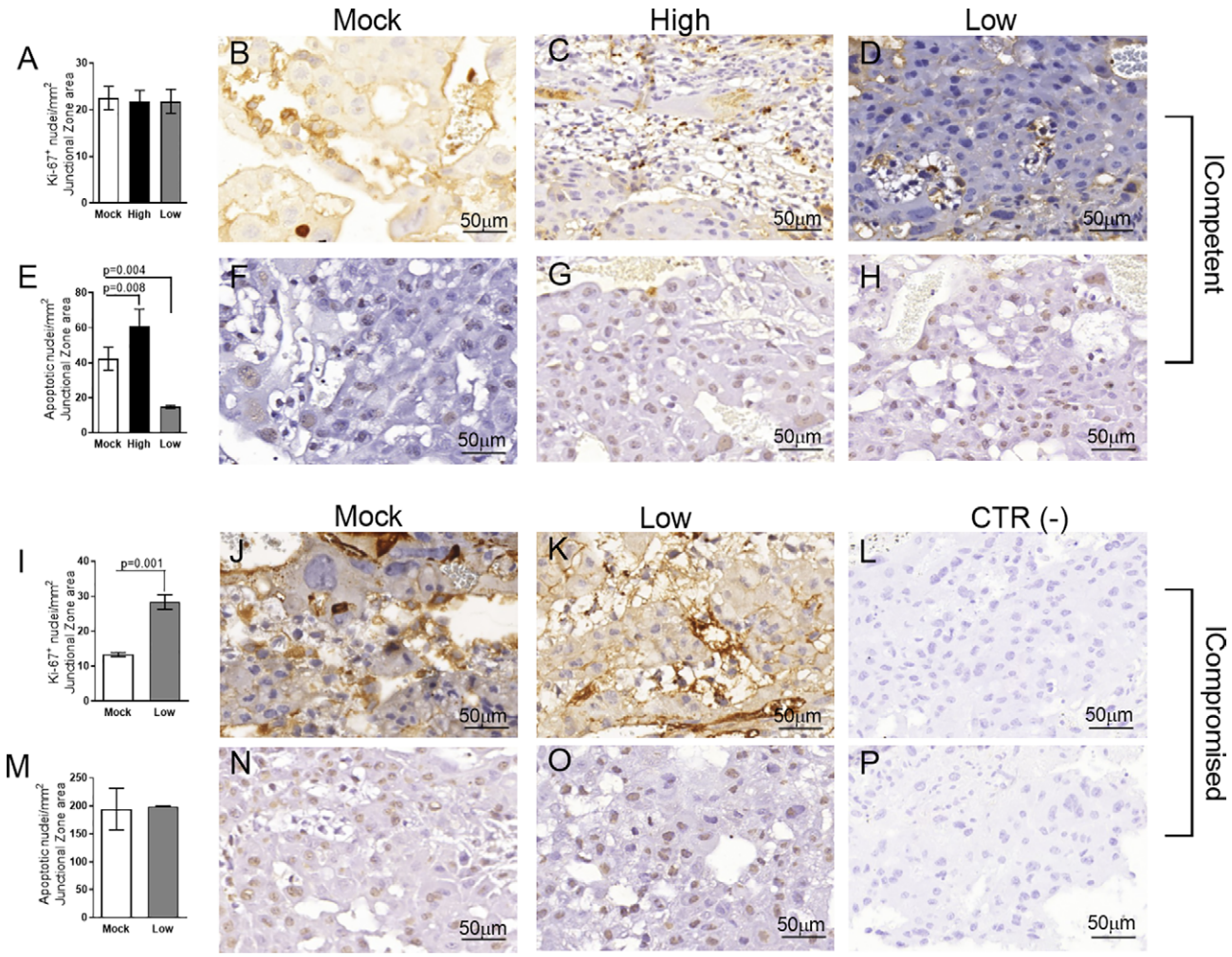

FIGURE 5 | Junctional zone remodeling in ICompetent and ICompromised placentae is affected by gestational ZIKV infection. A total of 180 digital images (40X) randomly captured from the whole junctional zone (Jz) of each placenta per dam were evaluated. Immunolabeled nuclei from each digital image were quantified and normalized by the total digital image area to obtain an index of the estimated number of proliferative and apoptotic nuclei in the entire histological section. **(A, I)** Quantification and **(B–D, J, K)** representative photomicrographs of Ki-67^{+} stained nuclei in the Jz of ICompetent (n=6 placentae from 6 independent dams/group) and ICompromised (n=3 placentae from 3 independent dams/group) placentae, respectively. **(E, M)** Quantification and **(F–H, N, O)** representative photomicrographs of apoptotic nuclei (TUNEL) in the Jz of ICompetent (n=5 placentae from 5 independent dams/group) and ICompromised (n=3 placentae from 3 independent dams/group) placentae, respectively. **(L, P)** Negative controls. One-way ANOVA followed by Tukey's posttest was used to assess changes among ICompetent groups, whereas an unpaired Student's t-test or nonparametric Mann-Whitney test was used to assess differences between ICompromised groups. The values are expressed as the mean ± SEM. Images were captured at 40X. Scale bar = 50 μm.

the fetal brain (at least at term), fetal and fetal head weights were lower in mice subjected to the high-ZIKV titer regimen, suggesting that high infective viral load in mid-pregnancy, even in ICompetent individuals, can induce IUGR and lower fetal head weight despite a lack of transmission to the fetal brain (47). On the other hand, ICompromised placentae and fetal brains had detectable viral transcripts, with no changes in weight, which is consistent with previous data (19). In fact, in our models, the presence (ICompromised) or absence (ICompetent) of the virus in the fetal brain did not correspond to fetal head size (decreased in only high ICompetent). The data from ICompetent and ICompromised placentae demonstrate how important the maternal immunological status is to control viremia, fetal survival and accessibility of the virus to the fetal brain. The reason for the reduction in fetal brain size in C57BL/6 mice in the absence of fetal brain infection requires further investigation. It is possible that fetal brains in the ICompetent mice may have been exposed to ZIKV earlier in pregnancy, when viremia was present in the maternal blood, and this may have severely compromised brain development. Of note, one limitation of our study is that we measured fetal head weight instead of cortical thickness. Future studies should investigate whether high- and low-ZIKV exposure alters cortical thickness in ICompetent and ICompromised offspring.

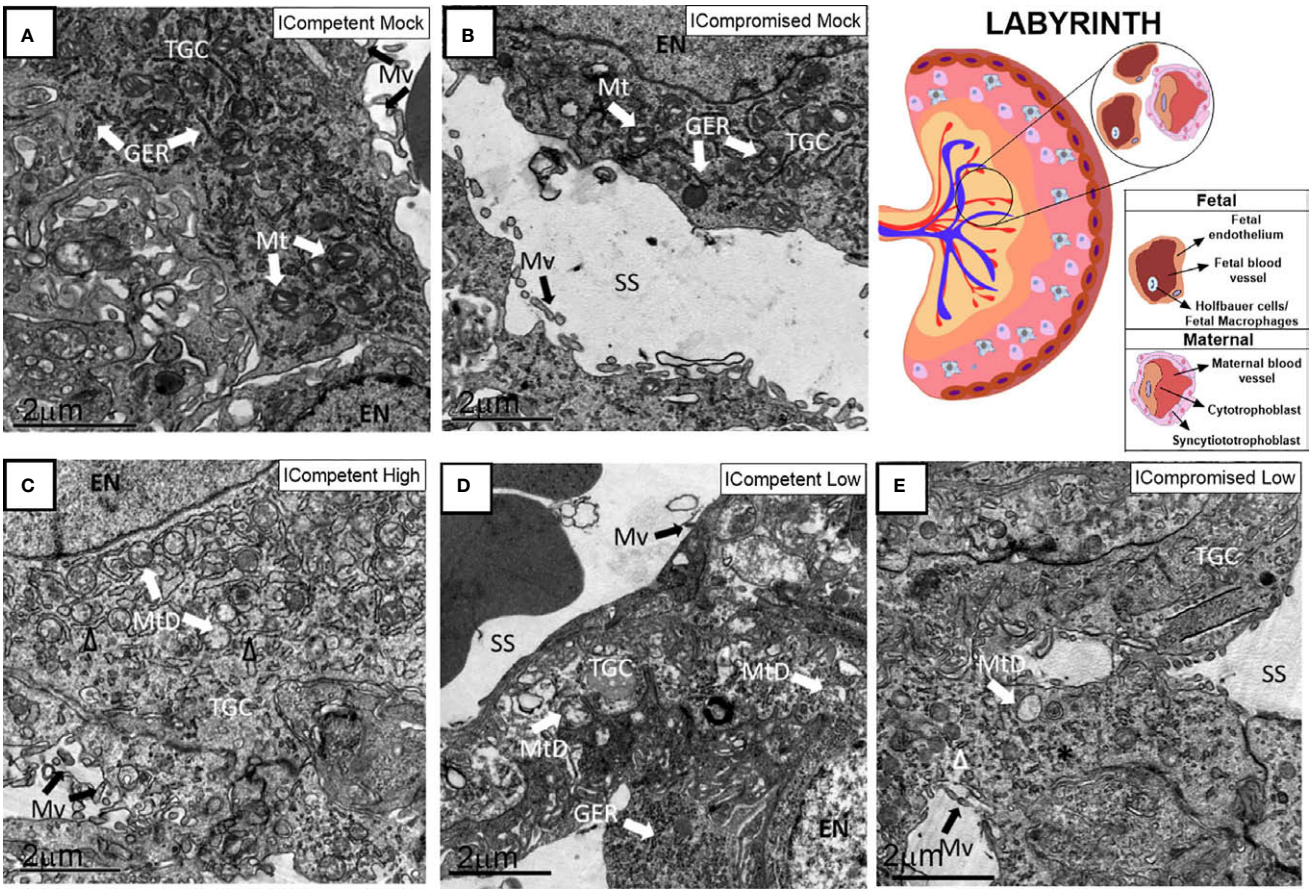

FIGURE 6 | Associated ultrastructural changes in the placental Lz after ZIKV infection. Transmission electron photomicrographs of ICompetent mock **(A)**, ICompromised mock **(B)**, ICompetent high **(C)**, ICompetent low **(D)** and ICompromised low **(E)** groups (n=5/group). We observed dilatation in the ER cisterns of ICompetent high placentas. Additionally, there was a reduction in the microvilli in both the ICompetent high and ICompetent low placentas. In the ICompromised low group, we found fragmented ER and microvillus reduction. All infected groups showed degenerate mitochondria. GER = granular endoplasmic reticulum; Δ = dilated granular endoplasmic reticulum; * = fragmented granular endoplasmic reticulum; Mt, mitochondria; MtD, degenerate mitochondria; Mv, microvilli; EN, euchromatic nuclei; SS, sinusoidal space; TGC, trophoblastic giant cell. Scale bar = 2 µm.

A distinct inflammatory profile was also detected in the three analyzed groups. At the protein level, low-ZIKV-ICompromised dams exhibited increased maternal IL-6 and CXCL-1 and placental CCL-2 and CXCL-1, whereas low-ZIKV-ICompetent dams had increased maternal CCL2 and placental IL-6 levels. CCCL-2 and CXCL-1 are related to fetal death and preterm delivery (43–45) and could be associated with pronounced fetal injury detected upon ICompromised pregnancy. In addition, IL-6 was previously demonstrated (48) to be related to fetal response syndrome, characterized by activation of the fetal immune system. This syndrome is known to increase fetal morbidity and affect several organs, such as the adrenal gland, brain and heart (32, 48–51). At the mRNA level, *Il6* expression was only detected in ICompromised placentae at term and may indicate a sustained harmful response in these mice until term. The IFN signaling pathway may be triggered by ZIKV (17) and is one of the key mechanisms of host defense and a viral target for immune evasion (20), but we only detected a slight increase in *Ifn1* in low-ZIKV ICompetent mice at term. However, we cannot rule out the possibility that these cytokines might have been produced earlier. Our findings showed that *Ifng* expression was significantly enhanced in both ICompetent and ICompromised low-ZIKV-derived placentae but not in high-ZIKV-infected mice. Although we could not assess cytokine expression in high-ZIKV ICompromised placentas, one may extrapolate that low-ZIKV infection could result in stimulation of *Ifng* producing cells, which has been previously shown to be protective for ZIKV-infected mice (52).

Both ICompromised and ICompetent mice showed increased expression of placental *Tnf* mRNA, which has been demonstrated to be directly related to placental damage, abortion and premature birth (53–56). In addition, an increased *Tnf* response is related to impaired placental hormone production and trophoblastic invasion and increased apoptosis in pregnancy (57, 58). Although we did not assess TNF-α protein levels in the placenta and maternal blood, this response could be implicated in the overall damage detected.

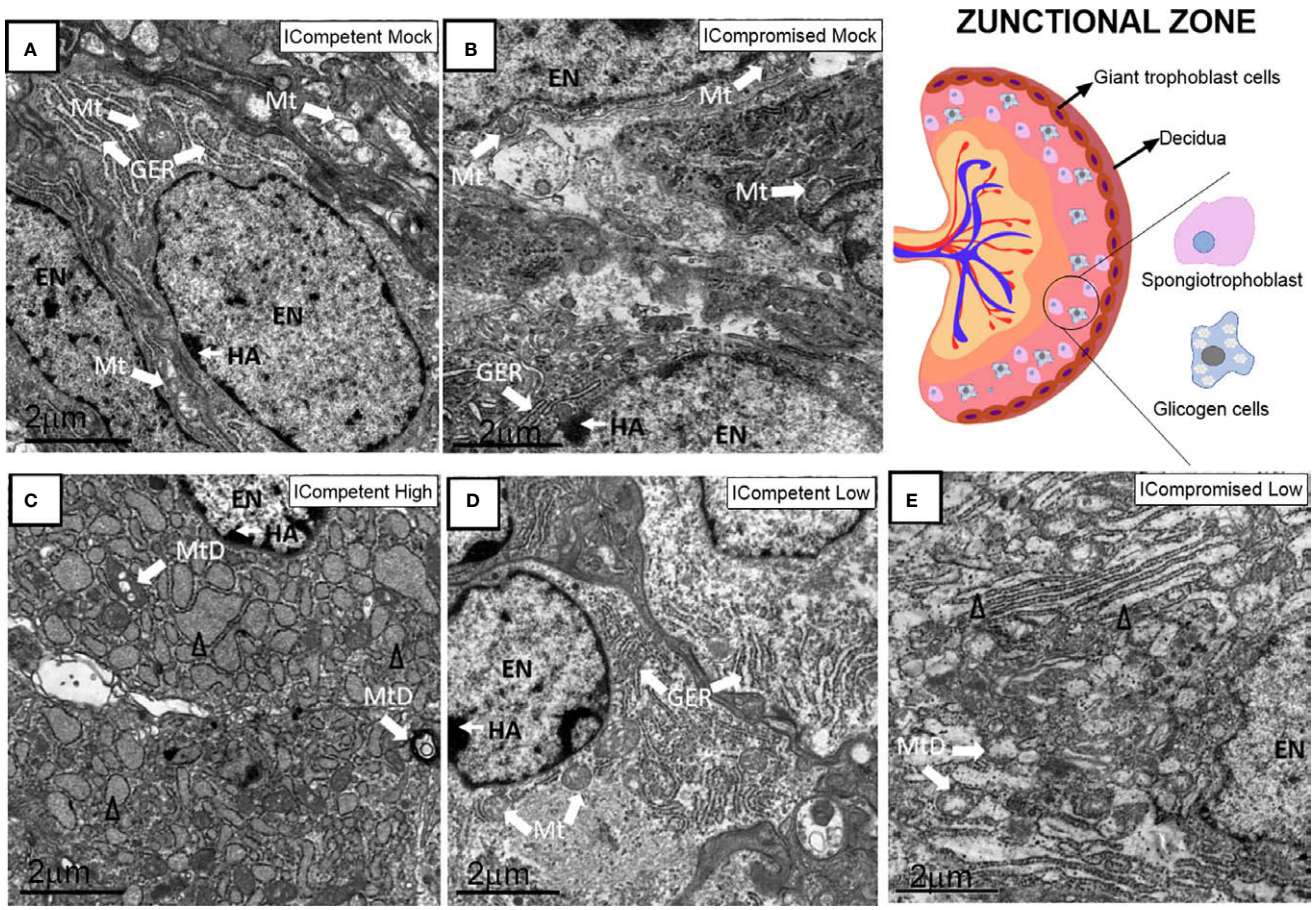

FIGURE 7 | Associated ultrastructural changes in the placental Jz after ZIKV infection. Transmission electron photomicrographs of ICompetent mock **(A)**, ICompromised mock **(B)**, ICompetent high **(C)**, ICompetent low **(D)** and ICompromised low **(E)** groups (n=5/group). We found deteriorating mitochondria and dilated reticulum endoplasmic cisterns in both the high ICompetent and low ICompromised groups. GER, granular endoplasmic reticulum; Δ, dilated granular endoplasmic reticulum; Mt, mitochondria; MtD, degenerate mitochondria; Mv, microvilli; EN, euchromatic nuclei; SS, sinusoidal space; TGC, trophoblastic giant cell; HA, heterochromatin area. Scale bar = 2 µm.

Although differences in placental weight were not observed, ZIKV infection mid-pregnancy had a profound effect on placental cellular turnover, dependent on virus titer, strain and/or placental compartment. The Lz is responsible for fetal and maternal nutrient, gas and waste exchange, while the Jz provides structural support, nutrient storage and hormone synthesis (35). ZIKV induced a consistent increase in Lz proliferation in all groups. However, the Lz apoptotic rate was increased only in the high-ZIKV-ICompetent and ICompromised groups and decreased in low-ZIKV-ICompetent mice. The mechanisms underlying these differences are unknown but may be related to the distinct maternal and placental proinflammatory responses and/or to the direct effect of the virus on the placenta (59). Increased Lz apoptosis in the high-ICompetent-ZIKV group may be one of the mechanisms driving the lower fetal and fetal head weight detected in this group. In this context, changes in placental turnover can determine placental maturation and function and lead to fetal distress and developmental abnormalities (60). An increase in the Lz apoptotic ratio may signify damage to this placental layer, which is consistent with the fact that diverse pathological lesions associated with congenital disorders were described in placentae from women infected by ZIKV at different stages of pregnancy (61). Conversely, no proliferative changes were observed in the Jz in high-ZIKV and low-ZIKV ICompetent mice, while increased and decreased apoptotic rates were detected. It follows that the lack of Jz-Ki-67 induction may suggest that this layer is less capable of restoring proliferation in response to high-ZIKV challenge, and this may be related to decreased fetal growth.

Our placental ultrastructural analysis detected consistent differences across ZIKV-exposed groups. The Lz and Jz layers from both strains exhibited signs of ER stress, i.e., dilated ER cisterns or fragmented ER granular structures. These alterations may result from the accumulation of folded or poorly folded viral proteins in the ER lumen (42, 62, 63). The *Flaviridae* family uses the ER to replicate (64), and according to Offerdahl et al. (63), there is evidence of ZIKV interacting with this organelle,

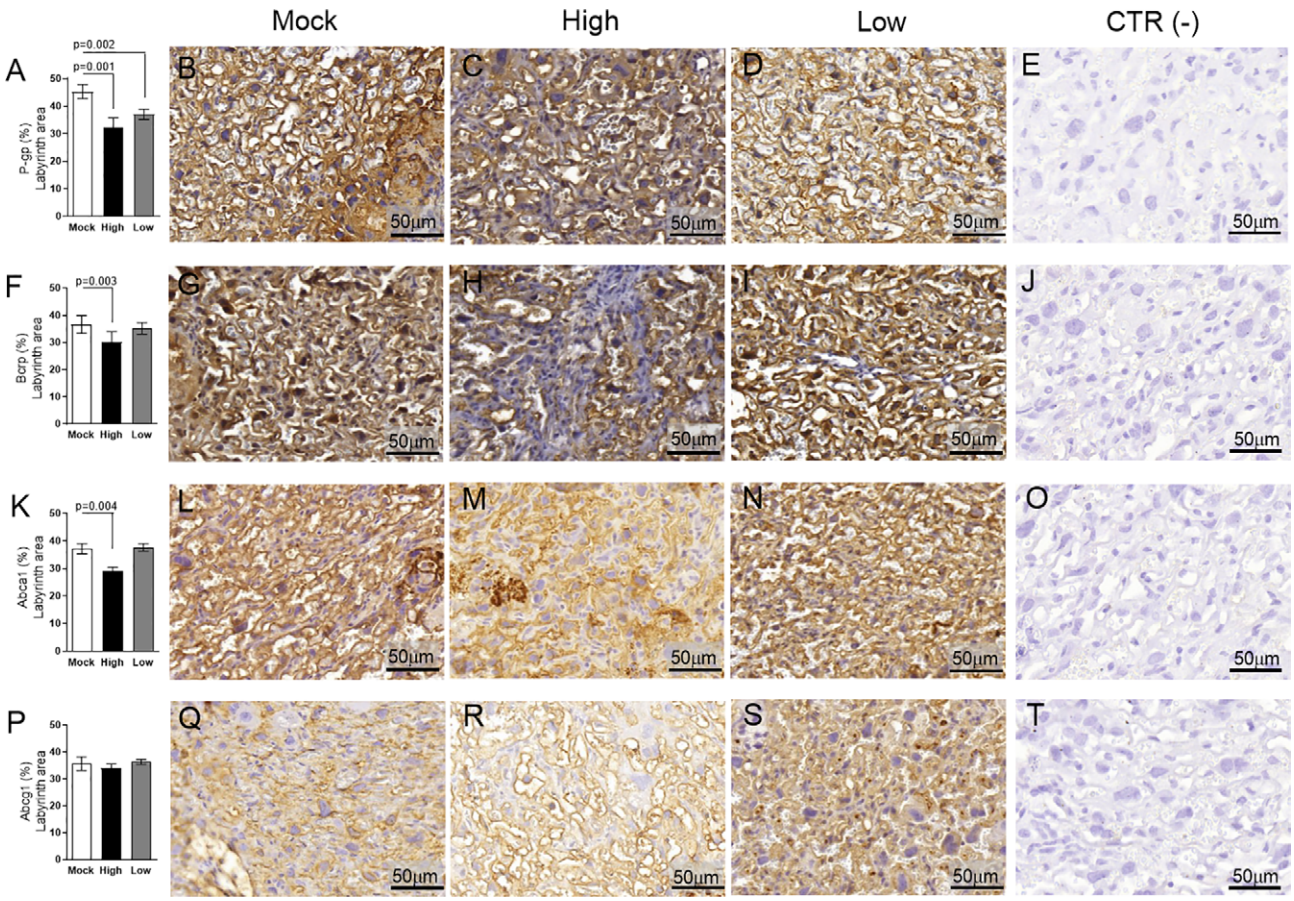

FIGURE 8 | ZIKV infection decreases P-gp, Bcrp and Abca1 expression in the placental Lz of infected mice in the ICompetent groups. A total of 180 digital images (40X) randomly captured from the whole labyrinth zone (Lz) of each placenta per dam were evaluated. Immunolabeling in each digital image was quantified by calculating the percentage area of the total stained labyrinthine tissue after exclusion of the total negative space. **(A)** Quantification and **(B–D)** representative photomicrographs of P-gp staining in the Lz of ICompetent (n=6 placentae from 6 independent dams/group) placenta. **(F)** Quantification and **(G–I)** representative photomicrographs of Bcrp staining in the Lz of ICompetent (n=6 placentae from 6 independent dams/group) placenta. **(K)** Quantification and **(L–N)** representative photomicrographs of Abca1 staining in the Lz of ICompetent (n=6 placentae from 6 independent dams/group) placenta. **(P)** Quantification and **(Q–S)** representative photomicrographs of Abcg1 staining in the Lz of ICompetent (n = 6 placentae from 6 independent dams/group) placenta. **(E, J, O, T)** Negative controls. One-way ANOVA followed by Tukey's post-test. The values are expressed as the mean ± SEM. Images were captured at 40X. Scale bar = 50 µm.

promoting an increased release of Ca^{+2} from the ER to the cell cytoplasm, thereby causing an increase in the production of reactive oxygen species (ROS) (65, 66).

The mitochondrial ultrastructure in the Lz and Jz layers was severely impacted by ZIKV exposure. We found evidence of mitochondrial degeneration, i.e., mitochondrial membrane rupture, absence of mitochondrial ridges and a less electron-dense mitochondrial matrix, in all the treated groups. Placental mitochondrial dysfunction is associated with IUGR (67, 68) and may be related, at least in part, to the lower fetal weight observed in high-ZIKV-ICompetent fetuses along with the altered placental apoptotic and proliferative patterns. Furthermore, mitochondrial dysfunction together with ER stress is likely to modify the placental ROS balance and generate local oxidative stress (69), which is associated with impaired fetal development (70). Of importance, associations between mitochondrial disruption, ER stress and placental cell senescence have been reported. Senescence is characterized as an irreversible interruption of the cell cycle and acquisition of a senescence-associated secretory phenotype (SASP) that promotes the release of cytokines, such as IL-1, IL-6, IL-8 and proinflammatory proteases (70). Therefore, the increased expression of IL-6 detected in the placentas of ICompromised mice suggests a SASP profile, which may be related to changes in the ER and mitochondrial ultrastructure, accompanied by important changes in apoptosis and cell proliferation. The interactions between mitochondria and the ER are critical for homeostasis and cell signaling (71). In conjunction with the ER, mitochondria can regulate cell death mediators in response to hypoxia and inflammation (72). The increase in apoptosis observed in the high-titer ICompetent groups and the low-titer ICompromised group may be related to the mitochondrial damage and ER stress observed. In fact, we observed an important decrease

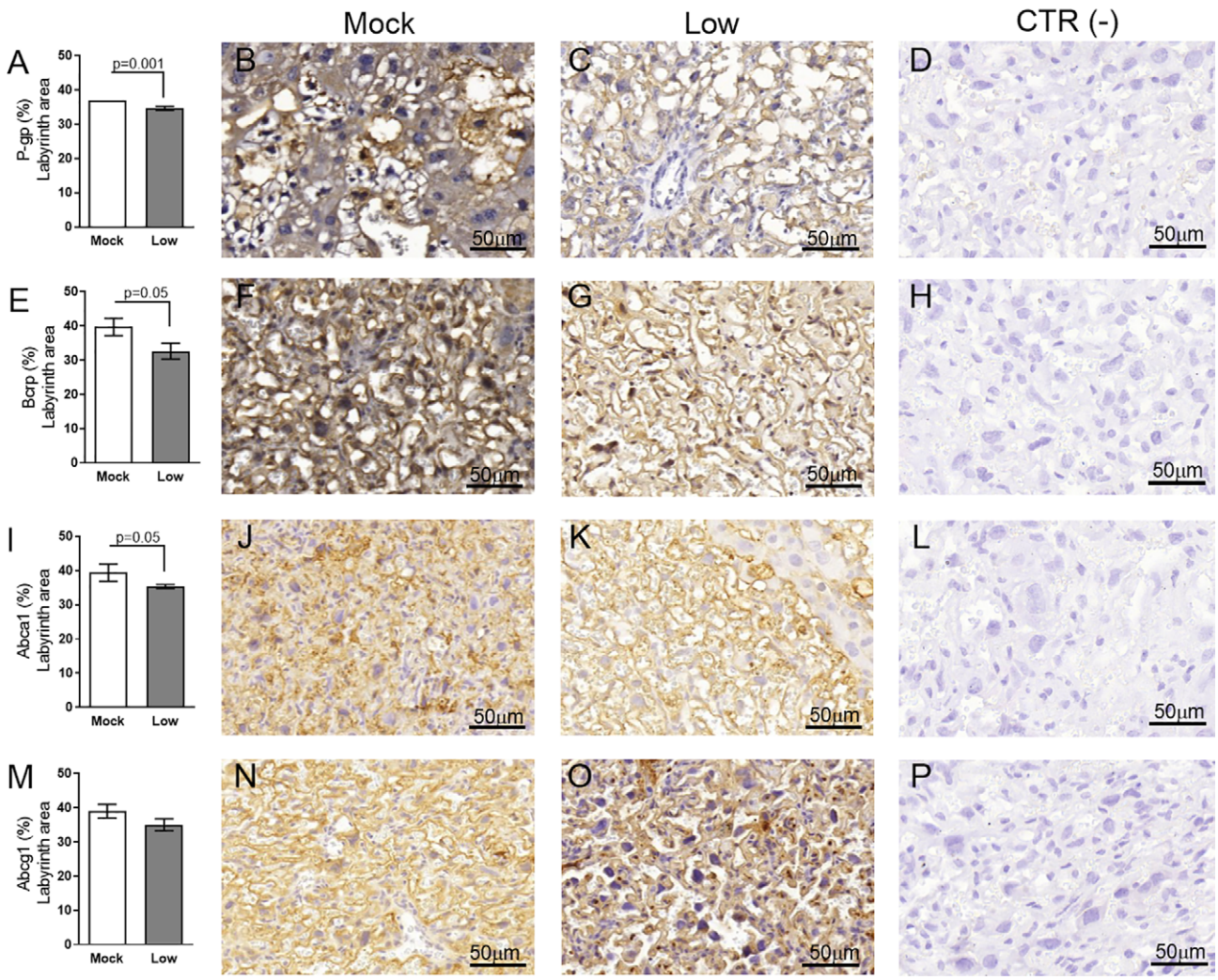

FIGURE 9 | ZIKV infection decreases P-gp, Bcrp and Abca1 protein expression in the placental Lz of infected mice in the ICompromised groups. A total of 180 digital images (40X) randomly captured from the whole labyrinth zone (Lz) of each placenta per dam were evaluated. Immunolabeling in each digital image was quantified by calculating the percentage area of the total stained labyrinth zone tissue after exclusion of the total negative space. **(A)** Quantification and **(B, C)** representative photomicrographs of P-gp staining in the Lz of ICompromised (n=3 placentae from 3 independent dams/group) placenta. **(E)** Quantification and **(F, G)** representative photomicrographs of Bcrp staining in the Lz of ICompromised (n=3 placentae from 3 independent dams/group) placenta. **(I)** Quantification and **(J, K)** representative photomicrographs of Abca1 staining in the Lz of ICompromised (n=3 placentae from 3 independent dams/group) placenta **(M)** quantification and **(N, O)** representative photomicrographs of Abcg1 staining in the Lz of ICompromised (n=3 placentae from 3 independent dams/group) placenta. **(D, H, L, P)** Negative controls. Unpaired Student's t-test or nonparametric Mann-Whitney test was used to assess differences between ICompromised groups. The values are expressed as the mean ± SEM. Images were captured at 40X. Scale ba r= 50 µm.

in microvillus abundance in sinusoidal giant trophoblast cells. Previously, we observed a decrease in microvillus density in the Lz of pregnancies exposed to malaria in pregnancy (MiP) (36). Together, our data show that different gestational infective stimuli (MiP and ZIKV) are capable of damaging placental microvillus abundance and impairing proper fetal-maternal exchange function and fetal growth/survival.

Next, to investigate whether maternal ZIKV exposure may influence fetal protection, we evaluated the placental localization and expression (semiquantitative) of the ABC efflux transporter systems P-gp, Bcrp, Abca1 and Abcg1, which are highly enriched in labyrinthine microvilli and in human syncytiotrophoblasts. These efflux transporters exchange drugs, environmental toxins, cytotoxic oxysterols and lipids within the maternal-fetal interface (26). We found a consistent decrease in labyrinthine P-gp expression in all ZIKV-exposed groups, demonstrating that ZIKV infection during pregnancy has the potential to increase fetal exposure to P-gp substrates, such as synthetic glucocorticoids, antibiotics, antiretrovirals, antifungals, stomach-protective drugs, and nonsteroidal anti-inflammatory drugs (26). Furthermore, Jz-P-gp was decreased in ICompromised placentae. Although little is known about the

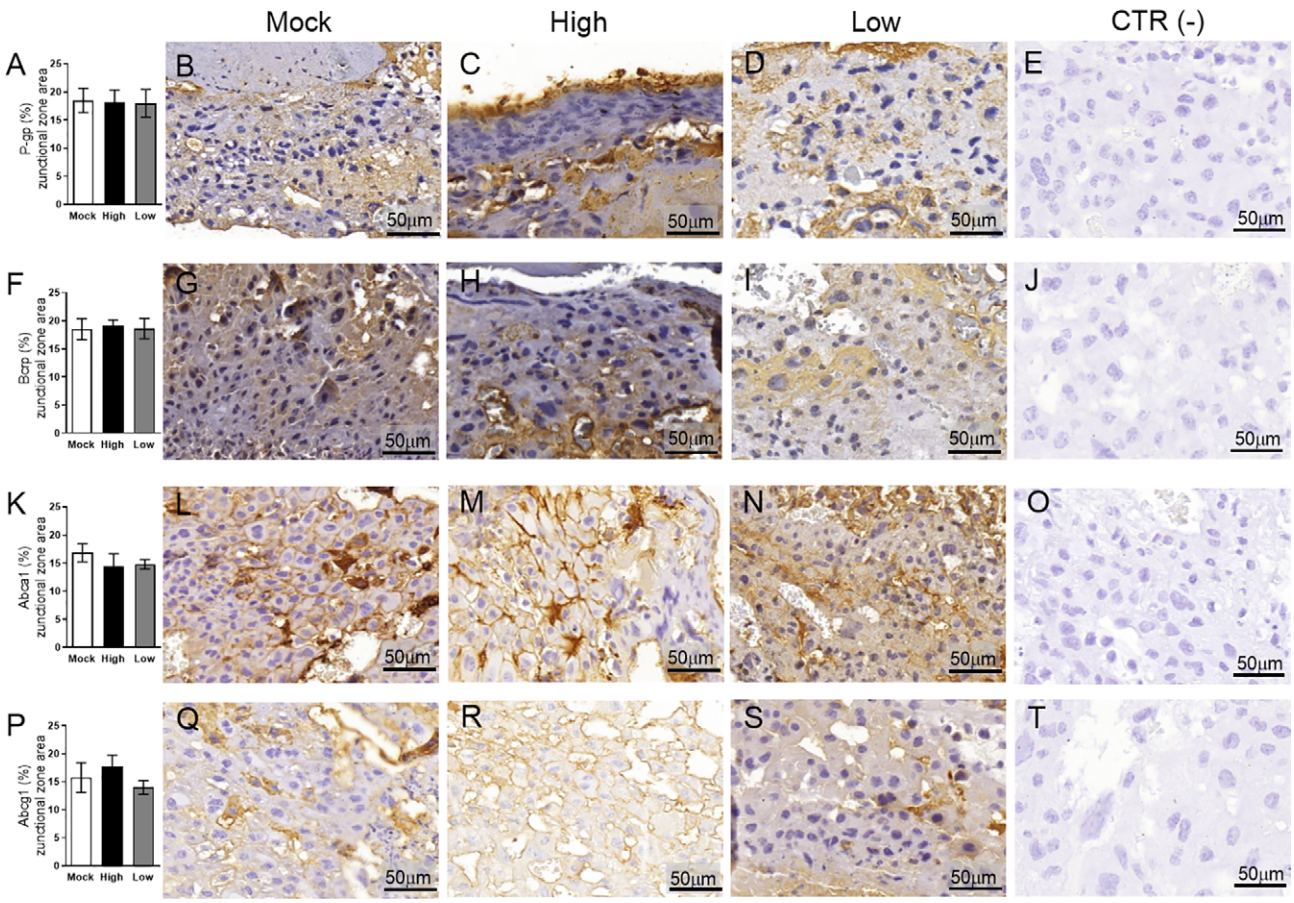

FIGURE 10 | ZIKV infection did not impact P-gp, Bcrp, Abca1 or Abcg1 protein expression in the placental Jz of infected mice in the ICompetent groups. A total of 180 digital images (40X) randomly captured from the whole junctional zone (Jz) of each placenta per dam were evaluated. Immunolabeling in each digital image was quantified by calculating the percentage area of the total stained junctional zone tissue after exclusion of the total negative space. **(A)** Quantification and **(B–D)** representative photomicrographs of P-gp staining in the Jz of ICompetent (n=6 placentae from 6 independent dams/group) placenta. **(F)** Quantification and **(G–I)** representative photomicrographs of Bcrp staining in the Jz of ICompetent (n=6 placentae from 6 independent dams/group) placenta. **(K)** Quantification and **(L–N)** representative photomicrographs of Abca1 staining in the Jz of ICompetent (n=6 placentae from 6 independent dams/group) placenta. **(P)** Quantification and **(Q–S)** representative photomicrographs of Abcg1 staining in the Jz of ICompetent (n=6 placentae from 6 independent dams/group) placenta. **(E, J, O, T)** Negative controls. One-way ANOVA followed by Tukey's post-test. The values are expressed as the mean ± SEM. Images were captured at 40X. Scale bar = 50 µm.

function of ABC transporters in the Jz, our data highlight the need for further studies investigating the biological importance of ABC transporters in the placental endocrine and structural zones of the rodent hemochorial placenta under normal and infective conditions.

ZIKV impaired Lz Bcrp and Abca1 expression in ICompetent (high) and ICompromised (low) mice. However, no effects were observed in ICompetent animals at a low ZIKV titer or in Abcg1 in any experimental setting. Thus, ZIKV also likely increases fetal accumulation of Bcrp substrates (antibiotics, antiretrovirals, sulfonylureas, folate, mercuric species, estrogenic mycotoxins, carcinogens and phototoxic compounds, among others) and disrupts placental lipid homeostasis (lipids, cholesterol, and cytotoxic oxysterols) by reducing placental Abca1 expression (26, 73–76). We can speculate that the increased fetal accumulation of the P-gp, Bcrp and Abca1 substrates during ZIKV infection may contribute to the establishment of congenital Zika syndrome, although additional studies are clearly required to answer this important question. The present data are in agreement with previous publications showing that bacterial, viral and protozoan inflammation alters the expression and/or function of P-gp, Bcrp and Abca1 in biological barriers, such as the placenta, yolk sac and blood-brain barriers (26, 27, 36, 64, 77–79).

CONCLUSION

Our data show that gestational ZIKV impacts the fetal phenotype independently of term fetal viremia. Abnormal placental cell turnover, ultrastructure and transporter expression may result from specific proinflammatory responses that depend on the ZIKV

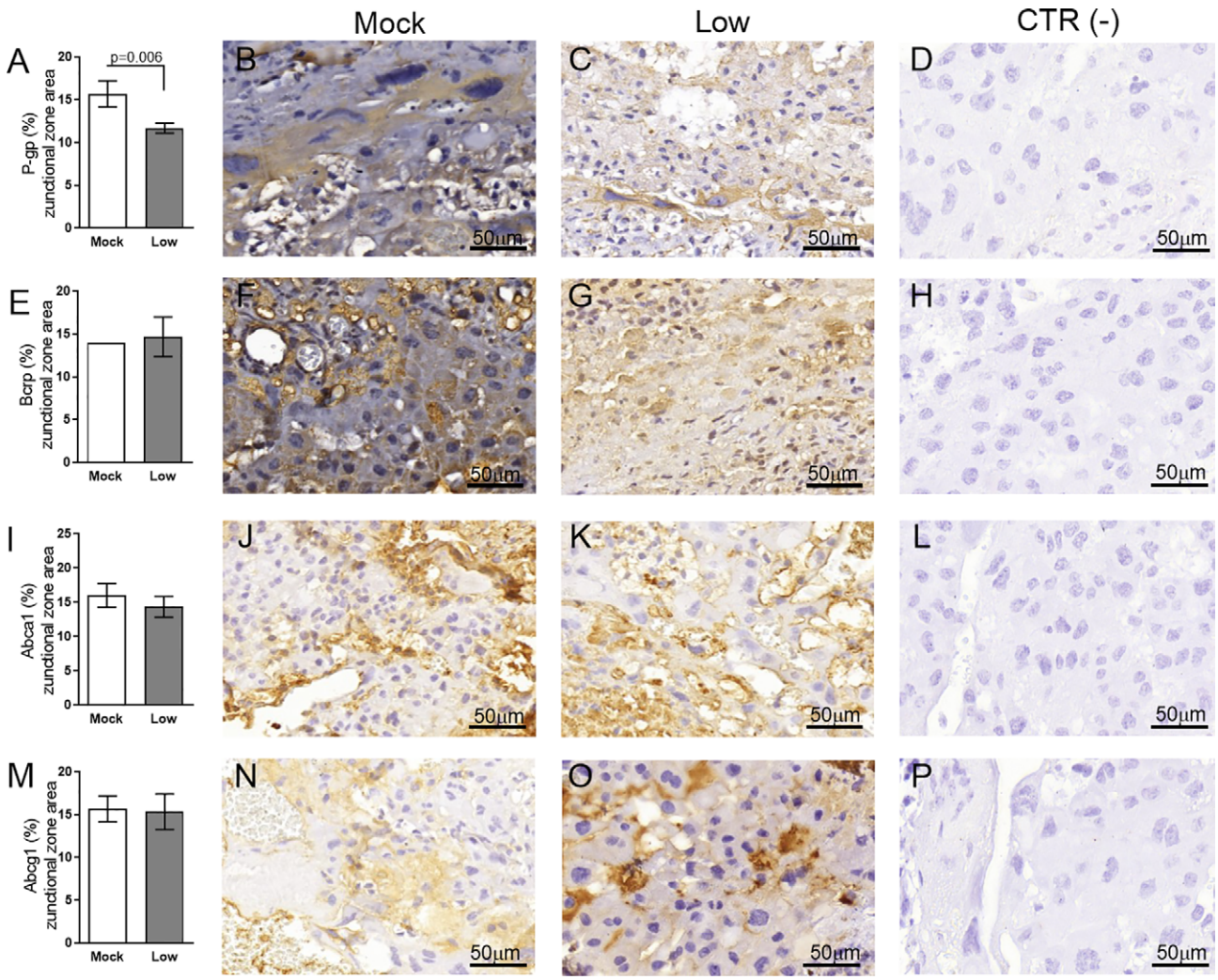

FIGURE 11 | ZIKV infection decreases Bcrp protein expression in the placental Jz of infected mice in the ICompromised group. A total of 180 digital images (40X) randomly captured from the whole junctional zone (Jz) of each placenta per dam were evaluated. Immunolabeling in each digital image was quantified by calculating the percentage area of the total stained junctional zone tissue after exclusion of the total negative space. **(A)** Quantification and **(B, C)** representative photomicrographs of P-gp staining in the Jz of ICompromised (n=3 placentae from 3 independent dams/group) placenta. **(E)** Quantification and **(F, G)** representative photomicrographs of Bcrp staining in the Jz of ICompromised (n=3 placentae from 3 independent dams/group) placenta. **(I)** Quantification and **(J, K)** representative photomicrographs of Abca1 staining in the Jz of ICompromised (n=3 placentae from 3 independent dams/group) placenta. **(M)** Quantification and **(N, O)** representative photomicrographs of Abcg1 staining in the Jz of ICompromised (n=3 placentae from 3 independent dams/group) placenta. **(D, H, L, P)** Negative controls. Unpaired Student's t-test or nonparametric Mann-Whitney test was used to assess differences between ICompromised groups. The values are expressed as the mean ± SEM. Images were captured at 40X. Scale bar = 50 µm.

infective load and maternal immune status. Fetal accumulation of drugs, environmental toxins and lipids within the fetal compartment may potentially be increased in ZIKV-infected pregnancies due to altered levels of key ABC transporters.

DATA AVAILABILITY STATEMENT

The datasets presented in this study can be found in online repositories. The names of the repository/repositories and accession number(s) can be found below: http://dx.doi.org/10.17632/xx5hgn7tjn.1.

ETHICS STATEMENT

The animal study was reviewed and approved by Animal Care Committee of the Health Sciences Center, Federal University of Rio de Janeiro (CEUA-036/16 and 104/16).

AUTHOR CONTRIBUTIONS

CA, FB, EB, LA, and TO-C conceived and designed the experiments. CA, VM, SC, HG, RS, and VN performed the experiments. CA, SC, FB, EB, SM, LA, and TO-C analyzed the data. CA, VM, EB, LA, and TO-C wrote the paper and edited the manuscript. All authors contributed to the article and approved the submitted version.

FUNDING

This work was supported, in whole or in part, by the Bill & Melinda Gates Foundation [OPP1107597]. Under the grant conditions of the Foundation, a Creative Commons Attribution 4.0 Generic License has already been assigned to the Author Accepted Manuscript version that might arise from this submission. This study was also supported by the Canadian Institutes for Health Research (SGM: Foundation-148368), Conselho Nacional de Desenvolvimento Científico e Tecnológico (CNPq; TMO-C: 304667/2016-1, 422441/2016-3, 303734/2012-4, 422410/2016-0, EB:310578/2020-5, LBA: 310867/2018-5), Coordenação de Aperfeiçoamento Pessoal de Nível Superior(CAPES, finance Code 001), and Fundação de Amparo à Pesquisa do Estado do Rio de Janeiro (FAPERJ, CBVA 2002/010/2016, TMO-C: 201.341/2016, SVAC: 200.302/2020, LBA: 201.324/2016.

ACKNOWLEDGMENTS

We would like to thank Alan Moraes for supporting the acquisition of electron microscopy images and the electron microscopy laboratory at the UFF Biology Institute for allowing the use of the JEM1011 transmission electron microscope. We would also like to thank Mauro Jorge Castro Cabral for the use of the MAGPIX® System equipment at the Paulo de Góes Institute of Microbiology/UFRJ, Ernesto T. Marques Jr. (Centro de Pesquisa Aggeu Magalhães, FIOCRUZ, PE) for providing ZIKV to the Institute of Microbiology Paulo de Góes, Federal University of Rio de Janeiro, and the technicians, Juliana Gonçalves, Rakel Alves, and Ronaldo Rocha for their support during all the experiments. This study was preprinted in the Biorxiv (https://www.biorxiv.org/content/10.1101/2020.12.17.423218v6).

REFERENCES

1. Garcez PP, Loiola EC, Madeiro da Costa R, Higa LM, Trindade P, Delvecchio R, et al. Zika Virus Impairs Growth in Human Neurospheres and Brain Organoids. *Science* (2016) 352(6287):816–8. doi: 10.1126/science.aaf6116
2. Brasil P, Calvet GA, Siqueira AM, Wakimoto M, de Sequeira PC, Nobre A, et al. Zika Virus Outbreak in Rio De Janeiro, Brazil: Clinical Characterization, Epidemiological and Virological Aspects. Powers am, Editor. *PloS Negl Trop Dis* (2016) 10(4):e0004636. doi: 10.1371/journal.pntd.0004636
3. Brasil P, Nielsen-Saines K. More Pieces to the Microcephaly–Zika Virus Puzzle in Brazil. *Lancet Infect Dis* (2016) 16(12):1307–9. doi: 10.1016/S1473-3099(16)30372-3
4. Brasil P, Pereira JP, Moreira ME, Ribeiro Nogueira RM, Damasceno L, Wakimoto M, et al. Zika Virus Infection in Pregnant Women in Rio De Janeiro. *N Engl J Med* (2016) 375(24):2321–34. doi: 10.1056/NEJMoa1602412
5. Jaenisch T, Rosenberger KD, Brito C, Brady O, Brasil P, Marques ET. Risk of Microcephaly After Zika Virus Infection in Brazil, 2015 to 2016. *Bull World Health Organ* (2017) 95(3):191–8. doi: 10.2471/BLT.16.178608
6. Proenca-Modena JL, Milanez GP, Costa ML, Judice CC, Maranhão Costa FT. Zika Virus: Lessons Learned in Brazil. *Microbes Infect* (2018) 20: (11–12):661–9. doi: 10.1016/j.micinf.2018.02.008
7. Jouannic J-M, Friszer S, Leparc-Goffart I, Garel C, Eyrolle-Guignot D. Zika Virus Infection in French Polynesia. *Lancet* (2016) 387(10023):1051–2. doi: 10.1016/S0140-6736(16)00625-5
8. Musso D, Ko AI, Baud D. Zika Virus Infection — After the Pandemic. Longo DL, Editor. *N Engl J Med* (2019) 381(15):1444–57. doi: 10.1056/NEJMra1808246
9. Kasprzykowski JI, Fukutani KF, Fabio H, Fukutani ER, Costa LC, Andrade BB, et al. A Recursive Sub-Typing Screening Surveillance System Detects the Appearance of the ZIKV African Lineage in Brazil: Is There a Risk of a New Epidemic? *Int J Infect Dis* (2020) 96:579–81. doi: 10.1016/j.ijid.2020.05.090
10. Miranda J, Martín-Tapia D, Valdespino-Vázquez Y, Alarcón L, Espejel-Nuñez A, Guzmán-Huerta M, et al. Syncytiotrophoblast of Placentae From Women With Zika Virus Infection has Altered Tight Junction Protein Expression and Increased Paracellular Permeability. *Cells* (2019) 8(10):1174. doi: 10.3390/cells8101174
11. Jurado KA, Simoni MK, Tang Z, Uraki R, Hwang J, Householder S, et al. Zika Virus Productively Infects Primary Human Placenta-Specific Macrophages. *JCI Insight* (2016) 1(13):e88461. doi: 10.1172/jci.insight.88461
12. Quicke KM, Bowen JR, Johnson EL, McDonald CE, Ma H, O'Neal JT, et al. Zika Virus Infects Human Placental Macrophages. *Cell Host Microbe* (2016) 20(1):83–90. doi: 10.1016/j.chom.2016.05.015
13. Tabata T, Petitt M, Puerta-Guardo H, Michlmayr D, Wang C, Fang-Hoover J, et al. Zika Virus Targets Different Primary Human Placental Cells, Suggesting Two Routes for Vertical Transmission. *Cell Host Microbe* (2016) 20(2):155–66. doi: 10.1016/j.chom.2016.07.002
14. Simoni MK, Jurado KA, Abrahams VM, Fikrig E, Guller S. Zika Virus Infection of Hofbauer Cells. *Am J Reprod Immunol* (2017) 77(2):e12613. doi: 10.1111/aji.12613
15. Rathore APS, Saron WAA, Lim T, Jahan N, John ALS. Maternal Immunity and Antibodies to Dengue Virus Promote Infection and Zika Virus–Induced Microcephaly in Fetuses. *Sci Adv* (2019) 5(2):eaav3208. doi: 10.1126/sciadv.aav3208
16. Lazear HM, Govero J, Smith AM, Platt DJ, Fernandez E, Miner JJ, et al. A Mouse Model of Zika Virus Pathogenesis. *Cell Host Microbe* (2016) 19(5):720–30. doi: 10.1016/j.chom.2016.03.010
17. Grant A, Ponia SS, Tripathi S, Balasubramaniam V, Miorin L, Sourisseau M, et al. Zika Virus Targets Human STAT2 to Inhibit Type I Interferon Signaling. *Cell Host Microbe* (2016) 19(6):882–90. doi: 10.1016/j.chom.2016.05.009
18. Yockey LJ, Varela L, Rakib T, Khoury-Hanold W, Fink SL, Stutz B, et al. Vaginal Exposure to Zika Virus During Pregnancy Leads to Fetal Brain Infection. *Cell* (2016) 166(5):1247–56. e4. doi: 10.1016/j.cell.2016.08.004
19. Garcez PP, Stolp HB, Sravanam S, Christoff RR, Ferreira JCCG, Dias AA, et al. Zika Virus Impairs the Development of Blood Vessels in a Mouse Model of Congenital Infection. *Sci Rep* (2018) 8(1):12774. doi: 10.1038/s41598-018-31149-3
20. Elong Ngono A, Shresta S. Immune Response to Dengue and Zika. *Annu Rev Immunol* (2018) 36(1):279–308. doi: 10.1146/annurev-immunol-042617-053142
21. Bayer A, Lennemann NJ, Ouyang Y, Bramley JC, Morosky S, Marques ETDAJ, et al. Type III Interferons Produced by Human Placental Trophoblasts Confer Protection Against Zika Virus Infection. *Cell Host Microbe* (2016) 19(5):705–12. doi: 10.1016/j.chom.2016.03.008
22. Luo H, Winkelmann ER, Fernandez-Salas I, Li L, Mayer SV, Danis-Lozano R, et al. Zika, Dengue and Yellow Fever Viruses Induce Differential Anti-Viral Immune Responses in Human Monocytic and First Trimester Trophoblast Cells. *Antiviral Res* (2018) 151:55–62. doi: 10.1016/j.antiviral.2018.01.003
23. Tanaka T, Narazaki M, Kishimoto T. IL-6 in Inflammation, Immunity, and Disease. *Cold Spring Harb Perspect Biol* (2014) 6(10):a016295. doi: 10.1101/cshperspect.a016295

24. Hunter CA, Jones SA. IL-6 as a Keystone Cytokine in Health and Disease. *Nat Immunol* (2015) 16(5):448–57. doi: 10.1038/ni.3153
25. Rabelo K, da Gonçalves AJS, de Souza LJ, Sales AP, de Lima SMB, Trindade GF, et al. Zika Virus Infects Human Placental Mast Cells and the HMC-1 Cell Line, and Triggers Degranulation, Cytokine Release and Ultrastructural Changes. *Cells* (2020) 9(4):975–90. doi: 10.3390/cells9040975
26. Bloise E, Ortiga-Carvalho TM, Reis FM, Lye SJ, Gibb W, Matthews SG. ATP-Binding Cassette Transporters in Reproduction: A New Frontier. *Hum Reprod Update* (2015) 22(2):164–81. doi: 10.1093/humupd/dmv049
27. do Imperio GE, Bloise E, Javam M, Lye P, Constantinof A, Dunk C, et al. Chorioamnionitis Induces a Specific Signature of Placental Abc Transporters Associated With an Increase of miR-331-5p in the Human Preterm Placenta. *Cell Physiol Biochem* (2018) 45(2):591–604. doi: 10.1159/000487100
28. Martinelli LM, Fontes KN, Reginatto MW, Andrade CBV, Monteiro VRS, Gomes HR, et al. Malaria in Pregnancy Regulates P-glycoprotein (P-Gp/Abcb1a) and ABCA1 Efflux Transporters in the Mouse Visceral Yolk Sac. *J Cell Mol Med* (2020) 00:1–12. doi: 10.1101/2020.06.27.175018
29. Reginatto MW, Fontes KN, Monteiro VRS, Silva NL, Andrade CBV, Gomes HR, et al. Effect of Sub-Lethal Prenatal Endotoxemia on Murine Placental Transport Systems and Lipid Homeostasis. *bioRxiv* (2020). doi: 10.1101/2020.08.04.236745
30. Martinelli LM, Reginatto MW, Fontes KN, Andrade CBV, Monteiro VRS, Gomes HR, et al. Breast Cancer Resistance Protein (Bcrp/Abcg2) is Selectively Modulated by Lipopolysaccharide (LPS) in the Mouse Yolk Sac. *Reprod Toxicol* (2020) 98:82–91. doi: 10.1016/j.reprotox.2020.09.001
31. Imperio GE, Javam M, Lye P, Constantinof A, Dunk CE, Reis FM, et al. Gestational Age-Dependent Gene Expression Profiling of ATP-binding Cassette Transporters in the Healthy Human Placenta. *J Cell Mol Med* (2019) 23(1):610–8. doi: 10.1111/jcmm.13966
32. Vermillion MS, Lei J, Shabi Y, Baxter VK, Crilly NP, McLane M, et al. Intrauterine Zika Virus Infection of Pregnant Immunocompetent Mice Models Transplacental Transmission and Adverse Perinatal Outcomes. *Nat Commun* (2017) 8(1):14575. doi: 10.1038/ncomms14575
33. Szaba FM, Tighe M, Kummer LW, Lanzer KG, Ward JM, Lanthier P, et al. Zika Virus Infection in Immunocompetent Pregnant Mice Causes Fetal Damage and Placental Pathology in the Absence of Fetal Infection. Coyne CB, Editor. *PloS Pathog* (2018) 14(4):e1006994. doi: 10.1371/journal.ppat.1006994
34. Coelho SVA, Neris RLS, Papa MP, Schnellrath LC, Meuren LM, Tschoeke DA, et al. Development of Standard Methods for Zika Virus Propagation, Titration, and Purification. *J Virol Methods* (2017) 246:65–74. doi: 10.1016/j.jviromet.2017.04.011
35. Connor KL, Kibschull M, Matysiak-Zablocki E, Nguyen TT-TN, Matthews SG, Lye SJ, et al. Maternal Malnutrition Impacts Placental Morphology and Transporter Expression: An Origin for Poor Offspring Growth. *J Nutr Biochem* (2020) 78:108329. doi: 10.1016/j.jnutbio.2019.108329
36. Fontes KN, Reginatto MW, Silva NL, Andrade CBV, Bloise FF, Monteiro VRS, et al. Dysregulation of Placental ABC Transporters in a Murine Model of Malaria-Induced Preterm Labor. *Sci Rep* (2019) 9(1):11488. doi: 10.1038/s41598-019-47865-3
37. Bloise E, Lin W, Liu X, Simbulan R, Kolahi KS, Petraglia F, et al. Impaired Placental Nutrient Transport in Mice Generated by *in Vitro* Fertilization. *Endocrinology* (2012) 153(7):3457–67. doi: 10.1210/en.2011-1921
38. Lanciotti RS, Kosoy OL, Laven JJ, Velez JO, Lambert AJ, Johnson AJ, et al. Genetic and Serologic Properties of Zika Virus Associated With an Epidemic, Yap State, Micronesia, 2007. *Emerg Infect Dis* (2008) 14(8):1232–9. doi: 10.3201/eid1408.080287
39. Livak KJ, Schmittgen TD. Analysis of Relative Gene Expression Data Using Real-Time Quantitative PCR and the 2–ΔΔct Method. *Methods* (2001) 25(4):402–8. doi: 10.1006/meth.2001.1262
40. Tschanz SA, Burri PH, Weibel ER. A Simple Tool for Stereological Assessment of Digital Images: The STEPanizer: Tool FOR Stereological Assessment. *J Microscopy* (2011) 243(1):47–59. doi: 10.1111/j.1365-2818.2010.03481.x
41. Sesso A, Belizário JE, Marques MM, Higuchi ML, Schumacher RI, Colquhoun A, et al. Mitochondrial Swelling and Incipient Outer Membrane Rupture in Preapoptotic and Apoptotic Cells. *Anatomical Rec* (2012) 295(10):1647. doi: 10.1002/ar.22553
42. Montalbano R, Waldegger P, Quint K, Jabari S, Neureiter D, Illig R, et al. Endoplasmic Reticulum Stress Plays a Pivotal Role in Cell Death Mediated by the Pan-Deacetylase Inhibitor Panobinostat in Human Hepatocellular Cancer Cells. *Trans Oncol* (2013) 6(2):143–IN6. doi: 10.1593/tlo.12271
43. Hamilton SA, Tower CL, Jones RL. Identification of Chemokines Associated With the Recruitment of Decidual Leukocytes in Human Labour: Potential Novel Targets for Preterm Labour. *PloS One* (2013) 8(2):e56946. doi: 10.1371/journal.pone.0056946
44. Bloise E, Bhuiyan M, Audette MC, Petropoulos S, Javam M, Gibb W, et al. Prenatal Endotoxemia and Placental Drug Transport in The Mouse: Placental Size-Specific Effects. *PloS One* (2013) 8(6):e65728. doi: 10.1371/journal.pone.0065728
45. Romero R, Mazor M, Brandt F, Sepulveda W, Avila C, Cotton DB, et al. Interleukin-1α and Interleukin-1 β in Preterm and Term Human Parturition. *Am J Reprod Immunol* (1992) 27(3-4):117–23. doi: 10.1111/j.1600-0897.1992.tb00737.x
46. Larocca RA, Abbink P, Peron JPS, de A, Zanotto PM, Iampietro MJ, et al. Vaccine Protection Against Zika Virus From Brazil. *Nature* (2016) 536(7617):474–8. doi: 10.1038/nature18952
47. Souza IN de O, Frost PS, França JV, Nascimento-Viana JB, Neris RLS, Freitas L, et al. Acute and Chronic Neurological Consequences of Early-Life Zika Virus Infection in Mice. *Sci Trans Med* (2018) 10(444):eaar2749. doi: 10.1126/scitranslmed.aar2749
48. Kalagiri RR, Carder T, Choudhury S, Vora N, Ballard AR, Govande V, et al. Inflammation in Complicated Pregnancy and Its Outcome. *Am J Perinatol* (2016) 33(14):1337–56. doi: 10.1055/s-0036-1582397
49. Barbeito-Andrés J, Pezzuto P, Higa LM, Dias AA, Vasconcelos JM, Santos TMP, et al. Congenital Zika Syndrome is Associated With Maternal Protein Malnutrition. *Sci Adv* (2020) 6(2):eaaw6284. doi: 10.1126/sciadv.aaw6284
50. Saito S, Nakashima A, Shima T, Ito M. Review ARTICLE: Th1/Th2/Th17 and Regulatory T-Cell Paradigm in Pregnancy. *Am J Reprod Immunol* (2010) 63(6):601–10. doi: 10.1111/j.1600-0897.2010.00852.x
51. Gotsch F, Romero R, Kusanovic JP, Mazaki-Tovi S, Pineles BL, Erez O, et al. The Fetal Inflammatory Response Syndrome. *Clin Obstet Gynecol* (2007) 50(3):652–83. doi: 10.1097/GRF.0b013e31811ebef6
52. Lucas CGO, Kitoko JZ, Ferreira FM, Suzart VG, Papa MP, Coelho SVA, et al. Critical Role of CD4 + T Cells and Ifnγ Signaling in Antibody-Mediated Resistance to Zika Virus Infection. *Nat Commun* (2018) 9(1):3136. doi: 10.1038/s41467-018-05519-4
53. Burdet J, Sacerdoti F, Cella M, Franchi AM, Ibarra C. Role of TNF-α in the Mechanisms Responsible for Preterm Delivery Induced by Stx2 in Rats. *Br J Pharmacol* (2013) 168(4):946. doi: 10.1111/j.1476-5381.2012.02239.x
54. Carpentier PA, Dingman AL, Palmer TD. Placental TNF-α Signaling in Illness-Induced Complications of Pregnancy. *Am J Pathol* (2011) 178(6):2802–10. doi: 10.1016/j.ajpath.2011.02.042
55. Romanowska-Próchnicka K, Felis-Giemza A, Olesińska M, Wojdasiewicz P, Paradowska-Gorycka A, Szukiewicz D. The Role of TNF-α and Anti-TNF-α Agents During Preconception, Pregnancy, and Breastfeeding. *Int J Mol Sci* (2021) 22(6):2922. doi: 10.3390/ijms22062922
56. Sarr D, Bracken TC, Owino SO, Cooper CA, Smith GM, Nagy T, et al. Differential Roles of Inflammation and Apoptosis in Initiation of Mid-Gestational Abortion in Malaria-Infected C57BL/6 and A/J Mice. *Placenta* (2015) 36(7):738. doi: 10.1016/j.placenta.2015.04.007
57. Galinsky R, Polglase GR, Hooper SB, Black MJ, Moss TJM. The Consequences of Chorioamnionitis: Preterm Birth and Effects on Development. *J Pregnancy* (2013) 2013:412831. doi: 10.1155/2013/412831
58. Mor G, Cardenas I, Abrahams V, Guller S. Inflammation and Pregnancy: The Role of the Immune System at the Implantation Site. *Ann N Y Acad Sci* (2011) 1221(1):80–7. doi: 10.1111/j.1749-6632.2010.05938.x
59. Ribeiro MR, Moreli JB, Marques RE, Papa MP, Meuren LM, Rahal P, et al. Zika-Virus-Infected Human Full-Term Placental Explants Display Pro-Inflammatory Responses and Undergo Apoptosis. *Arch Virol* (2018) 163(10):2687–99. doi: 10.1007/s00705-018-3911-x
60. Gown AM, Willingham MC. Improved Detection of Apoptotic Cells in Archival Paraffin Sections: Immunohistochemistry Using Antibodies to Cleaved Caspase 3. *J Histochem Cytochem* (2002) 50(4):449–54. doi: 10.1177/002215540205000401

61. de Noronha L, Zanluca C, Burger M, Suzukawa AA, Azevedo M, Rebutini PZ, et al. Zika Virus Infection at Different Pregnancy Stages: Anatomopathological Findings, Target Cells and Viral Persistence in Placental Tissues. *Front Microbiol* (2018) 9(2266):1–11. doi: 10.3389/fmicb.2018.02266
62. Lojpur T, Easton Z, Raez-Villanueva S, Laviolette S, Holloway AC, Hardy DB. Δ9-Tetrahydrocannabinol Leads to Endoplasmic Reticulum Stress and Mitochondrial Dysfunction in Human BeWo Trophoblasts. *Reprod Toxicol* (2019) 87:21–31. doi: 10.1016/j.reprotox.2019.04.008
63. Offerdahl DK, Dorward DW, Hansen BT, Bloom ME. Cytoarchitecture of Zika Virus Infection in Human Neuroblastoma and Aedes Albopictus Cell Lines. *Virology* (2017) 501:54–62. doi: 10.1016/j.virol.2016.11.002
64. Desuzinges-Mandon E, Arnaud O, Martinez L, Huché F, Di Pietro A, Falson P. Abcg2 Transports and Transfers Heme to Albumin Through Its Large Extracellular Loop. *J Biol Chem* (2010) 285(43):33123–33. doi: 10.1074/jbc.M110.139170
65. Ledur PF, Karmirian K, Pedrosa C da SG, Souza LRQ, Assis-de-Lemos G, Martins TM, et al. Zika Virus Infection Leads to Mitochondrial Failure, Oxidative Stress and DNA Damage in Human iPSC-derived Astrocytes. *Sci Rep* (2020) 10(1):1218. doi: 10.1038/s41598-020-57914-x
66. Reemst K, Noctor SC, Lucassen PJ, Hol EM. The Indispensable Roles of Microglia and Astrocytes During Brain Development. *Front Hum Neurosci* (2016) 10:566. doi: 10.3389/fnhum.2016.00566
67. Guitart-Mampel M, Gonzalez-Tendero A, Niñerola S, Morén C, Catalán-Garcia M, González-Casacuberta I, et al. Cardiac and Placental Mitochondrial Characterization in a Rabbit Model of Intrauterine Growth Restriction. *Biochim Biophys Acta (BBA) Gen Subj* (2018) 1862(5):1157–67. doi: 10.1016/j.bbagen.2018.02.006
68. Guitart-Mampel M, Juarez-Flores DL, Youssef L, Moren C, Garcia-Otero L, Roca-Agujetas V, et al. Mitochondrial Implications in Human Pregnancies With Intrauterine Growth Restriction and Associated Cardiac Remodelling. *J Cell Mol Med* (2019) 23(6):3962–73. doi: 10.1111/jcmm.14282
69. Zhang Z, Rong L, Li Y-P. Flaviviridae Viruses and Oxidative Stress: Implications for Viral Pathogenesis. *Oxid Med Cell Longev* (2019) 2019:1409582. doi: 10.1155/2019/1409582
70. Martínez F, Kiriakidou M, Strauss JF. Structural and Functional Changes in Mitochondria Associated With Trophoblast Differentiation: Methods to Isolate Enriched Preparations of Syncytiotrophoblast Mitochondria. *Endocrinology* (1997) 138(5):2172–83. doi: 10.1210/endo.138.5.5133
71. Burton GJ, Yung HW, Murray AJ. Mitochondrial – Endoplasmic Reticulum Interactions in the Trophoblast: Stress and Senescence. *Placenta* (2017) 52:146–55. doi: 10.1016/j.placenta.2016.04.001
72. Holland O, Dekker Nitert M, Gallo LA, Vejzovic M, Fisher JJ, Perkins AV. Review: Placental Mitochondrial Function and Structure in Gestational Disorders. *Placenta* (2017) 54:2–9. doi: 10.1016/j.placenta.2016.12.012
73. Bridges CC, Zalups RK, Joshee L. Toxicological Significance of Renal Bcrp: Another Potential Transporter in the Elimination of Mercuric Ions From Proximal Tubular Cells. *Toxicol Appl Pharmacol* (2015) 285(2):110–7. doi: 10.1016/j.taap.2015.03.027
74. Szilagyi JT, Gorczyca L, Brinker A, Buckley B, Laskin JD, Aleksunes LM. Placental BCRP/ABCG2 Transporter Prevents Fetal Exposure to the Estrogenic Mycotoxin Zearalenone. *Toxicol Sci* (2019) 168(2):394–404. doi: 10.1093/toxsci/kfy303
75. Scialis RJ, Aleksunes LM, Csanaky IL, Klaassen CD, Manautou JE. Identification and Characterization of Efflux Transporters That Modulate the Subtoxic Disposition of Diclofenac and Its Metabolites. *Drug Metab Dispos* (2019) 47(10):1080–92. doi: 10.1124/dmd.119.086603
76. Mao Q, Unadkat JD. Role of the Breast Cancer Resistance Protein (BCRP/ABCG2) in Drug Transport–an Update. *AAPS J* (2015) 17(1):65–82. doi: 10.1208/s12248-014-9668-6
77. Lye P, Bloise E, Javam M, Gibb W, Lye SJ, Matthews SG. Impact of Bacterial and Viral Challenge on Multidrug Resistance in First- and Third-Trimester Human Placenta. *Am J Pathol* (2015) 185(6):1666–75. doi: 10.1016/j.ajpath.2015.02.013
78. Girard S, Sebire G. Transplacental Transfer of Interleukin-1 Receptor Agonist and Antagonist Following Maternal Immune Activation. *Am J Reprod Immunol (N Y NY: 1989)* (2016) 75(1):8–12. doi: 10.1111/aji.12444
79. Bloise E, Petropoulos S, Iqbal M, Kostaki A, Ortiga-Carvalho TM, Gibb W, et al. Acute Effects of Viral Exposure on P-Glycoprotein Function in the Mouse Fetal Blood-Brain Barrier. *Cell Physiol Biochem: Int J Exp Cell Physiol Biochem Pharmacol* (2017) 41(3):1044–50. doi: 10.1159/000461569

Conflict of Interest: The authors declare that the research was conducted in the absence of any commercial or financial relationships that could be construed as a potential conflict of interest.

frontiers in Immunology

ORIGINAL RESEARCH
published: 26 May 2021
doi: 10.3389/fimmu.2021.685919

Association Between COVID-19 Pregnant Women Symptoms Severity and Placental Morphologic Features

Patricia Zadorosnei Rebutini[1], Aline Cristina Zanchettin[2], Emanuele Therezinha Schueda Stonoga[3], Daniele Margarita Marani Prá[1], André Luiz Parmegiani de Oliveira[1], Felipe da Silva Dezidério[1], Aline Simoneti Fonseca[2], Júlio César Honório Dagostini[3], Elisa Carolina Hlatchuk[3], Isabella Naomi Furuie[4], Jessica da Silva Longo[4], Bárbara Maria Cavalli[5], Carolina Lumi Tanaka Dino[5], Viviane Maria de Carvalho Hessel Dias[1], Ana Paula Percicote[3], Meri Bordignon Nogueira[5,6], Sonia Mara Raboni[7], Newton Sergio de Carvalho[5], Cleber Machado-Souza[2]* and Lucia de Noronha[1]*

[1] Postgraduate Program of Health Sciences, School of Medicine, Pontifícia Universidade Católica do Paraná-PUCPR, Curitiba, Brazil, [2] Postgraduate Program in Biotechnology Applied in Health of Children and Adolescent, Pelé Pequeno Príncipe, Research Institute, Faculdades Pequeno Príncipe, Curitiba, Brazil, [3] Department of Medical Pathology, Clinical Hospital, Universidade Federal do Paraná-UFPR, Curitiba, Brazil, [4] Department of Tocogynecology, Clinical Hospital, Universidade Federal do Paraná, UFPR, Curitiba, Brazil, [5] Postgraduate Program of Tocogynecology and Women's Health, Clinical Hospital, Universidade Federal do Paraná-UFPR, Curitiba, Brazil, [6] Virology Laboratory, Clinical Hospital, Universidade Federal do Paraná-UFPR, Curitiba, Brazil, [7] Department of Infectious Disease, Clinical Hospital, Universidade Federal do Paraná-UFPR, Curitiba, Brazil*

OPEN ACCESS

Edited by:
Abhay P.S. Rathore, Duke University, United States

Reviewed by:
David Alan Schwartz, Augusta University, United States
Jeffery A. Goldstein, Northwestern Medicine, United States

***Correspondence:**
Cleber Machado-Souza
Cleberius@gmail.com
Patricia Zadorosnei Rebutini
rebutini@gmail.com

Specialty section:
This article was submitted to Viral Immunology, a section of the journal Frontiers in Immunology

Received: *26 March 2021*
Accepted: *05 May 2021*
Published: *26 May 2021*

Citation:
Rebutini PZ, Zanchettin AC, Stonoga ETS, Prá DMM, de Oliveira ALP, Dezidério FdS, Fonseca AS, Dagostini JCH, Hlatchuk EC, Furuie IN, Longo JdS, Cavalli BM, Dino CLT, Dias VMdCH, Percicote AP, Nogueira MB, Raboni SM, de Carvalho NS, Machado-Souza C and de Noronha L (2021) Association Between COVID-19 Pregnant Women Symptoms Severity and Placental Morphologic Features. Front. Immunol. 12:685919. doi: 10.3389/fimmu.2021.685919

Since the beginning of the pandemic, few papers describe the placenta's morphological and morphometrical features in SARS-CoV-2–positive pregnant women. Alterations, such as low placental weight, accelerated villous maturation, decidual vasculopathy, infarcts, thrombosis of fetal placental vessels, and chronic histiocytic intervillositis (CHI), have been described.

Objective: To analyze clinical data and the placental morphological and morphometric changes of pregnant women infected with SARS-CoV-2 (COVID-19 group) in comparison with the placentas of non-infected pregnant women, matched for maternal age and comorbidities, besides gestational age of delivery (Control group).

Method: The patients in the COVID-19 and the Control group were matched for maternal age, gestational age, and comorbidities. The morphological analysis of placentas was performed using Amsterdam Placental Workshop Group Consensus Statement. The quantitative morphometric evaluation included perimeter diameter and number of tertiary villi, number of sprouts and knots, evaluation of deposition of villous fibrin, and deposition of intra-villous collagen I and III by Sirius Red. Additionally, Hofbauer cells (HC) were counted within villi by immunohistochemistry with CD68 marker.

Results: Compared to controls, symptomatic women in the COVID-19 group were more likely to have at least one comorbidity, to evolve to preterm labor and infant death, and to have positive SARS-CoV-2 RNA testing in their concepts. Compared to controls, placentas in the COVID-19 group were more likely to show features of maternal and

fetal vascular malperfusion. In the COVID-19 group, placentas of symptomatic women were more likely to show CHI. No significant results were found after morphometric analysis.

Conclusion: Pregnant women with symptomatic SARS-CoV-2 infection, particularly with the severe course, are more likely to exhibit an adverse fetal outcome, with slightly more frequent histopathologic findings of maternal and fetal vascular malperfusion, and CHI. The morphometric changes found in the placentas of the COVID-19 group do not seem to be different from those observed in the Control group, as far as maternal age, gestational age, and comorbidities are paired. Only the deposition of villous fibrin could be more accentuated in the COVID-19 group (p = 0.08 borderline). The number of HC/villous evaluated with CD68 immunohistochemistry did not show a difference between both groups.

Keywords: SARS-CoV-2, COVID-19, vertical transmission, placenta, morphometric analysis, placental histopathology

INTRODUCTION

One year after the recognition of the outbreak of the severe acute respiratory distress syndrome coronavirus 2 (SARS-CoV-2), it has spread all over the world, thus developing into a global pandemic with nearly 150 million confirmed infections and more than 3.1 million deaths worldwide so far (1). Fatalities and severe courses were primarily seen in elderly patients with relevant comorbidities, but soon there were reports of younger patients showing adverse outcomes (2, 3).

No longer after its first documented appearance, SARS-CoV-2 was suspected to be perinatally transmitted (4–8). This enveloped single-stranded RNA virus infects target cells by binding to angiotensin-converting enzyme 2 (ACE2) and entry into cells after spike protein cleavage by the transmembrane serine protease 2 (TMPRSS2). Since both proteins have been detected in the placenta and fetal tissues, a possible mechanism of intrauterine transmission and neonatal infection emerged (9–14), and the coronavirus disease 2019 (COVID-19) impact on pregnant women became of particular interest.

Along with the worldwide dissemination of COVID-19, reports of adverse pregnancy outcomes have emerged in the literature, such as preeclampsia, preterm delivery, miscarriage, intrauterine fetal demise, and neonatal death (15–18). Congenital infection can be challenging to characterize since pathogen detection usually requires specific methods, not always available, applied in a myriad of maternal and fetal samples. Despite that, antepartum or peripartum vertical transmission is now substantially documented. Almost 30% of neonatal infections reported to date occurred due to transplacental transmission, and the remaining due to environmental exposure. Additionally, Raschetti et al. observed that 55% of infected neonates developed COVID-19 (19–25).

It is well recognized that analysis of the placental histopathological changes can provide valuable information, considering that a variety of pathological agents, including infectious ones, are associated with characteristic morphological findings (26–29). Regardless, few papers describe the placenta's morphological and morphometrical features in SARS-CoV-2–positive pregnant women (30–34), and the association between maternal infection and abnormal placental findings is still to be determined.

Accordingly, the purpose of this study was to analyze clinical data and the morphological and morphometric changes in placentas of pregnant women infected with SARS-CoV-2 (COVID-19 group) and to compare the placentas of non-infected pregnant women (Control group) matched in a 1:1 fashion by gestational age at delivery, maternal age, and comorbidities.

MATERIALS AND METHODS

Ethical Approvals

The Brazilian National Ethics Committee approved the presented study of Human Experimentation under the protocol number CAAE: 35129820.6.0000.0096. Families signed the informed consent forms. The authors followed all relevant guidelines, regulations, and ethics and safety protocols during this study execution at all stages. The data that support the findings of this study are available from the corresponding author.

Study Design

A prospective observational case-control study.

Study Patients and Control Group Selection

For the COVID-19 group (study group), pregnant women with laboratory-confirmed infection, whose respective placenta specimens have been sent for histologic examination, were eligible for inclusion. This group comprises 19 women who had SARS-CoV-2 infection confirmed either in the second (n = 3) or in the third gestational trimester (n = 16). Initially, we included women who spontaneously sought treatment at Complexo Hospital de Clínicas, Universidade Federal do Paraná

(CHC-UFPR) or at Hospital Nossa Senhora das Graças (HNSG), Curitiba, Brazil, for symptoms of COVID-19 varying from mild to severe (n = 9). After the implementation of universal testing for SARS-CoV-2 infection for all obstetrical patients admitted to labor and delivery in both institutions, asymptomatic pregnant women were added thereafter (n=10).

For the Control group (n = 19), placentas of pregnant women who gave birth at CHC-UFPR in years prior to the SARS-CoV-2 outbreak were selected (from 2016 to 2018) and matched in a 1:1 fashion by gestational age at delivery, maternal age, and maternal comorbidities.

Historical controls were selected to ensure that women with false-negative test results for SARS-CoV-2 infection were excluded. Gestational age at delivery is a universally used matching variable since there is a correlation between placental development and the advancing gestation, which could interfere in the analysis. Maternal age and maternal comorbidities were also incorporated as matching variables, given their possible role as confounders when analyzing placental abnormalities.

Samples

Submission criteria for placental examination included maternal or fetal conditions previously diagnosed during prenatal care or gross abnormalities noted during delivery, as routinely implemented in both institutions. Therefore, the maternal-positive SARS-CoV-2 testing result was considered an abnormal maternal condition and a placental evaluation criterion.

All placentas were examined according to a standardized protocol that consisted of immediate fixation after delivery in 10 % buffered formalin for 72 h, gross examination with measurement of placental dimensions and chord length, weight evaluation of the placental disc after trimming of the fetal membranes and umbilical cord, followed by serial sectioning through 1.5-cm interval and cut surface examination. Macroscopic alterations were recorded and sampled. Additional representative samples of the umbilical cord (two sections), the membranes (one fetal membrane roll), and the chorionic plate (at least two full-thickness, non-peripheral sections including maternal and fetal surface) were submitted to paraffin embedding.

Clinical Information

Clinical and laboratory data were obtained from medical records during hospitalization; the mother and the newborn were followed up until discharge from the hospital.

Maternal information sought from each medical record for both groups comprised maternal age and comorbidities, parity, gestational age at delivery, mode of delivery, neonatal birth weight, and APGAR score. All pregnant women in both groups were tested for congenital intrauterine infections (TORCH) during prenatal care; only one (Patient code—PC 20-3744) tested positive for syphilis in the first trimester and received the preconized treatment.

For the study group, it was also retrieved the gestational age at and method used for SARS-CoV-2 infection diagnosis, presence or absence of symptoms typically attributed to COVID-19 (body temperature over 38°C, dyspnea, cough, myalgias, nausea and vomiting, diarrhea, headache, anosmia), disease severity (ranging from mild symptoms to critical organ dysfunction), and maternal outcome.

SARS-CoV-2 Testing

Maternal nasopharyngeal swabs specimens (n = 17) were tested for SARS-CoV-2 infection by real-time reverse transcriptase-polymerase chain reaction (RT-PCR). In the remaining two cases, the diagnosis was achieved by serologic testing (n = 2).

Detection of SARS-CoV-2 RNA in infants was performed in 13 case samples (n = 13), including umbilical cord blood (n = 13), amniotic fluid (n = 3), and infants' nasopharyngeal swabs specimens (n = 6), all of them collected immediately after birth. The mothers' milk was also tested in three cases.

Samples from formalin-fixed paraffin-embedded (FFPE) tissue were also tested to verify the presence of SARS-CoV-2 RNA in the placenta (n=11). Viral RNA extraction was performed with a commercially available paraffin extraction kit (Qiagen®) in Pelé Pequeno Príncipe Research Institute.

SARS-CoV-2 RNA identification tests were performed at CHC-UFPR and HNSG using XGEN MASTER COVID-19 Kit (Mobius Life Science, Inc, Brazil). Quantitative anti-SARS-CoV-2 IgM and IgG dosage was done in peripheral blood samples in both institutions.

Morphologic Analysis

All representative placental samples taken for microscopic assessment underwent routine processing, embedding, sectioning at 5 μm, and staining with hematoxylin and eosin (H&E).

The qualitative morphological analysis was performed in all placentas from the COVID-19 and Control groups (n = 38) using the Amsterdam Placental Workshop Group Consensus Statement (35). Histological sections containing at least one sample of the umbilical cord, membrane roll, and chorionic plate of every case from both groups were randomly selected and renamed by one research team member (blinding step). Two experienced perinatal pathologists systematically evaluated the slides.

Selected parameters were computed simply as "present" (yes) or "absent" (no). The extension and intensity of specific alterations were graded following Amsterdam protocol recommendations. The remaining parameters were subdivided into three quantitative categories: <30%, 30% to 70%, and > 70%, to record both the presence and extension of most alterations.

Assessed parameters included features of maternal vascular malperfusion (villous infarction, distal villous hypoplasia, accelerated villous maturation/increase in syncytial knots, decidual acute atherosis, decidual vascular fibrinoid necrosis with or without foam cells, decidual vascular mural hypertrophy, decidual chronic perivasculitis, absence of spiral artery remodeling, decidual arterial thrombosis, persistence of intramural endovascular trophoblast), features of fetal vascular malperfusion (fetal vascular thrombosis, fetal vascular intramural fibrin deposition, avascular villi, stem vessel obliteration/fibromuscular sclerosis, villous stromal-vascular karyorrhexis, vascular ectasia), delayed villous maturation, features of maternal inflammatory response (chorionitis, chorioamnionitis), features of fetal inflammatory response (umbilical vasculitis, funisitis), features

of chronic inflammation (chronic deciduous, villitis, intervillositis), intervillous thrombi, microcalcification foci, chorangiosis, and membrane meconium and hemosiderin staining.

Morphometric Analysis

The morphometric analysis included measurement of the perimeter and diameter of the villi, counting the number of tertiary villi, sprouts and knots of tertiary villi, quantifying the villous fibrin and the intra-villous collagen I and III depositions. It was performed in 11 cases of the COVID-19 group and eleven Control group cases (n = 22), matched for gestational age, maternal age, and maternal comorbidities.

One histological section stained with H&E containing at least one sample of the chorionic plate was randomly selected from every case in both groups (n = 22). Samples of grossly identified lesions were previously excluded. Each section was subsequently photographed at a magnification of 200× (medium power field—MPF) using the Scanner Axion Scan.Z1 (Zeiss AG, Oberkochen, Germany), resulting in about 5,000 high-resolution images for each case (ZEN Blue Edition, Zeiss, Germany). Following the exclusion of unfocused images, with artifacts, with non-villous tissue, or less than 100% of the field occupied with placental villi, the remaining images were randomized to obtain about 100 images for each case of both groups. The villi's perimeter and diameter were measured using Image-Pro Plus® 4 software, based on freehand drawing on 100 villi in consecutive images. At the end of each villus' contour, the program provided perimeter and minor diameter in micrometers (μm).

The variables number of tertiary villi, number of sprouts, and knots of tertiary villi were assessed by simply counting these microscopic structures by an experienced perinatal pathologist, in 30 of those 100 images, after a new cycle of randomization.

Histological sections were also stained with phosphotungstic hematoxylin (n = 22) and Sirius Red (n = 22), aiming to evaluate villous fibrin and intra-villous collagen I and III depositions, respectively. As previously described for H&E, the slides were photographed at MPF using the Scanner Axion Scan.Z1, and the resulting images were randomized to obtain about 200 images for every case of the COVID-19 and Control group for each stain. Positive control was chosen as a "mask," which contained adequate levels of specific pigment precipitation. The mask was then superimposed on the sample images, and Image-Pro Plus 4 software identified the positive areas, expressing the results as positive pigment deposition areas per μm^2. The values obtained for the collagen analysis were further divided by the observed field's total area, generating a percentage value for each image (36).

The morphometric analysis was also blind since each case was previously renamed by one member of the research team not involved in the data acquisition, and the images were also randomly generated by the software afterward, with no investigator's interference.

Immunohistochemistry

Histological sections of the placentas from both groups (n = 22) were fixed on electrically charged glass slides and subsequently dewaxed with heated xylol (37°C), dehydrated by successive baths of absolute ethyl alcohol with decreasing solution concentrations and rehydrated with water. Methyl alcohol and hydrogen peroxide were used to block endogenous peroxidase and distilled water and hydrogen peroxide for the second block. Next, incubation with anti-CD68 primary antibody (KP1 clone, monoclonal mouse, Biocare, California, USA) for 1 h and secondary antibody associated with the dextran polymer (Spring Bioscience, Pleasanton, USA) for 30 min. For development, DAB/substrate complex (DAB, DakoCytomation) was added onto the slides, followed by counterstaining with Mayer's hematoxylin, dehydration with ethyl alcohol baths in increasing concentrations, clarification with xylol, and blending with Canada balsam. The protocol developed and described above is already standardized and routinely used in CHC-UFPR. To quantify Hofbauer cells (HC), the number of villi and CD68+ cells in those villi were counted in 30 high-power random fields (HPF= 400×). Only positive cells morphologically compatible with histocytes, with visible nuclei, and located within villi were considered suitable for counting. Unspecific staining, staining of any other cells, and cells without visible nuclei were excluded.

All immunohistochemistry assays included a negative control (missing a primary antibody) and positive control (human lymph node).

Statistical Analysis

Means, standard deviations, medians, minimum, maximum values, frequencies, or percentages were used to describe the findings. The nominal variables are expressed as actual values and frequency and analyzed by Pearson chi-square test and or by Fisher exact test. Most of the quantitative variables exhibited normal distribution, as verified by the Shapiro–Wilk test, and were compared with the t-test. The Kruskal–Wallis non-parametric test was performed to compare the remaining quantitative variable between groups (fibrin deposition). For both tests, statistical significance was defined as a p-value of <0.05. The data were analyzed using the IBM SPSS Statistics v.20.0 software. Armonk, NY: IBM Corp.

RESULTS

Relevant clinical information about each case in both groups is summarized in **Tables 1** and **2**. Comparison between groups regarding clinical data and morphologic findings are resumed in **Table 3** (n = 38). In **Table 4**, morphometric data are presented along with clinical information of the cases evaluated from both groups (n = 22). **Figure 1** exemplifies morphometric and morphological parameters evaluated.

Maternal Clinical Profile and SARS-CoV-2 Testing Results

Among the nineteen patients testing positive for SARS-CoV-2 infection, almost half (9/19, 47.4%) were symptomatic. Three had COVID-19 symptoms varying from mild (fever, cough, among others, but without dyspnea) to moderate (with dyspnea, but without the necessity of complementary life

TABLE 1 | Clinical information of the COVID-19 group.

Patient code	Maternal age (yr)	Maternal Comorbidities	COVID-19 Symptoms/ Severe Disease	SARS-CoV-2 testing			Outcome			
				RT-PCR Maternal NS swab/ Trimester	Maternal Serology	RT-PCR placenta/ RT-PCR fetal samples	Gestational age at delivery	APGAR (1 min/5 min)/ Fetal-Maternal Outcome	Fetal weight (g)	Placental weight (g)/ Macroscopic alterations
20–3594	26	Hypertensive disorder in pregnancy and hypothyroidism	+/+	+/3rd	IgM+/IgG+	–/–	33	(5/9) Preterm newborn	2450	448/Infarcts (<5%)
20–3561	38	Hypothyroidism	+/+	*/2nd	IgM+/IgG+	–/–	28+2	(na) Preterm newborn	na	245
20–3282	40	*Situs inversus totalis* with metallic stent	+/+	+/3rd	na	–/+**	33+5	(0/0) Neonatal death/ Maternal death	2300	416
20–5379	38	Gestational diabetes	+/+	+/2nd	na	–/+**	23+6	(1/5) Neonatal death/ Maternal death	610	168/Placental hypoplasia
20–3744	29	Gestational diabetes, hypothyroidism, obesity, bipolar disorder, and syphilis (treated)	+/–	+/3rd	IgM+/IgG+	–/+**	34+1	(na) Preterm newborn	na	412/Infarcts (<5%)
20–5105	29	None	–	+/3rd	na	–/na	38+6	(9/10) Term newborn	2960	462
20–3369	29	Gestational diabetes and Hyperthyroidism	+/–	+/3rd	na	–/na	37+4	(8/9) Term newborn	2600	358/Infarcts (<5%)
20–3364	42	Hypertensive disorder in pregnancy	+/+	+/2nd	IgM+/IgG+	+/+§	28+3	Intrauterine death	1020	135/Placental hypoplasia and infarcts (30–40%)
20–5776	42	None	–	+/3rd	na	–/+**	36+5	(9/10) Preterm newborn	2605	382
20–5869	27	None	+/–	+/3rd	na	–/na	37+2	(9/10) Term newborn	2345	370
20–3916	24	None	–	+/3rd	IgM+/IgG+	–/na	38+6	(9/10) Term newborn	3030	650
20–4850	25	Obesity	+/+	+/3rd	na	na/–	30+2	(na) Preterm newborn	na	410
20–5006	22	Obesity	–	+/3rd	na	na/–	41+0	(4/9) Term newborn	3110	670
20–5009	23	Hypothyroidism	–	*/3rd	IgM+/IgG+	na/–	38+4	(5/9) Term newborn	3925	775/Hydropic placenta
20–5031	35	Gestational diabetes, obesity	–	+/3rd	na	na/–	36+4	(8/9) Preterm newborn	2720	450
20–6551	32	None	–	+/3rd	na	na/na	38+5	(8/9) Term newborn	3070	448
20–6680	38	None	–	+/3rd	na	na/na	37	(9/10) Term newborn	2875	318
20–7035	34	None	–	+/3rd	na	na/–	39	(9/9) Term newborn	3115	438
20–6071	34	Hypertensive disorder in pregnancy	–	+/3rd	na	na/–	34+6	(7/8) Preterm newborn	2370	384

**rt-PCR not available—diagnostic by serology.*

*RT-PCR positive in fetal samples: **Nasofaringeal swab and §Umbilical cord blood.*

na, not available.

TABLE 2 | Clinical information of the Control group.

Patient code	Maternal age (yr)	Maternal Comorbidities	Outcome			
			Gestational age at delivery	APGAR (1 min/5 min)/ Fetal Outcome	Fetal weight (g)	Placental weight (g) Macroscopic alterations
16–7859	20	Hypothyroidism	32+3	(3/7) Preterm newborn	1180	270/Placental hypoplasia
18–13016	23	Chronic hypertension and hypothyroidism	35+2	(4/8) Preterm newborn	2223	498/none
16–8315	18	Obesity	40+4	(7/9) Term newborn	3810	514 none
18–4906	20	None	28	(7/8) Preterm newborn	1205	248/none
18–14057	42	Diabetes, chronic hypertension, bipolar disorder	33+4	(2/8) Preterm newborn	1650	243/Placental hypoplasia
16–7599	25	Gestational diabetes	39	(8/10) Term newborn	3460	480/none
16–3340	39	None	38+3	(7/9) Term newborn	3005	395/none
18–9951	24	None	37+2	(8/9) Term newborn	3690	574/none
16–6144	29	None	39	(9/10) Term newborn	3345	394/none
17–2491	35	None	32+4	(8/9) Preterm newborn	2900	416/none
16–7667	36	None	36+4	(9/9) Preterm newborn	2315	319/none
18–5040	24	None	32+4	(1/6/8) Preterm newborn	1555	297/Infarcts (5%)
16–7155	25	Obesity	40	(7/9) Term newborn	2830	375/none
16–5762	39	Hypothyroidism	39+3	(8/9) Term newborn	3490	465/Infarcts (10%)
18–11859	38	Gestational diabetes, obesity	36+1	(6/9) Preterm newborn	2925	450/none
18–5502	27	None	37+2	(7/9) Term newborn	2500	552/none
16–3787	24	None	37+4	(9/10) Term newborn	2945	461/none
18–4510	19	None	40+2	(7/8) Term newborn	1990	413/none
18–6601	16	Hypertensive disorder in pregnancy	24+5	(8/9) Preterm newborn	2235	368/none

support) (3/9, 33.3%). Six developed severe courses, requiring orotracheal intubation and hemodynamic support within less than seven days after admission (6/9, 66.6%). Two of them died due to COVID-19 associated complications (2/6, 33.3%).

Twelve patients of the COVID-19 group had at least one comorbidity (12/19, 63.2%), such as hypertension (3/19, 15.8%), diabetes (4/19, 21%), obesity (4/19, 21%), and hypothyroidism (4/19, 21%). One patient had a diagnosis of Kartagener syndrome (chronic sinusitis, bronchiectasis, and situs inversus with dextrocardia) and had a cardiac valvar replacement (metallic) for 10 years (Patient code—PC 20-3282).

Most pregnant women tested positive for SARS-CoV-2 in the third gestational trimester (16/19, 84.2%), either immediately before delivery in asymptomatic patients or within less than 15 days from delivery in symptomatic ones.

Only three patients had a positive result in the second trimester, all of them with severe COVID-19 symptoms and equally close to delivery. In this subgroup, one woman died due to COVID-19 complications along with her infant (PC 20-5379). One had an intrauterine demise (PC 20-3364) and recovered utterly afterward. The third evolved to preterm labor (PC 20-3561).

Newborns Clinical Outcome and SARS-CoV-2 Testing Results

The mode of delivery, APGAR score, placental weight, fetal weight, fetal/placental weight ratio were similar between both groups (p=NS).

Among the 19 infants in the COVID-19 group, sixteen were born alive (16/19, 84.2%). We observed three infant deaths, being one intrauterine demise and two neonatal deaths within hours of delivery (3/19, 15.8%). All infant deaths occurred in women with severe COVID-19 symptoms, including the two who died due to COVID-19 complications (PC 20-3282 and 20-5379). In the Control group, all infants were born alive.

Preterm delivery was recorded in ten cases (10/19, 52.6%), including those with infant deaths mentioned above. In the Control group, nine pregnancies ended prematurely (9/19, 47.4%), a similarity that was expected due to methodological design. However, there were no recorded infant or maternal deaths.

SARS-CoV-2 RNA was detected in samples from five infants among thirteen tested (5/13, 38.4%). It was positive in one cord blood sample (PC 20-3364) and four newborns nasopharyngeal swabs specimens (PC 20-3282, 20-5379, 20-3744, and 20-5776). All amniotic fluid and mother's milk samples tests returned negative.

From all FFPE placental tissue tested (n = 11), only one case was positive for SARS-CoV-2 RNA, being the case of intrauterine demise (PC 20-3364).

Morphologic Alterations

All parameters enumerated in *Materials and Methods* were sought systematically. Many of them were not identified in any sample. The histopathological alterations identified in both groups are listed in **Table 3** and discussed below.

Morphometric Alterations and Immunohistochemistry Evaluation

The average number of sprouts and knots (per villous) of the COVID-19 group tertiary villi was 0.19 and 0.81, respectively, compared to 0.16 and 0.81 of the Control group (p=NS). The average perimeter of the COVID-19 group tertiary villi was 271.93 μm compared to 288.42 μm in the Control group (p=0.37).

TABLE 3 | Clinical and morphological comparisons between COVID-19 group (n=19) and Control group (n=19) placentas.

		Variable	Control	COVID-19	*p*-value
Clinical data	**Maternal**	Maternal age (years)	25 (16–42)	32 (22–42)	0.21
		Gestational age (weeks)	36 (23–40)	36 (23–41)	0.97
		Comorbidities	Hypertensive disorder (3) Gestational diabetes (3) Obesity (3) Hypothyroidism (3) None (11)	Hypertensive disorder (3) Gestational diabetes (4) Obesity (4) Hypothyroidism (4) None (7)	1
	Fetal	APGAR 1 min/5 min	7 (1–9)/9 (6–10)	8(0–9)/9 (0–10)	0.41/0.33
		Fetal weight (grams)	2865 (1,180–3,810)	2663 (610–3,925)	0,94
		Placental Weight (grams)	406 (243–573)	412 (135–775)	0,79
		Placental diameter (centimeters)	17 (12–19)	16 (12–22)	0,87
		Infant death	0	3	**0.09**
		Preterm delivery	9	10	0.74
		Term delivery	10	9	0.74
Morphological variables	**MVM**	Villous infarction	5	2	0.21
		Distal villous hypoplasia	6	4	0.46
		Accelerated villous maturation/increase in syncytial knots	5	8	0.30
		Decidual vascular mural hypertrophy	5	10	**0.09**
		Absence of spiral artery remodeling	1	6	**0.03**
		Decidual vascular fibrinoid necrosis without foam cells	1	3	0.29
		Decidual vascular fibrinoid necrosis with foam cells	0	2	0.14
		Decidual arterial thrombosis	0	1	0.31
	FVM	Avascular villi small foci	1	1	1.0
		Avascular villi intermediate foci	1	0	0.31
		Fetal vascular thrombosis	1	6	**0.03**
		Fetal vascular thrombosis—umbilical cord	0	5	**0.02**
		Fetal vascular intramural fibrin deposition (non-occlusive)	0	2	0.14
		Vascular ectasia	2	1	0.54
	DVM	Delayed villous maturation (focal - <30%)	1	4	0.15
		Delayed villous maturation (extensive - >70%)	2	2	1.0
	CI	Chronic deciduitis—non-intense	17	16	0.31
		Chronic deciduitis—intense	1	0	0.29
		Villitis—low grade	1	1	1.0
		Chronic intervillositis—low grade	3	2	0.63
		Chronic intervillositis—high grade	1	2	0.54
	MIR	Subchorionitis/chorionitis	5	6	0.72
		Chorioamnionitis—non-intense	2	0	0.14
		Chorioamnionitis (necrosis)—intense	0	1	0.31
	FIR	Umbilical vasculitis	2	1	0.63
	Others	Intervillous thrombi	3	1	0.29
		Villous fibrin (focal—<30%)	15	14	0.70
		Villous fibrin (multifocal 30–70%)	3	5	0.42
		Villous fibrin (extensive—>70%)	1	0	0.31
		Villous edema	3	4	0.70
		Chorangiosis	4	3	0.42

p-value refers to the comparison between COVID-19 vs. the Control group; relevant values are highlighted (bold). p-value < 0.05. MVM, maternal vascular malperfusion; FVM, fetal vascular malperfusion; DVM, delayed vilous maturation; CI, chronic inflammation; MIR, maternal inflammatory response; FIR, fetal inflammatory response.

The mean diameter of the COVID-19 group tertiary villi was 51.78 μm than 50.52 μm in the Control group (p=0.57).

The quantitative morphometric analysis of deposition of villous fibrin revealed an average area of 686.64 μm^2 in the COVID-19 group compared to 485.36 μm^2 in the Control group (p=0.08 - borderline).

The quantitative morphometric analysis of deposition of intra-villous collagen I and III revealed that COVID-19 group average areas were 36.40% and 63.60%, respectively, compared to 41.01% and 58.99% of the Control group (p=0.45).

HC counting revealed an average number of 1,7 CD68+ cell/villous in the COVID-19 group and 1,2 CD68+ cell/villous in the Control group (p=0.12).

DISCUSSION

New insights are being acquired on SARS-CoV-2 infection pathophysiology. COVID-19 is associated with an exaggerated inflammatory response, usually proportional to the disease's

TABLE 4 | Clinical and morphometrical comparisons between COVID-19 group (n=11) and Control group (n=11) placentas.

		Variable	Control	COVID-19	*p*-value
Clinical data	**Maternal**	Maternal age (years)	28.3 (18–42)	33 (26–42)	0.41
		Gestational age (weeks)	33.9 (23–39)	33.6 (23–38)	0.78
		Comorbidities	Hypertensive disorder (2) Gestational diabetes (2) Hypothyroidism (2) None (7)	Hypertensive disorder (2) Gestational diabetes (2) Hypothyroidism (2) None (4)	1
	Fetal	APGAR 1 min/5 min	6.5 (2–9)/8.7 (7–10)	6.6(0–9)/7 (0–10)	0.59/0.48
		Fetal weight (grams)	2656 (1,180–3,810)	2213 (610–3,030)	0.94
		Placental Weight (grams)	395 (243–573)	367 (135–650)	0.87
		Fetal/Placental ratio	6.74 (4.3–8.4)	5.96(3.63–7.55)	0.61
		Placental diameter (centimeters)	16.45 (13–19)	16.2 (12–20)	0.88
		Infant death	0	3	0.11
		Preterm newborn	7	6	0.66
		Term newborn	4	4	0.66
Morphometric variables	**HE**	Villi number	9.0 (5.3–14.5)	8.3 (4.7–10.9)	0.62
		Knots/villus	0.81 (0.6–1.0)	0.81 (0.6–1.0)	0.97
		Sprouts/villus	0.16 (0.1–0.3)	0.19 (0.1–0.5)	0.92
		Villus diameter	50.52 (43.4–58.8)	51.4 (45.5–63.0)	0.57
		Villus perimeter	288.42 (202.7–368.5)	271.93(213.8–358.4)	0.37
	HPt	Fibrin area (μm^2)	485.36(61.9–1749.6)	686.64 (170.3–2053.0)	**0.08**
	SiriusRed	Collagen I percentage	41.01(10.1–66.1)	36.40(13.8–68.6)	0.45
		Collagen III percentage	58.99(33.9–89.9)	63.60 (31.4–86.2)	0.45
Immunohistochemistry		CD68+ Hofbauer cell/villous	1.2	1.7	0.12

p-value refers to the comparison between COVID-19 vs. the Control group; relevant values are highlighted (bold). p-value < 0.05. HPt, phosphotungstic hematoxylin.

severity, recognized as a cytokine storm (37). Such inflammatory alterations cause endothelial damage and disruption in the coagulation system, which may play a direct pathogenic role in the disease (38). Reports of hypercoagulability, with d-dimer elevation, development of ischemic changes as gangrene of extremities, and even disseminated intravascular coagulopathy, are not uncommon. There is emerging evidence that at least part of COVID-19 manifestations is associated with a systemic thrombotic and microvascular injury (39–45). In pregnant women, when coagulation is already altered by pregnancy itself, the impact of COVID-19 is still the object of study.

In this context, placental findings are invaluable. To date, histopathological alterations described encompass maternal vascular malperfusion (MVM) features, including low placental weight, accelerated villous maturation, decidual vasculopathy, and infarcts. The MVM findings are frequently observed in placentas from pregnant women with hypertensive disorders, such as gestational hypertension and preeclampsia, and have been associated with oligohydramnios, preterm birth, and stillbirth. Fetal vascular malperfusion (FVM) alterations have been described as well, such as focal thrombosis of fetal placental vessels (30–34, 46). However, various authors did not identify a correlation between placental lesions and maternal infection, notably when the samples analyzed were obtained from uninfected placentas and infants (47).

Interestingly, in cases with confirmed transplacental infection, inflammatory alterations were more frequently observed, particularly chronic histiocytic intervillositis with trophoblast necrosis. In these cases, SARS-CoV-2 was detected in the syncytiotrophoblast by immunohistochemistry and or RNA *in situ* hybridization (48, 49). It is not yet clear if the syncytiotrophoblast destruction is caused by a direct viral effect or is secondary to inflammatory or ischemic injury. Whichever mechanism is involved, the damage of this protective villous layer can facilitate fetal infection.

Recognition of the disease's impact on the placenta, and the maternal-fetal response's nature, may help understand the processes involved in pathogenesis, and ultimately, it may lead to an explanation for an adverse outcome.

Maternal Clinical Profile and SARS-CoV-2 Testing Results

There were no significant differences in maternal age, gestational age at delivery, and maternal comorbidities profile between groups, thus corroborating that matching variables were adequately paired (p=NS).

In our COVID-19 group, the proportion of symptomatic patients is elevated (9/19, 47.4%). Since patients' recruitment was done at the beginning of the pandemic, almost half of our cases correspond to symptomatic patients. After the universal screening was adopted, asymptomatic patients were also incorporated into the study.

In the literature, pregnant women's outcomes have not been worse when compared to non-pregnant adult individuals. The severity of the COVID-19 seems to be related to existing comorbidities, like hypertension, obesity, among others (50–53), similarly to the general population. Most symptomatic patients in our study group had at least one comorbidity (8/9, 89%), including all the severely ill ones. In comparison, less than half of asymptomatic women had one comorbidity (4/10, 40%), and only one patient without comorbidities presented with mild symptoms (1/7, 15%—PC 20-5869).

Two women died from COVID-19 complications (PC 20-3282 and PC 20-5379). Both died shortly after hospitalization (three and one days after admission, respectively).

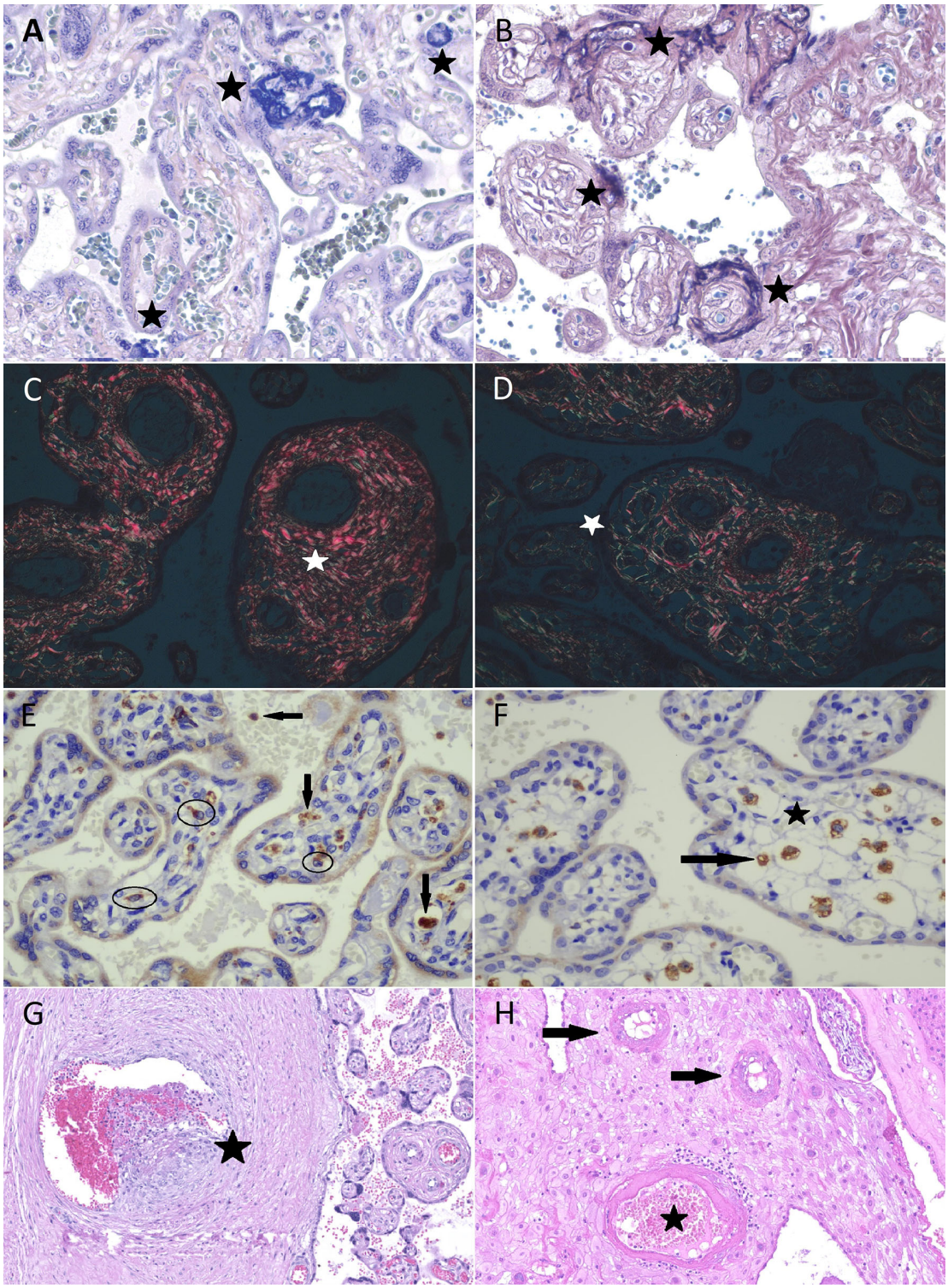

FIGURE 1 | Morphometric and morphological analysis of placental specimens from women infected with SARS-CoV-2 (COVID-19 group) and the Control Group. Fibrin deposition evaluation in COVID-19 group **(A)** and Control group **(B)** in phosphotungstic hematoxylin (star—deep blue amorphous material); both perivillous and intravillous deposition were included. Sirius Red: bright red collagen I **(C)** and green collagen III fibers **(D)** under polarized light. Photomicrography of immunostaining with CD68 (KP1 Clone, Biocare) in COVID-19 group **(E)** and in Control group **(F)**; eligible Hofbauer cells to counting (circled cells and those near the star). Macrophages outside villi and unspecific marking were excluded (arrows). Fetal vascular thrombosis **(G)** and decidual vasculopathy **(H)** in COVID-19 cases.

Newborns Clinical Outcome and SARS-CoV-2 Testing Results

The newborn outcome was directly related to the mother's health status among women with COVID-19. In patients with severe disease, the conceptus health deteriorated after Intensive Care Unit admission in all cases. Thus, not surprisingly, an adverse fetal outcome was more likely to occur in symptomatic patients (7/9, 77.7%) when compared to asymptomatic ones (3/10, 30%). Most of the asymptomatic patients had term deliveries (7/10, 70%) without recorded complications.

When considering patients with comorbidities (12/19, 63.2%), eight gestations ended prematurely (8/12, 66.6%). This proportion is slightly higher than what was observed in the Control group (5/9, 55.5%), even though clinical variables were adequately paired. Compared to the Control group, COVID-19 was also more frequently associated with maternal and infant deaths (although not statistically significant, p = 0.09).

Pertaining perinatal transmission of SARS-CoV-2, published reports to date suggest that it occurs, but is considered rare, with less than 2% of neonates with positive results until 24 h of life (54, 55).

Schwartz et al. proposed that positive samples for SARS-CoV-2 RNA collected within the initial 72 h of life can be considered diagnostic of early-onset COVID-19 infection. The probability that the infection resulted from the vertical transmission is even greater if the test is performed until 24 h of life (very early-onset COVID-19 infection). The authors also proposed that in cases where pregnant women and their neonates both tested positive for SARS-CoV-2, transplacental transmission could be confirmed by demonstrating the virus in fetal-derived placental tissue using immunohistochemistry to demonstrate SARS-CoV-2 antigens or RNA *in situ* hybridization to demonstrate viral nucleic acid (56). The World Health Organization recently published a manual with a definition and categorization of the timing of mother-to-child transmission of the SARS-CoV-2. Since various fetal samples are prone to cross-contamination, it preconizes rigorous methodology for sample gathering and strict criteria for establishing congenital transmission. Viral detection should be preferably performed in sterile samples, collected at birth, using nucleic acid detection techniques to confirm transplacental transmission (54).

From newborns' nasopharyngeal swabs and umbilical cord blood specimens tested, five resulted positive and were considered a possible congenital infection, or very early-onset COVID-19 infection, by the criteria above.

In two cases, the newborns were healthy until hospital discharge (PC 20-3744 and 20-5776). Two cases resulted in short-term neonatal deaths (PC 20-3282 and 20-5379); the families did not authorize postmortem evaluation in both cases. None of them exhibited symptoms attributable to SARS-CoV-2 disease.

In the fifth positive infant, a stillborn, SARS-CoV-2 RNA was detected in the umbilical cord blood sample collected immediately after delivery and in the placental FFPE tissue (PC 20-3364). An autopsy was performed, and evaluation of fetal tissues showed mild microglial hyperplasia, mild lymphocytic infiltrate, and edema in skeletal muscle. Other findings were unspecific and probably caused by intrauterine asphyxia. All fetal tissue samples tested negative for viral RNA. The authors (57) previously reported those results.

Morphologic Alterations

Our samples exhibited alterations spanning all major Amsterdam Placental Workshop Group Consensus Statement categories (MVM, FVM, delayed villous maturation, and inflammatory features). Most of them exhibited similar distribution between the two groups, which was expected due to the matching process. However, some results were unexpected.

Although maternal age and comorbidities were adequately matched, COVID-19 group placentas were more likely to show some MVM features when compared to controls, particularly signs of decidual vasculopathy. Decidual vascular mural hypertrophy was more frequently observed in the COVID-19 group (but did not reach statistical significance, p = 0.09). Ten patients exhibited this alteration (10/19, 56.6%), the majority without a recorded hypertensive disorder (7/10, 70%). In contrast, three of the five women with decidual vascular mural hypertrophy in the Control group had a hypertensive disorder.

The absence of spiral artery remodeling was significantly more frequent in the COVID-19 group (p=0,03). Six patients (6/19, 31.6%) exhibited this alteration combined with decidual vascular fibrinoid necrosis, mainly in women without the hypertensive disorder (5/6, 83.3%). In the Control group, those findings were noticed in only two cases, both in women with hypertension. Decidual arterial thrombosis was observed in only one case that ended with maternal and fetal death (PC 20-5379).

Accelerated villous maturation or increase in syncytial knots was similar in both groups, and those findings are supported by the morphometric analysis results discussed below. On the other hand, villous infarction and distal villous hypoplasia were less frequent in the study group.

Those findings are in consonance with previous reports describing higher decidual arteriopathy rates as a maternal vascular malperfusion feature in SARS-CoV-2 infected women. According to Shanes et al., though at least some of those alterations are thought to be chronic, its precise time of development is not precisely known, and as decidual arteriopathy appears to be more strongly related to COVID-19, it may be originating from a different mechanism (30).

Fetal vascular thrombosis was the FVM feature more frequently observed in our COVID-19 group. It was present in six cases (6/19, 31,5%), a significantly higher rate than in the Control group (p = 0.03). Of note, one case corresponded to the mother with Kartagener syndrome that evolved to maternal and neonatal death (PC 20-3282). In the Control group, this finding was detected only in one case, the mother showing no comorbidity (PC 20-5502). The distal lesions in villi indicative of fetal malperfusion were similar between both groups.

The frequency of inflammatory changes was similar between groups. Chronic histiocytic intervillositis, characterized by the accumulation of histocytes in the intervillous space, belongs to this category. In the context of COVID-19, such alteration is not frequently reported, and when present, was associated with

adverse fetal outcomes and or with documented newborn infection by SARS-CoV-2 (30–33, 48, 49).

We identified chronic histiocytic intervillositis in four of our cases (PC 20-3282, PC 20-5379, PC 20-3364, and PC 20-4850). All four mothers with placentas having this finding had a severe COVID-19 course; two of them died. Their infants were prematurely born; three of them were positive for SARS-CoV-2 RNA in nasopharyngeal swab or umbilical cord blood samples. Those three died as well.

In the three cases that resulted in maternal and or infant death (PC 20-3282, PC 20-5379, PC 20-3364), features of MVM, FVM, and inflammatory changes were identified in various combinations. However, only in one case (PC 20-3364), MVM and FVM features were more intense and exhibited a broader distribution throughout the placenta than other specimens from both groups. This patient had a hypertensive disorder as well; because of that, those alterations cannot be attributed entirely to viral injury, even though COVID-19 may have a contributory role in the pathophysiology. Of note, chronic histiocytic intervillositis was observed in all three, two of them categorized as high grade (PC 20-5379, PC 20-3364).

Considering only the two cases that resulted in maternal deaths, placental findings were similar to those observed in the COVID-19 group, except for the presence of chronic histiocytic intervillositis.

Although the frequency of chronic histiocytic intervillositis was similar in COVID-19 and Control groups, this finding was not associated with adverse outcomes in the Control group. Interestingly, in the COVID-19 group, this finding was more frequently observed in placentas of severely ill patients, including those that died from COVID-19 complications, those associated with infant deaths, and with a positive SARS-CoV-2 RNA test in fetal tissues.

Morphometric Alterations and Immunohistochemistry Evaluation

Measurements of villi, such as diameter and perimeter, and counting of sprouts and knots in tertiary villi, aimed to evaluate villi maturity objectively (58, 59). Changes found in the placentas of the COVID-19 group do not seem to be different from those observed in the Control group, as far as maternal age, gestational age, and comorbidities are paired. Those data corroborate the morphological impression that villous maturity retardation or acceleration was not different between our COVID-19 and Control groups.

Fibrosis can be the final event after villi damage, following inflammatory, infectious, or vascular insults, such as described in FVM physiopathology (60). The relative amount of villous fibrosis estimated by evaluation of collagen I and III depositions with Sirius Red histochemical stain showed no difference between groups. There was no difference between groups for global collagen deposition analysis as well, meaning that there was no relative increase in the amount of villous fibrosis in the COVID-19 group.

The amount of fibrin deposited in the villi evaluated by the phosphotungstic hematoxylin histochemical stain could be more accentuated in the COVID-19 group since the difference between groups was borderline. However, such borderline difference between COVID-19 and Control groups was not perceived at the morphological analysis. In the qualitative evaluation, fibrin deposition seemed to be similarly increased in both groups, both in perivillous and intravillous topography.

The number of HC per tertiary villi was also similar between groups. This finding suggests that, at least in perinatally infected women, villous histocytes did not proliferate, and HC hyperplasia may not be as involved in the physiopathology of COVID-19 in the placenta as described for other viruses like Zika virus or HIV (28, 61–63).

In conclusion, pregnant women with symptomatic SARS-CoV-2 infection, particularly with the severe course, are more likely to exhibit an adverse fetal outcome, with slightly more frequent histopathologic findings of maternal and fetal vascular malperfusion, and chronic histiocytic intervillositis. The morphometric changes found in the placentas of the COVID-19 group do not seem to be different from those observed in the Control group, as far as maternal age, gestational age, and comorbidities are paired. Only the deposition of villous fibrin could be more accentuated in the COVID-19 group ($p = 0.08$ borderline). The number of HC/villous evaluated with CD68 immunohistochemistry did not show a difference between both groups.

DATA AVAILABILITY STATEMENT

The original contributions presented in the study are included in the article/supplementary material. Further inquiries can be directed to the corresponding authors.

ETHICS STATEMENT

The studies involving human participants were reviewed and approved by Comitê de Ética em Pesquisa em Seres Humanos do Hospital de Clínicas da Universidade Federal do Paraná. The patients/participants provided their written informed consent to participate in this study.

AUTHOR CONTRIBUTIONS

DP, AO, and VD contributed to collecting SARS-CoV-2 patients' samples and medical records in HNSG. IF and JL contributed to the collection of SARS-CoV-2 patients' samples and medical records in CHC-UFPR. AZ and AF contributed to the RNA extraction and RT-PCR reactions in HNSG. MN, BC, and CD were responsible for the RT-PCR reactions in CHC-UFPR. ES was responsible for selecting the controls and contributed to the immunohistochemistry analysis. PR was responsible for morphological and morphometrical analysis, interpretation of data, and drafted the manuscript. JD and EH contributed to the literature review and morphometrical analysis (Phosphotungstic hematoxylin). FD contributed with morphometrical analysis (Sirius

Red). AP contributed with morphological analysis. SR supported the experiments and contributed to the RT-PCR reactions in CHC-UFPR. CM-S supported the experiments and was responsible for the statistical analysis. NC contributed to the manuscript revision. LN supported the experiments, supervised the project, and was a significant contributor to the manuscript review. All authors contributed to the article and approved the submitted version.

FUNDING

This research was funded by productivity research level 2 of the National Council for Scientific and Technological Development (CNPq) and by Pontificia Universidade Católica do Paraná with resources from BRDE, Banco Regional de Desenvolvimento do Extremo Sul.

ACKNOWLEDGMENTS

The authors express their gratitude to Seigo Nakashima for performing the image acquisition from slides and support with software usage (ZEN Blue Edition and Image-Pro Plus 4) and Maurício de Oliveira and Katiucia Thiara Fantinel Picolli for histochemical and immunohistochemical techniques. Also, to CAPES, CNPq, and BRDE/PUC-PR for financial support.

REFERENCES

1. World Health Organization. *Coronavirus (COVID-19) Dashboard* (2021). Available at: https://covid19.who.int/ (Accessed April 26, 2021).
2. Petrilli CM, Jones SA, Yang J, Rajagopalan H, O'Donnell L, Chernyak Y, et al. Factors Associated With Hospital Admission and Critical Illness Among 5279 People With Coronavirus Disease 2019 in New York City: Prospective Cohort Study. *BMJ* (2020) 369:m1966. doi: 10.1136/bmj.m1966
3. Docherty AB, Harrison EM, Green CA, Hardwick HE, Pius R, Norman L, et al. ISARIC4C Investigators. Features of 20 133 UK Patients in Hospital With covid-19 Using the ISARIC Who Clinical Characterization Protocol: Prospective Observational Cohort Study. *BMJ* (2020) 369:m1985. doi: 10.1136/bmj.m1985
4. Zhu H, Wang L, Fang C, Peng S, Zhang L, Chang G, et al. Clinical Analysis of 10 Neonates Born to Mothers With 2019-nCoV Pneumonia. *Transl Pediatr* (2020) 9(1):51–60. doi: 10.21037/tp.2020.02.06
5. Zeng H, Xu C, Fan J, Tang Y, Deng Q, Zhang W, et al. Antibodies in Infants Born to Mothers With COVID-19 Pneumonia. *JAMA* (2020) 323(18):1848–9. doi: 10.1001/jama.2020.4861
6. Dong L, Tian J, He S, Zhu C, Wang J, Liu C, et al. Possible Vertical Transmission of SARS-CoV-2 From an Infected Mother to Her Newborn. *JAMA* (2020) 323(18):1846–8. doi: 10.1001/jama.2020.4621
7. Alzamora MC, Paredes T, Caceres D, Webb CM, Valdez LM, La Rosa M. Severe COVID-19 During Pregnancy and Possible Vertical Transmission. *Am J Perinatol* (2020) 37(8):861–5. doi: 10.1055/s-0040-1710050
8. Zeng L, Xia S, Yuan W, Yan K, Xiao F, Shao J, et al. Neonatal Early-Onset Infection With SARS-CoV-2 in 33 Neonates Born to Mothers With COVID-19 in Wuhan, China. *JAMA Pediatr* (2020) 174(7):722–5. doi: 10.1001/jamapediatrics.2020.0878
9. Hecht JL, Quade B, Deshpande V, Mino-Kenudson M, Ting DT, Desai N, et al. SARS-CoV-2 can Infect the Placenta and is Not Associated With Specific Placental Histopathology: A Series of 19 Placentas From COVID-19-positive Mothers. *Mod Pathol* (2020) 33(11):2092–103. doi: 10.1038/s41379-020-0639-4
10. Mulvey JJ, Magro CM, Ma LX, Nuovo GJ, Baergen RN. Analysis of Complement Deposition and Viral RNA in Placentas of COVID-19 Patients. *Ann Diagn Pathol* (2020) 46:151530. doi: 10.1016/j.anndiagpath.2020.151530
11. Smithgall MC, Liu-Jarin X, Hamele-Bena D, Cimic A, Mourad M, Debelenko L, et al. Third-Trimester Placentas of Severe Acute Respiratory Syndrome Coronavirus 2 (SARS-CoV-2)-positive Women: Histomorphology, Including Viral Immunohistochemistry and in-Situ Hybridization. *Histopathology* (2020) 77(6):994–9. doi: 10.1111/his.14215
12. Penfield CA, Brubaker SG, Limaye MA, Lighter J, Ratner AJ, Thomas KM, et al. Detection of Severe Acute Respiratory Syndrome Coronavirus 2 in Placental and Fetal Membrane Samples. *Am J Obstet Gynecol MFM* (2020) 2(3):100133. doi: 10.1016/j.ajogmf.2020.100133
13. Patanè L, Morotti D, Giunta MR, Sigismondi C, Piccoli MG, Frigerio L, et al. Vertical Transmission of Coronavirus Disease 2019: Severe Acute Respiratory Syndrome Coronavirus 2 RNA on the Fetal Side of the Placenta in Pregnancies With Coronavirus Disease 2019-Positive Mothers and Neonates at Birth. *Am J Obstet Gynecol MFM* (2020) 2(3):100145. doi: 10.1016/j.ajogmf.2020.100145
14. Lamouroux A, Attie-Bitach T, Martinovic J, Leruez-Ville M, Ville Y. Evidence for and Against Vertical Transmission for Severe Acute Respiratory Syndrome Coronavirus 2. *Am J Obstet Gynecol* (2020) 223(1):91.e1–4. doi: 10.1016/j.ajog.2020.04.039
15. Joudi N, Henkel A, Lock WS, Lyell D. Preeclampsia Treatment in Severe Acute Respiratory Syndrome Coronavirus 2. *Am J Obstet Gynecol MFM* (2020) 2(3):100146. doi: 10.1016/j.ajogmf.2020.100146
16. Gidlöf S, Savchenko J, Brune T, Josefsson H. COVID-19 in Pregnancy With Comorbidities: More Liberal Testing Strategy is Needed. *Acta Obstet Gynecol Scand* (2020) 99(7):948–9. doi: 10.1111/aogs
17. Lokken EM, Walker CL, Delaney S, Kachikis A, Kretzer NM, Erickson A, et al. Clinical Characteristics of 46 Pregnant Women With a Severe Acute Respiratory Syndrome Coronavirus 2 Infection in Washington State. *Am J Obstet Gynecol* (2020) 223(6):911.e1–911.e14. doi: 10.1016/j.ajog.2020.05.031
18. Pierce-Williams RAM, Burd J, Felder L, Khoury R, Bernstein PS, Avila K, et al. Clinical Course of Severe and Critical Coronavirus Disease 2019 in Hospitalized Pregnancies: A United States Cohort Study. *Am J Obstet Gynecol MFM* (2020) 2(3):100134. doi: 10.1016/j.ajogmf.2020.100134
19. Kirtsman M, Diambomba Y, Poutanen SM, Malinowski A, Vlachodimitropoulou E, Parks W, et al. Probable Congenital SARS-CoV-2 Infection in a Neonate Born to a Woman With Active SARS-CoV-2 Infection. *CMAJ* (2020) 192(24):E647–50. doi: 10.1503/cmaj.200821
20. Vivanti AJ, Vauloup-Fellous C, Prevot S, Zupan V, Suffee C, Do Cao J, et al. Transplacental Transmission of SARS-CoV-2 Infection. *Nat Commun* (2020) 11(1):3572. doi: 10.1038/s41467-020-17436-6
21. Sisman J, Jaleel MA, Moreno W, Rajaram V, Collins RRJ, Savani RC, et al. Intrauterine Transmission of SARS-COV-2 Infection in a Preterm Infant. *Pediatr Infect Dis J* (2020) 39(9):e265–7. doi: 10.1097/INF.0000000000002815
22. Baud D, Greub G, Favre G, Gengler C, Jaton K, Dubruc E, et al. Second-Trimester Miscarriage in a Pregnant Woman With SARS-CoV-2 Infection. *JAMA* (2020) 323(21):2198–200. doi: 10.1001/jama.2020.7233
23. Walker KF, O'Donoghue K, Grace N, Dorling J, Comeau JL, Li W, et al. Maternal Transmission of SARS-COV-2 to the Neonate, and Possible Routes for Such Transmission: A Systematic Review and Critical Analysis. *BJOG* (2020) 127(11):1324–36. doi: 10.1111/1471-0528.16362
24. Schwartz DA, Thomas KM. Characterizing COVID-19 Maternal-Fetal Transmission and Placental Infection Using Comprehensive Molecular Pathology. *EBioMedicine* (2020) 60:102983. doi: 10.1016/j.ebiom.2020.102983
25. Raschetti R, Vivanti AJ, Vauloup-Fellous C, Loi B, Benachi A, De Luca D. Synthesis and Systematic Review of Reported Neonatal SARS-CoV-2 Infections. *Nat Commun* (2020) 11(1):5164. doi: 10.1038/s41467-020-18982-9
26. Benirschke B, Burton GJ, Baergen RN. *Pathology of the Human Placenta. 6th ed.* Berlin, Heidelberg: Springer (2012). doi: 10.1007/978-3-642-23941-0
27. Garcia AG, Fonseca EF, Marques RL, Lobato YY. Placental Morphology in Cytomegalovirus Infection. *Placenta* (1989) 10(1):1–18. doi: 10.1016/0143-4004(89)90002-7

28. de Noronha L, Zanluca C, Burger M, Suzukawa AA, Azevedo M, Rebutini PZ, et al. Zika Virus Infection at Different Pregnancy Stages: Anatomopathological Findings, Target Cells and Viral Persistence in Placental Tissues. *Front Microbiol* (2018) 9:2266. doi: 10.3389/fmicb.2018.02266
29. Ribeiro CF, Silami VG, Brasil P, Nogueira RM. Sickle-Cell Erythrocytes in the Placentas of Dengue-Infected Women. *Int J Infect Dis* (2012) 16(1):e72. doi: 10.1016/j.ijid.2011.09.005
30. Shanes ED, Mithal LB, Otero S, Azad HA, Miller ES, Goldstein JA. Placental Pathology in COVID-19. *Am J Clin Pathol* (2020) 154(1):23–32. doi: 10.1093/ajcp/aqaa089
31. Baergen RN, Heller DS. Placental Pathology in Covid-19 Positive Mothers: Preliminary Findings. *Pediatr Dev Pathol* (2020) 23(3):177–80. doi: 10.1177/1093526620925569
32. Hosier H, Farhadian SF, Morotti RA, Deshmukh U, Lu-Culligan A, Campbell KH, et al. SARS-CoV-2 Infection of the Placenta. *J Clin Invest* (2020) 130 (9):4947–53. doi: 10.1172/JCI139569
33. Gulersen M, Prasannan L, Tam Tam H, Metz CN, Rochelson B, Meirowitz N, et al. Histopathologic Evaluation of Placentas After Diagnosis of Maternal Severe Acute Respiratory Syndrome Coronavirus 2 Infection. *Am J Obstet Gynecol MFM* (2020) 2(4):100211. doi: 10.1016/j.ajogmf.2020.100211
34. Smithgall MC, Liu-Jarin X, Hamele-Bena D, Cimic A, Mourad M, Debelenko L, et al. Third-Trimester Placentas of Severe Acute Respiratory Syndrome Coronavirus 2 (SARS-CoV-2)-positive Women: Histomorphology, Including Viral Immunohistochemistry and in-Situ Hybridization. *Histopathology* (2020) 77(6):994–9. doi: 10.1111/his.14215
35. Khong TY, Mooney EE, Ariel I, Balmus NC, Boyd TK, Brundler MA, et al. Sampling and Definitions of Placental Lesions: Amsterdam Placental Workshop Group Consensus Statement. *Arch Pathol Lab Med* (2016) 140 (7):698–713. doi: 10.5858/arpa.2015-0225-CC
36. Malaquias MAS, Oyama LA, Jericó PC, Costa I, Padilha G, Nagashima S, et al. Effects of Mesenchymal Stromal Cells Play a Role the Oxidant/Antioxidant Balance in a Murine Model of Asthma. *Allergol Immunopathol* (2018) 46 (2):136–43. doi: 10.1016/j.aller.2017.06.003
37. Fajgenbaum DC, June CH. Cytokine Storm. *N Engl J Med* (2020) 383 (23):2255–73. doi: 10.1056/NEJMra2026131
38. Nagashima S, Mendes MC, Martins APC, Borges NH, Godoy TM, Miggiolaro AFRS, et al. Endothelial Dysfunction and Thrombosis in Patients With COVID-19—Brief Report. *Arterioscler Thromb Vasc Biol* (2020) 40:2404–7. doi: 10.1161/atvbaha.120.314860
39. Lippi G, Plebani M. Laboratory Abnormalities in Patients With COVID-2019 Infection. *Clin Chem Lab Med* (2020) 58(7):1131–4. doi: 10.1515/cclm-2020-0198
40. Lippi G, Plebani M, Henry BM. Thrombocytopenia is Associated With Severe Coronavirus Disease 2019 (COVID-19) Infections: A Meta-Analysis. *Clin Chim Acta* (2020) 506:145–8. doi: 10.1016/j.cca.2020.03.022
41. Tang N, Li D, Wang X, Sun Z. Abnormal Coagulation Parameters are Associated With Poor Prognosis in Patients With Novel Coronavirus Pneumonia. *J Thromb Haemost* (2020) 18(4):844–7. doi: 10.1111/jth.14768
42. Benhamou D, Keita H, Ducloy-Bouthors ASCARO Working Group. Coagulation Changes and Thromboembolic Risk in COVID-19 Obstetric Patients. *Anaesth Crit Care Pain Med* (2020) 39(3):351–3. doi: 10.1016/j.accpm.2020.05.003
43. Ribes A, Vardon-Bounes F, Mémier V, Poette M, Au-Duong J, Garcia C, et al. Thromboembolic Events and Covid-19. *Adv Biol Regul* (2020) 77:100735. doi: 10.1016/j.jbior.2020.100735
44. Klok FA, Kruip MJHA, van der Meer NJM, Arbous MS, Gommers D, Kant KM, et al. Confirmation of the High Cumulative Incidence of Thrombotic Complications in Critically Ill ICU Patients With COVID-19. *Thromb Res* (2020) 191:148–50. doi: 10.1016/j.thromres.2020.04.041
45. Zhang Y, Cao W, Xiao M, Li YJ, Yang Y, Zhao J, et al. [Clinical and Coagulation Characteristics of 7 Patients With Critical COVID-2019 Pneumonia and Acro-Ischemia]. *Zhonghua Xue Ye Xue Za Zhi* (2020) 41 (0):E006. doi: 10.3760/cma.j.issn.0253-2727.2020.0006
46. Menter T, Mertz KD, Jiang S, Chen H, Monod C, Tzankov A, et al. Placental Pathology Findings During and After SARS-CoV-2 Infection: Features of Villitis and Malperfusion. *Pathobiology* (2021) 88(1):69–77. doi: 10.1159/000511324
47. Levitan D, London V, McLaren RA, Mann JD, Cheng K, Silver M. Histologic and Immunohistochemical Evaluation of 65 Placentas From Women With Polymerase Chain Reaction-Proven Severe Acute Respiratory Syndrome Coronavirus 2 (SARS-CoV-2) Infection. *Arch Pathol Lab Med* (2021). doi: 10.5858/arpa.2020-0793-SA
48. Schwartz DA, Morotti D. Placental Pathology of COVID-19 With and Without Fetal and Neonatal Infection: Trophoblast Necrosis and Chronic Histiocytic Intervillositis as Risk Factors for Transplacental Transmission of SARS-CoV-2. *Viruses* (2020) 12(11):1308. doi: 10.3390/v12111308
49. Schwartz DA, Baldewijns M, Benachi A, Bugatti M, Collins RRJ, De Luca D, et al. Chronic Histiocytic Intervillositis With Trophoblast Necrosis are Risk Factors Associated With Placental Infection From Coronavirus Disease 2019 (COVID-19) and Intrauterine Maternal-Fetal Severe Acute Respiratory Syndrome Coronavirus 2 (SARS-CoV-2) Transmission in Liveborn and Stillborn Infants. *Arch Pathol Lab Med* (2020) 145(5):517–28. doi: 10.5858/arpa.2020-0771-SA
50. Knight M, Bunch K, Vousden N, Morris E, Simpson N, Gale C, et al. UK Obstetric Surveillance System SARS-CoV-2 Infection in Pregnancy Collaborative Group. Characteristics and Outcomes of Pregnant Women Admitted to Hospital With Confirmed SARS-CoV-2 Infection in UK: National Population-Based Cohort Study. *BMJ* (2020) 369:m2107. doi: 10.1136/bmj.m2107
51. Breslin N, Baptiste C, Gyamfi-Bannerman C, Miller R, Martinez R, Bernstein K, et al. Coronavirus Disease 2019 Infection Among Asymptomatic and Symptomatic Pregnant Women: Two Weeks of Confirmed Presentations to an Affiliated Pair of New York City Hospitals. *Am J Obstet Gynecol MFM* (2020) 2(2):100118. doi: 10.1016/j.ajogmf.2020.100118
52. Blitz MJ, Grünebaum A, Tekbali A, Bornstein E, Rochelson B, Nimaroff M, et al. Intensive Care Unit Admissions for Pregnant and Non-Pregnant Women With Coronavirus Disease 2019. *Am J Obstet Gynecol* (2020) 223 (2):290–1. doi: 10.1016/j.ajog.2020.05.004
53. Kayem G, Lecarpentier E, Deruelle P, Bretelle F, Azria E, Blanc J, et al. A Snapshot of the Covid-19 Pandemic Among Pregnant Women in France. *J Gynecol Obstet Hum Reprod* (2020) 49(7):101826. doi: 10.1016/j.jogoh.2020.101826
54. World Health Organization. *Definition and Categorization of the Timing of Mother-to-Child Transmission of SARS-CoV-2* (2021). Available at: https://www.who.int/publications/i/item/WHO-2019-nCoV-mother-to-child-transmission-2021 (Accessed April 26, 2021).
55. Egloff C, Vauloup-Fellous C, Picone O, Mandelbrot L, Roques P. Evidence and Possible Mechanisms of Rare Maternal-Fetal Transmission of SARS-CoV-2. *J Clin Virol* (2020) 128:104447. doi: 10.1016/j.jcv.2020.104447
56. Schwartz DA, Morotti D, Beigi B, Moshfegh F, Zafaranloo N, Patanè L. Confirming Vertical Fetal Infection With Coronavirus Disease 2019: Neonatal and Pathology Criteria for Early Onset and Transplacental Transmission of Severe Acute Respiratory Syndrome Coronavirus 2 From Infected Pregnant Mothers. *Arch Pathol Lab Med* (2020) 144(12):1451–6. doi: 10.5858/arpa.2020-0442-SA
57. Stonoga ES, de Almeida Lanzoni L, Rebutini P, Permegiani de Oliveira A, Chiste J, Fugaça C, et al. Intrauterine Transmission of SARS-CoV-2. *Emerg Infect Dis* (2021) 27(2):638–41. doi: 10.3201/eid2702.203824
58. Jackson MR, Mayhew TM, Boyd PA. Quantitative Description of the Elaboration and Maturation of Villi From 10 Weeks of Gestation to Term. *Placenta* (1992) 13(4):357–70. doi: 10.1016/0143-4004(92)90060-7
59. Vangrieken P, Vanterpool SF, van Schooten FJ, Al-Nasiry S, Andriessen P, Degreef E, et al. Histological Villous Maturation in Placentas of Complicated Pregnancies. *Histol Histopathol* (2020) 35(8):849–62. doi: 10.14670/HH-18-205
60. Redline RW, Ravishankar S. Fetal Vascular Malperfusion, An Update. *APMIS* (2018) 126(7):561–9. doi: 10.1111/apm.12849
61. Schwartz DA. Viral Infection, Proliferation, and Hyperplasia of Hofbauer Cells and Absence of Inflammation Characterize the Placental Pathology of Fetuses With Congenital Zika Virus Infection. *Arch Gynecol Obstet* (2017) 295 (6):1361–8. doi: 10.1007/s00404-017-4361-5
62. Simoni MK, Jurado KA, Abrahams VM, Fikrig E, Guller S. Zika Virus Infection of Hofbauer Cells. *Am J Reprod Immunol* (2017) 77(2):10.1111/aji.12613. doi: 10.1111/aji.12613

63. Rosenberg AZ, Yu W, Hill DA, Reyes CA, Schwartz DA. Placental Pathology of Zika Virus: Viral Infection of the Placenta Induces Villous Stromal Macrophage (Hofbauer Cell) Proliferation and Hyperplasia. *Arch Pathol Lab Med* (2017) 141(1):43–8. doi: 10.5858/arpa.2016-0401-OA

Conflict of Interest: The authors declare that the research was conducted in the absence of any commercial or financial relationships that could be construed as a potential conflict of interest.

frontiers in Immunology

PERSPECTIVE
published: 09 June 2021
doi: 10.3389/fimmu.2021.684194

Placental Morphologic Similarities Between ZIKV-Positive and HIV-Positive Pregnant Women

*Daiane Cristine Martins Ronchi[1], Mineia Alessandra Scaranello Malaquias[1], Patrícia Zadorosnei Rebutini[1], Letícia Arianne Panini do Carmo[1], Plínio Cézar Neto[1], Emily Scaranello Marini[1], Amanda Prokopenko[1], Seigo Nagashima[1], Camila Zanluca[2], Claudia Nunes Duarte dos Santos[2] and Lúcia de Noronha[1]**

[1] Laboratory of Experimental Pathology, Postgraduate Program of Health Sciences, School of Medicine, Pontifícia Universidade Católica do Paraná, Curitiba, Brazil, [2] Molecular Virology Laboratory, Instituto Carlos Chagas, Fundação Oswaldo Cruz, Curitiba, Brazil

OPEN ACCESS

Edited by:
Ashley L. St John, Duke-NUS Medical School, Singapore

Reviewed by:
Elizabeth Ann Lieser Enninga, Mayo Clinic, United States
Nicholas Lennemann, University of Alabama at Birmingham, United States

***Correspondence:**
Lúcia de Noronha
lnno.noronha@gmail.com

Specialty section:
This article was submitted to Viral Immunology, a section of the journal Frontiers in Immunology

Received: *22 March 2021*
Accepted: *19 May 2021*
Published: *09 June 2021*

Citation:
Martins Ronchi DC, Scaranello Malaquias MA, Rebutini PZ, Panini do Carmo LA, Neto PC, Marini ES, Prokopenko A, Nagashima S, Zanluca C, Duarte dos Santos CN and de Noronha L (2021) Placental Morphologic Similarities Between ZIKV-Positive and HIV-Positive Pregnant Women. Front. Immunol. 12:684194. doi: 10.3389/fimmu.2021.684194

Zika virus (ZIKV) caused global concern due to Brazil's unexpected epidemic, and it was associated with congenital microcephaly and other gestational intercurrences. The study aimed to analyze the placenta morphometric changes of ZIKV-infected pregnant women (ZIKV group; n = 23) compared to placentas of HIV-infected (HIV group; n = 24) and healthy pregnant women (N-control group; n = 22). It also analyzed the relationship between the morphometric results and pathological alterations on conventional microscopy, gestational trimester of infection, and presence of the congenital Zika syndrome (CZS). There was a significant increase in area ($p = 0.0172$), as well as a higher number of knots ($p = 0.0027$), sprouts ($p < 0.0001$), and CD163 +Hofbauer cells (HCs) ($p < 0.0001$) in the ZIKV group compared to the N-control group, suggesting that villous dysmaturity and HCs hyperplasia could be associated with ZIKV infections. The HIV group had a higher area ($p < 0.0001$), perimeter ($p = 0.0001$), sprouts ($p < 0.0001$), and CD163 + HCs ($p < 0.0001$) compared to the N-control group, demonstrating that the morphometric abnormalities found in the ZIKV and HIV group are probably similar. However, when ZIKV and HIV groups are compared, it was observed a higher number of sprouts ($p = 0.0066$) and CD163+ HCs ($p < 0.0001$) in the first one, suggesting that placental ZIKV congenital changes could be more pronounced.

Keywords: Zika virus, HIV, vertical transmission, placenta, morphometric analysis

INTRODUCTION

During pregnancy, Zika virus (ZIKV) infection has been associated with fetal malformations, such as microcephaly, lissencephaly, cerebellar hypoplasia, hydrocephalus, polymicrogyria, abnormal development of the corpus callosum, and changes in neuronal migration and subcortical calcifications that configure the Congenital Zika Syndrome (1–9).

Recently, ZIKV caused global concern due to the unexpected epidemic of infection in Brazil, associated with congenital microcephaly and abortions, both of which have been more common

when ZIKV infection occurred during the first trimester of gestation. Besides, severe cerebral malformations have not been described when the infection occurred in the third trimester, suggesting that the brain's abnormal development associated with ZIKV could become the organogenesis period (10, 11).

CZS has been associated with placental alterations like an increase in the number of syncytial knots and sprouts, stromal disorders, villous immaturity, Hofbauer cells (HCs) hyperplasia, and vascular abnormalities (12, 13). The direct infection and replication of ZIKV in placenta tissues can be triggered by the infection of HCs (placental macrophage) in the chorionic villi (10). HCs appear to be the most frequently observed ZIKV-positive cells in the naturally infected human placentas and also may remain persistently infected until delivery. Even in the placenta samples with a short interval between the acute phase of infection and delivery time, ZIKV appears to be detected exclusively in HCs. Furthermore, villous immaturity may be related to congenital disorders caused by ZIKV infection, and it is also associated with an increase in HCs. The persistence of ZIKV-positive HCs in full-term placentas may indicate that these cells could provide a viral source for continued fetal infection and may be responsible for the transplacental transmission mediated by its migratory ability to reach the fetal vessels (12).

Human immunodeficiency virus (HIV) has also been associated with abortion, stillborn, preterm delivery, and other gestational intercurrences, but not with the congenital syndrome. However, the effects of HIV on the placentas remain poorly understood. The main target of HIV is CD4 T lymphocytes, but other cells expressing CD4 are also infected, like monocytes, macrophages, and dendritic cells, where HCs are included. Some of the alterations described include chorioamnionitis and deciduitis, and villitis, an increase in the number of syncytial knots and sprouts, stromal disorders like fibrin deposition and fibrosis, abnormalities of the villous maturation and infarction. Other authors have described placentas of HIV-infected pregnant with no pathological alterations on the conventional microscopy. On the other hand, morphometric techniques have usually shown alterations in villus diameter and perimeter, suggesting changes in villous maturation (14–18).

Given that, despite having different vertical transmission routes and outcomes, both HIV and ZIKV may produce similar morphological changes in placental tissues, such as villous immaturity and hyperplasia of HCs. Severe villitis, for example, does not appear to be a common form of placental injury in both cases. In addition, these two viruses can break through the placental barrier causing only subtle morphological alterations, resulting in placentas of the usual histological aspect under conventional microscopy (14–18).

Because of this, the present study aimed to analyze the placental morphometric changes in ZIKV-infected pregnant women and compare these changes with that found in HIV-infected pregnant women, considering gestational trimester of infection, presence of CZS, and pathological alterations on conventional microscopy as variables. In addition, this study also compares both groups (ZIKV and HIV) to the placentas of healthy (non-infected) pregnant women.

MATERIALS AND METHODS

Ethical Approvals

The Brazilian National Ethics Committee approved the presented study under the number CAAE: 42481115.7.0000.5248. The authors confirm that all methods were carried out following relevant guidelines and regulations. Furthermore, the sample collection followed all relevant ethics and safety protocols. The data that support the findings of this study are available from the corresponding author upon reasonable request.

Samples

The ZIKV-infected placenta group (ZIKV group) comprises 23 placentas that were formalin-fixed paraffin-embedded (FFPE) (12). The 23 patients gave birth to 15 term healthy and eight malformed babies, between 34 and 40 gestational weeks (average = 38; median = 38; SD = 2.17). All the 15 term healthy babies (37–40 gestational weeks) are alive. Of the eight malformed babies, five were preterm (34–36 gestational weeks). Still, regarding this group of malformed babies, four of them are alive, two had perinatal death and two were stillborn. The 23 mothers have at least two positive tests for ZIKV infection: anti-ZIKV IgM positive in the maternal blood and/or colostrum, positive RT-PCR in the maternal blood and/or urine, positive RT-PCR in the frozen placenta samples, positive RT-PCR and/or immunohistochemical test in the FFPE placenta samples. The newborn/stillborn additional samples were also positive: brain tissue RT-PCR and anti-ZIKV IgM in the blood (12).

The HIV-infected placenta group (HIV group) consisted of 24 FFPE placenta samples of HIV-positive pregnant women with no comorbidities. Pregnant women gave birth to healthy newborns between 33 and 40 weeks (average = 38.08; median = 38; SD = 1.99) of gestation in 2004 to 2005, when ZIKV was not circulating in Brazil. The placentas showed no pathological changes on the conventional microscopy. We did not observe villous maturation changes, and weights of the newborns were normal for gestational age (average = 2789.29 g; median = 2730 g; SD = 497.19 g; min-max = 1780–3890 g). Maternal age of this group ranged from 17 to 42 years (average = 26; median = 26; SD = 6.53). The placentas were from pregnant women who had been diagnosed with HIV before or during their pregnancy. The newborns were followed up until their HIV infection condition was defined as negative. All the babies are alive e HIV-seronegative. The viral loads and CD4/CD8 ratio were measured three to six times for most patients. The viral loads ranged from 13047.5 to 5760 (copies), and the CD4/CD8 ratio ranged from 0.65 to 0.35 during the 9 months of pregnancy. Antiretroviral therapy was administered at least 1 month before the birth in all patients (16).

The non-infected placenta group (N-control group) comprises 22 pregnant women that had prenatal without comorbidities. They gave birth to healthy newborns, between 34 and 40 gestational weeks (average = 38.19; median = 38; SD = 1.65), from 2004 to 2005, when ZIKV was not circulating in Brazil. The placentas did not present anatomopathological alterations. We did not observe villous maturation changes,

and weights of the newborns were normal for gestational age (average = 2957.27 g; median = 2887.5 g; SD = 762.63 g; min–max = 1770–4410 g). Maternal age of this group ranged from 15 to 40 years (average = 26.06; median = 24; SD = 7.14). The pregnant woman and the newborn were followed up until discharge from the hospital (16).

The samples of three groups were matched by gestational age, which varied from 33 to 38 weeks. All the pregnant women were submitted to laboratory tests for congenital intrauterine infections (*TORCH = toxoplasmosis, rubella, cytomegalovirus, syphilis, and herpes*) with negative results. Analysis of gestational age showed no significant differences between the groups.

Morphometric Analysis

Histological sections of all placentas were stained with hematoxylin & eosin (H&E) to evaluate the perimeter, diameter, and area of villi, the number of sprouts, syncytial knots, and villi numbers per medium power field (MPF). H&E sections were photographed at a magnification of 200× (MPF) using the Scanner Axion Scan.Z1, generating an average of 5,000 images. Unfocused, with artifacts, non-villous tissue representative (membranes, cord, decidua) images were excluded. The remaining images selected (about 1,000) had 100% of the field occupied with placental villi and were randomized to obtain about 100 images for each case of the three groups.

For all placentas, the perimeter, diameter, area of the villi, and basal membrane thickness were measured using Image-Pro Plus® 4 software, based on freehand drawing on 100 consecutive villi. After freehand villus' contour, the program provided perimeter, diameters (major), area, and basal membrane thickness in micrometers or square micrometers ($\mu m/\mu m^2$) (16).

To evaluate the syncytial knots and sprouts per villi, the same 100 MPF/H&E images were used and submitted to simple counting of these microscopic structures (12).

Immunohistochemical Analysis

Histological sections of the placentas were fixed on electrically charged glass slides and subsequently dewaxed with heated xylol (37°C), dehydrated with successive baths of absolute ethyl alcohol, and rehydrated with water. Methyl alcohol and hydrogen peroxide were used to block endogenous peroxidase and distilled water and hydrogen peroxide for the second block. They were incubated with anti-CD163 primary antibody (type: polyclonal/rabbit; clone/code: 14215; dilution: 1:1000; source: Thermo Fisher) for 1 h and with secondary antibody associated with the dextran polymer (Spring Bioscience, Pleasanton, USA) for 30 min. DAB/substrate complex (DAB, DakoCytomation) was added onto the slides, followed by counterstaining with Mayer's hematoxylin, dehydration with ethyl alcohol baths, clarification with xylol, and blending with Canada balsam (12).

The 30 HPF (high power field = 400×) were analyzed by counting the number of villi and CD163+ HCs per villi in all three study groups.

The images were obtained from random sample regions without the interference of an observer. The morphometric measurements and the score of CD163 positive cells were performed blindly.

Statistical Analyses

The results were described by means, standard deviations, medians, minimum, and maximum values. The comparison of the groups concerning quantitative variables was performed using the non-parametric Kruskal-Wallis test or t-test. The Shapiro-Wilk test evaluated the normality condition. Values of $p < 0.05$ indicated statistical significance. The data were analyzed using the IBM SPSS Statistics v.20.0 software. Armonk, NY, USA: IBM Corp.

RESULTS

Morphometric Alterations of the HIV and ZIKV Groups

The analysis of the area ($p = 0.0172$) and the number of knots ($p = 0.0027$), sprouts ($p < 0.0001$), and CD163+ HCs ($p < 0.0001$) in the ZIKV group demonstrated larger immature chorionic villi with a higher number of knots and sprouts and HCs hyperplasia when compared with the N-control group (**Figure 1** and **Supplementary Figure 1**).

HIV group placentas with no pathological alterations on conventional microscopy also showed changes in villous maturation and HC hyperplasia by morphometry analysis compared to the N-control group. The area ($p < 0.0001$), perimeter (p = 0.0001), number sprouts ($p < 0.0001$), and CD163+ HCs ($p < 0.0001$) of HIV group were higher than the N-control group (**Figure 1** and **Supplementary Figure 1**).

The ZIKV group placentas showed higher values of the number of sprouts ($p < 0.0066$) and CD163+ HCs ($p < 0.0001$) compared to the HIV group (**Figure 1** and **Supplementary Figure 1**).

Trimester of ZIKV Infection

Morphometric analyses were performed in placental samples from mothers who were infected with ZIKV during the first (n = 4), second (n = 8), and third trimesters of pregnancy (n = 6). In five placenta samples, the trimester of infection was unknown. The perimeter ($p = 0.0292$), number of knots ($p = 0.0062$), sprouts ($p < 0.0001$), and CD163+ HCs ($p < 0.0001$) showed significant differences by the trimester of infection. The most relevant differences were observed between the second trimester and third trimester of infection versus the N-control group, revealing second-/third-trimester ZIKV placentas with villous dysmaturity and HCs hyperplasia compared to the control placentas (**Table 1**).

Pathological Alterations

ZIKV group placentas with and without pathological alterations by conventional microscopy were compared. It was observed that placentas with pathological changes presented higher diameter ($p = 0.0226$), perimeter ($p = 0.0212$), number of knots ($p = 0.0101$), number of sprouts ($p < 0.0001$), and CD163+ HCs ($p < 0.0001$) compared to placentas without pathological alterations (**Table 1**). However, placentas considered within normal standards also presented morphometric changes characterized by higher area, perimeter, number of knots, sprouts, and CD163+ HCs compared to the N-control group ($p < 0.05$).

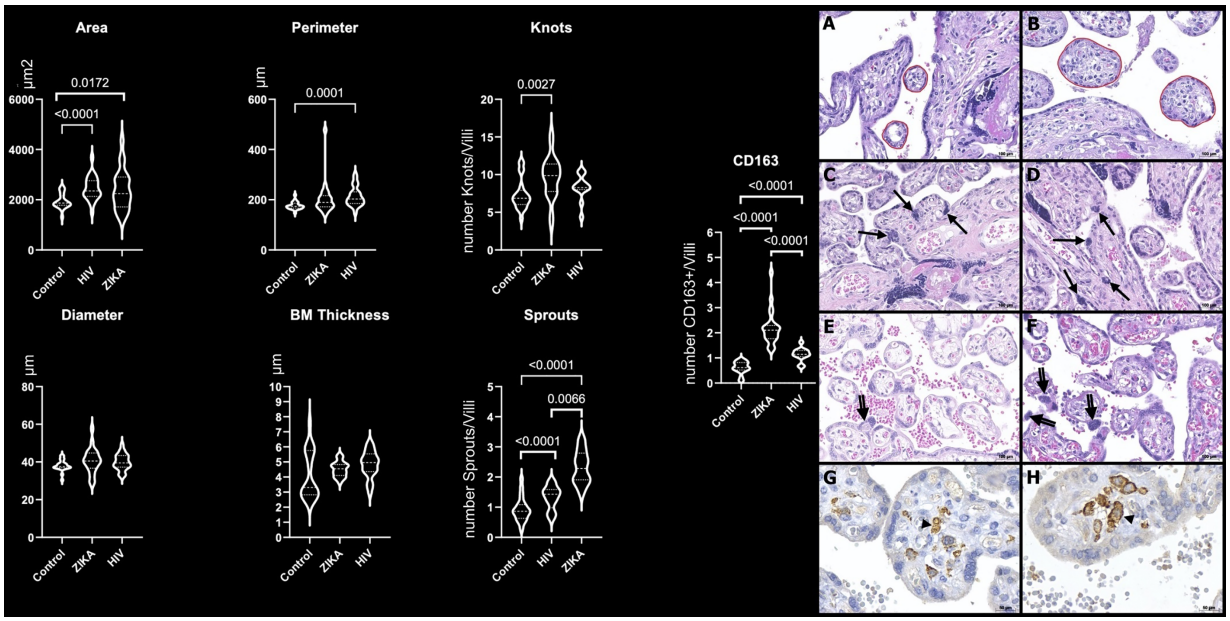

FIGURE 1 | Morphometric analysis of placental specimens from women infected with ZIKV during the pregnancy compared to the HIV and N-control groups. Perimeter, diameter, and basal membrane (BM) thickness in μm; area in μm^2; number of knots, sprouts, and CD163+ HCs per villi (CD163/villi). Photomicrography of a placental sample stained with H&E showing the perimeter of villi (red freehand drawing) in N-control group **(A)** and ZIKV group **(B)**; the number of syncytial knots/villi (arrows) in N-control group **(C)** and ZIKV-group **(D)**; the number of sprouts/villi (double arrows) in N-control group **(E)** and ZIKV group **(F)**. Original magnification: 200×. Scale bars: 100 μm. Photomicrography of immunostaining with CD163 highlighting Hofbauer cell (arrowhead) in the N-control group **(G)** and ZIKV group **(H)**. Original magnification: 400×. Scale bars: 50 μm.

Congenital Zika Syndrome

The status of the newborns (with or without CZS) was also analyzed. The diameter ($p = 0.0109$), area ($p = 0.0102$), perimeter ($p = 0.0035$), number of knot ($p = 0.0054$), number of sprouts ($p < 0.0001$), and CD163+ HCs ($p < 0.0001$) were higher in placentas of newborns with CZS compared with placentas of newborns without this condition (**Table 1**).

DISCUSSION

Morphometric Alterations of HIV and ZIKV Groups

The findings showed significant enlargement of the area of the ZIKV group when compared with the N-control group. A higher number of knots, sprouts, and CD163+ HCs were also noticed.

Syncytial knots are syncytiotrophoblasts' specializations, and their severe increase in late gestation indicates early maturation (12). Syncytial sprouts are markers of trophoblast proliferation; they are seen frequently during early pregnancy and are increased in the villous dysmaturity (19, 20).

HCs, the most frequently ZIKV-positive cells, are placental villous macrophages of fetal origin, and alterations in their numbers (hyperplasia) and biological features are associated with complications in pregnancy. HCs play a role in diverse functions, such as placental vasculogenesis, immune regulation, and the secretion of enzymes and cytokines across the maternal-fetal barrier. In addition, there is some evidence suggesting the involvement of HCs in the development of placental villi (12).

This study's findings corroborate with studies that showed a delay in villous maturation and signs of the HCs hyperplasia in ZIKV-infected placentas. These alterations could damage the chorionic villi, such as calcification, necrosis, Wharton jelly sclerosis, fibrin deposition, and a significant villi size increase (11, 21–23). We could conclude that all of the anatomopathological parameters could be confirmed by the morphometric data and may be used to describe ZIKV-infected placentas.

Other findings showed that the HIV group had a larger area, perimeter, number of sprouts, and CD163+ HCs compared to the N-control group. Studies also revealed that placentas exposed to HIV infection exhibited the following microscopic features: edema, villous immaturity, focal necrosis of trophoblasts, numerous HCs, intervillous fibrin deposition, and chorangiosis (17, 18, 24). However, when those patterns are subtle or minimal, pathologists cannot make the diagnosis. Given that, morphometric techniques may be helpful to identify subtle abnormalities.

Rabelo et al. (22) showed ZIKV NS1 protein in the decidual and endothelial cells of the maternal decidua and CTB, STB, and HCs in the third trimester placental tissues associated with an HIV-exposed, but uninfected, infant with severe congenital Zika syndrome. Nonetheless, the maternal HIV infection could have contributed to the permissiveness of other placental cell types to ZIKV infection.

Finally, when both groups (ZIKV and HIV) were compared, no statistically significant results were found, except for the number of

TABLE 1 | Median (max-min) and *p*-value of morphometric data in the gestational trimester of infection, presence of placenta pathological alterations, and CZS.

Variables	N-CONTROL	Gestational Trimester of Infection†			Pathological Alterations of Placenta on Conventional Microscopy§		Congenital Zika Syndrome*	
		First (n = 4)	Second (n = 8)	Third (n = 6)	No (n = 15)	Yes (n = 8)	No (n = 15)	Yes (n = 8)
Diameter (μm)	37.6 (43.4–30.4)	38.3 (46.3–29.1)	40.2 (45.3–32.1)	39.8 (44.6–29.1)	40.1 (50.6–29.1)	44.9 (57.7–36.6)	40.0 (45.3–29.1)	45.5 (57.7–36.6)
			NS		**0.0226**		**0.0109**	
Area (μm^2)	1867 (2496–1314)	1812.9 (3536.9–1228.8)	2119.4 (2927.2–1377.9)	2241.8 (2917.7–1527.3)	2165.1 (3671.2–1228.8)	2907.4 (4354.4–1673.3)	2119.4 (2927.2–1228.8)	2897.1 (4354.4–1673.3)
			NS		NS		**0.0102**	
Perimeter (μm)	174 (219–148)	174.2 (237.2–142.2)	182.1 (477.7–163.2)	186.2 (203.8–154.3)	181.2 (477.7–142.2)	208.9 (257.6–163.2)	180.3 (477.7–142.2)	214.0 (257.6–176.9)
			0.0292[a]		**0.0212**		**0.0035**	
Number of knots/villi	6.9 (11.7–4.2)	9.9 (11.6–7.9)	11.1 (14.3–9.3)	8.6 (15.5–4.7)	9.8 (15.5–4.7)	10.2 (11.6–3.5)	10.1 (15.5–4.7)	9.8 (11.6–3.5)
			0.0062[a]		**0.0101**		**0.0054**	
Number of sprouts/villi	0.9 (1.9–0.3)	1.9 (3.2–1.6)	2.4 (3.1–1.4)	2.1 (2.6–1.8)	2.4 (3.2–1.6)	2.0 (3.3–1.4)	2.2 (3.2–1.4)	2.8 (3.3–1.7)
			<0.0001[b]		**<0.0001**		**<0.0001**	
Number of cells CD163+/villi	0.6 (1.0–0.1)	2.7 (3.3–2.0)	2.2 (2.3–1.7)	1.9 (2.3–1.7)	2.0 (2.4–1.3)	2.5 (4.4–1.7)	2.0 (2.4–1.3)	2.8 (4.4–1.4)
			<0.0001[c]		**<0.0001**		**<0.0001**	

Analysis only for the ZIKV group.

†Five cases of unknown gestational trimester.

§Main pathological findings: umbilical artery agenesis (1), mild acute funisitis (1), and villous immaturity (6).

**Major central nervous malformations: microcephaly (3), spina bifida (1), hydrocephalus (2), and encephalocele (1).*

[a]p value refers to the second trimester vs. N-control.

[b]p-value refers to the e third trimester vs. N-control and first vs. the third trimester.

[c]p-value refers to the third trimester vs. N-control; first vs. the second and third trimester. Kruskal-Wallis test and t-test; values of $p < 0.05$ indicated statistical significance.

NS, not significant p-value.

Bold values = Statistically significant values.

sprouts and CD163+ HCs higher in the ZIKV group. Thus, it seems that HCs hyperplasia and sprouting/dysmaturity villi may be more pronounced and characteristic in the ZIKV-infected placentas (12, 17). Even though placental changes, such as dysmaturity and hyperplasia of HCs, can be seen in other maternal-fetal diseases, such as congenital infections (TORCH) and diabetes, in the absence of these comorbidities, this aspect may help the pediatric pathologists to suspect the diagnosis of ZIKV vertical transmission. This study also demonstrates that the morphometrical abnormalities finding in ZIKV and HIV groups are very similar, despite having different vertical transmission routes and outcomes since ZIKV is a teratogenic virus and HIV is not. In addition, vertical HIV transmission is much rarer than that of ZIKV, but it can increase perinatal and intrauterine deaths (**Supplementary Figure 1**) (14, 17, 18).

Trimester of ZIKV Infection

When the gestational trimester of infection was analyzed, it was observed that most of the differences between the ZIKV and N-control groups appear to be when infection occurred in the second or third trimester. Since all newborns of this study were in the third trimester (term or preterm), the shorter time that elapsed between the moment of ZIKV infection and the birth may be an explanation for more pronounced changes in these placentas.

The number of HCs also showed differences between groups, suggesting that these cells may have early hyperplasia, and this hyperplasia seems to be maintained throughout the gestational period, although it decreases in intensity over the months. This fact appears to agree with the hypothesis that these cells can work as a reservoir of ZIKV (12, 25).

Regardless of the trimester in which the infection occurred, as ZIKV is detected in placental cells until the end of pregnancy, it is plausible to speculate that the infection of the fetus could happen as a secondary event. In some cases, those abnormalities are only detected months after the delivery (20, 26–29).

Pathological Alterations

Fifteen of 23 ZIKV group placentas were diagnosed without pathological alterations for the pediatric pathologist. However, eight of them had pathological alterations on conventional microscopy, mainly villous immaturity. When placentas with and without pathological alterations were compared, placentas diagnosed with villous immaturity had a higher diameter, perimeter, number of knots, and CD163+ cells. This means that pathologists probably identified those alterations on conventional microscopy and, altogether, termed villous immaturity, so they did not need morphometry techniques to make these diagnoses.

On the other hand, ZIKV-group placentas with no pathological alterations also showed higher diameter, perimeter, and number of knots, sprouts, and CD163+ cells to the N-control group. Therefore, conventional microscopy cannot identify subtle alterations that morphometry could find.

Congenital Zika Syndrome

This study showed significant enlargement of the villi's diameter, area, and perimeter and the number of sprouts and CD163+ HCs in the group that had CZS. In addition, eight infants had fetal malformations related to ZIKV infection during pregnancy. However, 15 women had the onset of ZIKV symptoms during pregnancy and gave birth to infants without CZS.

This study observed that ZIKV causes essential alterations in the placenta's villous, leading to congenital disorders, stillborn, and neonatal death. We could also conclude that morphometric parameters may be biomarkers for CZS since they are more pronounced in malformed newborns. These data could help in the clinical follow-up of newborns with subclinical congenital disorders or even unapparent at birth.

In conclusion, there are placental dysmaturity alterations after ZIKV infection during pregnancy. Very similar placental alterations could be demonstrated on the HIV-infected pregnant women, but sprouting and HCs hyperplasia may be less pronounced in this group. Also, the morphometric analysis revealed villous dysmaturity even in placentas diagnosed within the usual standards by the routine exams. The second and third gestational trimester infections generated more villous dysmaturity and HCs hyperplasia than those pregnant women who became infected in the first trimester. In addition, placentas whose babies had CZS showed more pronounced changes than those without CZS. These alterations may help understand the aspect of ZIKV infection related to placental damage and congenital disabilities and possible deficiencies that might appear after birth.

DATA AVAILABILITY STATEMENT

The raw data supporting the conclusions of this article will be made available by the authors, without undue reservation.

ETHICS STATEMENT

The studies involving human participants were reviewed and approved by the ethics committee of the Oswaldo Cruz Foundation (Fiocruz) Brazilian National Ethics Committee of Human Experimentation. The patients/participants provided their written informed consent to participate in this study.

AUTHOR CONTRIBUTIONS

LN, CZ, and CNDS contributed to the study design. CZ performed the experiments. SN prepared the materials for analyses. DCMR, PZR, LAPC, PCN, and AP performed the morphometric analyses. PZR participated in the patient follow-up. MASM and ESM participated in sample identification/distribution. DCMR, MASM, PZR, and LN analyzed the results and wrote the manuscript. All authors contributed to the article and approved the submitted version.

FUNDING

This research was funded by Fiocruz, CNPq (439968/2016-0), CAPES Zika Fast Track 481-2016 (88887.116626/2016-01), and

Fundação Araucária (CP04/2016). CNDS and LN have a CNPq fellowship.

SUPPLEMENTARY MATERIAL

The Supplementary Material for this article can be found online at: https://www.frontiersin.org/articles/10.3389/fimmu.2021.684194/full#supplementary-material

Supplementary Figure 1 | Illustrative figure shows the morphometric differences between N-control and ZIKV group and between N-control and HIV group, respectively. However, it also represents similar morphometrics results when the ZIKV group was compared with the HIV group. The N-control group's syncytial membranes are more efficient in exchanges because the vessels are closer to the cytotrophoblast. In ZIKV- and HIV-infected placentas, villus increases in size, moving the vessel away from the trophoblast layer, distancing the syncytiotrophoblast membranes cause intrauterine death, premature, low birth weight babies, and/or other malformations. Created with www.biorender.com.

REFERENCES

1. Neu N, Duchon J, Zachariah P. TORCH Infections. *Clin Perinatol* (2015) 42 (1):77–103(viii). doi: 10.1016/j.clp.2014.11.001
2. Noronha Ld, Zanluca C, Azevedo ML, Luz KG, Santos CN. Zika Virus Damages the Human Placental Barrier and Presents Marked Fetal Neurotropism. *Mem Inst Oswaldo Cruz* (2016) 111(5):287–93. doi: 10.1590/0074-02760160085
3. Ayres CFJ. Identification of Zika Virus Vectors and Implications for Control. *Lancet Infect Dis* (2016) 16(3):278–9. doi: 10.1016/S1473-3099
4. Solomon IH, Milner DA, Folkerth RD. Neuropathology of Zika Virus Infection. *J Neuroinfect Dis* (2016) 7(2):220. doi: 10.4172/2314-7326.1000220
5. Hughes BW, Addanki KC, Sriskanda AN, McLean E, Bagasra O. Infectivity of Immature Neurons to Zika Vírus: A Link to Congenital Zika Syndrome. *EBioMedicine* (2016) 10):65–70. doi: 10.1016/j.ebiom.2016.06.026
6. Oehler E, Watrin L, Larre P, Leparc-Goffart I, Lastère S, Valour F, et al. ZIKV Infection Complicated by Guillain-Barré Syndrome: Case Report, French Polinesia, December 2013. *Euro Surveill* (2014) 19(9):1–3. doi: 10.2807/1560-7917.es2014.19.9.20720
7. Brasil P, Pereira JP, Moreira ME, Nogueira RMR, Damasceno L, Wakimoto M, et al. Zika Virus Infection in Pregnant Women in Rio De Janeiro. *N Engl J Med* (2016) 375:2321–34. doi: 10.1056/NEJMoa1602412
8. Melo AS, Aguiar RS, Amorim MMR, Arruda MB, Melo FO, Ribeiro STC, et al. Congenital Zika Virus Infection: Beyond Neonatal Microcephaly. *JAMA Neurol* (2016) 73:1407–16. doi: 10.1001/jamaneurol.2016.3720
9. Schuler-Faccini L, Ribeiro EM, Feitosa IM, Horovitz DDG, Cavalcanti DP, Pessoa A, et al. Brazilian Medical Genetics Society–Zika Embryopathy Task Forceet. Possible Association Between Zika Virus Infection and Microcephaly–Brazil, 2015. Morb. *Mortal Wkly Rep* (2016) 65:59–62. doi: 10.15585/mmwr.mm6503e2
10. Petersen LR, Jamieson DJ, Powers AM, Honein MA. Zika Virus. Baden LR, Editor. *N Engl J Med* (2016) 374(16):1552–63. doi: 10.1056/NEJMra1602113
11. Bhatnagar J, Rabeneck DB, Martines RB, Reagan-Steiner S, Ermias Y, Estetter LBC, et al. Zika Vírus RNA Replication and Persistence in Brain and Placental Tissue. *Emerging Infect Dis* (2017) 23(3):405–14. doi: 10.3201/eid2303.161499
12. Noronha L, Zanluca C, Burger M, Suzukawa AA, Azevedo M, Rebutini PZ, et al. Zika Virus Infection At Different Pregnancy Stages: Anatomopathological Findings, Target Cells and Viral Persistence in Placental Tissues. *Front Microbiol* (2018) 9:2266. doi: 10.3389/fmicb.2018.02266
13. Souza AS, Dias CM, Braga FDCB, Terzian ACB, Estofolete CF, Oliani AH, et al. Fetal Infection by Zika Virus in the Third Trimester: Report of 2 Cases. *Clin Infect Dis* (2016) 63:1622–5. doi: 10.1093/cid/ciw613
14. Maartens G, Celum C, Lewin SR. HIV Infection: Epidemiology, Pathogenesis, Treatment, and Prevention. *Lancet* (2014) 384(9939):258–71. doi: 10.1016/S0140-6736(14)60164-1
15. Yang SW, Cho EH, Choi SY, Lee YK, Park JH, Kim MK, et al. Dc-SIGN Expression in Hofbauer Cells may Play an Important Role in Immune Tolerance in Fetal Chorionic Villi During the Development of Preeclampsia. *J Reprod Immunol* (2017) 124:30–7. doi: 10.1016/j.jri.2017.09.012
16. Baurakiades E, Martins APC, Moreschi V, Souza CDA, Abujamra K, Saito AO, et al. Histomorphometric and Immunohistochemical Analysis of Infectious Agents, T-cell Subpopulations and Inflammatory Adhesion Molecules in Placentas From HIV-seropositive Pregnant Women. *Diagn Pathol* (2011) 6:101. doi: 10.1186/1746-1596-6-101
17. López CL, Pires ARC, Fonseca EC, Rodrigues FR, Braga Neto AR, Herdy GVH, et al. Anatomopathological Characterization of Placentas From HIV+ Patients Associated With p24 Expression. *J Bras Patol Med Lab* (2013) 49 (6):437–45. doi: 10.1590/S1676-24442013000600010
18. Obimbo MM, Zhou Y, McMaster MT, Cohen CR, Qureshi Z, Ong'ech J, et al. Placental Structure in Preterm Birth Among HIV-positive Versus HIV-negative Women in Kenya. *J Acquir Immune Defic Syndr* (2019) 80(1):94–102. doi: 10.1097/QAI.0000000000000187
19. Loukeris K, Sela R, Baergen RN. Syncytial Knots as a Reflection of Placental Maturity: Reference Values for 20 to 40 Weeks Gestational Age. *Pediatr Dev Pathol* (2010) 13:305–9. doi: 10.2350/09-08-0692-OA.1
20. Aagaard KM, Lahon A, Suter MA, Arya RP, Seferovic MD, Vogt MB, et al. Primary Human Placental Trophoblasts are Permissive for Zika Virus (ZIKV) Replication. *Sci Rep* (2017) 7:41389. doi: 10.1038/srep41389
21. Tabata T, Petitt M, Puerta-Guardo H, Michlmayr D, Wang C, Fang-Hoover J, et al. Zika Virus Targets Different Primary Human Placental Cells, Suggesting Two Routes for Vertical Transmission. *Cell Host Microbe* (2016) 20(2):155–66. doi: 10.1016/j.chom.2016.07.002
22. Rabelo K, Fernandes RCSC, Souza LJ, Souza TL, Santos FB, Nunes PCG, et al. Placental Histopathology and Clinical Presentation of Severe Congenital Zika Syndrome in a Human Immunodeficiency Virus-Exposed Uninfected Infant. *Front Immunol* (2017) 8:1704. doi: 10.3389/fimmu.2017.01704
23. Zare Mehrjardi M, Shobeirian F. The Role of the Placenta in Prenatally Acquired Zika Virus Infection. *Virus Dis* (2017) 28(3):247–9. doi: 10.1007/s13337-017-0399-z
24. Anderson VM. The Placental Barrier to Maternal HIV Infection. *Obstet Gynecol Clin North Am* (1997) 24(4):797–820. doi: 10.1016/s0889-8545(05)70345-4
25. Zanluca C, De Melo VCA, Mosimann ALP, dos Santos GIV, dos Santos CND, Luz K. First Report of Autochthonous Transmission of Zika Virus in Brazil. *Mem Inst Oswaldo Cruz* (2015) 110(4):569–72. doi: 10.1590/0074-02760150192
26. Aragão M, Holanda A, Brainer-Lima A, Petribu NCL, Castillo M, van der Linden V, et al. Nonmicrocephalic Infants With Congenital Zika Syndrome Suspected Only After Neuroimaging Evaluation Compared With Those With Microcephaly At Birth and Postnatally: How Large is the Zika Virus "Iceberg"? *AJNR Am J Neuroradiol* (2017) 38:1427–34. doi: 10.3174/ajnr.A5216
27. Ventura L, Ventura C, Lawrence L, van der Linden V, van der Linden A, Gois AL, et al. Visual Impairment in Children With Congenital Zika Syndrome. *J AAPOS* (2017) 21:295–9. doi: 10.1016/j.jaapos.2017.04.003
28. Luo H, Winkelmann ER, Fernandez-Salas I, Li L, Mayer SV, Danis-Lozano R, et al. Zika, Dengue and Yellow Fever Viruses Induce Differential Anti-Viral Immune Responses in Human Monocytic and First Trimester Trophoblast Cells. *Antiviral Res* (2018) 151:55–62. doi: 10.1016/j.antiviral.2018.01.003
29. Sheridan MA, Yunusov D, Balaraman V, Alexenko AP, Yabe S, Verjovski-Almeida S, et al. Vulnerability of Primitive Human Placental Trophoblast to Zika Virus. *Proc Natl Acad Sci* (2017) 114(9):E1587–96. doi: 10.1073/pnas.1616097114

Conflict of Interest: The authors declare that the research was conducted in the absence of any commercial or financial relationships that could be construed as a potential conflict of interest.

frontiers in Immunology

ORIGINAL RESEARCH
published: 15 June 2021
doi: 10.3389/fimmu.2021.686415

The Placental Response to Guinea Pig Cytomegalovirus Depends Upon the Timing of Maternal Infection

*Zachary W. Berkebile[1], Dira S. Putri[1], Juan E. Abrahante[2], Davis M. Seelig[3], Mark R. Schleiss[1] and Craig J. Bierle[1]**

[1] Department of Pediatrics, Division of Pediatric Infectious Diseases, University of Minnesota, Minneapolis, MN, United States, [2] Informatics Institute, University of Minnesota, Minneapolis, MN, United States, [3] Department of Veterinary Clinical Sciences, University of Minnesota, Minneapolis, MN, United States

Human cytomegalovirus (HCMV) infects the placenta, and these placental infections can cause fetal injury and/or demise. The timing of maternal HCMV infection during pregnancy is a determinant of fetal outcomes, but how development affects the placenta's susceptibility to infection, the likelihood of placental injury post-infection, and the frequency of transplacental HCMV transmission remains unclear. In this study, guinea pig cytomegalovirus (GPCMV) was used to model primary maternal infection and compare the effects of infection at two different times on the placenta. When guinea pigs were infected with GPCMV at either 21- or 35-days gestation (dGA), maternal and placental viral loads, as determined by droplet digital PCR, were not significantly affected by the timing of maternal infection. However, when the transcriptomes of gestational age-matched GPCMV-infected and control placentas were compared, significant infection-associated changes in gene expression were only observed after maternal infection at 35 dGA. Notably, transcripts associated with immune activation (e.g. *Cxcl10*, *Ido1*, *Tgtp1*, and *Tlr8*) were upregulated in the infected placenta. A GPCMV-specific *in situ* hybridization assay detected rare infected cells in the main placenta after maternal infection at either time, and maternal infection at 35 dGA also caused large areas of GPCMV-infected cells in the junctional zone. As GPCMV infection after mid-gestation is known to cause high rates of stillbirth and/or fetal growth restriction, our results suggest that the placenta becomes sensitized to infection-associated injury late in gestation, conferring an increased risk of adverse pregnancy outcomes after cytomegalovirus infection.

Keywords: cytomegalovirus, congenital infection, inflammation, placenta, fetal membranes, guinea pig

OPEN ACCESS

Edited by:
Ashley L. St John, Duke-NUS Medical School, Singapore

Reviewed by:
Stephanie N. Langel, Duke University, United States
Daniel Malouli, Oregon Health and Science University, United States

***Correspondence:**
Craig J. Bierle
cjbierle@umn.edu

Specialty section:
This article was submitted to Viral Immunology, a section of the journal Frontiers in Immunology

Received: *26 March 2021*
Accepted: *25 May 2021*
Published: *15 June 2021*

Citation:
Berkebile ZW, Putri DS, Abrahante JE, Seelig DM, Schleiss MR and Bierle CJ (2021) The Placental Response to Guinea Pig Cytomegalovirus Depends Upon the Timing of Maternal Infection. Front. Immunol. 12:686415. doi: 10.3389/fimmu.2021.686415

INTRODUCTION

Congenital cytomegalovirus infection (cCMV), a leading cause of sensorineural hearing loss and neurocognitive disability in children, occurs in roughly 1 in 200 pregnancies (1–3). cCMV is also a cause of intrauterine growth restriction, preterm birth, and fetal demise (4–8). The timing of maternal human cytomegalovirus (HCMV) infection during pregnancy affects the rate of congenital transmission and fetal outcomes post-infection (9–18). Neurologic sequelae are most frequently

observed in congenitally infected children when maternal infection occurs in the first trimester (14–17). Maternal infection late in pregnancy is associated with the highest rates of intrauterine growth restriction (IUGR) and congenital infection (9–13, 15, 18).

HCMV infects the placenta and these placental infections can cause fetal injury, including spontaneous abortion and neonatal demise, even in the absence of detectable viral transmission to the fetus (4, 5, 19–22). HCMV-associated placental pathology includes chronic villitis, cytomegalic cells, and areas of necrosis and calcification (19, 22–24). HCMV was detected in 15% of fetal remains and/or placenta after stillbirth and infection was found to be associated with fetal thrombotic vasculopathy (4). In a cohort of women with a prenatal diagnosis of fetal growth restriction, the detection of HCMV antigen in the placenta correlated with higher rates of villitis and more severe growth restriction than cases of IUGR without HCMV involvement (21). While HCMV appears to cause a hypoxia-like condition in infected placenta, how HCMV causes placental dysfunction remains poorly understood (22).

HCMV and other viruses may injure the placenta either directly by causing cytopathic effects in infected cells or by activating the maternal or fetal immune system and triggering placental immunopathology (25). Dysmature villi were frequently observed in HCMV-infected placentas, suggesting that infection can interfere with early placental development (19). Trophoblast progenitor cells can be infected by HCMV, and HCMV infection both limits the capacity of trophoblast progenitors to differentiate *in vitro* and disrupts the formation of anchoring villi in first trimester placental explants (26–28). The inflammatory response to viral infection during pregnancy can also cause placental dysfunction and adverse pregnancy outcomes (29). For example, type I interferon signaling triggered by Zika virus can cause abnormal placental development in mice and syncytial knot formation in villous explants (30). cCMV causes a proinflammatory cytokine bias in the placenta and amniotic fluid, but whether this host response disrupts normal placental function has yet to be determined (31, 32).

As the species-specificity of HCMV precludes its study in animals, guinea pig cytomegalovirus (GPCMV) has become the most widely used experimental model of cCMV (33, 34). Guinea pigs deliver precocious pups after gestational periods that average 65 days. Similarities between guinea pigs and humans include hemomonochorial placentas that invade deeply into the decidua and the prenatal development of major organs and the immune system (35–37). These similarities between human and guinea pig placentation and development make the rodent a uniquely powerful comparative model for understanding the developmental origins of health and disease (35). GPCMV infection studies have revealed that placental and fetal infection occur sequentially after maternal inoculation (34, 38–41). If maternal infection occurs early in pregnancy, infectious virus may not be detected in pup organs and evidence of prior fetal infection can be limited to the presence of infection-associated histologic lesions in pup organs (41–43). Maternal GPCMV infection after mid-gestation has been found to cause high rates of stillbirth and IUGR in pups (42–44).

In this study, we investigated whether the susceptibility and antiviral responses of the placenta to GPCMV infection varied across gestation. Time mated guinea pigs were infected either at 21 days gestation (dGA, "early") or at 35 dGA ("late"). No significant differences in maternal or placental viral loads were noted between the two groups at 21 days post-infection (dpi). However, infection after mid-gestation caused more frequent fetal membrane infections and significant changes in placental gene expression that were not observed after infection at the earlier time point. Furthermore, *in situ* hybridization revealed that GPCMV infection primarily localized to the junctional zone after maternal infection at the later time. Our observations lead us to propose that GPCMV-associated stillbirth and IUGR are the result of developmentally regulated changes in the placenta that predispose the organ to infection-associated injury late in gestation.

MATERIALS AND METHODS

Cells and Virus

A minimally tissue culture adapted stock of GPCMV 22122 (ATCC VR-682), prepared as previously described by passaging guinea pig salivary gland homogenate twice on JH4 guinea pig lung fibroblasts (ATCC CCL-158), was used for this study (33, 45, 46). JH4 cells were purchased from ATCC and propagated according to their specifications excepting that the growth media was supplemented with sodium bicarbonate (47). GPCMV stocks were prepared as previously described and titered on JH4 cells (48). For animal studies, virus was aliquoted into single-use units, flash-frozen, and stored at -80°C. These aliquots were routinely re-titered as guinea pigs were infected to confirm that the stock did not deteriorate during storage.

Ethics Statement

All animal procedures were conducted in accordance with protocols approved by the Institutional Animal Care and Use Committee (IACUC) at the University of Minnesota, Minneapolis (Protocol ID: 1810-36403A). Experimental protocols and endpoints were developed in strict accordance to the National Institutes of Health Office of Laboratory Animal Welfare (Animal Welfare Assurance #A3456-01), Public Health Service Policy on Humane Care and Use of Laboratory Animals, and United States Department of Agriculture Animal Welfare Act guidelines and regulations (USDA Registration # 41-R-0005) with the oversight and approval of the IACUC. Outbred Hartley guinea pigs were initially purchased from Elm Hill Laboratories (Chelmsford, MA). Breeding pairs of strain 2 and strain 13 guinea pigs were generously shared by MS and the U.S. Army Medical Research Institute of Infectious Diseases, respectively. Guinea pigs were housed in a facility maintained by the University of Minnesota Research Animal Resources, who were accredited through the Association for Assessment and Accreditation of Laboratory Animal Care, International (AAALAC). All procedures were conducted by trained personnel under the supervision of veterinary staff.

Animal Pathogenicity Study

The GPCMV serostatus of all animals received from an external source was tested by ELISA within one week of receipt and again after one month of housing at the University of Minnesota (49). Only GPCMV seronegative animals were used for infection studies. Female guinea pigs were bred at two to three months of age. After the delivery of their first litter, the animals were bred a second time during postpartum estrus to establish timed pregnancies by housing with a male for three days postpartum. These second pregnancies were confirmed by progesterone ELISA (DRG International); only animals with plasma progesterone concentrations exceeding 15 ng/ml by 20 days postpartum were included in this study (50).

At either 21 (range 18 to 23) or 35 (range 33 to 35) dGA guinea pigs were injected subcutaneously into the scruff of the neck with 0.5 ml of PBS containing $2x10^5$ PFU of GPCMV or PBS alone. Blood and plasma were collected from dams every seven days post-infection (dpi) until they were euthanized at 14, 21, or 28 dpi. After euthanasia, blood and plasma were collected from the dams and amniotic fluid was collected from the pups. Pup tissue samples were divided and frozen for DNA extraction, stabilized in RNAlater (ThermoFisher) for RNA extraction, embedded in optimal cutting temperature (O.C.T.) compound (Fisher Scientific), or immersion-fixed using Shandon Formal-Fixx (ThermoFisher) and embedded in paraffin.

Viral Load Quantification by Droplet Digital PCR

After DNA was extracted from whole blood, tissue, and amniotic fluid, GPCMV genomes were quantified by droplet digital PCR (ddPCR) using primers and probes specific to *GP54* using the Bio-Rad QX200 system as previously described (46). ddPCR results were analyzed using the QuantaSoft™ Analysis Pro software (Bio-Rad); GPCMV viral loads are presented as the number of copies genome per ml of fluid or mg of tissue.

RNA Sequencing

RNA was extracted from guinea pig placentas that had been stabilized in RNAlater (ThermoFisher) and stored at -20°C using the RNAeasy Mini Kit (Qiagen). ~30 mg pieces of placenta were combined with 0.6 ml of β-mercaptoethanol-containing RLT buffer and Lysing Matrix D (MP Biomedicals) and pulsed at 6 m/s for 30 seconds in a FastPrep 24 (MP Biomedicals). RNA was extracted from 0.45 ml of the resulting homogenate using the manufacturer's standard protocol, including the optional on-column DNase I digest (Qiagen), Total RNA integrity was assessed by capillary electrophoresis using an Agilent TapeStation; all samples used for library creation had RNA integrity numbers that exceeded 7.0.

Dual indexed TruSeq stranded mRNA libraries were prepared and sequenced using a NextSeq 550 high-output 75-bp single-end run (mean of $22.4x10^6$ reads/sample). FastQ reads were trimmed using Trimmomatic (v 0.33) enabled with the optional "-q" option; 3bp sliding-window trimming from 3' end requiring minimum Q30 (51). Quality control on raw sequence data for each sample was performed with FastQC. Read mapping was performed *via* Hisat2 (v2.1.0) using the "Cavpor3.0" genome (GCF_000151735.1) as reference (52). Gene quantification was done *via* Cuffquant for FPKM values and Feature Counts for raw read counts (53, 54). Differentially expressed genes were identified using the edgeR (negative binomial) feature in CLCGWB (Qiagen) using raw read counts (55). The generated list was filtered based on a minimum 2X Absolute Fold Change and False Discovery Rate corrected $p < 0.05$. Raw and processed RNA-Seq data have been deposited in NCBI's Gene Expression Omnibus and are accessible through GEO Series accession number GSE169358 (56). Normalized gene expression data (FPKM) was uploaded to ClustVis for data visualization and heat map analysis (57). Gene Ontology (GO) analysis was performed by uploading a list of differentially expressed transcripts to g:Profiler (58). Results from this GO analysis were visualized using Cytoscape, Enrichment Map, ClusterMaker2, and WordCloud (59–63).

Real-Time Droplet Digital PCR Analyses

RNA was extracted from placenta as described above. A two-step reverse transcriptase ddPCR (RT-ddPCR) protocol was used to quantify transcript abundance (46). cDNA was synthesized from total RNA using the Maxima™ H Minus cDNA Synthesis Master Mix (ThermoFisher). PCR primers targeting guinea pig transcripts were designed using the Primer Quest tool and were ordered from Integrated DNA Technologies (**Table S2**). ddPCR reactions were prepared using the EvaGreen Digital PCR Supermix (Bio-Rad) using a primer concentration of 250 nM and cycled using the following thermal conditions: 95°C for 5 min; 40 cycles of 95°C for 30 s and 60°C for 30s; 4°C for 5 min; 90°C for 5 min; hold at 4°C. The ddPCR data were analyzed with QuantaSoft™ Analysis Pro software (Bio-Rad). Absolute quantification of gene expression was presented as copies per nanogram of total RNA.

In Situ Hybridization

5-μm sections of paraffin-embedded placenta were mounted onto Superfrost Plus slides (ThermoFisher). After air drying the tissue sections overnight, the slides were baked at 60°C for 1 hr. Tissue was deparaffinized and pretreated using the recommended protocol for RNAscope® 2.5 Assays (ACD Document #322452). For target retrieval, samples were incubated at 99°C for 15 minutes, and the slides were treated with RNAscope Protease Plus for 30 minutes. Slides were stained using either the RNAscope 2.5 HD Detection Reagent – RED (ACD Document # 322360-USM) or the RNAscope 2.5 HD Duplex Reagent (322500-USM) and the RNAscope Probe V-CavHV-2-gp3. Stained slides were scanned using a Huron TissueScope LE and the number of *gp3*+ foci and areas of *gp3*-staining were counted and calculated using NIS-Elements BR (Nikon).

RESULTS

The Timing of Maternal GPCMV Infection Affects the Rate of Fetal Membrane Infection but Not Placental Viral Loads

To study how the timing of maternal GPCMV infection affects viral loads in the placenta, extraplacental membranes, and fetus, guinea pigs were time mated during postpartum estrus and

infected at either 21 or 35 days gestation (dGA) (**Figure 1**). HCMV infection during the first trimester causes most cases of neurologic disability in congenitally infected children, and infecting guinea pigs at 21 dGA exposes the pup and placenta to virus during a comparable period of late embryonic/early fetal development (14–17, 65). GPCMV infection after mid-gestation has been found to often cause fetal growth restriction and/or stillbirth (42–44). As high rates of ischemic injury and virus-specific focal necrosis and inflammation had been reported 21 days after maternal infection at 30 dGA, we elected to infect animals at 35 dGA and analyze matched pups and placentas at 21 dpi, before expected still- or preterm birth, to identify mechanisms that could cause these adverse pregnancy outcomes (39).

Five groups of animals were used in this study. Three groups of Hartley guinea pigs were infected at 21 dGA and euthanized at either 14, 21, or 28 dpi. The remaining two groups were inbred strain 2 females bred with strain 13 males to create hybrid pregnancies (2X13) and were infected with GPCMV at either at 21 or 35 dGA and euthanized at 21 dpi (66). This study compared GPCMV pathogenesis between the outbred and inbred guinea pigs and examined the effect of maternal infection at the two different times on the placenta. Most prior GPCMV research has been done in Hartley guinea pigs, and the few studies that compared GPCMV infection between inbred and outbred guinea pigs have yielded conflicting results as to whether strain 2 or strain 13 animals are more susceptible to infection than Hartley guinea pigs (67–69).

Guinea pigs were infected with $2X10^5$ PFU of GPCMV or mock-infected by subcutaneous injection. While Hartley dams were on-average larger than strain 2 females, no differences in maternal weight gain were noted between GPCMV-infected and control dams (**Figure S1**). Maternal blood and serum were collected weekly until each animal's predetermined endpoint. GPCMV viral load was quantified using a droplet digital PCR (ddPCR) assay targeting *GP54* (46). When maternal viremia at 7 dpi and viral loads in spleen were quantified, infection was confirmed in all dams and no significant differences were noted between the five groups (**Table S1** and **Figure S2A**).

The placentas from the two groups of guinea pigs that were infected at 21 dGA and euthanized at 21 dpi were compared, and significantly higher viral loads were detected in the strain 2X13 placentas than in their Hartley counterparts (Mann–Whitney U test, P<0.0001) (**Figure 2A**). No other significant differences in placental viral load were noted in the remaining groups. When viral loads were assessed in the extraplacental membranes, GPCMV was detected in both the amnion and visceral yolk sac (**Table 1** and **Figure S2B**) (46). A significant correlation (Pearson r=0.5056, $p<0.001$) in GPCMV viral loads was observed in the amnion and yolk sac of individual fetuses (**Figure 2B**). The highest frequencies of fetal membrane infection and the highest viral loads in the membranes were observed in the dams infected at 35 dGA. GPCMV was only detected in a handful of amniotic fluid samples collected from guinea pigs infected at 35 dGA, consistent with previous observations that GPCMV generally does not accumulate in amniotic fluid (43, 46, 69).

Fetal infection was assayed by quantifying viral loads in the brain. GPCMV was most often detected at 14 dpi and occasionally at later times post-infection. As the brain is less frequently infected by GPCMV than other fetal tissues, these results may underreport the actual rate of congenital GPCMV infection in this experiment and/or indicate that fetal infections resolved *in utero* (42, 43). The fetuses of GPCMV infected dams trended smaller than their mock-infected counterparts in most cases (**Table S1** and **Figure S2C**). However, due in part to unexpectedly large variation in litter sizes, this study was underpowered to determine whether GPCMV caused fetal growth restriction. Guinea pigs bred during postpartum estrus had significantly larger litters than expected, including many large litters of 6-8 pups, and fetal weights correlate with litter size after mid-gestation (37).

To summarize, our animal studies found that maternal infection at 35 dGA resulted in higher rates of fetal membrane

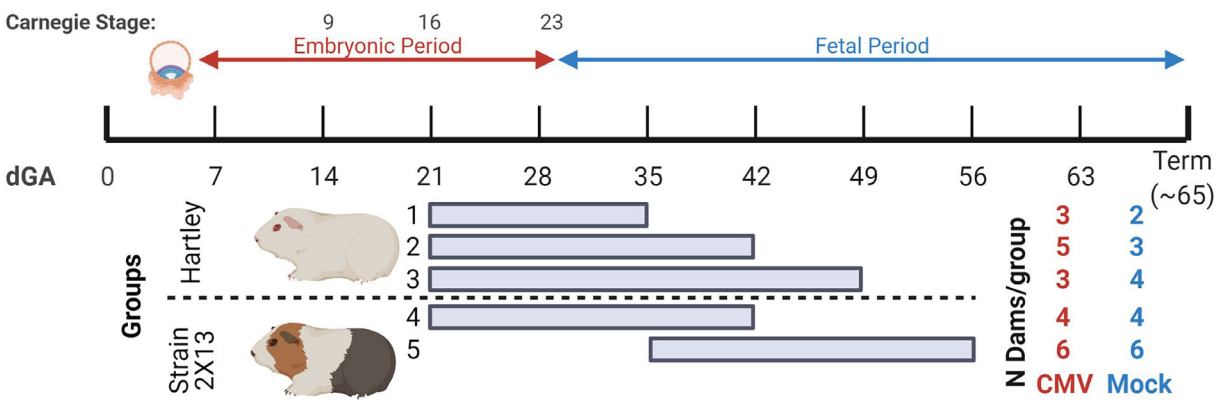

FIGURE 1 | Summary of GPCMV infections in time mated guinea pigs. The ~65-day gestational period of guinea pigs is diagramed. Implantation occurs at 5-6 dGA and the embryonic period ends at 29 dGA. Reference Carnegie stages for guinea pig development are indicated (64). Five groups of GPCMV-infected and control guinea pigs were used in this study, including outbred Hartley guinea pigs and inbred strain 2 females that were bred to strain 13 males (producing semi-allogenic, hybrid pregnancies). Guinea pigs were infected either at 21 dGA (embryonic period) or at 35 dGA (fetal period). The number of GPCMV- and mock-infected dams for each group is shown. Figure created with BioRender.com.

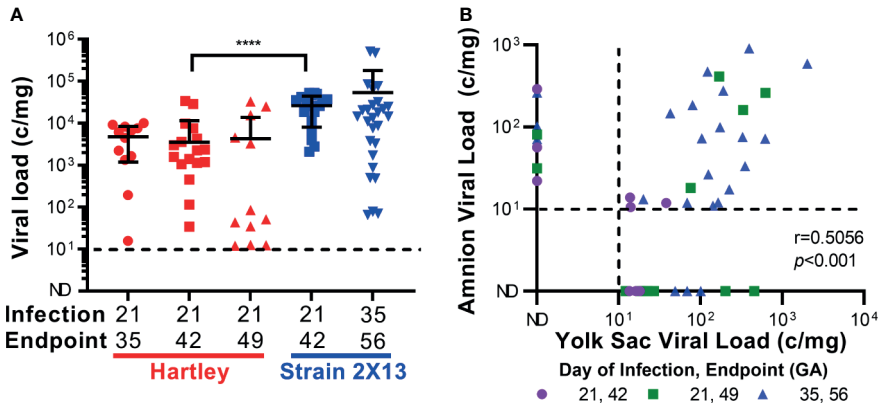

FIGURE 2 | GPCMV viral loads after maternal infection during pregnancy. Time mated guinea pigs were infected at either 21 or 35 dGA with $2X10^5$ PFU of GPCMV and euthanized 14, 21, or 28 days later. DNA was extracted from tissues and GPCMV viral loads were determined using a ddPCR assay specific to *GP54*. The limit of detection for this assay is indicated by the dashed line. **(A)** Viral load in placentas. Significantly higher viral loads (Mann-Whitney test, **** $p < 0.0001$) were observed in the placentas of strain 2X13 hybrids than in the placentas of Hartley guinea pigs. **(B)** Viral loads in infected fetal membranes. The number of GPCMV genome copies detected in the amnion and visceral yolk sac of individual fetuses was significantly correlated (Pearson r=0.5056, $p < 0.001$).

TABLE 1 | Summary of GPCMV viral load data.

Strain	dGA of infection, endpoint	Placenta		Amnion		Yolk Sac		Fetus[3]	AF[4]
		CMV+[1]	MVL[2]	CMV+[1]	MVL[2]	CMV+[1]	MVL[2]	CMV+[1]	CMV+[1]
Hartley	21,35	12/12	$5.7x10^3$	0/10	N/A	0/10	N/A	9/10	0/10
	21,42	17/29	$6.0x10^3$	4/29	$1.5x10^1$	4/28	$2.0x10^1$	9/29	0/29
	21,49	12/19	$6.8x10^3$	6/19	$1.6x10^2$	11/19	$1.8x10^2$	9/19	0/18
2X13	21,42	18/19	$2.8x10^4$	2/18	$1.7x10^2$	2/18	$1.7x10^1$	0/18	0/18
	35,56	27/27	$5.4x10^4$	18/24	$1.8x10^2$	22/24	$2.5x10^2$	4/27	4/21

[1]*Samples containing detectable GPCMV DNA/total number of samples.*
[2]*Mean viral load (MVL) expressed as copies/ml for infected blood and amniotic fluid or copies/mg for infected tissue.*
[3]*Viral load in fetal brain quantified.*
[4]*Amniotic fluid.*

infection and higher viral loads in the amnion and yolk sac than infection at 21 dGA. However, neither the timing of maternal infection nor the experimental endpoint had a significant effect on placental viral load. Higher viral loads were noted in placentas from our strain 2X13 hybrid pregnancies when compared to Hartley guinea pigs, but there was no other evidence that indicated that infection was more severe in the inbred animals. Presuming that there would be minimal animal-to-animal variation in the placental response to infection in guinea pigs with a consistent maternal and fetal genetic background, we focused on the strain 2X13 animals in our subsequent analysis of the effect of infection on placental function.

GPCMV Infection After Mid-Gestation Significantly Alters Placental Gene Expression

Having found that the timing of maternal GPCMV infection did not affect placental viral loads, we next compared how infection at our earlier and later time point affected placental gene expression. For this analysis, placentas were randomly selected from inbred guinea pigs that had been GPCMV- or mock-infected either at 21 or 35 dGA and euthanized at 21 dpi. RNA was extracted from four placentas from four GPCMV-infected dams and four placentas from three control dams per group and sequenced (**Table S1**). A principal component analysis of RNA-Seq data revealed that the samples clustered based upon the gestational age of placenta (**Figure 3A**). GPCMV- infected and control placenta from the early infection groups clustered tightly, while there was clear separation between GPCMV- and mock-infected samples after maternal infection at 35 dGA. Pairwise gene expression comparisons between age-matched groups of GPCMV and mock-infected tissues affirmed these findings. GPCMV infection at 21 dGA had a limited effect on placental gene expression at 21 dpi: only 8 transcripts were differentially regulated (≥2 fold, $p < 0.05$). In contrast, maternal infection at 35 dGA resulted in the differential regulation of 126 transcripts (≥2 fold, $p < 0.05$) at 21 dpi. A gene set enrichment analysis was performed on the transcripts that were differentially expressed after GPCMV infection late in pregnancy (58). This analysis found that several gene ontology terms related to the immune response (including GO:0002376, immune system process) were significantly enriched after GPCMV infection at 35 dGA (**Figure S3A**).

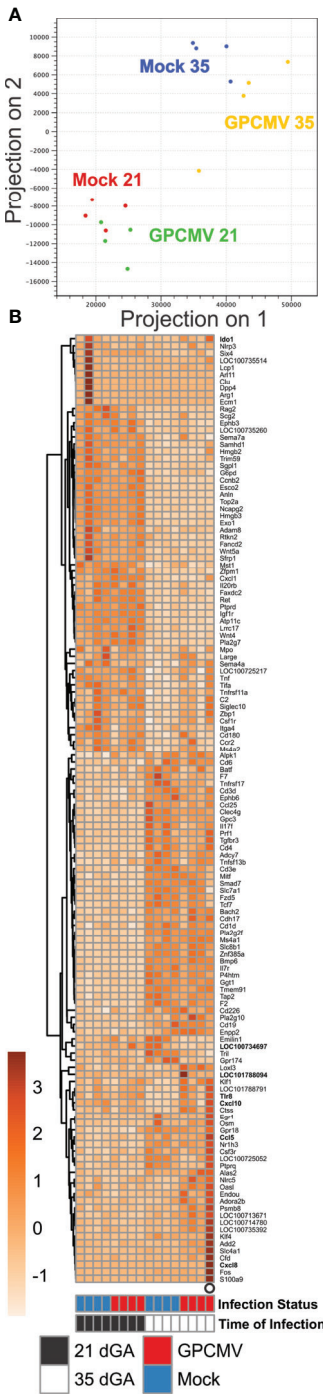

FIGURE 3 | Transcriptome profiling of GPCMV-infected placenta. Time mated guinea pigs were GPCMV- or mock-infected at 21 or 35 dGA and euthanized 21 days later. RNA was extracted from placentas (N=4/group) and gene expression was quantified by Illumina RNA-Seq. **(A)** Principal component analysis illustrating the similarity in gene expression between samples. **(B)** Heat map illustrating the relative expression of transcripts that function as part of an immune system processes (GO:0002376) that were differentially expressed in placenta either during normal development or after GPCMV infection. Transcripts that were also analyzed by RT-ddPCR are shown in bold.

In a pairwise gene expression analysis that compared the two groups of mock-infected placentas, the gestational age of placentas was found to have a much more significant effect on gene expression than GPCMV infection: 1438 transcripts were differentially regulated (≥2 fold, $p < 0.05$) between the two groups of control tissue. Gene ontogeny analysis found numerous terms related to the regulation of the mitotic cell, signaling receptor activity, and condensed chromosome regions were enriched in this pairwise comparison (**Figure S3B**). Many of the gene expression differences between normal placenta from 42 and 56 dGA appear to be related to the relatively higher expression of transcripts involved in cell division and the cell cycle by the younger tissue. While transcripts that function as part of an immune system process were not found to be significantly enriched in our comparison of normal placentas, 116 transcripts related to the immune response were differentially expressed between the two groups (**Figure 3B**, **Table S3**). We hypothesize that these normal changes in placental immunity may cause GPCMV infection after mid-gestation to significantly affect placental gene expression.

As only four samples of placenta per group were analyzed by RNA-seq, sample-to-sample variation in gene expression could be caused either by regional differences in transcription in the relatively large guinea pig placenta or represent the unique responses of individual fetuses to GPCMV infection. To better elucidate host factors that regulate the placenta's response to GPCMV, we used reverse transcriptase droplet digital PCR (RT-ddPCR) to measure the expression of select transcripts that function as part of the inflammatory response in additional placenta samples. For this experiment, RNA was extracted from two placentas per dam (including the samples that had been previously analyzed by RNA-Seq). RT-ddPCR confirmed that four genes– *Cxcl10*, *Ido1*, *Tgtp1*, and *Tlr8*–were significantly upregulated after maternal infection at 35 dGA when compared to age-matched control placentas (**Figure 4**). This analysis also found that *Cxcl10* and *Ido1* are normally downregulated as the guinea pig placenta matures and that GPCMV infection at 21 dGA leads to decreased *Ido1* expression relative to age-matched normal placenta. RT-ddPCR analysis did not support the RNA-Seq finding that several other inflammatory mediators—*Ccl5*, *Ccl15-l*, *Cxcl8*, *Il1b*, and *Il36b-l*—were differentially regulated by maternal GPCMV infection at 35 dGA (**Figure S4**). In the case of *Cxcl8* and *Il1b*, high levels of cytokine transcription were noted in the placenta of a dam that had been euthanized while delivering stillborn pups at 56 dGA (these placentas are represented as open circles in **Figures 3**, **4**, and **Figure S4**). The elevated transcription of these cytokines may not be specific to GPCMV infection and instead be inflammatory markers of preterm labor or *in utero* fetal demise (70, 71). Cumulatively, our gene expression analyses of GPCMV-infected placenta suggest that the immune response is dysregulated by GPCMV infection after mid-gestation but not after infection earlier in pregnancy.

The Junctional Zone Becomes Infected by GPCMV After Maternal Infection After Mid-Gestation

Finally, we compared the frequency and localization of GPCMV-infected cells in the placenta using *in situ* hybridization. For this

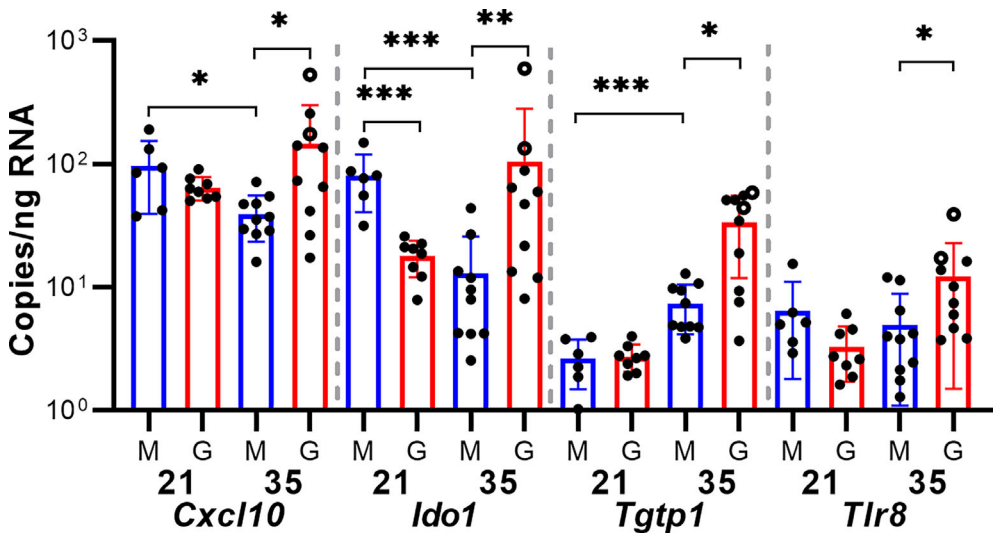

FIGURE 4 | GPCMV infection dysregulates immune gene transcription. A two-step RT-ddPCR protocol was used to quantify the expression of select transcripts in GPCMV- (G) and mock-infected (M) placentas after maternal infection at either 21 or 35 dGA. Data from two placentas per dam is shown. Statistically significant differences were calculated by Mann-Whitney test (*$p < 0.05$, **$p < 0.01$, ***$p < 0.001$).

study, we designed an RNAscope probe specific to the GPCMV transcript *gp3*. RNA-Seq analysis had revealed that *gp3* is highly expressed during all phases of GPCMV replication (**Figure S5**) (46). *gp3*+ foci, each representing either an individual infected cell or a group of infected cells, were manually counted in stained placenta sections (**Figure 5**). A small number of *gp3*+ foci were observed in the interlobium and labyrinth of all GPCMV-infected placenta (**Figure 5C**). When the placentas of dams infected at 21 and 35 dGA were compared, significantly more GPCMV infected cells were noted in the margin of placentas, including either the parietal yolk sac or marginal syncytium, after infection at the later time. Large areas of *gp3*+ cells were detected in the junctional zone in eight of ten of the placentas from the late infection group (**Figures 5A, B, D**). These large areas of GPCMV-infected cells were often adjacent to either the subplacenta or large blood vessels and were never detected after maternal infection at 21 dGA. Whether GPCMV infection of the junctional zone reflects the recruitment of infected cells to the placenta late in pregnancy or if there is a cell type in this region that becomes permissive to GPCMV infection as the placenta matures remains to be determined.

DISCUSSION

The timing of HCMV infection during pregnancy is a determinant of fetal outcomes, yet how placental development affects the course and severity of cCMV remains poorly understood (25, 72). Using the GPCMV model, we assessed how the placenta and fetal membranes are differentially affected by maternal infection at two times: 21 and 35 dGA. Prior research has found that GPCMV infection early in pregnancy can resolve prenatally while infection after mid-gestation often causes stillbirth and fetal growth restriction (42–44). Our study identified several possible explanations for these adverse pregnancy outcomes, including an increased rate of fetal membrane and junctional zone infection late in gestation and a transcriptional response to GPCMV that may indicate that placental immunopathology only occurs after maternal infection at later times in pregnancy.

This study found that GPCMV infects both the amnion and the yolk sack, that viral loads in the two membranes are correlated, and that the highest rates of infection and viral loads in the membranes occur after maternal infection late in pregnancy (46). While GPCMV joins HCMV on a short list of viruses that have been observed to infect the fetal membranes, it remains unclear whether or how viral infections of the fetal membrane affect the fetus (24, 73). In contrast, ascending bacterial infections, a significant cause of preterm labor, have a much better understood effect on fetal membrane physiology. Bacterial infection, treatment with inflammatory cytokines, or exposure to pathogen-associated molecular patterns can all trigger preterm labor in animal models and/or cause fetal membrane explants to biomechanically weaken *ex vivo* (71, 74–76). Several studies have suggested that viral infection may sensitize the fetal membranes to later damage from bacteria (77–79). It has also been hypothesized that fetal membrane infection may allow viruses to circumvent the potent antiviral defense of the placenta to infect the fetus (80). In this paraplacental route of infection, viruses that infect the chorioamnion may be shed into amniotic fluid and infect the fetus. Given that this study's primary focus was on the effect of infection on the placenta, future experiments that specifically analyze the effect of GPCMV on the fetal membranes are merited.

Developmentally programmed changes in maternal, placental, and fetal immunity are critical for healthy

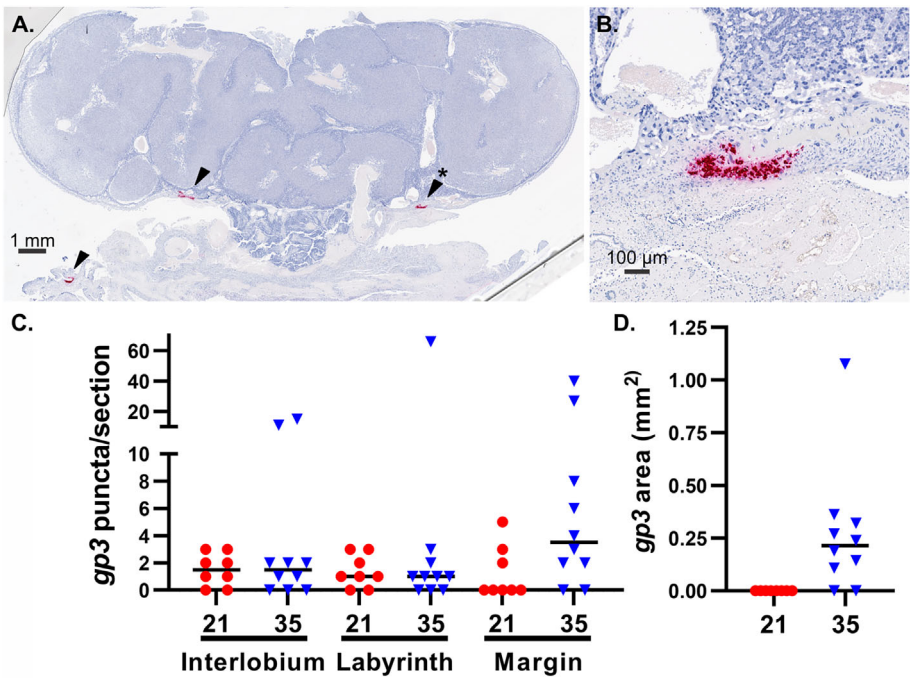

FIGURE 5 | GPCMV localization in infected placenta. An RNAscope probe specific to GPCMV *gp3* was used to detect infected cells in sections of placenta by *in situ* hybridization. **(A)** A representative section of a placenta from a dam infected at 35 dGA, illustrating large areas of GPCMV infected cells in the junctional zone and decidua (red, indicated by arrows). **(B)** High-magnification image of infected cells in the junctional zone (*). **(C)** *gp3*+ puncta, representing individual infected cells or small groups of infected cells, were counted based on their localization in the placenta after maternal infection at 21 or 35 dGA and collection at 21 dpi. **(D)** The measured area of *gp3*+ stained cells in the junctional zone of placentas is shown.

pregnancy, helping to establish and maintain maternal-fetal tolerance, remodel the uterus, and regulate parturition (30, 71). Alterations in maternal immunity can increase the severity of viral infections late in pregnancy (81). Severe, third-trimester infections caused by viruses such as influenza and hepatitis E can cause fetal injury or demise. High rates of maternal demise have been reported in some GPCMV infection studies (38, 82). However, HCMV infections are typically mild and there is no evidence that the virus causes more severe illness in pregnant individuals (83). We found that the timing of maternal GPCMV infection did not significantly affect maternal, placental, or fetal viral loads, and severe illness was not noted in dams that had been infected at the later time. Having eliminated severe maternal illnesses as a cause of adverse pregnancy outcomes in our experiments, the remainder of this study focused on the placental response to GPCMV infection.

Prior work in placental cells and explants has found that gestational age affects how permissive the cells or tissue are to viral infection and the nature of the inflammatory response that is triggered by infection (84, 85). Our study found that maternal infection at 35 dGA significantly altered placental gene expression while infection at 21 dGA had remarkably little effect on placental gene expression. Infection after mid-gestation upregulated numerous transcripts that function as part of an immune system process. Two transcripts that are dysregulated by placental GPCMV infection, *Cxcl10* and *Ido1*, are particularly relevant to the pathogenesis of cCMV. CXCL10, a biomarker of VUE, chronic chorioamnionitis, and late preterm birth, is found at elevated concentrations in amniotic fluid and maternal sera during cCMV (31, 86–89). Curiously, while the concentration of CXCL10 in amniotic fluid correlates with CMV genome abundance, the chemokine does not appear to accumulate in amniotic fluid when other viruses cause intrauterine infections (32). We and others have found that CXCL10 transcription is upregulated when placental cells or tissue are infected with HCMV or GPCMV *in vitro* (46, 84, 85). Indoleamine-2,3-dioxygenase (IDO) is an enzyme that is encoded by two genes, *IDO1* and *IDO2*, that catalyze the rate-limiting step in tryptophan catabolism. IDO production by the placenta and the subsequent metabolism of tryptophan prevents the rejection of the allogeneic fetus by suppressing T cell proliferation and activity (90). IDO is more highly expressed by the human placenta during the first-trimester than at term and HCMV infection suppressed IDO expression in early placenta (91). While our gene expression analysis was limited to a single time point post-infection, GPCMV may cause placental immunopathology but only after maternal infection relatively late in pregnancy.

In an analysis of placental pathology after GPCMV infection, pregnant Hartley guinea pigs were inoculated with GPCMV at 30 dGA. Infection caused ischemic injury and necrosis associated with acute or chronic inflammation beginning at 14 dpi and

GPCMV-specific antigens and viral particles were most frequently observed at 28 dpi in the marginal and interlobar transitional zones of the main placenta (39). We used *in situ* hybridization to compare the localization of GPCMV in the placenta 21 days after infection at 21 or 35 dGA. Like Griffith and colleagues, we detected occasional infected cells in the main placenta after infection at either time. However, the most consistent pattern of infection and largest lesions localized to the junctional zone, which is situated between the main placenta and the maternal decidua. These lesions were only found after infection at 35 dGA and may indicate that a ring of GPCMV-sensitive cells develop at the base of the placenta as term approaches. Given how frequently we detected this pattern of junctional zone infection, we were surprised it had not been previously reported. However, because our RNAscope assay targets a viral transcript (*gp3*) that is highly expressed during all phases of GPCMV's replication, *in situ* hybridization may be more sensitive than electron microscopy or immunohistochemistry for detecting GPCMV infected cells.

Cumulatively, our data suggests the placenta becomes more sensitized to GPCMV infection-associated injury late in gestation either due to a potentially pathogenic immune response or by the fetal membranes and junctional zone becoming more permissive to infection. Numerous questions remain. Because GPCMV-associated lesions had previously been reported exclusively in the main placenta, we extracted DNA and RNA for viral load quantification and gene expression analyses from this tissue (37, 39). A more nuanced analysis that compares the rate of GPCMV infection and the immune response in the decidua, junctional zone, and main placenta is justified. Our study did not investigate the effects of infection during the earliest stages of pregnancy. One report has noted that maternal GPCMV infection immediately prior to conception caused high rates of fetal demise, suggesting that the virus may perturb early placental development and function (40). Due to the limited availability of normal tissue between twenty weeks gestation and term, how viral infection effects the function of the human placenta after mid-gestation remains poorly characterized. Given similarities in the placental response of humans and guinea pigs to CMV infection and that comparative gene expression analyses suggest that murine placental development largely parallels the first half of human pregnancy, guinea pigs may be particularly well suited to model intrauterine infection after mid-gestation (92).

DATA AVAILABILITY STATEMENT

The datasets presented in this study can be found in online repositories. The names of the repository/repositories and accession number(s) can be found in the article/**Supplementary Material**.

ETHICS STATEMENT

The animal study was reviewed and approved by Institutional Animal Care and Use Committee at the University of Minnesota.

AUTHOR CONTRIBUTIONS

CB conceived and designed the study. CB, ZB, and DP collected the data. All authors participated in data analysis and interpretation. CB drafted the manuscript. All authors contributed to the article and approved the submitted version.

FUNDING

This project was supported by grants from the Minnesota Masonic Charities (Masonic Early Investigator Award) and the National Institutes of Health (R21HD087496, R01HD098866, and UL1TR002494).

ACKNOWLEDGMENTS

Breeding pairs of strain 13 guinea pigs were generously shared by the U.S. Army Medical Research Institute of Infectious Diseases. Next-generation sequencing library generation and Illumina sequencing were completed by the University of Minnesota Genomics Center. Histopathologic studies were supported by Colleen Forster of the University of Minnesota Histology and Research Laboratory, which is supported by the National Institutes of Health's National Center for Advancing Translational Sciences, grant UL1TR002494, and the resources and staff of the University of Minnesota University Imaging Centers (UIC, SCR_020997). Grants from the National Institutes of Health (R21HD087496 to CB and R01HD098866 to MS) and the Minnesota Masons (Masonic Early Investigator Award to CB) supported this work. The funders had no role in study design, data collection, analysis, decision to publish, or preparation of the manuscript.

SUPPLEMENTARY MATERIAL

The Supplementary Material for this article can be found online at: https://www.frontiersin.org/articles/10.3389/fimmu.2021.686415/full#supplementary-material

REFERENCES

1. Pereira L. Congenital Viral Infection: Traversing the Uterine-Placental Interface. *Annu Rev Virol* (2018) 5(1):273–99. doi: 10.1146/annurev-virology-092917-043236
2. Kenneson A, Cannon MJ. Review and Meta-Analysis of the Epidemiology of Congenital Cytomegalovirus (Cmv) Infection. *Rev Med Virol* (2007) 17 (4):253–76. doi: 10.1002/rmv.535
3. Mocarski ESJr., Shenk T, Griffiths PD, Pass RF. Cytomegaloviruses. In: Knipe DM, Howley PM, editors. *Fields Virology, 6th*. Philadelphia, PA: Wolters Kluwer/Lippincott Williams & Wilkins Health (2013). p. 1960–2014.

4. Iwasenko JM, Howard J, Arbuckle S, Graf N, Hall B, Craig ME, et al. Human Cytomegalovirus Infection Is Detected Frequently in Stillbirths and Is Associated With Fetal Thrombotic Vasculopathy. *J Infect Dis* (2011) 203 (11):1526–33. doi: 10.1093/infdis/jir121
5. Pereira L, Petitt M, Fong A, Tsuge M, Tabata T, Fang-Hoover J, et al. Intrauterine Growth Restriction Caused by Underlying Congenital Cytomegalovirus Infection. *J Infect Dis* (2014) 209(10):1573–84. doi: 10.1093/infdis/jiu019
6. Panhani S, Heinonen KM. Screening for Congenital Cytomegalovirus Infection Among Preterm Infants Born Before the 34th Gestational Week in Finland. *Scand J Infect Dis* (1994) 26(4):375–8. doi: 10.3109/00365549409008607
7. Gibson CS, Goldwater PN, MacLennan AH, Haan EA, Priest K, Dekker GA, et al. Fetal Exposure to Herpesviruses May Be Associated With Pregnancy-Induced Hypertensive Disorders and Preterm Birth in a Caucasian Population. *BJOG* (2008) 115(4):492–500. doi: 10.1111/j.1471-0528.2007.01653.x
8. Shi TL, Huang LJ, Xiong YQ, Zhong YY, Yang JJ, Fu T, et al. The Risk of Herpes Simplex Virus and Human Cytomegalovirus Infection During Pregnancy Upon Adverse Pregnancy Outcomes: A Meta-Analysis. *J Clin Virol* (2018) 104:48–55. doi: 10.1016/j.jcv.2018.04.016
9. Preece PM, Blount JM, Glover J, Fletcher GM, Peckham CS, Griffiths PD. The Consequences of Primary Cytomegalovirus Infection in Pregnancy. *Arch Dis Child* (1983) 58(12):970–5. doi: 10.1136/adc.58.12.970
10. Bodeus M, Hubinont C, Goubau P. Increased Risk of Cytomegalovirus Transmission In Utero During Late Gestation. *Obstet Gynecol* (1999) 93(5 Pt 1):658–60. doi: 10.1097/00006250-199905000-00005
11. Gindes L, Teperberg-Oikawa M, Sherman D, Pardo J, Rahav G. Congenital Cytomegalovirus Infection Following Primary Maternal Infection in the Third Trimester. *BJOG* (2008) 115(7):830–5. doi: 10.1111/j.1471-0528.2007.01651.x
12. Bodeus M, Kabamba-Mukadi B, Zech F, Hubinont C, Bernard P, Goubau P. Human Cytomegalovirus in Utero Transmission: Follow-Up of 524 Maternal Seroconversions. *J Clin Virol* (2010) 47(2):201–2. doi: 10.1016/j.jcv.2009.11.009
13. Picone O, Vauloup-Fellous C, Cordier AG, Guitton S, Senat MV, Fuchs F, et al. A Series of 238 Cytomegalovirus Primary Infections During Pregnancy: Description and Outcome. *Prenat Diagn* (2013) 33(8):751–8. doi: 10.1002/pd.4118
14. Pass RF, Fowler KB, Boppana SB, Britt WJ, Stagno S. Congenital Cytomegalovirus Infection Following First Trimester Maternal Infection: Symptoms at Birth and Outcome. *J Clin Virol* (2006) 35(2):216–20. doi: 10.1016/j.jcv.2005.09.015
15. Faure-Bardon V, Magny JF, Parodi M, Couderc S, Garcia P, Maillotte AM, et al. Sequelae of Congenital Cytomegalovirus Following Maternal Primary Infections Are Limited to Those Acquired in the First Trimester of Pregnancy. *Clin Infect Dis* (2019) 69(9):1526–32. doi: 10.1093/cid/ciy1128
16. Lipitz S, Yinon Y, Malinger G, Yagel S, Levit L, Hoffman C, et al. Risk of Cytomegalovirus-Associated Sequelae in Relation to Time of Infection and Findings on Prenatal Imaging. *Ultrasound Obstet Gynecol* (2013) 41(5):508–14. doi: 10.1002/uog.12377
17. Foulon I, Naessens A, Foulon W, Casteels A, Gordts F. A 10-Year Prospective Study of Sensorineural Hearing Loss in Children With Congenital Cytomegalovirus Infection. *J Pediatr* (2008) 153(1):84–8. doi: 10.1016/j.jpeds.2007.12.049
18. Elkan Miller T, Weisz B, Yinon Y, Weissbach T, De Castro H, Avnet H, et al. Congenital Cytomegalovirus Infection Following Second and Third Trimester Maternal Infection Is Associated With Mild Childhood Adverse Outcome Not Predicted by Prenatal Imaging. *J Pediatr Infect Dis Soc* (2021) 10(5):562–8. doi: 10.1093/jpids/piaa154
19. Garcia AG, Fonseca EF, Marques RL, Lobato YY. Placental Morphology in Cytomegalovirus Infection. *Placenta* (1989) 10(1):1–18. doi: 10.1016/0143-4004(89)90002-7
20. Muhlemann K, Miller RK, Metlay L, Menegus MA. Cytomegalovirus Infection of the Human Placenta: An Immunocytochemical Study. *Hum Pathol* (1992) 23(11):1234–7. doi: 10.1016/0046-8177(92)90290-j
21. Tsuge M, Hida AI, Minematsu T, Honda N, Oshiro Y, Yokoyama M, et al. Prospective Cohort Study of Congenital Cytomegalovirus Infection During Pregnancy With Fetal Growth Restriction: Serologic Analysis and Placental Pathology. *J Pediatr* (2019) 206:42–8 e2. doi: 10.1016/j.jpeds.2018.10.003
22. Maidji E, Nigro G, Tabata T, McDonagh S, Nozawa N, Shiboski S, et al. Antibody Treatment Promotes Compensation for Human Cytomegalovirus-Induced Pathogenesis and a Hypoxia-Like Condition in Placentas With Congenital Infection. *Am J Pathol* (2010) 177(3):1298–310. doi: 10.2353/ajpath.2010.091210
23. Sinzger C, Muntefering H, Loning T, Stoss H, Plachter B, Jahn G. Cell Types Infected in Human Cytomegalovirus Placentitis Identified by Immunohistochemical Double Staining. *Virchows Arch A Pathol Anat Histopathol* (1993) 423(4):249–56. doi: 10.1007/BF01606887
24. Uenaka M, Morizane M, Tanimura K, Deguchi M, Kanzawa M, Itoh T, et al. Histopathological Analysis of Placentas With Congenital Cytomegalovirus Infection. *Placenta* (2019) 75:62–7. doi: 10.1016/j.placenta.2019.01.003
25. Yockey LJ, Lucas C, Iwasaki A. Contributions of Maternal and Fetal Antiviral Immunity in Congenital Disease. *Science* (2020) 368(6491):608–12. doi: 10.1126/science.aaz1960
26. Tabata T, Petitt M, Zydek M, Fang-Hoover J, Larocque N, Tsuge M, et al. Human Cytomegalovirus Infection Interferes With the Maintenance and Differentiation of Trophoblast Progenitor Cells of the Human Placenta. *J Virol* (2015) 89(9):5134–47. doi: 10.1128/JVI.03674-14
27. Tabata T, Petitt M, Fang-Hoover J, Rivera J, Nozawa N, Shiboski S, et al. Cytomegalovirus Impairs Cytotrophoblast-Induced Lymphangiogenesis and Vascular Remodeling in an In Vivo Human Placentation Model. *Am J Pathol* (2012) 181(5):1540–59. doi: 10.1016/j.ajpath.2012.08.003
28. Zydek M, Petitt M, Fang-Hoover J, Adler B, Kauvar LM, Pereira L, et al. Hcmv Infection of Human Trophoblast Progenitor Cells of the Placenta is Neutralized by a Human Monoclonal Antibody to Glycoprotein B and Not by Antibodies to the Pentamer Complex. *Viruses* (2014) 6(3):1346–64. doi: 10.3390/v6031346
29. Mor G, Aldo P, Alvero AB. The Unique Immunological and Microbial Aspects of Pregnancy. *Nat Rev Immunol* (2017) 17(8):469–82. doi: 10.1038/nri.2017.64
30. Yockey LJ, Iwasaki A. Interferons and Proinflammatory Cytokines in Pregnancy and Fetal Development. *Immunity* (2018) 49(3):397–412. doi: 10.1016/j.immuni.2018.07.017
31. Scott GM, Chow SS, Craig ME, Pang CN, Hall B, Wilkins MR, et al. Cytomegalovirus Infection During Pregnancy With Maternofetal Transmission Induces a Proinflammatory Cytokine Bias in Placenta and Amniotic Fluid. *J Infect Dis* (2012) 205(8):1305–10. doi: 10.1093/infdis/jis186
32. Gervasi MT, Romero R, Bracalente G, Chaiworapongsa T, Erez O, Dong Z, et al. Viral Invasion of the Amniotic Cavity (VIAC) in the Midtrimester of Pregnancy. *J Matern Fetal Neonatal Med* (2012) 25(10):2002–13. doi: 10.3109/14767058.2012.683899
33. Hartley JW, Rowe WP, Huebner RJ. Serial Propagation of the Guinea Pig Salivary Gland Virus in Tissue Culture. *Proc Soc Exp Biol Med* (1957) 96 (2):281–5. doi: 10.3181/00379727-96-23455
34. Choi YC, Hsiung GD. Cytomegalovirus Infection in Guinea Pigs. II. Transplacental and Horizontal Transmission. *J Infect Dis* (1978) 138 (2):197–202. doi: 10.1093/infdis/138.2.197
35. Morrison JL, Botting KJ, Darby JRT, David AL, Dyson RM, Gatford KL, et al. Guinea Pig Models for Translation of the Developmental Origins of Health and Disease Hypothesis Into the Clinic. *J Physiol* (2018) 596(23):5535–69. doi: 10.1113/JP274948
36. Mess A, Zaki N, Kadyrov M, Korr H, Kaufmann P. Caviomorph Placentation as a Model for Trophoblast Invasion. *Placenta* (2007) 28(11-12):1234–8. doi: 10.1016/j.placenta.2007.08.003
37. Kaufmann P, Davidoff M. The Guinea-Pig Placenta. *Adv Anat Embryol Cell Biol* (1977) 53(2):5–91. doi: 10.1007/978-3-642-66618-6
38. Auerbach MR, Yan D, Vij R, Hongo JA, Nakamura G, Vernes JM, et al. A Neutralizing Anti-Gh/Gl Monoclonal Antibody is Protective in the Guinea Pig Model of Congenital Cmv Infection. *PloS Pathog* (2014) 10(4):e1004060. doi: 10.1371/journal.ppat.1004060
39. Griffith BP, McCormick SR, Fong CK, Lavallee JT, Lucia HL, Goff E. The Placenta as a Site of Cytomegalovirus Infection in Guinea Pigs. *J Virol* (1985) 55(2):402–9. doi: 10.1128/JVI.55.2.402-409.1985
40. Harrison CJ, Myers MG. Relation of Maternal Cmv Viremia and Antibody Response to the Rate of Congenital Infection and Intrauterine Growth Retardation. *J Med Virol* (1990) 31(3):222–8. doi: 10.1002/jmv.1890310309
41. Kumar ML, Prokay SL. Experimental Primary Cytomegalovirus Infection in Pregnancy: Timing and Fetal Outcome. *Am J Obstet Gynecol* (1983) 145 (1):56–60. doi: 10.1016/0002-9378(83)90339-3
42. Griffith BP, Lucia HL, Hsiung GD. Brain and Visceral Involvement During Congenital Cytomegalovirus Infection of Guinea Pigs. *Pediatr Res* (1982) 16 (6):455–9. doi: 10.1203/00006450-198206000-00010

43. Griffith BP, Hsiung GD. Cytomegalovirus Infection in Guinea Pigs. IV. Maternal Infection at Different Stages of Gestation. *J Infect Dis* (1980) 141 (6):787–93. doi: 10.1093/infdis/141.6.787
44. Harrison CJ, Britt WJ, Chapman NM, Mullican J, Tracy S. Reduced Congenital Cytomegalovirus (Cmv) Infection After Maternal Immunization With a Guinea Pig CMV Glycoprotein Before Gestational Primary Cmv Infection in the Guinea Pig Model. *J Infect Dis* (1995) 172(5):1212–20. doi: 10.1093/infdis/172.5.1212
45. Yang D, Tamburro K, Dittmer D, Cui X, McVoy MA, Hernandez-Alvarado N, et al. Complete Genome Sequence of Pathogenic Guinea Pig Cytomegalovirus From Salivary Gland Homogenates of Infected Animals. *Genome Announc* (2013) 1(2):e0005413. doi: 10.1128/genomeA.00054-13
46. Putri DS, Berkebile ZW, Mustafa HJ, Fernandez-Alarcon C, Abrahante JE, Schleiss MR, et al. Cytomegalovirus Infection Elicits a Conserved Chemokine Response From Human and Guinea Pig Amnion Cells. *Virology* (2020) 548:93–100. doi: 10.1016/j.virol.2020.06.005
47. Hoying JJ. *Selection and Histochemical Identification of Epithelial-Like Cells From Guinea Pig Lung. [M.s.]*. Dayton, Ohio: W.S.U. Printing Service: Wright State University (1975).
48. Britt WJ. Human Cytomegalovirus: Propagation, Quantification, and Storage. *Curr Protoc Microbiol* (2010) 18:14E.3.1–3.17. doi: 10.1002/97804717 29259.mc14e03s18
49. Schleiss MR, Bourne N, Stroup G, Bravo FJ, Jensen NJ, Bernstein DI. Protection Against Congenital Cytomegalovirus Infection and Disease in Guinea Pigs, Conferred by a Purified Recombinant Glycoprotein B Vaccine. *J Infect Dis* (2004) 189(8):1374–81. doi: 10.1086/382751
50. Bierle CJ, Fernandez-Alarcon C, Hernandez-Alvarado N, Zabeli JC, Janus BC, Putri DS, et al. Assessing Zika Virus Replication and the Development of Zika-Specific Antibodies After a Mid-Gestation Viral Challenge in Guinea Pigs. *PloS One* (2017) 12(11):e0187720. doi: 10.1371/journal.pone.0187720
51. Bolger AM, Lohse M, Usadel B. Trimmomatic: A Flexible Trimmer for Illumina Sequence Data. *Bioinformatics* (2014) 30(15):2114–20. doi: 10.1093/bioinformatics/btu170
52. Siren J, Valimaki N, Makinen V. Indexing Graphs for Path Queries With Applications in Genome Research. *IEEE/ACM Trans Comput Biol Bioinform* (2014) 11(2):375–88. doi: 10.1109/TCBB.2013.2297101
53. Trapnell C, Roberts A, Goff L, Pertea G, Kim D, Kelley DR, et al. Differential Gene and Transcript Expression Analysis of RNA-seq Experiments With TopHat and Cufflinks. *Nat Protoc* (2012) 7(3):562–78. doi: 10.1038/nprot.2012.016
54. Liao Y, Smyth GK, Shi W. The Subread Aligner: Fast, Accurate and Scalable Read Mapping by Seed-and-Vote. *Nucleic Acids Res* (2013) 41(10):e108. doi: 10.1093/nar/gkt214
55. Robinson MD, McCarthy DJ, Smyth GK. Edger: A Bioconductor Package for Differential Expression Analysis of Digital Gene Expression Data. *Bioinformatics* (2010) 26(1):139–40. doi: 10.1093/bioinformatics/btp616
56. Edgar R, Domrachev M, Lash AE. Gene Expression Omnibus: NCBI Gene Expression and Hybridization Array Data Repository. *Nucleic Acids Res* (2002) 30(1):207–10. doi: 10.1093/nar/30.1.207
57. Metsalu T, Vilo J. ClustVis: a web tool for visualizing clustering of multivariate data using Principal Component Analysis and heatmap. *Nucleic Acids Res* (2015) 43(W1):W566–70. doi: 10.1093/nar/gkv468
58. Raudvere U, Kolberg L, Kuzmin I, Arak T, Adler P, Peterson H, et al. G: Profiler: A Web Server for Functional Enrichment Analysis and Conversions of Gene Lists (2019 Update). *Nucleic Acids Res* (2019) 47(W1):W191–W8. doi: 10.1093/nar/gkz369
59. Shannon P, Markiel A, Ozier O, Baliga NS, Wang JT, Ramage D, et al. Cytoscape: A Software Environment for Integrated Models of Biomolecular Interaction Networks. *Genome Res* (2003) 13(11):2498–504. doi: 10.1101/gr.1239303
60. Merico D, Isserlin R, Stueker O, Emili A, Bader GD. Enrichment Map: A Network-Based Method for Gene-Set Enrichment Visualization and Interpretation. *PloS One* (2010) 5(11):e13984. doi: 10.1371/journal.pone.0013984
61. Oesper L, Merico D, Isserlin R, Bader GD. Wordcloud: A Cytoscape Plugin to Create a Visual Semantic Summary of Networks. *Source Code Biol Med* (2011) 6:7. doi: 10.1186/1751-0473-6-7
62. Morris JH, Apeltsin L, Newman AM, Baumbach J, Wittkop T, Su G, et al. Clustermaker: A Multi-Algorithm Clustering Plugin for Cytoscape. *BMC Bioinf* (2011) 12:436. doi: 10.1186/1471-2105-12-436
63. Reimand J, Isserlin R, Voisin V, Kucera M, Tannus-Lopes C, Rostamianfar A, et al. Pathway Enrichment Analysis and Visualization of Omics Data Using G: Profiler, GSEA, Cytoscape and Enrichmentmap. *Nat Protoc* (2019) 14(2):482–517. doi: 10.1038/s41596-018-0103-9
64. Butler H. *An Atlas for Staging Mammalian and Chick Embryos*. In: Juurlink BHJ, editor. Boca Raton, Fla: CRC Press (1987).
65. Harman MT, Dobrovolny MP. The Development of the External Form of the Guinea-Pig (Cavia Cobaya) Between the Ages of 21 Days and 35 Days of Gestation. *J Morphol* (1933) 54(3):493–519. doi: 10.1002/jmor.1050540306
66. Wright S. *The Effects of Inbreeding and Crossbreeding on Guinea Pigs: I. Decline in Vigor : II. Differentiation Among Inbred Families*. Washington, D.C: U.S. Dept. of Agriculture (1922).
67. Fong CK, Lucia H, Bia FJ, Hsiung GD. Histopathologic and Ultrastructural Studies of Disseminated Cytomegalovirus Infection in Strain 2 Guinea Pigs. *Lab Invest* (1983) 49(2):183–94.
68. Nozawa N, Yamamoto Y, Fukui Y, Katano H, Tsutsui Y, Sato Y, et al. Identification of a 1.6 Kb Genome Locus of Guinea Pig Cytomegalovirus Required for Efficient Viral Growth in Animals But Not in Cell Culture. *Virology* (2008) 379(1):45–54. doi: 10.1016/j.virol.2008.06.018
69. Griffith BP, McCormick SR, Booss J, Hsiung GD. Inbred Guinea Pig Model of Intrauterine Infection With Cytomegalovirus. *Am J Pathol* (1986) 122(1):112–9.
70. Goldstein JA, Gallagher K, Beck C, Kumar R, Gernand AD. Maternal-Fetal Inflammation in the Placenta and the Developmental Origins of Health and Disease. *Front Immunol* (2020) 11:531543. doi: 10.3389/fimmu.2020.531543
71. Romero R, Espinoza J, Goncalves LF, Kusanovic JP, Friel L, Hassan S. The Role of Inflammation and Infection in Preterm Birth. *Semin Reprod Med* (2007) 25(1):21–39. doi: 10.1055/s-2006-956773
72. Chatzakis C, Ville Y, Makrydimas G, Dinas K, Zavlanos A, Sotiriadis A. Timing of Primary Maternal Cytomegalovirus Infection and Rates of Vertical Transmission and Fetal Consequences. *Am J Obstet Gynecol* (2020) 223 (6):870–83.e11. doi: 10.1016/j.ajog.2020.05.038
73. Tabata T, Petitt M, Fang-Hoover J, Zydek M, Pereira L. Persistent Cytomegalovirus Infection in Amniotic Membranes of the Human Placenta. *Am J Pathol* (2016) 186(11):2970–86. doi: 10.1016/j.ajpath.2016.07.016
74. Kumar D, Moore RM, Mercer BM, Mansour JM, Redline RW, Moore JJ. The Physiology of Fetal Membrane Weakening and Rupture: Insights Gained From the Determination of Physical Properties Revisited. *Placenta* (2016) 42:59–73. doi: 10.1016/j.placenta.2016.03.015
75. Yoshimura K, Hirsch E. Effect of Stimulation and Antagonism of Interleukin-1 Signaling on Preterm Delivery in Mice. *J Soc Gynecol Investig* (2005) 12 (7):533–8. doi: 10.1016/j.jsgi.2005.06.006
76. McCarthy R, Martin-Fairey C, Sojka DK, Herzog ED, Jungheim ES, Stout MJ, et al. Mouse Models of Preterm Birth: Suggested Assessment and Reporting Guidelines. *Biol Reprod* (2018) 99(5):922–37. doi: 10.1093/biolre/ioy109
77. Potter JA, Tong M, Aldo P, Kwon JY, Pitruzzello M, Mor G, et al. Viral Infection Dampens Human Fetal Membrane Type I Interferon Responses Triggered by Bacterial Lps. *J Reprod Immunol* (2020) 140:103126. doi: 10.1016/j.jri.2020.103126
78. Cross SN, Potter JA, Aldo P, Kwon JY, Pitruzzello M, Tong M, et al. Viral Infection Sensitizes Human Fetal Membranes to Bacterial Lipopolysaccharide by MERTK Inhibition and Inflammasome Activation. *J Immunol* (2017) 199 (8):2885–95. doi: 10.4049/jimmunol.1700870
79. Bakaysa SL, Potter JA, Hoang M, Han CS, Guller S, Norwitz ER, et al. Single- and Double-Stranded Viral RNA Generate Distinct Cytokine and Antiviral Responses in Human Fetal Membranes. *Mol Hum Reprod* (2014) 20(7):701–8. doi: 10.1093/molehr/gau028
80. Tabata T, Petitt M, Puerta-Guardo H, Michlmayr D, Wang C, Fang-Hoover J, et al. Zika Virus Targets Different Primary Human Placental Cells, Suggesting Two Routes for Vertical Transmission. *Cell Host Microbe* (2016) 20(2):155–66. doi: 10.1016/j.chom.2016.07.002
81. Kourtis AP, Read JS, Jamieson DJ. Pregnancy and Infection. *N Engl J Med* (2014) 370(23):2211–8. doi: 10.1056/NEJMra1213566
82. Griffith BP, Lucia HL, Tillbrook JL, Hsiung GD. Enhancement of Cytomegalovirus Infection During Pregnancy in Guinea Pig. *J Infect Dis* (1983) 147(6):990–8. doi: 10.1093/infdis/147.6.990
83. Davis NL, King CC, Kourtis AP. Cytomegalovirus Infection in Pregnancy. *Birth Defects Res* (2017) 109(5):336–46. doi: 10.1002/bdra.23601

84. Weisblum Y, Panet A, Zakay-Rones Z, Vitenshtein A, Haimov-Kochman R, Goldman-Wohl D, et al. Human Cytomegalovirus Induces a Distinct Innate Immune Response in the Maternal-Fetal Interface. *Virology* (2015) 485:289–96. doi: 10.1016/j.virol.2015.06.023
85. Weisblum Y, Oiknine-Djian E, Vorontsov OM, Haimov-Kochman R, Zakay-Rones Z, Meir K, et al. Zika Virus Infects Early- and Midgestation Human Maternal Decidual Tissues, Inducing Distinct Innate Tissue Responses in the Maternal-Fetal Interface. *J Virol* (2017) 91(4):e01905–16. doi: 10.1128/JVI.01905-16
86. Lee J, Romero R, Chaiworapongsa T, Dong Z, Tarca AL, Xu Y, et al. Characterization of the Fetal Blood Transcriptome and Proteome in Maternal Anti-Fetal Rejection: Evidence of a Distinct and Novel Type of Human Fetal Systemic Inflammatory Response. *Am J Reprod Immunol* (2013) 70(4):265–84. doi: 10.1111/aji.12142
87. Romero R, Chaemsaithong P, Chaiyasit N, Docheva N, Dong Z, Kim CJ, et al. CXCL10 and IL-6: Markers of Two Different Forms of Intra-Amniotic Inflammation in Preterm Labor. *Am J Reprod Immunol* (2017) 78(1):e12685. doi: 10.1111/aji.12685
88. Gervasi MT, Romero R, Bracalente G, Erez O, Dong Z, Hassan SS, et al. Midtrimester Amniotic Fluid Concentrations of Interleukin-6 and Interferon-Gamma-Inducible Protein-10: Evidence for Heterogeneity of Intra-Amniotic Inflammation and Associations With Spontaneous Early (<32 Weeks) and Late (>32 Weeks) Preterm Delivery. *J Perinat Med* (2012) 40(4):329–43. doi: 10.1515/jpm-2012-0034
89. Lee J, Kim JS, Park JW, Park CW, Park JS, Jun JK, et al. Chronic Chorioamnionitis is the Most Common Placental Lesion in Late Preterm Birth. *Placenta* (2013) 34(8):681–9. doi: 10.1016/j.placenta.2013.04.014
90. Munn DH, Zhou M, Attwood JT, Bondarev I, Conway SJ, Marshall B, et al. Prevention of Allogeneic Fetal Rejection by Tryptophan Catabolism. *Science* (1998) 281(5380):1191–3. doi: 10.1126/science.281.5380.1191
91. Lopez H, Benard M, Saint-Aubert E, Baron M, Martin H, Al Saati T, et al. Novel Model of Placental Tissue Explants Infected by Cytomegalovirus Reveals Different Permissiveness in Early and Term Placentae and Inhibition of Indoleamine 2,3-Dioxygenase Activity. *Placenta* (2011) 32(7):522–30. doi: 10.1016/j.placenta.2011.04.016
92. Soncin F, Khater M, To C, Pizzo D, Farah O, Wakeland A, et al. Comparative Analysis of Mouse and Human Placentae Across Gestation Reveals Species-Specific Regulators of Placental Development. *Development* (2018) 145(2):dev156273. doi: 10.1242/dev.156273
93. Kearse M, Moir R, Wilson A, Stones-Havas S, Cheung M, Sturrock S, et al. Geneious Basic: An Integrated and Extendable Desktop Software Platform for the Organization and Analysis of Sequence Data. *Bioinformatics* (2012) 28(12):1647–9. doi: 10.1093/bioinformatics/bts199

Conflict of Interest: The authors declare that the research was conducted in the absence of any commercial or financial relationships that could be construed as a potential conflict of interest.

frontiers in Immunology

ORIGINAL RESEARCH
published: 18 June 2021
doi: 10.3389/fimmu.2021.686411

Evaluating the Safety of West Nile Virus Immunity During Congenital Zika Virus Infection in Mice

Joshua A. Acklin[1,2], *Javier D. Cattle*[1,3], *Arianna S. Moss*[1], *Julia A. Brown*[1,2], *Gregory A. Foster*[4], *David Krysztof*[4], *Susan L. Stramer*[4] *and Jean K. Lim*[1*]

[1] Department of Microbiology, Icahn School of Medicine at Mount Sinai, New York, NY, United States, [2] Graduate School of Biomedical Sciences, Icahn School of Medicine at Mount Sinai, New York, NY, United States, [3] Department of Epidemiology, Mailman School of Public Health, Columbia University, New York, NY, United States, [4] Scientific Affairs, American Red Cross, Gaithersburg, MD, United States

Antibody-dependent enhancement (ADE) is a phenomenon that occurs when cross-reactive antibodies generated from a previous flaviviral infection increase the pathogenesis of a related virus. Zika virus (ZIKV) is the most recent flavivirus introduced to the Western Hemisphere and has become a significant public health threat due to the unanticipated impact on the developing fetus. West Nile virus (WNV) is the primary flavivirus that circulates in North America, and we and others have shown that antibodies against WNV are cross-reactive to ZIKV. Thus, there is concern that WNV immunity could increase the risk of severe ZIKV infection, particularly during pregnancy. In this study, we examined the extent to which WNV antibodies could impact ZIKV pathogenesis in a murine pregnancy model. To test this, we passively transferred WNV antibodies into pregnant *Stat2*$^{-/-}$ mice on E6.5 prior to infection with ZIKV. Evaluation of pregnant dams showed weight loss following ZIKV infection; however, no differences in maternal weights or viral loads in the maternal brain, spleen, or spinal cord were observed in the presence of WNV antibodies. Resorption rates, and other fetal parameters, including fetal and placental size, were similarly unaffected. Further, the presence of WNV antibodies did not significantly alter the viral load or the inflammatory response in the placenta or the fetus in response to ZIKV. Our data suggest that pre-existing WNV immunity may not significantly impact the pathogenesis of ZIKV infection during pregnancy. Our findings are promising for the safety of implementing WNV vaccines in the continental US.

Keywords: flavivirus, congenital Zika syndrome, antibody dependent enhancement, vaccines, placenta

OPEN ACCESS

Edited by:
Ashley L. St John, Duke-NUS Medical School, Singapore

Reviewed by:
Amelia K. Pinto, Saint Louis University, United States
Annie Elong Ngono, La Jolla Institute for Immunology (LJI), United States

***Correspondence:**
Jean K. Lim
jean.lim@mssm.edu

Specialty section:
This article was submitted to Viral Immunology, a section of the journal Frontiers in Immunology

Received: *26 March 2021*
Accepted: *24 May 2021*
Published: *18 June 2021*

Citation:
Acklin JA, Cattle JD, Moss AS, Brown JA, Foster GA, Krysztof D, Stramer SL and Lim JK (2021) Evaluating the Safety of West Nile Virus Immunity During Congenital Zika Virus Infection in Mice. Front. Immunol. 12:686411. doi: 10.3389/fimmu.2021.686411

INTRODUCTION

Antibody-dependent enhancement (ADE) is a phenomenon by which antibodies elicited from a previous infection facilitate viral entry into a susceptible cell through the engagement of Fc gamma receptors (FcγRs) (1, 2). The most established example of ADE in humans occurs between the four serotypes of dengue virus (DENV), a mosquito-transmitted flavivirus that is estimated to cause ~390 million infections annually around the globe (3, 4). Studies show that while primary infections

with DENV are typically mild, secondary infections with a heterotypic DENV serotype are more frequently severe, with increased incidence of dengue hemorrhagic fever (DHF) and dengue shock syndrome (DSS) (5, 6). ADE between the DENV serotypes is poised to occur due to the unique degree of cross-reactivity between the antigenic envelope proteins, and the fact that the four serotypes co-circulate (7–12). While high concentrations of cross-reactive antibodies may offer protection in the short term, these same antibodies can promote pathogenesis through ADE if secondary infection occurs during a time when the concentration of antibodies falls below the neutralization threshold (13, 14). Observing ADE in human populations is difficult and requires prospective studies in flavivirus endemic areas (15). In the case of dengue, while the phenomenon of severe secondary infections has been observed for decades, the correlation between antibody titers and severe disease was only directly demonstrated recently (16). A major question in the field that remains is whether this occurs with other flaviviruses in humans. In the absence of human data, *in vitro* and *in vivo* models can offer clues into this possibility. The data generated by such studies hold broad implications for the development of any flavivirus vaccine (17).

In 2016, Zika virus (ZIKV), a flavivirus closely related to DENV, received global attention after it was found to be the cause of a large outbreak that started in Brazil and spread to nearly every South and Central American country. While ZIKV has historically been associated with mild disease, this recent outbreak was much more severe (18–23). The most concerning disease outcomes were observed in pregnant women, where the virus impacted the developing fetus, resulting in spontaneous abortions and fetal abnormalities such as microcephaly (24). Based on confirmed ZIKV infections, the CDC estimates that 10% of pregnancies resulted in some form of fetal abnormality; this number increased to 15% when evaluating infections that occured during the first trimester (22, 25). Additionally, two recent studies showed that children that were exposed to ZIKV *in utero* were at greater risk of developing neurological deficits and developmental delays in their early years of life despite no overt signs of ZIKV-related damage at birth (26, 27). It remains unclear what factors may have led to the increased pathogenesis of ZIKV in the most recent outbreaks, but one possibility is the involvement of ADE. Given that antibodies against DENV can both bind to and enhance ZIKV *in vitro* and *in vivo*, and since DENV is endemic in ZIKV outbreak regions, pre-existing immunity to DENV could have been a contributing factor to the severity of the recent ZIKV outbreak (28–35). We have previously reported that passive transfer of DENV reactive antibodies can potently enhance ZIKV infection in pregnant mice. Enhanced infection resulted in heightened maternal weight loss, fetal developmental delays, damage to the developing placenta, and finally increased resorption. We further showed the dependency on antibodies as this process was maintained with purified DENV reactive IgG and reversed with FcγR blocking (32).

In the United States, DENV does not regularly circulate as it does in South and Central America. However, West Nile virus (WNV), another closely related flavivirus, causes annual outbreaks of neurological disease, primarily meningitis, encephalitis, and acute flaccid paralysis (36). WNV is estimated to have infected at least 7 million people since its introduction into the Western Hemisphere in 1999 (37, 38). There is a great need for a WNV vaccine for human use, and should one be approved, WNV seropositivity would increase significantly. This is concerning because we and others have demonstrated that antibodies elicited by WNV are cross-reactive to ZIKV, suggesting that preexisting WNV immunity has the potential to impact ZIKV pathogenesis (31, 39, 40). In fact, during the 2016 outbreak, mosquito transmission of ZIKV occurred in both Texas and Florida, demonstrating the potential for ZIKV to expand into WNV-endemic areas (41). This risk is expected to increase as global temperatures rise (42). In this manuscript, we seek to understand the extent to which pre-existing WNV immunity impacts ZIKV outcomes during pregnancy using a *Stat2*$^{-/-}$ mouse model of ZIKV ADE.

MATERIALS AND METHODS

Generation of Human Immune Plasma

WNV-infected blood donors were identified through screening 52,355,427 blood donations in the United States between August 2003-December 2011. Initial screening was conducted through WNV nucleic acid testing (NAT). Blood donors were identified as WNV-infected if the initial WNV NAT was reactive, repeat WNV NAT was also reactive, and WNV-specific IgM and/or IgG antibody testing results were positive on the initial blood donation or upon follow up testing. Testing for WNV antibodies was conducted by Abbott Laboratories (2003-2004; Abbott Park IL) or Focus Diagnostics (2003-2011; San Juan Capistrano CA). We received plasma from 471 WNV-infected blood donors that met these criteria. Among these, we included only those samples where positive reactivity for WNV-specific IgG on the index sample was documented (n = 146). DENV-immune plasma samples were collected as previously described (31). Random blood donor plasma samples (n = 54) that were negative for all infectious pathogens were used as negative controls. All plasma samples were individually tested for reactivity to ZIKV E protein by ELISA as previously described (31). 15 individual donors with the highest reactivity to ZIKV E protein from the DENV or WNV cohorts were pooled and used for these experiments. All control plasma failed to react to ZIKV E protein, and 15 random donors were pooled and used for the CTRL-immune plasma condition.

Neutralization Assays

Neutralization titers were determined by co-incubating serially diluted, heat-inactivated pooled immune plasma with 10 50% tissue culture infectious doses ($TCID_{50}$) of WNV Kunjin isolate (CH16532), DENV-1 (BC89/94), or ZIKV (PRVABC-59) in DMEM with 2% FBS. After shaking at room temperature for 1 hour, the virus-antibody mixture was added to a monolayer of Vero cells in 96 well format. Following a two-day incubation at

37°C, cells were detached from the plate using trypsin/EDTA, fixed with 4% PFA, permeabilized with PBS containing 0.2% BSA and 0.05% saponin, and stained with 4G2 antibody (1 µg/ml) for 1 hour at room temperature. After washing, cells were incubated with goat anti-mouse IgG conjugated to phycoerythrin (1µg/ml, Invitrogen) for 1 hour at room temperature. The percentage of infected cells was determined by flow cytometry using a FACS Caliber and analyzed using FlowJo2 software version 10.1.r7. The 50% inhibitory doses (IC_{50}) of each plasma pool was calculated by using the four-parameter logarithmic regression in GraphPad Prism.

In Vitro Antibody-Dependent Enhancement of ZIKV Infection

Antibody-dependent enhancement of ZIKV infection was measured using a flow cytometry-based assay. Briefly, serial dilutions of either non-reactive (CTRL), DENV-immune or WNV-immune human plasma were pre-incubated with ZIKV strain PRVABC-59 at an MOI of 1 for 1 hour at 37°C. Immune complexes were then co-incubated with K562 cells (5×10^4) in 96 well U-bottom plates in RPMI 1640 media supplemented with 10% FBS, 2 mM L-glutamine, 10 µg/ml penicillin, and 10µg/ml streptomycin. After incubation for 48 hours at 37°C, cells were fixed with 4% PFA, permeabilized with PBS containing 0.2% BSA and 0.05% saponin, and stained with 4G2 antibody (1 µg/ml) for 1 hour at room temperature. After washing, cells were incubated with goat anti-mouse IgG conjugated to phycoerythrin (1µg/ml, Invitrogen) for 1hr at room temperature. The percentage of infected cells was determined by flow cytometry using a FACS Caliber and analyzed using FlowJo2 software version 10.1.r7. The data were then fit to a Gaussian distribution utilizing the non-linear regression functionality of GraphPad Prism, and the enhancing concentration at which 50% of maximum enhancement was reached (EC_{50}) was determined utilizing the Gaussian fit.

ZIKV Infection of *Stat2*$^{-/-}$ Mice

Mouse studies were carried out in an animal Biosafety Level 2+ facility under a protocol approved by the Icahn School of Medicine at Mount Sinai Animal Care and Use Committee. Breeding pairs were formed using *Stat2*$^{-/-}$ mice (provided by Christian Schindler; 8-10 week old nulliparous females and >8 week old non-virgin males). Females were then separated after plugs were detected (defined as E0.5) and infected at E6.5. Pregnant *Stat2*$^{-/-}$ mice were injected intraperitoneally with 20 µl of CTRL-, WNV- or DENV- immune plasma two hours prior to intradermal infection with 5×10^3 PFU ZIKV (strain PRVABC-59, GenBank: KU501215.1). ZIKV was obtained originally from the CDC, passaged once in Vero cells, and sequence verified. Mice were monitored daily for weight loss. Fetal and maternal tissues were harvested at E13.5 for analysis.

ZIKV Quantification

Total RNA was isolated from tissue homogenates using Direct-zol RNA MiniPrep Plus (Zymo Research) according to manufacturer's protocol, and 1 µg of RNA was reverse transcribed into cDNA using the High Capacity Reverse Transcription Kit (Applied Biosciences) with random hexamer primers. The following ZIKV-specific primers (5′-TTGGTCATGATACTGCTGATTGC-3′ and 5′-CCYTCCACRAAGTCYCTATTGC-3′) were used for qRT-PCR (43), and detection of amplification was determined *via* PerfeCTa SYBR Green fast mix (Quanta) following the manufacturer's protocol. PCR amplification was conducted in 384-well format using the Roche LightCycler 480 System. RNA quantification was determined by fitting to an *in vitro*-transcribed RNA standard.

Cytokine and Chemokine Protein Quantification

Tissue homogenates were evaluated for 23 cytokines/chemokines by multiplexed ELISA for the following analytes: IL-17A, IL-22, IL-10, IL-2, IL-4, IFNγ, IL-21, TNFα, IL-5, IL-6, Cxcl16, Ccl4/MIP-1β, Ccl3/MIP-1α, IL-12(p70), Ccl11, IL-1β, Cxcl1/GROα, Cxcl2/GROβ, Ccl5/RANTES, Ccl7/MCP-3, Ccl2/MCP-1, Ccl12, and Cxcl10/IP-10 as previously described (44). Samples were analyzed on a Luminex MAGPIX platform. For each bead region, >50 beads were collected per analyte. The median fluorescence intensity was recorded and used to extrapolate pg/ml based on a 5P regression fitting of a standard curve of each analyte. Heat maps for median fold induction were generated in R by logarithmic base 2 transformation of the median cytokine level in the ZIKV-infected conditions divided by the median cytokine level of uninfected controls. Hierarchical clustering was performed using the hclust function in R, which stratifies based on Euclidean distance.

Histological and Tissue Analysis

Tissues were fixed in 10% neutral-buffered formalin before embedding into paraffin and cutting into 5 µm sections. Deparaffinization and antigen retrieval was performed as previously described (31). Slides were stained with hematoxylin (Gill's formula, Vector Laboratories H3401) and eosin Y (Sigma Aldrich E4009) according to manufacturer's instructions. For vimentin staining, slides were blocked in Tris-buffered saline containing 0.01% Tween-20 (TBST) and 2.5% normal goat serum for 40 minutes at room temperature. After washing, slides were incubated with rabbit monoclonal anti-vimentin antibody (1:1000, clone EPR3776, Abcam) for 1 hour at 4°C, then washed and incubated with goat anti-rabbit Alexa Fluor 488 before mounting with Vectashield hard-set mounting medium with DAPI (Vector Laboratories). Full-slice images were taken with an AxioImager Z2 microscope (Zeiss) and Zen 2012 software.

In situ hybridization using RNAscope® (ACDBio) was performed on 5 µm paraffin-embedded sections. Slides were baked at 55°C for twenty minutes for deparaffinization. Slides were then washed twice with xylene, twice in ethanol, and dried at 60°C. Slides were then incubated with hydrogen peroxide for 10 minutes at RT, and then rinsed in diH2O. Antigen retrieval was performed as per the manufacturer's guidelines, and slides were washed with water, transferred into 100% ethanol for three minutes and air dried. Sections were treated with RNAscope Protease Plus at 40°C for 30 minutes and washed with diH2O. Fluorescence *in situ* hybridization was subsequently performed according to the manufacturer's protocol (ACD# 323110) with RNAscope Probe V-ZIKVsph2015 (ACD #467871; binds sense

RNA) as previously described (Cao et al., 2017). Slides were mounted with Vectashield hard-set mounting medium with DAPI (Vector Laboratories). Full-slice images were taken with an AxioImager Z2 microscope (Zeiss) and Zen 2012 software. Images were rendered in FIJI for final visualization.

Quantification and Statistical Analysis

For all statistical significance indications in this manuscript, **** indicates a p-value ≤ 0.0001, *** indicates a p-value ≤ 0.001, ** indicates a p-value ≤ 0.01, and * indicates a p-value ≤ 0.05. NS indicates non significance. All sample sizes, replicate numbers, statistical tests and significance can be found in the figures and figure legends of this manuscript. Graphical representations were rendered in GraphPad Prism 8.0.1.

RESULTS

In Vitro Characterization of WNV Antibodies Elicited Through Natural Infection

To study how WNV antibodies could impact ZIKV pathogenesis, we utilized a cohort of individuals that were naturally infected with WNV identified through routine screening of the blood supply in the United States (31). To confirm antibody reactivity to WNV, we conducted a neutralization assay using the Kunjin isolate of WNV (WNV^{KUN}), which is 97.7% identical at the amino acid level to the NY99 strain that was introduced to the US (45). In brief, plasma from 15 WNV-seropositive blood donors were pooled and tested for the ability to neutralize WNV^{KUN} using a flow-cytometry based microneutralization assay. Compared to plasma from geographically-matched WNV-uninfected control (CTRL) individuals, immune plasma from WNV-infected individuals showed a strong capacity to neutralize WNV (IC_{50} = 1:5,770), while the CTRL plasma showed no activity (**Figure 1A**). Given that WNV antibodies have previously been shown to cross-react with ZIKV, we next sought to assess the ability of WNV immune plasma to neutralize and enhance ZIKV (31, 40). For comparison, we used DENV immune plasma, which is known to neutralize and enhance ZIKV both *in vitro* and *in vivo* (31–34). To directly compare WNV plasma potential with DENV immune plasma, we first needed to characterize the neutralization capacity of our DENV plasma against DENV. As shown in **Figure 1A**, DENV plasma potently neutralizes DENV-1, while non-reactive CTRL plasma is incapable. Indeed, the neutralization potential of DENV plasma against DENV-1 (IC_{50} = 1:10,021) is comparable to that of WNV plasma to neutralize WNV. Therefore, any differences in the potential to neutralize and enhance ZIKV are a result of antigenic cross-reactivity, and not of differing concentrations of virus-specific antibodies. We next conducted neutralization assays against ZIKV, utilizing our CTRL, WNV, and DENV plasma. Consistent with the relative antigenic distance from ZIKV, DENV immune plasma showed ~10-fold increased capacity to neutralize ZIKV (IC_{50} = 1:4,320) compared to WNV immune plasma (**Figure 1B**) (46, 47).

Having shown the neutralizing potential of the WNV and DENV plasma against ZIKV, we next asked to what extent these samples could enhance ZIKV. WNV, DENV or CTRL plasma were serially-diluted and co-incubated with ZIKV. These virus-antibody complexes were then used to infect K562 cell, which are only susceptible to ZIKV infection through antibody-mediated entry (48). After 2 days, we evaluated infection using flow cytometry to determine fold enhancement in the presence of varying concentrations of antibodies. Enhancement potential was quantified by fitting data to a Gaussian curve, and calculating the enhancing concentration at which 50% of maximum enhancement was achieved (EC_{50}). While WNV antibodies could enhance infection (EC_{50} = 390), DENV antibodies were more potent (EC_{50} = 3,470), showing ~10 fold increase in potency relative to WNV (**Figure 1C**). Together, these results demonstrate that WNV antibodies can modulate ZIKV infection *in vitro*, but to a lesser extent compared to DENV antibodies.

Impact of WNV Antibodies on the Pathogenesis of ZIKV in Pregnant Mice

Given that WNV antibodies can both bind and enhance ZIKV *in vitro*, we next evaluated how WNV antibodies could alter the course of ZIKV disease during pregnancy. To do this, we utilized ZIKV-infected pregnant *Stat2*$^{-/-}$ mice, a model we have

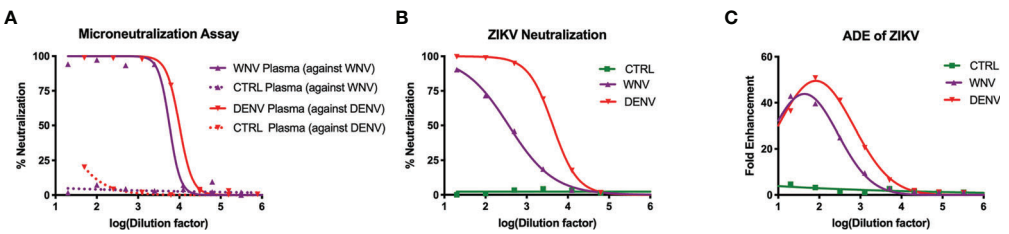

FIGURE 1 | Neutralization and enhancement potential of WNV immune plasma. **(A)** The capacity of plasma from WNV-infected individuals to neutralize WNV (Kunjin isolate) was compared to the capacity of plasma from DENV-infected individuals to neutralize DENV (serotype 1) in Vero cells. Non-reactive CTRL plasma was used as a negative control for each. Neutralization is represented by the percent reduction in infection compared to virus alone. **(B)** Neutralization of ZIKV (strain PRVABC-59) by WNV, DENV, and CTRL immune plasma in Vero cells is shown. **(C)** Enhancement of ZIKV by WNV, DENV, and CTRL immune plasma was tested in K562 cells. Enhancement was determined based on percent infection over the virus alone condition. All assays were completed in technical triplicate.

previously employed to evaluate the enhancement of ZIKV infection in the presence of DENV antibodies (32). Pregnant *Stat2*$^{-/-}$ mice were infected on E6.5 with 5,000 PFU of the PRVABC-59 strain of ZIKV, a clinical strain from the 2015 outbreak in Puerto Rico. Two hours prior to infection, mice were injected intraperitoneally with either WNV-immune plasma, DENV-immune plasma or CTRL plasma. Uninfected control mice were also treated with either WNV (n = 2) or CTRL (n = 2) plasma. No differences were observed for maternal weights or any fetal parameters between the uninfected groups (**Figure S1**) and thus were combined into a single group. Maternal weights were monitored through E13.5, at which point maternal organs and uterine horns were evaluated. We found that while all ZIKV-infected mice lost weight over the course of pregnancy compared to uninfected mice, no significant differences were observed in the presence or absence of WNV antibodies (**Figure 2A**). Pregnant mice that received DENV plasma prior to infection steadily lost weight over the course of pregnancy, consistent with our previous findings (32). Evaluation of viremia revealed a significant increase in mice that received DENV plasma at 3 days post infection, but not in mice that received WNV plasma, compared to CTRL (**Figure 2B**). However, viral loads in maternal brains, spleens, and spinal cords revealed no significant differences in the presence of WNV antibodies or DENV antibodies by qRT-PCR (**Figures 2C–E**). While the presence of DENV antibodies in ZIKV-infected mice elevated the broad inflammatory response significantly, no striking differences existed between mice that received WNV antibodies or CTRL (**Figure 2F**).

Impact of WNV Antibodies on ZIKV Induced Fetal Tissue Damage

We next investigated how the presence of WNV antibodies altered fetal outcomes during pregnancy in this model. We evaluated uterine horns and individual fetal-placental pairs for morphological differences upon infection to determine if the presence of WNV antibodies impacted ZIKV associated fetal damage (**Figure 3A**). Uterine horns from ZIKV infected dams, irrespective of plasma group, were darker in color and morphologically damaged compared to those from uninfected dams, with DENV plasma showing the most damage, CTRL plasma showing the least, and WNV plasma showing an intermediate phenotype. This observation was supported by quantifying the resorption rates between groups. Although the resorption rates among ZIKV-infected dams treated with WNV plasma revealed a trend towards an increase in resorption, this was not statistically significant compared to mice that received CTRL antibodies ($p > 0.99$; **Figure 3B**). This was in contrast to the mice that received DENV antibodies, where a significant increase in the resorption rate was observed (**Figure 3B**). We next evaluated fetuses and placentas for developmental defects compared to uninfected fetuses. Due to the high resorption rate, we were unable to include fetuses from dams that received the DENV antibodies in subsequent analyses and instead limited our comparisons to fetuses from pregnant dams that received WNV and CTRL antibodies. While fetuses from infected dams were significantly smaller than fetuses from uninfected dams, there were no significant differences in fetal size, fetal mass, placental length or placental mass between mice that received WNV plasma or CTRL plasma (**Figures 3C–F**).

In our previous reports, we showed that much of the damage caused by cross-reactive DENV antibodies was the result of higher viral loads in the placenta, which led to greater inflammation and placental damage (32). Therefore, we next asked whether viral replication differed in the fetal tissue in the presence of WNV antibodies by qRT-PCR. While all placentas from infected mice had viral loads in the placentas, there were no differences in viral load in mice that received WNV antibodies compared to mice that received non-specific CTRL antibodies (**Figure 4A**). Evaluation of viral loads in the fetal heads showed the same trend, with no significant differences between the two groups (**Figure 4B**).

We also asked whether the presence of WNV antibodies could alter the inflammatory landscape in the placentas and fetal heads during ZIKV infection. We examined fetal and placental homogenates from mice that received either WNV or CTRL antibodies for chemokine and cytokine production by multiplex ELISA. Examination across 21 cytokines showed no significant differences in the inflammatory milieu in either the placentas or the fetal heads obtained from ZIKV-infected pregnant dams that received WNV or CTRL antibodies (**Figure 4C**).

Pathogenesis of ZIKV in the Placenta in the Presence of WNV Antibodies

Our previous study evaluating ADE caused by the presence of DENV antibodies implicated increased damage to the labyrinth zone of the placenta during ZIKV infection. Therefore, we wondered whether WNV antibodies had any impact on placental structure in ZIKV-infected mice. Harvested placentas across numerous pregnancies were evaluated for overall pathological changes by H&E staining (**Figure 5A**, left) as well as the density and structure of the labyrinth zone using Vimentin staining (**Figure 5A**, right). In all cases, we found a pronounced reduction in the size and density of the labyrinth zone due to ZIKV infection; however, there were no obvious differences in the placentas harvested from mice that received WNV plasma or CTRL plasma (**Figure 5A**). The extent of viral infection between mice that received CTRL or WNV antibodies was similar, consistent with the qRT-PCR results, and infection was limited to the decidual-placental interface (**Figure 5B**, red arrows) as examined by fluorescence RNA *in situ* hybridization. This is consistent with our previous findings during ZIKV infections in the absence of cross-reactive antibodies in this model (32). Together, our findings show no significant impact of WNV antibodies on the pathogenesis of ZIKV during pregnancy.

DISCUSSION

Our study is the first to examine the potential for WNV antibodies to enhance ZIKV infection in the context of pregnancy. We found no significant evidence that WNV

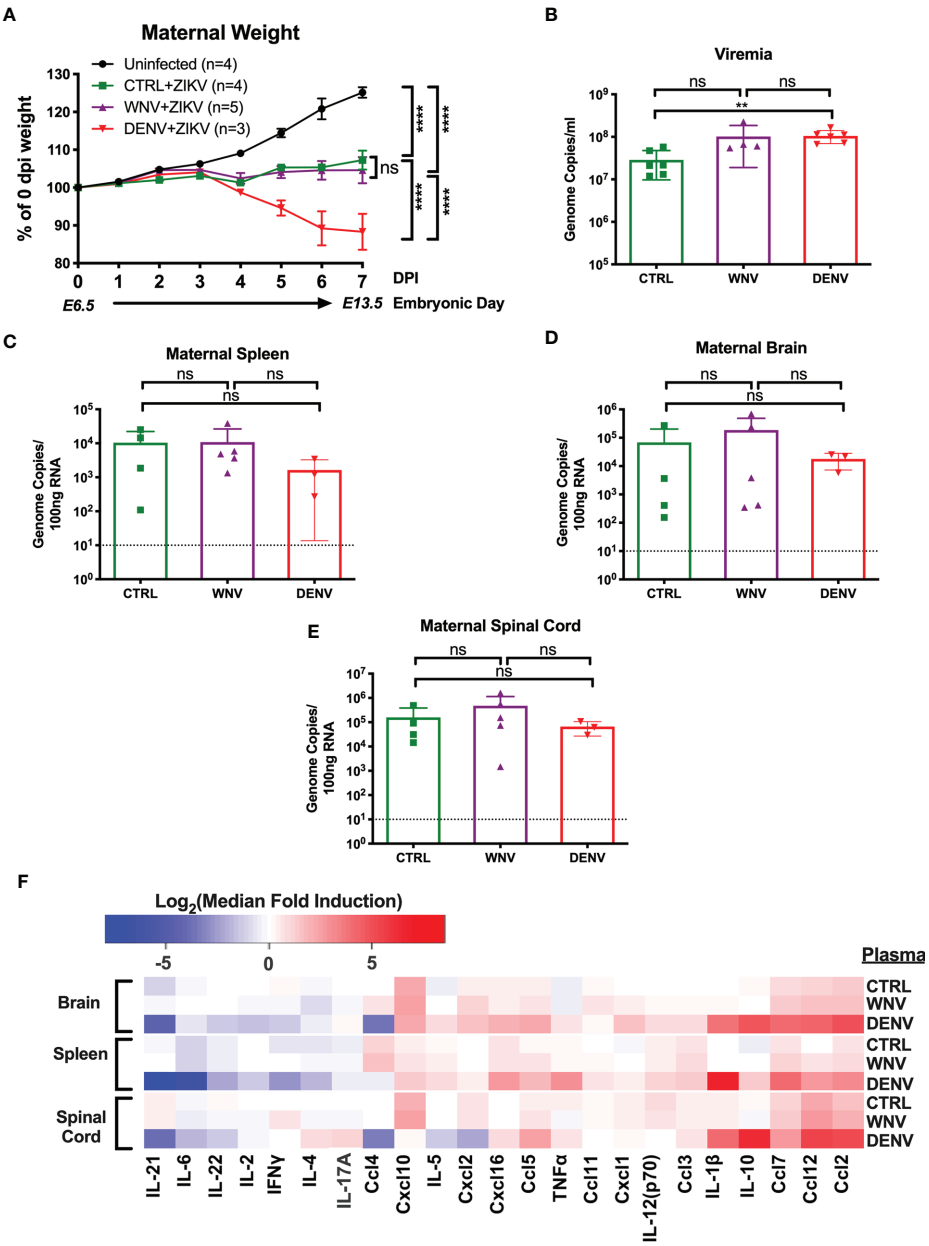

FIGURE 2 | Impact of WNV antibodies on ZIKV infected dams. ZIKV-infected *Stat2*$^{-/-}$ dams that received 20µl of either CTRL (n=4), WNV (n=5) or DENV (n=3) plasma were compared to uninfected dams that also received WNV or CTRL plasma (n=4; See **Figure S1**). **(A)** Maternal weights between infection at E6.5 and tissue collection at E13.5 are shown as a percentage of starting weight at E6.5. Significance was determined by two-way ANOVA, and error bars represents SD. **(B)** Viremia was determined at 3 days post infection in ZIKV-infected dams by qRT-PCR. Mice included in this subfigure are from an unmatched cohort of CTRL (n=6), WNV (n=4), and DENV (n=6) mice. Viral loads in dams from **(A)** were determined in the maternal spleens **(C)**, brains **(D)**, and spinal cords **(E)** by qRT-PCR. For **(C–E)**, dotted lines indicate the limit of detection, and mean values with SD are depicted with the overlaid bar plots. Significance was determined by Mann-Whitney U-test. **(F)** Tissue homogenates from brain, spleen and spinal cords from ZIKV-infected mice in **(A)** were evaluated for inflammatory markers by multiplex ELISA. Data are shown as a $\log_2$ transformed median fold induction over the median pg/ml expression in the uninfected condition. ns, not significant; $^{**}p < 0.01$, $^{****}p < 0.0001$.

antibodies mediate enhancement of ZIKV in pregnant mice. In the absence of thorough prospective human studies on the influence of WNV immunity on ZIKV infections, we hope that these data provide the first insights into the safety of introducing greater WNV immunity into ZIKV endemic regions and regions at risk of ZIKV expansion. This finding has major implications for WNV vaccine development and begins to address larger questions about the process of ADE.

ADE is known to be a function of antigenic distance, with a 'sweet spot' level of antigenic relatedness resulting in the

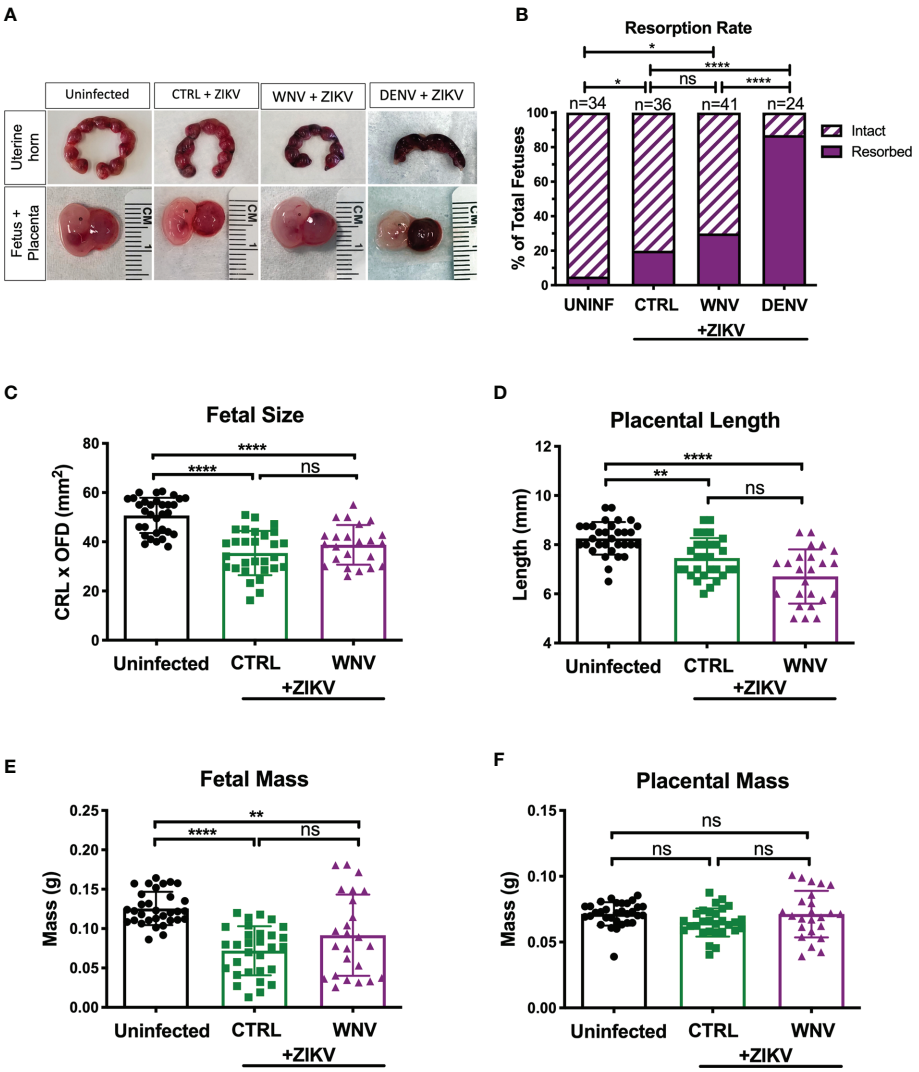

FIGURE 3 | Impact of WNV antibodies on ZIKV-infected fetuses. Uterine horns were harvested and morphologically examined at E13.5 from ZIKV-infected or uninfected dams (**A**, top). Fetal and placental pairs were isolated from each harvested conceptus, and representative images are shown (**A**, bottom). The resorption rate across all pregnancies are represented by the proportion of resorbed and intact fetuses **(B)**; uninfected mice (n=34), CTRL (n=36), WNV (n=41), and DENV (n=24). Significance between groups was determined by χ^2 analysis. Intact fetuses and placentas were measured for fetal size **(C)** by multiplying the crown-to-rump length (CRL) by the occipital-frontal diameter (OFD), placental length **(D)**, represented by diameter, fetal mass **(E)**, and placental mass **(F)**. Significance for **(C–F)** was determined by a one-way ANOVA, with a Kruskal-Wallis post-test for multiple comparisons between uninfected mice (n=32), CTRL (n=29) and WNV (n=24). Bar plot overlays for **(C–F)** depict mean and SD. Resorbed and partially resorbed fetuses were excluded from the analysis in **(C–F)**. ns, not significant; $^{*}p < 0.05$, $^{**}p < 0.01$, $^{****}p < 0.0001$.

possibility of enhancement. In general, higher relatedness will result in greater antigenic affinity and neutralization, while lower relatedness will result in less binding and weak or no enhancement potential. Based on ADE observed between the DENV serotypes, ~68% identity at the amino acid level for the E proteins appears to be sufficient for enhancement to be observed (49). ZIKV and the four serotypes of DENV are on average 55% similar at the antigenic E level, and *in vitro/in vivo* data suggest that enhancement *can* occur between the two viruses (50). Consistent with this notion, a recently published study showed that antibodies against ZIKV could enhance infection in children subsequently infected with DENV (51–53). However, studies that have evaluated the impact of DENV immunity on ZIKV pathogenesis in humans have largely shown that DENV immunity is protective, with one study showing a concentration dependent loss of protection against ZIKV at intermediate DENV antibody levels (54). It is possible that these seemingly conflicting data, where enhancement occurs in one direction but not the other, are the result of a wider window of severe symptomology for DENV infections compared to ZIKV infections. Alternatively, perhaps the order in which infection occurs generates antibodies against antigenic epitopes that are

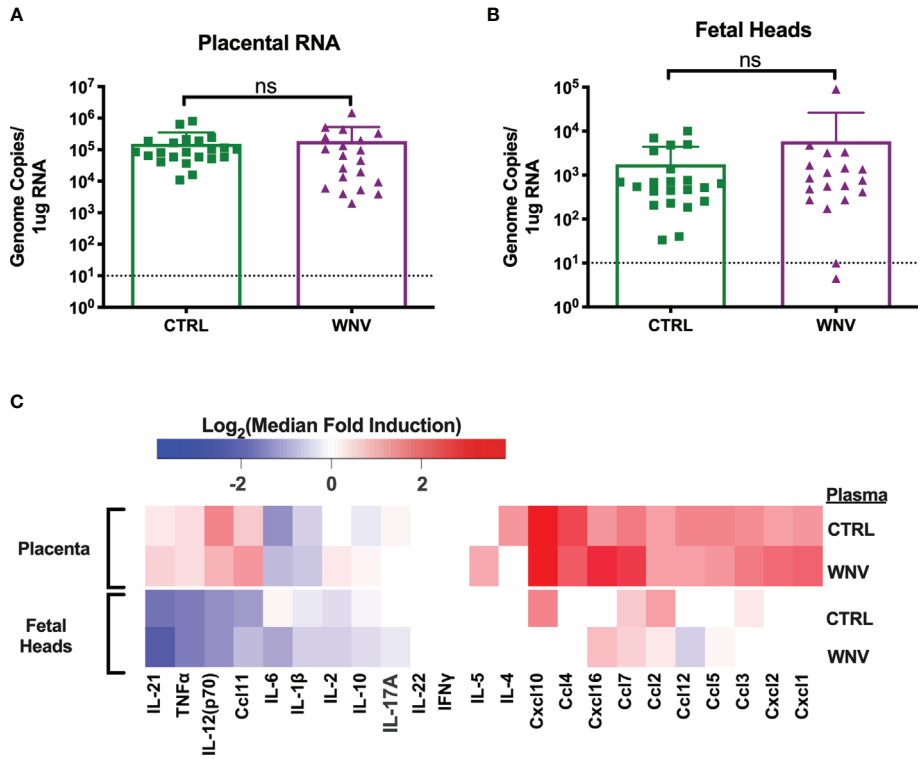

FIGURE 4 | Molecular characterization of ZIKV infection in the fetus and placenta. RNA was extracted from **(A)** placentas (CTRL n=22; WNV n=20) and **(B)** fetal heads (CTRL n=22; WNV= 19) to examine viral loads by qRT-PCR. Significance was determined by Mann-Whitney U-test, and the dashed lines represent the limit of detection. Overlaid bar plots depict mean and SD. **(C)** Tissue homogenates from placentas and fetal heads were evaluated for inflammatory markers by multiplex ELISA. Data are shown as a log_2 transformed median fold induction over the median pg/ml expression in the uninfected condition. ns, not significant.

more or less potently neutralizing or enhancing. WNV is slightly more antigenically distant from ZIKV (~54% amino acid identity to the E protein) (49). Our study showed that WNV antibodies could enhance ZIKV at the *in vitro* level, but not at the *in vivo* level in ZIKV-infected pregnant mice. Given that the mouse model is a very sensitive model for detecting ADE, our results suggest that WNV is unlikely to alter ZIKV pathogenesis in humans, at least in the context of pregnancy. However, carefully designed prospective human studies need to test this hypothesis considering that the antigenic relatedness of these two viruses suggests that ADE could be possible. Further, the role of ZIKV specific antibodies impacting the pathogenesis of WNV has yet to be examined.

Our data also provide further evidence for how enhancement might influence ZIKV pathogenesis in pregnancy. In our report on DENV enhancement of ZIKV in this model, we identified that the placenta was the primary target for enhanced ZIKV damage (32). We found that enhancing antibodies expanded the tropism of ZIKV from the decidual-placental interface into the cytotrophoblast layer, which correlated with an increase in cytokine production, as well as in the disruption of the placental labyrinth zone. The labyrinth zone is a bed of fetal derived endothelium essential for maternal-fetal blood and nutrient transfer, and thus we hypothesized that the disruption of this zone was responsible for the fetal abnormalities noted (55). In this work, we did not find any evidence of enhancement by increased pathogenesis, inflammation or viral load. Infection was limited to the decidual interface, demonstrating cross-reactive antibodies which are not capable of increasing the infectious range of ZIKV in the placenta. It is not clear if ZIKV gains access to this compartment through direct Fc-mediated endocytosis, or if this is the result of increased access to the compartment during inflammatory responses. However, we believe that based on our data, infection of this zone is critical for the ZIKV mediated pathology observed in enhanced infections.

Our study has several limitations. One major limitation is that we only assessed a single concentration of WNV antibodies in this study (20µl/mouse). This concentration was chosen because it is the concentration where DENV antibodies can potently enhance ZIKV. However, as we showed that the enhancement potential for DENV antibodies for ZIKV is ~1 log greater than that of WNV antibodies *in vitro* (**Figure 1C**), it is possible that WNV antibodies would require ~10-fold higher concentration to achieve enhancement. Our previous data suggest that increasing the antibody concentration 10-fold would also increase mortality non-specifically due to the non-physiological concentration of circulating antibodies (31). One possibility for why DENV plasma enhances while WNV plasma does not in our

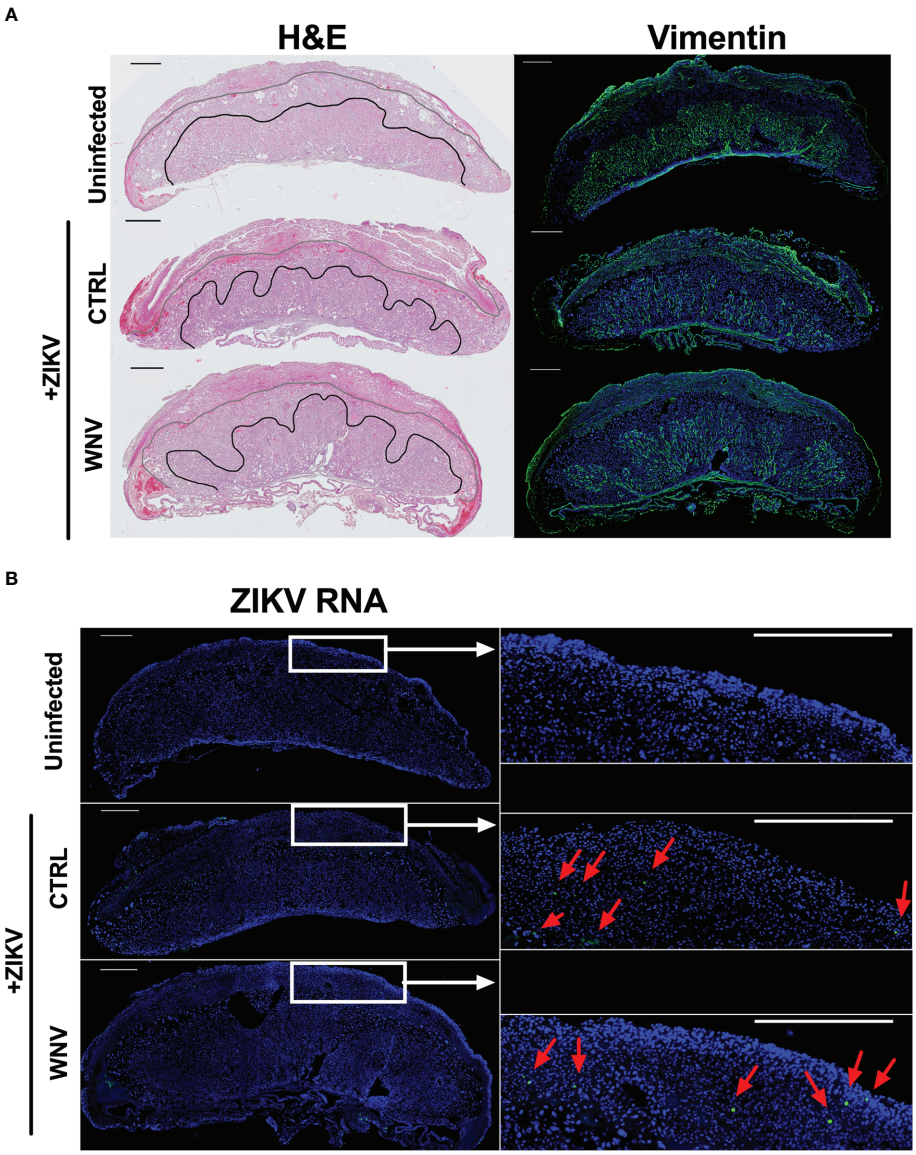

FIGURE 5 | ZIKV-induced damage in the developing placenta. Placentas harvested at E13.5 from uninfected of ZIKV-infected dams that received either WNV or CTRL plasma were examined for **(A)** the disruption of the placental labyrinth zone by both hematoxylin and eosin (H&E) staining (left) and immunofluorescence staining for vimentin (right), which marks fetal endothelium (green). DAPI is shown in blue. **(B)** Placentas were evaluated for ZIKV RNA localization by *in situ* hybridization. Tiled images of representative whole placentas are shown on the left, with tiles from white boxed regions shown on the right for ease of comparison (scale = 500μm). ZIKV-infected cells (green) are highlighted with red arrows and DAPI is shown in blue.

experiments is because the concentration of WNV-specific antibodies is lower in the pooled WNV plasma than the concentration of DENV-specific antibodies in the DENV plasma. To address this, we quantified the number of WNV specific IC_{50}'s we injected per mouse of WNV plasma and compared that to the number of DENV specific IC_{50}'s injected per mouse of DENV plasma. We found that we were using a comparable concentration of IC_{50}'s (<2-fold difference). Therefore, we find it unlikely that the differences observed between the WNV and DENV groups in our mouse studies are a result of differing amounts of WNV and DENV specific IgG. Instead, these data suggest that the differences we have observed are due to the relative antigenic cross-reactivity to ZIKV.

An additional limitation of this study is the use of *Stat2*$^{-/-}$ mice. ZIKV NS5 is known to bind and degrade human STAT2, but not mouse Stat2, resulting in a species barrier (56). To overcome this, the human STAT2 knock-in mouse model has recently been described for ZIKV infection in non-pregnant adult mice. Our future work will aim to utilize the human *STAT2* knock-in model for studying ADE in the context of pregnancy (34), which may be more translatable to human disease.

Ultimately, the goal of studying ADE should be to model the relative risk that immunity to any one virus poses to the severity of another. Understanding this would provide risk assessments for severe outbreak zones, vaccine development, and identification of patients at risk for severe disease sequelae. As one could imagine, this model will likely be complex and multifactorial – with antibody concentration already having been identified to be a major risk factor for ADE. Antigenic distance, neutralization capacity, antibody durability, antibody subclass, infection order and many other factors are still under investigation for their role in predisposing enhanced infection (57). This current study has begun to address the role of cross reactivity, and we hope that our findings will be helpful in building this risk model.

DATA AVAILABILITY STATEMENT

The raw data supporting the conclusions of this article will be made available by the authors, without undue reservation.

ETHICS STATEMENT

The animal study was reviewed and approved by Icahn School of Medicine at Mount Sinai Animal Care and Use Committee.

AUTHOR CONTRIBUTIONS

JA conceptualized the project, conducted the experiments, data analysis, drafting and editing of the manuscript. JC conducted experiments and edited the manuscript. AM conducted experiments and edited the manuscript. JB conceptualized the project and conducted experiments. GF, DK, and SS contributed critical reagents and edited the manuscript. JL conceptualized the project, managed the project and edited the manuscript. All authors contributed to the article and approved the submitted version.

FUNDING

This work was funded by NIAID grant R01AI150837 and NHLBI F31HL149295.

SUPPLEMENTARY MATERIAL

The Supplementary Material for this article can be found online at: https://www.frontiersin.org/articles/10.3389/fimmu.2021.686411/full#supplementary-material

REFERENCES

1. Takada A, Kawaoka Y. Antibody-dependent Enhancement of Viral Infection: Molecular Mechanisms and In Vivo Implications. *Rev Med Virol* (2003) 13:387–98. doi: 10.1002/rmv.405
2. Taylor A, Foo SS, Bruzzone R, Dinh LV, King NJ, Mahalingam S. Fc Receptors in Antibody-Dependent Enhancement of Viral Infections. *Immunol Rev* (2015) 268:340–64. doi: 10.1111/imr.12367
3. Narayan R, Tripathi S. Intrinsic ADE: The Dark Side of Antibody Dependent Enhancement During Dengue Infection. *Front Cell Infect Microbiol* (2020) 10:580096. doi: 10.3389/fcimb.2020.580096
4. Gyawali N, Bradbury RS, Taylor-Robinson AW. The Epidemiology of Dengue Infection: Harnessing Past Experience and Current Knowledge to Support Implementation of Future Control Strategies. *J Vector Borne Dis* (2016) 53:293–304.
5. Soo KM, Khalid B, Ching SM, Chee HY. Meta-Analysis of Dengue Severity During Infection by Different Dengue Virus Serotypes in Primary and Secondary Infections. *PLoS One* (2016) 11:e0154760. doi: 10.1371/journal.pone.0154760
6. Halstead SB. Dengue Antibody-Dependent Enhancement: Knowns and Unknowns. *Microbiol Spectr* (2014) 2. doi: 10.1128/microbiolspec.AID-0022-2014
7. Toh YX, Gan V, Balakrishnan T, Zuest R, Poidinger M, Wilson S, et al. Dengue Serotype Cross-Reactive, Anti-E Protein Antibodies Confound Specific Immune Memory for 1 Year After Infection. *Front Immunol* (2014) 5:388. doi: 10.3389/fimmu.2014.00388
8. Zidane N, Dussart P, Bremand L, Bedouelle H. Cross-reactivities Between Human IgMs and the Four Serotypes of Dengue Virus as Probed With Artificial Homodimers of domain-III From the Envelope Proteins. *BMC Infect Dis* (2013) 13:302. doi: 10.1186/1471-2334-13-302
9. Moi ML, Takasaki T, Kurane I. Human Antibody Response to Dengue Virus: Implications for Dengue Vaccine Design. *Trop Med Health* (2016) 44:1. doi: 10.1186/s41182-016-0004-y
10. Khan E, Prakoso D, Imtiaz K, Malik F, Farooqi JQ, Long MT, et al. The Clinical Features of Co-circulating Dengue Viruses and the Absence of Dengue Hemorrhagic Fever in Pakistan. *Front Public Health* (2020) 8:1–10. doi: 10.3389/fpubh.2020.00287
11. Hamel R, Surasombatpattana P, Wichit S, Dauvé A, Donato C, Pompon J, et al. Phylogenetic Analysis Revealed the Co-Circulation of Four Dengue Virus Serotypes in Southern Thailand. *PLoS One* (2019) 14:e0221179. doi: 10.1371/journal.pone.0221179
12. Racherla RG, Pamireddy ML, Mohan A, Mudhigeti N, Mahalakshmi PA, Nallapireddy U, et al. Co-circulation of Four Dengue Serotypes at South Eastern Andhra Pradesh, India: A Prospective Study. *Indian J Med Microbiol* (2018) 36:236–40. doi: 10.4103/ijmm.IJMM_18_109
13. Moi ML, Takasaki T, Saijo M, Kurane I. Determination of Antibody Concentration as the Main Parameter in a Dengue Virus Antibody-Dependent Enhancement Assay Using Fcγr-Expressing BHK Cells. *Arch Virol* (2014) 159:103–16. doi: 10.1007/s00705-013-1787-3
14. Ripoll DR, Wallqvist A, Chaudhury S. Molecular Simulations Reveal the Role of Antibody Fine Specificity and Viral Maturation State on Antibody-Dependent Enhancement of Infection in Dengue Virus. *Front Cell Infect Microbiol* (2019) 9:200. doi: 10.3389/fcimb.2019.00200
15. Katzelnick LC, Harris E. The Use of Longitudinal Cohorts for Studies of Dengue Viral Pathogenesis and Protection. *Curr Opin Virol* (2018) 29:51–61. doi: 10.1016/j.coviro.2018.03.004
16. Katzelnick LC, Gresh L, Halloran ME, Mercado JC, Kuan G, Gordon A, et al. Antibody-dependent Enhancement of Severe Dengue Disease in Humans. *Science* (2017) 358:929–32. doi: 10.1126/science.aan6836
17. Fischer C, de Oliveira-Filho EF, Drexler JF. Viral Emergence and Immune Interplay in Flavivirus Vaccines. *Lancet Infect Dis* (2020) 20:15–7. doi: 10.1016/S1473-3099(19)30697-8
18. Lazear HM, Diamond MS. Zika Virus: New Clinical Syndromes and Its Emergence in the Western Hemisphere. *J Virol* (2016) 90:4864–75. doi: 10.1128/JVI.00252-16
19. Brasil P, Pereira JP Jr., Moreira ME, Ribeiro Nogueira RM, Damasceno L, Wakimoto M, et al. Zika Virus Infection in Pregnant Women in Rio De Janeiro. *N Engl J Med* (2016) 375:2321–34. doi: 10.1056/NEJMoa1602412
20. Coyne CB, Lazear HM. Zika Virus - Reigniting the TORCH. *Nat Rev Microbiol* (2016) 14:707–15. doi: 10.1038/nrmicro.2016.125

21. Honein MA, Dawson AL, Petersen EE, Jones AM, Lee EH, Yazdy MM, et al. Birth Defects Among Fetuses and Infants of US Women With Evidence of Possible Zika Virus Infection During Pregnancy. *JAMA* (2017) 317:59–68. doi: 10.1001/jama.2016.19006
22. Reynolds MR, Jones AM, Petersen EE, Lee EH, Rice ME, Bingham A, et al. Vital Signs: Update on Zika Virus-Associated Birth Defects and Evaluation of All U.s. Infants With Congenital Zika Virus Exposure - U.S. Zika Pregnancy Registry, 2016. *MMWR Morb Mortal Wkly Rep* (2017) 66:366–73. doi: 10.15585/mmwr.mm6613e1
23. Schaub B, Vouga M, Najioullah F, Gueneret M, Monthieux A, Harte C, et al. Analysis of Blood From Zika Virus-Infected Fetuses: A Prospective Case Series. *Lancet Infect Dis* (2017) 17:520–7. doi: 10.1016/S1473-3099(17)30102-0
24. Wheeler AC. Development of Infants With Congenital Zika Syndrome: What Do We Know and What can We Expect? *Pediatrics* (2018) 141:S154–s160. doi: 10.1542/peds.2017-2038D
25. Shapiro-Mendoza CK, Rice ME, Galang RR, Fulton AC, VanMaldeghem K, Prado MV, et al. Pregnancy Outcomes After Maternal Zika Virus Infection During Pregnancy - U.s. *Territories* (2017). *MMWR Morb Mortal Wkly Rep* (2017) 66(23):615–21. doi: 10.15585/mmwr.mm6623e1
26. Mulkey SB, Arroyave-Wessel M, Peyton C, Bulas DI, Fourzali Y, Jiang J, et al. Neurodevelopmental Abnormalities in Children With In Utero Zika Virus Exposure Without Congenital Zika Syndrome. *JAMA Pediatr* (2020) 174:269–76. doi: 10.1001/jamapediatrics.2019.5204
27. Pereira H, Dos Santos SP, Amâncio A, de Oliveira-Szejnfeld PS, Flor EO, de Sales Tavares J, et al. Neurological Outcomes of Congenital Zika Syndrome in Toddlers and Preschoolers: A Case Series. *Lancet Child Adolesc Health* (2020) 4:378–87. doi: 10.1016/S2352-4642(20)30041-9
28. Barba-Spaeth G, Dejnirattisai W, Rouvinski A, Vaney MC, Medits I, Sharma A, et al. Structural Basis of Potent Zika-dengue Virus Antibody Cross-Neutralization. *Nature* (2016) 536:48–53. doi: 10.1038/nature18938
29. Kostyuchenko VA, Lim EX, Zhang S, Fibriansah G, Ng TS, Ooi JS, et al. Structure of the Thermally Stable Zika Virus. *Nature* (2016) 533:425–8. doi: 10.1038/nature17994
30. Sirohi D, Chen Z, Sun L, Klose T, Pierson TC, Rossmann MG, et al. The 3.8 Å Resolution cryo-EM Structure of Zika Virus. *Science* (2016) 352:467–70. doi: 10.1126/science.aaf5316
31. Bardina SV, Bunduc P, Tripathi S, Duehr J, Frere JJ, Brown JA, et al. Enhancement of Zika Virus Pathogenesis by Preexisting Antiflavivirus Immunity. *Science* (2017) 356:175–80. doi: 10.1126/science.aal4365
32. Brown JA, Singh G, Acklin JA, Lee S, Duehr JE, Chokola AN, et al. Dengue Virus Immunity Increases Zika Virus-Induced Damage During Pregnancy. *Immunity* (2019) 50:751–762.e5. doi: 10.1016/j.immuni.2019.01.005
33. Zimmerman MG, Quicke KM, O'Neal JT, Arora N, Machiah D, Priyamvada L, et al. Cross-Reactive Dengue Virus Antibodies Augment Zika Virus Infection of Human Placental Macrophages. *Cell Host Microbe* (2018) 24:731–742.e6. doi: 10.1016/j.chom.2018.10.008
34. Rathore APS, Saron WAA, Lim T, Jahan N, St John AL. Maternal Immunity and Antibodies to Dengue Virus Promote Infection and Zika Virus-Induced Microcephaly in Fetuses. *Sci Adv* (2019) 5:eaav3208. doi: 10.1126/sciadv.aav3208
35. Li M, Zhao L, Zhang C, Wang X, Hong W, Sun J, et al. Dengue Immune Sera Enhance Zika Virus Infection in Human Peripheral Blood Monocytes Through Fc Gamma Receptors. *PLoS One* (2018) 13:e0200478. doi: 10.1371/journal.pone.0200478
36. Petersen LR, Brault AC, Nasci RS. West Nile Virus: Review of the Literature. *JAMA* (2013) 310:308–15. doi: 10.1001/jama.2013.8042
37. Murray KO, Mertens E, Despres P. West Nile Virus and its Emergence in the United States of America. *Vet Res* (2010) 41:67. doi: 10.1051/vetres/2010039
38. Ronca SE, Murray KO, Nolan MS. Cumulative Incidence of West Nile Virus Infection, Continental United States, 1999-2016. *Emerg Infect Dis* (2019) 25:325–7. doi: 10.3201/eid2502.180765
39. Keasey SL, Pugh CL, Jensen SMR, Smith JL, Hontz RD, Durbin AP, et al. Antibody Responses to Zika Virus Infections in Environments of Flavivirus Endemicity. *Clin Vaccine Immunol* (2017) 24:e00036–17. doi: 10.1128/CVI.00036-17
40. Willis E, Hensley SE. Characterization of Zika Virus Binding and Enhancement Potential of a Large Panel of Flavivirus Murine Monoclonal Antibodies. *Virology* (2017) 508:1–6. doi: 10.1016/j.virol.2017.04.031
41. Adams LE, Martin SW, Lindsey NP, Lehman JA, Rivera A, Kolsin J, et al. Epidemiology of Dengue, Chikungunya, and Zika Virus Disease in U.S. States and Territories, 2017. *Am J Trop Med Hyg* (2019) 101:884–90. doi: 10.4269/ajtmh.19-0309
42. Messina JP, Brady OJ, Golding N, Kraemer MUG, Wint GRW, Ray SE, et al. The Current and Future Global Distribution and Population at Risk of Dengue. *Nat Microbiol* (2019) 4:1508–15. doi: 10.1038/s41564-019-0476-8
43. Schwarz MC, Sourisseau M, Espino MM, Gray ES, Chambers MT, Tortorella D, et al. Rescue of the 1947 Zika Virus Prototype Strain With a Cytomegalovirus Promoter-Driven cDNA Clone. *mSphere* (2016) 1:e00246–16. doi: 10.1128/mSphere.00246-16
44. Aguado LC, Schmid S, Sachs D, Shim JV, Lim JK, tenOever BR. Microrna Function is Limited to Cytokine Control in the Acute Response to Virus Infection. *Cell Host Microbe* (2015) 18:714–22. doi: 10.1016/j.chom.2015.11.003
45. Daffis S, Lazear HM, Liu WJ, Audsley M, Engle M, Khromykh AA, et al. The Naturally Attenuated Kunjin Strain of West Nile Virus Shows Enhanced Sensitivity to the Host Type I Interferon Response. *J Virol* (2011) 85:5664–8. doi: 10.1128/JVI.00232-11
46. Heinz FX, Stiasny K. The Antigenic Structure of Zika Virus and Its Relation to Other Flaviviruses: Implications for Infection and Immunoprophylaxis. *Microbiol Mol Biol Rev* (2017) 81. doi: 10.1128/MMBR.00055-16
47. Gupta SK, Singh S, Nischal A, Pant KK, Seth PK. Molecular-based Identification and Phylogeny of Genomic and Proteomic Sequences of Mosquito-Borne Flavivirus. *Genes Genomics* (2014) 36:31–43. doi: 10.1007/s13258-013-0137-x
48. Castanha PMS, Nascimento EJM, Braga C, Cordeiro MT, de Carvalho OV, de Mendonça LR, et al. Dengue Virus-Specific Antibodies Enhance Brazilian Zika Virus Infection. *J Infect Dis* (2017) 215:781–5. doi: 10.1093/infdis/jiw638
49. Xu X, Vaughan K, Weiskopf D, Grifoni A, Diamond MS, Sette A, et al. Identifying Candidate Targets of Immune Responses in Zika Virus Based on Homology to Epitopes in Other Flavivirus Species. *PLoS Curr* (2016) 8. doi: 10.1371/currents.outbreaks.9aa2e1fb61b0f632f58a098773008c4b
50. Wen J, Shresta S. Antigenic Cross-Reactivity Between Zika and Dengue Viruses: Is it Time to Develop a Universal Vaccine? *Curr Opin Immunol* (2019) 59:1–8. doi: 10.1016/j.coi.2019.02.001
51. Katzelnick LC, Narvaez C, Arguello S, Lopez Mercado B, Collado D, Ampie O, et al. Zika Virus Infection Enhances Future Risk of Severe Dengue Disease. *Science* (2020) 369:1123–8. doi: 10.1126/science.abb6143
52. Gordon A, Gresh L, Ojeda S, Katzelnick LC, Sanchez N, Mercado JC, et al. Prior Dengue Virus Infection and Risk of Zika: A Pediatric Cohort in Nicaragua. *PLoS Med* (2019) 16:e1002726. doi: 10.1371/journal.pmed.1002726
53. Rodriguez-Barraquer I, Costa F, Nascimento EJM, Nery NJ, Castanha PMS, Sacramento GA, et al. Impact of Preexisting Dengue Immunity on Zika Virus Emergence in a Dengue Endemic Region. *Science* (2019) 363:607–10. doi: 10.1126/science.aav6618
54. Terzian ACB, Schanoski AS, Mota MTO, da Silva RA, Estofolete CF, Colombo TE, et al. Viral Load and Cytokine Response Profile Does Not Support Antibody-Dependent Enhancement in Dengue-Primed Zika Virus-Infected Patients. *Clin Infect Dis* (2017) 65:1260–5. doi: 10.1093/cid/cix558
55. Woods L, Perez-Garcia V, Hemberger M. Regulation of Placental Development and Its Impact on Fetal Growth—New Insights From Mouse Models. *Front Endocrinol* (2018) 9:1–18. doi: 10.3389/fendo.2018.00570
56. Grant A, Ponia SS, Tripathi S, Balasubramaniam V, Miorin L, Sourisseau M, et al. Zika Virus Targets Human STAT2 to Inhibit Type I Interferon Signaling. *Cell Host Microbe* (2016) 19:882–90. doi: 10.1016/j.chom.2016.05.009
57. Guzman MG, Vazquez S. The Complexity of Antibody-Dependent Enhancement of Dengue Virus Infection. *Viruses* (2010) 2:2649–62. doi: 10.3390/v2122649

Conflict of Interest: The authors declare that the research was conducted in the absence of any commercial or financial relationships that could be construed as a potential conflict of interest.

frontiers in Immunology

ORIGINAL RESEARCH
published: 15 July 2021
doi: 10.3389/fimmu.2021.702048

Inhibition of Tryptophan Catabolism Is Associated With Neuroprotection During *Zika* Virus Infection

Fernanda Martins Marim[1,2,3], *Danielle Cunha Teixeira*[2,3], *Celso Martins Queiroz-Junior*[2,3,4], *Bruno Vinicius Santos Valiate*[1,3], *Jose Carlos Alves-Filho*[5], *Thiago Mattar Cunha*[5], *Robert Dantzer*[6], *Mauro Martins Teixeira*[1,2,3], *Antonio Lucio Teixeira*[7*] and *Vivian Vasconcelos Costa*[2,3,4*]

[1] Department of Biochemistry and Immunology, Institute of Biological Sciences, Universidade Federal de Minas Gerais, Belo Horizonte, Brazil, [2] Research Group in Arboviral Diseases, Institute of Biological Sciences, Universidade Federal de Minas Gerais, Belo Horizonte, Brazil, [3] Center for Drug Research and Development of Pharmaceuticals, Institute of Biological Sciences, Universidade Federal de Minas Gerais, Belo Horizonte, Brazil, [4] Departament of Morphology, Institute of Biological Sciences, Universidade Federal de Minas Gerais, Belo Horizonte, Brazil, [5] Center for Research in Inflammatory Diseases (CRID), Department of Pharmacology, Ribeirao Preto Medical School, Universidade de São Paulo, Ribeirão Preto, Brazil, [6] Department of Symptom Research, The University of Texas MD Anderson Cancer Center, Houston, TX, United States, [7] Department of Psychiatry and Behavioral Sciences, McGovern Medical Houston, The University of Texas Health Science Center at Houston, Houston, TX, United States

OPEN ACCESS

Edited by:
Carl G. Feng,
The University of Sydney, Australia

Reviewed by:
Amelia K. Pinto,
Saint Louis University, United States
Ali Zaid,
Griffith University, Australia

***Correspondence:**
Vivian Vasconcelos Costa
vivianvcosta@gmail.com;
vivianvcosta@ufmg.br
Antonio Lucio Teixeira
altexr@gmail.com

Specialty section:
This article was submitted to Viral Immunology, a section of the journal Frontiers in Immunology

Received: 29 April 2021
Accepted: 30 June 2021
Published: 15 July 2021

Citation:
Marim FM, Teixeira DC, Queiroz-Junior CM, Valiate BVS, Alves-Filho JC, Cunha TM, Dantzer R, Teixeira MM, Teixeira AL and Costa VV (2021) Inhibition of Tryptophan Catabolism Is Associated With Neuroprotection During Zika Virus Infection. Front. Immunol. 12:702048. doi: 10.3389/fimmu.2021.702048

Zika virus (ZIKV) is an arbovirus belonging to *Flaviviridae* family that emerged as a global health threat due to its association with microcephaly and other severe neurological complications, including Guillain-Barré Syndrome (GBS) and Congenital Zika Syndrome (CZS). ZIKV disease has been linked to neuroinflammation and neuronal cell death. Neurodegenerative processes may be exacerbated by metabolites produced by the kynurenine pathway, an important pathway for the degradation of tryptophan, which induces neuronal dysfunction due to enhanced excitotoxicity. Here, we exploited the hypothesis that ZIKV-induced neurodegeneration can be rescued by blocking a target enzyme of the kynurenine pathway, the Indoleamine 2,3-dioxygenase (IDO-1). RT-PCR analysis showed increased levels of IDO-1 RNA expression in undifferentiated primary neurons isolated from wild type (WT) mice infected by ZIKV *ex vivo*, as well as in the brain of ZIKV-infected A129 mice. Pharmacological inhibition of IDO-1 enzyme with 1-methyl-D-tryptophan (1-MT), in both *in vitro* and *in vivo* systems, led to significant reduction of ZIKV-induced neuronal death without interfering with the ability of ZIKV to replicate in those cells. Furthermore, *in vivo* analyses using both genetically modified mice ($IDO^{-/-}$ mice) and A129 mice treated with 1-MT resulted in reduced microgliosis, astrogliosis and Caspase-3 positive cells in the brain of ZIKV-infected A129 mice. Interestingly, increased levels of CCL5 and CXCL-1 chemokines were found in the brain of 1-MT treated-mice. Together, our data indicate that IDO-1 blockade provides a

neuroprotective effect against ZIKV-induced neurodegeneration, and this is amenable to inhibition by pharmacological treatment.

Keywords: *Zika virus*, IDO-1, neuroinflammation, neuronal death, microgliosis

INTRODUCTION

ZIKV is an arbovirus belonging to the family *Flaviviridae*, genus *Flavivirus*, composed of positive sense, single-stranded RNA. ZIKV was first isolated from a rhesus monkey in 1947 in the Zika forest (Uganda) and humans' infection was reported in Nigeria in 1954 (1). Epidemiological studies suggest that *Zika virus* had a wide geographical distribution, being introduced in Brazil between 2013 and 2015, causing a major epidemic (2) when there was an increase in cases of microcephaly and the incidence of Guillain-Barré syndrome (GBS) (3). ZIKV transmission occurs mainly by culicids of the genus *Aedes* (4), however, other transmission routes such as blood transfusion, sexual transmission and maternal-fetal transmission have already been demonstrated (5).

In humans, the disease caused by ZIKV manifests in about 20% of cases and is characterized by mild clinical symptoms such as fever, headache, myalgia, rash, conjunctivitis and joint pain (6). However, fetal brain samples from infected mothers have shown that ZIKV is able to break through biological placental barriers to infect developing neural cells inducing neuroinflammation, neuronal death, and neurodegeneration, therefore, leading to microcephaly and congenital Zika syndrome, both of which eventually manifest as fetal brain abnormalities (7–11).

The mechanism by which ZIKV exerts these neurological effects has been related to induction of neuronal excitotoxicity, a pathological process mediated by excessive glutamatergic activity (12), infection, activation, and apoptosis of neural progenitor cells, mature neurons, and glial cells with concomitant inflammation (13). Cell death and neurodegenerative processes can be exacerbated by metabolites produced by the kynurenine pathway (KP), an important pathway of degradation of tryptophan, at least in part due to excitotoxicity. Kynurenine pathway is induced by the activation of Indoleamine-2,3-dioxygenase (IDO-1) enzyme in the presence of proinflammatory cytokines, generating several neuroprotective and neurotoxic metabolites (14, 15).

IDO-1 is found in macrophages, monocytes, microglia, astrocytes, and neurons (16, 17) and is considered the major enzyme involved in tryptophan degradation (18). Imbalances in levels of KP metabolites have been associated with neurodegenerative disorders including Huntington's, Alzheimer's, and Parkinson's diseases and other brain disorders as well as several cancers (19). IDO-1 has been linked to neurodegenerative diseases, and have been studied as a possible therapeutic target (19–23).

1-methyl-D-tryptophan (1-MT) is a methylated tryptophan, acting as a competitive IDO-1 inhibitor (24). Recent studies have shown its ability to improve responses to many anticancer therapies and to boost immunity in infectious diseases (24).

In this study we explored the hypothesis that ZIKV-induced neurodegeneration can be rescued by blocking the enzyme IDO-1 that catalyzes the rate-limiting step in KP.

MATERIAL AND METHODS

Animals and Ethics

This study was carried out in accordance with the recommendations of the Brazilian Government (law 11794/2008a) and approved by the Committee on Animal Ethics of Universidade Federal de Minas Gerais (UFMG) (protocol no.106/2020 CEUA/UFMG). All mice were 5 to 8 weeks old and were kept under specific-pathogen-free conditions at 23°C on a 12-h light/12-h dark cycle with food and water provided *ad libitum*. Experiments were conducted using wild-type C57BL/6 mice, type I interferon receptor deficient mice (A129) on SV129/Ev background, and deficient mice in the enzyme indoleamine 2,3-dioxygenase (IDO-$1^{-/-}$) on C57BL/6 background at the Immunopharmacology Laboratory at ICB-UFMG. C57BL/6 mice were purchased from Biotério Central of UFMG, A129 mice were originally purchased from B&K Universal Limited (United Kingdom) and IDO-$1^{-/-}$ were kindly provided by Universidade de São Paulo (USP).

Mouse Experiments

Mice were inoculated with ZIKV by intravenous (I.V) route (tail vein) with $4x10^3$ PFU of ZIKV in a volume of 200 µl PBS or by intracranial (i.c) route with $1x\ 10^6$ PFU of ZIKV in a volume of 20 µl PBS. In some experiments, mice were treated orally with 10 mg/animal of the Indoleamine 2,3-dioxygenase enzyme inhibitor (1-MT), 1 hour after infection and every 24 hours. Clinical symptoms were monitored daily and severely ill mice with a ≥ 20% weight decrease were euthanized. On day 5 after infection (the peak of ZIKV infection), the animals were euthanized to obtain spleen, brain, optic nerve and eye. For primary culture experiments (neurons), brains from mouse embryos on the fifteenth day of the embryonic period (E15) were collected to obtain neuronal cultures.

Virus

A low-passage-number clinical isolate of ZIKV (HS-2015-BA-01), isolated from a viremic patient with symptomatic infection in Bahia State, Brazil, in 2015, was used. The complete genome of the virus is available at GenBank under the accession no. KX520666. Virus stocks were propagated in C6/36 *Aedes albopictus* cells and were titrated in CCL-81 Vero cells as described previously (25).

Intraocular Pressure Measurement (IOP)

The IOP was measured on days 0, 3 and 5 after ZIKV infection using an applanation tonometer (Tono-Pen Vet - Reichert Technologies, NY, USA), as previously described (26–28).

Virus Titration

The viral load on mouse tissues (brain, eye, optic nerve and spleen) and in the supernatant of cell culture samples was determined by plaque assay in CCL-81 Vero cells, as previously described (25). Plaque counts were computed as p.f.u. per gram of tissue mass or milliliter of supernatant.

Evaluation of Inflammatory Markers

The brain tissue was homogenized in a buffer containing protease inhibitors (100 mg of tissue per 1 mL of extraction solution; 0.4 mol/L NaCl, 0.05% Tween 20, 0.5% BSA, 0.1 mmol/L phenylmethyl sulfonil fluoride, 0.1 mmol/L benzethonium chloride, 10 mmol/L EDTA, and 20 KI aprotinin). The brain homogenate was centrifuged at 3000 × *g* for 10 min at 4°C, and the supernatant was collected to determine the concentration of cytokines by ELISA. The cytokines (TNF and IL-1β) and chemokines (CCL5 and CXCL1) levels in the brain of mice were measured using DuoSet ELISA kits antibodies (R&D Systems) in accordance with the manufacturer's instructions. Neutrophil accumulation in mouse brains was also indirectly measured by determining the level of myeloperoxidase activity, according to a previous study (29).

Brains Sections and Staining

For histopathological scoring, brain samples were stained with hematoxylin and eosin (H&E) and the analyses was performed in cerebral cortex and hippocampus sections in a blinded manner according to previous studies (29, 30). Briefly, each brain region was graded on a four-point scale: 0, no tissue damage; 1, minimal tissue damage and/or mild inflammation; 2, mild tissue damage and/or moderate inflammation; 3, severe tissue damage and high inflammation; 4, necrosis with loss of tissue elements and presence of cellular debris. Meningeal inflammation was also graded on a four-point scale: 0, no inflammation; and points between 1 and 4 were assigned when there were one to four layers of cellular inflammation, respectively. The final score was calculated as a sum of cerebral cortex added to the score obtained from the meningeal inflammation analysis, totalizing a maximum of 8 points. For immunostaining analyses, brain samples were processed and sections from hippocampus, striatum, and prefrontal and motor cortex of mice were stained for microglia (IBA1 Polyclonal Antibody – Invitrogen), astrocytes (S100-β polyclonal antibody – Abcam) and apoptosis (Caspase-3 Monoclonal Antibody – Invitrogen) according to manufacturer's instructions (Vector Elite kit - Vector Laboratories) as described in as previously described (31). Image acquisition and analysis were performed using an Olympus BX 41 microscope (Olympus). The images presented in the article are representative of one of those experiments.

Primary Neurons Cell Cultures

Neuronal cultures were prepared from the cortex and striatal regions of E15 of C57BL/6 wild-type mouse embryo brains. After dissection, the brain tissue was submitted to trypsin digestion followed by cell dissociation using a fire-polished Pasteur pipette. Neuronal cells were plated onto poly-L-ornithine-coated dishes in neurobasal medium supplemented with N2 and B27 supplements (Gibco), 2 mM GlutaMAX (Gibco) and 50 g/ml penicillin/streptomycin (Sigma), incubated at 37°C and 5% CO_2 for 5 days. Infection was performed with ZIKV (MOI of 0.1), followed by an adsorption period of 1 h. Wells were washed with incomplete medium and each well was replaced by a final volume of complete neurobasal medium. In some experiments, neuronal cultures were treated with 3, 10, 30 or 100 μM of the Indoleamine 2,3-dioxygenase enzyme inhibitor every 24h. Beside the kinetic experiments, all experiments evaluating the effects of 1-MT on primary neurons were performed after 48 h of ZIKV infection. At the time point, the supernatant was collected for quantification of viral load while the cells adhered to the plate were used in the cell death assay.

Neuronal Cell Viability

Neuronal cell death was assessed by LIVE/DEAD Cell Viability Assays after 48 hours of ZIKV infection, as previously described (27). Briefly, the neuronal cell culture was stained with 2 μM calcein acetoxymethyl ester (AM) and 2 μM ethidium homodimer -1. After 10 minutes, the neuronal culture was immediately visualized by a FLoid Cell Imaging Station fluorescence microscope (Thermo Fisher Scientific). Images were captured and the fractions of live (green, calcein AM) and dead (red, ethidium homodimer -1) cells in the same field of view were evaluated. Cell viability was analyzed, and the quantification was performed using the ImageJ software. Data are reported as the percentage of dead cells out of the total number of cells.

Real-Time RT-PCR

RNA was isolated using TRIzol™ reagent in accordance with the manufacturer's instructions (Invitrogen). RNA was resuspended in 30 μL of nuclease-free water, and its concentration was analyzed by Nanodrop spectrophotometer. cDNAs were prepared from 2 μg of total RNA extracted in a 10 μL final reverse transcription reaction. RT-qPCR was performed from 10x diluted cDNA using SYBR Green PCR Master Mix (Applied Biosystems). Real-time was performed in a 7500 Fast Real-Time PCR System (Applied Biosystems). The appropriate primers were used to amplify a specific fragment corresponding to specific gene targets as follows: GAPDH F: 5'-ACG GCC GCA TCT TCT TGT GCA- 3'; GAPDH R: 5' -CGC CCA AAT CCG TTC ACA CCG A- 3; IDO-1 F: 5'-TCA AAG CAA TCC CCA CTG TAT CC- 3'; IDO-1 R: 5' -TCC ACA AAG TCA CGC ATC CTC- 3'. All data are presented as relative expression units after normalization to GAPDH gene, and measurements were conducted in duplicate.

Statistical Analysis

Results were expressed as Mean ± SEM for the number of independent experiments. GraphPad Prism (GraphPad Software, Inc) was used to analyze data using different-tests as appropriate and $P < 0.05$, $P < 0.01$, $P < 0.001$ and $P < 0.0001$

indicate the levels of statistical significance. Additional information is indicated in *Figure Legends*.

RESULTS

IDO-1 Expression Is Enhanced Upon ZIKV Infection *In Vitro* and *In Vivo*

The KP is segregated into two distinct branches triggering neurotoxic and neuroprotective metabolites. The first step of KP converts the essential amino acid L-tryptophan to N-formylkynurenine and is regulated by rate-limiting enzymes, being the Indoleamine 2,3-dioxygenase 1 (IDO-1) the main enzyme contributing to the production of kynurenines during inflammatory conditions (32). Therefore, differential mRNA expression of IDO-1 was investigated in non-infected and ZIKV-infected primary neuron cultures from cortex and striatal regions obtained from wild type (WT) C57BL/6 mice embryo brains. After 48 hours of ZIKV infection, there was an increase in the levels of IDO-1 when compared to Mock control in primary neuron cultures (**Figure 1A**). Additionally, increased levels of IDO-1 expression were also seen in the brain of A129 mice infected with ZIKV, 5 days upon infection, peak of disease manifestation in these mice, when compared to Mock littermates (**Figure 1B**). These results clearly demonstrate that ZIKV infection induced increased expression of IDO-1 enzyme *in vitro* and *in vivo*.

1-MT Inhibitor Reduces Neuronal Death in ZIKV Primary Neurons

Subsequently, we evaluated the effect of blockade of IDO-1 enzyme *in vitro*. Previous studies by our group have shown that undifferentiated neuronal cultures are highly susceptible to ZIKV infection, inducing neuronal death (27, 33). Then, we tested whether the IDO-I inhibitor, 1-methyl-D-tryptophan (1-MT) would reduce ZIKV-induced neuronal cell death. For that, primary neuronal cultures obtained from the corticostriatal region of C57BL/6 embryo brains were infected with ZIKV (MOI 0.1) and treated with 1-MT at concentrations of 3; 10; 30 and 100 μM. After 48 hours following infection, the supernatant was collected to evaluate viral load by plaque assay and cells were subjected to cell viability assays. ZIKV neuronal infection resulted in 10^9 PFU/mL in the culture supernatants, and *in vitro* IDO-1 inhibition with 1-MT did not interfere with ability of the virus to replicate in these cells. The highest 1-MT concentration triggered some reduction of the viral load (**Figure 2A**). Nevertheless, 1-MT treatment induced a significant reduction of neuronal cell death, in all evaluated concentrations (**Figures 2B, C**). At the concentration of 100 μM 1-MT, cytotoxicity was detected in infected cells, but without reaching statistical difference.

IDO-1 Inhibition Did Not Prevent ZIKV-Induced Clinical Manifestations as Well as Virus Replication in A129 Mice

Further, we investigated the effects of IDO-1 inhibition during ZIKV infection *in vivo*. For that, A129 mice were inoculated (i.v) with 4 x 10^3 PFU of ZIKV and, after 1 hour, they were treated with 1-MT and every 24 hours until euthanasia (**Figure 3A**). Five days after infection, peak of disease manifestation in this model, spleen, brain, optic nerve and eye of the animals were collected. In accordance with previous studies from our group (27), there was significant body weight loss in the ZIKV group when compared to Mock control. Similarly, infected mice treated

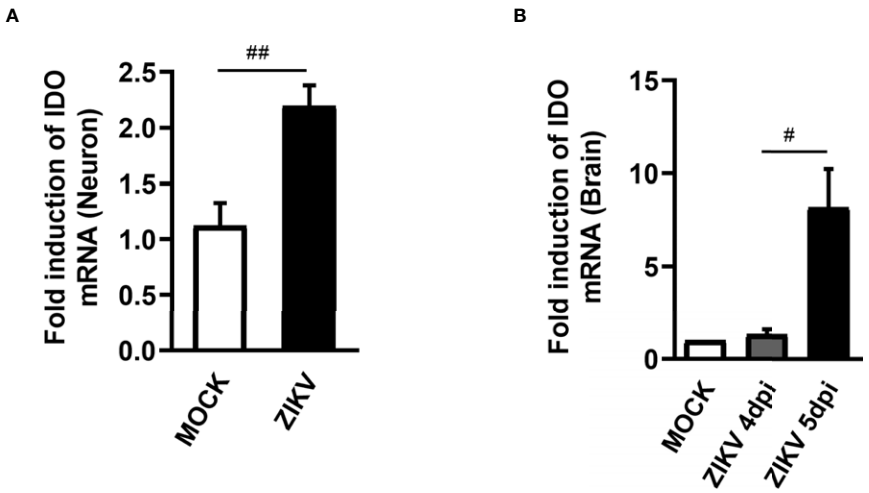

FIGURE 1 | IDO-1 expression induced by ZIKV infection. **(A)** Primary culture of cortical-striatal neurons from C57BL/6 mice on D5 were infected with ZIKV (MOI 0.1) and after 48 hours the cells were harvested. **(B)** Type I interferon receptor deficient mice (A129) were inoculated (i.v) with 4x10^3 PFU/200 μL of ZIKV. At day 4 and 5 of infection, the brain was harvested. RNA extraction and subsequent Real time PCR analysis of IDO-1 expression in the brain and neuronal primary culture was done. Results are expressed as mean ± SEM and are representative of two independent experiments. Statistically significant differences were assessed by Mann Whitney test. (#) for $P < 0.05$ and (##) for $P < 0.01$.

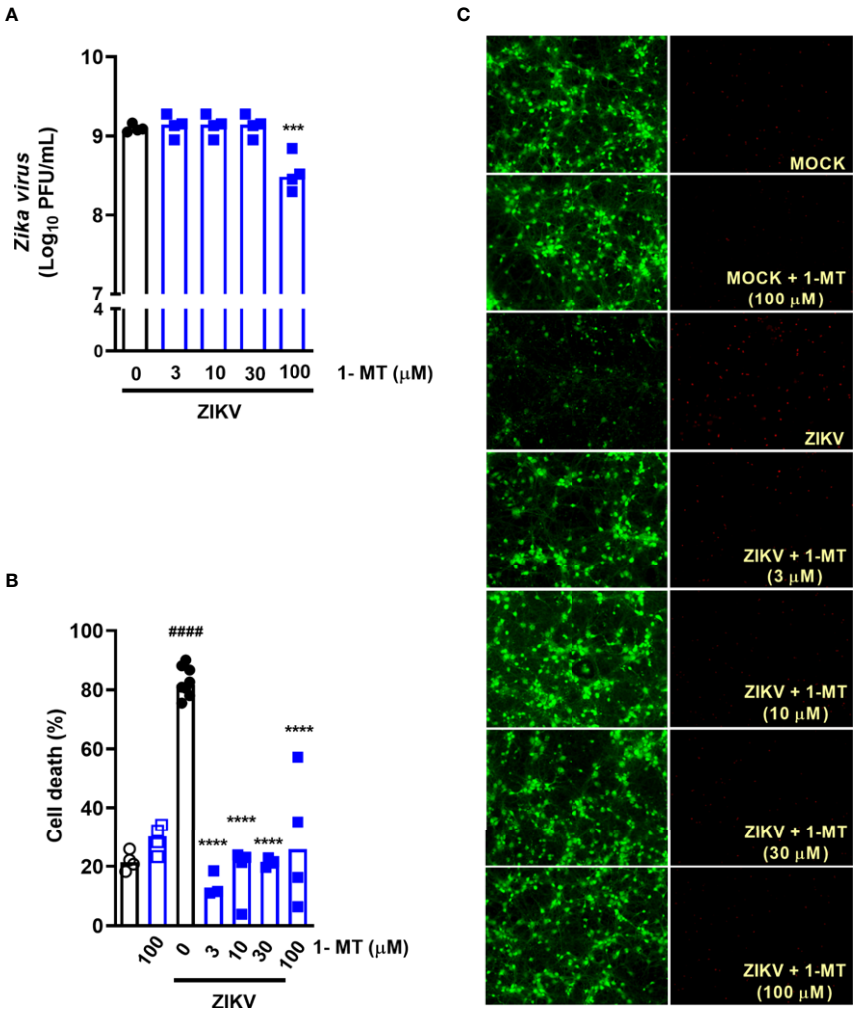

FIGURE 2 | IDO-1 inhibition in primary undifferentiated neurons infected by ZIKV. Primary culture of cortical-striatal neurons on D5. Neuronal culture from C57BL/6 mice were infected with ZIKV (MOI 0.1) and treated with 1-MT inhibitor at concentrations of 3; 10; 30 and 100 μM. After 48 hours, **(A)** the supernatant was collected to assess viral load, **(B)** cell death was assessed using the LIVE/DEAD Cell Viability Assay. **(C)** Representative images of infected and uninfected neurons stained with calcein AM (green indicates live cells) and ethidium homodimer (red indicates dead cells). All results are expressed as median and are representative of at least two independent experiments. Statistically significant differences were assessed by One-way ANOVA plus Holm-Sidak's or Tukey's comparisons test. (####) for $P < 0,0001$ compared to the MOCK group; (***) for $P < 0,001$ and (****) for $P < 0,0001$ compared to the ZIKV group.

with 1-MT lost as much weight as the ZIKV group (**Figure 3B**). Ophthalmic alterations induced by ZIKV infection were also evaluated through the measurement of intraocular pressure (IOP), but no significant differences were detected between infected groups, treated or not with 1-MT (**Figure 3C**). Moreover, 1-MT treatment of ZIKV-infected mice did not interfere with viral loads detected in the brain (**Figure 3D**), optic nerve (**Figure 3E**), eye (**Figure S1A**) or spleen (**Figure S1B**). No significant differences were detected in neutrophils recruitment to the brain (**Figure 3F**). Although 1-MT did not prevent viral replication, it induced larger production of the chemokines CCL5 (**Figure 3G**) and CXCL1 (**Figure 3H**) in the brain of infected mice when compared to non-treated ZIKV group, but there was no difference in TNF (**Figure 3I**) and IL -1β (**Figure 3J**) levels. Overall, the results show that IDO-1 inhibition was not able to reduce clinical manifestations induced by ZIKV-infection, as well as virus replication in A129 mice.

IDO-1 Inhibition Prevents Microgliosis, Astroglioses and Caspase-3 Expression of Cells in the Brain of ZIKV Infected Mice

Infection of A129 mice with ZIKV triggered histopathological signs of brain inflammation and tissue damage. Histopathological analysis of the brain revealed mild gliosis and meningitis 5 days after ZIKV infection. Such changes were similar in non-treated and 1-MT-treated ZIKV-infected mice (**Figures 4A, B**). Despite such evidence, 1-MT treatment prompted a significant reduction in the number of IBA-1

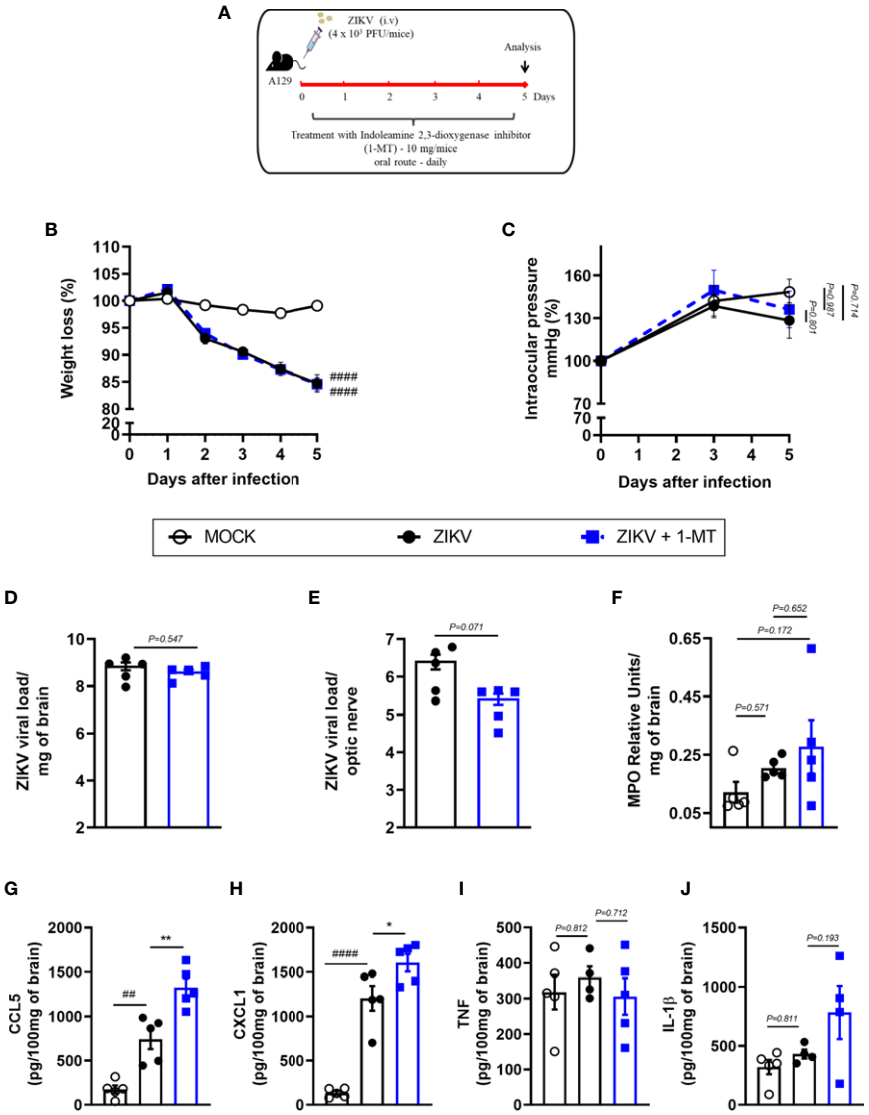

FIGURE 3 | Clinical signs and inflammatory parameters in A129 mice infected by ZIKV treated or not with 1-MT inhibitor. **(A)** Experimental schematic representation of experimental strategy. A129 were inoculated (i.v) with $4x10^3$ PFU/200μL of ZIKV and treated daily with 1-MT. **(B)** The body weight was evaluated daily and **(C)** the intraocular pressure was analyzed on days 0, 3 and 5. At day 5 of infection, **(D)** the brain and **(E)** optical nerve was harvested for plaque assay analysis. **(F)** Measurement of myeloperoxidase activity (neutrophil accumulation) and **(G–J)** chemokine/cytokine production was assessed in mouse brain of animals. All results are expressed as mean and error bar indicate the standard error (SEM) and are representative of at least two independent experiments. Statistically significant differences were assessed by Two-way ANOVA plus Tukey's comparisons test **(A, B)**, Mann Whitney test **(D, E)** and One-way ANOVA **(F–J)** plus Tukey's comparisons test. (##) for $P < 0,01$ and (####) for $P < 0,0001$ when compared to the MOCK group. (*) for $P < 0,05$ and (**) for $P < 0,001$ compared to the ZIKV group.

positive cells (IBA-1^+ cells) in the cerebral cortex of infected mice (**Figures 4C, D**). In addition, there was significant reduction in the number of astrocytes (S100β^+ cells) in 1-MT-treated group when compared to non-treated ZIKV infected group (**Figures 4E, F**). Another important feature of ZIKV infection is neurodegeneration, including cell death. In this regard, treatment of infected mice with 1- MT decreased the number of brain Caspase-3-positive cells (Caspase-3^+ cells), which is suggestive of reduced apoptosis (**Figures 4G, H**).

Effects of ZIKV Infection in Indoleamine 2,3-Dioxigenase 1 (IDO-$1^{-/-}$) Deficient Mice

In view of the effects observed after 1-MT treatment and the potential contribution of this pathway in preventing neurodegeneration, we also evaluated ZIKV infection in genetically modified Indoleamine 2,3-dioxigenase 1 deficient (IDO-$1^{-/-}$) mice. Since C57BL/6 mice are resistant to ZIKV infection (27, 34, 35), ZIKV infection was performed by intracerebral route by inoculation of with 1 x 10^6 PFU of

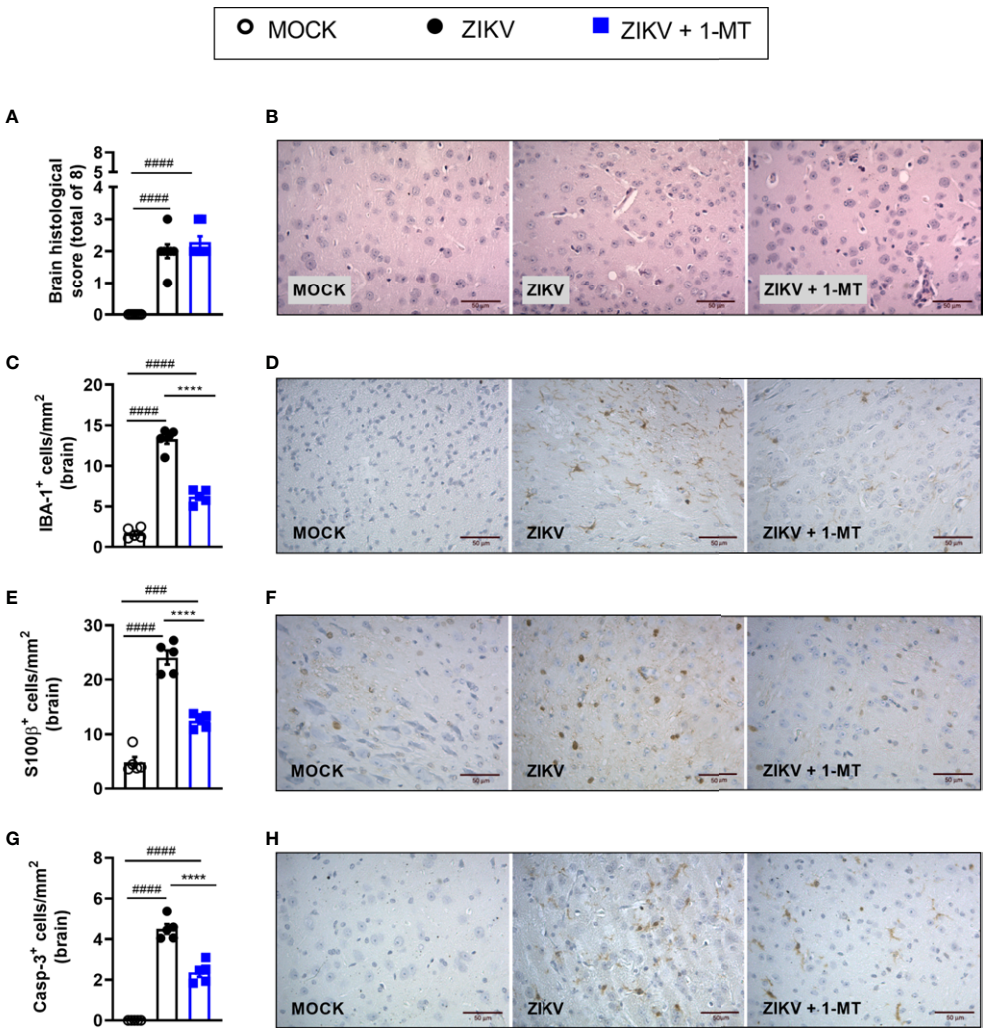

FIGURE 4 | Morphometric analysis of the brain of A129 mice infected by ZIKV, treated or not with 1-MT inhibitor. A129 were inoculated (i.v) with $4x10^3$ PFU/200µL of ZIKV and treated daily with 1-MT. **(A)** Semiquantitative analysis (histopathological score) after H&E staining of brain sections of ZIKV-infected mice 5 days after infection. **(C, E, G)** Immunostaining of **(C)** IBA-1^+, **(E)** S100-β^+ and **(G)** Caspase-3 was performed in the brains of mice. **(B, D, F, H)** Representative images from brain sections. All results are expressed as mean and error bar indicate the standard error (SEM) and are representative of at least two independent experiments. Statistically significant differences were assessed by One-way ANOVA plus Tukey's comparisons test. (###) for $P < 0,001$ and (####) for $P < 0,0001$ when compared to the MOCK group. (****) for $P < 0,0001$ compared to the ZIKV group.

ZIKV (i.c) in both WT C57BL/6 and IDO-$1^{-/-}$ mice (**Figure 5A**). Body weight loss was significantly higher in C57BL/6 and IDO-$1^{-/-}$ mice infected with ZIKV than in their respective controls (**Figure 5B**). Furthermore, there was no significant change in the IOP levels between WT and IDO-$1^{-/-}$ ZIKV-infected groups (**Figure 5C**). Regarding viral replication, no viable virus (assessed by plaque assay) or ZIKV genome (RT-PCR) was detected in the brain of ZIKV-infected WT or IDO-$1^{-/-}$ mice. Accordingly, no difference in MPO levels was detected into mice's brains (**Figure 5D**). Finally, as demonstrated during 1-MT treatment, intracranial ZIKV infection also led to increased production of inflammatory mediators, such as CCL5 (**Figure 5E**) and CXCL1 (**Figure 5F**) in both WT and IDO-$1^{-/-}$ ZIKV mice. Production of TNF and IL-1β in WT and IDO-$1^{-/-}$ was analogous to Mock (**Figures 5G, H**). Additionally, in a pattern similar to that observed in A129 mice treated with 1-MT, brain histopathological analysis of C57BL/6 and IDO-$1^{-/-}$ infected mice revealed mild gliosis and meningitis in both infected experimental groups (**Figures 6A, B**). Accordingly, reduced microgliosis, astrogliosis and apoptosis were found in infected IDO-$1^{-/-}$ mice in comparison to ZIKV infected WT littermates as demonstrated by reduction of the number of IBA-1 (**Figures 6C, D**), S100β (**Figures 6E, F**) and Caspase-3 (**Figures 6G, H**) positive cells of mice's brain sections. Furthermore, the morphology of the Caspase-3-stained cells, especially the nucleus morphology, comprised both neurons and glial cells.

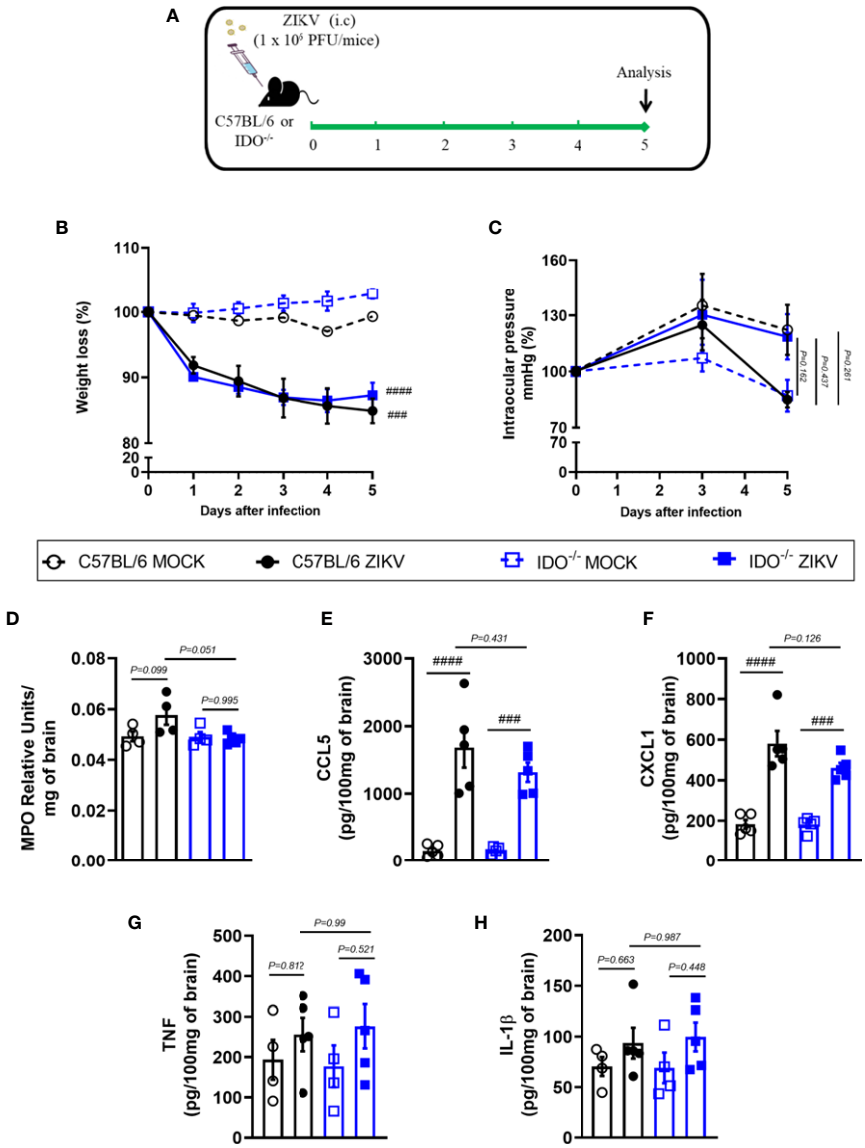

FIGURE 5 | Clinical signs and inflammatory parameters after ZIKV infection of WT and IDO$^{-/-}$ mice infected by ZIKV. **(A)** Experimental schematic representation of experimental strategy. C57BL/6 and IDO-1$^{-/-}$ were inoculated (intracranial) with 1x10^{6} PFU/20µL of ZIKV. **(B)** The body weight was evaluated daily and **(C)** the intraocular pressure was analyzed on days 0, 3 and 5. At day 5 of infection, **(D)** the brain was harvested and myeloperoxidase absorbance analysis and **(E–H)** chemokine/cytokine production was assessed. All results are expressed as mean and error bar indicate the standard error (SEM) and are representative of at least two independent experiments. Statistically significant differences were assessed by Two-way ANOVA plus Tukey's comparisons test **(B, C)** and One-way ANOVA plus Tukey's comparisons test (D-H). (###) for *P < 0,001* and (####) for *P < 0,0001* compared to the MOCK group.

DISCUSSION

Several studies have reported the tropism of the ZIKV to different cellular types, tissues and body fluids. Meanwhile, ZIKV-tropism to the CNS is the most harmful feature to the host and may cause neurodegeneration and other neuronal dysfunctions. Despite its association with neurological diseases, such as microcephaly, GBS and CZS, there are no current approved therapies for the treatment of this important pathogen (36). In order to develop effective therapies, a better understanding of the pathogenicity resulting from the virus-host interaction is required. Global analysis of gene expression shows that ZIKV infection prompts significant dysregulation of several host factors associated with neural development, immune response, cell death, among others (37, 38). In the present study, we evaluated the potential neuroprotective effect of the blockade of IDO-1 enzyme by using a genetically approach (IDO-1$^{-/-}$ mice) or a pharmacological strategy (1-MT inhibitor), *in vitro* and *in vivo*. The main results

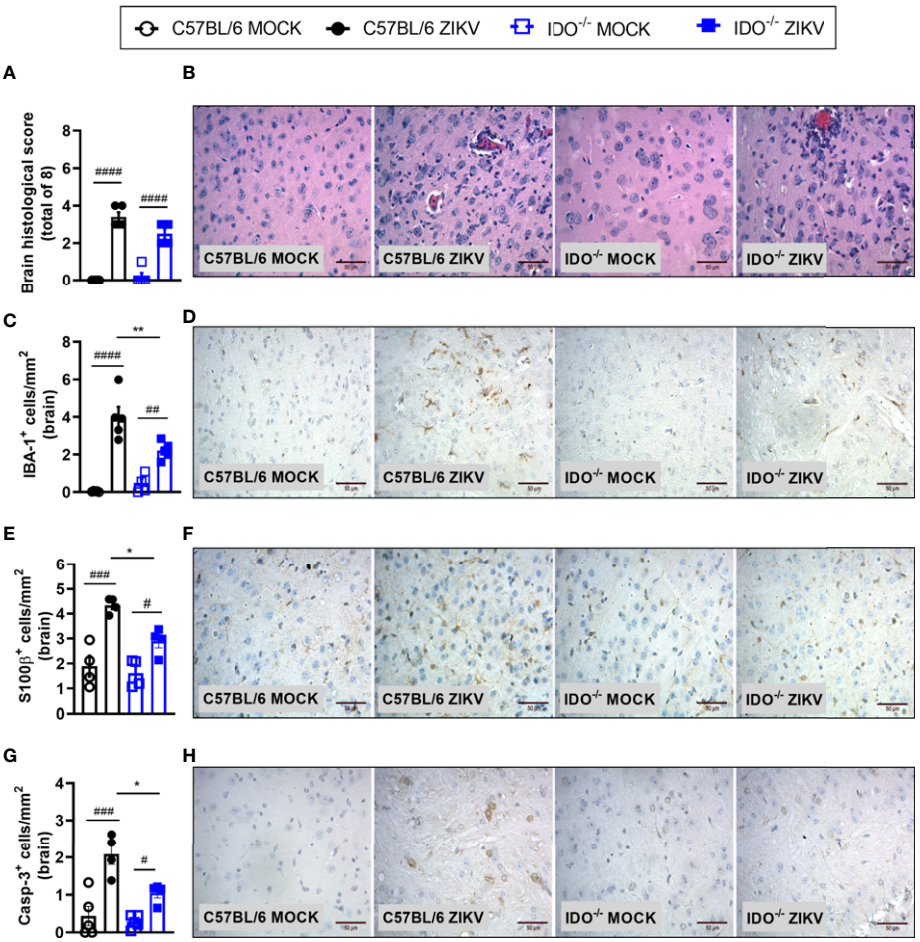

FIGURE 6 | Morphometric analysis of the brain of WT and IDO$^{-/-}$ mice infected by ZIKV. C57BL/6 and IDO-1$^{-/-}$ were inoculated (intracranial) with 1x10^{6} PFU/20µL of ZIKV. **(A)** Semiquantitative analysis (histopathological score) after H&E staining of brain sections of ZIKV-infected mice 5 days after infection. **(C, E, G)** Immunostaining of **(C)** IBA-1^{+}, **(E)** S100-β^{+} and **(G)** Caspase-3 was performed in the brains of mice. **(B, D, F, H)** Representative images from brain sections. Results are expressed as mean and error bar indicate the standard error (SEM) and are representative of at least two independent experiments. Statistically significant differences were assessed by One-way ANOVA plus Tukey's comparisons test (#) for $P < 0,05$, (##) for $P < 0,01$ and (###) for $P < 0,001$ and (####) for $P < 0,0001$ when compared to the MOCK group. (*) for $P < 0,05$ and (**) for $P < 0,01$ compared to the ZIKV group.

were: (I) increased levels of IDO-1 expression after ZIKV infection; (II) reduction of neuronal death upon 1-MT treatment; (III); massive reduction of ZIKV-induced microgliosis, astrogliosis and apoptosis in IDO$^{-/-}$ mice and after 1-MT administration in A129 mice. Overall, these data indicate a neuroprotective effect induced by IDO-1 inhibition after ZIKV infection *in vivo* and *in vitro*.

IDO-1 is the first rate-limiting of the KP responsible for converting tryptophan into several downstream kynurenine metabolites. This enzyme is expressed by many cell types, including macrophages, microglia, dendritic cells, astrocytes, fibroblasts, and epithelial cells (32) and is commonly induced by proinflammatory cytokines. In the current study, we showed that ZIKV infection increased levels of IDO-1 expression in mice's brain and also in primary neuron culture obtained from embryonic brains of mice. These results demonstrate that Indoleamine-2,3-dioxygenase, or IDO-1, is activated by the inflammatory response induced by ZIKV. In this context, we next, evaluated the effects of the inhibition of IDO-1 on ZIKV infection *in vitro* and *in vivo* systems. We found that a pharmacological inhibition in primary neurons infected by ZIKV did not prevent viral replication but induced less cell death. Likewise, human monocyte-derived macrophages induce IDO-1 expression upon West Nile virus (WNV), *via* TNF and NF-KB signaling, but IDO was not essential for the control of WNV infection (39). Similarly, 1-MT treatment of ZIKV-infected mice did not interfere with the ability of ZIKV to replicate in the brain, optic nerve, eye or spleen tissues. Additionally, no significant difference in neutrophil recruitment was observed between treated and non-treated ZIKV-infected mice. At the same time, chemokines relevant for the migration of monocytes, lymphocytes, as well as for neutrophil traffic, such as CCL5 and CXCL1, respectively, had

increased levels in 1-MT treated ZIKV mice. We also evaluated ZIKV infection in IDO-1$^{-/-}$ mice and WT mouse model. Corroborating the pharmacological data, the absence of IDO did not interfere with clinical signs, viral replication or inflammatory parameters, although microgliosis, astrogliosis and caspase-3 expression reduced after infection. Chemokine signaling plays an important homeostatic role and modulates neuroprotective processes on different stimuli, orchestrating the action of neurons-microglia-astrocytes to preserve brain damage (40). In pathological processes, pro-inflammatory cytokines and chemokines are robustly induced and can lead IDO-1 activity and tryptophan associated metabolites (39, 41, 42). IDO-1 inhibition in Influenza virus infection does not affect leukocyte infiltration or viral clearance, thus, blockade of IDO-1 could play a beneficial role in host protection (43–45). These data show that pharmacological inhibition or genetic ablation of IDO-1 did not completely prevent brain inflammation, but reduced brain damage and cell death.

ZIKV can infect almost all CNS cells, including neurons, glial cells, endothelial cells and pericytes. Activated CNS-resident cells could be the source of proinflammatory cytokines and chemokines such as CCL5 and CXCL1, found in ZIKV-infected brain tissue. ZIKV infection and replication are associated with brain damage and, as consequence, severe neurological symptoms (8, 27). The mechanisms by which ZIKV exert these effects involve neuronal excitotoxicity and apoptosis of microglia, astrocytes and other cells. Our group has shown that neuronal cell death induced by ZIKV is associated with excitotoxicity mediated by the release of glutamate and other neurotoxic factors such as TNF and IL-1β, inducing the activation of NMDA (N-methyl-d-aspartate receptor) receptors (27, 33). Accordingly, treatment with Memantine (an FDA-approved allosteric NMDA receptor antagonist) *in vivo* and *in vitro* was effective to prevent ZIKV-induced cell death and neurodegeneration but did not interfere with the ability of the virus to replicate. Furthermore, administration of Ifenprodil (a selective inhibitor of the NMDA receptor, specifically for the GluN1 and GluN2B subunits) in a primary neuron culture rescues ZIKV-induced neurotoxicity (27, 33). IDO expression in Huntington's disease is chronically elevated, inducing neurotoxicity, and IDO inhibition reduces neurotoxicity sensitivity and neuroprotective role (46).

Cell death and neurodegenerative processes can be exacerbated by metabolites produced by KP. Kynurenine metabolism is directly associated with several neurodegenerative and neurological diseases, such as Alzheimer's disease, multiple sclerosis, and stroke (23, 47). In accordance with recent studies from our group (27, 33, 48), infection of A129 mice induced brain inflammation and tissue damage, and we found mild gliosis and meningitis in all infected mice groups. However, pharmacological inhibition or deletion of IDO-1 (IDO$^{-/-}$) prompted a significant reduction of IBA-1 positive cells in the brain's mice, suggesting less microglia activation. It appears that microglia activation is dependent on IDO-1 (49, 50). In a similar pattern, we found a reduction in the number of astrocytes (S100β positive cells). Microglia and activated astrocytes produce several inflammatory mediators, including IL-1β, TNF, glutamate, nitric oxide (NO) among others, which can trigger neuronal death after ZIKV infection (33). In addition, ZIKV-induced neurodegeneration can be caused by loss of structure or function of neurons. Recent studies demonstrated that ZIKV is able to induce apoptosis of neuronal cells *in vitro* (33) and *in vivo* (28). In this regard, we have shown that treatment of infected mice with 1-MT decreased the number of brain Caspase-3-positive cells, which is suggestive of reduced apoptosis. According to cell morphology, especially the nucleus, these cells comprised both neurons and glial cells, however, co-localization assays were not performed (Caspase-3/IBA-1 or Caspase-3/S100β or NeuN/Caspase-3). Although ZIKV-induces neuronal damage, it is unclear whether neuronal death is due to direct neurotoxicity or secondary to the activation of microglia and astrocytes. Apoptosis can be a result from inflammatory mediators released by the activated microglia or induced in a non-cell autonomous manner, triggering cell death of uninfected neurons by releasing cytotoxic factors (33). These data suggest the pharmacological or genetic inhibition of IDO-1 prevents microglial activation, astrogliosis and apoptosis in the brain of ZIKV infected, without preventing clinical outcomes.

Development of efficient therapies against viral infections, such as ZIKV, is important for the control and reduction of clinical symptoms, viral load, neuroinflammation, and mainly, neurodegeneration. A combination of compounds that could prevent ZIKV-induced neurodegeneration with viral replication (antiviral drugs) represents the ideal treatment. Meanwhile, no approved antiviral drugs are available. Recently, our group showed that a therapeutic administration of an antiviral peptide (AH-D) significantly reduced viral loads in serum, spleen, brain and optical nerve throughout the course of ZIKV infection (30). Additionally, we also demonstrated the efficacy of the 7-Deaza-7-fluoro-2'-C-methyl adenosine (DFMA), a nucleoside analogue, which showed significant antiviral effects against ZIKV *in vitro* and *in vivo* systems, especially when administered prophylactically and at early times after ZIKV infection (48). These compounds open a new perspective to evaluate the synergic effect of a neuroprotective drug such as 1-MT along with an antiviral drug against ZIKV-induced disease in an early future.

In conclusion, our data indicate that IDO-1 inhibition exerts a neuroprotective role in CNS reducing the microglial activation, astrogliosis and apoptosis without antiviral effect. Further studies are required to elucidate the mechanisms of neuroprotection obtained by ablation of IDO-1 and it will be important to evaluate whether the combination of neuroprotective drugs, such 1-MT, and antiviral like AH-D or DFMA could be the treatment for ZIKV infection.

DATA AVAILABILITY STATEMENT

The raw data supporting the conclusions of this article will be made available by the authors, without undue reservation.

ETHICS STATEMENT

The animal study was reviewed and approved by Committee on Animal Ethics of Universidade Federal de Minas Gerais (UFMG) (protocol no.106/2020 CEUA/UFMG).

AUTHOR CONTRIBUTIONS

FM, JA-F, TC, MT, AT, and VC designed the study. FM, DT, CQ-J, and BV conducted the experiments and analysis of the data. FM, AT, and VC interpreted the results. FM, CQ-J, AT, and VC wrote the first draft of the paper. RD, MT, AT, and VC obtained funding. All authors contributed to the article and approved the submitted version.

FUNDING

This work was supported by the Grants from National Institute of Science and Technology in Dengue and Host-microorganism Interaction (INCT dengue), which is a programme sponsored by the Brazilian National Science Council (CNPq, Brazil) and the Minas Gerais Foundation for Science (FAPEMIG, Brazil). This work also received support from Coordenação de Aperfeiçoamento de Pessoal de Nível Superior – CAPES/Brazil (grant no CAPES: 88881.130741), ZIKALLIANCE consortium – 734548, Financiadora de Estudos e Pesquisa (FINEP 01.16.0050.00, Brazil), Conselho Nacional de Desenvolvimento Cientifico e Tecnológico (CNPq) under grants: 425359/2018 and 440423/2016-13, Fundação de Amparo à Pesquisa do Estado de Minas Gerais (FAPEMIG, Brazil) - APQ-02281- 18) and by L'Oréal-Unesco-ABC For Women in Science Program). Also, this work was funded by NIH (R01 CA193522 and R01 NS073939) and an MD Anderson Cancer Support Grant (P30 CA016672).

ACKNOWLEDGMENTS

We thank Ilma Marçal and Tania Colina for technical support during the study.

SUPPLEMENTARY MATERIAL

The Supplementary Material for this article can be found online at: https://www.frontiersin.org/articles/10.3389/fimmu.2021.702048/full#supplementary-material

Supplementary Figure 1 | Viral load in the eye and spleen of A129 mice infected by ZIKV, treated or not with 1-MT inhibitor. A129 were inoculated (i.v) with $4x10^3$ PFU/200µL of ZIKV and treated daily with 1-MT. **(A)** Eye and **(B)** spleen was harvested for plaque assay analysis. All results are expressed as mean and error bar indicate the standard error (SEM) and are representative of at least two independent experiments. Statistically significant differences were assessed by One-way ANOVA plus Tukey's comparisons test.

REFERENCES

1. Macnamara FN. Zika Virus: A Report on Three Cases of Human Infection During an Epidemic of Jaundice in Nigeria. *Trans R Soc Trop Med Hyg* (1954) 48(2):139–45. doi: 10.1016/0035-9203(54)90006-1
2. Baud D, Gubler DJ, Schaub B, Lanteri MC, Musso D. An Update on Zika Virus Infection. *Lancet* (2017) 390(10107):2099–109. doi: 10.1016/S0140-6736(17)31450-2
3. Campos GS, Bandeira AC, Sardi SI. Zika Virus Outbreak, Bahia, Brazil. *Emerg Infect Dis* (2015) 21(10):1885–6. doi: 10.3201/eid2110.150847
4. Cunha MS, Esposito DL, Rocco IM, Maeda AY, Vasami FG, Nogueira JS, et al. First Complete Genome Sequence of Zika Virus (Flaviviridae, Flavivirus) From an Autochthonous Transmission in Brazil. *Genome Announc* (2016) 4 (2):e00032–16. doi: 10.1128/genomeA.00032-16
5. Kurscheidt FA, Mesquita CSS, Damke G, Damke E, Carvalho A, Suehiro TT, et al. Persistence and Clinical Relevance of Zika Virus in the Male Genital Tract. *Nat Rev Urol* (2019) 16(4):211–30. doi: 10.1038/s41585-019-0149-7
6. Duffy MR, Chen TH, Hancock WT, Powers AM, Kool JL, Lanciotti RS, et al. Zika Virus Outbreak on Yap Island, Federated States of Micronesia. *N Engl J Med* (2009) 360(24):2536–43. doi: 10.1056/NEJMoa0805715
7. Cugola FR, Fernandes IR, Russo FB, Freitas BC, Dias JL, Guimaraes KP, et al. The Brazilian Zika Virus Strain Causes Birth Defects in Experimental Models. *Nature* (2016) 534(7606):267–71. doi: 10.1038/nature18296
8. Garcez PP, Loiola EC, Madeiro da Costa R, Higa LM, Trindade P, Delvecchio R, et al. Zika Virus Impairs Growth in Human Neurospheres and Brain Organoids. *Science* (2016) 352(6287):816–8. doi: 10.1126/science.aaf6116
9. Noronha L, Zanluca C, Azevedo ML, Luz KG, Santos CN. Zika Virus Damages the Human Placental Barrier and Presents Marked Fetal Neurotropism. *Mem Inst Oswaldo Cruz* (2016) 111(5):287–93. doi: 10.1590/0074-02760160085
10. Dallmeier K, Neyts J. Zika and Other Emerging Viruses: Aiming at the Right Target. *Cell Host Microbe* (2016) 20(4):420–2. doi: 10.1016/j.chom.2016.09.011
11. Saiz JC, Martin-Acebes MA. The Race To Find Antivirals for Zika Virus. *Antimicrob Agents Chemother* (2017) 61(6):e00411–17. doi: 10.1128/AAC.00411-17
12. Dong XX, Wang Y, Qin ZH. Molecular Mechanisms of Excitotoxicity and Their Relevance to Pathogenesis of Neurodegenerative Diseases. *Acta Pharmacol Sin* (2009) 30(4):379–87. doi: 10.1038/aps.2009.24
13. Marim FM, Camargos VN, Queiroz-Junior CM, Costa VV. Zika Virus Infection and Potential Mechanisms Implicated in Neuropsychiatric Complications. In: AL Teixeira, D Macedo, BT Baune, editors. *Perinatal Inflammation and Adult Psychopathology: From Preclinical Models to Humans*. Springer (2020). p. 207–22.
14. O'Connor JC, Andre C, Wang Y, Lawson MA, Szegedi SS, Lestage J, et al. Interferon-Gamma and Tumor Necrosis Factor-Alpha Mediate the Upregulation of Indoleamine 2,3-Dioxygenase and the Induction of Depressive-Like Behavior in Mice in Response to Bacillus Calmette-Guerin. *J Neurosci* (2009) 29(13):4200–9. doi: 10.1523/JNEUROSCI.5032-08.2009
15. Campbell BM, Charych E, Lee AW, Moller T. Kynurenines in CNS Disease: Regulation by Inflammatory Cytokines. *Front Neurosci* (2014) 8:12. doi: 10.3389/fnins.2014.00012
16. Guillemin GJ, Cullen KM, Lim CK, Smythe GA, Garner B, Kapoor V, et al. Characterization of the Kynurenine Pathway in Human Neurons. *J Neurosci* (2007) 27(47):12884–92. doi: 10.1523/JNEUROSCI.4101-07.2007
17. Jones SP, Guillemin GJ, Brew BJ. The Kynurenine Pathway in Stem Cell Biology. *Int J Tryptophan Res* (2013) 6:57–66. doi: 10.4137/IJTR.S12626
18. Lob S, Konigsrainer A, Zieker D, Brucher BL, Rammensee HG, Opelz G, et al. IDO1 and IDO2 Are Expressed in Human Tumors: Levo- But Not Dextro-1-Methyl Tryptophan Inhibits Tryptophan Catabolism. *Cancer Immunol Immunother* (2009) 58(1):153–7. doi: 10.1007/s00262-008-0513-6
19. Maddison DC, Giorgini F. The Kynurenine Pathway and Neurodegenerative Disease. *Semin Cell Dev Biol* (2015) 40:134–41. doi: 10.1016/j.semcdb.2015.03.002
20. Zadori D, Klivenyi P, Szalardy L, Fulop F, Toldi J, Vecsei L. Mitochondrial Disturbances, Excitotoxicity, Neuroinflammation and Kynurenines: Novel Therapeutic Strategies for Neurodegenerative Disorders. *J Neurol Sci* (2012) 322(1-2):187–91. doi: 10.1016/j.jns.2012.06.004

21. Giil LM, Midttun O, Refsum H, Ulvik A, Advani R, Smith AD, et al. Kynurenine Pathway Metabolites in Alzheimer's Disease. *J Alzheimers Dis* (2017) 60(2):495–504. doi: 10.3233/JAD-170485
22. Hestad KA, Engedal K, Whist JE, Farup PG. The Relationships Among Tryptophan, Kynurenine, Indoleamine 2,3-Dioxygenase, Depression, and Neuropsychological Performance. *Front Psychol* (2017) 8:1561. doi: 10.3389/fpsyg.2017.01561
23. Colpo GD, Venna VR, McCullough LD, Teixeira AL. Systematic Review on the Involvement of the Kynurenine Pathway in Stroke: Pre-Clinical and Clinical Evidence. *Front Neurol* (2019) 10:778. doi: 10.3389/fneur.2019.00778
24. Fox E, Oliver T, Rowe M, Thomas S, Zakharia Y, Gilman PB, et al. Indoximod: An Immunometabolic Adjuvant That Empowers T Cell Activity in Cancer. *Front Oncol* (2018) 8:370. doi: 10.3389/fonc.2018.00370
25. Costa VV, Fagundes CT, Valadao DF, Avila TV, Cisalpino D, Rocha RF, et al. Subversion of Early Innate Antiviral Responses During Antibody-Dependent Enhancement of Dengue Virus Infection Induces Severe Disease in Immunocompetent Mice. *Med Microbiol Immunol* (2014) 203(4):231–50. doi: 10.1007/s00430-014-0334-5
26. Foureaux G, Franca JR, Nogueira JC, Fulgencio Gde O, Ribeiro TG, Castilho RO, et al. Ocular Inserts for Sustained Release of the Angiotensin-Converting Enzyme 2 Activator, Diminazene Aceturate, to Treat Glaucoma in Rats. *PloS One* (2015) 10(7):e0133149. doi: 10.1371/journal.pone.0133149
27. Costa VV, Del Sarto JL, Rocha RF, Silva FR, Doria JG, Olmo IG, et al. N-Methyl-D-Aspartate (NMDA) Receptor Blockade Prevents Neuronal Death Induced by Zika Virus Infection. *mBio* (2017) 8(2):e00350–17. doi: 10.1128/mBio.00350-17
28. Camargos VN, Foureaux G, Medeiros DC, da Silveira VT, Queiroz-Junior CM, Matosinhos ALB, et al. In-Depth Characterization of Congenital Zika Syndrome in Immunocompetent Mice: Antibody-Dependent Enhancement and an Antiviral Peptide Therapy. *EBioMedicine* (2019) 44:516–29. doi: 10.1016/j.ebiom.2019.05.014
29. Amaral DC, Rachid MA, Vilela MC, Campos RD, Ferreira GP, Rodrigues DH, et al. Intracerebral Infection With Dengue-3 Virus Induces Meningoencephalitis and Behavioral Changes That Precede Lethality in Mice. *J Neuroinflamm* (2011) 8:23. doi: 10.1186/1742-2094-8-23
30. Jackman JA, Costa VV, Park S, Real A, Park JH, Cardozo PL, et al. Therapeutic Treatment of Zika Virus Infection Using a Brain-Penetrating Antiviral Peptide. *Nat Mater* (2018) 17(11):971–7. doi: 10.1038/s41563-018-0194-2
31. Doria JG, de Souza JM, Silva FR, Olmo IG, Carvalho TG, Alves-Silva J, et al. The mGluR5 Positive Allosteric Modulator VU0409551 Improves Synaptic Plasticity and Memory of a Mouse Model of Huntington's Disease. *J Neurochem* (2018) 147(2):222–39. doi: 10.1111/jnc.14555
32. Fujigaki H, Yamamoto Y, Saito K. L-Tryptophan-Kynurenine Pathway Enzymes are Therapeutic Target for Neuropsychiatric Diseases: Focus on Cell Type Differences. *Neuropharmacology* (2017) 112(Pt B):264–74. doi: 10.1016/j.neuropharm.2016.01.011
33. Olmo IG, Carvalho TG, Costa VV, Alves-Silva J, Ferrari CZ, Izidoro-Toledo TC, et al. Zika Virus Promotes Neuronal Cell Death in a Non-Cell Autonomous Manner by Triggering the Release of Neurotoxic Factors. *Front Immunol* (2017) 8:1016. doi: 10.3389/fimmu.2017.01016
34. Rossi SL, Tesh RB, Azar SR, Muruato AE, Hanley KA, Auguste AJ, et al. Characterization of a Novel Murine Model to Study Zika Virus. *Am J Trop Med Hyg* (2016) 94(6):1362–9. doi: 10.4269/ajtmh.16-0111
35. Dowall SD, Graham VA, Rayner E, Atkinson B, Hall G, Watson RJ, et al. A Susceptible Mouse Model for Zika Virus Infection. *PloS Negl Trop Dis* (2016) 10(5):e0004658. doi: 10.1371/journal.pntd.0004658
36. Boldescu V, Behnam MAM, Vasilakis N, Klein CD. Broad-Spectrum Agents for Flaviviral Infections: Dengue, Zika and Beyond. *Nat Rev Drug Discov* (2017) 16(8):565–86. doi: 10.1038/nrd.2017.33
37. Sun X, Hua S, Chen HR, Ouyang Z, Einkauf K, Tse S, et al. Transcriptional Changes During Naturally Acquired Zika Virus Infection Render Dendritic Cells Highly Conducive to Viral Replication. *Cell Rep* (2017) 21(12):3471–82. doi: 10.1016/j.celrep.2017.11.087
38. Chang Y, Jiang Y, Li C, Wang Q, Zhang F, Qin CF, et al. Different Gene Networks are Disturbed by Zika Virus Infection in a Mouse Microcephaly Model. *Genomics Proteomics Bioinf* (2021). doi: 10.1016/j.gpb.2019.06.004
39. Yeung AW, Wu W, Freewan M, Stocker R, King NJ, Thomas SR. Flavivirus Infection Induces Indoleamine 2,3-Dioxygenase in Human Monocyte-Derived Macrophages *Via* Tumor Necrosis Factor and NF-kappaB. *J Leukoc Biol* (2012) 91(4):657–66. doi: 10.1189/jlb.1011532
40. Trettel F, Di Castro MA, Limatola C. Chemokines: Key Molecules That Orchestrate Communication Among Neurons, Microglia and Astrocytes to Preserve Brain Function. *Neuroscience* (2020) 439:230–40. doi: 10.1016/j.neuroscience.2019.07.035
41. Ito H, Ando T, Ogiso H, Arioka Y, Saito K, Seishima M. Inhibition of Indoleamine 2,3-Dioxygenase Activity Accelerates Skin Wound Healing. *Biomaterials* (2015) 53:221–8. doi: 10.1016/j.biomaterials.2015.02.098
42. Hoshi M, Osawa Y, Ito H, Ohtaki H, Ando T, Takamatsu M, et al. Blockade of Indoleamine 2,3-Dioxygenase Reduces Mortality From Peritonitis and Sepsis in Mice by Regulating Functions of CD11b+ Peritoneal Cells. *Infect Immun* (2014) 82(11):4487–95. doi: 10.1128/IAI.02113-14
43. Fox JM, Sage LK, Huang L, Barber J, Klonowski KD, Mellor AL, et al. Inhibition of Indoleamine 2,3-Dioxygenase Enhances the T-Cell Response to Influenza Virus Infection. *J Gen Virol* (2013) 94(Pt 7):1451–61. doi: 10.1099/vir.0.053124-0
44. Lin YT, Lin CF, Yeh TH. Influenza A Virus Infection Induces Indoleamine 2,3-Dioxygenase (IDO) Expression and Modulates Subsequent Inflammatory Mediators in Nasal Epithelial Cells. *Acta Otolaryngol* (2020) 140(2):149–56. doi: 10.1080/00016489.2019.1700304
45. Kim SB, Choi JY, Uyangaa E, Patil AM, Hossain FM, Hur J, et al. Blockage of Indoleamine 2,3-Dioxygenase Regulates Japanese Encephalitis *Via* Enhancement of Type I/II IFN Innate and Adaptive T-Cell Responses. *J Neuroinflamm* (2016) 13(1):79. doi: 10.1186/s12974-016-0551-5
46. Mazarei G, Budac DP, Lu G, Lee H, Moller T, Leavitt BR. The Absence of Indoleamine 2,3-Dioxygenase Expression Protects Against NMDA Receptor-Mediated Excitotoxicity in Mouse Brain. *Exp Neurol* (2013) 249:144–8. doi: 10.1016/j.expneurol.2013.08.007
47. Huang YS, Ogbechi J, Clanchy FI, Williams RO, Stone TW. IDO and Kynurenine Metabolites in Peripheral and CNS Disorders. *Front Immunol* (2020) 11:388. doi: 10.3389/fimmu.2020.00388
48. Del Sarto JL, Rocha RPF, Bassit L, Olmo IG, Valiate B, Queiroz-Junior CM, et al. 7-Deaza-7-Fluoro-2'-C-Methyladenosine Inhibits Zika Virus Infection and Viral-Induced Neuroinflammation. *Antiviral Res* (2020) 180:104855. doi: 10.1016/j.antiviral.2020.104855
49. Herrera-Rios D, Mughal SS, Teuber-Hanselmann S, Pierscianek D, Sucker A, Jansen P, et al. Macrophages/Microglia Represent the Major Source of Indolamine 2,3-Dioxygenase Expression in Melanoma Metastases of the Brain. *Front Immunol* (2020) 11:120. doi: 10.3389/fimmu.2020.00120
50. Zhang S, Zong Y, Ren Z, Hu J, Wu X, Xiao H, et al. Regulation of Indoleamine 2, 3-Dioxygenase in Hippocampal Microglia by NLRP3 Inflammasome in Lipopolysaccharide-Induced Depressive-Like Behaviors. *Eur J Neurosci* (2020) 52(11):4586–601. doi: 10.1111/ejn.15016

Conflict of Interest: RD has done consultancy work for Compass Pathways, UK.

The remaining authors declare that the research was conducted in the absence of any commercial or financial relationships that could be construed as a potential conflict of interest.

frontiers in Immunology

ORIGINAL RESEARCH
published: 26 July 2021
doi: 10.3389/fimmu.2021.720716

Immediate Pre-Partum SARS-CoV-2 Status and Immune Profiling of Breastmilk: A Case-Control Study

Laura Sánchez García[1†], Natalia Gómez-Torres[2†], Fernando Cabañas[3], Raquel González-Sánchez[4], Manuela López-Azorín[4], M. Teresa Moral-Pumarega[5], Diana Escuder-Vieco[5], Esther Cabañes-Alonso[6], Irma Castro[2], Claudio Alba[2], Juan Miguel Rodríguez Gómez[2] and Adelina Pellicer[1]*

[1] Neonatology Department, Biomedical Research Foundation-IDIPAZ, La Paz University Hospital, Madrid, Spain, [2] Nutrition and Food Science Department, Complutense University, Madrid, Spain, [3] Neonatology Department, Quironsalud Madrid University Hospital and Quironsalud San José Hospital, Biomedical Research Foundation-IDIPAZ, La Paz University Hospital, Madrid, Spain, [4] Neonatology Department, Quironsalud Madrid University Hospital and Quironsalud San José Hospital, Madrid, Spain, [5] Neonatology Department, 12 Octubre University Hospital, Madrid, Spain, [6] Neonatology Department and Regional Human Milk Bank, 12 Octubre University Hospital, Madrid, Spain

OPEN ACCESS

Edited by:
Abhay P. S. Rathore, Duke University, United States

Reviewed by:
Steffanie Sabbaj, University of Alabama at Birmingham, United States
Laxmi Yeruva, University of Arkansas for Medical Sciences, United States

***Correspondence:**
Laura Sánchez García
laurasg_alcobendas@yahoo.es

†These authors have contributed equally to this work and share first authorship

Specialty section:
This article was submitted to Viral Immunology, a section of the journal Frontiers in Immunology

Received: *04 June 2021*
Accepted: *07 July 2021*
Published: *26 July 2021*

Citation:
Sánchez García L, Gómez-Torres N, Cabañas F, González-Sánchez R, López-Azorín M, Moral-Pumarega MT, Escuder-Vieco D, Cabañes-Alonso E, Castro I, Alba C, Rodríguez Gómez JM and Pellicer A (2021) Immediate Pre-Partum SARS-CoV-2 Status and Immune Profiling of Breastmilk: A Case-Control Study. Front. Immunol. 12:720716. doi: 10.3389/fimmu.2021.720716

Objetive: To address the prevalence of SARS-CoV-2 and the evolutionary profile of immune compounds in breastmilk of positive mothers according to time and disease state.

Methods: Forty-five women with term pregnancies with confirmed non-severe SARS-CoV-2 infection (case group), and 96 SARS-CoV-2 negative women in identical conditions (control group) were approached, using consecutive sample. Weekly (1st to 5th week postpartum) reverse transcription polymerase chain reaction (RT-PCR) in nasopharyngeal swabs (cases) and breastmilk (cases and controls) were obtained. Concentration of cytokines, chemokines, and growth factors in breastmilk (cases and controls) were determined at 1st and 5th week post-partum.

Results: Thirty-seven (study group) and 45 (control group) women were enrolled. Symptomatic infection occurred in 56.8% of women in the study group (48% fever, 48% anosmia, 43% cough). SARS-CoV-2 RNA was not found in breastmilk samples. Concentrations of cytokines (IFN-γ, IL-1ra, IL-4, IL-6, IL-9, IL-13, and TNF-α) chemokines (eotaxin, IP-10, MIP-1α, and RANTES) and growth factors (FGF, GM-CSF, IL7, and PDGF-BB) were higher in breastmilk of the study compared with the control group at 1st week postpartum. Immune compounds concentrations decreased on time, particularly in the control group milk samples. Time of nasopharyngeal swab to become negative influenced the immune compound concentration pattern. Severity of disease (symptomatic or asymptomatic infection) did not affect the immunological profile in breast milk.

Conclusions: This study confirms no viral RNA and a distinct immunological profile in breastmilk according to mother's SARS-CoV-2 status. Additional studies should address

whether these findings indicate efficient reaction against SARS-CoV-2 infection, which might be suitable to protect the recipient child.

Keywords: COVID-19, vertical infectious disease transmission, breastfeeding, immunologic factors, immune system

INTRODUCTION

During the first months of COVID-19 pandemic, some concerns arose about the safety of breastfeeding because of the potential risk of viral transmission. However, most of the human milk samples assayed for SARS-CoV-2 RNA Reverse Transcription Polymerase Chain Reaction (RT-PCR) have yielded negative results (1–5), whereas no evidence of SARS-CoV-2 transmission through human milk has been provided yet (6, 7).

With regard to the efficacy of breastmilk to provide protecting anti-SARS-CoV-2 antibodies (3, 8, 9), most studies carried so far have addressed their presence. However, information regarding the impact of COVID-19 on other immune compounds, such as cytokines, chemokines, and growth factors, is lacking. These immune factors act in the prevention of infantile infection and can modulate the immunological development of the infant (10–15). In fact, their abundance in human milk is often inversely related to their scarcity in the infant's gut, characterized by a deficit of mucosal-related anti-inflammatory mechanisms, a limited production of secretory IgA, and a poor innate effector cell function (15).

Activation of inflammatory signaling pathway is a critical mediator in the pathophysiology of COVID-19 (16–18), and maternal environmental factors, including viral infections and previous antigenic exposures, are known to affect immunological composition of human milk (19–23). Therefore, a deeper insight on the impact of SARS-CoV-2 infection on the composition of breastmilk is needed.

This research aims to address questions related on the safety and the efficacy of breastmilk feeding of neonates born to mothers with non-severe SARS-CoV-2 infection, through the systematic assessment of: (a) the prevalence of viral RNA in breastmilk according to SARS-CoV-2 status, (b) the impact of SARS-CoV-2 infection on the milk profile of cytokines, chemokines, and growth factors, and (c) the evolution of their concentrations during the first five weeks of lactation.

METHODS

This multicenter, prospective case-control study was conducted in Madrid, between April and July 2020. Since March 2020, maternity hospitals tested pregnant woman for SARS-CoV-2 infection by routine nasopharyngeal RT-PCR as screening prior delivery. Given the high incidence of COVID-19 disease at the start of the study, the Spanish Ministry of Health considered a patient had confirmed SARS-CoV-2 infection whenever the RT-PCR was positive, regardless of clinical features. Four level 3 institutions of the health system of the Madrid region (Spain) (La Paz University Hospital, 12 de Octubre University Hospital, Quironsalud Madrid University Hospital and Quironsalud San José Hospital) participated in this study. The protocol was approved by the reference Clinical Research Ethics Committee. Informed consent was obtained from mothers before enrolment. Every mother-infant's information was treated anonymously.

Eligibility Criteria

Women with term pregnancies with confirmed SARS-CoV-2 infection at the time of delivery, who were in good clinical condition and had a decision to breastfeed were considered eligible for the study (study group). For each positive case, two consecutive women with term pregnancies, in identical conditions, who were SARS-CoV-2 negative were approached (control group). Prospective data recording of participant mothers (age, underlying pathology, type of delivery, time of positive SARS-CoV-2 RT-PCR and related clinical features/treatment) and their infants (gestational age, birth weight, neonatal diagnoses) were obtained.

Study Procedures

During the first month after delivery, breastmilk (case and control groups) and nasopharyngeal swabs (case group) were collected by the participant mothers, who were instructed on accomplishment and storage of samples. Breastmilk samples were collected every 72 h from delivery after careful hand, breast, and nipple hygiene, with the mouth and nose covered by a mask. Milk was collected either by pump or manual extraction, and kept in individual sterile container for each aliquot. After milk extraction, breast pump was cleaned with soap and water, and disinfected by alcohol or immersion in boiling water. Case group mothers self-performed weekly nasopharyngeal smear using swab kits and the corresponding RT-PCR transport medium. Control group mothers underwent a serological study prior to hospital discharge. Blood samples were centrifuged and stored for analysis. Presence of IgG and IgM antibodies against SARS-CoV-2 was assessed using the IgG+IgM Combo Detection Kit (SD Biosensor, Korea).

All biological samples were identified by a study code and date of extraction, immediately frozen at −20°C, periodically collected at home by a specialized transport system and shipped on dry ice (−78.5°C) to the Nutrition and Food Science Department, Complutense University of Madrid where the samples were analyzed. To eliminate or minimize potential lab biases, all the samples were submitted to a single freeze–thaw cycle and were analyzed by the same researchers. After hospital discharge, follow up of the infants was done by serial phone calls during the first month of age.

RT-PCR Assays

RNA extraction from the nasopharyngeal and milk samples (200 μl) was carried out using the KINGFISHER FLEX 96

extraction robot (ThermoFisher), the MagMax_Core_Flex extraction program and the MagMAX Viral/Pathogen II Nucleic Acid Isolation kit (Applied Biosistems, ThermoFisher). For the detection of SARS-CoV-2, the TaqPath COVID-19 CE-IVD RT-PCR kit (Applied Biosystems, Thermo Fisher Scientific) was used in a 384-well format with the QuantStudio 7 Flex System equipment (Applied Biosystems). All procedures were performed following the manufacturer's instructions.

Immunoassays in Breastmilk Samples

Concentration and frequency of detection of 30 soluble immune factors in the milk samples were determined by magnetic bead-based multiplex immunoassays using a Bioplex 200 instrument (Bio-Rad, Hercules, CA, USA) and the pro-human cytokine 27-plex assay (Bio-Rad). The immune factors included in this study were interleukin (IL) 1β, IL1ra, IL2, IL4, IL5, IL6, IL7, IL8, IL9, IL10, IL12(p70), IL13, IL15, and IL17, interferon-gamma (IFN-γ), granulocyte colony stimulating factor (G-CSF), granulocyte-macrophage colony stimulating factor (GM-CSF), monocyte chemoattractant protein-1 (MCP-1), macrophage inflammatory protein 1α and 1β (MIP-1α, MIP-1β), eotaxin, basic fibroblast growth factor (Basic FGF), tumor necrosis factor-alpha (TNF-α), inferon γ-induced protein (IP-10), platelet-derived growth factor-BB (PDGF-BB), regulated on activation normal T-cells expressed and secreted (RANTES), and vascular endothelial growth factor (VEGF). In addition, levels of transforming growth factor-beta 2 (TGF-β2), epidermal growth factor (EGF), and growth-related oncogene-α (Groα) were measured, respectively, by the human TGF-β2, human EGF, and human GRO alpha (CXCL1) ELISA kits (RayBiotech, Norcross, GA, USA).

To avoid interferences, the fatty layer and the somatic cells were removed from the milk samples. Briefly, sample aliquots (1 ml) were centrifuged at 11,000g for 15 min at 4°C, the intermediate aqueous phase was collected and stored at −20°C until analysis. Every assay was run in duplicate according to the manufacturer's instructions using the same reagents' batches and equipment; standard curves were performed for each analyte in every assay. All the concentrations were expressed as nanograms per liter (ng/L), except IP-10, VEGF, TGFβ2, EGF, and Groα, which were expressed as micrograms per liter (μg/L).

Statistical Analysis

Demographic data with normal distribution were presented as the mean and standard deviation (SD). Regarding immune factors, normality of data distribution was examined through visual inspection of histograms and Shapiro-Wilks tests, both evidencing a non-normal distribution for all tested parameters ($\rho < 0.05$). Accordingly, nonparametric statistical analyses were performed, and data were expressed as the median and interquartile range (IQR). Immune factor concentrations were logarithmically transformed prior to statistical analysis. Differences in the relative abundance of the immune compounds were compared by Wilcoxon rank test and Mann-Whitney *U* test. To compare multiple comparisons, Bonferroni-adjusted *post hoc* significance levels were performed. Fisher's exact probability test was performed to compare the frequency of detection of different immunological compounds. Significance was declared at $\rho < 0.05$ for all analyses. All analyses were performed with the R software version 4.0.3 (R-project, http://www.r-project.org). For the purpose of this report, immune factor concentration on one of the milk samples obtained during week 1 (day 3 to day 6) and week 5 (beyond day 28) postpartum were used for comparisons.

RESULTS

During the study period a total of 141 term-pregnant women who fulfilled eligibility criteria were approached. Of them, 37 study group and 45 control group women were included in the final analyses. Details on participants' chart flow and reasons for exclusion are described in **Figure 1**.

No differences in maternal age [33.9 (5.4) *vs* 34.5 (5.1) years, p=0.612], previous maternal health problems prevalence (19% *vs* 13%, p= 0.493, only 1 case of obesity in study group), rates of vaginal delivery (73% *vs* 89%, p= 0.064), gestational age at birth [39.1 (1.8) *vs* 39.1 (1.6) weeks, p= 0.852], or birth weight [3187 (543) *vs* 3240 (469) grams, p= 0.639] between study and control group were found.

By hospital protocol, nasopharyngeal PCR was performed at 24 h and at 36 to 48 h from birth on infants of positive SARS-COV-2 mothers, resulting negative in all cases. None of infants of mothers in study and control group presented clinical signs of SARS-COV-2 infection in the first month of life.

Among the study group, 21 (56.8%) women presented mild SARS-CoV-2 infection related symptoms, consisting of fever (48%), anosmia (48%), cough (43%), ageusia (14%), odynophagia (10%), myalgia (10%), diarrhea (10%), or headache (5%). Nineteen (51.3%) received medication (anticoagulation, antibiotics, hydroxychloroquine, oxygen therapy) around labor. Serological analyses of control women were negative.

RT-PCR Assays

Nasopharyngeal RT-PCR tests were serially conducted in 30 of the 37 SARS-CoV-2–positive women [four samples (1 per week), n=25; three samples (weeks 1–3), n=5; no samples, n=7]. Nasopharyngeal RT-PCR tests attained negative results at week 2 (n=7, 23.3%), at week 3 (n=9, 30%), and at week 4 (n=9, 30%) postpartum and remained positive at the last sample that was tested in 5 (16.6%) participants (3 at week 3, and 2 at week 4).

All human milk samples analyzed were negative for SARS-CoV-2 RNA as assessed by RT-PCR.

Immunological Assays in Breastmilk Samples

All of the 30 immunological factors that were searched for in breastmilk could be detected in, at least, some of the milk samples. IFN-γ, IL-8, IL-12(p70), IL-17, IP-10, MIP-1β, TNF-α, VEGF, TGFβ2, EGF, and GROα displayed the highest frequencies of detection (100% of the samples), closely followed by eotaxin, G-CSF, IL-1β, IL-1ra, IL-2, IL-4, IL-6, IL-7, IL-9, and RANTES, which were detected in >95% of the samples. In contrast, IL-5 and IL-15 were the least frequently detected compounds (≤70% of the samples).

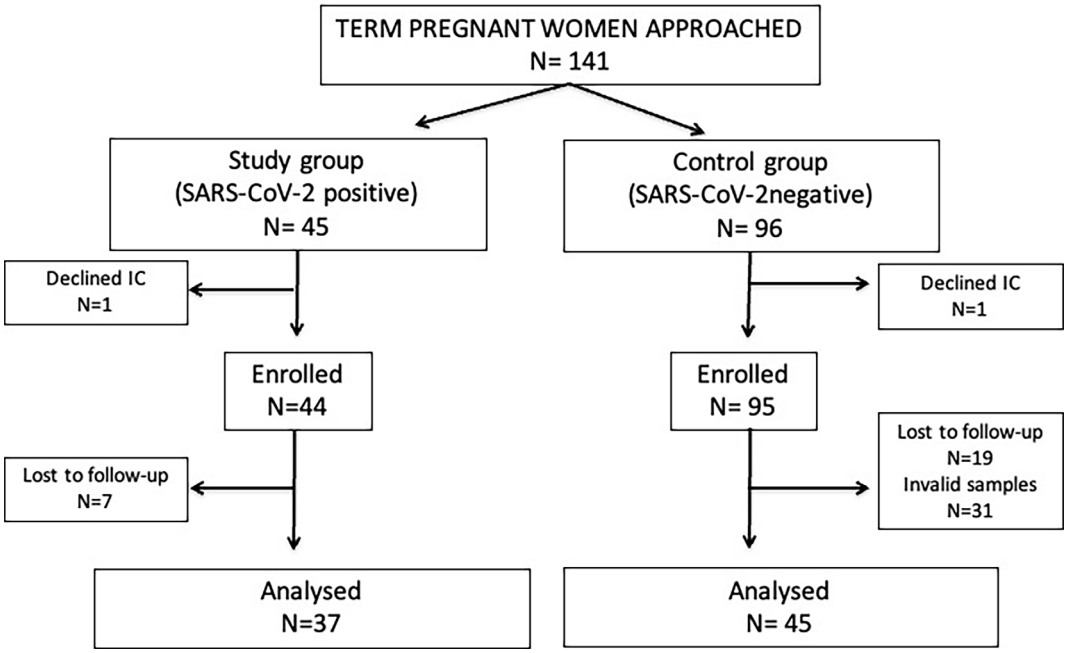

FIGURE 1 | Flow diagram of participants. IC, informed consent; Invalid samples, non-availability of all samples to be compared, inadequate sample identification or conservation.

No differences were observed between samples collected in week 1 or week 5 postpartum, with the exception of GM-CSF, which frequency of detection in week 1 (79%) was lower than that in week 5 (90%) (p=0.047).

Breastmilk Cytokine Pattern

Table 1 displays concentration of cytokines in breastmilk samples. IFN-γ, IL-1ra, IL-4, IL-6, IL-9, IL-13, and TNF-α showed higher concentrations in study than in the control group at both sampling times. In addition, IL-1β and IL-2 at week 5 postpartum were higher in breastmilk samples of the study group.

Evolution of cytokine concentration on breastmilk samples over time showed no differences in the study group women, with the exception of IFN-γ, IL1ra, IL4, IL9 that significantly decreased between week 1 and week 5 postpartum. In the control group women, all the tested cytokines decreased over time, with the exception of IL10, IL12, and IL13 that remained stable. Time of nasopharyngeal swab to become negative influenced the cytokines pattern in breastmilk (**Figure 2**).

Breastmilk Chemokine Pattern

Table 2 displays concentration of chemokines in breastmilk samples. Eotaxin, IP-10, MIP-1α, and RANTES showed higher breastmilk concentration among the study group than in the control group at week 1 postpartum; at week 5, the concentration of chemokines, except for GRO-α, was significantly higher in breastmilk samples of the study group than in the control group.

Concentration of chemokines decreased over time, it being statistically significant for most of them in the study group and for all tested chemokines in the control group. Time of nasopharyngeal swab to become negative influenced the chemokines pattern in breastmilk (**Figure 3**).

Breastmilk Growth Factor Pattern

Table 3 displays concentration of growth factors in breastmilk samples. Overall, concentrations of growth factors were higher in the breastmilk samples of the study group compared with the control group women. The differences were statistically significant for basic FGF, GM-CSF, IL7, and PDGF-BB at week 1 postpartum, and for all of them, with the exception of IL-5 and EGF, in the samples collected at week 5.

Most growth factor concentrations remained stable over time in study group; in contrast, concentrations of basic FGF, G-CSF, VEGF, TGF-β2, and EGF significantly decreased from week 1 to week 5 postpartum in the control group breastmilk samples. Time of nasopharyngeal swab to become negative influenced the growth factor pattern in breastmilk (**Figure 4**).

Breastmilk Immunological Pattern According to Disease State

Concentration of immune factors in breastmilk samples in the SARS-CoV-2–positive women depending on the presence or not of COVID-19-related symptoms did not show relevant differences, neither in the first sampling time (lower IL-12 in symptomatic than in asymptomatic women, $p<0.01$) nor in the second (higher IL-15 ($p<0.01$) and lower GM-CSF ($p<0.03$) in symptomatic women).

TABLE 1 | Concentration (ng/l) of cytokines in milk samples of study and control group women over time.

	Week 1 postpartum			Week 5 postpartum				
	STUDY GROUP (n = 36)	CONTROL GROUP (n = 45)		STUDY GROUP (n = 37)	CONTROL GROUP (n = 45)			
Immune Factors	**Median (IQR)**	**Median (IQR)**	ρ^a	**Median (IQR)**	**Median (IQR)**	$^b\rho$	$^c\rho$	$^d\rho$
IFN- γ	160.5 (78.8-301.8)	50.4 (23.7-117.7)	0.003	135.8 (18.3-151.6)	11.8 (4.3-23)	<0.001	<0.001	<0.001
IL-1β	3.2 (1.5-5.0)	2.1 (1.4-3.7)	0.273	2.7 (1.8-3.3)	1.0 (0.7-1.4)	<0.001	0.117	<0.001
IL-1ra	5966.4 (1642.5-62227.1)	1444.3 (676.2-3939.5)	0.023	5896.3 (662.9-5979.4)	443.6 (271.9-852.4)	<0.001	0.004	<0.001
IL-2	5.8 (3.8-7.8)	4.2 (3.0-6.1)	0.164	4.7 (2.4-6.7)	3.1 (2.3-3.8)	0.014	0.300	0.002
IL-4	3.9 (1.3-3.7)	1.0 (0.6-2.1)	0.001	2.6 (1.6-2.7)	0.5 (0.3-0.7)	<0.001	0.007	<0.001
IL-6	208.5 (28.5-223.7)	17.7 (7.5-46.2)	<0.001	207.1 (21.1-212.1)	3.6 (2.3-10.9)	<0.001	0.075	<0.001
IL-9	29.8 (14.8-40.8)	13.1 (8.6-20.0)	0.005	27.3 (11.1-29.7)	5.4 (3.9-8.4)	<0.001	0.041	< 0.001
IL-10	3.3 (1.8-4.8)	3.7 (2.0-4.7)	0.795	2.9 (1.9-4.2)	3.3 (2.7-4.3)	0.363	0.279	0.565
IL-12 (p70)	3.9 (3.0-4.5)	3.8 (3.4-4.3)	0.890	3.4 (2.8-4.1)	3.8 (3.4-4.1)	0.052	0.505	0.712
IL-13	1.4 (0.9-1.9)	0.9 (0.7-1.3)	0.007	1.4 (0.8-1.9)	0.9 (0.7-1.3)	0.043	0.260	0.756
IL-15	94.3 (59.9-164.7)	99.2 (82.6-137.2)	0.921	90.7 (67.5-149.9)	90.7 (49.1-128.3)	0.560	0.734	0.039
IL-17	13.2 (5.4-15.9)	11.3 (10.4-16.7)	0.436	11.8 (5.0-15.3)	9.7 (8.1-12.5)	0.567	0.915	0.007
TNF-α	106.3 (67.9-130.2)	35.5 (25.9-75.8)	0.001	92.2 (73.0-112.4)	17.7 (11.5-50.8)	<0.001	0.314	<0.001

[a]*ρ: Mann-Whitney U test was used to evaluate differences in concentration of cytokines between milk samples from STUDY GROUP and CONTROL GROUP collected in week 1 postpartum.*
[b]*ρ: Mann-Whitney U was used to evaluate differences in concentration of cytokines between milk samples STUDY GROUP and CONTROL GROUP collected in week 5 postpartum.*
[c]*ρ: Wilcoxon signed rank test was used to evaluate differences in the concentration of cytokines of the milk samples of STUDY GROUP between week 1 and week 5 postpartum.*
[d]*ρ: Wilcoxon signed rank test was used to evaluate differences in the concentration of cytokines of the milk samples of CONTROL GROUP between week 1 and week 5 postpartum.*

DISCUSSION

This study confirms that in the asymptomatic or non-severe infected pregnant woman, breastmilk samples do not carry SARS-CoV-2 RNA. These results coincide with those found in previous studies (1–3, 7, 24–26), although a very low rate of positive milk samples (4) or isolated case reports (27–31) have also been published. This information is crucial as neonatal infection by SARS-CoV-2 is uncommon and usually asymptomatic (32–34). The lack of viral RNA in breastmilk supports its safety, and it is in accord with recent epidemiological data, as several small observational studies reported on the absence of infection in infants fed by breastmilk of SARS-CoV-2 positive woman (35, 36) or inadvertently fed with SARS-CoV-2 RNA-positive milk (29).

SARS-CoV-2 RNA seems to be widespread on surfaces from COVID-19 patient rooms (37) and, also, on the breast skin of lactating mothers (3). This suggests that milk samples may become contaminated with viral RNA when a mother and/or

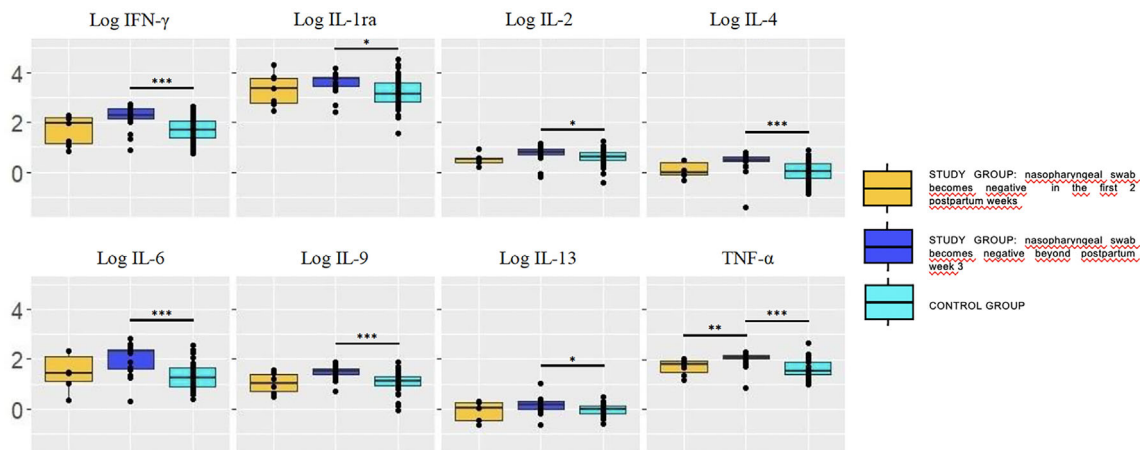

FIGURE 2 | Concentration (log) of cytokines in breastmilk of study group women according to the moment in which the nasopharyngeal test becomes negative (pooling samples obtained at weeks 1 and 5). Cytokine concentrations were significantly higher in breastmilk samples of mothers whose RT-PCR remained positive at postpartum week 3 (dark blue box) compared with the control group. Trends also pointed toward higher concentrations in the former compared with those who became negative sooner, within the first 2 postpartum weeks (yellow box). The values are expressed as $\log_{10}$ of the concentrations (ng/L). Statistical differences on pairwise *post hoc* comparisons between the study and control groups are indicated with an asterisk (*p < 0.05; **p ≤ 0.01; ***p ≤ 0.001, Wilcoxon rank test, Bonferroni *post hoc* test).

TABLE 2 | Concentration* of chemokines in milk samples of study group and control group women over time.

	Week 1 postpartum			Week 5 postpartum				
	STUDY GROUP (n = 36)	CONTROL GROUP (n = 45)		STUDY GROUP (n = 37)	CONTROL GROUP (n = 45)			
Immune Factors	**Median (IQR)**	**Median (IQR)**	**[a]ρ**	**Median (IQR)**	**Median (IQR)**	**[b]ρ**	**[c]ρ**	**[d]ρ**
Eotaxin	24.2 (14.6-32.9)	14.5 (4.3-23.3)	0.020	16.9 (10.4-21)	3.1 (1.8-5.3)	<0.001	<0.001	<0.001
IL-8	1919.0 (299.7-2606.6)	584.2 (234.7-1916.7)	0.137	1921.4 (213.4-2021.5)	47.7 (20.5-167.7)	<0.001	0.001	<0.001
IP-10	18.2 (7.2-53)	10.5 (4.1-18.5)	0.025	21.9 (10.0-58.3)	2.8 (1.2-11.8)	<0.001	0.750	0.002
MCP-1	2078.4 (650.8-2738.4)	892.7 (544.1-2601.7)	0.221	2010.2 (730.6-2288.2)	123.1 (53.4-732.4)	<0.001	0.027	<0.001
MIP-1α	43.9 (10.3-47.1)	13.4 (5.3-41.9)	0.040	43.4 (26.1-44.0)	2.5 (1.0-6.7)	<0.001	0.041	<0.001
MIP-1β	212.7 (81.2-344.9)	112.9 (38.3-293.6)	0.270	191.6 (88.2-204.3)	10.5 (7.3-44.3)	<0.001	0.054	<0.001
RANTES	84.5 (48.7-115.0)	44.3 (26.2-84.1)	0.032	81.0 (61.1-142.1)	18.5 (14-39.8)	<0.001	0.427	0.011
GRO-α	7.4 (4.8-8.9)	7.9 (6.6-8.5)	0.314	7.3 (4.7-8.7)	7.3 (6.0-8.1)	0.856	<0.001	<0.001

Concentrations are expressed as ng/L, with the exception of IP-10 and GRO-α (expressed as μg/L).

[a]ρ: Mann-Whitney U test was used to evaluate differences in concentration of chemokines between milk samples of STUDY GROUP and CONTROL GROUP collected in week 1 postpartum.

[b]ρ: Mann-Whitney U test was used to evaluate differences in concentration of chemokines between milk samples of STUDY GROUP and CONTROL GROUP collected in week 5 postpartum.

[c]ρ: Wilcoxon signed rank test was used to evaluate differences in the concentration of chemokines of milk the samples of STUDY GROUP between week 1 and week 5 postpartum.

[d]ρ: Wilcoxon signed rank test was used to evaluate differences in the concentration of chemokines of the milk samples of CONTROL GROUP between week 1 and week 5 postpartum.

her neonate are positive; therefore, caution should be extreme to avoid contaminations when performing SARS-CoV-2 assessments of human milk. In addition, it must be highlighted that RT-PCR assays can only detect viral RNA but not viable infectious viruses. A detailed virological assessment of some COVID-19 cases showed that, although high concentrations of viral RNA were found both in pharyngeal and fecal samples, the virus itself could be readily isolated from throat or lung samples but not from the fecal ones (38). A study involving 64 milk samples from 18 women who had confirmed SARS-CoV-2 supported this affirmation. Only one sample had a detectable level of viral RNA but no replication-competent virus was detectable in any sample, including the sample that was positive for SARS-CoV-2 RNA (2). To date, no study has described presence of infectious SARS-CoV-2 in colostrum and milk.

The second objective of this study was the profiling of cytokines, chemokines, and growth factors in the milk samples. Overall, the concentrations of most of the immune factors analyzed were higher in the samples of positive women than in those of negative ones. This activation of innate and adaptative immune response constitutes the first line of defense against viral infections (16–18, 39).

A study involving the assessment of immunological compounds in milk produced by healthy women, found a higher co-occurrence

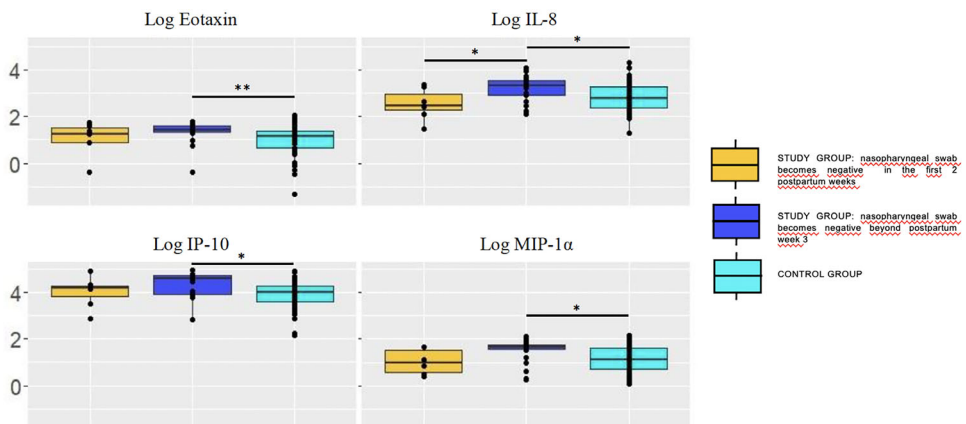

FIGURE 3 | Concentration (log) of chemokines in breastmilk of study group women according to the moment in which the nasopharyngeal test becomes negative (pooling samples obtained at weeks 1 and 5). Chemokyne concentrations were significantly higher in breastmilk samples of mothers whose RT-PCR remained positive at postpartum week 3 (dark blue box) compared with the control group. Trends also pointed toward higher concentrations in the former compared with those who became negative sooner, within the first 2 postpartum weeks (yellow box). The values are expressed as $\log_{10}$ of the concentrations (ng/L), with the exception of IP-10 (μg/L). Statistical differences on pairwise *post hoc* comparisons between the study and control groups are indicated with an asterisk (*p < 0.05; **p ≤ 0.01; ***p ≤ 0.001, Wilcoxon rank test, Bonferroni *post hoc* test).

TABLE 3 | Concentration* of growth factors in milk samples from study group and control group women over time.

	Week 1 postpartum			Week 5 postpartum				
	STUDY GROUP (n = 36)	CONTROL GROUP (n = 45)		STUDY GROUP (n = 37)	CONTROL GROUP (n = 45)			
Immune Factors	**Median (IQR)**	**Median (IQR)**	[a]ρ	**Median (IQR)**	**Median (IQR)**	[b]ρ	[c]ρ	[d]ρ
Basic FGF	64.0 (28.6-73.3)	22.5 (16.4-46.3)	<0.001	59.4 (55.1-64.3)	12.8 (9.6-21.7)	<0.001	0.394	<0.001
G-CSF	178.6 (116.1-287.1)	104.3 (68.1-224.6)	0.227	147.8 (121.9-203.5)	32.4 (12-110.9)	<0.001	0.245	<0.001
GM-CSF	13.5 (12.9-14.6)	1.4 (0.8-2.7)	<0.001	13.6 (7.8-16.1)	2 (0.8-11)	0.006	0.086	0.016
IL-5	17.4 (7.9-24.3)	23.7 (10.9-36.9)	0.321	21.1 (14.8-35.7)	20.8 (9.8-29.5)	0.540	0.275	0.612
IL-7	114.7 (33.3-147.7)	27.5 (19.3-33.4)	<0.001	113.9 (53.2-135.0)	28.2 (21.1-52.3)	<0.001	0.225	0.052
PDGF-BB	54.8 (28.7-70.7)	23.6 (14.9-31.5)	<0.001	40.9 (35.7-67.5)	23.6 (13.3-34.8)	<0.001	0.458	0.786
VEGF	11.5 (4.5-16.4)	7.6 (3.8-11.2)	0.090	10.4 (3.7-11.5)	2.7 (1.8-3.4)	<0.001	0.007	<0.001
TGF-β2	2.5 (1.7-3.0)	2.1 (1.7-2.5)	0.164	2.7 (1.7-3.0)	1.9 (1.7-2.1)	0.003	0.014	<0.001
EGF	5.6 (4.5-6.6)	5.4 (4.9-5.9)	0.768	5.4 (4.3-6.0)	5 (4.3-5.5)	0.120	<0.001	<0.001

Concentrations are expressed as ng/L, with the exception of VEGF, TFG-β2 and EFG (expressed as μg/L).

[a]*ρ: Mann-Whitney U test was used to evaluate differences in concentration of growth factors between milk samples of STUDY GROUP and CONTROL GROUP collected in week 1 postpartum.*

[b]*ρ: Mann-Whitney U test was used to evaluate differences in concentration of growth factors between t milk samples of STUDY GROUP and CONTROL GROUP collected in week 5 postpartum.*

[c]*ρ: Wilcoxon signed rank test was used to evaluate differences in the concentration of growth factors of the milk samples of STUDY GROUP between week 1 and week 5 postpartum.*

[d]*ρ: Wilcoxon signed rank test was used to evaluate differences in the concentration of growth factors of the milk samples of CONTROL GROUP between week 1 and week 5postpartum.*

of immune factors and higher TNFα to IL10 ratios in milk samples from healthy women with a higher level of exposure to microorganisms (40). In our study, the same was observed in the milk of SARS-CoV-2-positive women, a finding which is consistent with a wider plasticity of the immune responses.

Concentrations of most of the immune factors analyzed remained stable over time in SARS-CoV-2-positive women milk samples. In contrast, most of these compounds significantly decreased from the first to the fifth week postpartum in negative women. Previous studies have reported notably higher concentrations of several cytokines, chemokines, growth factors, and immunoglobulins in colostrum than in mature milk (13, 41–44). Although this could simply be a physiological response from the mother to infection and not enough proof for it to be protective, our findings could also suggest that, in the presence of a viral infection, the immunological profile of human milk may be adapted to provide additional infant's protection against the maternal infection. Evidences for an immunological cross-talk between mothers and their breast-fed infants during infections, including severe viral respiratory infections, have already been provided (45, 46). In our study, positive women were either asymptomatic or suffered mild disease, therefore the evolutive profile of immunological compounds in breastmilk was related to the time when RT-PCR swabs became negative, as a marker of disease state. Mothers who later became negative for nasopharyngeal RT-PCR presented persistently higher levels of

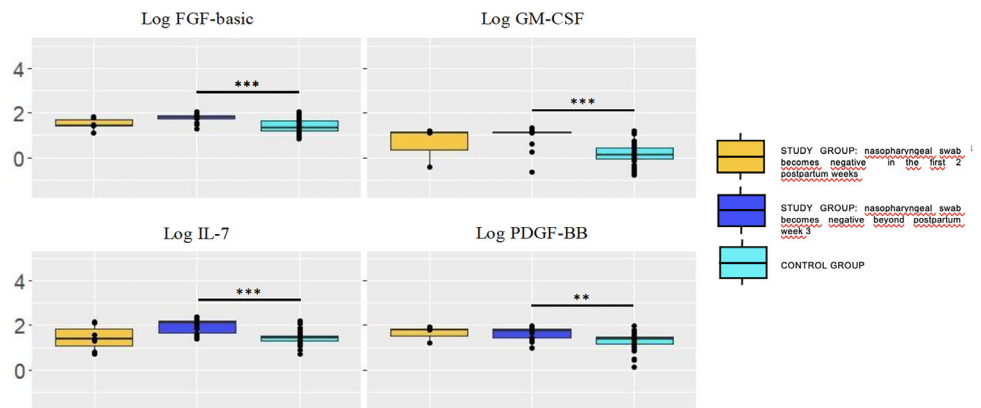

FIGURE 4 | Concentration (log) of growth factors in breastmilk of study group women according to the moment in which the nasopharyngeal test becomes negative (pooling samples obtained at week 1 and 5). Growth factors concentrations were significantly higher in breastmilk samples of mothers whose RT-PCR remained positive at postpartum week 3 (dark blue box) compared with the control group. Trends also pointed toward higher concentrations in the former compared with those who became negative sooner, within the first two postpartum weeks (yellow box). The values are expressed as $\log_{10}$ of the concentrations (ng/L). Statistical differences on pairwise *post hoc* comparisons between the study and control groups are indicated with an asterisk (*p < 0.05; **p ≤ 0.01; ***p ≤ 0.001, Wilcoxon rank test, Bonferroni *post hoc* test).

several immunological factors. This immunological profile has been described in COVID19 pathophysiology related to the severity of the infection (16–18, 39). Of note, all the newborns in the study and control group remained free of clinical signs of SARS-COV-2 infection in the first month of life.

In this study, VEGF, TGF-β2 and EGF were the most abundant growth factors found in the milk samples, independently of the SARS-CoV-2 status or the sampling time, the concentration being 50- to 100-fold higher, coinciding with those detected in healthy women as reported in a previous study (40). These three immune compounds play critical roles in infants' health and development, including protection against infectious diseases, modulation of inflammatory processes, and establishment of food tolerance (12, 40, 47–49).

This study has several limitations. There is a lack of comparison between serum and milk immune factors profile, and the antibody levels were not assayed. The distinct profile in immune compounds in breast milk of SARS-CoV-2 positive women could not be translated into effective gastrointestinal absorption and in a functional form to impact the infant immune system. Follow-up losses in the control group could eventually modify the results. Finally, the analysis of the immune compounds was limited to two milk samples, with an interval of approximately 1 month. We took this decision after confirmation of the lack of viral RNA in any of the milk samples over time. Therefore, we considered that the observation period was adequate to see eventual evolution of the immune compounds related to mother's infection status. On the other hand, a strength of this work is the huge variety of compounds that have been analyzed, and the systematic approach to both SARS-CoV-2 documented infection and control women.

In summary, the results of this study provide additional evidence to the safety of breastfeeding in SARS-CoV-2 infected women, as RNA was not detected in any of the milk samples tested throughout the observation period. Our results also suggest that the immune system of the infected women reacted efficiently against SARS-CoV-2 as a distinct pattern of cytokines, chemokines, and growth factors was observed in the milk samples of infected women, that persisted over time. However, this cannot be directly extrapolated to a beneficial effect in the infant. More studies are required to elucidate if this pattern only reflects the inflammatory status of the mother or if it may be linked to the development of an integration of the mother-infant immune systems, being especially suitable to protect recipient child.

DATA AVAILABILITY STATEMENT

The raw data supporting the conclusions of this article will be made available by the authors, without undue reservation.

ETHICS STATEMENT

The studies involving human participants were reviewed and approved by Ethical committee of clinical research of La Paz University Hospital. Written informed consent to participate in this study was provided by the participants' legal guardian/next of kin.

AUTHOR CONTRIBUTIONS

LS conceptualized and designed the study, participated in patient's enrolment, data gathering and analysis, drafted the initial manuscript, and reviewed and approved the final version. AP and JR conceptualized and designed the study, and participated in data analyses, drafted the initial manuscript, and reviewed and approved the final version. FC conceptualized and designed the study, and reviewed and approved the final version of the manuscript. RG-S, ML-A, MM-P, DE-V and EC-A participated in patient's enrolment and data gathering, and reviewed and approved the final version of the manuscript. NG-T and IC participated in sampling management and analysis, drafted the initial manuscript, and reviewed and approved the final version. CA participated in statistical and data analyses. All authors contributed to the article and approved the submitted version.

FUNDING

This work was supported by Instituto de Salud San Carlos III [COV20/01046]; Ministerio de Ciencia, Innovación y Universidades (Spain) by Irma Castro predoctoral contract [BES-2017-080713] and RETICS "Maternal and Child Health and Development Network" (SAMID Network), funded by the PN I+D+i 2013-2016 (Spain), ISCIII-Sub-Directorate General for Research Assessment and Promotion and the European Regional Development Fund (ERDF) [RD16/0022].

REFERENCES

1. Marín Gabriel MA, Cuadrado I, Álvarez Fernández B, González Carrasco E, Alonso Díaz C, Neo-COVID-19 Research Group, et al. Multicenter Spanish Study Found No Incidences of Viral Transmission in Infants Born to Mothers With COVID-19. *Acta Paediatr* (2020) 109(11):2302–8. doi: 10.1111/apa.15474
2. Chambers CD, Krogstad P, Bertrand K, Contreras D, Tobin NH, Bode L, et al. Evaluation of SARS-CoV-2 in Breastmilk From 18 Infected Women. *JAMA* (2020) 324(13):1347–8. doi: 10.1001/jama.2020.15580
3. Pace RM, Williams JE, Järvinen KM, Belfort MB, Dw Pace C, Lackey KA, et al. COVID-19 and Human Milk: SARS-CoV-2, Antibodies, and Neutralizing Capacity. (2020). doi: 10.1101/2020.09.16.20196071. medRxiv.
4. Bertino E, Moro GE, De Renzi G, Viberti G, Cavallo RCollaborative Research Group on SARS-CoV-2 in Human Milk, et al. Detection of SARS-CoV-2 in Milk From COVID-19 Positive Mothers and Follow-Up of Their Infants. *Front Pediatr* (2020) 27:8:597699. doi: 10.3389/fped.2020.597699
5. Cheema R, Partridge E, Kair LR, Kuhn-Riordon K, Silva AI, Bettinelli ME, et al. Protecting Breastfeeding During the COVID-19 Pandemic. *Am J Perinatol* (2020). doi: 10.1055/s-0040-1714277
6. Centeno-Tablante E, Medina-Rivera M, Finkelstein JL, Rayco-Solon P, García-Casal MN, Rogers L, et al. Transmission of SARS-CoV-2 Through Breast Milk and Breastfeeding: A Living Systematic Review. *Ann N Y Acad Sci* (2021) 1484(1):32–54. doi: 10.1111/nyas.14477
7. Martins-Filho PR, Santos VS, Santos HPJr. To Breastfeed or Not to Breastfeed? Lack of Evidence on the Presence of SARS-CoV-2 in

Breastmilk of Pregnant Women With COVID-19. *Rev Panam Salud Publica* (2020) 44:e59. doi: 10.26633/RPSP.2020.59
8. Demers-Mathieu V, Do DM, Mathijssen GB, Sela DA, Seppo A, Järvinen KM, et al. Difference in Levels of SARS-CoV-2 S1 and S2 Subunits- and Nucleocapsid Protein-Reactive SIgM/IgM, IgG and SIgA/IgA Antibodies in Human Milk. *J Perinatol* (2020). doi: 10.1038/s41372-020-00805-w
9. Fox A, Marino J, Amanat F, Krammer F, Hanh-Holbrook J, Zolla-Pazner S, et al. Robust and Specific Secretory IgA Against SARS-CoV-2 Detected in Human Milk. *iScience* (2020) 23(11):101735. doi: 10.1016/j.isci.2020.101735
10. Garofalo RP, Goldman AS. Cytokines, Chemokines, and Colony-Stimulating Factors in Human Milk: The 1997 Update. *Biol Neonate* (1998) 4(2):134–42. doi: 10.1159/000014019
11. Field CJ. The Immunological Components of Human Milk and Their Effect on Immune Development in Infants. *J Nutr* (2005) 135:1–4. doi: 10.1093/jn/135.1.1
12. Dvorak B. Milk Epidermal Growth Factor and Gut Protection. *J Pediatr* (2010) 156(2 Suppl):S31–5. doi: 10.1016/j.jpeds.2009.11.018
13. Garofalo RP. Cytokines in Human Milk. *J Pediatr* (2010) 156:S36–40. doi: 10.1016/j.jpeds.2009.11.019
14. Dawod B, Marshall JS. Cytokines and Soluble Receptors in Breast Milk as Enhancers of Oral Tolerance Development. *Front Immunol* (2019) 10:16. doi: 10.3389/fimmu.2019.00016
15. Ruiz L, Fernández L, Rodríguez JM. *Immune Factors in Human Milk. In Human Milk: Sampling and Measurement of Energy-Yielding Nutrients and Other Macromolecules*. M McGuire, D O'Connor, editors. London: Academic Press (2020).
16. Azkur AK, Akdis M, Azkur D, Sokolowska M, van de Veen W, Brüggen MC. Immune Response to SARS-CoV-2 and Mechanisms of Immunopathological Changes in COVID-19. *Allergy* (2020) 75(7):1564–81. doi: 10.1111/all.14364
17. Chatterjee SK, Saha S, Munoz MNM. Molecular Pathogenesis, Immunopathogenesis and Novel Therapeutic Strategy Against COVID-19. *Front Mol Biosci* (2020) 7:196. doi: 10.3389/fmolb.2020.00196
18. Choudhary S, Sharma K, Silakari O. The Interplay Between Inflammatory Pathways and COVID-19: A Critical Review on Pathogenesis and Therapeutic Options. *Microb Pathog* (2020) 150:104673. doi: 10.1016/j.micpath.2020.104673
19. Farquhar C, Mbori-Ngacha DA, Redman MW, Bosire RK, Lohman BL, Piantadosi AL, et al. CC and CXC Chemokines in Breastmilk are Associated With Mother-to-Child HIV-1 Transmission. *Curr HIV Res* (2005) 3:361–9. doi: 10.2174/157016205774370393
20. Bosire R, Guthrie BL, Lohman-Payne B, Mabuka J, Majiwa M, Wariua G, et al. Longitudinal Comparison of Chemokines in Breastmilk Early Postpartum Among HIV-1-Infected and Uninfected Kenyan Women. *Breastfeed Med Off J Acad Breastfeed Med* (2007) 2:129–38. doi: 10.1089/bfm.2007.0009
21. Walter J, Ghosh MK, Kuhn L, Semrau K, Sinkala M, Kankasa C, et al. High Concentrations of Interleukin 15 in Breast Milk are Associated With Protection Against Postnatal HIV Transmission. *J Infect Dis* (2009) 200:1498–502. doi: 10.1086/644603
22. de Quental OB, França EL, Honório-França AC, Morais TC, Daboin BEG, Bezerra IMP, et al. Zika Virus Alters the Viscosity and Cytokines Profile in Human Colostrum. *J Immunol Res* (2019) 2019:9020519. doi: 10.1155/2019/9020519
23. Rabe T, Lazar K, Cambronero C, Goelz R, Hamprecht K. Human Cytomegalovirus (HCMV) Reactivation in the Mammary Gland Induces a Proinflammatory Cytokine Shift in Breast Milk. *Microorganisms* (2020) 8 (2):289. doi: 10.3390/microorganisms8020289
24. Lackey KA, Pace RM, Williams JE, Bode L, Donovan SM, Järvinen KM, et al. SARS-CoV-2 and Human Milk: What Is the Evidence? *Matern Child Nutr* (2020) 16(4):e13032. doi: 10.1111/mcn.13032
25. Yang N, Che S, Zhang J, Wang X, Tang YCOVID-19 Evidence and Recommendations Working Group, et al. Breastfeeding of Infants Born to Mothers With COVID-19: A Rapid Review. *Ann Transl Med* (2020) 8 (10):618. doi: 10.21037/atm-20-3299
26. Chen L, Li Q, Zheng D, Jiang H, Wei Y, Zou L, et al. Clinical Characteristics of Pregnant Women With Covid-19 in Wuhan, China. *N Engl J Med* (2020) 382 (25):e100. doi: 10.1056/NEJMc2009226
27. Groß R, Conzelmann C, Müller JA, Stenger S, Steinhart K, Kirchhoff F, et al. Detection of SARS-CoV-2 in Human Breastmilk. *Lancet* (2020) 395 (10239):1757–8. doi: 10.1016/S0140-6736(20)31181-8
28. Hinojosa-Velasco A, de Oca PVB, García-Sosa LE, Mendoza-Durán JG, Pérez-Méndez MJ, Dávila-González E, et al. A Case Report of Newborn Infant With Severe COVID-19 in Mexico: Detection of SARS-CoV-2 in Human Breast Milk and Stool. *Int J Infect Dis* (2020) 100:21–4. doi: 10.1016/j.ijid.2020.08.055
29. Lugli L, Bedetti L, Lucaccioni L, Gennari W, Leone C, Ancora G, et al. An Uninfected Preterm Newborn Inadvertently Fed SARS-CoV-2-Positive Breast Milk. *Pediatrics* (2020) 146(6):e2020004960. doi: 10.1542/peds.2020-004960
30. Costa S, Posteraro B, Marchetti S, Tamburrini E, Carducci B, Lanzone A, et al. Excretion of SARS-CoV-2 in Human Breast Milk. *Clin Microbiol Infect* (2020) 26(10):1430–2. doi: 10.1016/j.cmi.2020.05.027
31. De Rose DU, Piersigilli F, Ronchetti MP, Santisi A, Bersani I. Study Group of Neonatal Infectious Diseases of The Italian Society of Neonatology (SIN), et al. Novel Corornavirus Disease (COVID-19) in Newborns and Infants: What We Know So Far. *Ital J Pediatr* (2020) 46(1):56. doi: 10.1186/s13052-020-0820-x
32. Fernández Colomer B, Sánchez-Luna M, de Alba Romero C, Alarcón A, Baña Souto A, Camba Longueira F, et al. Neonatal Infection Due to SARS-CoV-2: An Epidemiological Study in Spain. *Front Pediatr* (2020) 8:580584.
33. White A, Mukherjee P, Stremming J, Sherlock LG, Reynolds RM, Smith D, et al. Neonates Hospitalized With Community-Acquired SARS-CoV-2 in a Colorado Neonatal Intensive Care Unit. *Neonatology* (2020) 117(5):641–5. doi: 10.1159/000508962
34. Wei M, Yuan J, Liu Y, Fu T, Yu X, Zhang ZJ. Novel Coronavirus Infection in Hospitalized Infants Under 1 Year of Age in China. *JAMA* (2020) 323 (14):1313–4. doi: 10.1001/jama.2020.2131
35. Walker KF, O'Donoghue K, Grace N, Dorling J, Comeaud JL, Li W, et al. Maternal Transmission of SARS-COV-2 to the Neonate, and Possible Routes for Such Transmission: A Systematic Review and Critical Analysis. *BJOG* (2020) 127(11):1324–36. doi: 10.1111/1471-0528.16362
36. Pereira A, Cruz-Melguizo S, Adrien M, Fuentes L, Marin E, Forti Z, et al. Breastfeeding Mothers With COVID-19 Infection: A Case Series. *Int Breastfeed J* (2020) 15(1):69. doi: 10.1186/s13006-020-00314-8
37. Marotz C, Belda-Ferre P, Ali F, Das P, Huang S, Cantrel K, et al. Microbial Context Predicts SARS-CoV-2 Prevalence in Patients and the Hospital Built Environment. (2020). doi: 10.1101/2020.11.19.20234229. medRxiv.
38. Wölfel R, Corman VM, Guggemos W, Seilmaier M, Zange S, Müller MA, et al. Virological Assessment of Hospitalized Patients With COVID-2019. *Nature* (2020) 581(7809):465–9. doi: 10.1038/s41586-020-2196-x
39. Tay MZ, Poh CM, Rénia L, MacAry PA, Ng LFP. The Trinity of COVID-19: Immunity, Inflammation and Intervention. *Nat Rev Immunol* (2020) 20 (6):363–74. doi: 10.1038/s41577-020-0311-8
40. Ruiz L, Espinosa-Martos I, García-Carral C, Manzano S, McGuire MK, Meehan CL, et al. What's Normal? Immune Profiling of Human Milk From Healthy Women Living in Different Geographical and Socioeconomic Settings. *Front Immunol* (2017) 8:696. doi: 10.3389/fimmu.2017.00696
41. Chollet-Hinton LS, Stuebe AM, Casbas-Hernandez P, Chetwynd E, Troester MA. Temporal Trends in the Inflammatory Cytokine Profile of Human Breastmilk. *Breastfeed Med* (2014) 9(10):530–7. doi: 10.1089/bfm.2014.0043
42. Moles L, Manzano S, Fernández L, Montilla A, Corzo N, Ares S, et al. Bacteriological, Biochemical, and Immunological Properties of Colostrum and Mature Milk From Mothers of Extremely Preterm Infants. *J Pediatr Gastroenterol Nutr* (2015) 60(1):120–6. doi: 10.1097/MPG.0000000000000560
43. Collado MC, Santaella M, Mira-Pascual L, Martínez-Arias E, Khodayar-Pardo P, Ros G, et al. Longitudinal Study of Cytokine Expression, Lipid Profile and Neuronal Growth Factors in Human Breast Milk From Term and Preterm Deliveries. *Nutrients* (2015) 7(10):8577–91. doi: 10.3390/nu7105415
44. Trend S, Strunk T, Lloyd ML, Heen Kok C, Metcalfe J, Geddes DT, et al. Levels of Innate Immune Factors in Preterm and Term Mother's Breast Milk During the 1st Month Postpartum. *Br J Nutr* (2016) 115(7):1178–93. doi: 10.1017/S0007114516000234
45. Bryan DL, Hart PH, Forsyth KD, Gibson RA. Immunomodulatory Constituents of Human Milk Change in Response to Infant Bronchiolitis. *Pediatr Allergy Immunol* (2007) 18(6):495–502. doi: 10.1111/j.1399-3038.2007.00565.x
46. Riskin A, Almog M, Peri R, Halasz K, Srugo I, Kessel A. Changes in Immunomodulatory Constituents of Human Milk in Response to Active Infection in the Nursing Infant. *Pediatr Res* (2012) 71(2):220–5. doi: 10.1038/pr.2011.34

47. Veldhoen M, Hocking RJ, Atkins CJ, Locksley RM, Stockinger B. TGFbeta in the Context of an Inflammatory Cytokine Milieu Supports *De Novo* Differentiation of IL-17-Producing T Cells. *Immunity* (2006) 24:179–89. doi: 10.1016/j.immuni.2006.01.001
48. Verhasselt V. Neonatal Tolerance Under Breastfeeding Influence: The Presence of Allergen and Transforming Growth Factor-β in Breast Milk Protects the Progeny From Allergic Asthma. *J Pediatr* (2010) 156:S16–20. doi: 10.1016/j.jpeds.2009.11.015
49. Penttila IA. Milk-Derived Transforming Growth Factor-β and the Infant Immune Response. *J Pediatr* (2010) 156:S21–5. doi: 10.1016/j.jpeds.2009.11.016

Conflict of Interest: The authors declare that the research was conducted in the absence of any commercial or financial relationships that could be construed as a potential conflict of interest.

Publisher's Note: All claims expressed in this article are solely those of the authors and do not necessarily represent those of their affiliated organizations, or those of the publisher, the editors and the reviewers. Any product that may be evaluated in this article, or claim that may be made by its manufacturer, is not guaranteed or endorsed by the publisher.

frontiers in Immunology

ORIGINAL RESEARCH
published: 29 July 2021
doi: 10.3389/fimmu.2021.719810

Immune Profile of the Normal Maternal-Fetal Interface in Rhesus Macaques and Its Alteration Following Zika Virus Infection

*Matilda J. Moström[1,2], Elizabeth A. Scheef[1], Lesli M. Sprehe[1], Dawn Szeltner[1], Dollnovan Tran[1], Jon D. Hennebold[3], Victoria H. J. Roberts[3], Nicholas J. Maness[2,4], Marissa Fahlberg[1] and Amitinder Kaur[1,2]**

[1] Division of Immunology, Tulane National Primate Research Center, Covington, LA, United States, [2] Department of Microbiology and Immunology, Tulane School of Medicine, New Orleans, LA, United States, [3] Division of Reproductive and Developmental Sciences, Oregon National Primate Research Center, Beaverton, OR, United States, [4] Division of Microbiology, Tulane National Primate Research Center, Covington, LA, United States

OPEN ACCESS

Edited by:
Ashley L. St. John, Duke-NUS Medical School, Singapore

Reviewed by:
Lucia De Noronha, Pontifical Catholic University of Parana, Brazil
Abhay P. S. Rathore, Duke University, United States

***Correspondence:**
Amitinder Kaur
akaur@tulane.edu

Specialty section:
This article was submitted to Viral Immunology, a section of the journal Frontiers in Immunology

Received: *03 June 2021*
Accepted: *05 July 2021*
Published: *29 July 2021*

Citation:
Moström MJ, Scheef EA, Sprehe LM, Szeltner D, Tran D, Hennebold JD, Roberts VHJ, Maness NJ, Fahlberg M and Kaur A (2021) Immune Profile of the Normal Maternal-Fetal Interface in Rhesus Macaques and Its Alteration Following Zika Virus Infection. Front. Immunol. 12:719810. doi: 10.3389/fimmu.2021.719810

The maternal decidua is an immunologically complex environment that balances maintenance of immune tolerance to fetal paternal antigens with protection of the fetus against vertical transmission of maternal pathogens. To better understand host immune determinants of congenital infection at the maternal-fetal tissue interface, we performed a comparative analysis of innate and adaptive immune cell subsets in the peripheral blood and decidua of healthy rhesus macaque pregnancies across all trimesters of gestation and determined changes after Zika virus (ZIKV) infection. Using one 28-color and one 18-color polychromatic flow cytometry panel we simultaneously analyzed the frequency, phenotype, activation status and trafficking properties of αβ T, γδ T, iNKT, regulatory T (Treg), NK cells, B lymphocytes, monocytes, macrophages, and dendritic cells (DC). Decidual leukocytes showed a striking enrichment of activated effector memory and tissue-resident memory CD4+ and CD8+ T lymphocytes, CD4+ Tregs, CD56+ NK cells, CD14+CD16+ monocytes, CD206+ tissue-resident macrophages, and a paucity of B lymphocytes when compared to peripheral blood. t-distributed stochastic neighbor embedding (tSNE) revealed unique populations of decidual NK, T, DC and monocyte/macrophage subsets. Principal component analysis showed distinct spatial localization of decidual and circulating leukocytes contributed by NK and CD8+ T lymphocytes, and separation of decidua based on gestational age contributed by memory CD4+ and CD8+ T lymphocytes. Decidua from 10 ZIKV-infected dams obtained 16-56 days post infection at third (n=9) or second (n=1) trimester showed a significant reduction in frequency of activated, CXCR3+, and/or Granzyme B+ memory CD4+ and CD8+ T lymphocytes and γδ T compared to normal decidua. These data suggest that ZIKV induces local

immunosuppression with reduced immune recruitment and impaired cytotoxicity. Our study adds to the immune characterization of the maternal-fetal interface in a translational nonhuman primate model of congenital infection and provides novel insight in to putative mechanisms of vertical transmission.

Keywords: fetal-maternal immunity, decidua, Zika, gammadelta T cells, dNK, decidual T cells, Treg, congenital viral infection

INTRODUCTION

Successful maintenance of pregnancy requires a balance between sustaining an immune tolerant state to prevent rejection of foreign paternal-origin fetal antigens and at the same time protect the fetus against vertical transmission of microbial pathogens (1). The maternal-fetal interface is a rich and complex immune environment essential to fetal growth and survival that consists of maternal decidual tissue and fetal-origin cells such as placental trophoblasts, endothelial cells and Hofbauer cells (2, 3). The decidua contains a myriad of immune cells including antigen-presenting cells (DC and macrophages), stromal cells, NK cells, neutrophils, mast cells, regulatory T (Treg) cells, and adaptive T lymphocytes that are geared towards a dual role of establishing a tolerogenic environment conducive to placental embedding while maintaining local immunity against infections (1, 4, 5). Decidual leukocytes are phenotypically and functionally distinct from peripheral blood and change with gestational age. Most of the data in humans are from first trimester pregnancy with fewer studies in the second or third trimester (6–8). Studies in the first trimester of pregnancy in humans have shown that NK cells account for 50-90% of the decidual leukocyte population and predominantly have a CD56bright CD16– phenotype (7, 9). Despite the presence of cytolytic granules, decidual NK are poorly cytotoxic and differ from circulating NK cells in their functionality, expression of inhibitory and cytotoxicity receptors, and at the level of gene expression (7, 10–13). A similar dominant population of CD56+ NK cells has been described in rhesus macaque decidua (14–16). Along with decidual NK cells, Tregs and macrophages play a key role in maintaining an anti-inflammatory environment in the decidua (17, 18). Among adaptive immune subsets, CD3+ T lymphocytes constitute 5-20% of the decidual leukocyte population in early pregnancy and increase with gestational age; in contrast, B lymphocytes are rare (6, 19). Decidual T lymphocytes are enriched for differentiated CD8+ effector memory T cells that have reduced cytotoxic granule content and a transcriptional profile of exhaustion and activation genes distinct from circulating effector memory CD8+ T lymphocytes (20, 21). Decidual CD8+ T cells are also key players in recognition of foreign antigen and have been shown to contain fetal-specific CD8+ T cells (22–25). It is not known however whether decidual CD8+ T lymphocytes mount an antigen-specific response against pathogens; one study demonstrating decidual CD8+ T cells binding to EBV-specific tetramers was not conclusive (26, 27). Although the maternal-fetal interface has been extensively investigated for mechanisms underlying preterm birth and preeclampsia, relatively little is known about factors that prevent or allow maternal-fetal transmission of pathogens. We are using the rhesus macaque nonhuman primate (NHP) model to study factors predisposing to placental transmission of congenital infections such as cytomegalovirus (CMV) and Zika virus (ZIKV) (28–30).

Important similarities in placental biology make NHPs a suitable animal model to study vertical transmission of pathogens. Rhesus macaque placentation resembles humans in consisting of a hemochorial placenta with trophoblast invasion of the uterine wall (31, 32). However, macaque placentation is less deep with trophoblast invasion restricted to spiral arteries in the decidua and only occurring *via* the endovascular route (33). Macaque extravillous trophoblasts express the HLA-G ortholog, Mamu-AG, which has features of a nonclassical MHC class I molecule and was shown to be a ligand for the inhibitory killer immunoglobulin-like receptor Mamu-KIR3DL05 (34, 35). A recent transcriptomic analysis of human and macaque placenta revealed that the majority of human placental marker genes were shared between the two species, further validating the relevance of the NHP model (36). Of particular interest to the current study are the immune determinants at the maternal-fetal interface that protect against vertical transmission. A single-cell transcriptomics study of normal human pregnancy demonstrated the complexity of the immune populations in the maternal-fetal interface (37). The maternal-fetal interface of NHPs is less well delineated. Currently data are lacking on the decidual T lymphocyte phenotype, presence of nontraditional T cells, NK cell subsets, B cells, and myeloid cells in rhesus macaques across different gestational ages and their comparison to peripheral blood. The aim of this study was to conduct a comprehensive analysis of the immune composition of decidual and circulating leukocytes in normal rhesus macaque pregnancies throughout gestation and investigate changes in congenital infection. To this end we developed one 28-color and one 18-color flow cytometry panel to simultaneously analyze multiple innate and adaptive immune subsets in the decidua and blood of healthy rhesus macaques in the first, second and third trimester of pregnancy. We compared the frequency, phenotype, function and trafficking properties of decidual leukocytes with that of circulating leukocytes. In addition, we correlated changes in the decidual leukocyte composition with increasing gestational age. We then investigated changes following ZIKV infection in pregnancy by comparing normal decidua with decidual leukocytes and peripheral blood mononuclear cells from a previously reported study on ZIKV infection in pregnant rhesus macaques (29).

MATERIALS AND METHODS

Animals and Study Design

Rhesus macaque dams of Indian ancestry from the Tulane National Primate Research Center (TNPRC) and the Oregon National Primate Research Center (ONPRC) were used for this study. All macaques were from the specific pathogen free (SPF) colonies of the respective primate centers. SPF macaques are CMV-seropositive but free of SIV, STLV, Type D retrovirus, and herpes B virus. At both institutions all animal procedures were performed according to approved Institutional Animal Care and Use Committee protocols. Peripheral blood (n=24) and decidua (n=11) from normal pregnant dams aged 3.6-17.0 years (mean=7.7 years, median=6.7 years) were collected for cross-sectional analysis of first, second, and third trimester gestation (**Table 1**). Information regarding timed-mating, housing, and mode of sampling are detailed in **Supplemental Table 1**. Decidua was obtained in 1st trimester from day 44-50 gestation (n=3), 2nd trimester at day 100 gestation (n=3), and 3rd trimester from day 130-167 gestation (n=5) (**Supplemental Table 1**).

Blood and decidua were also collected close to or at the time of Caesarian section (C-section) from a cohort of ZIKV-infected dams (n=10) enrolled in a separate previously published study (29). The group consisted of pregnant Indian-ancestry rhesus macaques inoculated subcutaneously with a single dose of 1x10^4 PFU ZIKV Rio-U1 at the first (n=1), second (n=3), or third trimester (n=6) gestation followed by C-section and decidua collection at 2nd or 3rd trimester gestation (**Table 1** and **Supplemental Table 2**). Peripheral blood was obtained 5-41 days post ZIKV infection while placenta was collected at the time of study C-section or spontaneous abortion which ranged from 16-56 days post ZIKV infection (**Supplemental Table 2**). One decidua was collected in the second trimester at 64 days gestation age while the remaining 9 decidua samples were collected in the third trimester at 142 to 157 days gestation age (**Table 1** and **Supplemental Table 2**).

Isolation of Leukocytes From Blood and Decidual Tissue

Peripheral blood mononuclear cells (PBMC) were isolated from blood collected in anticoagulant EDTA or heparin tubes by density gradient centrifugation with Lymphocyte Separation Medium (LSM; MP Biomedicals) or Lymphoprep (Stemcell Technologies). Isolated PBMC were cryopreserved using serum-free Bambanker cryopreservation media (Bulldog Bio) and stored in liquid nitrogen until use.

Following C-section, decidua from ONPRC study animals was dissected from the maternal side of the placenta and shipped overnight to TNPRC in R10 media (RPMI supplemented with Hepes, L-glutamine, and 10%FBS) on ice for decidual leukocyte isolation. Placental samples collected at TNPRC were immediately processed for decidual leukocyte isolation. Blood clots were removed from the maternal side of the placenta and decidual tissue carefully dissected away from the placenta. Visible blood vessels were removed and decidual tissue pieces were then washed extensively with sodium chloride 0.9% (Hanna Pharmaceutical Supply Co.) to remove any debris and remaining blood. Clean decidua was dissected into 2 mm^2 pieces and subjected to three rounds of digestion by shaking at 60 RPM at 37°C for 30 minutes in digestion media containing 0.1mg/mL DNAse I (Millipore Sigma 11284932001) and collagenase IV 1 mg/mL (Millipore Sigma C5138-100MG). Released cells in solution were collected in between each digestion and washed. After the last digestion, residual cells were passed repeatedly through a sterile 18-gauge animal feeding needle (Fisherbrand^{TM}) for gentle mechanical sheering before straining through sterile 70μm filters. Cells from each digestion were pooled. The resulting single cell suspension was layered over a density gradient LSM (MP Biomedicals) and spun at 1500 rpm for 45 minutes with no brakes. Lymphocytes were carefully collected from the top layer, washed, and cryopreserved in DMSO supplemented with 90% FBS or in serum-free Bambanker cryopreservation medium (Bulldog Bio).

Phenotyping by Multicolor Flow Cytometry

Two flow cytometry panels were used to phenotype the leukocytes, one adaptive 28-color panel, and one innate 18-color panel (**Supplemental Table 3**). In the same batch experiment, decidual leukocytes and PBMC from normal and ZIKV-infected animals were gently thawed using standard protocols supplemented with 17.5μg/mL DNAse I (Millipore Sigma 11284932001). 1-3 million live lymphocytes were used for staining. Briefly, cells were stained with live/dead discriminating dye for 20min at room temperature (RT). Cell suspensions were washed with 2% FBS/PBS buffer and the 28-color panel was stained sequentially with anti-Vα24-PE and BV421-CD1d tetramer first (20 minutes incubation at RT), followed by addition of the chemokine receptor antibodies anti-CCR5-BUV737 and anti-CXCR3-PE-Cy7 (20 minutes incubation at 37°C), and finally by addition of the chemokine receptor antibodies anti-CCR4-BV510 and anti-CCR6-BV650 (20 minutes incubation at 37°C) with no washes in between. Last, the remaining surface cocktail was added and the tubes incubated for 20 minutes at RT with antibodies outlined in **Supplemental Table 3**. Cells were then washed with 2% FBS/PBS prior to incubating with BD Cytofix/Cytoperm^{TM} solution (BD Biosciences) for 20 minutes at RT followed by washing with BD Perm/Wash^{TM} buffer (BD Biosciences). Intracellular antibodies

TABLE 1 | Description of study cohort.

Trimester	1st Trimester		2nd Trimester		3rd Trimester	
Sample type	**Decidua**	**PBMC**	**Decidua**	**PBMC**	**Decidua**	**PBMC**
Uninfected (n)	3	6	3	11	5	7
Zika (n)	0	0	1	1	9	8

were then added for a 20-minute incubation at RT. The 18-color panel was stained using the same applicable steps. Cells were fixed with Stabilizing Fixative (BD Biosciences; Cat# 338036) and acquired the next day on the BD FACSymphony A5 and BD LSRFortessa X-20 using BD FACSDiva version 9.1 and 9.0 respectively. A mean of 244,000 (50,000 to 718,000) Time/CD45+/Live events were collected. FMO controls included in the experiments were BB700-PD-1, BV650-CCR6, PE-Cy7-CXCR3, AL647-CX3CR1, PE-Vα24, and APC-NKG2D. Single color controls were acquired in all experiments and compensation and analysis was performed in FlowJo software v10.7 (BD Biosciences).

Data Analysis

Flow cytometry data was analyzed using FlowJo v10.7 (BD Biosciences). Statistical analysis was performed using GraphPad Prism version 9.0.1 (GraphPad Software Inc.) and R (CRAN). tSNEs were calculated in FlowJo using the default settings for opt-SNE. An equal number of cells per tissue were used when analyzing PBMC *versus* decidua in uninfected animals. An equal number of cells per condition were used when analyzing ZIKV-infection *versus* uninfected decidua. Boxplots and tSNE renderings were created using the tidyverse and ggpubr packages in R. Data throughout the result section are reported as mean ± standard deviation (SD) unless noted.

RESULTS

Circulating and Decidual Leukocyte Composition in Normal Pregnancy

To examine immune cell populations at the maternal-fetal interface in normal rhesus macaques, we conducted a cross-sectional analysis of first (n=3), second (n=3), and third (n=5) trimester decidua obtained at the time of C-section in healthy pregnancy and compared it with blood obtained from gestation-matched healthy, uninfected dams experiencing normal pregnancies (**Table 1**). PBMC and decidual leukocytes were evaluated with two flow cytometry panels, one 28-color panel focused on adaptive immunity, and one 18-color innate cell focused panel (**Supplemental Table 3**). T lymphocytes, NK cells, B lymphocytes, and cells of the myeloid lineage were enumerated using the gating strategy in **Figures 1A–C**. Definitions used in this study for each analyzed cell type in the two flow panels were based on markers in NHPs that are equal to their human counterparts (**Table 2**). For example, NK cells which are CD3– CD16^{bright} CD56^{dim} or CD16$^{-/dim}$ CD56^{bright} in humans are defined as CD3– HLA-DR$^{lo/-}$ CD8+ in rhesus macaques (38). T lymphocytes were the predominant leukocytes in both PBMC (mean ± SD; 48.0 ± 14.7%) and decidua (54.2 ± 12.6%) but not significantly different between the two compartments (**Figures 2A, B**). NK cells were significantly increased in the decidua with ~3-fold greater frequency compared to PBMC, and were highest in the 2nd trimester (**Figures 2A, B**). No relationship between NK cells and gestational age was found in the decidua (**Supplemental Figure 1**). B lymphocytes were close to absent in decidual tissue in contrast to PBMC where they made up 25.3 ± 10.8% of the live CD45+ leukocytes (**Figures 2A, B**). In the myeloid antigen presenting compartment, which was defined as CD3– CD20– CD8$^{lo/-}$ HLA-DR+ (**Table 2**), a population of CD14+ tissue macrophages expressing both CD163+ and CD206+ were found in the decidua (**Figures 2C, D**). This population was virtually absent in PBMC (0.1 ± 1.2%) but represented 28.1 ± 14.7% of HLA-DR+ leukocytes in the decidua (**Figure 2D**). CD14+ CD163+ CD206– myeloid cells were found in PBMC and decidua at 54.1 ± 25.8% and 18.3 ± 12.8% respectively of myeloid HLA-DR+ expressing cells (**Figure 2D**). These cells are a mix of classical and intermediate monocytes in the PBMC and recently infiltrated monocytes and macrophages in tissues (39, 40). CD14+ CD163– CD206– cells were significantly increased in the decidua compared to PBMC (**Figure 2D**). Plasmacytoid DC (pDC) frequency ranged between 0.3 to 14.7% of HLA-DR-expressing cells in decidua but were not significantly different from PBMC (**Figure 2D**). CD14– CD123– HLA-DR+ leukocytes, which can be either conventional DCs or CD14– CD16+ non-classical monocytes in circulation, were similar between PBMC and decidua (34.4 ± 21.3% and 29.8 ± 15.8% respectively of HLA-DR-expressing cells).

To further probe differences and assess global changes of PBMC *vs*. decidua that may have been missed during manual gating, we performed an unbiased clustering analysis by t-distributed stochastic neighbor embedding (tSNE) using CD45+ live+ single cells in the 28-color panel focused on T, NK, and B cells. There were clear differences in leukocyte populations between sample types (**Figure 3**). Gradients colored by MFI depicted distinct CD3+ CD4+ (clusters 3 and 6) and CD3+ CD8+ T cells (clusters 8, 9, and 10) between the circulation and the decidual T cells (**Figure 3**). The near absence of B cells in decidua observed by manual gating was confirmed by the cluster of HLA-DR+ CD20+ (cluster 2) events only found in PBMC (**Figure 3**). CD95/Fas receptor, a marker of T cell memory in NHPs, was found in cluster 9, representing CD8+ T cells, which was predominantly found in the decidua. Granzyme B was found in both tissues but in different clusters which represented unique types of NK cells (**Figure 3**). An additional 17 more markers used to perform the tSNE algorithm are found in **Supplemental Figure 2**.

Classical and Unconventional T Lymphocytes Distribution in PBMC and Decidua

αβ T and γδ T cells were distinguished by expression of the pan-γδ T cell marker on total CD3+ T lymphocytes (**Figure 1A**). In classical αβ T lymphocytes, the CD4+ T cells were reduced in decidua compared to PBMC from 37.4 ± 12.0% to 20.7 ± 4.1% (**Figure 4A**). Consistent with human data, CD8+ T cells were the dominant T lymphocyte population in macaque decidua and present at significantly higher frequencies (63.1 ± 7.4%) compared to PBMC (47.5 ± 11.6%) (6, 19). No significant differences were found in double-positive (DP) or double-negative (DN) T cells (**Figure 4A**). In the non-classical T lymphocyte subset, γδ T cells were increased in decidua compared to PBMC but did not reach statistical significance

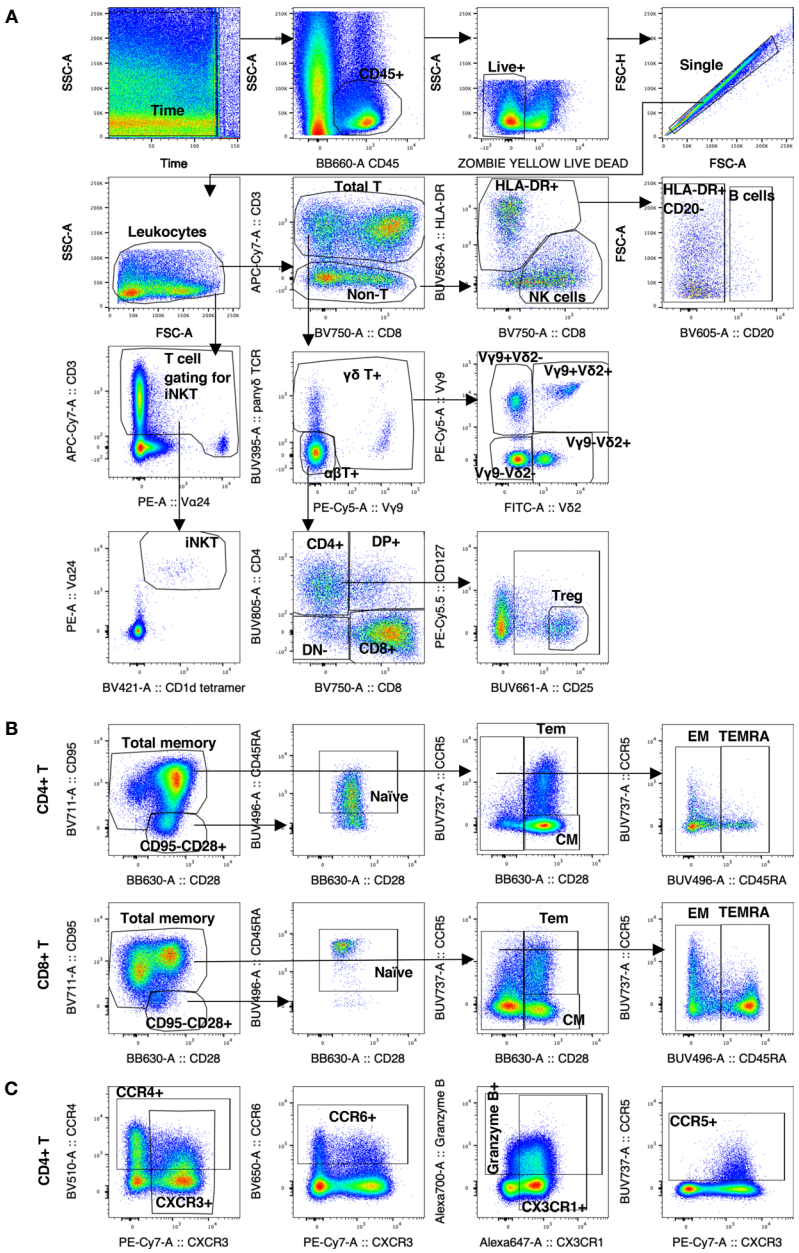

FIGURE 1 | Gating strategy of decidual leukocytes and PBMC in normal rhesus macaques. **(A)** Gating strategy in 28-color panel to identify αβ T cells, NK cells, B cells, myeloid cells (HLA-DR+ CD20-), iNKTs, γδ T cells, Tregs. **(B)** Gating strategy in CD4+ T and CD8+ T to delineate the naïve memory T cells subsets of CM, Tem, EM, and TEMRA. **(C)** Gating strategy of chemokine receptor expression.

unless only third trimester animals were compared (two-tailed unpaired t-test, p-value = 0.0008) (**Figure 4A**).

Among unconventional T lymphocytes, we evaluated invariant natural killer T (iNKT) cells. iNKT are an innate subset of T lymphocytes that respond to glycolipid antigens presented on CD1d molecules. These cells have been reported in human decidua but there are no data in NHPs (41, 42). Here, we sought to identify their presence in rhesus macaque decidua using the stringent identifying criteria of Vα24 TCR-expressing T lymphocytes binding to α-galactoslyceramide (αGC)-loaded CD1d tetramers (41–44). A detectable but sparse population of iNKTs with frequencies ranging between 0.036 to 0.918% of CD3+ T lymphocytes were detected in 6 of 9 decidua samples and at frequencies ranging between 0.005 to 4.4% in 17 out of 24 PBMC samples. We did not detect any difference in iNKT frequency between PBMC and decidua (**Figure 4A**).

In agreement with data from humans (6, 19), the decidua had a significantly increased frequency of CD4+ T regulatory cells

TABLE 2 | Flow cytometric definition of cell types.

Cell type*	Definition	Panel
αβ T cells	$CD3^+$ pan$\gamma\delta^-$	Adaptive 28-color
	CD4+: $CD4^+$ $CD8^-$	
	CD8+: $CD4^-$ $CD8^+$	
	Double Positive (DP+): CD4+ CD8+	
	Double Negative (DN–): CD4– CD8–	
γδ T cells	CD3+ pan$\gamma\delta$+	Adaptive 28-color
	Vγ9+ Vδ2+	
	Vγ9+ Vδ2–	
	Vγ9– Vδ2+	
	Vγ9– Vδ2–	
iNKT	CD3+ Vα24+ CD1d tetramer+	Adaptive 28-color
T regulatory cells	CD3+ CD4+ CD127– $CD25^{hi}$	Adaptive 28-color
Memory T cells	Naïve: CD95– CD28+ CD45RA+	Adaptive 28-color
In CD4+ αβ T	Total Memory: CD95+ CD28+/–	
In CD8+ αβ T	Central Memory (CM): CD95+ CD28+ CCR5–	
In γδ T	Transitional Effector Memory (Tem): CD95+ CD28+ CCR5+	
	Effector Memory (EM): CD95+ CD28– CD45RA–	
	Terminal Effector Memory (TEMRA): CD95+ CD28– CD45RA+	
	Tissue Resident Memory (Trm): CD95+ CD28+/– CD103+ CD69+	
T helper subsets	CD3+ CD4+	Adaptive 28-color
	CXCR3+ CCR5+/– Th1-like	
	CCR4+ Th2-like	
	CCR6+ Th17-like	
NK cells	CD3– HLA-$DR^{lo/-}$ CD8+	Innate 18-color and adaptive 28-color
	CD16+ CD56–	
	CD16– CD56+	
	CD16+ CD56+	
	CD16– CD56–	
B cells	CD3– HLA-DR^{hi} CD20+	Adaptive 28-color
Macrophages in Decidua	CD3– CD20– HLA-DR+ CD8– CD14+	Innate 18-color
	CD163+ CD206+	
	CD163+ CD206–	
	CD163– CD206–	
Monocytes in PBMC	CD3– CD20– HLA-DR+ CD8–	Innate 18-color
	Classical monocytes: CD14+ CD16–	
	Intermediate monocytes: CD14+ CD16+	
	Non-classical monocytes and DCs: CD14– CD16+	
Dendritic cells (DC)	CD3– CD20– HLA-DR+ CD14–	Innate 18-color
	Conventional DC, myeloid DC, and non-classical monocytes: CD123–	
	Plasmacytoid DC: CD123+	

**Cells are pre-gated as Live+ Single CD45+ Leukocytes.*

(Tregs) when compared to PBMC (**Figure 4A**). In this study, CD4+ Tregs were defined based on low CD127 expression on CD25hi CD4+ T lymphocytes, a population that has previously been shown in both humans and macaques to be FoxP3-positive and display Treg functionality of suppressive activity (45). Tregs accounted for 7.9 ± 5.5% of decidual CD4+ T lymphocytes while they were present in only 0.5 ± 0.4% of circulating CD4+ T lymphocytes. If assessed as a fraction of T cells, Tregs were 1.7 ± 1.4% in decidua and 0.2 ± 0.2% in PBMC. Decidual Tregs increased with gestation as a positive correlation (R^2 = 0.5392, p-value = 0.0243) between Treg frequency and days of gestation was detected (**Supplemental Figure 1**).

Memory CD4+ and CD8+ T Lymphocytes in PBMC and Decidua

Using a combination of CD95, CD28, CCR5, CD45RA, CD69, and CD103 we delineated naïve (CD95– CD28+ CD45RA+) and five populations of CD95+ memory CD4+ T or CD8+ T lymphocytes (**Table 2** and **Figure 1B**). Memory subsets included CD95+ CD28+ CCR5–CD45RA– central memory (CM), CD95+ CD28– CCR5+/– CD45RA– effector memory (EM), CD95+ CD28+ CCR5+ CD45RA–transitional effector memory (Tem), CD95+ CD28– CCR5+/– CD45RA+ terminally differentiated effector memory (TEMRA), and CD95+ CD69+ CD103+ tissue-resident memory (Trm).

The decidua exhibited a distinct phenotype of memory cells and a near absence of naïve cells (**Figure 4B**). The majority of CD4+ T memory lymphocytes in decidua and PBMC were CM but PBMC had an increased frequency of CM CD4+ T compared to decidua, whereas decidua had higher frequencies of EM and Tem CD4+ T lymphocytes (**Figure 4C**). CD4+ Trm were present at a small frequency of 0.7 ± 0.5% of CD4+ memory while no cells of this phenotype were found in PBMC (**Figure 4C**). Effector memory (EM) constituted the predominant subset of CD8+ T memory lymphocytes in decidua at a frequency of 67.0 ± 13.4% that was significantly higher than PBMC. Conversely, in

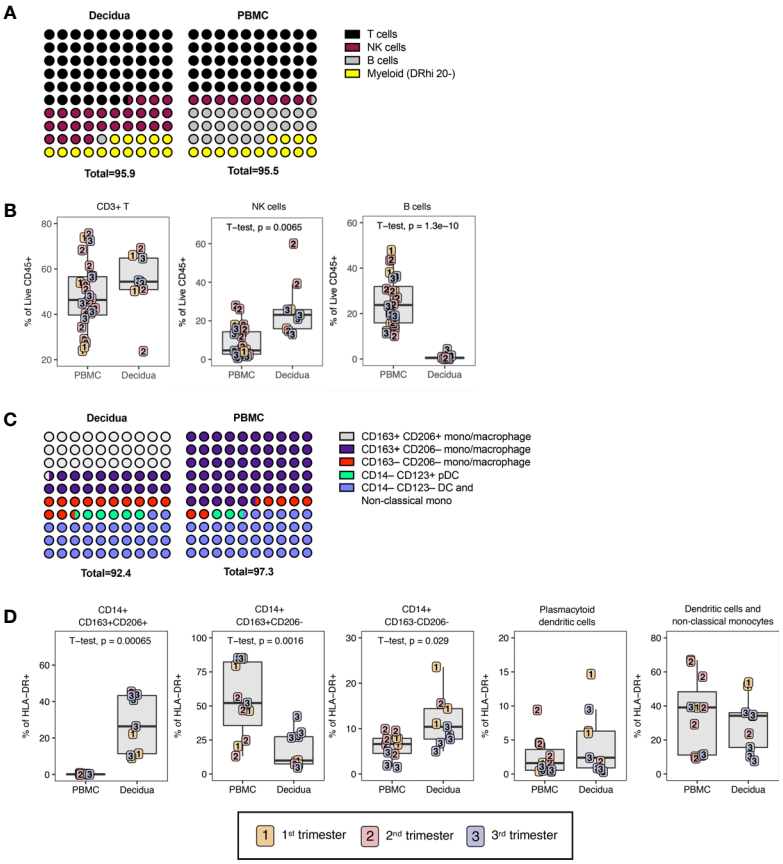

FIGURE 2 | Leukocyte composition of PBMC and decidua in normal rhesus macaques. **(A)** Comparison of relative proportions of the CD45+ leukocytes in decidua and PBMC. **(B)** Frequency of total T lymphocytes, NK cells, and B lymphocytes in PBMC and decidua during the first (yellow), second (red) and third trimester (blue) of pregnancy in normal rhesus macaques. **(C)** Comparison of relative proportions of the myeloid cells (CD3-CD20-HLA-DR+) in decidua and PBMC. **(D)** Frequency of myeloid cells (CD3-CD20-HLA-DR+) in PBMC and decidua of monocyte/macrophages subsets, and dendritic cells (DC). P-values <0.05 (unpaired t-test) shown on the plots.

PBMC, the majority of CD8+ memory T cells showed a terminally differentiated TEMRA phenotype of 65.6 ± 16.7%. The decidua had a reduced frequency of CD8+ T CM at 13.1 ± 4.9% compared to 18.7 ± 9.4% in the PBMC, which is similar to what was seen in the CD4+ T lymphocyte memory compartment (**Figure 4D**). Decidua also had a clear population of CD8+ Trm cells (6.8 ± 5.4%), which was completely absent in the PBMC (**Figure 4D**).

To evaluate the functional potential of circulatory T cells to those at the maternal-fetal interface, markers related to exhaustion, cytotoxicity, and activation were investigated using the gating strategy shown in **Supplemental Figure 3**. The exhaustion marker PD-1 was significantly elevated in decidual CD4+ and CD8+ T lymphocytes compared to PBMC with roughly 4-fold higher frequencies of PD-1+ CD4 + or CD8+ T lymphocytes in the decidua (**Figures 5A, B**). This is similar to what has been observed for effector memory T lymphocytes in humans between PBMC and decidual T lymphocytes (25). Despite high expression levels of PD-1, memory CD4+ and CD8+ T lymphocytes in the decidua were highly activated with significantly increased frequencies of CD69+ and HLA-DR+ cells as compared to PBMC (**Figures 5A, B**). CD25, a marker of activation, was significantly increased on CD4+ T lymphocytes in the decidua compared to PBMC (**Figure 5A**).

To investigate cytotoxic potential, we examined granzyme B expression in memory CD4+ and CD8+ memory T lymphocytes. Although decidual CD8+ memory T cells as a whole had lower frequencies of granzyme B-positive cells compared to PBMC (38.6 ± 9.9 *versus* 48.4 ± 17.4), these differences did not reach statistical significance (**Figure 5B**). However, evaluation of memory subsets yielded clear differences between PBMC and decidua. Among circulating CD8+ memory T lymphocytes, TEMRA contained the highest frequency of granzyme B-positive cells (62.0 ± 15.9) followed by EM at 55.5 ± 17.2%, and Tem and CM at <50% (**Figure 5C**). Comparison between the two compartments showed significantly higher frequency of granzyme B-positive Tem and CM CD8+ T lymphocytes in the decidua compared to PBMC (**Figure 5C**). No difference was found in CD8+ EM or

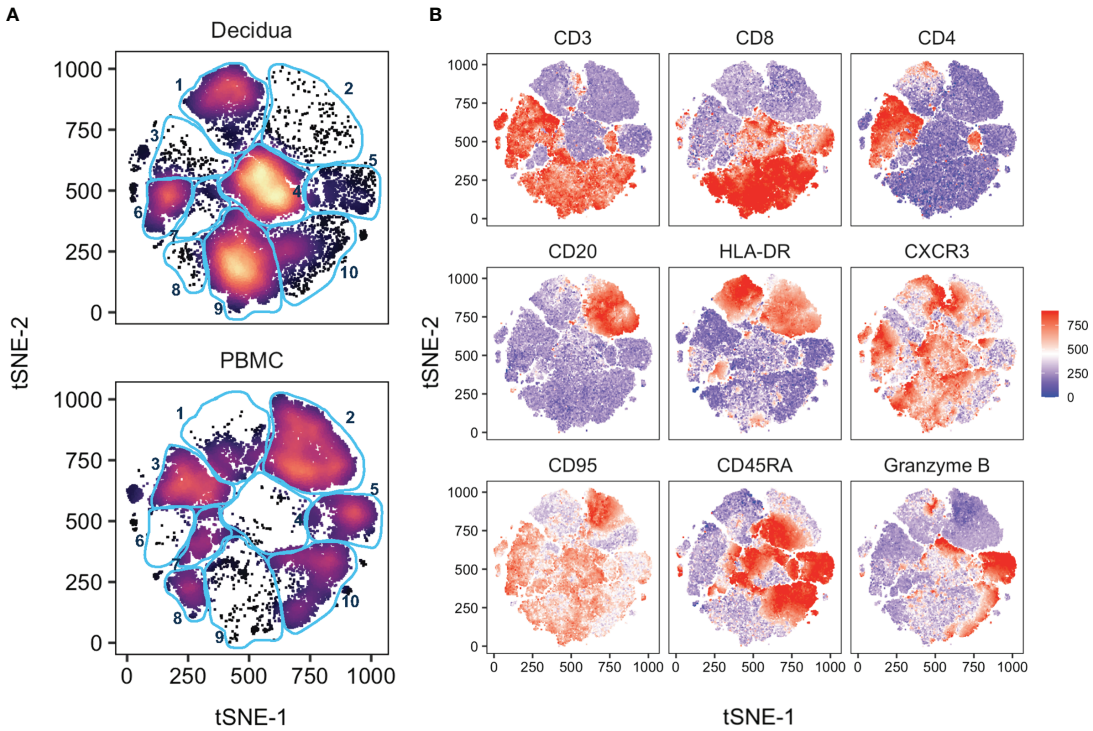

FIGURE 3 | tSNE analysis of PBMC and decidua in normal rhesus macaques. **(A)** tSNE plot representing an equal number of CD45+/live/single cell/leukocytes from decidua (n = 9) and PBMC (n = 24) of normal pregnant rhesus macaque samples. The 28-color adaptive panel was used to generate this plot. Blue gates were manually drawn based on clustering patterns. **(B)** Individual MFI gradients of nine markers on the tSNE map. Red coloring represents high MFI and blue coloring represents low MFI. Remaining gradients are found in **Supplemental Figure 2**.

TEMRA. To further assess granzyme B expression in decidual and PBMC CD8+ T lymphocytes, we measured the median fluorescence intensity (MFI) of granzyme B in the different CD8+ T lymphocyte memory subsets as an approximation of granzyme B content. Across the memory subsets of TEMRA, EM and CM, granzyme B MFI in decidual leukocytes was significantly lower compared to their circulating counterparts (**Figure 5D**). Therefore, despite similar frequencies of granzyme B-positive cells, the predominant decidual subsets of EM and TEMRA CD8+ T memory have reduced granzyme B content and are potentially less cytotoxic compared to the corresponding memory subsets in circulation. It is noteworthy that the granzyme B content as measured by MFI was significantly lower in decidual CM compared to PBMC CM despite the frequency of granzyme B-positive CM CD8+ T lymphocytes being significantly higher in decidua (**Figures 5C, D**).

In memory T cells, the trafficking phenotype was also investigated by Th-subset associated receptors CXCR3, CCR6, CCR5, and CCR4 (**Figures 1C**, **5E, F**). Consistent with previous reports in humans (25), decidual memory CD4+ T lymphocytes have an increased frequency of CXCR3 expression in contrast to the peripheral leukocytes from 87.3 ± 7.5% in decidua to 52.7 ± 10.8% in PBMC indicating Th1 skewing (**Figure 5E**). The same is true for CD8+ T lymphocytes where 90.0 ± 7.6% expressed CXCR3 and only 66.2 ± 13.6% did so in PBMC (**Figure 5F**). CCR5 was also increased in decidual CD4+ and CD8+ T lymphocytes compared to PBMC. Little to no CCR4 and CCR6 expression was found in the decidua, which was significantly different from PBMC where these chemokines were well-expressed (**Figures 5E, F**).

γδ T Lymphocytes in PBMC and Decidua

Next, the non-classical T lymphocytes were investigated. There are limited data on γδ T at the maternal-fetal interface. In one study in humans, γδ T cells were shown to be increased in the decidua in contrast to peripheral blood while having a reduced Vδ2 frequency (46). We investigated the frequency, CD4/CD8 phenotype, memory phenotype, and activation status of total γδ T lymphocytes detected by the pan- γδ TCR antibody. We also evaluated γδ T subsets based on TCR chain usage of total γδ T by using NHP cross-reactive antibodies against the Vγ9 TCR and Vδ2 TCR chain.

The majority of both decidual and peripheral blood γδ T lymphocytes were CD8+ or DN for CD4 and CD8 (**Figure 6A**). They were nearly entirely of a memory phenotype in both PBMC and decidua; however, CD8+ EM predominated in the decidua (42.6 ± 10.0) and TEMRA were most abundant in the PBMC (49.9 ± 14.8%) (**Figure 6B**). As expected, tissue resident Trm were detected in the decidua (5.5 ± 4.1%) but not in PBMC (**Figure 6B**). Similar to what was observed in αβ T lymphocytes,

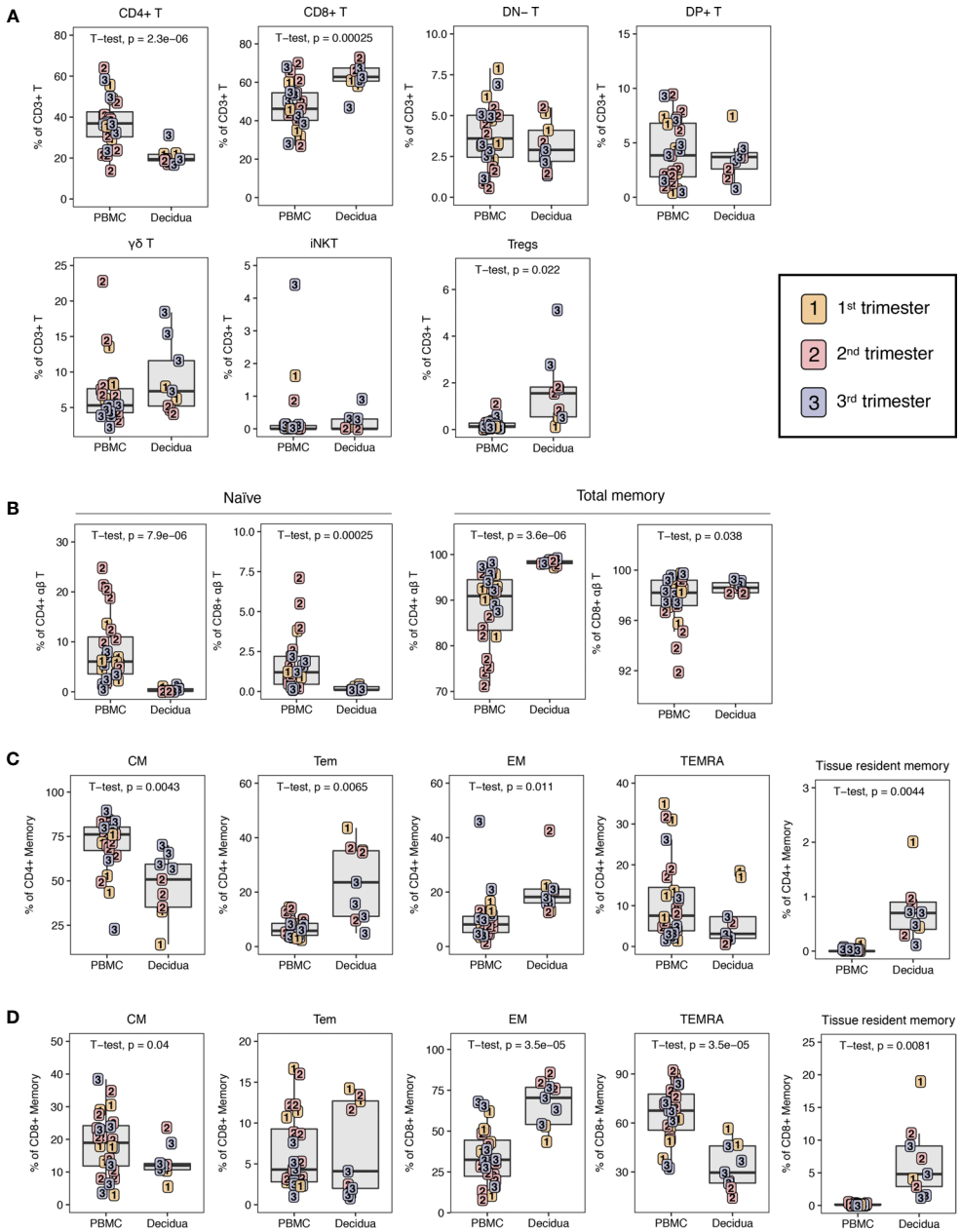

FIGURE 4 | T lymphocyte composition in PBMC and decidua from first to third trimester in normal pregnant rhesus macaques. **(A)** Frequency of conventional and innate T cells in first (yellow), second (red) and third trimester (blue) of pregnancy in PBMC and decidua of normal rhesus macaques. **(B)** CD4+ T and CD8+ T naive and total memory. **(C)** CD4+ T memory subsets. **(D)** CD8+ T memory subsets. P-values <0.05 (unpaired t-test) shown on the plots.

total γδ T lymphocytes appeared to be more activated in the decidua. Expression of CD25, CD69 and HLA-DR were significantly increased compared to PBMC, and this was accompanied with a concurrent increase of PD-1 expression in the decidua (**Figure 6C**). Like the αβ T lymphocytes, there was a significant reduction in the frequency of CCR6-expressing cells in the decidual γδ T cells (**Figure 6C**).

Using the individual gamma and delta TCR chains, four subsets of γδ T cells could be distinguished. The double positive, Vγ9+ Vδ2+ was present at significantly lower frequencies in the decidua compared to PBMC (**Figure 6D**). The single positive Vγ9+ Vδ2– and Vγ9– Vδ2+ γδ T were minor populations in both PBMC and decidua ranging in frequency from 1.0 to 21.8% of γδ T cells (**Figure 6D**). The innate-like

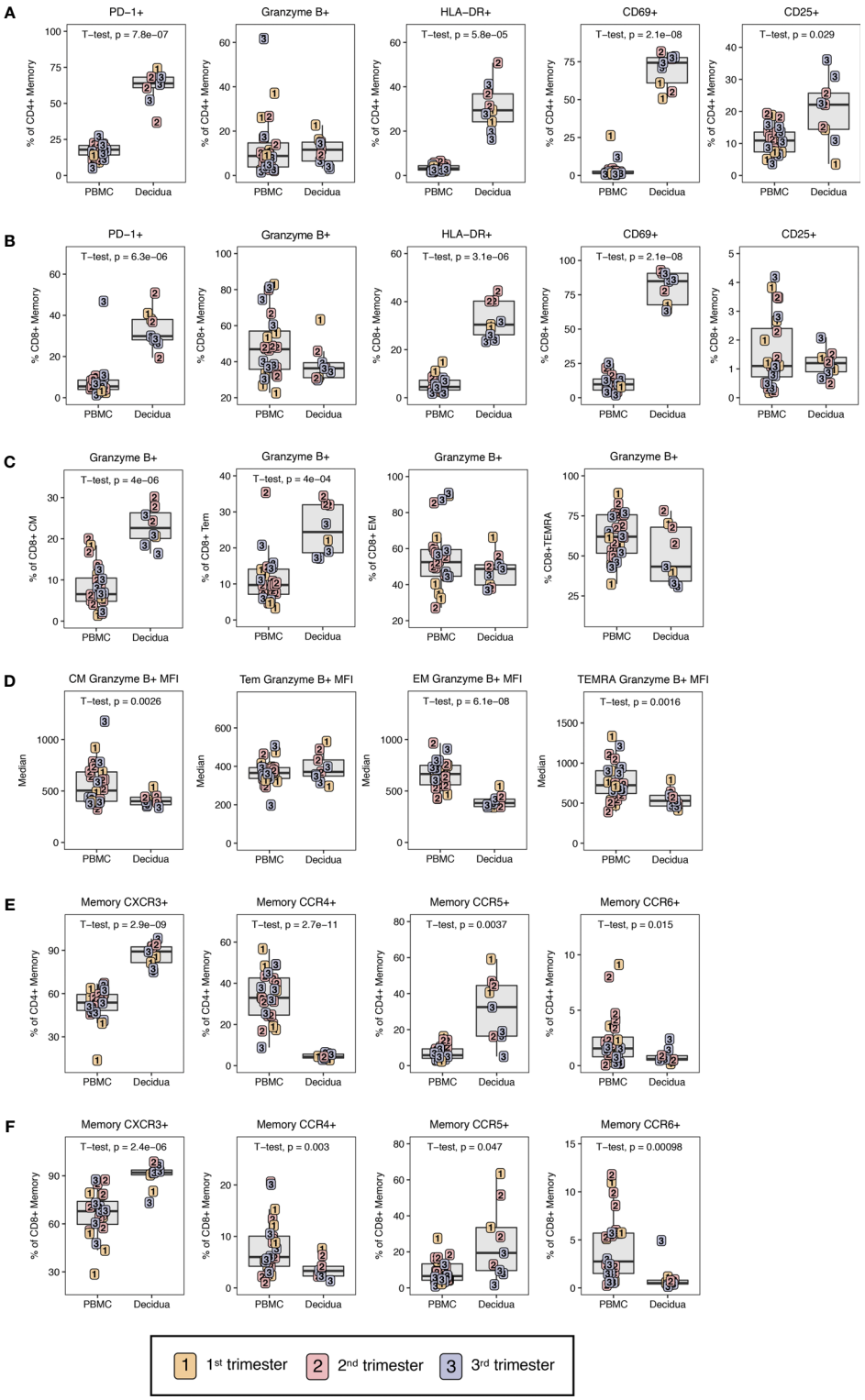

FIGURE 5 | Phenotypic characterization of T lymphocyte memory. **(A)** Phenotype of CD4+ T cell and **(B)** CD8+ T cell memory by PD-1, Granzyme B, HLA-DR, CD69, and CD25 in first (yellow), second (red) and third trimester (blue) of pregnancy in PBMC and decidua of normal rhesus macaques. **(C)** Cytotoxic potential in CD8+ T memory subsets by Granzyme B frequency in CM, Tem, EM, and TEMRA. **(D)** MFI of Granzyme B in CD8+ T memory subsets. **(E)** Chemokine receptor expression on memory CD4+ and **(F)** CD8+ T cells. P-values < 0.05 (unpaired t-test) shown on the plots.

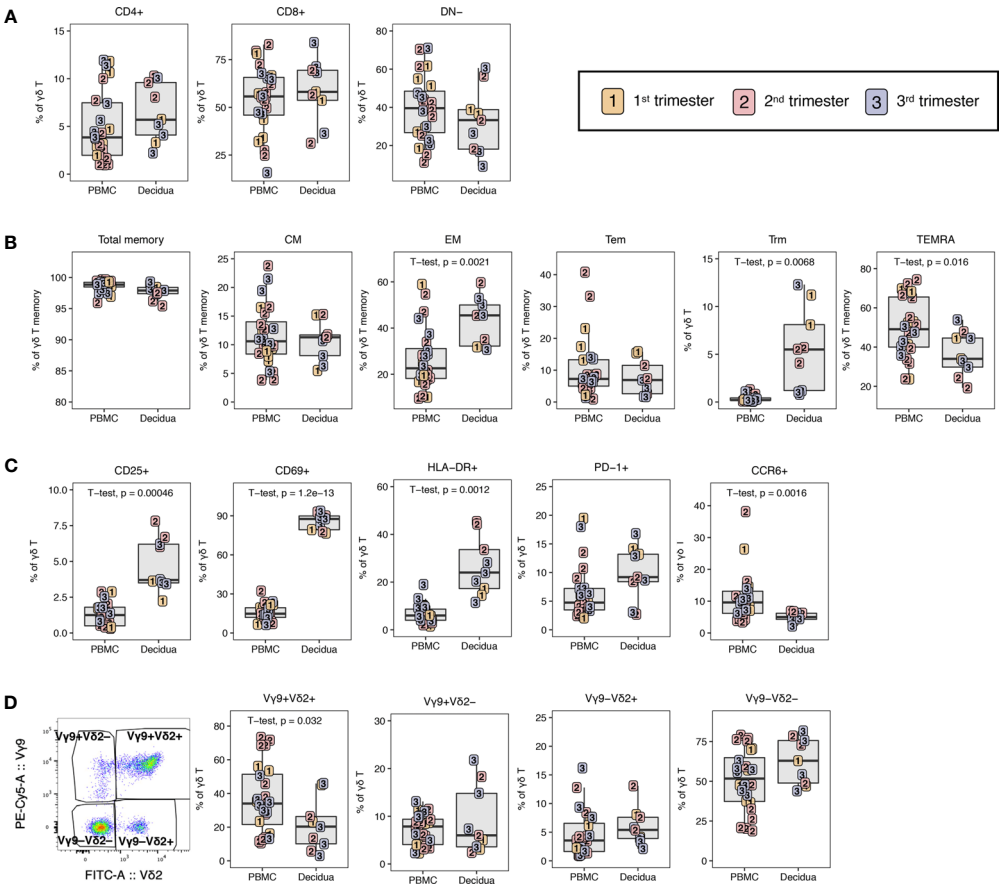

FIGURE 6 | γδ T lymphocytes in PBMC and decidua of normal rhesus macaque pregnancies. **(A)** CD4 and CD8 expression on γδ T lymphocytes in PBMC and decidua in first (yellow), second (red) and third trimester (blue) of pregnancy of normal rhesus macaques. **(B)** Memory phenotype of γδ T lymphocytes. **(C)** Phenotype of activation, exhaustion, cytotoxic potential and chemokine receptor expression in γδ T lymphocytes. **(D)** Representative flow plot of Vγ9 and Vδ2 chains and the Vγ9 and Vδ2 subsets in PBMC and decidua. P-values < 0.05 (unpaired t-test) shown on the plots.

double negative Vγ9– Vδ2– subset was increased in the decidua, although not significantly (**Figure 6D**).

Global Analysis of Innate Immune Cells in Decidua and PBMC

To analyze global differences of innate leukocytes of the peripheral blood compared to decidua, we performed a tSNE analysis on the 18-color innate cell panel. Only live CD45+ CD3– CD20–cells were included in the computation. Stark differences could be observed between the PBMC and the decidual cells (**Figure 7A**). The top half of the tSNE shows clusters 1,2,3,4,5 which consist of NK cells based on their CD8+ and HLA-DRlo/– expression (**Figures 7A, B**). In decidua, cluster 4 was a dominant cluster of CD16– CD56+ NK cells which was absent in the PBMC tSNE. On the other hand, peripheral blood NK cells like those present in cluster 3 exhibited a CD16+ CD56– or CD16– CD56– phenotype (**Figures 7A, B**). The lower half of the tSNE expresses HLA-DR+ which by the removal of CD20+ cells in the gating preceding tSNE analysis is consistent with myeloid antigen-presenting cells (APCs). Cluster 8 is the major myeloid APC subset in the decidua which is absent in PBMC and is likely mostly comprised of monocytes or macrophages based on CD14 and CD163 expression (**Figures 7A, B**). In the PBMC, clusters 7 and 9 are predominant subsets which are rare in the decidua. Based on gradient expression of CD14, CD16, and CD163, cluster 7 is likely classical monocytes based on CD14+ CD16– CD163+ events, while cluster 9 is consistent with intermediate, non-classical monocytes, or conventional DCs (**Figures 7A, B**). Cluster 10 appears to be a pDC population based on CD123 expression. Four additional markers used to perform the tSNE clustering algorithm are shown in **Supplemental Figure 4**.

NK Cells in PBMC and Decidua

The decidual tissue has been reported to be enriched with innate cells such as NK cells in previous non-human primate studies (15). Here, we sought to complement these data by identifying the activation status of innate cells and their unique phenotypes. A distinct phenotype of CD16– CD56+ single-positive NK cells was found to predominate in the decidua (55.3 ± 16.1%), in stark contrast to PBMC where the major NK cell subset identified were

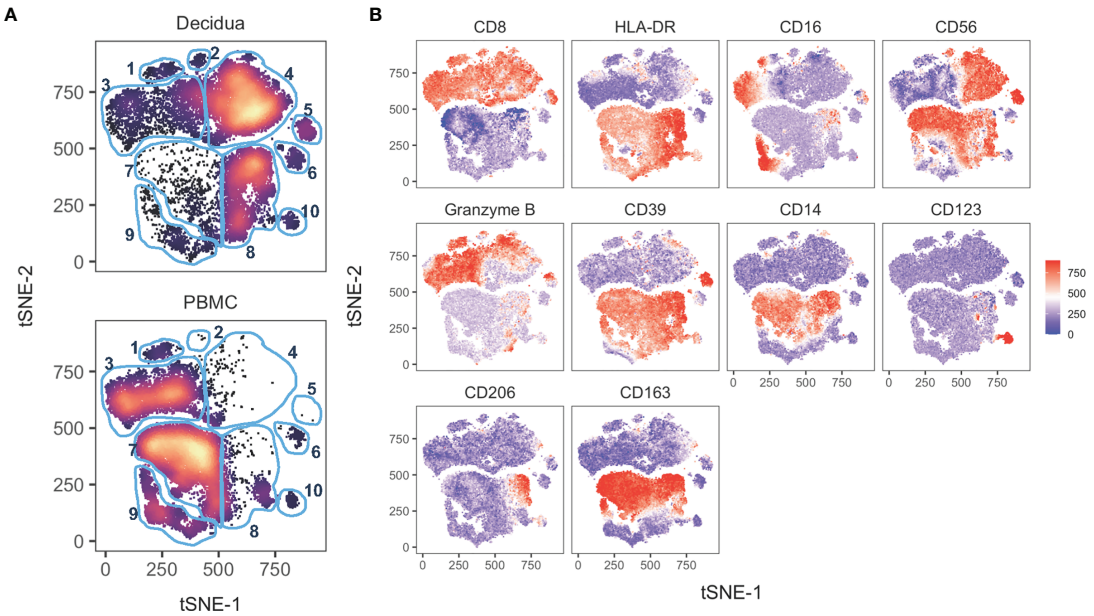

FIGURE 7 | tSNE of 14 innate cell markers of PBMC and decidual leukocytes in normal pregnant rhesus macaques. **(A)** tSNE plot representing an equal number of CD45+/live/single cells/CD3-CD20- cells from decidua (n = 8) and PBMC (n = 11) of rhesus macaques experiencing a normal pregnancy. The 18-color innate panel was used to generate this plot. Blue gates were manually drawn based on clustering patterns. **(B)** Individual MFI gradients of ten markers on the tSNE map. Red coloring represents high MFI and blue coloring represents low MFI. Remaining gradients are found in **Supplemental Figure 4**.

CD16+ CD56– cells (48.2 ± 20.2%) (**Figures 8A, B**). Interestingly, a distinct CD16+ CD56+ population of NK cells was found in the decidual tissue (8.4 ± 5.2%) which was virtually absent in PBMC (**Figure 8B**). These have been described in human decidua as CD56bright and CD16+/dim NK cells (9). In addition, double-negative CD16– CD56– NK cells were significantly increased in the PBMC compared to decidua (**Figure 8B**). NKG2A and NKG2D dual positivity also defined a subset of NK cells found almost exclusively in the decidua (62.9 ± 12.1%) (**Figures 8C, D**). NKG2D+ NKG2A– cells were greatly reduced in decidual NK cells as compared to peripheral NK cells (**Figures 8C, D**).

To analyze the cytotoxic capacity of these cells, we measured the frequency of granzyme B+ cells as well as the MFI, a proxy of intracellular granzyme B content. The frequency and MFI of granzyme B in the cytotoxic CD16+ CD56– and the double-positive CD16+ CD56+ NK subsets were significantly lower in the decidua compared to PBMC (**Figure 8E**). Interestingly, the frequency of granzyme B-positive CD16– CD56+ NK cells was significantly higher in the decidua compared to PBMC; however, the granzyme B MFI of this decidual subset was significantly lower as was true of the other decidual NK subsets (**Figure 8E**). These data show that the dominant decidual CD16– CD56+ NK subset contain high proportions of cytotoxic NK, albeit with less cytotoxicity. It is noteworthy that the frequency of the granzyme B-positive cells in all the NK subsets was highest in third trimester decidua (**Figure 8E**).

Similar to T lymphocytes, decidual NK cells expressed more CXCR3 in both CD56– and CD56+ subsets compared to PBMC (**Figure 8F**). We also evaluated expression of CX3CR1, a chemokine receptor which is upregulated in cells that home to sites experiencing endothelial inflammation and is elevated on a subset of memory CD8+ T lymphocytes and myeloid cells (47). We found decreased expression of CX3CR1 on CD56– NK cells of the decidua (47.8 ± 4.6) compared to PBMC (71.1 ± 11.1) but not in CD56+ NK cells where similar expression levels were found (**Figure 8F**). All of the NK cells in the decidua expressed high levels of the activation marker CD69 ranging from 42.7% to 94.9%, which is similar to levels observed in αβ and γδ T cells (**Figures 5A, B**, **6C**, **8F**). In contrast, CD69 expression on peripheral blood NK cells never exceeded 39.3% (**Figure 8F**). We also evaluated expression of the sialo-adhesin molecule CD169, a marker of activation, which has been previously reported to be present on >60% of CD16+ decidual NK cells in macaques (48). The frequency of CD169+ NK cells was significantly higher in decidua compared to PBMC, but was only found on 0.4-4.4% of total NK cells in our study (**Figure 8F**).

In a recent single cell RNA sequencing analysis of human first trimester maternal-fetal interface, three NK cells subsets were defined by combinations of NKG2A, NKG2C, CD39, Granzyme B, and CD103 expression (37). These were termed dNK1, dNK2, and dNK3 where dNK1 expressed many HLA-C binding molecules and was the only subset to express LILRB1 that can bind dimeric HLA-G. dNK1 was found to be the subset with most cytotoxic potential by granzyme A, granzyme B, perforin, and granulysin followed by dNK2 and dNK3. We defined dNK1 as NKG2A+, CD39+, granzyme B+ NK; dNK2 as NKG2A+, CD39–, Granzyme B+ NK; and dNK3 as CD103+ granzyme B– NK (**Figure 8G**). Between the 28-color and 18-color flow panels, we

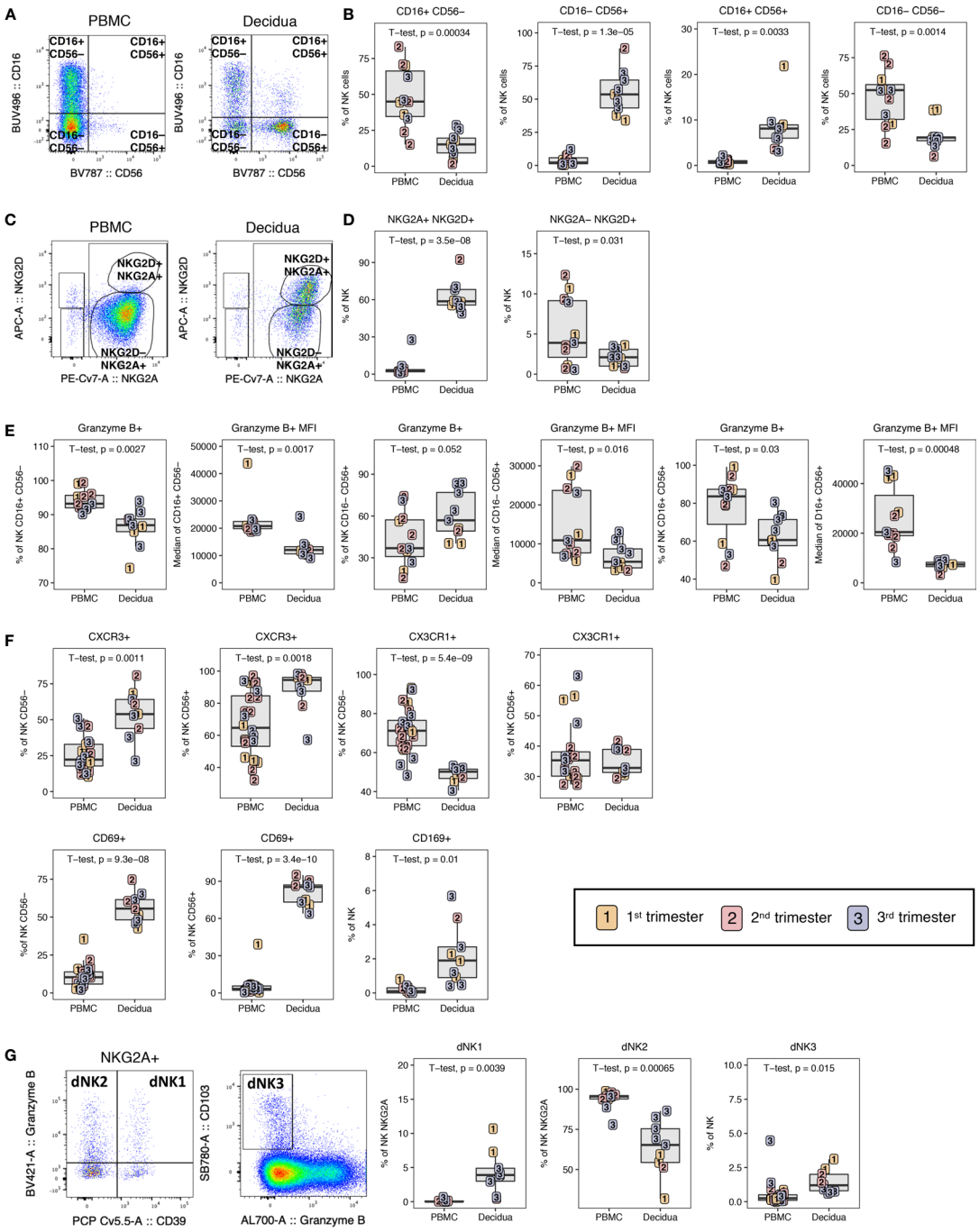

FIGURE 8 | NK cell composition in PBMC and decidua of normal rhesus macaque pregnancies. **(A)** Representative flow plots of NK cells CD16/CD56 subsets. **(B)** NK cell subset frequencies in PBMC and decidua first (yellow), second (red) and third trimester (blue) of normal pregnant rhesus macaques. **(C)** NKG2A/NKG2D flow plots with representative gating of PBMC and decidua. **(D)** Frequency of NKG2A+NKG2D+ and NKG2A-NKG2D+ NK cells in PBMC and decidua. **(E)** Granzyme B expression frequency and MFI on NK cell subsets. **(F)** CD56- *vs* CD56+ NK cell expression of CXCR3, CX3CR1, CD69 and the CD169 on total NK cells. **(G)** Representative flow plot of dNK1, dNK2, and dNK3 subsets with box plots showing their frequency in PBMC and decidua. P-values < 0.05 (unpaired t-test) shown on the plots.

could readily identify all three dNK subsets in decidua samples from the rhesus macaques (**Figure 8G**). dNK2 was the most common phenotype in both PBMC and decidua while dNK1 and dNK3 were only consistently found in decidua (**Figure 8G**).

Myeloid Cells in PBMC and Decidua

Using the gating strategy shown in **Figure 9A** on HLA-DR+ CD3– CD20– CD45+ leukocytes in the 18-color innate panel, we identified a similar proportion of classical monocytes or

macrophages (CD14+ CD16–) in PBMC and decidua (**Figure 9B**). CD14+ CD16+ intermediate monocytes were significantly increased in the decidua while non-classical monocytes and dendritic cells (CD14– CD16+/– CD123–) were found at a higher frequency in the PBMC compared to decidua (**Figure 9B**). pDCs, which express CD123, were more abundant in the decidua compared to the PBMC, though not significantly. CD14+ CD163+ CD206+ macrophages were detected at high frequency in the decidua (44.7 ± 16.2%) and were not detected in PBMC (**Figure 9B**). In contrast, single positive CD14+ CD163+ CD206– myeloid cells were predominantly found in the PBMC (84.4 ± 11.3%). Double negative CD14+ CD163– CD206– myeloid cells were highest at the first and second trimester of gestation but were not significantly different between PBMC and decidua (**Figure 9B**). We also assessed the expression of CD169 and CD69 on myeloid cells to determine their activation status. We found that the decidual classical and intermediate monocytes had an increased expression of CD169 (34.2% ± 21.5% and 70.5% ± 20.7 respectively) compared to PBMC (1.0% ± 1.7 and 11.8% ± 9.4 respectively) (**Figure 9C**). DC and monocyte/macrophage subsets (HLA-DR+ CD14– CD123–) in decidua also contained significantly higher frequencies of CD69+ and CX3CR1+ cells when compared to PBMC (**Figure 9C**). These data support increased activation status and migration capability of decidual macrophages and DC populations.

Changes in Decidual Leukocytes With Gestation Age

To assess temporal gestational effects on decidual immune cell composition, the frequency of major decidual cell populations were correlated with gestational age in days (**Supplemental Figure 1**). Neither T nor B lymphocytes showed a change with gestation (**Supplemental Figure 1**). In contrast, Tregs had a correlative increase with gestation while γδ T cells and iNKTs trended towards an increase (**Supplemental Figure 1**). In the innate compartment, neither total NK cell frequency nor any NK cell subset proportion were significantly different with gestation (**Supplemental Figure 1**). We identified a significant increase in CD14+ CD163+ CD206– decidual macrophages cells with gestation, with a corresponding decrease of CD14+ CD163– CD206– macrophages (**Supplemental Figure 1**). Both pDCs and DC/non-classical monocytes decreased with gestation, though the decrease in pDCs was not significant (**Supplemental Figure 1**).

Among naïve and memory T lymphocyte subsets, several memory CD4+ T lymphocyte subsets showed significant changes with gestational age (**Supplemental Figure 5**). These included gestational dependency of central memory CD4+ T lymphocytes with a highly significant positive correlation (R^2 0.8267; p-value >0.001) with increasing gestation age (**Supplemental Figure 5**). This coincided with significant declines in CD4+ Tem, CD4+ TEMRA and activated/proliferating Ki67+ memory CD4+ T lymphocytes in the decidua (**Supplemental Figure 5**). Expression of CCR5 on CD4+ and CD8+ T memory cells also showed significant negative correlation with gestational age (**Supplemental Figure 5**). For Th1-like cells assessed by CXCR3 expression, Th2-like cells assessed by CCR4 expression, and Th17-like cells assessed by CCR6, no correlative relationships were observed with gestational age (**Supplemental Figure 5**). A significant positive correlation between CD4+ memory T lymphocytes PD-1 and HLA-DR expression was observed in the PBMC but not the decidua (**Supplemental Figure 5**) indicating a discordance of activated/exhausted memory CD4+ T between the two compartments.

PCA Analysis of PBMC and Decidual Leukocytes

To help interpret what most distinguishes the PBMC and decidual leukocytes in normal rhesus macaques, a Principal Component Analysis (PCA) was performed using all of the populations manually gated from samples stained with both the 28-color adaptive panel and 18-color innate focused panel (**Figure 10**). Despite a range in gestation, the PBMC samples from pregnant macaques clustered tightly in the right-hand quadrant. The decidual leukocytes clustered away from the PBMC by principal component 1 (PC1) and were more spread, indicating their lack of similarity to PBMC and highlighting the heterogeneity of the tissue. Populations which contributed most prominently to PC1 were innate NK cells and many types of T lymphocytes expressing the activation marker CD69. This coincides with differences manifest in the tSNE analysis in **Figures 3**, **7**. By principal component 2 (PC2), the decidual leukocytes are less well-clustered together while a longitudinal pattern of gestational age is apparent. The major contributors to PC2 are memory CD4+ T lymphocyte proliferation markers and frequencies of different innate cells (**Figure 10**).

ZIKV Impact on Maternal Immunity

To investigate the impact of ZIKV on the leukocytes of the peripheral blood and decidua, we studied dams infected with ZIKV during pregnancy in comparison to normal, uninfected rhesus macaques. Placenta was collected from 10 ZIKV-infected dams either at second trimester spontaneous abortion (n=1) or at near term C-section (n=9); details are described in **Supplementary Table 2**. We found that the frequency of total T lymphocytes out of live CD45+ leukocytes was increased in the ZIKV-infected dams compared to the uninfected dams (**Figure 11A**). Within the traditional αβ T cells there were no indications of changes in CD4/CD8 proportions or their memory subtypes to explain the increase in T cells (data not shown).

To determine whether ZIKV infection affected immune function, we assessed the expression of HLA-DR (activation), CXCR3 (activation and trafficking), Ki67 (activation and proliferation), and granzyme B (cytotoxicity) on decidual T lymphocytes in ZIKV-infected dams and compared with decidua of normal pregnancies. A significant decline in HLA-DR+ activated memory CD4+ and CD8+ T lymphocytes was observed in ZIKV-infected decidua as compared to normal decidua (**Figures 11B, C**). Coinciding with the lack of HLA-DR, Ki67+ memory CD4+ T lymphocytes were also significantly decreased in the infected animals compared to normal decidua (**Figure 11B**). Other notable changes on memory T lymphocytes in decidua of ZIKV-infected dams including a significant decrease in frequency of CXCR3 positive cells in both CD4+

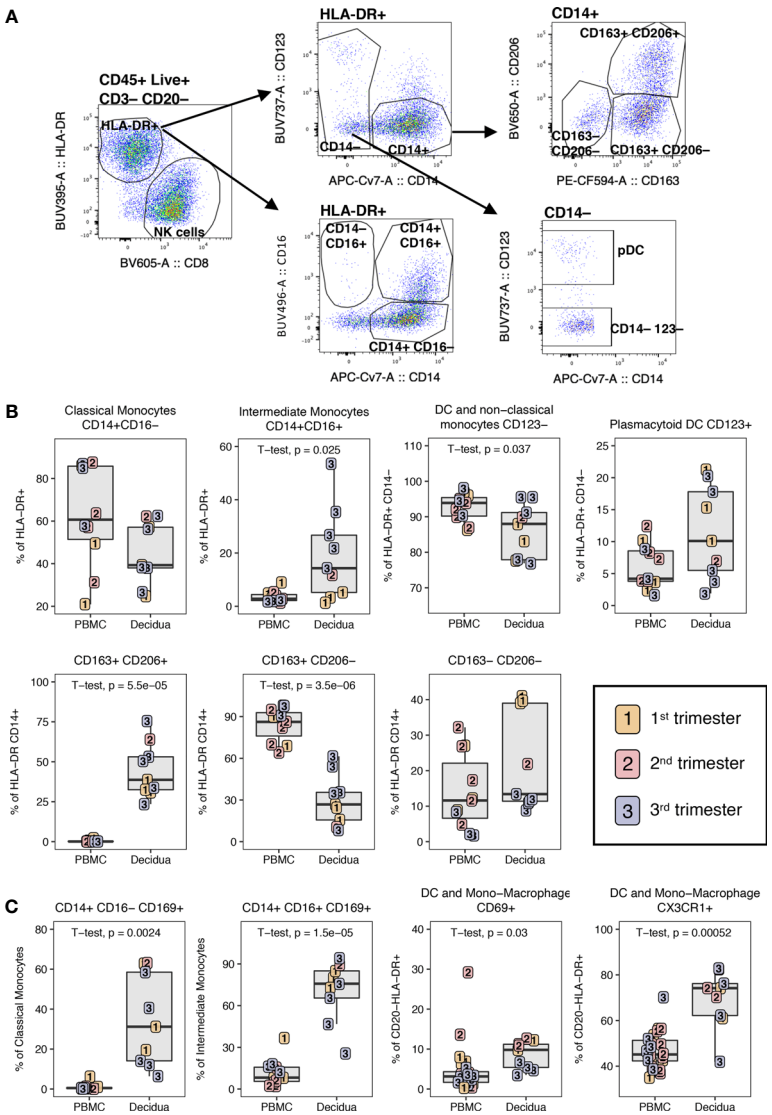

FIGURE 9 | Phenotype of dendritic cells and monocyte/macrophage in PBMC and decidua of normal pregnant rhesus macaques. **(A)** Representative flow plot and gating of HLA-DR+ myeloid cells. **(B)** Frequency of monocyte/macrophage and DC subsets in PBMC and decidua first (yellow), second (red) and third trimester (blue) of normal pregnant rhesus macaques. **(C)** Phenotype of monocyte/macrophages and DCs with box plots showing their frequency. P-values < 0.05 (unpaired t-test) shown on the plots.

and CD8+ T lymphocytes, and reduced frequency of granzyme B-positive CD4+ T memory cells compared to uninfected decidua (**Figures 11B, C**). A similar pattern of perturbation was observed in decidual γδ T cells of ZIKV-infected dams, namely a significant decrease in HLA-DR, Ki67, PD-1, and granzyme B, indicative of inhibition of activation, proliferation and cytotoxicity of γδ T (**Figure 11D**). Vγ9 and Vδ2 subsets likewise showed a general reduction of proliferative and activation potential by Ki67+ suggesting that the effect was global and not confined to a particular subset of γδ T (**Figure 11E**). In contrast to Ki67, decreased granzyme B expression was confined to the Vγ9+ Vδ2+ subset of γδ T (**Figure 11E**). This subset was recently shown to have the greatest cytotoxic potential and cytokine secretory capacity in healthy adults (49). In addition, decreased PD-1 expression and HLA-DR was confined to the Vγ9+ Vδ2– and Vγ9– Vδ2+ subsets respectively.

To study changes in the innate compartment, we found a loss of total NK cells in ZIKV-infected compared to uninfected dams (**Figure 12A**). These decreases were subset specific, in that the decidual CD16+ CD56+ NK subset showed a significant decrease whereas the CD16– CD56– NK cell subset showed a proportional increase in frequency in ZIKV-infected compared to uninfected macaques (**Figure 12A**). We observed an increase in dNK2 in ZIKV-infected dams while dNK1 and dNK3 were comparable to normal decidua (**Figure 12**). Similar to the changes observed in T cells of ZIKV-infected macaques, CD69

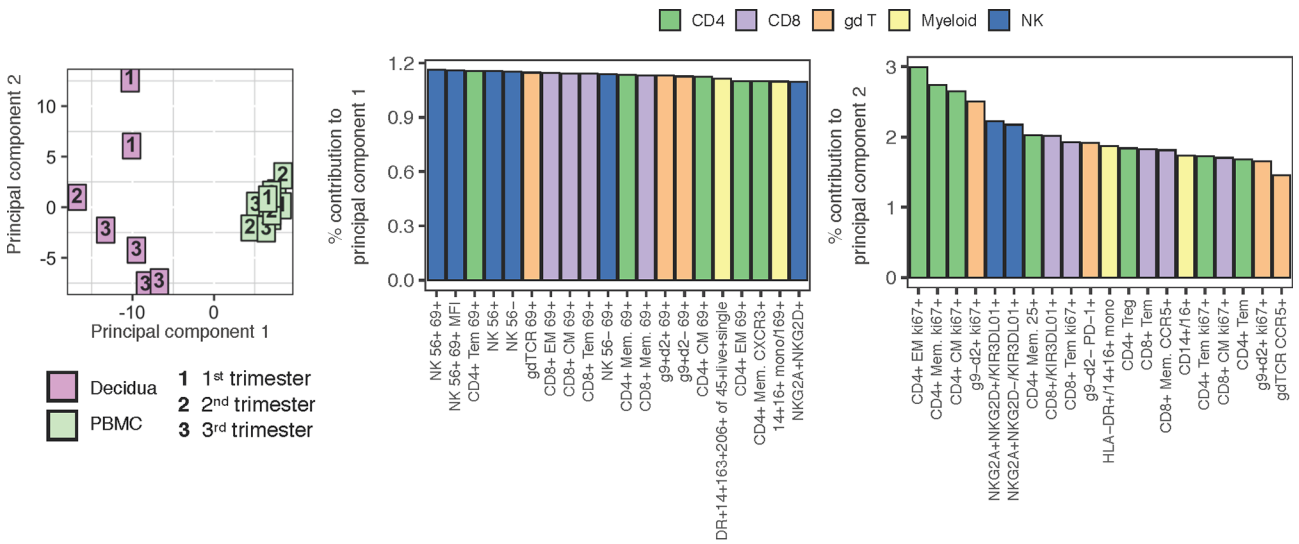

FIGURE 10 | PCA plot using adaptive and innate cell data of PBMC and decidual leukocytes in normal rhesus macaques. A PCA plot was generated using a combination of adaptive and innate immune cells and their features. 217 variables describing frequencies of unique cell types and MFI when applicable (e.g. Granzyme B MFI) were used to contrast PBMC (n = 9) (green) to decidua (n = 7) (pink) samples across 1st, 2nd, and 3rd trimester (left). The top 20 contributing variables to principal component 1 (middle) and principal component 2 (right) are shown and color coded according to major cell populations, CD4+ T (green), CD8+ T (purple), γδ T (orange), myeloid CD20-HLA-DR+ (yellow), and NK cells (blue).

expression on both CD56– and CD56+ NK cells were reduced compared to normal decidua (**Figure 12A**). We did not observe increased CD169 expression on NK cells contrary to a recent study that reported an increase in CD169-positive CD16+ NK cells in the decidua of ZIKV-infected dams (48). Few changes in myeloid cell proportions were observed following ZIKV-infection, although CD14+ CD163– CD206– cells were higher in the decidua of uninfected macaques compared to ZIKV-infected macaques (22.0 ± 13.1% and 8.5 ± 6.4%, respectively, $p = 0.025$).

Similar to changes observed in the decidua, the majority of changes observed in PBMC of ZIKV-infected dams were confined to the T lymphocyte compartment and manifest as a decrease in markers of activation of HLA-DR, Ki67, and PD-1 expression on CD4+ and CD8+ T lymphocyte subsets compared to normal pregnant macaques (**Supplemental Table 4**). In addition to the reduced activation of αβ T lymphocytes, γδ T lymphocytes appeared to be more differentiated by increased TEMRA memory phenotype and the Vγ9+ Vδ2+ had a reduced activation status. Both the CD56– NK cells, and myeloid cells (HLA-DR+ CD20–) showed decreased Ki67 compared to uninfected macaques (**Supplemental Table 3**).

Global Analysis of the Impact of ZIKV on the Maternal-Fetal Interface

To further understand the impact of ZIKV on pregnancy and specifically in the decidua, we performed tSNE and PCA analysis of the decidual leukocytes in comparison to uninfected animals (**Figures 13A–C**). A tSNE analysis of decidual cells computed with data from a 28-color panel focused on the adaptive immune system resolved several notable differences (**Figures 13A, B**). In particular, clusters 2 and 8 appear to be affected by ZIKV infection (**Figure 13A**). Cluster 2 is consistent with CD8 memory T cells by CD3+ CD8+ CD95+ CD28– cells, and cluster 8 are likely myeloid cells defined by CD3– HLA-DR+ CD20– expression (**Figure 13B** and **Supplemental Figure 6**). An additional 16 markers used to compute the tSNE are found in **Supplemental Figure 6**.

tSNE analysis of innate markers using an 18-color panel focusing on the innate immune system further highlighted differences in decidual immune composition after Zika virus infection (**Figures 13C, D**). Prior to computing the tSNE map, dead cells and CD45+ CD3+ or CD45+ CD20+ cells were excluded. The most notable differences appear in clusters 4, 6, and 7. Cluster 4 are tissue macrophages defined by their HLA-DR+ CD14+ CD163+ CD206+ CD39+ CD169+ phenotype (**Figures 13C, D** and **Supplemental Figure 7**). Cluster 7 are CD16– CD56+ NK cells defined by the presence of CD8+ HLA-DR–/lo CD16– and CD56+, and cluster 6 are also NK CD16– CD56+ NK cells with the additional expression of CD39 (**Figures 13C, D** and **Supplemental Figure 7**).

PCA analysis shown in **Figure 13E** determined immune cell subsets that most contributed to the separation between infected and uninfected decidua. The uninfected decidua is found to cluster away from infected tissues by PC1. The top contributors to PC1 were memory T lymphocytes expressing activation and proliferation markers (**Figure 13F**). PC2 did not well separate uninfected from infected samples (**Figure 13E**). Little to no clustering effect was observed between animals with congenital transmission and no congenital transmission of ZIKV (**Figure 13E**). Like the uninfected decidua, there was also wide heterogeneity among ZIKV-infected decidua.

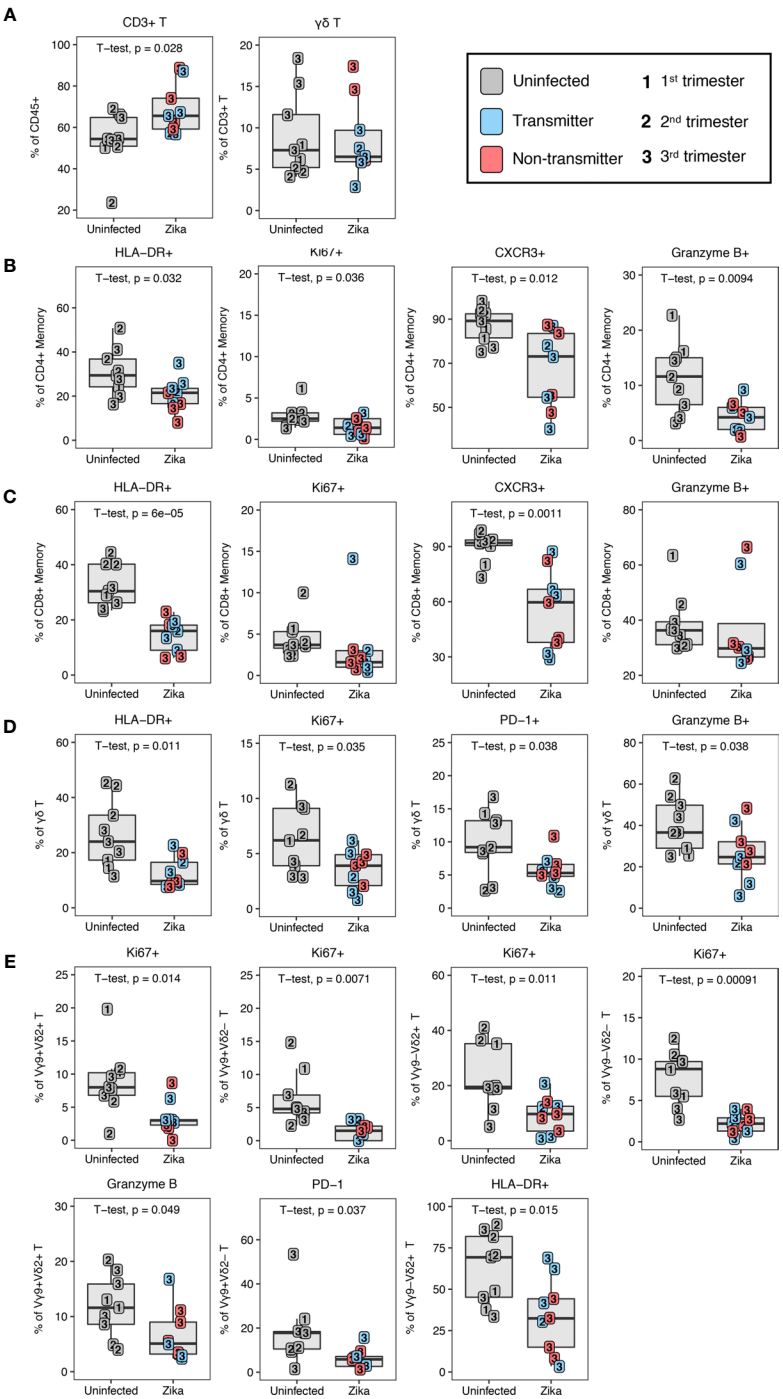

FIGURE 11 | T lymphocyte changes in ZIKV-infected macaques. **(A)** T and γδ T lymphocytes in uninfected (n = 9) (grey) and ZIKV-infected (n = 9) decidual leukocytes. In the ZIKV-infected group, animals with detected amniotic fluid transmission displayed in blue and non-transmitters in red **(B)** Decreased activation of CD4+ T memory in the ZIKV-infected group. **(C)** Decreased activation of CD8+ T memory in the ZIKV-infected group. **(D)** Decreased activation of γδ T lymphocytes in the ZIKV-infected group. **(E)** Decreased decidual γδ T lymphocyte subset activation in ZIKV-infected macaques. P-values < 0.05 (unpaired t-test) shown on the plots.

ZIKV Non-Transmitters Compared to Transmitters

Five of the 10 ZIKV-infected dams had ZIKV RNA detected by PCR in the amniotic fluid. Although we cannot definitively exclude absence of placental transmission in the PCR-negative dams, we compared immune parameters in the amniotic fluid ZIKV PCR positive (transmitters) and negative (non-transmitters) dams. The frequency of single positive CD16–

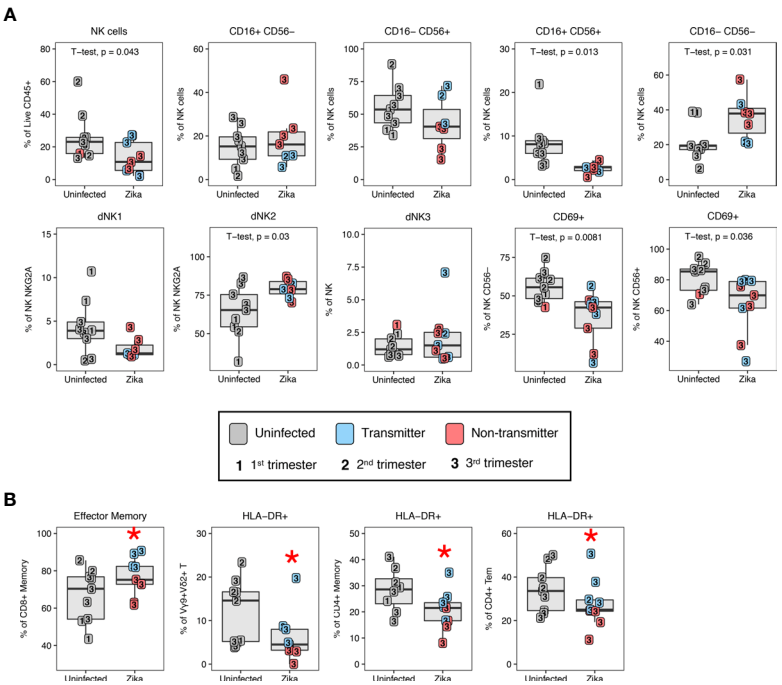

FIGURE 12 | Changes in decidual NK cells in ZIKV-infected dams and immune correlates of transmission. **(A)** Altered NK cell subsets by CD16/CD56, granzyme B, KIR3DL01, and CD169 in the decidual leukocytes of uninfected (n=9) (grey) and ZIKV-infected (n=9) dams. In the ZIKV-infected group, animals with detected amniotic fluid transmission displayed in blue and non-transmitters in red. P-values < 0.05 (unpaired t-test) shown on the plots. **(B)** Immune parameters significantly different between transmitter and non-transmitter dams. P-value <0.05 between transmitters and non-transmitters shown as red asterisk. Normal decidual leukocytes are displayed for comparison.

CD56+ NK cells in the non-transmitter dams (24.4 ± 14.1%) was reduced compared to the transmitter dams (59.7 ± 12.2% (**Figure 12A**). Animals that transmitted also had higher frequencies of CD8+ T effector memory cells compared to non-transmitters (83.5 ± 6.3% compared to 68.2 ± 5.9%, respectively) (**Figure 12B**). Interestingly, macaques that did not transmit ZIKV had the greatest reduction of T cell activation compared to both uninfected and ZIKV-transmitters (**Figure 12B**). For example, HLA-DR expression in Vγ9+ Vδ2+ was reduced from 9.2 ± 5.6% to 2.4 ± 1.4% in non-transmitters, and HLA-DR expression on total CD4+ memory T cells was reduced from 24.6 ± 6.0% to 15.2 ± 4.8% in non-transmitters (**Figure 12B**). CD4+ Tem cells also had a reduced expression of HLA-DR in non-transmitters compared to transmitters (**Figure 12B**).

DISCUSSION

This is the first comprehensive single-cell phenotypic analysis of multiple immune cell subsets in the decidua and peripheral blood of healthy rhesus macaques across the three trimesters of pregnancy. By simultaneously probing conventional T lymphocytes, iNKT, Tregs, γδ T, B lymphocytes, NK cells, monocytes, macrophages and dendritic cells (DC), we could evaluate components of both the innate and adaptive immune system and study their interaction in the setting of normal pregnancy and after ZIKV infection of pregnant macaque. Several findings reported in blood and decidua of human pregnancy were recapitulated in normal rhesus macaque pregnancy reinforcing the value of this NHP model for the study of congenital viral infections. Notable among the similarities between human and NHP decidua were the predominance of the CD16–CD56+ phenotype of NK cells, enrichment of CD4+ Tregs, enrichment of memory CD4+ and CD8+ T lymphocytes, increased activation but decreased cytotoxicity of decidual NK cells and CD8+ T lymphocytes, a predominance of CD206+ macrophages, and a paucity of B lymphocytes (6, 20, 50–52). tSNE analysis of CD45+ live leukocytes on the 28-color adaptive lymphocyte-focused flow cytometry panel and on CD3–CD20–CD45+ live leukocytes on the 18-color innate cell-focused flow panel revealed several clusters representing populations of CD4+ and CD8+ T lymphocytes, NK cells, monocytes or macrophages and DCs that were unique to either peripheral blood or decidua. The immune cell diversity between decidua and PBMC was similar to what was recently reported in humans using a similar approach (53).

Memory T lymphocytes comprise roughly 5-20% of the CD45+ leukocyte population in human decidua from the first trimester and increase with gestational age. As part of the adaptive immune system they are key players in mounting an immune response against foreign antigens in pregnancy (10, 22). Decidual CD8+ T lymphocytes are unique in that they recognize

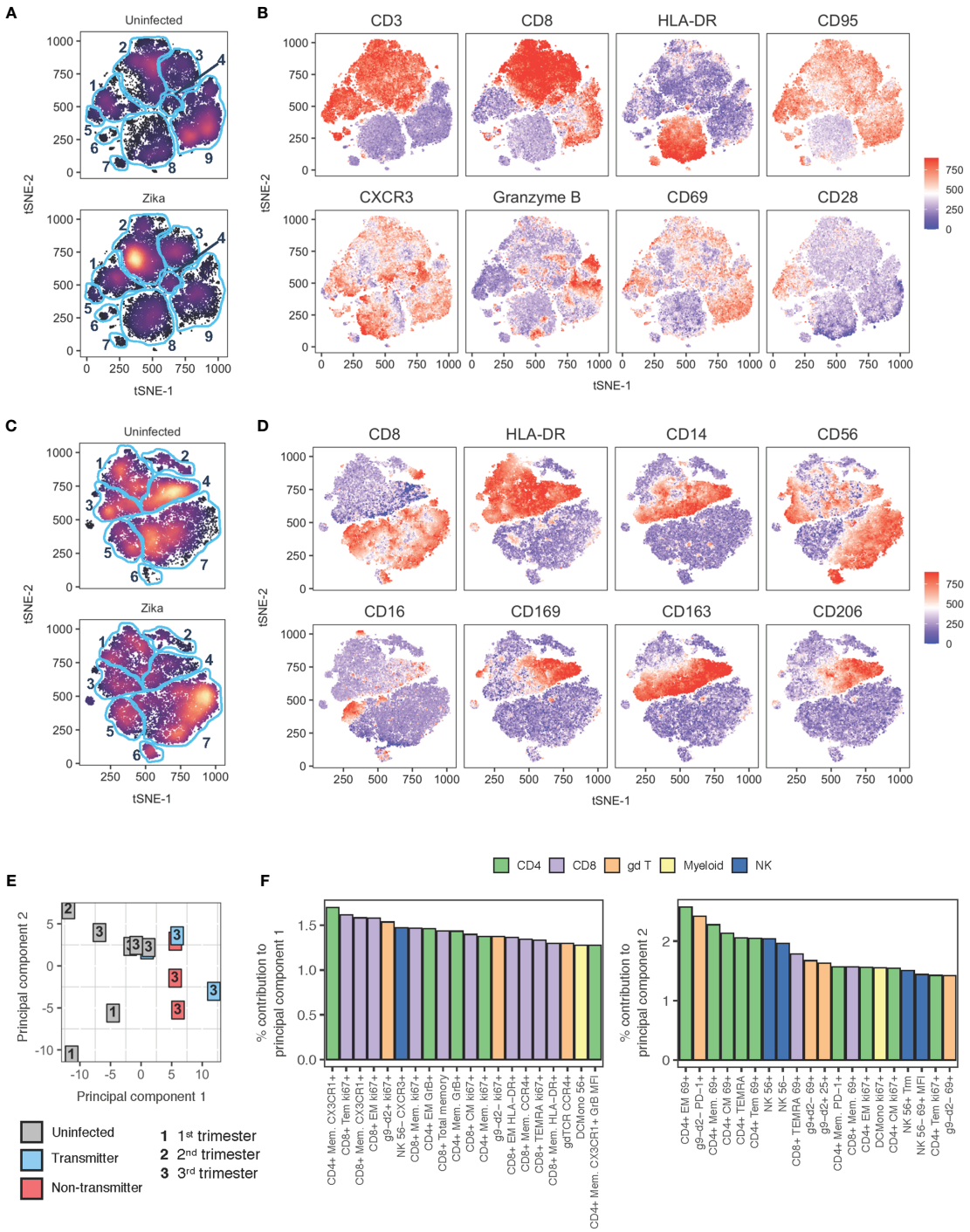

FIGURE 13 | tSNE and PCA analysis of decidual leukocytes of uninfected and ZIKV-infected rhesus macaques. **(A)** tSNE plot representing an equal number of CD45+/live/single cells/leukocytes cells from decidua of rhesus macaques experiencing a normal pregnancy (n = 9) or after ZIKV infection (n = 8). The 28-color adaptive panel was used to generate this plot. Blue gates were manually drawn based on clustering patterns. **(B)** Individual MFI gradients of eight markers on the tSNE map. Red coloring represents high MFI and blue coloring represents low MFI. **(C)** tSNE plot representing an equal number of CD45+/live/single cells/CD3-/CD20- cells from decidua of rhesus macaques experiencing a normal pregnancy (n = 8) or after ZIKV infection (n = 7). The 18-color innate panel was used to generate this plot. Blue gates were manually drawn based on clustering patterns. **(D)** Individual MFI gradients of eight markers on the tSNE map. Red coloring represents high MFI and blue coloring represents low MFI. **(E)** PCA plot of decidual leukocytes of uninfected and ZIKV-infected dams. **(F)** The top 20 contributing variables to principal component 1 (left) and principal component 2 (right) are shown and color coded according to major cell populations, CD4+ T (green), CD8+ T (purple), γδ T (orange), myeloid CD20-HLA-DR+ (yellow), and NK cells (blue).

fetal antigens but remain tolerant to avoid fetal rejection. However, their role in pathogen-specific immunity and the properties of the immune response necessary to clear infections without harming the fetus are not known (23). In our study, we performed an extensive evaluation of the memory phenotype, activation status, cytotoxic granule content, and chemokine receptor expression on memory subsets of both circulating and decidual CD4+ and CD8+ T lymphocytes in pregnancy. T lymphocytes were the dominant leukocyte population in the decidua across all three trimesters with the exception of one second trimester dam in whom NK cells comprised roughly 60% of the decidual leukocyte population (**Figure 2B**). Reciprocally, we did not find NK cells as the dominant decidual population in first trimester. Neither was there a clear trend of decidual NK cells declining with gestation age. These findings are in contrast with humans where NK cells are the dominant leukocyte population in first trimester decidua. Whether this observation represents a species-specific difference in decidual leukocyte composition will require further study in a larger cohort of animals.

Relative to studies on decidual NK cells, data on decidual T lymphocytes are limited particularly for rhesus macaque decidua. A recent study in rhesus macaques at the third trimester of pregnancy used mass cytometry to examine multiple immune subsets including memory T lymphocytes in choriodecidual cells in decidua parietalis as well as in placental villi (54). The decidual leukocytes evaluated in our study were primarily isolated from tissue removed from the maternal surface of the placenta (decidua basalis) and stripped away from chorionic tissue. Using a combination of CD95, CD28, CCR5, CD45RA, CD69 and CD103, we delineated CM, EM, TEM, TEMRA, and tissue-resident Trm memory. Rhesus macaques had significantly higher proportions of EM CD8+ and CD4+ T in the decidua compared to peripheral blood consistent with human data (20, 25, 55). Less clear is the concordance between rhesus macaque and human decidua for other memory subsets. CM CD8+ and CD4+ T lymphocytes were present at significantly lower frequencies in rhesus macaque decidua. One study showed higher frequencies of CM CD4+ and CD8+ T lymphocytes in term human decidua compared to peripheral blood (55). CD4+ TEMRA lymphocytes did not differ between peripheral blood and decidua; however, CD8+ TEMRA were significantly lower in the decidual compartment, contrary to human studies showing a higher proportion of CD8+ TEMRA in the decidua (22). It is noteworthy that in rhesus macaques, the proportion of decidual CM CD4+ T was lowest in the first trimester and highest in the third trimester, a finding that has not previously been reported. The increase in decidual CM CD4+ T with increasing gestation age was associated with a decline in Ki67+ activated memory CD4+ T (both CM and EM subsets) and a decline in CCR5+ CD4 memory and CD8 memory. These changes with gestational age were confined to the decidua and not observed in circulating lymphocytes. Reduced decidual CCR5+ memory CD4+ T with gestation age may have implications for the relative risk of mother-to-child transmission of HIV in different trimesters of pregnancy (56).

Consistent with findings in humans, decidual EM, CM and TEMRA CD8+ T had lower granzyme B content compared to their circulating memory counterparts (20). Of note, the proportion of granzyme B+ TEM and CM CD8+ T lymphocytes was significantly higher in the decidua but their granzyme B content measured by MFI was lower. Thus, decidual CD8+ T contain substantial proportions of Granzyme B-positive cells but likely are less cytotoxic compared to circulating memory CD8+ T lymphocytes. With respect to effector function, the majority of decidual memory CD4+ and CD8+ T were highly activated and skewed to a Th1 phenotype as evidenced by high proportions expressing CD69, HLA-DR, and CXCR3. This was in striking contrast to circulating memory T lymphocytes that were less activated and showed a mixture of Th1 (CXCR3+), Th2 (CCR4+), and Th17 (CCR6+, CCR4+) cells and is similar to findings in humans (55). In concert with high levels of activation, decidual CD4+ and CD8+ T lymphocytes contained significantly higher levels of PD-1+ cells compared to circulating memory T lymphocytes but not in a correlative manner like the PBMC. This is not surprising in light of studies showing expression of immune inhibitory check-point receptors on human decidual T lymphocytes as one likely mechanism by which decidual T lymphocytes maintain concurrent effector function and a tolerogenic phenotype during pregnancy (21, 57).

In addition to conventional T lymphocytes, CD4+ Tregs, iNKT and γδ T lymphocytes accounted for roughly 20% of the total decidual T (CD3+) lymphocyte population. Tregs play an essential immunosuppressive role in inhibiting alloreactive T cells and maintaining tolerance during normal pregnancy. As in humans, CD4+ CD25bright CD127lo Tregs in rhesus macaques were present at significantly higher frequencies in the decidua compared to peripheral blood and showed a significant increase with gestation age. Human studies of normal pregnancy have shown that decidual Treg frequencies remain unchanged (d. basalis) or increase (d. parietalis) at term gestation (51, 58–60). A recent study provided evidence for clonally expanded effector Tregs, likely containing fetal antigen-specific Tregs, increasing in the 3rd trimester of normal pregnancy but decreasing in preeclampsia (61). While we did not characterize the type of decidual Tregs in this study, the findings of CD4+ Tregs enrichment in macaque decidua and its relationship to gestation age appear similar to human decidua.

Among other immunomodulatory T lymphocytes, low frequencies of decidual iNKT were detected at levels comparable to peripheral blood. It should be noted that the method of iNKT detection is an important consideration for comparison with studies reporting on NKT lymphocytes. Several publications including one on macaque decidua have defined NKT as CD3+CD56+ T lymphocytes (62). This is erroneous and does not represent genuine iNKT lymphocytes (63). We used T lymphocyte expression of the Vα24 TCR along with binding to α-galactoslyceramide(GC)-loaded CD1d tetramers for specific and stringent identification of iNKT lymphocytes as described in humans and nonhuman primates (43, 64). In our study, CD3+CD56+ T lymphocytes were enriched in the decidua with mean frequency of 21.7% of T lymphocytes as compared to <5%

of T lymphocytes in peripheral blood. Yet, less than 1% of decidual CD56+ T were genuine iNKT as defined by Vα24+ T lymphocytes binding to αGC-loaded CD1d tetramer. Moreover, all Vα24+ CD1d-tetramer-positive iNKT lymphocytes did not express CD56. In two studies in humans that used stringent criteria for identification, iNKT were detected in first trimester decidua at low frequencies of <0.5% of CD3+ decidual leukocytes and were present at significantly higher frequencies in the decidua compared to peripheral blood (41, 42).

γδ T lymphocytes are another unconventional T lymphocyte subset that recognize non-peptide antigens in an MHC-independent manner and respond to bacterial and viral infections (65). Early trimester decidua is enriched for γδ T but their role in pregnancy is not well understood (46). In utero CMV infection is associated with expansion of fetal Vγ9– γδ T lymphocytes (66). In one study ZIKV infection in humans was associated with expansion of Vδ2+ γδ T in the peripheral blood (67). To our knowledge there are no published data on decidual γδ T in rhesus macaques. Using a NHP cross-reactive pan-γδ TCR antibody along with antibodies specific for the Vγ9 and Vδ2 TCR chain, four populations of γδ T were defined of which the Vγ9–Vδ2– subset formed the bulk of the γδ T lymphocytes in the decidua and peripheral blood. γδ T lymphocytes showed higher frequencies in the decidua particularly at third trimester gestation. Of total γδ T cells, the Vδ2 subset is significantly higher in blood of healthy human donors compared to early gestation decidua (46). The same conclusion can be inferred in rhesus macaques as the dominant Vγ9+Vδ2+ population was significantly higher in the peripheral blood compared to the decidua. Similar to the conventional T lymphocytes, decidual γδ T were highly activated and enriched for effector memory cells in the decidua. These data suggest that despite being a relatively small population, decidual γδ T also have the capability to be potent effectors. Their role in protective immunity at the maternal-fetal interface remains to be determined. Of interest, ZIKV-infected pregnant dams in our study had increased levels of circulating Vδ2+ γδ T compared to normal pregnancies. In the ZIKV-infected dams, the decidual γδ T had a reduced proliferation potential similar to the memory CD4+ T but also reduced PD-1 expression. This may suggest that decidual γδ T are less exhausted and could have effector function in the face of a viral infection.

Among innate leukocytes we evaluated NK cells, monocytes/macrophages and dendritic cells in the decidua and peripheral blood of normal pregnancy. Based on co-expression of the scavenger receptor CD163 and the mannose receptor CD206, three populations of decidual macrophages were detected of which the dual positive CD163+ CD206+ subset was only seen in the decidua. A CD163+ CD206– decidual macrophage population was present but at a significantly lower frequency compared to peripheral blood where this monocyte subset was dominant. The two populations of CD163+ decidual macrophages appear to be phenotypically analogous to the CD11c(lo) and CD11c(hi) subsets with distinct gene expression profiles described in humans (50). Although neither subset is precisely M1- or M2-polarized, the gene profile of the CD11c(lo) CD206+ subset resembles M2-polarized macrophages. It is noteworthy that the CD163+CD206– decidual macrophage population increased with gestational age as did the frequency of CD14+CD16+ inflammatory monocytes. These changes likely reflect the plasticity of the decidual macrophages moving to a more inflammatory phenotype as pregnancy progresses to term.

NK cells are the most abundant decidual leukocyte population in the first trimester of pregnancy and essential for implantation of the placenta through their interactions with extravillous trophoblasts. Decidual NK cells are phenotypically and functionally distinct from NK cells in the circulation and at other tissue sites and constitute a diverse population of tissue-resident innate lymphoid cells (68). Recent studies on first trimester human decidua using single cell RNAseq and mass cytometry have revealed several novel populations including dNK1, dNK2, and dNK3 based on their gene expression profile, phenotypic markers and function (11, 37). In this study we complemented evaluation of macaque NK subsets based on CD16 and CD56 co-expression patterns with NKG2A, CD39, CD103 and Granzyme B to define putative dNK1, dNK2 and dNK3 populations in macaques. These definitions were adapted from and based on the single cell gene expression, flow cytometry and mass cytometry profile of human first trimester decidua (11, 37). By flow cytometry, we defined dNK1 as NKG2A+ CD39+ granzymeB+ NK; dNK2 as NKG2A+ CD39+ granzymeB+ NK; and dNK3 as CD103+ granzymeB– NK. CD39 is a surface bound ectonucleosidase enzyme which is upregulated during inflammatory conditions. It is constitutively expressed in the placenta and is found on many immune cell subsets such as Tregs, NK cells, monocyte/macrophages, and dendritic cells. CD39 along with CD73 can convert ATP to adenosine leading the extracellular environment from a proinflammatory to immunosuppressive environment (69). tSNE analysis of the 28-color and 18-color flow cytometry panel revealed several unique non-overlapping clusters for NK cells in decidual and circulating leukocytes. With manual gating, several expected and novel observations were made. Consistent with previous studies in humans and macaques, the majority of decidual NK cells were CD56+CD16– (7, 9, 15, 16). This was in contrast to circulating NK cells in macaques that are predominantly CD16+CD56– (38). Macaque decidua also contained a clearly discernible population of CD16+ CD56+ double-positive NK cells that were not detected in peripheral blood. A similar double-positive NK population has been reported in vaginal and rectal mucosal tissues of rhesus macaques (70). To our knowledge this is the first report of CD16+CD56+ NK cells in macaque decidua. Similar to humans, granzyme B content in the decidual NK subsets was lower than their circulating phenotypic counterparts. When analyzed for dNK1-3 subsets on the basis of CD39, granzyme B and CD103 expression, the dominant dNK2 population was significantly lower in the decidua compared to peripheral blood. The dNK1 and dNK3 subsets constituted a small population of NK cells which was present at higher frequencies in the decidua. The dNK1 and dNK3

decidual populations were lower in the third trimester compared to the first trimester, whereas the dNK2 decidual population increased from the first to the third trimester. These data are consistent with the known functions of human dNK1 cells expressing high levels of KIRs and interacting with HLA-C molecules on extra-villous trophoblasts to promote placentation in the first trimester (11). Macaque decidual NK cells also contained a high frequency of NKG2A+NKG2D+ NK cells that were absent or detected at low frequencies in the circulation. NKG2D is a C-type lectin-like activating receptor expressed on NK cells and T lymphocyte subsets. In a study of first trimester human decidua, NKG2D was expressed on all CD56+ decidual NK and surface expression of the NKG2D ligands, UL16 binding protein and the stress-inducible MHC-Class I related chain molecules (MIC), was detected on extra-villous trophoblasts, villous trophoblasts, and decidual macrophages (71). A significant increase in NKG2D expression was observed in second trimester decidual NK as compared to first trimester (72). NKG2D was also shown to be involved in the cytotoxic effector function that decidual NK acquire *in vitro* on exposure to human CMV-infected autologous fibroblasts (73). Because the anti-NKG2A antibody in rhesus macaques does not differentiate between the inhibitory receptor NKG2A and the activating receptor NKG2C, we cannot be certain whether the NKG2D+ decidual NK cells co-express NKG2A or NKG2C (74). However, in light of the human data, it is likely that the NKG2A+NKG2D+ NK population in macaque decidua is a cytotoxic population. Similar to the T lymphocyte subsets in macaque decidua, the majority of decidual NK cells were significantly more activated than circulating NK cells as evidenced by surface expression of CD69, CXCR3 and CD169 molecules. The chemokine receptor CX3CR1 was also expressed on decidual NK cells but at lower frequencies compared to circulating NK cells.

Our analysis of decidual and circulating leukocytes from a ZIKV infection study in pregnancy in comparison to normal decidua yielded unexpected and interesting findings. In human studies, patients with ZIKV infection are reported to have increased DN T cells and increased activated CD8+ T cells when compared to healthy controls. Furthermore, nonclassical T cell subsets such as double negative (CD4-CD8-) Vδ2 TCR+ T cells are increased in ZIKV infected individuals which correlate with acute resolution of symptoms. This suggests that Vδ2 TCR+ T cells play a role in resolution in ZIKV symptoms (67). Based on these data, ZIKV could potentially disturb the balance at the maternal-fetal interface, as early gestation decidua has an increased frequency of γδ T cells compared to matched maternal blood (46). *In vitro* studies have shown that ZIKV can infect and replicate in human placental macrophages or Hofbauer cells, viral replication coincides with type I interferon induction, and anti-viral gene expression and pro-inflammatory cytokines (75). The mechanism of transmission is thought to by direct infection of Hofbauer cells and disrupting placental barrier. The role of decidual immunity is unknown as few studies have investigated tissue level cellular immunity to ZIKV despite its broad tissue trophism (76). To our surprise, the most striking finding in decidual cells from ZIKV-infected dams was a decrease in NK cells and increase in total T lymphocytes with significant reduction in activated (HLA-DR+ and/or Ki67+) memory CD4+ and CD8+ T and γδ T lymphocytes, reduced frequency of decidual Granzyme B+ CD4+ T and γδ T lymphocytes and reduction in CXCR3+ memory CD4+ and CD8+ T lymphocytes. We also saw a reduction in circulating DN T lymphocytes and a significant reduction in activated, proliferating, and PD-1-positive memory CD4+ T, memory CD8+ T, γδ T, and NK cells in ZIKV-infected dams as compared to healthy pregnant macaques. Overall, these data suggest an immunosuppressive effect with suppression of inflammation and decreased immune recruitment of decidual memory T cells at the maternal-fetal interface. Our findings raise the possibility that the prolonged ZIKV viremia reported in pregnant humans and macaques (29, 77, 78) is related to the immunosuppressive effect of ZIKV infection. Immunosuppression has been reported with Asian-lineage ZIKV related to suppression of type I interferon responses and induction of a M2 anti-inflammatory type transcription phenotype of monocytes ex vivo. But no changes in T cell phenotype were observed in this study (79).

The immunosuppressive effects we have observed in this study are in contrast to the autoimmunity (loss of immune suppression) type of symptoms by Guillain-Barré syndrome that may arise in conjunction with ZIKV infection (76). It is possible that ZIKV induces autoimmunity of the circulating leukocytes while at the tissue-level of the already tolerant maternal-fetal interface, the immune cell environment is silenced by loss of T cell activation and reduced infiltration of CXCR3-expressing CD4+ and CD8+ T lymphocytes which are inflammation-homing T cells. The CXCL10-CXCR3 axis is important in attracting effector T cells to decidual tissue (23). In mice epigenetic silencing of T cell chemoattractant genes in decidual stromal cells led to impaired accumulation of decidual effector T lymphocytes (80). CXCR3 blockade eliminated decidual CD8+ T cell infiltration and protected against in utero fetal infection and immunopathogenesis in a murine model of Listeria infection (81). The question of whether or not the immunosuppressive effects in the maternal decidua reflected an impaired virus-specific cellular immune response or protected against immunopathology are unresolved and will require future prospective studies.

The overall picture of the NHP maternal-fetal interface emerging from our study is that of a complex, dynamic immune environment with capability of robust effector activity balanced with features of a tolerogenic phenotype. Normal macaque decidua is populated with a dominance of memory T lymphocytes, CD8+ more than CD4+, throughout the gestation period with a subset showing markers of tissue-resident memory. The majority of memory CD4+ and CD8+ T, and γδ T lymphocytes are highly activated with a CXCR3+ Th1 phenotype but a significant proportion also express PD-1. Higher frequencies of cytotoxic memory T lymphocytes with less granzyme B content at the single cell level compared to their circulating counterparts are detected in the decidua. Decidual

NK cells are phenotypically distinct with a dominance of cytotoxic CD56+ NK cells that co-express NKG2D and NKG2a/c. Similar to memory T lymphocytes, the majority of decidual NK cells are activated and express CXCR3 but have lower granzyme B content compared to their circulating counterparts. In the myeloid lineage, we found a population of tissue-resident CD163+ CD206+ macrophages which were unique to the decidual environment. We also found a strong presence of tolerogenic CD4+ Tregs which correlated with gestational age in the decidua. In all, these features identify the maternal-fetal interface as a distinct and unique environment that pathogens need to navigate for vertical transmission to the fetus. Our findings of reduced activation, reduced CXCR3 expression and reduced cytotoxicity of decidual memory T lymphocytes in ZIKV infection indicate local immunosuppression and impaired immune recruitment as possible mechanisms of vertical transmission.

In conclusion, we have reported on the first deep and comprehensive analysis of immune cells at the maternal-fetal interface and its comparison to circulating leukocytes in a normal rhesus macaque pregnancy model. By extending our analysis to an investigation of changes in the maternal decidua in a cohort of ZIKV-infected dams, we provide novel insights in to immune perturbations following a congenital viral infection. The stark contrasts of the circulating to decidual leukocytes highlights the immunological barrier formed by the maternal-fetal interface and the need to study this in the context of pathogenic infections that can be transmitted from mother to fetus. Such studies are needed to find vaccine targets against congenital infections.

DATA AVAILABILITY STATEMENT

The raw data supporting the conclusions of this article will be made available by the authors, without undue reservation.

ETHICS STATEMENT

The animal study was reviewed and approved by TNPRC and ONPRC IACUC.

AUTHOR CONTRIBUTIONS

MM and AK conceived the study. MM, MF, and AK wrote the manuscript. MM, AK, MF, JH, VR, and NM reviewed the manuscript. MM, LS, ES, DT, DS, JH, and VR helped procure and process samples. MM, LS, and ES performed the experiment. MM, MF, and AK analyzed the data. MM and MF prepared and processed the data for presentation. AK, JH, VR, and NM were responsible for the support of experiments. All authors contributed to the article and approved the submitted version.

FUNDING

Funding was provided by NIH by 1P01AI129859, TNPRC Base Grant OD011104, and ONPRC Base Grant OD011092. Additional funding for the ZIKV-infected study group was provided by the Bill and Melinda Gates Foundation (OPP1152818). Animal samples were available through the ONPRC Pathology tissue distribution program, which is supported by ONPRC NIH Base Grant OD011092.

ACKNOWLEDGMENTS

The authors would like to acknowledge the TNPRC Flow Core, Megan Varnado, Natalie Guy, and Kaitlin Didier for the flow cytometry support. Both the TNPRC and ONPRC veterinary medicine teams provided animal care and procured samples. Teresa Beechwood for shipping samples from OHSU to Tulane. In addition, Blake Schouest is acknowledged for assisting with literature references. The authors would like to thank the NIH Tetramer Core facility for provision of the CD1dTM conjugated to BV421.

SUPPLEMENTARY MATERIAL

The Supplementary Material for this article can be found online at: https://www.frontiersin.org/articles/10.3389/fimmu.2021.719810/full#supplementary-material

REFERENCES

1. Mor G, Aldo P, Alvero AB. The Unique Immunological and Microbial Aspects of Pregnancy. *Nat Rev Immunol* (2017) 17(8):469–82. doi: 10.1038/nri.2017.64
2. Ander SE, Diamond MS, Coyne CB. Immune Responses at the Maternal-Fetal Interface. *Sci Immunol* (2019) 4(31):1–10. doi: 10.1126/sciimmunol.aat6114
3. Schumacher A, Sharkey DJ, Robertson SA, Zenclussen AC. Immune Cells at the Fetomaternal Interface: How the Microenvironment Modulates Immune Cells To Foster Fetal Development. *J Immunol* (2018) 201(2):325–34. doi: 10.4049/jimmunol.1800058
4. Robson A, Harris LK, Innes BA, Lash GE, Aljunaidy MM, Aplin JD, et al. Uterine Natural Killer Cells Initiate Spiral Artery Remodeling in Human Pregnancy. *FASEB J* (2012) 26(12):4876–85. doi: 10.1096/fj.12-210310
5. Tessier DR, Yockell-Lelievre J, Gruslin A. Uterine Spiral Artery Remodeling: The Role of Uterine Natural Killer Cells and Extravillous Trophoblasts in Normal and High-Risk Human Pregnancies. *Am J Reprod Immunol* (2015) 74(1):1–11. doi: 10.1111/aji.12345
6. Bartmann C, Segerer SE, Rieger L, Kapp M, Sutterlin M, Kammerer U. Quantification of the Predominant Immune Cell Populations in Decidua Throughout Human Pregnancy. *Am J Reprod Immunol* (2014) 71(2):109–19. doi: 10.1111/aji.12185
7. Koopman LA, Kopcow HD, Rybalov B, Boyson JE, Orange JS, Schatz F, et al. Human Decidual Natural Killer Cells Are a Unique NK Cell Subset With Immunomodulatory Potential. *J Exp Med* (2003) 198(8):1201–12. doi: 10.1084/jem.20030305
8. Williams PJ, Searle RF, Robson SC, Innes BA, Bulmer JN. Decidual Leucocyte Populations in Early to Late Gestation Normal Human Pregnancy. *J Reprod Immunol* (2009) 82(1):24–31. doi: 10.1016/j.jri.2009.08.001
9. Nishikawa K, Saito S, Morii T, Hamada K, Ako H, Narita N, et al. Accumulation of CD16-CD56+ Natural Killer Cells With High Affinity

Interleukin 2 Receptors in Human Early Pregnancy Decidua. *Int Immunol* (1991) 3(8):743–50. doi: 10.1093/intimm/3.8.743
10. Crespo AC, van der Zwan A, Ramalho-Santos J, Strominger JL, Tilburgs T. Cytotoxic Potential of Decidual NK Cells and CD8+ T Cells Awakened by Infections. *J Reprod Immunol* (2017) 119:85–90. doi: 10.1016/j.jri.2016.08.001
11. Huhn O, Ivarsson MA, Gardner L, Hollinshead M, Stinchcombe JC, Chen P, et al. Distinctive Phenotypes and Functions of Innate Lymphoid Cells in Human Decidua During Early Pregnancy. *Nat Commun* (2020) 11(1):381. doi: 10.1038/s41467-019-14123-z
12. Jabrane-Ferrat N. Features of Human Decidual NK Cells in Healthy Pregnancy and During Viral Infection. *Front Immunol* (2019) 10:1397. doi: 10.3389/fimmu.2019.01397
13. Siewiera J, Gouilly J, Hocine HR, Cartron G, Levy C, Al-Daccak R, et al. Natural Cytotoxicity Receptor Splice Variants Orchestrate the Distinct Functions of Human Natural Killer Cell Subtypes. *Nat Commun* (2015) 6:10183. doi: 10.1038/ncomms10183
14. Dambaeva SV, Breburda EE, Durning M, Garthwaite MA, Golos TG. Characterization of Decidual Leukocyte Populations in Cynomolgus and Vervet Monkeys. *J Reprod Immunol* (2009) 80(1-2):57–69. doi: 10.1016/j.jri.2008.12.006
15. Dambaeva SV, Durning M, Rozner AE, Golos TG. Immunophenotype and Cytokine Profiles of Rhesus Monkey CD56bright and CD56dim Decidual Natural Killer Cells. *Biol Reprod* (2012) 86(1):1–10. doi: 10.1095/biolreprod.111.094383
16. Slukvin II, Watkins DI, Golos TG. Phenotypic and Functional Characterization of Rhesus Monkey Decidual Lymphocytes: Rhesus Decidual Large Granular Lymphocytes Express CD56 and Have Cytolytic Activity. *J Reprod Immunol* (2001) 50(1):57–79. doi: 10.1016/S0165-0378(00)00090-5
17. Laskarin G, Kammerer U, Rukavina D, Thomson AW, Fernandez N, Blois SM. Antigen-Presenting Cells and Materno-Fetal Tolerance: An Emerging Role for Dendritic Cells. *Am J Reprod Immunol* (2007) 58(3):255–67. doi: 10.1111/j.1600-0897.2007.00511.x
18. Vacca P, Cantoni C, Vitale M, Prato C, Canegallo F, Fenoglio D, et al. Crosstalk Between Decidual NK and CD14+ Myelomonocytic Cells Results in Induction of Tregs and Immunosuppression. *Proc Natl Acad Sci U S A* (2010) 107(26):11918–23. doi: 10.1073/pnas.1001749107
19. Tilburgs T, Claas FH, Scherjon SA. Elsevier Trophoblast Research Award Lecture: Unique Properties of Decidual T Cells and Their Role in Immune Regulation During Human Pregnancy. *Placenta* (2010) 31 Suppl:S82–6. doi: 10.1016/j.placenta.2010.01.007
20. Tilburgs T, Schonkeren D, Eikmans M, Nagtzaam NM, Datema G, Swings GM, et al. Human Decidual Tissue Contains Differentiated CD8+ Effector-Memory T Cells With Unique Properties. *J Immunol* (2010) 185(7):4470–7. doi: 10.4049/jimmunol.0903597
21. van der Zwan A, Bi K, Norwitz ER, Crespo AC, Claas FHJ, Strominger JL, et al. Mixed Signature of Activation and Dysfunction Allows Human Decidual CD8(+) T Cells to Provide Both Tolerance and Immunity. *Proc Natl Acad Sci U S A* (2018) 115(2):385–90. doi: 10.1073/pnas.1713957115
22. Kieffer TEC, Laskewitz A, Scherjon SA, Faas MM, Prins JR. Memory T Cells in Pregnancy. *Front Immunol* (2019) 10:625. doi: 10.3389/fimmu.2019.00625
23. Lissauer D, Kilby MD, Moss P. Maternal Effector T Cells Within Decidua: The Adaptive Immune Response to Pregnancy? *Placenta* (2017) 60:140–4. doi: 10.1016/j.placenta.2017.09.003
24. Lissauer D, Piper K, Goodyear O, Kilby MD, Moss PA. Fetal-Specific CD8+ Cytotoxic T Cell Responses Develop During Normal Human Pregnancy and Exhibit Broad Functional Capacity. *J Immunol* (2012) 189(2):1072–80. doi: 10.4049/jimmunol.1200544
25. Powell RM, Lissauer D, Tamblyn J, Beggs A, Cox P, Moss P, et al. Decidual T Cells Exhibit a Highly Differentiated Phenotype and Demonstrate Potential Fetal Specificity and a Strong Transcriptional Response to IFN. *J Immunol* (2017) 199(10):3406–17. doi: 10.4049/jimmunol.1700114
26. Parker EL, Silverstein RB, Verma S, Mysorekar IU. Viral-Immune Cell Interactions at the Maternal-Fetal Interface in Human Pregnancy. *Front Immunol* (2020) 11:522047. doi: 10.3389/fimmu.2020.522047
27. van Egmond A, van der Keur C, Swings GM, Scherjon SA, Claas FH. The Possible Role of Virus-Specific CD8(+) Memory T Cells in Decidual Tissue. *J Reprod Immunol* (2016) 113:1–8. doi: 10.1016/j.jri.2015.09.073
28. Bialas KM, Tanaka T, Tran D, Varner V, Cisneros de la Rosa E, Chiuppesi F, et al. Maternal CD4+ T Cells Protect Against Severe Congenital Cytomegalovirus Disease in a Novel Nonhuman Primate Model of Placental Cytomegalovirus Transmission. *Proc Natl Acad Sci U S A* (2015) 112(44):13645–50. doi: 10.1073/pnas.1511526112
29. Magnani DM, Rogers TF, Maness NJ, Grubaugh ND, Beutler N, Bailey VK, et al. Fetal Demise and Failed Antibody Therapy During Zika Virus Infection of Pregnant Macaques. *Nat Commun* (2018) 9(1):1624. doi: 10.1038/s41467-018-04056-4
30. Schouest B, Beddingfield BJ, Gilbert MH, Bohm RP, Schiro F, Aye PP, et al. Zika Virus Infection During Pregnancy Protects Against Secondary Infection in the Absence of CD8(+) Cells. *Virology* (2021) 559:100–10. doi: 10.1016/j.virol.2021.03.019
31. Carter AM, Enders AC, Pijnenborg R. The Role of Invasive Trophoblast in Implantation and Placentation of Primates. *Philos Trans R Soc Lond B Biol Sci* (2015) 370(1663):20140070. doi: 10.1098/rstb.2014.0070
32. Furukawa S, Kuroda Y, Sugiyama A. A Comparison of the Histological Structure of the Placenta in Experimental Animals. *J Toxicol Pathol* (2014) 27(1):11–8. doi: 10.1293/tox.2013-0060
33. Carter AM. Comparative Studies of Placentation and Immunology in Non-Human Primates Suggest a Scenario for the Evolution of Deep Trophoblast Invasion and an Explanation for Human Pregnancy Disorders. *Reproduction* (2011) 141(4):391–6. doi: 10.1530/REP-10-0530
34. Banerjee P, Ries M, Janaka SK, Grandea AG3rd, Wiseman R, O'Connor DH, et al. Diversification of Bw4 Specificity and Recognition of a Nonclassical MHC Class I Molecule Implicated in Maternal-Fetal Tolerance by Killer Cell Ig-Like Receptors of the Rhesus Macaque. *J Immunol* (2018) 201(9):2776–86. doi: 10.4049/jimmunol.1800494
35. Boyson JE, Iwanaga KK, Urvater JA, Hughes AL, Golos TG, Watkins DI. Evolution of a New Nonclassical MHC Class I Locus in Two Old World Primate Species. *Immunogenetics* (1999) 49(2):86–98. doi: 10.1007/s002510050467
36. Rosenkrantz JL, Gaffney JE, Roberts VHJ, Carbone L, Chavez SL. Transcriptomic Analysis of Primate Placentas and Novel Rhesus Trophoblast Cell Lines Informs Investigations of Human Placentation. *BMC Biol* (2021) 19(1):127. doi: 10.1186/s12915-021-01056-7
37. Vento-Tormo R, Efremova M, Botting RA, Turco MY, Vento-Tormo M, Meyer KB, et al. Single-Cell Reconstruction of the Early Maternal-Fetal Interface in Humans. *Nature* (2018) 563(7731):347–53. doi: 10.1038/s41586-018-0698-6
38. Webster RL, Johnson RP. Delineation of Multiple Subpopulations of Natural Killer Cells in Rhesus Macaques. *Immunology* (2005) 115(2):206–14. doi: 10.1111/j.1365-2567.2005.02147.x
39. Cai Y, Sugimoto C, Arainga M, Alvarez X, Didier ES, Kuroda MJ. *In Vivo* Characterization of Alveolar and Interstitial Lung Macrophages in Rhesus Macaques: Implications for Understanding Lung Disease in Humans. *J Immunol* (2014) 192(6):2821–9. doi: 10.4049/jimmunol.1302269
40. Takahashi N, Sugimoto C, Allers C, Alvarez X, Kim WK, Didier ES, et al. Shifting Dynamics of Intestinal Macrophages During Simian Immunodeficiency Virus Infection in Adult Rhesus Macaques. *J Immunol* (2019) 202(9):2682–9. doi: 10.4049/jimmunol.1801457
41. Boyson JE, Rybalov B, Koopman LA, Exley M, Balk SP, Racke FK, et al. CD1D and Invariant NKT Cells at the Human Maternal-Fetal Interface. *Proc Natl Acad Sci U S A* (2002) 99(21):13741–6. doi: 10.1073/pnas.162491699
42. Tsuda H, Sakai M, Michimata T, Tanebe K, Hayakawa S, Saito S. Characterization of NKT Cells in Human Peripheral Blood and Decidual Lymphocytes. *Am J Reprod Immunol* (2001) 45(5):295–302. doi: 10.1111/j.8755-8920.2001.450505.x
43. Rout N, Else JG, Yue S, Connole M, Exley MA, Kaur A. Paucity of CD4+ Natural Killer T (NKT) Lymphocytes in Sooty Mangabeys Is Associated With Lack of NKT Cell Depletion After SIV Infection. *PLoS One* (2010) 5(3):e9787. doi: 10.1371/journal.pone.0009787

44. Rout N, Greene J, Yue S, O'Connor D, Johnson RP, Else JG, et al. Loss of Effector and Anti-Inflammatory Natural Killer T Lymphocyte Function in Pathogenic Simian Immunodeficiency Virus Infection. *PLoS Pathog* (2012) 8 (9):e1002928. doi: 10.1371/journal.ppat.1002928
45. Hartigan-O'Connor DJ, Poon C, Sinclair E, McCune JM. Human CD4+ Regulatory T Cells Express Lower Levels of the IL-7 Receptor Alpha Chain (CD127), Allowing Consistent Identification and Sorting of Live Cells. *J Immunol Methods* (2007) 319(1-2):41–52. doi: 10.1016/j.jim.2006.10.008
46. Terzieva A, Dimitrova V, Djerov L, Dimitrova P, Zapryanova S, Hristova I, et al. Early Pregnancy Human Decidua Is Enriched With Activated, Fully Differentiated and Pro-Inflammatory Gamma/Delta T Cells With Diverse TCR Repertoires. *Int J Mol Sci* (2019) 20(3):1–18. doi: 10.3390/ijms 20030687
47. Bottcher JP, Beyer M, Meissner F, Abdullah Z, Sander J, Hochst B, et al. Functional Classification of Memory CD8(+) T Cells by CX3CR1 Expression. *Nat Commun* (2015) 6:8306. doi: 10.1038/ncomms9306
48. Hirsch AJ, Roberts VHJ, Grigsby PL, Haese N, Schabel MC, Wang X, et al. Zika Virus Infection in Pregnant Rhesus Macaques Causes Placental Dysfunction and Immunopathology. *Nat Commun* (2018) 9(1):263. doi: 10.1038/s41467-017-02499-9
49. Papadopoulou M, Dimova T, Shey M, Briel L, Veldtsman H, Khomba N, et al. Fetal Public Vgamma9Vdelta2 T Cells Expand and Gain Potent Cytotoxic Functions Early After Birth. *Proc Natl Acad Sci U S A* (2020) 117(31):18638–48. doi: 10.1073/pnas.1922595117
50. Houser BL, Tilburgs T, Hill J, Nicotra ML, Strominger JL. Two Unique Human Decidual Macrophage Populations. *J Immunol* (2011) 186(4):2633–42. doi: 10.4049/jimmunol.1003153
51. Tilburgs T, Roelen DL, van der Mast BJ, van Schip JJ, Kleijburg C, de Groot-Swings GM, et al. Differential Distribution of CD4(+)CD25(bright) and CD8 (+)CD28(-) T-Cells in Decidua and Maternal Blood During Human Pregnancy. *Placenta* (2006) 27(Suppl A):S47–53. doi: 10.1016/ j.placenta.2005.11.008
52. Vacca P, Pietra G, Falco M, Romeo E, Bottino C, Bellora F, et al. Analysis of Natural Killer Cells Isolated From Human Decidua: Evidence That 2b4 (CD244) Functions as an Inhibitory Receptor and Blocks NK-Cell Function. *Blood* (2006) 108(13):4078–85. doi: 10.1182/blood-2006-04-017343
53. Vazquez J, Chavarria M, Li Y, Lopez GE, Stanic AK. Computational Flow Cytometry Analysis Reveals a Unique Immune Signature of the Human Maternal-Fetal Interface. *Am J Reprod Immunol* (2018) 79(1):1–9. doi: 10.1111/aji.12774
54. Toothaker JM, Presicce P, Cappelletti M, Stras SF, McCourt CC, Chougnet CA, et al. Immune Cells in the Placental Villi Contribute to Intra-Amniotic Inflammation. *Front Immunol* (2020) 11:866. doi: 10.3389/fimmu. 2020.00866
55. Feyaerts D, Benner M, van Cranenbroek B, van der Heijden OWH, Joosten I, van der Molen RG. Human Uterine Lymphocytes Acquire a More Experienced and Tolerogenic Phenotype During Pregnancy. *Sci Rep* (2017) 7(1):2884. doi: 10.1038/s41598-017-03191-0
56. Johnson EL, Chakraborty R. HIV-1 at the Placenta: Immune Correlates of Protection and Infection. *Curr Opin Infect Dis* (2016) 29(3):248–55. doi: 10.1097/QCO.0000000000000267
57. Meggyes M, Miko E, Szigeti B, Farkas N, Szereday L. The Importance of the PD-1/PD-L1 Pathway at the Maternal-Fetal Interface. *BMC Pregnancy Childbirth* (2019) 19(1):74. doi: 10.1186/s12884-019-2218-6
58. Erlebacher A. Immunology of the Maternal-Fetal Interface. *Annu Rev Immunol* (2013) 31:387–411. doi: 10.1146/annurev-immunol-032712-100003
59. Salvany-Celades M, van der Zwan A, Benner M, Setrajcic-Dragos V, Bougleux Gomes HA, Iyer V, et al. Three Types of Functional Regulatory T Cells Control T Cell Responses at the Human Maternal-Fetal Interface. *Cell Rep* (2019) 27(9):2537–47 e5. doi: 10.1016/j.celrep.2019.04.109
60. Tilburgs T, Roelen DL, van der Mast BJ, de Groot-Swings GM, Kleijburg C, Scherjon SA, et al. Evidence for a Selective Migration of Fetus-Specific CD4 +CD25bright Regulatory T Cells From the Peripheral Blood to the Decidua in Human Pregnancy. *J Immunol* (2008) 180(8):5737–45. doi: 10.4049/ jimmunol.180.8.5737
61. Tsuda S, Zhang X, Hamana H, Shima T, Ushijima A, Tsuda K, et al. Clonally Expanded Decidual Effector Regulatory T Cells Increase in Late Gestation of Normal Pregnancy, But Not in Preeclampsia, in Humans. *Front Immunol* (2018) 9:1934. doi: 10.3389/fimmu.2018.01934
62. Presicce P, Senthamaraikannan P, Alvarez M, Rueda CM, Cappelletti M, Miller LA, et al. Neutrophil Recruitment and Activation in Decidua With Intra-Amniotic IL-1beta in the Preterm Rhesus Macaque. *Biol Reprod* (2015) 92(2):56. doi: 10.1095/biolreprod.114.124420
63. Boyson JE, Aktan I, Barkhuff DA, Chant A. NKT Cells at the Maternal-Fetal Interface. *Immunol Invest* (2008) 37(5):565–82. doi: 10.1080/ 08820130802191409
64. Lee PT, Benlagha K, Teyton L, Bendelac A. Distinct Functional Lineages of Human V(alpha)24 Natural Killer T Cells. *J Exp Med* (2002) 195(5):637–41. doi: 10.1084/jem.20011908
65. Lawand M, Dechanet-Merville J, Dieu-Nosjean MC. Key Features of Gamma-Delta T-Cell Subsets in Human Diseases and Their Immunotherapeutic Implications. *Front Immunol* (2017) 8:761. doi: 10.3389/fimmu.2017.00761
66. Vermijlen D, Brouwer M, Donner C, Liesnard C, Tackoen M, Van Rysselberge M, et al. Human Cytomegalovirus Elicits Fetal Gammadelta T Cell Responses In Utero. *J Exp Med* (2010) 207(4):807–21. doi: 10.1084/ jem.20090348
67. Cimini E, Castilletti C, Sacchi A, Casetti R, Bordoni V, Romanelli A, et al. Human Zika Infection Induces a Reduction of IFN-Gamma Producing CD4 T-Cells and a Parallel Expansion of Effector Vdelta2 T-Cells. *Sci Rep* (2017) 7 (1):6313. doi: 10.1038/s41598-017-06536-x
68. Bjorkstrom NK, Ljunggren HG, Michaelsson J. Emerging Insights Into Natural Killer Cells in Human Peripheral Tissues. *Nat Rev Immunol* (2016) 16(5):310–20. doi: 10.1038/nri.2016.34
69. Antonioli L, Pacher P, Vizi ES, Hasko G. CD39 and CD73 in Immunity and Inflammation. *Trends Mol Med* (2013) 19(6):355–67. doi: 10.1016/ j.molmed.2013.03.005
70. Reeves RK, Gillis J, Wong FE, Yu Y, Connole M, Johnson RP. CD16- Natural Killer Cells: Enrichment in Mucosal and Secondary Lymphoid Tissues and Altered Function During Chronic SIV Infection. *Blood* (2010) 115(22):4439–46. doi: 10.1182/blood-2010-01-265595
71. Apps R, Gardner L, Traherne J, Male V, Moffett A. Natural-Killer Cell Ligands at the Maternal-Fetal Interface: UL-16 Binding Proteins, MHC Class-I Chain Related Molecules, HLA-F and CD48. *Hum Reprod* (2008) 23(11):2535–48. doi: 10.1093/humrep/den223
72. Zhang J, Dunk CE, Kwan M, Jones RL, Harris LK, Keating S, et al. Human dNK Cell Function Is Differentially Regulated by Extrinsic Cellular Engagement and Intrinsic Activating Receptors in First and Second Trimester Pregnancy. *Cell Mol Immunol* (2017) 14(2):203–13. doi: 10.1038/ cmi.2015.66
73. Siewiera J, El Costa H, Tabiasco J, Berrebi A, Cartron G, Le Bouteiller P, et al. Human Cytomegalovirus Infection Elicits New Decidual Natural Killer Cell Effector Functions. *PLoS Pathog* (2013) 9(4):e1003257. doi: 10.1371/ journal.ppat.1003257
74. Biassoni R, Fogli M, Cantoni C, Costa P, Conte R, Koopman G, et al. Molecular and Functional Characterization of NKG2D, Nkp80, and NKG2C Triggering NK Cell Receptors in Rhesus and Cynomolgus Macaques: Monitoring of NK Cell Function During Simian HIV Infection. *J Immunol* (2005) 174(9):5695–705. doi: 10.4049/jimmunol. 174.9.5695
75. Quicke KM, Bowen JR, Johnson EL, McDonald CE, Ma H, O'Neal JT, et al. Zika Virus Infects Human Placental Macrophages. *Cell Host Microbe* (2016) 20(1):83–90. doi: 10.1016/j.chom.2016.05.015
76. Miner JJ, Diamond MS. Zika Virus Pathogenesis and Tissue Tropism. *Cell Host Microbe* (2017) 21(2):134–42. doi: 10.1016/j.chom. 2017.01.004
77. Driggers RW, Ho CY, Korhonen EM, Kuivanen S, Jaaskelainen AJ, Smura T, et al. Zika Virus Infection With Prolonged Maternal Viremia and Fetal Brain Abnormalities. *N Engl J Med* (2016) 374(22):2142–51. doi: 10.1056/ NEJMoa1601824
78. Dudley DM, Aliota MT, Mohr EL, Weiler AM, Lehrer-Brey G, Weisgrau KL, et al. A Rhesus Macaque Model of Asian-Lineage Zika Virus Infection. *Nat Commun* (2016) 7:12204. doi: 10.1038/ncomms 12204
79. Foo SS, Chen W, Chan Y, Bowman JW, Chang LC, Choi Y, et al. Asian Zika Virus Strains Target CD14(+) Blood Monocytes and Induce M2-Skewed

Immunosuppression During Pregnancy. *Nat Microbiol* (2017) 2(11):1558–70. doi: 10.1038/s41564-017-0016-3
80. Nancy P, Tagliani E, Tay CS, Asp P, Levy DE, Erlebacher A. Chemokine Gene Silencing in Decidual Stromal Cells Limits T Cell Access to the Maternal-Fetal Interface. *Science* (2012) 336(6086):1317–21. doi: 10.1126/science.1220030
81. Chaturvedi V, Ertelt JM, Jiang TT, Kinder JM, Xin L, Owens KJ, et al. CXCR3 Blockade Protects Against Listeria Monocytogenes Infection-Induced Fetal Wastage. *J Clin Invest* (2015) 125(4):1713–25. doi: 10.1172/JCI78578

Conflict of Interest: The authors declare that the research was conducted in the absence of any commercial or financial relationships that could be construed as a potential conflict of interest.

Publisher's Note: All claims expressed in this article are solely those of the authors and do not necessarily represent those of their affiliated organizations, or those of the publisher, the editors and the reviewers. Any product that may be evaluated in this article, or claim that may be made by its manufacturer, is not guaranteed or endorsed by the publisher.

frontiers in Immunology

REVIEW
published: 21 October 2021
doi: 10.3389/fimmu.2021.757400

Understanding Viral and Immune Interplay During Vertical Transmission of HIV: Implications for Cure

Omayma Amin[1], *Jenna Powers*[1], *Katherine M. Bricker*[1] *and Ann Chahroudi*[1,2*]

[1] *Department of Pediatrics, Emory University School of Medicine, Atlanta, GA, United States,* [2] *Center for Childhood Infections and Vaccines of Children's Healthcare of Atlanta and Emory University, Atlanta, GA, United States*

Despite the significant progress that has been made to eliminate vertical HIV infection, more than 150,000 children were infected with HIV in 2019, emphasizing the continued need for sustainable HIV treatment strategies and ideally a cure for children. Mother-to-child-transmission (MTCT) remains the most important route of pediatric HIV acquisition and, in absence of prevention measures, transmission rates range from 15% to 45% *via* three distinct routes: *in utero*, intrapartum, and in the postnatal period through breastfeeding. The exact mechanisms and biological basis of these different routes of transmission are not yet fully understood. Some infants escape infection despite significant virus exposure, while others do not, suggesting possible maternal or fetal immune protective factors including the presence of HIV-specific antibodies. Here we summarize the unique aspects of HIV MTCT including the immunopathogenesis of the different routes of transmission, and how transmission in the antenatal or postnatal periods may affect early life immune responses and HIV persistence. A more refined understanding of the complex interaction between viral, maternal, and fetal/infant factors may enhance the pursuit of strategies to achieve an HIV cure for pediatric populations.

Keywords: HIV, MTCT, cure, pediatric, shock and kill, antiretroviral, breast milk, reservoir

OPEN ACCESS

Edited by:
Ashley L. St John, Duke-NUS Medical School, Singapore

Reviewed by:
Maria Blasi, Duke University, United States
Florence Buseyne, Institut Pasteur, France

****Correspondence:***
Ann Chahroudi
ann.m.chahroudi@emory.edu

Specialty section:
This article was submitted to Viral Immunology, a section of the journal Frontiers in Immunology

Received: *12 August 2021*
Accepted: *27 September 2021*
Published: *21 October 2021*

Citation:
Amin O, Powers J, Bricker KM and Chahroudi A (2021) Understanding Viral and Immune Interplay During Vertical Transmission of HIV: Implications for Cure. Front. Immunol. 12:757400. doi: 10.3389/fimmu.2021.757400

INTRODUCTION

Pediatric AIDS was first described in 1982, shortly after the first adult cases were reported (1). Of the estimated 37.5 million people currently living with HIV-1 as of 2020, 1.7 million of those individuals are children (2). While heterosexual transmission is the major transmission mode in adults, the majority of pediatric infections occur through mother-to-child transmission (MTCT) during pregnancy, labor and delivery, and postpartum through breastfeeding. Tremendous progress has been made in both prevention and treatment of HIV in children. However, despite the implementation of prevention of mother-to-child transmission (PMTCT) measures that decrease the risk of vertical HIV transmission to less than 5% (3, 4), approximately 150,000 children were newly infected with HIV in 2020, the majority of whom live in sub-Saharan Africa (5). As with HIV infection in adults, the primary targets for infection are activated CD4+ T cells expressing the

CCR5 co-receptor. Risk of MTCT transmission is influenced by geography, maternal viral load, co-infections, delivery mode, and breast-feeding (6), among other factors. The precise mechanisms of MTCT and how its timing influences establishment of HIV infection and persistence have not been fully elucidated. In this review, we aim to summarize what is known about HIV MTCT, the immunologic and virologic factors involved in HIV transmission in the fetal and neonatal/infant periods, and provide implications for HIV cure strategies targeting perinatally infected children.

ROUTES AND MECHANISMS OF VERTICAL TRANSMISSION

Mother-to-child transmission (MTCT) remains the most important route of pediatric HIV acquisition and, in the absence of preventative measures, transmission rates range from 15% to 45% *via* three distinct routes: *in utero*, intrapartum, and in the postnatal period through breastfeeding. Overall, it is estimated that 20-25%, 35-50% and 25-45% of perinatal HIV transmissions occur *in utero*, intrapartum, and through breastfeeding, respectively (7–9). It is important to note that despite the prolonged exposure to HIV during fetal development, delivery, and breastfeeding, MTCT of HIV is relatively inefficient, and many children born to women with HIV do not become infected, even in absence of preventative services. Here, we will discuss the biological mechanisms of HIV MTCT and with emphasis on the factors influencing transmission. While this is still an active area of research, further elucidating these mechanisms of transmission is likely to inform cure approaches that should be considered for the almost 2 million children living with HIV.

In Utero Transmission

Transmission of HIV *in utero* is the least efficient route of MTCT, accounting for an estimated absolute rate of 5-10% of MTCT for women not receiving antiretroviral therapy (ART) (7, 8). The major risk factors for *in utero* transmission are high maternal viral loads and placental inflammation (8, 10, 11). The mechanisms of *in utero* HIV transmission are incompletely understood, but some have been proposed. Early studies suggested that *in utero* transmission may occur though HIV in the amniotic fluid coming into contact with fetal mucosal surfaces (12). Although the fetal gastrointestinal tract is populated with targets for HIV infection (e.g., CD4+CCR5+ T cells) (13), more recent studies have found that even in women with detectable virus in the plasma, HIV is not detected in the amniotic fluid (14–16). Another study found that amniotic fluid has innate inhibitory activity against the replication of HIV (17). Consequently, it is more likely that *in utero* transmission occurs primarily through the placenta. The placenta is a highly effective barrier that successfully inhibits most pathogens from reaching fetal circulation through various protective mechanisms. The placenta is composed of fetal-derived trophoblast progenitor cells that differentiate into specialized cell layers. These specialized trophoblasts have broad antiviral activity in addition to acting as a physical barrier to pathogens (18). Maternal blood comes into direct contact with the placenta by 10-12 weeks of gestation when trophoblasts form the placental villi and mediate the exchange of gases, nutrients, and waste products between maternal and fetal tissue (18).

While *in utero* transmission of HIV has been documented to occur as early as 8 weeks gestation (19), the vast majority of transmissions *via* this mode occur in the third trimester (20, 21). There are two mechanisms of transplacental transmission: infection of the trophoblasts and transcytosis across the trophoblastic layer. Although trophoblasts have low to no expression of CD4 receptors, multiple studies have detected HIV in these cells (22–24). More recent evidence suggests that transmission occurs primarily through cell-associated virus, as trophoblasts appear to be naturally nonpermissive to cell-free HIV (25). In a study designed to mimic the complex cellular architecture of the placenta, transcytosis and infection of the trophoblastic layer were only accomplished by cell-associated virus (26). New evidence suggests that cell-associated HIV enters trophoblasts *via* fusion with maternal lymphocytes (27). This cell-fusion mediated spread of HIV may be less sensitive to ART than cell-free infection, causing the placenta to become a potential reservoir for the virus during pregnancy (27). It is important to note that even when HIV successfully traverses the placenta, transmission to the fetus is not guaranteed. Studies have shown that both infected and uninfected infants had maternal cells with HIV DNA in their dried cord blood, and there was no significant difference between the rate of infection and the presence of HIV-infected cells in cord blood (28, 29). These findings suggest that there are likely more factors, some of which we will discuss in later sections of this paper, governing *in utero* transmission of HIV.

Intrapartum Transmission

The most common route of HIV MTCT occurs during labor and delivery, accounting for an absolute rate of 10-20% of infections in children born to women not receiving ART (7, 8). A major risk factor for intrapartum transmission is again maternal viral load (30–32), and while in the United States the current standard of care is delivery by Caesarian section unless women are on ART with low viral loads, most women deliver vaginally elsewhere in the world (33). Although multiple mechanisms of intrapartum transmission have been proposed, most of the evidence supports infection *via* exposure of infant mucosal surfaces to maternal secretions and blood during birth. The fetal intestines are populated with high levels CD4+CCR5+ T cells (13), and evidence suggests that higher viral loads in the birth canal correlate with increased transmission rates (10). Additionally, factors that would increase contact of fetal mucosal surfaces with maternal viral secretions also increase transmission rates. For example, genital ulcers have been shown to cause an increase in intrapartum transmission rates (34). This association remained significant even after adjusting for plasma HIV viral load. Several possible mechanisms are thought to explain this association including increased recruitment of HIV-infected CD4+ T cells to the mucosal surface of the genital lesions resulting in increased

viral load in the genital tract (35, 36). Finally, the protective effect of elective Caesarian section against MTCT of HIV is attributed to the reduction of fetal contact with the birth canal (37–39).

Another proposed mechanism of intrapartum transmission is maternal-fetal microtransfusion (also called placental microtransfusion) causing fetal exposure to maternal blood containing both cell-free HIV RNA and cell-associated HIV DNA. Although the cause is unknown, microtransfusions occur at or near time of delivery when there is a disruption of the placental barrier and are thought to increase when uterine contractions intensify causing membranes to rupture. One study done using placental alkaline phosphatase (PLAP) as a marker for microtransfusions found that in women who had vaginal deliveries, high levels of PLAP were associated with higher intrapartum transmission risk (40). However, there was no significant association between PLAP (microtransfusion) levels and perinatal transmission as a whole. As described above, further studies designed to detect maternal cells in dried fetal cord blood as a proxy for microtransfusion also found no correlation (28, 29). Maternal-fetal microtransfusions are still relatively understudied, however.

Postpartum Transmission

Breastfeeding contributes to a considerable proportion of pediatric HIV infections accounting for an estimated absolute rate of 5-15% of MTCT for women not receiving ART (8). Premastication, where an adult chews foods before feeding it to the child, is also a risk factor for MTCT and this risk is associated with predisposing oral conditions that lead to the presence of blood in the mouth (41). It was recognized early on that breastfeeding was a potential mechanism for HIV transmission; however, the World Health Organization recommends that women in sub-Saharan Africa (with high HIV prevalence) breastfeed their children due to lack of consistent access to a safe water supply (42). Other factors such as the cost of formula and the stigma associated with not breastfeeding play into this decision (7). In order for MTCT to occur during breast feeding, the virus must first pass through the mammary epithelium, remain infectious within breast milk, traverse the infant mucosal barriers and establish infection. Studies in *ex vivo* organ tissue model systems and *in vivo* animal models have provided evidence that transmission can occur *via* the oral route (43, 44). Oral inoculations of simian immunodeficiency virus (SIV) have been shown to cause infection in infant rhesus macaques, providing proof of concept, although often these experimental inoculums contained higher doses of virus than would be seen in normal levels in breast milk (45–47). Cord blood and neonatal blood contain low levels of CD4+ T cells expressing CCR5, but, as described above, CD4+CCR5+ T cells populating the fetal intestines are abundant (13), a finding that has also been described in infant rhesus macaques (48–50). The mammary epithelium, like the placenta, however, successfully inhibits many pathogens from entering the breast milk through various protective mechanisms. Additionally, there is evidence that breast milk and saliva have innate inhibitory activity that restricts HIV transmission (51–54). The protective mechanisms of the maternal and fetal immune responses that limit breast milk transmission will be discussed in more detail below.

One major risk factor for MTCT during breastfeeding is viral load in the breast milk (10), and both cell-free and cell-associated HIV are thought to contribute to transmission. HIV RNA levels in breast milk correlate with plasma levels but are generally 100-fold lower (8, 55). Conditions that increase breast milk viral shedding are associated with higher transmission rates. Nonexclusive breastfeeding and infrequent emptying of the breast can lead to breast inflammation secondary to milk stasis, which in turn increases the viral load and has a strong association with increased MTCT (56–61). However, conflicting research found that nonexclusive breast feeding and mastitis do not significantly increase viral loads in breast milk (56). Still, HIV transmission was increased in breastfed infants who also received solid foods when compared to exclusively breastfed children (58). This mixed feeding is thought to cause disruption of the infant's gut mucosal lining secondary to the introduction of non-breast-milk foods and early introduction of pathogens or foreign antigens, leading to immune activation and increased susceptibility to infection (62–64). Microbiome differences between mixed fed and exclusively breastfed infants may also impact transmission (65). Multiple studies suggested that cell-associated viruses also have a role in transmission during breastfeeding (66, 67). Understanding these biological mechanisms of breast milk viral spread is an important first step in characterizing the establishment of HIV reservoirs during this period. Further, it should be recognized that breastfeeding transmission can occur outside of the neonatal period and infants may be diagnosed after more time has elapsed since infection than occurs with *in utero* and intrapartum transmission. This later diagnosis, coupled with rapid immune system changes in early life, likely leads to a unique immunovirologic environment defining HIV persistence in children infected through the breastfeeding route.

FACTORS INFLUENCING VERTICAL TRANSMISSION

MTCT is multifactorial, with different viral, maternal, and fetal/infant factors at play that influence the risk of HIV transmission (**Figure 1**). Knowledge of these risk factors and understanding of their roles in MTCT have been crucial to develop preventative measures and here we postulate that their consideration should also inform the investigation into curative approaches.

Viral Factors Impacting MTCT

Viral Burden

Maternal viral load has been shown to be the strongest predictor of perinatal HIV transmission. Many studies have demonstrated increased risk of transmission with high levels of maternal viremia and high p24 antigenemia (68–71). Acute infection during pregnancy is associated with increased risk of perinatal transmission and is likely related to the high viral loads in plasma

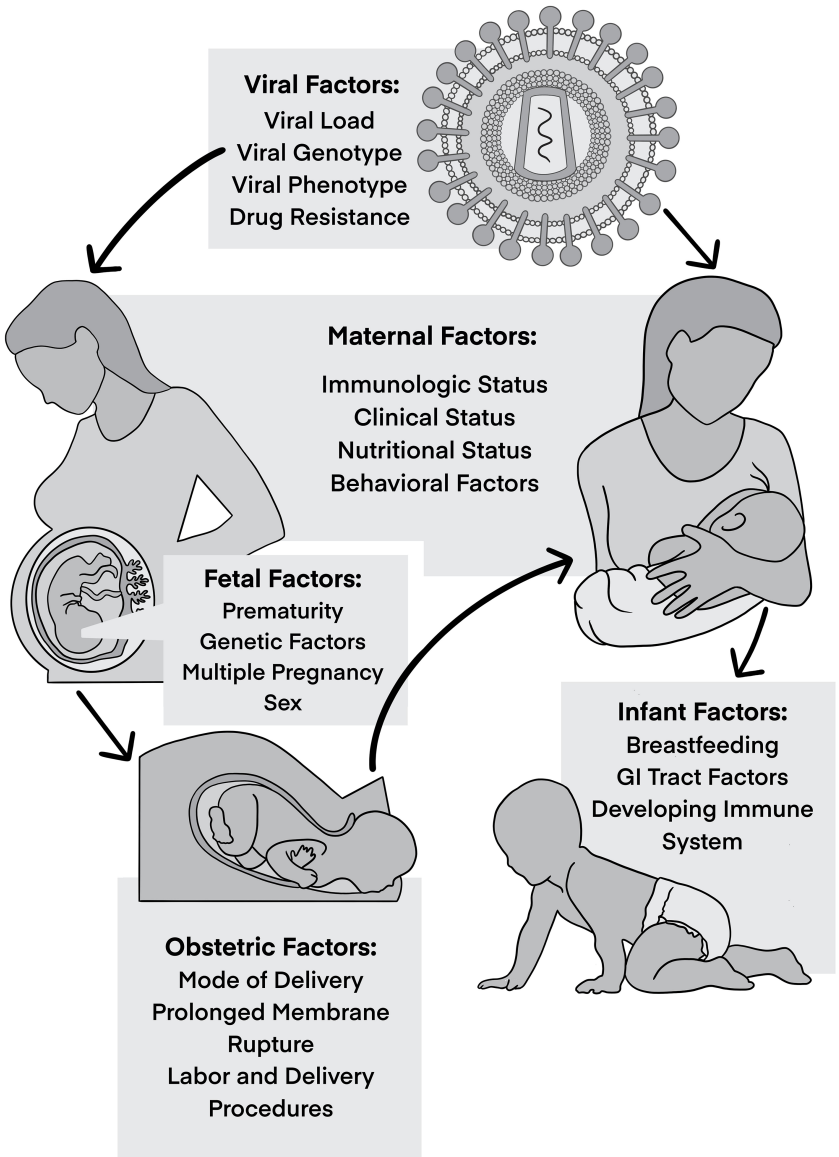

FIGURE 1 | Factors influencing vertical transmission.

and the genital tract (72). Consequently, maternal viral suppression *via* use of ART during pregnancy has been proven to lower the risk of perinatal transmission. This was first supported by the 076 trial which showed that administration of zidovudine during pregnancy, delivery, and to the newborn for the first 6 months of life reduced transmission by nearly 70% in women with HIV who did not breast-feed (73). Subsequent studies have indicated that transmission is reduced even further with triple-drug regimens (74). Several studies have tried to establish a threshold of maternal viral load below which transmission does not occur (75); however, it has been demonstrated that transmission can occur in some cases where women have low levels of HIV RNA in the blood, indicating the presence of other factors influencing the transmission process. In one study that included 320 women from 18 different centers in France showed that perinatal transmission occurred in 12% of the women at less than 1000 copies/ml compared to 29% in women with more than 10,000 copies/ml (76). In contrast, in Bangkok 281 pregnant women were followed and no transmission occurred in those with virus load less than 2,000 copies/ml (77).

Several behavioral practices have been associated with increased risk of maternal to infant HIV transmission due to resultant increases in viral load. These behavioral factors include illicit drug use (IDU), cigarette smoking, and alcohol use. IDU is associated with increased risk of MTCT (78–81). Alcohol and drug use like heroin, amphetamine and cocaine, may be associated with failure to control viral load in the presence of

ART, hence increased transmission rate (82–85). Additionally, transmission may be increased through drug interactions with ART and placental injury (86). Some have demonstrated an association between IDU and lack of adherence to ART which can lead to increased viral load (83, 85–87).

In addition to plasma viral load, viral levels in cervicovaginal fluid and breast milk are also thought to influence transmission risk in the intrapartum and postnatal periods (56, 88–90). As referenced above, levels of HIV DNA in breast milk cells (ie, CD4+ T cells) are positively correlated with postnatal transmission, and this intracellular HIV DNA is not significantly reduced by maternal ART. Risk of transmission is higher during early lactation due to the increased cellular content of colostrum (91). Both maternal ART and extended infant prophylaxis (at least with a single agent) during breastfeeding significantly reduces but does not eliminate MTCT, an observation that likely reflects virus persistence in CD4+ T cells (92–97).

Viral Genotype and Phenotype

Several studies of viral variants in mothers and infants attempted to characterize HIV quasispecies associated with MTCT and have yielded conflicting results. Major, minor, and multiple variant transmission events have been described (98–100). Most evidence suggests that a single or restricted subset of maternal viral variants establish infection in the infant suggesting selective pressure during the transmission process. However, the basis and the factors controlling MTCT bottleneck are not yet fully understood. Different properties of virus populations have been reported in studies analyzing vertical transmission stratified by timing, with transmission during the intrapartum period found to be primarily associated with the transmission of minor maternal variants while *in utero* transmission was more likely to occur with single or multiple HIV variants (100–104). Maternal antiretroviral drug resistance is associated with transmission during breastfeeding, but not during the *in utero*/intrapartum periods (105).

Phylogenetic analyses of HIV *env* in infected infants showed that they have a more homogenous virus population when compared to their mothers (106, 107). Studies have also shown that macrophage-tropic and non-syncytium-inducing (NSI) or CCR5-utilizing HIV viral strains are selectively transmitted (108). Another characteristic found in transmitted viruses was shorter variable loops and fewer putative N-linked glycosylation (PNG) sites encoded in *env* (70, 109–111). Different HIV subtypes may also have distinct MTCT rates. Work conducted in Tanzania showed that subtype C is preferentially transmitted from mother to child compared to subtype A and D (100). In another study from Kenya, the MTCT rate appeared to be higher among mothers infected with subtype D compared with subtype A (112). However, no such differences have been observed in other cohorts (100, 112–115).

Host Factors Impacting MTCT

Genetic Factors

Genetic polymorphisms in the coding and regulatory regions of HIV receptors and their ligands influence the risk of HIV acquisition. Infants with a single nucleotide polymorphism (SNP) in the CD4 gene at position C868T that may modify the tertiary structure of CD4 were more likely to acquire HIV compared to infants with wild type CD4 (116). In the setting of MTCT, most of the transmitted viruses use CCR5 as a coreceptor (117). As has been shown for horizontal infection in adults, the presence of a 32-bp deletion in the coding region of the *CCR5* gene (*CCR5*-Δ32) in the homozygous state in infants results in non-functional coreceptors and confers protection from vertical infection (118, 119). Heterozygosity also exerts a protective effect when carried by mothers due to lower maternal viral burden (107). Conversely, polymorphisms in the CCR5 promoter region at positions 59029 and 59353T increase the expression of CCR5 leading to increased risk of MTCT when carried by infants (120–123).

Increased risk of vertical transmission was also seen with genetic polymorphisms resulting in decreased expression of the natural ligands for HIV coreceptors (CCL3, CCL4, and CCL5) (124).

Genetic variations affecting innate immunity may also influence MTCT. Defensins are antimicrobial peptides that are expressed by epithelial cells, known for innate mucosal defense and antiviral activities. Defensins inhibit HIV infection *via* different mechanisms including direct binding to virions as well as disturbing intracellular signaling by modulation of host cell surface receptors. Three SNPs in the 5′ untranslated region of β-defensin-1 (*DEFB1*) gene were reported to modulate risk of MTCT: −52G/A, -20(G/A) and −44C/G (125–127). Braida et al. described an association between -44(C/G) and HIV infection in Italian pediatric population (125). Another study found a lower copy number of *DEFB104* among HIV-infected children when compared to HIV-exposed children and healthy controls, suggesting that *DEFB104* may have a potential protective role against vertical transmission (128).

Multiple studies have investigated the influence of HLA concordance between mother and infant on vertical transmission and as well as risk of disease progression in infected infants (129–131). Specific maternal HLA polymorphisms, including B4901, B5301, A2/6802 and B18, have also been associated with decreased risk of MTCT (132–134). HLA-G, a non-classical class I MHC gene highly expressed in placental trophoblasts, has several SNPs found to be associated with decreased risk of vertical transmission (135, 136). Certain class II MHC alleles have also been reported to influence MTCT among certain ethnicities such as *DQB1*0604*, *DR3*, *DR13*, *DRB1*1501* (137–139).

Gender specific differences in MTCT have been reported in several cohorts (140, 141). Female infants are reported to have two- to three-fold increased risk of infection at birth compared to male infants (7, 140, 141). This increased susceptibility has been linked to subversion of innate immunity, with female fetuses acquiring maternal variants resistant to type I interferons (142). Sex-specific differences in *in utero* infection have also been attributed to the fact that *in utero* mortality rates of HIV-infected male infants are disproportionately higher and thus more HIV-infected female infants are liveborn. It is also proposed that a minor histocompatibility reaction between infant male Y chromosome-derived antigens and maternal lymphocytes reduce the risk of MTCT to boys (140).

Maternal Co-Infections

Several coexisting maternal infections have been found to be associated with increased MTCT of HIV. Multiple studies demonstrated an increased risk of vertical transmission in the setting of chorioamnionitis (143–145), primarily related to disruption of the placental barrier and entrance of HIV-infected cells into the amniotic fluid (143, 144, 146). Chorioamnionitis complications including preterm labor and premature rupture of membranes can also lead to increased risk of MTCT related to immaturity of the skin and mucosal membranes as well as the premature fetal immune system. In a multicenter prospective cohort, clinical and biologic factors that contributed to MTCT were studied. Histologic chorioamnionitis was found to be a major risk factor for transmitting HIV (147).

Adachi and colleagues evaluated the effect of sexually transmitted infections (STIs) on risk of MTCT in a large cohort of HIV-infected pregnant women and found increased rates of HIV transmission in the presence of a another sexually transmitted disease (148). In general, inflammation of the maternal genital tract mucosa has been shown to increase rate of vertical transmission independent of maternal plasma HIV load (59). Infections resulting in genital ulcer disease such as HSV-2 are also associated with increased genital shedding of HIV (35, 149, 150). Conflicting data exist regarding maternal syphilis infection and MTCT of HIV. A study in Zimbabwe showed that active maternal syphilis at the time of delivery was not associated with intra-partum MTCT risk while several other groups have demonstrated an increased risk of vertical HIV acquisition in the setting of maternal syphilis (146, 151). HIV and Hepatitis B virus (HBV) co-infection are associated with increased HBV, but not HIV transmission to the infant. Maternal Hepatitis C virus (HCV) co-infection has been linked to higher rates of vertical HIV transmission (152–160).

Unprotected sexual intercourse during pregnancy itself is thought to be associated with increased risk of MTCT (161, 162). Bulterys et al. conducted a prospective cohort study in Rwanda that showed that unprotected sexual intercourse with multiple partners before and during pregnancy in a population with high HIV-1 seroprevalence may increase risk of transmission from infected mother to infants (161). Another study by Burns and colleagues also found higher frequency of intercourse during pregnancy among women transmitting HIV to their infants (163). Potential mechanisms include increased HIV strain diversity (i.e., superinfection) (164, 165) and vaginal or cervical inflammation due to microabrasions or STIs that result in chorioamnionitis and/or increased viral shedding in genital fluids (164).

Tuberculosis (TB) is one of the most important causes of mortality and morbidity in HIV infection, especially in women residing in TB endemic areas. Active TB infection increases HIV viral load which is a known risk factor for perinatal transmission (166–168). Gupta et al., found a 2.5-fold increase in the odds of MTCT of HIV in pregnant women with TB/HIV coinfection, after adjusting for maternal and infant factors (169). Similarly, malaria and HIV coinfection is associated with an increased risk of adverse outcomes in pregnant women (170) as well as increased HIV viral load (171). As such, a few studies have suggested an increased risk of perinatal transmission with maternal malaria (172–174), yet others failed to demonstrate this relationship (144, 175, 176). Finally, other common viral infections, such as Cytomegalovirus (CMV), may play a critical role in influencing MTCT. One described mechanism has been through enhancement of placental susceptibility to HIV infection (177).

Maternal Immunological Factors

There are multiple maternal immunological factors associated with increased risk of perinatal transmission, including low CD4+ T cell count, CD4+ T cell percentage, and CD4/CD8 ratio (178). Shivakoti et al. showed that high maternal soluble CD14 concentration during the peripartum period was associated with increased risk of MTCT, independent of maternal viral load, CD4+ T cell count and ART exposure (179), implicating immune activation in transmission.

Adaptive immune responses play an important role in transmission from mother to infant. MTCT is a unique setting where HIV-1 acquisition occurs in the presence of naturally elicited HIV-specific antibodies that are passively transferred prior to birth. Several studies have examined the impact of maternal antibodies on MTCT; however, there have been conflicting results and their role in protecting infants against HIV-1 transmission remains unclear. These contradicting results may be explained by small cohort sizes, lack of control for the other known risk factors for HIV transmission, timing, and methods used in infant diagnosis, and potential clade-specific differences in virus–antibody interactions. Initial studies demonstrated that higher levels of maternal HIV-1 envelope (Env)-specific IgG antibody responses were associated with reduced transmission risk (180, 181).This association was not observed in subsequent studies and research focus was shifted to examine the effect of neutralizing antibodies (nAbs) and their role in modulating the risk of transmission (182, 183). Work conducted in nonhuman primates showed that passive immunization of infants with a cocktail of HIV-1-neutralizing antibodies provided partial protection against oral simian-human immunodeficiency virus transmission (184). Subsequent human studies showed that high levels of maternal nAbs were correlated with reduced MTCT rates while others failed to confirm this association (185–188). However, founder viruses in infants are generally more resistant to neutralization by maternal antibodies (189, 190), suggesting that the transmitted variants are able to escape nAbs and supportive of the idea that maternal antibodies may confer partial protection.

In a large cohort of non-breastfeeding HIV-1 infected women enrolled in the pre-ART era Women and Infant Transmission Study (WITS), Permar and her group found that maternal V3-specific IgG binding responses and CD4 binding site-blocking responses correlated and were independently predictive of reduced MTCT risk (191). They also found that both binding and neutralizing responses targeting the C-terminal region of HIV envelope (Env) were associated with decreased risk of transmission (191). Antibody effector functions beyond neutralization have also been examined for their contribution

to MTCT. Maternal antibody-dependent cellular cytotoxicity (ADCC) is thought to have a role in protection against HIV-1 transmission. In one such investigation, plasma and breast milk obtained soon after delivery from 9 transmitting and 10 non-transmitting women in Kenya demonstrated that breast milk Env-specific IgG responses with ADCC activity were associated with decreased MTCT risk (192). However, Pollara et al. found no association of ADCC-mediating responses and MTCT risk in HIV clade C breastfeeding women in Malawi (193). In addition to antibodies and antibody effector functions, Lohman-Payne et al. also reported breast milk HIV gag-specific IFNg responses to be associated with protection from MTCT *via* breastfeeding in a Kenyan cohort (194).

Infant Immunological Factors

Most infants born to HIV-1 infected mothers do not become infected despite having an immature immune system and repeated exposures to HIV-1 throughout the peripartum and breastfeeding periods. To survive to term, the developing fetus must avoid generating an inflammatory response to the many foreign maternal antigens to which it is exposed during development resulting in a predominantly tolerogenic immune system in the fetus and newborn (195). The tolerogenic environment is facilitated by high levels of anti-inflammatory cytokines such as TGFb and IL-10 (196), which likely subvert immune activation and establishment of infection upon HIV exposure. TGFb also directs naïve CD4+ T cell to differentiate to Tregs resulting in a larger Treg pool in infants, representing 15% of fetal blood T cells compared to 5% of adult blood T cells. These Tregs promote immune tolerance and are long-lived (196, 197). Much of these regulatory cells reside in intestinal tissue and are critical for mucosal immune homeostasis. In addition to higher levels of Tregs, the CD4+ effector cells of infants are predominantly of the Th17 and Th2 phenotype (rather than Th1 as in adults) (198, 199). Th17 cells are critical to maintaining the integrity of the intestinal mucosal barrier and may thus restrict dissemination of infection. Conversely, Tugizov and colleagues have reported lower levels of innate proteins that restrict infection, such as defensins, in infant compared to adult oral epithelia (43).

In the mother-child transmission pair, the infant may be disadvantaged in that the transmitted virus in has already adapted to evade a genetically similar immune system. Anti-HIV-1 antibodies and T cells transferred to the child either *in utero* or through breastmilk have pre-adapted to the transmitted virus and may be ineffective. Additionally, because of shared HLA alleles the transmitted virus may be preadapted to escape CD8+ T cells targeting HIV epitopes restricted by HLA alleles inherited from the mother further complicating pediatric HIV-1 infection (200, 201). HIV-specific cellular immune responses are detected in exposed uninfected infants, but their role in influencing virus acquisition is uncertain (202, 203).

IMPLICATIONS FOR CURE APPROACHES

The World Health Organization recommendations state that all infants and children under two years of age with confirmed HIV-1 begin ART immediately at the time of diagnosis irrespective of CD4+ T cell counts (204). Despite this recommendation, HIV-1-infected children are one third less likely to receive ART than infected adults (205). Reasons for this include fewer drugs available for use by children, higher treatment cost, and dependence on a caregiver to provide ART (206). These factors can complicate the design and implementation of cure studies in children.

A major barrier to HIV cure is the establishment of a reservoir of HIV-infected cells that persists despite suppressive ART and can give rise to rebound viremia if ART is interrupted. In adults, it is well documented that viral reservoirs are established during early stages of HIV infection (207) and this finding is supported by the SIV/macaque model in which rapid seeding of the viral reservoir within 3 days of infection has been described (208). Furthermore, rebound of viremia is almost always seen after ART discontinuation in both horizontally infected adults and perinatally-infected children (209–211). However, little is known about the exact timing of reservoir seeding in different MTCT settings and whether there are differences in reservoir establishment in relation to time of infection and mode of transmission. Increased understanding of these factors may aid in the development of approaches to eradicate viral reservoirs and/or induce viral remission (sustained viral suppression in absence of ART) in children.

The uniqueness of the in-utero transmission window allows for rapid detection and treatment as children born to women with HIV can be screened at birth. Such early detection is not generally feasible in adult transmissions. Infants diagnosed at birth *via* rapid point-of-care testing can begin ART within the first few hours of life (212). Infections arising from intra- or post-partum transmission will not be detected at the time of birth, so follow-up care and repeated testing are required to monitor these transmission modes. In these instances, early ART initiation is not as practical in resource limited settings, although current United States guidelines recommend triple drug prophylaxis (given at therapeutic dosing) for neonates with high risk of acquiring HIV infection.

Contemporary studies of HIV reservoirs in perinatally infected infants and children have focused on *in utero* transmission, following the description of the 'Mississippi child'. This child received ART between 30 hours and 18 months of age, and then remained persistently aviremic for 27 months after discontinuation of ART before rebound (209, 213). *In utero* infection was documented, but the child did not develop HIV-specific antibody or T cell responses, thought due to the very early initiation of ART. Despite the eventual rebound, this partial remission led to several clinical trials of very early ART (typically considered to be within 48 hours) to limit the size of the HIV reservoir and investigate the possibility of achieving post-treatment control after ART interruption. Results from the Early Infant Treatment (EIT) study in Botswana have demonstrated that very early ART leads to an exceptionally small reservoir of intact proviral HIV DNA as well as an improved innate and adaptive antiviral immune response compared to delayed ART (214). As of this writing, results from the ART interruption phase of the very early ART trials,

including EIT and IMPAACT P1115 (215), have not been published. Kuhn and colleagues describe challenges in meeting predetermined virologic and immunologic criteria for ART interruption in the LEOPARD trial of very early/early ART conducted in South Africa (216).

The South African Children with HIV Early antiRetroviral therapy (CHER) trial (217), that included children with *in utero* and intrapartum HIV infection, has led to a number of key findings regarding persistent HIV reservoirs. One report demonstrated rare intact proviral sequences in children after 6-9 years of ART initiated after 2 months of age but within the first year of life using near full-length proviral amplification and sequencing (218). This group further identified clones of infected cells shortly after birth that could also be detected after almost a decade on ART, suggesting that clonal expansion of reservoir cells maintains HIV persistence in children as it does for adults (219). Two additional case reports of long-term HIV remission have emerged, one from the CHER trial, with unknown timing of infection (*in utero vs* intrapartum) (220) and the other from a French cohort, with presumed intrapartum transmission (221), both of whom started ART at 2-3 months of life.

There have been relatively fewer studies of reservoir characteristics in children infected postpartum through breastfeeding. However, presently over half of new infections occur postnatally through breast milk (9). As this route has become predominant in perinatal HIV infection, a nonhuman primate model has been established to better understand virologic and immunologic features of lentivirus infection following postpartum transmission, more precisely define anatomic sites of virus persistence, and test strategies to promote reservoir eradication or remission (46, 47, 222–224). These and other ongoing studies may inform the design of future cure-directed clinical trials in children with HIV infection acquired through breast milk.

Regardless of the mode of transmission earlier ART is generally associated with a smaller reservoir during viremia suppression (210, 214, 225–237), although starting ART within 14 days of life may not lead to significantly greater HIV DNA persistence compared to within 48 hours of life (238). ART initiation within 8 days has also been associated with a faster HIV DNA decay compared to ART started at 5 months (239). Female sex and maternal acute HIV infection during pregnancy have been associated with higher levels of persistent HIV DNA (240).

While protocol-specified ART interruption has not occurred in recent clinical trials, studies of intermittent viremia *vs*. sustained viral suppression can be informative to identify biomarkers that may be predictive of viral rebound dynamics. These findings are by nature complicated by behavioral factors, including adherence to ART regimens. Millar and colleagues assessed factors associated with intermittent viremia in *in utero* infected infants started on early ART (in the first 3 weeks of life) (240). A smaller reservoir size as measured by total HIV DNA in PBMCs was not correlated with maintained viral suppression whereas a longer time to initial viral suppression was, implicating immunologic contributions to aviremia, although this finding may have been influenced by ART nonadherence. In children in the EIT study who started on ART at < 7 days of life, sustained HIV RNA suppression was associated with negative HIV serostatus and negative qualitative HIV DNA PCR at ~20 months (225). HIV seronegativity has also been described in other studies of early or very early ART and has been proposed as an estimate for reservoir size (227, 228, 241–244).

Identification of cure strategies that target latently infected cells, allow immune recognition and clearance of the reservoir, and/or promote viral remission are currently considered extremely high priority for the field. Unlike in adults, few cure strategies have been tested in children to date, with the exception of very early ART that it is now understood is insufficient to lead to cure in the majority of individuals. However, there are several approaches that may provide benefit in the setting of perinatal HIV transmission, and their study should be carefully considered for certain populations (**Figure 2**). The design of such studies should take into consideration not only the timing of ART initiation, but also the duration of ART (and therefore age of the trial participant), as well as the known or presumed mode of HIV transmission (*in utero*, intrapartum, or postpartum). For example, a neonate infected *in utero* and initiating very early ART is likely to be vastly different both virologically and immunologically from an adolescent who acquired HIV through breastfeeding with delayed ART initiation and periods of unsuppressed viremia over years. In the former case, adding the cure directed therapy at the time of early ART initiation may lead to an extremely small reservoir size (or even prevent reservoir establishment in the best-case scenario). This cure-directed therapy might include one or multiple broadly neutralizing antibodies delivered by passive (as is being tested in IMPAACT 2008 (215) or active immunization along with ART. A novel proposed strategy, termed "surge and purge," combines very early ART, passive antibody administration, and immune stimulation to destabilize reservoir establishment (245). Infants and children with very small reservoirs may also be good candidates for approaches designed to silence HIV expression ("block and lock"). For the school aged or adolescent child with a larger reservoir size, the "kick and kill" approach may be more effective, with a latency reversal agent used to reactivate virus expression followed by immune-based clearance of infected cells. Studies in nonhuman primates support the notion that pre-existing reservoir size as well as age-related factors may influence susceptibility to latency reversal (246, 247). Therapeutic HIV vaccines designed to boost antiviral T cell responses may have benefit in kick and kick strategies targeting established infection (223, 248) and possibly in limiting reservoir size early in infection, although in both settings the impact may depend on the child's age at vaccination, the timing of ART, and the degree of immune exhaustion present. Results from the HVRRICANE trial are forthcoming, in which a prime-boost vaccine strategy will be tested in combination with a TLR4 adjuvant (hypothesized to reverse latency) in HIV-1-infected children with history of early ART or previous immunization with one of the vaccine components (215).

In summary, HIV MTCT is promoted by distinct immunopathogenesis for the three different routes of transmission that may also affect HIV persistence. Consideration of the complex interaction between viral, maternal, and fetal/infant factors may enhance the pursuit of strategies to achieve an

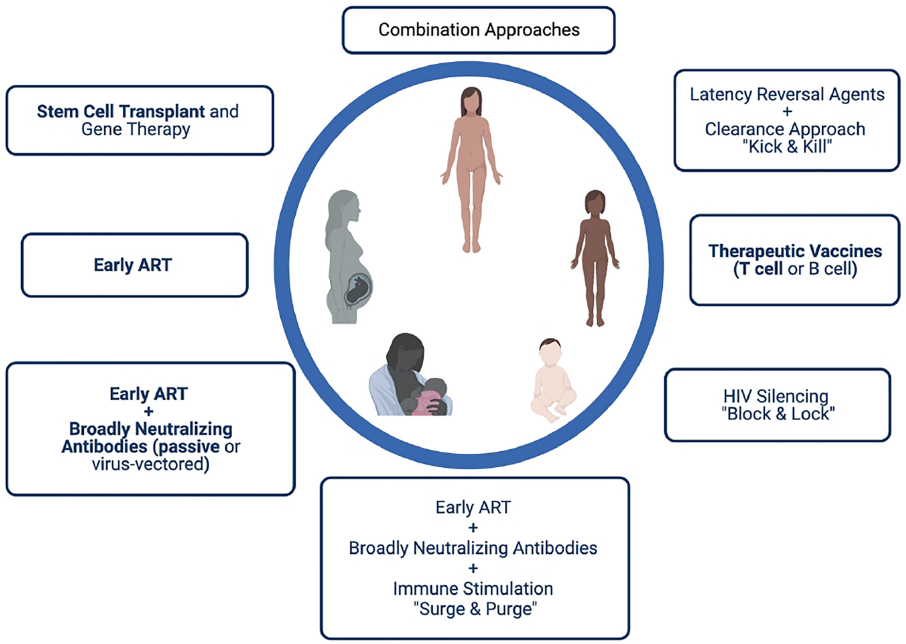

FIGURE 2 | Possible HIV cure approaches for perinatally infected infants, children and adolescents. Strategies in bold have been or are being studied in pediatric clinical trials.

HIV cure for pediatric populations. Future preclinical and clinical trials from the neonatal period through adolescence will further elucidate how MTCT influences the potential for HIV cure.

AUTHOR CONTRIBUTIONS

OA is the first author, the rest of the coauthors AC, KB, JP contributed to the manuscript. All authors reviewed the final manuscript. All authors contributed to the article and approved the submitted version.

FUNDING

AC would like to acknowledge funding support from the NIH (R01 AI133706, P01 AI131276, R37 AI157862, and UM1 AI164566).

REFERENCES

1. Centers for Disease C. Unexplained Immunodeficiency and Opportunistic Infections in Infants–New York, New Jersey, California. *MMWR Morb Mortal Wkly Rep* (1982) 31(49):665–7.
2. UNAIDS. *Global HIV & AIDS Statistics - Fact Sheet*. UNAIDS (2011). Available at: https://www.unaids.org/en/resources/fact-sheet (Accessed 10/06/2020).
3. WHO. *Antiretroviral Drugs for Treatment Pregnant Women and Preventing HIV Infection in Infants: Recommendations for a Public Health Approach*. Geneva: WHO (2010).
4. HIV/AIDS) UJUNPo. *Press Release: "World Leaders Launch Plan to Eliminate New HIV Infections Among Children by 2015"*. Geneva: UNAIDS (2011).
5. UNAIDS. *Global HIV & AIDS Statistics*. UNAIDS (2020).
6. Goulder PJ, Lewin SR, Leitman EM. Paediatric HIV Infection: The Potential for Cure. *Nat Rev Immunol* (2016) 16(4):259–71. doi: 10.1038/nri.2016.19
7. Lehman DA, Farquhar C. Biological Mechanisms of Vertical Human Immunodeficiency Virus (HIV-1) Transmission. *Rev Med Virol* (2007) 17 (6):381–403. doi: 10.1002/rmv.543
8. Tobin NH, Aldrovandi GM. Immunology of Pediatric HIV Infection. *Immunol Rev* (2013) 254(1):143–69. doi: 10.1111/imr.12074
9. Luzuriaga K, Mofenson LM. Challenges in the Elimination of Pediatric HIV-1 Infection. *N Engl J Med* (2016) 374(8):761–70. doi: 10.1056/NEJMra1505256
10. John GC, Nduati RW, Mbori-Ngacha DA, Richardson BA, Panteleeff D, Mwatha A, et al. Correlates of Mother-to-Child Human Immunodeficiency Virus Type 1 (HIV-1) Transmission: Association With Maternal Plasma HIV-1 RNA Load, Genital HIV-1 DNA Shedding, and Breast Infections. *J Infect Dis* (2001) 183(2):206–12. doi: 10.1086/317918
11. Kumar SB, Rice CE, Milner DA Jr., Ramirez NC, Ackerman WE 4th, Mwapasa V, et al. Elevated Cytokine and Chemokine Levels in the Placenta Are Associated With in-Utero HIV-1 Mother-to-Child Transmission. *AIDS* (2012) 26(6):685–94. doi: 10.1097/QAD.0b013e3283519b00
12. Fazely F, Sharma PL, Fratazzi C, Greene MF, Wyand MS, Memon MA, et al. Simian Immunodeficiency Virus Infection *via* Amniotic Fluid: A Model to Study Fetal Immunopathogenesis and Prophylaxis. *J Acquir Immune Defic Syndr (1988)* (1993) 6(2):107–14.
13. Bunders MJ, van der Loos CM, Klarenbeek PL, van Hamme JL, Boer K, Wilde JCH, et al. Memory CD4(+)CCR5(+) T Cells Are Abundantly Present in the Gut of Newborn Infants to Facilitate Mother-to-Child Transmission of HIV-1. *Blood* (2012) 120(22):4383–90. doi: 10.1182/blood-2012-06-437566

14. Lobato AC, Aguiar RA, Aleixo AW, Andrade BA, Cavallo IK, Kakehasi FM, et al. HIV-1 RNA Detection in the Amniotic Fluid of HIV-Infected Pregnant Women. *Mem Inst Oswaldo Cruz* (2010) 105(5):720–1. doi: 10.1590/S0074-02762010000500021
15. Maiques V, García-Tejedor A, Perales A, Córdoba J, Esteban RJ. HIV Detection in Amniotic Fluid Samples. Amniocentesis Can Be Performed in HIV Pregnant Women? *Eur J Obstet Gynecol Reprod Biol* (2003) 108 (2):137–41. doi: 10.1016/S0301-2115(02)00405-0
16. Mohlala BK, Tucker TJ, Besser MJ, Williamson C, Yeats J, Smit L, et al. Investigation of HIV in Amniotic Fluid From HIV-Infected Pregnant Women at Full Term. *J Infect Dis* (2005) 192(3):488–91. doi: 10.1086/431604
17. Farzin A, Boyer P, Ank B, Nielsen-Saines K, Bryson Y. Amniotic Fluid Exhibits an Innate Inhibitory Activity Against HIV Type 1 Replication *In Vitro*. *AIDS Res Hum Retroviruses* (2013) 29(1):77–83. doi: 10.1089/aid.2011.0355
18. Arora N, Sadovsky Y, Dermody TS, Coyne CB. Microbial Vertical Transmission During Human Pregnancy. *Cell Host Microbe* (2017) 21 (5):561–7. doi: 10.1016/j.chom.2017.04.007
19. Lewis SH, Reynolds-Kohler C, Fox HE, Nelson JA. HIV-1 in Trophoblastic and Villous Hofbauer Cells, and Haematological Precursors in Eight-Week Fetuses. *Lancet* (1990) 335(8689):565–8. doi: 10.1016/0140-6736(90)90349-A
20. Rouzioux C, Costagliola D, Burgard M, Blanche S, Mayaux MJ, Griscelli C, et al. Estimated Timing of Mother-To-Child Human Immunodeficiency Virus Type 1 (HIV-1) Transmission by Use of a Markov Model. *Am J Epidemiol* (1995) 142(12):1330–7. doi: 10.1093/oxfordjournals.aje.a117601
21. Chouquet C, Richardson S, Burgard M, Blanche S, Mayaux MJ, Rouzioux C, et al. Timing of Human Immunodeficiency Virus Type 1 (HIV-1) Transmission From Mother to Child: Bayesian Estimation Using a Mixture. *Stat Med* (1999) 18 (7):815–33. doi: 10.1002/(SICI)1097-0258(19990415)18:7<815::AID-SIM74>3.0.CO;2-G
22. Menu E, Mbopi-Keou FX, Lagaye S, Pissard S, Mauclère P, Scarlatti G, et al. Selection of Maternal Human Immunodeficiency Virus Type 1 Variants in Human Placenta. European Network for *In Utero* Transmission of HIV-1. *J Infect Dis* (1999) 179(1):44–51. doi: 10.1086/314542
23. Zachar V, Zacharova V, Fink T, Thomas RA, King BR, Ebbesen P, et al. Genetic Analysis Reveals Ongoing HIV Type 1 Evolution in Infected Human Placental Trophoblast. *AIDS Res Hum Retroviruses* (1999) 15(18):1673–83. doi: 10.1089/088922299309711
24. De Andreis C, Simoni G, Rossella F, Castagna C, Pesenti E, Porta G, et al. HIV-1 Proviral DNA Polymerase Chain Reaction Detection in Chorionic Villi After Exclusion of Maternal Contamination by Variable Number of Tandem Repeats Analysis. *AIDS* (1996) 10(7):711–5. doi: 10.1097/00002030-199606001-00004
25. Ross AL, Cannou C, Barré-Sinoussi F, Menu E. Proteasome-Independent Degradation of HIV-1 in Naturally Non-Permissive Human Placental Trophoblast Cells. *Retrovirology* (2009) 6:46. doi: 10.1186/1742-4690-6-46
26. Lagaye S, Derrien M, Menu E, Coïto C, Tresoldi E, Mauclère P, et al. Cell-To-Cell Contact Results in a Selective Translocation of Maternal Human Immunodeficiency Virus Type 1 Quasispecies Across a Trophoblastic Barrier by Both Transcytosis and Infection. *J Virol* (2001) 75(10):4780–91. doi: 10.1128/JVI.75.10.4780-4791.2001
27. Tang Y, Woodward BO, Pastor L, George AM, Petrechko O, Nouvet FJ, et al. Endogenous Retroviral Envelope Syncytin Induces HIV-1 Spreading and Establishes HIV Reservoirs in Placenta. *Cell Rep* (2020) 30(13):4528–39.e4. doi: 10.1016/j.celrep.2020.03.016
28. Biggar RJ, Lee TH, Wen L, Broadhead R, Kumwenda N, Taha TE, et al. The Role of Transplacental Microtransfusions of Maternal Lymphocytes in HIV Transmission to Newborns. *AIDS* (2008) 22(17):2251–6. doi: 10.1097/QAD.0b013e328314e36b
29. Lee TH, Chafets DM, Biggar RJ, McCune JM, Busch MP. The Role of Transplacental Microtransfusions of Maternal Lymphocytes in *In Utero* HIV Transmission. *J Acquir Immune Defic Syndr* (2010) 55(2):143–7. doi: 10.1097/QAI.0b013e3181eb301e
30. Magder LS, Mofenson L, Paul ME, Zorrilla CD, Blattner WA, Tuomala RE, et al. Risk Factors for *In Utero* and Intrapartum Transmission of HIV. *J Acquir Immune Defic Syndr* (2005) 38(1):87–95. doi: 10.1097/00126334-200501010-00016
31. Fawzi W, Msamanga G, Renjifo B, Spiegelman D, Urassa E, Hashemi L, et al. Predictors of Intrauterine and Intrapartum Transmission of HIV-1 Among Tanzanian Women. *AIDS* (2001) 15(9):1157–65. doi: 10.1097/00002030-200106150-00011
32. Mofenson LM, Lambert JS, Stiehm ER, Bethel J, Meyer WA, Whitehouse J, et al. Risk Factors for Perinatal Transmission of Human Immunodeficiency Virus Type 1 in Women Treated With Zidovudine. Pediatric AIDS Clinical Trials Group Study 185 Team. *N Engl J Med* (1999) 341(6):385–93. doi: 10.1056/NEJM199908053410601
33. Briand N, Jasseron C, Sibiude J, Azria E, Pollet J, Hammou Y, et al. Cesarean Section for HIV-Infected Women in the Combination Antiretroviral Therapies Era, 2000-2010. *Am J Obstet Gynecol* (2013) 209(4):335.e1–12. doi: 10.1016/j.ajog.2013.06.021
34. Drake AL, John-Stewart GC, Wald A, Mbori-Ngacha DA, Bosire R, Wamalwa DC, et al. Herpes Simplex Virus Type 2 and Risk of Intrapartum Human Immunodeficiency Virus Transmission. *Obstet Gynecol* (2007) 109(2 Pt 1):403–9. doi: 10.1097/01.AOG.0000251511.27725.5c
35. Mbopi-Kéou FX, Legoff J, Grésenguet G, Si-Mohamed A, Matta M, Mayaud P, et al. Genital Shedding of Herpes Simplex Virus-2 DNA and HIV-1 RNA and Proviral DNA in HIV-1- and Herpes Simplex Virus-2-Coinfected African Women. *J Acquir Immune Defic Syndr* (2003) 33(2):121–4. doi: 10.1097/00126334-200306010-00001
36. McClelland RS, Wang CC, Overbaugh J, Richardson BA, Corey L, Ashley RL, et al. Association Between Cervical Shedding of Herpes Simplex Virus and HIV-1. *AIDS* (2002) 16(18):2425–30. doi: 10.1097/00002030-200212060-00007
37. Parazzini F, Ricci E, Chiaffarino F, Di Cintio E, Di Cintio E, Pardi G, et al.Elective Caesarean-Section *Versus* Vaginal Delivery in Prevention of Vertical HIV-1 Transmission: A Randomised Clinical Trial. *Lancet* (1999) 353(9158):1035–9. doi: 10.1016/s0140-6736(98)08084-2
38. Andiman W, Bryson Y, de Martino M, Bryson Y, Farley J, Fowler H, et al. The Mode of Delivery and the Risk of Vertical Transmission of Human Immunodeficiency Virus Type 1–A Meta-Analysis of 15 Prospective Cohort Studies. *N Engl J Med* (1999) 340(13):977–87. doi: 10.1056/NEJM199904013401301
39. Kennedy CE, Yeh PT, Pandey S, Betran AP, Narasimhan M. Elective Cesarean Section for Women Living With HIV: A Systematic Review of Risks and Benefits. *AIDS* (2017) 31(11):1579–91. doi: 10.1097/QAD.0000000000001535
40. Kwiek JJ, Mwapasa V, Milner DA Jr, Alker AP, Miller WC, Tadesse E, et al. Maternal-Fetal Microtransfusions and HIV-1 Mother-to-Child Transmission in Malawi. *PloS Med* (2006) 3(1):e10. doi: 10.1371/journal.pmed.0030010
41. Ivy WI, Dominguez KL, Rakhmanina NY, Iuliano AD, Danner SP, Borkowf CB, et al. Premastication as a Route of Pediatric HIV Transmission: Case–Control and Cross-Sectional Investigations. *JAIDS J Acquired Immune Defic Syndr* (2012) 59(2):207–12. doi: 10.1097/QAI.0b013e31823b4554
42. Organization WH. *Breastfeeding and HIV*. World Health Organization (2016).
43. Tugizov SM, Herrera R, Veluppillai P, Greenspan D, Soros V, Greene WC, et al. Differential Transmission of HIV Traversing Fetal Oral/Intestinal Epithelia and Adult Oral Epithelia. *J Virol* (2012) 86(5):2556–70. doi: 10.1128/JVI.06578-11
44. Milush JM, Kosub D, Marthas M, Schmidt K, Scott F, Wozniakowski A, et al. Rapid Dissemination of SIV Following Oral Inoculation. *AIDS* (2004) 18 (18):2371–80.
45. Van Rompay KK, Abel K, Lawson JR, Singh RP, Schmidt KA, Evans T, et al. Attenuated Poxvirus-Based Simian Immunodeficiency Virus (SIV) Vaccines Given in Infancy Partially Protect Infant and Juvenile Macaques Against Repeated Oral Challenge With Virulent SIV. *J Acquir Immune Defic Syndr* (2005) 38(2):124–34. doi: 10.1097/00126334-200502010-00002
46. Obregon-Perko V, Bricker KM, Mensah G, Uddin F, Kumar MR, Fray EJ, et al. Simian-Human Immunodeficiency Virus SHIV.C.CH505 Persistence in ART-Suppressed Infant Macaques Is Characterized by Elevated SHIV RNA in the Gut and a High Abundance of Intact SHIV DNA in Naive CD4+ T Cells. *J Virol* (2020) 95(2):e01669–20. doi: 10.1128/JVI.01669-20
47. Mavigner M, Habib J, Deleage C, Rosen E, Mattingly C, Bricker K, et al. Simian Immunodeficiency Virus Persistence in Cellular and Anatomic Reservoirs in Antiretroviral Therapy-Suppressed Infant Rhesus Macaques. *J Virol* (2018) 92(18):e00562–18. doi: 10.1128/JVI.00562-18

48. Chahroudi A, Cartwright E, Lee ST, Mavigner M, Carnathan DG, Lawson B, et al. Target Cell Availability, Rather Than Breast Milk Factors, Dictates Mother-To-Infant Transmission of SIV in Sooty Mangabeys and Rhesus Macaques. *PloS Pathog* (2014) 10(3):e1003958. doi: 10.1371/journal.ppat.1003958
49. Veazey RS, Lifson JD, Pandrea I, Purcell J, Piatak M, Lackner AA. Simian Immunodeficiency Virus Infection in Neonatal Macaques. *J Virol* (2003) 77 (16):8783–92. doi: 10.1128/jvi.77.16.8783-8792.2003
50. Wang X, Xu H, Pahar B, Alvarez X, Green LC, Dufour J, et al. Simian Immunodeficiency Virus Selectively Infects Proliferating CD4+ T Cells in Neonatal Rhesus Macaques. *Blood* (2010) 116(20):4168–74. doi: 10.1182/blood-2010-03-273482
51. Lyimo MA, Howell AL, Balandya E, Eszterhas SK, Connor RI. Innate Factors in Human Breast Milk Inhibit Cell-Free HIV-1 But Not Cell-Associated HIV-1 Infection of CD4+ Cells. *J Acquir Immune Defic Syndr* (2009) 51 (2):117–24. doi: 10.1097/QAI.0b013e3181a3908d
52. Fouda GG, Jaeger FH, Amos JD, Ho C, Kunz EL, Anasti K, et al. Tenascin-C Is an Innate Broad-Spectrum, HIV-1-Neutralizing Protein in Breast Milk. *Proc Natl Acad Sci USA* (2013) 110(45):18220–5. doi: 10.1073/pnas.1307336110
53. Mall AS, Habte H, Mthembu Y, Peacocke J, de Beer C. Mucus and Mucins: Do They Have a Role in the Inhibition of the Human Immunodeficiency Virus? *Virol J* (2017) 14(1):192. doi: 10.1186/s12985-017-0855-9
54. Kazmi SH, Naglik JR, Sweet SP, Evans RW, O'Shea S, Banatvala JE, et al. Comparison of Human Immunodeficiency Virus Type 1-Specific Inhibitory Activities in Saliva and Other Human Mucosal Fluids. *Clin Vaccine Immunol* (2006) 13(10):1111–8. doi: 10.1128/CDLI.00426-05
55. Milligan C, Overbaugh J. The Role of Cell-Associated Virus in Mother-To-Child HIV Transmission. *J Infect Dis* (2014) 210(suppl_3):S631–40. doi: 10.1093/infdis/jiu344
56. Lunney KM, Iliff P, Mutasa K, Ntozini R, Magder LS, Moulton LH, et al. Associations Between Breast Milk Viral Load, Mastitis, Exclusive Breast-Feeding, and Postnatal Transmission of HIV. *Clin Infect Dis* (2010) 50 (5):762–9. doi: 10.1086/650535
57. Kuhn L, Sinkala M, Kankasa C, Semrau K, Kasonde P, Scott N, et al. High Uptake of Exclusive Breastfeeding and Reduced Early Post-Natal HIV Transmission. *PloS One* (2007) 2(12):e1363. doi: 10.1371/journal.pone.0001363
58. Coovadia HM, Rollins NC, Bland RM, Little K, Coutsoudis A, Bennish ML, et al. Mother-To-Child Transmission of HIV-1 Infection During Exclusive Breastfeeding in the First 6 Months of Life: An Intervention Cohort Study. *Lancet* (2007) 369(9567):1107–16. doi: 10.1016/S0140-6736(07)60283-9
59. Coutsoudis A, Dabis F, Fawzi W, Gaillard P, Haverkamp G, Harris DR, et al. Late Postnatal Transmission of HIV-1 in Breast-Fed Children: An Individual Patient Data Meta-Analysis. *J Infect Dis* (2004) 189(12):2154–66. doi: 10.1086/420834
60. Gejo NG, Weldearegay HG, W/tinsaie KT, Mekango DE, Woldemichael ES, Buda AS, et al. Exclusive Breastfeeding and Associated Factors Among HIV Positive Mothers in Northern Ethiopia. *PloS One* (2019) 14(1):e0210782. doi: 10.1371/journal.pone.0210782
61. Coutsoudis A, Pillay K, Spooner E, Kuhn L, Coovadia HM. Influence of Infant-Feeding Patterns on Early Mother-to-Child Transmission of HIV-1 in Durban, South Africa: A Prospective Cohort Study. South African Vitamin A Study Group. *Lancet* (1999) 354(9177):471–6. doi: 10.1016/S0140-6736(99)01101-0
62. Semrau K, Kuhn L, Brooks DR, Cabral H, Sinkala M, Kankasa C, et al. Exclusive Breastfeeding, Maternal HIV Disease, and the Risk of Clinical Breast Pathology in HIV-Infected, Breastfeeding Women. *Am J Obstet Gynecol* (2011) 205(4):344.e1–8. doi: 10.1016/j.ajog.2011.06.021
63. Semba RD, Kumwenda N, Hoover DR, Taha TE, Quinn TC, Mtimavalye L, et al. Human Immunodeficiency Virus Load in Breast Milk, Mastitis, and Mother-to-Child Transmission of Human Immunodeficiency Virus Type 1. *J Infect Dis* (1999) 180(1):93–8. doi: 10.1086/314854
64. Embree JE, Njenga S, Datta P, Nagelkerke NJD, Ndinya-Achola JO, Mohammed Z, et al. Risk Factors for Postnatal Mother-Child Transmission of HIV-1. *AIDS* (2000) 14(16):2535–41. doi: 10.1097/00002030-200011100-00016
65. Wood LF, Brown BP, Lennard K, Karaoz U, Havyarimana E, Passmore J-AS, et al. Feeding-Related Gut Microbial Composition Associates With Peripheral T-Cell Activation and Mucosal Gene Expression in African Infants. *Clin Infect Dis* (2018) 67(8):1237–46. doi: 10.1093/cid/ciy265
66. Rousseau CM, Nduati RM, Richardson BA, John-Stewart GC, Mbori-Ngacha DA, Kreiss JK, et al. Association of Levels of HIV-1–Infected Breast Milk Cells and Risk of Mother-To-Child Transmission. *J Infect Dis* (2004) 190(10):1880–8. doi: 10.1086/425076
67. Ndirangu J, Viljoen J, Bland RM, Danaviah S, Thorne C, Vande Perre P, et al. Cell-Free (RNA) and Cell-Associated (DNA) HIV-1 and Postnatal Transmission Through Breastfeeding. *PloS One* (2012) 7(12):e51493. doi: 10.1371/journal.pone.0051493
68. Thea DM, Steketee RW, Pliner V, Bornschlegel K, Brown T, Orloff S, et al. The Effect of Maternal Viral Load on the Risk of Perinatal Transmission of HIV-1. *AIDS* (1997) 11(4):437–44. doi: 10.1097/00002030-199704000-00006
69. Cao Y, Krogstad P, Korber BT, Koup RA, Muldoon M, Macken C, et al. Maternal HIV-1 Viral Load and Vertical Transmission of Infection: The Ariel Project for the Prevention of HIV Transmission From Mother to Infant. *Nat Med* (1997) 3(5):549–52. doi: 10.1038/nm0597-549
70. Scarlatti G, Hodara V, Rossi P, Muggiasca L, Bucceri A, Albert J, et al. Transmission of Human Immunodeficiency Virus Type 1 (HIV-1) From Mother to Child Correlates With Viral Phenotype. *Virology* (1993) 197 (2):624–9. doi: 10.1006/viro.1993.1637
71. O'Shea S, Newell M-L, Dunn DT, Garcia-Rodriguez M-C, Bates I, Mullen J, et al. Maternal Viral Load, CD4 Cell Count and Vertical Transmission of HIV-1. *J Med Virol* (1998) 54(2):113–7. doi: 10.1002/(SICI)1096-9071(199802)54:2<113::AID-JMV8>3.0.CO;2-9
72. Morrison CS, Demers K, Kwok C, Bulime S, Rinaldi A, Munjoma M, et al. Plasma and Cervical Viral Loads Among Ugandan and Zimbabwean Women During Acute and Early HIV-1 Infection. *AIDS* (2010) 24(4):573–82. doi: 10.1097/QAD.0b013e32833433df
73. Connor EM, Sperling RS, Gelber R, Kiselev P, Scott G, O'Sullivan MJ, et al. Reduction of Maternal-Infant Transmission of Human Immunodeficiency Virus Type 1 With Zidovudine Treatment. Pediatric AIDS Clinical Trials Group Protocol 076 Study Group. *N Engl J Med* (1994) 331(18):1173–80. doi: 10.1056/NEJM199411033311801
74. Cooper ER, Charurat M, Mofenson L, Hanson CI, Pitt J, Diaz C, et al. Combination Antiretroviral Strategies for the Treatment of Pregnant HIV-1-Infected Women and Prevention of Perinatal HIV-1 Transmission. *J Acquir Immune Defic Syndr* (2002) 29(5):484–94. doi: 10.1097/00042560-200204150-00009
75. Dickover RE, Garratty EM, Herman SA, Sim MS, Plaeger S, Boyer PJ, et al. Identification of Levels of Maternal HIV-1 RNA Associated With Risk of Perinatal Transmission: Effect of Maternal Zidovudine Treatment on Viral Load. *JAMA* (1996) 275(8):599–605. doi: 10.1001/jama.1996.03530320023029
76. Mayaux MJ, Dussaix E, Isopet J, Rekacewicz C, Mandelbrot L, Ciraru-Vigneron N, et al. Maternal Virus Load During Pregnancy and Mother-To-Child Transmission of Human Immunodeficiency Virus Type 1: The French Perinatal Cohort Studies. *J Infect Dis* (1997) 175(1):172–5. doi: 10.1093/infdis/175.1.172
77. Shaffer N, Roongpisuthipong A, Siriwasin W, Chotpitayasunondh T, Chearskul S, Young NL, et al. Maternal Virus Load and Perinatal Human Immunodeficiency Virus Type 1 Subtype E Transmission, Thailand. *J Infect Dis* (1999) 179(3):590–9. doi: 10.1086/314641
78. Burns DN, Landesman S, Muenz LR, Nugent RP, Goedert JJ, Minkoff H, et al. Cigarette Smoking, Premature Rupture of Membranes, and Vertical Transmission of HIV-1 Among Women With Low CD4+ Levels. *J Acquir Immune Defic Syndr (1988)* (1994) 7(7):718–26.
79. Turner BJ, Hauck WW, Fanning TR, Markson LE. Cigarette Smoking and Maternal-Child HIV Transmission. *J Acquir Immune Defic Syndr Hum Retrovirol* (1997) 14(4):327–37. doi: 10.1097/00042560-199704010-00004
80. Matheson PB, Schoenbaum E, Greenberg B, Pliner V. Association of Maternal Drug Use During Pregnancy With Mother-to-Child HIV Transmission. New York City Perinatal HIV Transmission Collaborative Study. *AIDS* (1997) 11(7):941–2.
81. Rodriguez EM, Mofenson LM, Chang BH, Rich KC, Fowler MG, Smeriglio V, et al. Association of Maternal Drug Use During Pregnancy With Maternal HIV Culture Positivity and Perinatal HIV Transmission. *AIDS* (1996) 10 (3):273–82. doi: 10.1097/00002030-199603000-00006

82. Carrico AW, Johnson MO, Moskowitz JT, Neilands TB, Morin SF, Charlebois ED, et al. Affect Regulation, Stimulant Use, and Viral Load Among HIV-Positive Persons on Anti-Retroviral Therapy. *Psychosom Med* (2007) 69(8):785–92. doi: 10.1097/PSY.0b013e318157b142
83. Baum MK, Rafie C, Lai S, Sales S, Page B, Campa A. Crack-Cocaine Use Accelerates HIV Disease Progression in a Cohort of HIV-Positive Drug Users. *J Acquir Immune Defic Syndr* (2009) 50(1):93–9. doi: 10.1097/QAI.0b013e3181900129
84. Ellis RJ, Childers ME, Cherner M, Lazzaretto D, Letendre S, Grant I. Increased Human Immunodeficiency Virus Loads in Active Methamphetamine Users Are Explained by Reduced Effectiveness of Antiretroviral Therapy. *J Infect Dis* (2003) 188(12):1820–6. doi: 10.1086/379894
85. Chander G, Lau B, Moore RD. Hazardous Alcohol Use: A Risk Factor for Non-Adherence and Lack of Suppression in HIV Infection. *J Acquir Immune Defic Syndr* (2006) 43(4):411–7. doi: 10.1097/01.qai.0000243121.44659.a4
86. Purohit V, Rapaka RS, Schnur P, Shurtleff D. Potential Impact of Drugs of Abuse on Mother-to-Child Transmission (MTCT) of HIV in the Era of Highly Active Antiretroviral Therapy (HAART). *Life Sci* (2011) 88(21-22):909–16. doi: 10.1016/j.lfs.2011.03.022
87. Arnsten JH, Demas PA, Grant RW, Gourevitch MN, Farzadegan H, Howard AA. Impact of Active Drug Use on Antiretroviral Therapy Adherence and Viral Suppression in HIV-Infected Drug Users. *J Gen Intern Med* (2002) 17(5):377–81. doi: 10.1007/s11606-002-0044-3
88. John GC, Nduati RW, Mbori-Ngacha D, Overbaugh J, Welch M, Richardson BA, et al. Genital Shedding of Human Immunodeficiency Virus Type 1 DNA During Pregnancy: Association With Immunosuppression, Abnormal Cervical or Vaginal Discharge, and Severe Vitamin A Deficiency. *J Infect Dis* (1997) 175(1):57–62. doi: 10.1093/infdis/175.1.57
89. Clemetson DBA. Detection of HIV DNA in Cervical and Vaginal Secretions. *JAMA* (1993) 269(22):2860. doi: 10.1001/jama.1993.03500220046024
90. Loussert-Ajaka I, Mandelbrot L, Delmas MC, Bastian H, Benifla JL, Farfara I, et al. HIV-1 Detection in Cervicovaginal Secretions During Pregnancy. *AIDS* (1997) 11(13):1575–81. doi: 10.1097/00002030-199713000-00005
91. Rousseau CM, Nduati RM, Richardson BA, Steele MS, John-Stewart GC, Mbori-Ngacha DA, et al. Longitudinal Analysis of Human Immunodeficiency Virus Type 1 RNA in Breast Milk and of Its Relationship to Infant Infection and Maternal Disease. *J Infect Dis* (2003) 187(5):741–7. doi: 10.1086/374273
92. Nagot N, Kankasa C, Tumwine JK, Meda N, Hofmeyr GJ, Vallo R, et al. Extended Pre-Exposure Prophylaxis With Lopinavir–Ritonavir *Versus* Lamivudine to Prevent HIV-1 Transmission Through Breastfeeding Up to 50 Weeks in Infants in Africa (ANRS 12174): A Randomised Controlled Trial. *Lancet* (2016) 387(10018):566–73. doi: 10.1016/S0140-6736(15)00984-8
93. Flynn PM, Taha TE, Cababasay M, Fowler MG, Mofenson LM, Owor M, et al. Prevention of HIV-1 Transmission Through Breastfeeding: Efficacy and Safety of Maternal Antiretroviral Therapy *Versus* Infant Nevirapine Prophylaxis for Duration of Breastfeeding in HIV-1-Infected Women With High CD4 Cell Count (IMPAACT PROMISE): A Randomi. *JAIDS J Acquir Immune Defic Syndr* (2018) 77(4):383–92. doi: 10.1097/QAI.0000000000001612
94. Flynn PM, Taha TE, Cababasay M, Butler K, Fowler MG, Mofenson LM, et al. Association of Maternal Viral Load and CD4 Count With Perinatal HIV-1 Transmission Risk During Breastfeeding in the PROMISE Postpartum Component. *JAIDS J Acquired Immune Deficiency Syndromes* (2021) 88(2):206–13. doi: 10.1097/QAI.0000000000002744
95. Shapiro RL, Hughes MD, Ogwu A, Kitch D, Lockman S, Moffat C, et al. Antiretroviral Regimens in Pregnancy and Breast-Feeding in Botswana. *New Engl J Med* (2010) 362(24):2282–94. doi: 10.1056/NEJMoa0907736
96. Luoga E, Vanobberghen F, Bircher R, Nyuri A, Ntamatungiro AJ, Mnzava D, et al. Brief Report: No HIV Transmission From Virally Suppressed Mothers During Breastfeeding in Rural Tanzania. *J Acquir Immune Defic Syndr* (2018) 79(1):e17–20. doi: 10.1097/QAI.0000000000001758
97. Giuliano M, Andreotti M, Liotta G, Jere H, Sagno J-B, Maulidi M, et al. Maternal Antiretroviral Therapy for the Prevention of Mother-To-Child Transmission of HIV in Malawi: Maternal and Infant Outcomes Two Years After Delivery. *PloS One* (2013) 8(7):e68950. doi: 10.1371/journal.pone.0068950
98. Kliks S, Contag CH, Corliss H, Learn G, Rodrigo A, Wara D, et al. Genetic Analysis of Viral Variants Selected in Transmission of Human Immunodeficiency Viruses to Newborns. *AIDS Res Hum Retroviruses* (2000) 16(13):1223–33. doi: 10.1089/08892220050116998
99. Zhang H, Tully DC, Hoffmann FG, He J, Kankasa C, Wood C. Phylogenetic and Phenotypic Analysis of HIV Type 1 Env Gp120 in Cases of Subtype C Mother-to-Child Transmission. *AIDS Res Hum Retroviruses* (2002) 18 (18):1415–23. doi: 10.1089/088922202320935492
100. Renjifo B, Chung M, Gilbert P, Mwakagile D, Msamanga G, Fawzi W, et al. In-Utero Transmission of Quasispecies Among Human Immunodeficiency Virus Type 1 Genotypes. *Virology* (2003) 307(2):278–82. doi: 10.1016/S0042-6822(02)00066-1
101. Dickover RE, Garratty EM, Plaeger S, Bryson YJ. Perinatal Transmission of Major, Minor, and Multiple Maternal Human Immunodeficiency Virus Type 1 Variants *In Utero* and Intrapartum. *J Virol* (2001) 75(5):2194–203. doi: 10.1128/JVI.75.5.2194-2203.2001
102. Kwiek JJ, Russell ES, Dang KK, Burch CL, Mwapasa V, Meshnick SR, et al. The Molecular Epidemiology of HIV-1 Envelope Diversity During HIV-1 Subtype C Vertical Transmission in Malawian Mother–Infant Pairs. *AIDS* (2008) 22(7):863–71. doi: 10.1097/QAD.0b013e3282f51ea0
103. Ahmad N, Baroudy BM, Baker RC, Chappey C. Genetic Analysis of Human Immunodeficiency Virus Type 1 Envelope V3 Region Isolates From Mothers and Infants After Perinatal Transmission. *J Virol* (1995) 69(2):1001–12. doi: 10.1128/jvi.69.2.1001-1012.1995
104. Wolinsky S, Wike C, Korber B, Hutto C, Parks WP, Rosenblum L, et al. Selective Transmission of Human Immunodeficiency Virus Type-1 Variants From Mothers to Infants. *Science* (1992) 255(5048):1134–7. doi: 10.1126/science.1546316
105. Boyce CL, Sils T, Ko D, Wong-On-Wing A, Beck IA, Styrchak SM, et al. Maternal HIV Drug Resistance Is Associated With Vertical Transmission and Is Prevalent in Infected Infants. *Clin Infect Dis* (2021). doi: 10.1093/cid/ciab744
106. Baan E, de Ronde A, Luchters S, Vyankandondera J, Lange JM, Pollakis G, et al. HIV Type 1 Mother-to-Child Transmission Facilitated by Distinctive Glycosylation Sites in the Gp120 Envelope Glycoprotein. *AIDS Res Hum Retroviruses* (2012) 28(7):715–24. doi: 10.1089/aid.2011.0023
107. Ometto L, Zanchetta M, Mainardi M, De Salvo GL, Garcia-Rodriguez MC, Gray L, et al. Co-Receptor Usage of HIV-1 Primary Isolates, Viral Burden, and CCR5 Genotype in Mother-to-Child HIV-1 Transmission. *AIDS* (2000) 14(12):1721–9. doi: 10.1097/00002030-200008180-00006
108. Derdeyn CA, Hunter E. Viral Characteristics of Transmitted HIV. *Curr Opin HIV AIDS* (2008) 3(1):16–21. doi: 10.1097/COH.0b013e3282f2982c
109. John GC, Kreiss J. Mother-To-Child Transmission of Human Immunodeficiency Virus Type 1. *Epidemiologic Rev* (1996) 18(2):149–57. doi: 10.1093/oxfordjournals.epirev.a017922
110. Bryson YJ. Perinatal HIV-1 Transmission: Recent Advances and Therapeutic Interventions. *AIDS* (1996) 10 Suppl 3:S33–42.
111. Van'T Wout AB, Kootstra NA, Mulder-Kampinga GA, Albrecht-van Lent N, Scherpbier HJ, Veenstra J, et al. Macrophage-Tropic Variants Initiate Human Immunodeficiency Virus Type 1 Infection After Sexual, Parenteral, and Vertical Transmission. *J Clin Invest* (1994) 94(5):2060–7. doi: 10.1172/JCI117560
112. Yang C, Li M, Newman RD, Shi Y-P, Ayisi J, van Eijk AM, et al. Genetic Diversity of HIV-1 in Western Kenya: Subtype-Specific Differences in Mother-to-Child Transmission. *AIDS* (2003) 17(11):1667–74. doi: 10.1097/00002030-200307250-00011
113. Walter J, Kuhn L, Aldrovandi GM. Advances in Basic Science Understanding of Mother-to-Child HIV-1 Transmission. *Curr Opin HIV AIDS* (2008) 3 (2):146–50. doi: 10.1097/COH.0b013e3282f50bb2
114. Koulinska IN, Villamor E, Chaplin B, Msamanga G, Fawzi W, Renjifo B, et al. Transmission of Cell-Free and Cell-Associated HIV-1 Through Breast-Feeding. *J Acquir Immune Defic Syndr (1999)* (2006) 41(1):93–9. doi: 10.1097/01.qai.0000179424.19413.24
115. Eshleman SH, Church JD, Chen S, Guay LA, Mwatha A, Fiscus SA, et al. Comparison of HIV-1 Mother-to-Child Transmission After Single-Dose Nevirapine Prophylaxis Among African Women With Subtypes A, C and D. *J Acquir Immune Defic Syndr* (2006) 42(4):518–21. doi: 10.1097/01.qai.0000221676.22069.b8
116. Choi RY, Farquhar C, Juno J, Mbori-Ngacha D, Lohman-Payne B, Vouriot F, et al. Infant CD4 C868T Polymorphism Is Associated With Increased

Human Immunodeficiency Virus (HIV-1) Acquisition. *Clin Exp Immunol* (2010) 160(3):461–5. doi: 10.1111/j.1365-2249.2010.04096.x

117. Shearer WT, Kalish LA, Zimmerman PA. CCR5 HIV-1 Vertical Transmission. Women and Infants Transmission Study Group. *J Acquir Immune Defic Syndr Hum Retrovirol* (1998) 17(2):180–1. doi: 10.1097/00042560-199802010-00014
118. Mandl CW, Aberle SW, Henkel JH, Puchhammer-Stöckl E, Heinz FX. Possible Influence of the Mutant CCR5 Allele on Vertical Transmission of HIV-1. *J Med Virol* (1998) 55(1):51–5. doi: 10.1002/(SICI)1096-9071(199805)55:1<51::AID-JMV9>3.0.CO;2-N
119. Philpott S, Burger H, Charbonneau T, Grimson R, Vermund SH, Visosky A, et al. CCR5 Genotype and Resistance to Vertical Transmission of HIV-1. *J Acquir Immune Defic Syndr* (1999) 21(3):189–93. doi: 10.1097/00126334-199907010-00002
120. Kostrikis LG, Neumann AU, Thomson B, Korber BT, McHardy P, Karanicolas R, et al. A Polymorphism in the Regulatory Region of the CC-Chemokine Receptor 5 Gene Influences Perinatal Transmission of Human Immunodeficiency Virus Type 1 to African-American Infants. *J Virol* (1999) 73(12):10264–71. doi: 10.1128/JVI.73.12.10264-10271.1999
121. Pedersen BR, Kamwendo D, Blood M, Mwapasa V, Molyneux M, North K, et al. CCR5 Haplotypes and Mother-to-Child HIV Transmission in Malawi. *PloS One* (2007) 2(9):e838. doi: 10.1371/journal.pone.0000838
122. Singh KK, Hughes MD, Chen J, Phiri K, Rousseau C, Kuhn L, et al. Associations of Chemokine Receptor Polymorphisms With HIV-1 Mother-to-Child Transmission in Sub-Saharan Africa: Possible Modulation of Genetic Effects by Antiretrovirals. *J Acquir Immune Defic Syndr* (2008) 49(3):259–65. doi: 10.1097/QAI.0b013e318186eaa4
123. Salkowitz JR, Bruse SE, Meyerson H, Valdez H, Mosier DE, Harding CV, et al. CCR5 Promoter Polymorphism Determines Macrophage CCR5 Density and Magnitude of HIV-1 Propagation *in vitro*. *Clin Immunol* (2003) 108(3):234–40. doi: 10.1016/S1521-6616(03)00147-5
124. De Rossi A. Virus-Host Interactions in Paediatric HIV-1 Infection. *Curr Opin HIV AIDS* (2007) 2(5):399–404. doi: 10.1097/COH.0b013e3282ced163
125. Braida L, Boniotto M, Pontillo A, Tovo PA, Amoroso A, Crovella S. A Single-Nucleotide Polymorphism in the Human Beta-Defensin 1 Gene Is Associated With HIV-1 Infection in Italian Children. *AIDS* (2004) 18(11):1598–600. doi: 10.1097/01.aids.0000131363.82951.fb
126. Ricci E, Malacrida S, Zanchetta M, Montagna M, Giaquinto C, De Rossi A. Role of Beta-Defensin-1 Polymorphisms in Mother-to-Child Transmission of HIV-1. *J Acquir Immune Defic Syndr* (2009) 51(1):13–9. doi: 10.1097/QAI.0b013e31819df249
127. Milanese M, Segat L, Pontillo A, Arraes LC, de Lima Filho JL, Crovella S. DEFB1 Gene Polymorphisms and Increased Risk of HIV-1 Infection in Brazilian Children. *AIDS* (2006) 20(12):1673–5. doi: 10.1097/01.aids.0000238417.05819.40
128. Milanese M, Segat L, Arraes LC, Garzino-Demo A, Crovella S. Copy Number Variation of Defensin Genes and HIV Infection in Brazilian Children. *J Acquir Immune Defic Syndr* (2009) 50(3):331–3. doi: 10.1097/QAI.0b013e3181945f39
129. Polycarpou A, Ntais C, Korber BT, Elrich HA, Winchester R, Krogstad P, et al. Association Between Maternal and Infant Class I and II HLA Alleles and of Their Concordance With the Risk of Perinatal HIV Type 1 Transmission. *AIDS Res Hum Retroviruses* (2002) 18(11):741–6. doi: 10.1089/08892220260139477
130. Aikhionbare FO, Hodge T, Kuhn L, Bulterys M, Abrams EJ, Bond VC. Mother-To-Child Discordance in HLA-G Exon 2 Is Associated With a Reduced Risk of Perinatal HIV-1 Transmission. *AIDS* (2001) 15(16):2196–8. doi: 10.1097/00002030-200111090-00019
131. MacDonald KS, Embree J, Njenga S, Nagelkerke NJD, Ngatia I, Mohammed Z, et al. Mother-Child Class I HLA Concordance Increases Perinatal Human Immunodeficiency Virus Type 1 Transmission. *J Infect Dis* (1998) 177(3):551–6. doi: 10.1086/514243
132. MacDonald KS, Embree JE, Nagelkerke NJ, Castillo J, Ramhadin S, Njenga S, et al. The HLA A2/6802 Supertype Is Associated With Reduced Risk of Perinatal Human Immunodeficiency Virus Type 1 Transmission. *J Infect Dis* (2001) 183(3):503–6. doi: 10.1086/318092
133. Farquhar C, Rowland-Jones S, Mbori-Ngacha D, Redman M, Lohman B, Slyker J, et al. Human Leukocyte Antigen (HLA) B*18 and Protection Against Mother-to-Child HIV Type 1 Transmission. *AIDS Res Hum Retroviruses* (2004) 20(7):692–7. doi: 10.1089/0889222041524616
134. Mackelprang RD, John-Stewart G, Carrington M, Richardson B, Rowland-Jones S, Gao X, et al. Maternal HLA Homozygosity and Mother-Child HLA Concordance Increase the Risk of Vertical Transmission of HIV-1. *J Infect Dis* (2008) 197(8):1156–61. doi: 10.1086/529528
135. Fabris A, Catamo E, Segat L, Morgutti M, Arraes LC, de Lima-Filho JL, et al. Association Between HLA-G 3'UTR 14-Bp Polymorphism and HIV Vertical Transmission in Brazilian Children. *AIDS* (2009) 23(2):177–82. doi: 10.1097/QAD.0b013e32832027bf
136. Aikhionbare FO, Kumaresan K, Shamsa F, Bond VC. HLA-G DNA Sequence Variants and Risk of Perinatal HIV-1 Transmission. *AIDS Res Ther* (2006) 3:28. doi: 10.1186/1742-6405-3-28
137. Kilpatrick DC, Hague RA, Yap PL, Mok JY. HLA Antigen Frequencies in Children Born to HIV-Infected Mothers. *Dis Markers* (1991) 9(1):21–6.
138. Winchester R, Chen Y, Rose S, Selby J, Borkowsky W. Major Histocompatibility Complex Class II DR Alleles DRB1*1501 and Those Encoding HLA-DR13 Are Preferentially Associated With a Diminution in Maternally Transmitted Human Immunodeficiency Virus 1 Infection in Different Ethnic Groups: Determination by an Automated Sequence-Based Typing Method. *Proc Natl Acad Sci USA* (1995) 92(26):12374–8. doi: 10.1073/pnas.92.26.12374
139. Just JJ, Abrams E, Louie LG, Urbano R, Wara D, Nicholas SW, et al. Influence of Host Genotype on Progression to Acquired Immunodeficiency Syndrome Among Children Infected With Human Immunodeficiency Virus Type 1. *J Pediatr* (1995) 127(4):544–9. doi: 10.1016/S0022-3476(95)70110-9
140. Biggar RJ, Taha TE, Hoover DR, Yellin F, Kumwenda N, Broadhead R. Higher *In Utero* and Perinatal HIV Infection Risk in Girls Than Boys. *J Acquir Immune Defic Syndr* (2006) 41(4):509–13. doi: 10.1097/01.qai.0000191283.85578.46
141. Taha TE, Nour S, Kumwenda NI, Broadhead RL, Fiscus SA, Kafulafula G, et al. Gender Differences in Perinatal HIV Acquisition Among African Infants. *Pediatrics* (2005) 115(2):e167–72. doi: 10.1542/peds.2004-1590
142. Adland E, Millar J, Bengu N, Muenchhoff M, Fillis R, Sprenger K, et al. Author Correction: Sex-Specific Innate Immune Selection of HIV-1 In Utero Is Associated With Increased Female Susceptibility to Infection. *Nat Commun* (2020) 11(1). doi: 10.1038/s41467-020-16215-7
143. St Louis ME, Kamenga M, Brown C, Tarande Manzila AMNM, Batter V, Behets F, et al. Risk for Perinatal HIV-1 Transmission According to Maternal Immunologic, Virologic, and Placental Factors. *Jama* (1993) 269(22):2853–9. doi: 10.1001/jama.1993.03500220039023
144. Mwanyumba F, Gaillard P, Inion I, Verhofstede C, Claeys P, Chohan V, et al. Placental Inflammation and Perinatal Transmission of HIV-1. *J Acquir Immune Defic Syndr* (2002) 29(3):262–9. doi: 10.1097/00042560-200203010-00006
145. Temmerman M, Nyong'o AO, Bwayo J, Fransen K, Coppens M, Piot P. Risk Factors for Mother-to-Child Transmission of Human Immunodeficiency Virus-1 Infection. *Am J Obstet Gynecol* (1995) 172(2 Pt 1):700–5. doi: 10.1016/0002-9378(95)90597-9
146. Wabwire-Mangen F, Gray RH, Mmiro FA, Ndugwa C, Abramowsky C, Wabinga H, et al. Placental Membrane Inflammation and Risks of Maternal-to-Child Transmission of HIV-1 in Uganda. *J Acquir Immune Defic Syndr* (1999) 22(4):379–85. doi: 10.1097/00126334-199912010-00009
147. Van Dyke RB, Korber BT, Popek E, Macken C, Widmayer SM, Bardeguez A, et al. The Ariel Project: A Prospective Cohort Study of Maternal-Child Transmission of Human Immunodeficiency Virus Type 1 in the Era of Maternal Antiretroviral Therapy. *J Infect Dis* (1999) 179(2):319–28. doi: 10.1086/314580
148. Adachi K, Xu J, Yeganeh N, Camarca M, Morgado MG, Watts D, et al. Combined Evaluation of Sexually Transmitted Infections in HIV-Infected Pregnant Women and Infant HIV Transmission. *PloS One* (2018) 13(1):e0189851. doi: 10.1371/journal.pone.0189851
149. Hitti J, Watts DH, Burchett SK, Schacker T, Selke S, Brown ZA, et al. Herpes Simplex Virus Seropositivity and Reactivation at Delivery Among Pregnant Women Infected With Human Immunodeficiency Virus-1. *Am J Obstet Gynecol* (1997) 177(2):450–4. doi: 10.1016/S0002-9378(97)70214-X
150. McClelland RS, Wang CC, Richardson BA, Corey L, Ashley RL, Mandaliya K, et al. A Prospective Study of Hormonal Contraceptive Use and Cervical

Shedding of Herpes Simplex Virus in Human Immunodeficiency Virus Type 1-Seropositive Women. *J Infect Dis* (2002) 185(12):1822–5. doi: 10.1086/340639

151. Gray RH, Wabwire-Mangen F, Kigozi G, Sewankambo NK, Serwadda D, Moulton LH, et al. Randomized Trial of Presumptive Sexually Transmitted Disease Therapy During Pregnancy in Rakai, Uganda. *Am J Obstet Gynecol* (2001) 185(5):1209–17. doi: 10.1067/mob.2001.118158
152. Menendez C, Sanchez-Tapias JM, Kahigwa E, Mshinda H, Costa J, Vidal J, et al. Prevalence and Mother-to-Infant Transmission of Hepatitis Viruses B, C, and E in Southern Tanzania. *J Med Virol* (1999) 58(3):215–20. doi: 10.1002/(SICI)1096-9071(199907)58:3<215::AID-JMV5>3.0.CO;2-K
153. Tess BH, Rodrigues LC, Newell ML, Dunn DT, Lago TD. Breastfeeding, Genetic, Obstetric and Other Risk Factors Associated With Mother-to-Child Transmission of HIV-1 in Sao Paulo State, Brazil. Sao Paulo Collaborative Study for Vertical Transmission of HIV-1. *AIDS* (1998) 12(5):513–20. doi: 10.1097/00002030-199805000-00013
154. England K, Thorne C, Newell ML. Vertically Acquired Paediatric Coinfection With HIV and Hepatitis C Virus. *Lancet Infect Dis* (2006) 6 (2):83–90. doi: 10.1016/S1473-3099(06)70381-4
155. Giovannini M, Tagger A, Ribero ML, Zuccotti G, Pogliani L, Grossi A, et al. Maternal-Infant Transmission of Hepatitis C Virus and HIV Infections: A Possible Interaction. *Lancet* (1990) 335(8698):1166. doi: 10.1016/0140-6736(90)91174-9
156. Hershow RC, Riester KA, Lew J, Quinn TC, Mofenson LM, Davenny K, et al. Increased Vertical Transmission of Human Immunodeficiency Virus From Hepatitis C Virus-Coinfected Mothers. Women and Infants Transmission Study. *J Infect Dis* (1997) 176(2):414–20. doi: 10.1086/514058
157. Paccagnini S, Principi N, Massironi E, Tanzi E, Romanò L, Muggiasca ML, et al. Perinatal Transmission and Manifestation of Hepatitis C Virus Infection in a High Risk Population. *Pediatr Infect Dis J* (1995) 14(3):195–9. doi: 10.1097/00006454-199503000-00005
158. Papaevangelou V, Pollack H, Rochford G, Kokka R, Hou Z, Chernoff D, et al. Increased Transmission of Vertical Hepatitis C Virus (HCV) Infection to Human Immunodeficiency Virus (HIV)-Infected Infants of HIV- and HCV-Coinfected Women. *J Infect Dis* (1998) 178(4):1047–52. doi: 10.1086/515668
159. Thomas DL, Villano SA, Riester KA, Hershow R, Mofenson LM, Landesman SH, et al. Perinatal Transmission of Hepatitis C Virus From Human Immunodeficiency Virus Type 1-Infected Mothers. Women and Infants Transmission Study. *J Infect Dis* (1998) 177(6):1480–8. doi: 10.1086/515315
160. Tovo PA, Palomba E, Ferraris G, Principi N, Ruga E, Dallacasa P, et al. Increased Risk of Maternal-Infant Hepatitis C Virus Transmission for Women Coinfected With Human Immunodeficiency Virus Type 1. Italian Study Group for HCV Infection in Children. *Clin Infect Dis* (1997) 25 (5):1121–4. doi: 10.1086/516102
161. Bulterys M, Landesman S, Burns DN, Rubinstein A, Goedert JJ. Sexual Behavior and Injection Drug Use During Pregnancy and Vertical Transmission of HIV-1. *JAIDS J Acquired Immune Deficiency Syndromes* (1997) 15(1):76–82. doi: 10.1097/00042560-199705010-00012
162. Matheson PB, Thomas PA, Abrams EJ, Pliner V, Lambert G, Bamji M, et al. Heterosexual Behavior During Pregnancy and Perinatal Transmission of HIV-1. New York City Perinatal HIV Transmission Collaborative Study Group. *AIDS* (1996) 10(11):1249–56. doi: 10.1097/00002030-199609000-00011
163. Burns DN, Landesman S, Wright DJ, Waters D, Mitchell RM, Rubinstein A, et al. Influence of Other Maternal Variables on the Relationship Between Maternal Virus Load and Mother-to-Infant Transmission of Human Immunodeficiency Virus Type 1. *J Infect Dis* (1997) 175(5):1206–10. doi: 10.1086/593569
164. Taha TE, Gray RH. Genital Tract Infections and Perinatal Transmission of HIV. *Ann N Y Acad Sci* (2000) 918:84–98. doi: 10.1111/j.1749-6632.2000.tb05477.x
165. Bulterys M, Chao A, Dushimimana A, Phocas NP, Kurawige J-B, Musanganire F, et al. Multiple Sexual Partners and Mother-to-Child Transmission of HIV-1. *AIDS* (1993) 7(12):1639–45. doi: 10.1097/00002030-199312000-00015
166. Day JH, Grant AD, Fielding KL, Morris L, Moloi V, Charalambous S, et al. Does Tuberculosis Increase HIV Load? *J Infect Dis* (2004) 190(9):1677–84. doi: 10.1086/424851
167. Goletti D, Weissman D, Jackson RW, Graham NM, Vlahov D, Klein RS, et al. Effect of Mycobacterium Tuberculosis on HIV Replication. Role of Immune Activation. *J Immunol* (1996) 157(3):1271–8.
168. Toossi Z, Mayanja-Kizza H, Hirsch CS, Edmonds KL, Spahlinger T, Hom DL, et al. Impact of Tuberculosis (TB) on HIV-1 Activity in Dually Infected Patients. *Clin Exp Immunol* (2001) 123(2):233–8. doi: 10.1046/j.1365-2249.2001.01401.x
169. Gupta A, Bhosale R, Kinikar A, Gupte N, Bharadwaj R, Kagal A, et al. Maternal Tuberculosis: A Risk Factor for Mother-to-Child Transmission of Human Immunodeficiency Virus. *J Infect Dis* (2011) 203(3):358–63. doi: 10.1093/jinfdis/jiq064
170. Taha TE, Canner JK, Dallabetta GA, Chiphangwi JD, Liomba G, Wangel AM, et al. Childhood Malaria Parasitaemia and Human Immunodeficiency Virus Infection in Malawi. *Trans R Soc Trop Med Hyg* (1994) 88(2):164–5. doi: 10.1016/0035-9203(94)90277-1
171. Hoffman IF, Jere CS, Taylor TE, Munthali P, Dyer JR, Wirima JJ, et al. The Effect of Plasmodium Falciparum Malaria on HIV-1 RNA Blood Plasma Concentration. *AIDS* (1999) 13(4):487–94. doi: 10.1097/00002030-199903110-00007
172. Brahmbhatt H, Sullivan D, Kigozi G, Askin F, Wabwire-Mangenm F, Serwadda D, et al. Association of HIV and Malaria With Mother-to-Child Transmission, Birth Outcomes, and Child Mortality. *J Acquir Immune Defic Syndr* (2008) 47(4):472–6. doi: 10.1097/QAI.0b013e318162afe0
173. Brahmbhatt H, Kigozi G, Wabwire-Mangen F, Serwadda D, Sewankambo N, Lutalo T, et al. The Effects of Placental Malaria on Mother-to-Child HIV Transmission in Rakai, Uganda. *AIDS* (2003) 17(17):2539–41. doi: 10.1097/00002030-200311210-00020
174. Ayouba A, Badaut C, Kfutwah A, Cannou C, Juillerat A, Gangnard S, et al. Specific Stimulation of HIV-1 Replication in Human Placental Trophoblasts by an Antigen of Plasmodium Falciparum. *AIDS* (2008) 22(6):785–7. doi: 10.1097/QAD.0b013e3282f560ee
175. Mwapasa V, Rogerson SJ, Molyneux ME, Abrams ET, Kamwendo DD, Lema VM, et al. The Effect of Plasmodium Falciparum Malaria on Peripheral and Placental HIV-1 RNA Concentrations in Pregnant Malawian Women. *AIDS* (2004) 18(7):1051–9. doi: 10.1097/00002030-200404300-00014
176. Msamanga GI, Taha TE, Young AM, Brown ER, Hoffman IF, Read JS, et al. Placental Malaria and Mother-to-Child Transmission of Human Immunodeficiency Virus-1. *Am J Trop Med Hyg* (2009) 80(4):508–15. doi: 10.4269/ajtmh.2009.80.508
177. Johnson EL, Chakraborty R. HIV-1 at the Placenta: Immune Correlates of Protection and Infection. *Curr Opin Infect Dis* (2016) 29(3):248–55. doi: 10.1097/QCO.0000000000000267
178. Fowler MG, Rogers MF. Overview of Perinatal HIV Infection. *J Nutr* (1996) 126(suppl_10):2602S–7S. doi: 10.1093/jn/126.suppl_10.2602S
179. Shivakoti R, Gupta A, Ray JC, Uprety P, Gupte N, Bhosale R, et al. Soluble CD14: An Independent Biomarker for the Risk of Mother-To-Child Transmission of HIV in a Setting of Preexposure and Postexposure Antiretroviral Prophylaxis. *J Infect Dis* (2016) 213(5):762–5. doi: 10.1093/infdis/jiv479
180. Rossi P, Moschese V, Broliden PA, Fundaró C, Quinti I, Plebani A, et al. Presence of Maternal Antibodies to Human Immunodeficiency Virus 1 Envelope Glycoprotein Gp120 Epitopes Correlates With the Uninfected Status of Children Born to Seropositive Mothers. *Proc Natl Acad Sci* (1989) 86(20):8055–8. doi: 10.1073/pnas.86.20.8055
181. Broliden PA, Moschese V, Ljunggren K, Rosen J, Fundaro C, Plebani A, et al. Diagnostic Implication of Specific Immunoglobulin G Patterns of Children Born to HIV-Infected Mothers. *AIDS (London England)* (1989) 3(9):577–82. doi: 10.1097/00002030-198909000-00004
182. Pancino G, Leste-Lasserre T, Burgard M, Costagliola D, Ivanoff S, Blanche S, et al. Apparent Enhancement of Perinatal Transmission of Human Immunodeficiency Virus Type 1 by High Maternal Anti-Gp160 Antibody Titer. *J Infect Dis* (1998) 177(6):1737–41. doi: 10.1086/517435
183. Guevara H, Casseb J, Zijenah LS, Mbizvo M, Oceguera LF 3rd, Hanson CV, et al. Maternal HIV-1 Antibody and Vertical Transmission in Subtype C Virus Infection. *J Acquir Immune Defic Syndr* (2002) 29(5):435–40. doi: 10.1097/00042560-200204150-00002
184. Hofmann-Lehmann R, Vlasak J, Rasmussen RA, Smith BA, Baba TW, Liska V, et al. Postnatal Passive Immunization of Neonatal Macaques With a Triple Combination of Human Monoclonal Antibodies Against Oral Simian-Human Immunodeficiency Virus Challenge. *J Virol* (2001) 75 (16):7470–80. doi: 10.1128/JVI.75.16.7470-7480.2001
185. Dickover R, Garratty E, Yusim K, Miller C, Korber B, Bryson Y. Role of Maternal Autologous Neutralizing Antibody in Selective Perinatal

Transmission of Human Immunodeficiency Virus Type 1 Escape Variants. *J Virol* (2006) 80(13):6525–33. doi: 10.1128/JVI.02658-05
186. Ugen KE, Goedert JJ, Boyer J, Refaeli Y, Frank I, Williams WV, et al. Vertical Transmission of Human Immunodeficiency Virus (HIV) Infection. Reactivity of Maternal Sera With Glycoprotein 120 and 41 Peptides From HIV Type 1. *J Clin Invest* (1992) 89(6):1923–30. doi: 10.1172/JCI115798
187. Broliden K, Sievers E, Tovo PA, Moschese V, Scarlatti G, Broliden PA, et al. Antibody-Dependent Cellular Cytotoxicity and Neutralizing Activity in Sera of HIV-1-Infected Mothers and Their Children. *Clin Exp Immunol* (2008) 93 (1):56–64. doi: 10.1111/j.1365-2249.1993.tb06497.x
188. Omenda MM, Milligan C, Odem-Davis K, Nduati R, Richardson BA, Lynch J, et al. Evidence for Efficient Vertical Transfer of Maternal HIV-1 Envelope–Specific Neutralizing Antibodies But No Association of Such Antibodies With Reduced Infant Infection. *JAIDS J Acquired Immune Deficiency Syndromes* (2013) 64(2):163–6. doi: 10.1097/QAI.0b013e31829f6e41
189. Kliks SC. Features of HIV-1 That Could Influence Maternal-Child Transmission. *JAMA: J Am Med Assoc* (1994) 272(6):467.
190. Wu X, Parast AB, Richardson BA, Nduati R, John-Stewart G, Mbori-Ngacha D, et al. Neutralization Escape Variants of Human Immunodeficiency Virus Type 1 Are Transmitted From Mother to Infant. *J Virol* (2006) 80(2):835–44. doi: 10.1128/JVI.80.2.835-844.2006
191. Martinez DR, Vandergrift N, Douglas AO, McGuire E, Bainbridge J, Nicely NI, et al. Maternal Binding and Neutralizing IgG Responses Targeting the C-Terminal Region of the V3 Loop Are Predictive of Reduced Peripartum HIV-1 Transmission Risk. *J Virol* (2017) 91(9): e02422–16. doi: 10.1128/JVI.02422-16
192. Mabuka J, Nduati R, Odem-Davis K, Peterson D, Overbaugh J. HIV-Specific Antibodies Capable of ADCC Are Common in Breastmilk and Are Associated With Reduced Risk of Transmission in Women With High Viral Loads. *PloS Pathog* (2012) 8(6):e1002739. doi: 10.1371/journal.ppat.1002739
193. Pollara J, McGuire E, Fouda GG, Rountree W, Eudailey J, Overman RG, et al. Association of HIV-1 Envelope-Specific Breast Milk IgA Responses With Reduced Risk of Postnatal Mother-To-Child Transmission of HIV-1. *J Virol* (2015) 89(19):9952–61. doi: 10.1128/JVI.01560-15
194. Lohman-Payne B, Slyker JA, Moore S, Maleche-Obimboe E, Wamalwae DC, Richardson BA, et al. Breast Milk Cellular HIV-Specific Interferon γ Responses Are Associated With Protection From Peripartum HIV Transmission. *AIDS* (2012) 26(16):2007–16. doi: 10.1097/QAD.0b013e328359b7e0
195. Mor G, Aldo P, Alvero AB. The Unique Immunological and Microbial Aspects of Pregnancy. *Nat Rev Immunol* (2017) 17(8):469–82. doi: 10.1038/nri.2017.64
196. Mold JE, Michaelsson J, Burt TD, Muench MO, Beckerman KP, Busch MP, et al. Maternal Alloantigens Promote the Development of Tolerogenic Fetal Regulatory T Cells *In Utero*. *Science* (2008) 322(5907):1562–5. doi: 10.1126/science.1164511
197. Takahata Y, Nomura A, Takada H, Ohga S, Furuno K, Hikino S, et al. CD25 +CD4+ T Cells in Human Cord Blood: An Immunoregulatory Subset With Naive Phenotype and Specific Expression of Forkhead Box P3 (Foxp3) Gene. *Exp Hematol* (2004) 32(7):622–9. doi: 10.1016/j.exphem.2004.03.012
198. Hebel K, Weinert S, Kuropka B, Knolle J, Kosak B, Jorch G, et al. CD4+ T Cells From Human Neonates and Infants Are Poised Spontaneously to Run a Nonclassical IL-4 Program. *J Immunol* (2014) 192(11):5160–70. doi: 10.4049/jimmunol.1302539
199. Siegrist CA. Neonatal and Early Life Vaccinology. *Vaccine* (2001) 19(25-26):3331–46. doi: 10.1016/S0264-410X(01)00028-7
200. Goulder PJ, Brander C, Tang Y, Tremblay C, Colbert RA, Addo MM, et al. Evolution and Transmission of Stable CTL Escape Mutations in HIV Infection. *Nature* (2001) 412(6844):334–8. doi: 10.1038/35085576
201. Wilson CC, Brown RC, Korber BT, Wilkes BM, Ruhl DJ, Sakamoto D, et al. Frequent Detection of Escape From Cytotoxic T-Lymphocyte Recognition in Perinatal Human Immunodeficiency Virus (HIV) Type 1 Transmission: The Ariel Project for the Prevention of Transmission of HIV From Mother to Infant. *J Virol* (1999) 73(5):3975–85. doi: 10.1128/JVI.73.5.3975-3985.1999
202. Liu AY, Lohman-Payne B, Chung MH, Kiarie J, Kinuthia J, Slyker J, et al. Maternal Plasma and Breastmilk Viral Loads Are Associated With HIV-1-Specific Cellular Immune Responses Among HIV-1-Exposed, Uninfected Infants in Kenya. *Clin Exp Immunol* (2015) 180(3):509–19. doi: 10.1111/cei.12599
203. Lohman-Payne B, Sandifer T, Ohainle M, et al. In-Uteroinfection With HIV-1 Associated With Suppressed Lymphoproliferative Responses at Birth. *Clin Exp Immunol* (2014) 178(1):86–93. doi: 10.1111/cei.12386
204. *The Use of Antiretroviral Drugs for Treating and Preventing HIV Infection*. Available at: http://apps.who.int/iris/bitstream/handle/10665/85321/9789241505727_eng.pdf?sequence=1 (Accessed 11/23/2018).
205. UNAIDS. *The Gap Report*. Available at: http://www.unaids.org/sites/default/files/media_asset/UNAIDS_Gap_report_en.pdf (Accessed 11/26/2018).
206. Organization GWH. *WHO Recommendations on the Diagnosis of HIV Infection in Infants and Children* (2010). Available at: http://whqlibdoc.who.int/publications/2010/9789241599085_eng.pdf?ua=1 (Accessed 11/26/2018).
207. Takata H, Buranapraditkun S, Kessing C, Fletcher JLK, Muir R, Tardif V, et al. Delayed Differentiation of Potent Effector CD8+T Cells Reducing Viremia and Reservoir Seeding in Acute HIV Infection. *Sci Trans Med* (2017) 9(377):eaag1809. doi: 10.1126/scitranslmed.aag1809
208. Whitney JB, Hill AL, Sanisetty S, Penaloza-MacMaster P, Liu J, Shetty M, et al. Rapid Seeding of the Viral Reservoir Prior to SIV Viraemia in Rhesus Monkeys. *Nature* (2014) 512(7512):74–7. doi: 10.1038/nature13594
209. Luzuriaga K, Gay H, Ziemniak C, Sanborn KB, Somasundaran M, Rainwater-Lovett K, et al. Viremic Relapse After HIV-1 Remission in a Perinatally Infected Child. *New Engl J Med* (2015) 372(8):786–8. doi: 10.1056/NEJMc1413931
210. Bitnun A, Samson L, Chun TW, Kakkar F, Brophy J, Murray D, et al. Early Initiation of Combination Antiretroviral Therapy in HIV-1-Infected Newborns Can Achieve Sustained Virologic Suppression With Low Frequency of CD4+ T Cells Carrying HIV in Peripheral Blood. *Clin Infect Dis* (2014) 59(7):1012–9. doi: 10.1093/cid/ciu432
211. Giacomet V, Trabattoni D, Zanchetta N, Biasin M, Gismondo M, Clerici M, et al. No Cure of HIV Infection in a Child Despite Early Treatment and Apparent Viral Clearance. *Lancet* (2014) 384(950):1320. doi: 10.1016/S0140-6736(14)61405-7
212. Jani IV, Meggi B, Mabunda N, Vubil A, Sitoe NE, Tobaiwa O, et al. Accurate Early Infant HIV Diagnosis in Primary Health Clinics Using a Point-of-Care Nucleic Acid Test. *J Acquir Immune Defic Syndr* (2014) 67(1):e1–4. doi: 10.1097/QAI.0000000000000250
213. Persaud D, Gay H, Ziemniak C, Chen YH, Piatak M Jr, Chun T-W, et al. Absence of Detectable HIV-1 Viremia After Treatment Cessation in an Infant. *N Engl J Med* (2013) 369(19):1828–35. doi: 10.1056/NEJMoa1302976
214. Garcia-Broncano P, Maddali S, Einkauf KB, Jiang C, Gao C, Chevalier J, et al. Early Antiretroviral Therapy in Neonates With HIV-1 Infection Restricts Viral Reservoir Size and Induces a Distinct Innate Immune Profile. *Sci Trans Med* (2019) 11(520):eaax7350. doi: 10.1126/scitranslmed.aax7350
215. Safety and Effects of Using Prime-boost HIVIS DNA and MVA-CMDR Vaccine Regimens With or Without Toll-like Receptor 4 Agonist on HIV Reservoirs in Perinatally HIV Infected Children and Youth (HVRRICANE). Available at: https://clinicaltrials.gov/ct2/show/NCT04301154.
216. Kuhn L, Strehlau R, Shiau S, Patelc F, Shena Y, Technauc K-G, et al. Early Antiretroviral Treatment of Infants to Attain HIV Remission. *EClinicalMedicine* (2020) 18:100241. doi: 10.1016/j.eclinm.2019.100241
217. Violari A, Cotton MF, Gibb DM, Babiker AG, Steyn J, Madhi SA, et al. Early Antiretroviral Therapy and Mortality Among HIV-Infected Infants. *New Engl J Med* (2008) 359(21):2233–44. doi: 10.1056/NEJMoa0800971
218. Katusiime MG, Halvas EK, Wright I, Joseph K, Bale MJ, Kirby-McCullough B, et al. Intact HIV Proviruses Persist in Children Seven to Nine Years After Initiation of Antiretroviral Therapy in the First Year of Life. *J Virol* (2020) 94 (4):e01519–19. doi: 10.1128/JVI.01519-19
219. Bale M, Katusiime M-G, Wells D, Wu X, Spindler J, Halvas EK, et al. Early Emergence and Long-Term Persistence of HIV-Infected T-Cell Clones in Children. *mBio* (2021) 12:e00568–21. doi: 10.1128/mBio.00568-21
220. Violari A, Cotton MF, Kuhn L, Schramm DB, Paximadis M, Loubser S, et al. A Child With Perinatal HIV Infection and Long-Term Sustained Virological Control Following Antiretroviral Treatment Cessation. *Nat Commun* (2019) 10(1):412–23. doi: 10.1038/s41467-019-08311-0
221. Frange P, Faye A, Avettand-Fenoël V, Bellaton E, Descamps D, Angin M, et al. HIV-1 Virological Remission Lasting More Than 12 Years After Interruption of Early Antiretroviral Therapy in a Perinatally Infected Teenager Enrolled in

the French ANRS EPF-CO10 Paediatric Cohort: A Case Report. *Lancet HIV* (2016) 3(1):e49–54. doi: 10.1016/S2352-3018(15)00232-5
222. Goswami R, Nelson AN, Tu JJ, Dennis M, Feng L, Kumar A, et al. Analytical Treatment Interruption After Short-Term Antiretroviral Therapy in a Postnatally Simian-Human Immunodeficiency Virus-Infected Infant Rhesus Macaque Model. *mBio* (2019) 10(5):e01971–19. doi: 10.1128/mBio.01971-19
223. Bricker KM, Obregon-Perko V, Uddin F, Williams B, Uffman E, Garrido C, et al. Therapeutic Vaccination of SIV-Infected, ART-Treated Infant Rhesus Macaques Using Ad48/MVA in Combination With TLR-7 Stimulation. *PloS Pathog* (2020) 16(10):e1008954. doi: 10.1371/journal.ppat.1008954
224. Obregon-Perko V, Bricker K, Chahroudi A. The Brain Retains: Nonhuman Primate Models for Pediatric HIV-1 in the CNS. *Curr HIV/AIDS Rep* (2020) 17(4):343–53. doi: 10.1007/s11904-020-00503-4
225. Ajibola G, Garcia-Broncano P, Maswabi K, Bennett K, Hughes MD, Moyo S, et al. Viral Reservoir in Early-Treated Human Immunodeficiency Virus-Infected Children and Markers for Sustained Viral Suppression. *Clin Infect Dis* (2021) 22:e997–1003. doi: 10.1093/cid/ciab143
226. Martínez-Bonet M, Puertas MC, Fortuny C, Ouchi D, Mellado MJ, Rojo P, et al. Establishment and Replenishment of the Viral Reservoir in Perinatally HIV-1-Infected Children Initiating Very Early Antiretroviral Therapy. *Clin Infect Dis* (2015) 61(7):1169–78. doi: 10.1093/cid/civ456
227. Persaud D, Patel K, Karalius B, Rainwater-Lovett K, Ziemniak C, Ellis A, et al. Influence of Age at Virologic Control on Peripheral Blood Human Immunodeficiency Virus Reservoir Size and Serostatus in Perinatally Infected Adolescents. *JAMA Pediatr* (2014) 168(12):1138. doi: 10.1001/jamapediatrics.2014.1560
228. Rocca S, Zangari P, Cotugno N, Ferns B, Foster C, De Rossi A, et al. Human Immunodeficiency Virus (HIV)-Antibody Repertoire Estimates Reservoir Size and Time of Antiretroviral Therapy Initiation in Virally Suppressed Perinatally HIV-Infected Children. *J Pediatr Infect Dis Soc* (2019) 8(5):433–8. doi: 10.1093/jpids/piy080
229. Tagarro A, Chan M, Zangari P, Ferns B, Foster C, De Rossi A, et al. Early and Highly Suppressive Antiretroviral Therapy Are Main Factors Associated With Low Viral Reservoir in European Perinatally HIV-Infected Children. *J Acquired Immune Deficiency Syndromes (1999)* (2018) 79(2):269–76. doi: 10.1097/QAI.0000000000001789
230. Kuhn L, Paximadis M, Da Costa Dias B, Loubser S, Strehlau R, Patel F, et al. Age at Antiretroviral Therapy Initiation and Cell-Associated HIV-1 DNA Levels in HIV-1-Infected Children. *PloS One* (2018) 13(4):e0195514. doi: 10.1371/journal.pone.0195514
231. Ananworanich J, Avihingsanon A. HIV and Noncommunicable Diseases: The Asian Perspective. *J Acquir Immune Defic Syndr* (2014) 67 Suppl 1:S99–103. doi: 10.1097/QAI.0000000000000262
232. Uprety P, Chadwick EG, Rainwater-Lovett K, Ziemniak C, Luzuriaga K, Capparelli EV, et al. Cell-Associated HIV-1 DNA and RNA Decay Dynamics During Early Combination Antiretroviral Therapy in HIV-1-Infected Infants. *Clin Infect Dis* (2015) 61(12):1862–70. doi: 10.1093/cid/civ688
233. Luzuriaga K, Tabak B, Garber M, Chen YH, Ziemniak C, McManus MM, et al. HIV Type 1 (HIV-1) Proviral Reservoirs Decay Continuously Under Sustained Virologic Control in HIV-1–Infected Children Who Received Early Treatment. *J Infect Dis* (2014) 210(10):1529–38. doi: 10.1093/infdis/jiu297
234. Massanella M, Puthanakit T, Leyre L, Jupimai T, Sawangsinth P, de Souza M, et al. Continuous Prophylactic ARV/ART Since Birth Reduces Seeding and Persistence of the Viral Reservoir in Vertically HIV-Infected Children. *Clin Infect Dis* (2020) 73:427–38. doi: 10.1093/cid/ciaa718
235. Foster C, Domínguez-Rodríguez S, Tagarro A, Gkouleli T, Heaney J, Watters S, et al. The CARMA Study: Early Infant Antiretroviral Therapy—Timing Impacts on Total HIV-1 DNA Quantitation 12 Years Later. *J Pediatr Infect Dis Soc* (2021) 10(3):295–301. doi: 10.1093/jpids/piaa071
236. Van Zyl GU, Bedison MA, Van Rensburg AJ, Laughton B, Cotton MF, Mellors JW. Early Antiretroviral Therapy in South African Children Reduces HIV-1-Infected Cells and Cell-Associated HIV-1 RNA in Blood Mononuclear Cells. *J Infect Dis* (2015) 212(1):39–43. doi: 10.1093/infdis/jiu827
237. Avettand-Fenoel V, Lechenadec J, Diallo MS, Fillion M, Melard A, Samri A, et al. Initiating Antiretroviral Treatment Early in Infancy Has Long-Term Benefits on the Human Immunodeficiency Virus Reservoir in Late Childhood and Adolescence. *Clin Infect Dis* (2021). doi: 10.1093/cid/ciaa1931
238. Kuhn L. Early Infant Treatment: Still a Long Way to Go to Reach Human Immunodeficiency Virus Remission. *Clin Infect Dis* (2021) 72(3):394–5. doi: 10.1093/cid/ciaa033
239. Veldsman KA, Rensburg A, Isaacs S, Naidoo S, Laughton B, Lombard C, et al. HIV-1 DNA Decay Is Faster in Children Who Initiate ART Shortly After Birth Than Later. *J Int AIDS Soc* (2019) 22(8):e25368. doi: 10.1002/jia2.25368
240. Millar JR, Bengu N, Vieira VA, Adland E, Roider J, Muenchhoff M, et al. Early Initiation of Antiretroviral Therapy Following In Utero HIV Infection Is Associated With Low Viral Reservoirs But Other Factors Determine Subsequent Plasma Viral Rebound. *J Infect Dis* (2021). doi: 10.1093/infdis/jiab223
241. Veldsman KA, Laughton B, Janse van Rensburg A, Zuidewind P, Dobbels E, Barnabas S, et al. Viral Suppression Is Associated With HIV-Antibody Level and HIV-1 DNA Detectability in Early Treated Children at 2 Years of Age. *AIDS* (2021) 35(8):1247–52. doi: 10.1097/QAD.0000000000002861.
242. McManus WR, Bale MJ, Spindler J, Wiegand A, Musick A, Patro SC, et al. HIV-1 in Lymph Nodes Is Maintained by Cellular Proliferation During Antiretroviral Therapy. *J Clin Invest* (2019) 129(11):4629–42. doi: 10.1172/JCI126714
243. Bitnun A, Ransy DG, Brophy J, Kakkar F, Hawkes M, Samson L, et al. Clinical Correlates of Human Immunodeficiency Virus–1 (HIV-1) DNA and Inducible HIV-1 RNA Reservoirs in Peripheral Blood in Children With Perinatally Acquired HIV-1 Infection With Sustained Virologic Suppression for at Least 5 Years. *Clin Infect Dis* (2020) 70(5):859–66. doi: 10.1093/cid/ciz251
244. Palma P, McManus M, Cotugno N, Rocca S, Rossi P, Luzuriaga K. The HIV-1 Antibody Response: A Footprint of the Viral Reservoir in Children Vertically Infected With HIV. *Lancet HIV* (2020) 7(5):e359–65. doi: 10.1016/S2352-3018(20)30100-4
245. Singh V, Dashti A, Mavigner M, Chahroudi A. Latency Reversal 2.0: Giving the Immune System a Seat at the Table. *Curr HIV/AIDS Rep* (2021) 18(2):117–27. doi: 10.1007/s11904-020-00540-z
246. Nixon CC, Mavigner M, Sampey GC, Brooks AD, Spagnuolo RA, Irlbeck DM, et al. Systemic HIV and SIV Latency Reversal *via* Non-Canonical NF-κb Signalling *In Vivo*. *Nature* (2020) 578(7793):160–5. doi: 10.1038/s41586-020-1951-3
247. Dashti A, Waller C, Mavigner M, Schoof N, Bar KJ, Shaw GM, et al. SMAC Mimetic Plus Triple-Combination Bispecific HIVxCD3 Retargeting Molecules in SHIV.C.CH505-Infected, Antiretroviral Therapy-Suppressed Rhesus Macaques. *J Virol* (2020) 94(21):e00793–20. doi: 10.1128/JVI.00793-20
248. Palma P, Romiti ML, Montesano C, Santilli V, Mora N, Aquilani A, et al. Therapeutic DNA Vaccination of Vertically HIV-Infected Children: Report of the First Pediatric Randomised Trial (PEDVAC). *PloS One* (2013) 8(11):e79957. doi: 10.1371/journal.pone.0079957

Conflict of Interest: The authors declare that the research was conducted in the absence of any commercial or financial relationships that could be construed as a potential conflict of interest.

Advantages of publishing in Frontiers

OPEN ACCESS
Articles are free to read for greatest visibility and readership

FAST PUBLICATION
Around 90 days from submission to decision

HIGH QUALITY PEER-REVIEW
Rigorous, collaborative, and constructive peer-review

TRANSPARENT PEER-REVIEW
Editors and reviewers acknowledged by name on published articles

Frontiers
Avenue du Tribunal-Fédéral 34
1005 Lausanne | Switzerland

Visit us: www.frontiersin.org
Contact us: frontiersin.org/about/contact

REPRODUCIBILITY OF RESEARCH
Support open data and methods to enhance research reproducibility

DIGITAL PUBLISHING
Articles designed for optimal readership across devices

FOLLOW US
@frontiersin

IMPACT METRICS
Advanced article metrics track visibility across digital media

EXTENSIVE PROMOTION
Marketing and promotion of impactful research

LOOP RESEARCH NETWORK
Our network increases your article's readership